Value-added Chemicals from Biomass by Heterogeneous Catalysis

Voss, Bodil

Publication date:
2011

Value-added Chemicals from Biomass by Heterogeneous Catalysis

Bodil Voss

Ph.D. Thesis

Department of Chemical and Biochemical Engineering,
Technical University of Denmark

and

Haldor Topsøe A/S

April 2011

Preface

This dissertation is submitted in partial fulfilment of the requirements for receiving the PhD degree.

The dissertation covers the main part of the research work carried out in the period May 1st 2008 to April 30th 2011 (hereinafter referred to as the project) under my PhD study. The project was conducted as an industrial PhD project in collaboration between Haldor Topsøe A/S and the Technical University of Denmark, funded partly by the government (FI). The subject for the thesis is within a new technology area in the company. This has set a lot of challenges to the people involved. But it has been refreshing and interesting to turn the new pages.

I wish to thank my company for having supported me in this endeavour. I thank my colleague, Executive Vice President Jesper Nerlov, who actually commenced this process by offering me the opportunity of undertaking a PhD study after having been with the company for 17 years. Naturally, I am grateful for the guidance and instructions I received during my study from my first company supervisor PhD Simon Ivar Andersen (former Project Manager at Haldor Topsøe A/S, currently Reservoir Fluid Chemistry Discipline Manager at Schlumberger, Canada), Professor Jan-Dierk Grunwaldt, first as my primary university supervisor and later faithfully as my third party supervisor, and Professor John Woodley for taking me the rest of the way as my university supervisor. Thanks are also given to PhD Claus Hviid Christensen who took part in the initiation of the project as the then Director of Chemical Institute, Center for Sustainable and Green Chemistry, DTU, and who was my university supervisor for the very first few months. I specially want to thank my dear colleague Senior Scientist PhD Niels Christian Schjødt, who was there all the time during the project and took over the last 11 months as my company supervisor when Simon resigned. Thank you so much.

Generally, I found tremendous helpfulness all the way from everybody else involved, all the hardworking technicians, analysis experts and other colleagues, especially in our bio-group, who contributed. I thank you all. I indeed owe many thanks to Anders Kallesøe, Mai-Britt Jannie Metzon and Peter Mune for your effort, focus and clever observations.

Last but not least, special thanks to my family for being behind me and helping me distinguish the important matters from the even more important matters.

Bodil Voss

Table of Contents

Summary

In the contemporary debate on resource utilisation, biomass has been discussed as an alternative carbon source to fossil reserves in order to reduce the emission of CO_2 to the atmosphere. The replacement or supplement of oil based transportation fuels through biomass based conversions has already been implemented. The subject on chemical production has received less attention.

This thesis describes and evaluates the quest for an alternative conversion route, based on a biomass feedstock and employing a heterogeneous catalyst capable of converting the feedstock, to a value-added chemical. The project work to fulfil the above objective has been conducted with a multi-disciplinary approach ranging from fundamental catalyst research, through experiments, characterisation and process evaluation to market analysis.

The motivation herein is sought in the assets of sustainable resource utilisation obtained for such a process and the hypothesis that process feasibility in comparison with the conventional synthesis gas based technologies may further be attainable, taking advantage of the conservation of chemical C-C bonds in biomass based feedstocks. With ethanol as one example of a biomass based feedstock, having retained one C-C bond originating from the biomass precursor, the aspects of utilising heterogeneous catalysis for its conversion to value added chemicals is investigated. Through a simple analysis of known, but not industrialised catalytic routes, the direct conversion of ethanol to acetic acid product is identified to show good perspectives.

The nesting of a useful catalyst and an effective process is crucial to the potential of the overall process innovation. In a pre-screening study, a group of Cu based catalysts active in the conversion have been identified. Considering the freedom to operate, the prospects of process development are further identified through process calculations based on the experimental evidence attained, theory and the process elements described in literature (primarily patent-related). The protection of the process inventions made in relation to this is sought through the filing of three patent applications. The most important contributions of this thesis are reflected in the eventual conclusion that an ethanol to acetic acid process and a related catalyst, both subject to further development, are identified.

The understanding of the catalytic behaviour of down-selected catalysts, Cu spinel ($CuAl_2O_4$) and Cu/SiO_2, is obtained through characterisation as well as activity, selectivity and stability studies in appropriately developed experimental set-ups. Through numerous characterisation analyses (XAFS, XRPD, SEM, TEM, TPR, carbon analysis etc.) the rapid deactivation of the Cu spinel catalyst may be concluded to be attributed to the formation of high molecular carbonaceous compounds covering the catalytic surface, being catalysed by acidic alumina sites present during and after catalyst activation. This theory explains several phenomena observed for this catalyst. The Cu/SiO_2 catalyst, having an inert support, shows far higher robustness to process variations, but immediately exhibits a too low activity from an industrial angle. Several means of improving its activity are elucidated. For example an activity dependence on the Cu crystal size is indicated by the comparison of the activity and XRPD analyses obtained for crushed and whole catalyst pellets. Empirical kinetic models, in good agreement with the experimental data obtained for the Cu/SiO_2 catalyst, are developed

in order to support the establishment of an improved economic evaluation of the investigated process. Extrapolation of the derived model to the industrial pressure regime indicates a satisfactory activity. The Cu/SiO_2 catalyst is further able to withstand partly oxidative dehydrogenation conditions, allowing for immense process improvements. Finally, the ethanol to acetic acid process is put into a broader context, by reviewing the methods used in this work, the market influence on its fate, the conclusions and suggested improvements listed. Eventually, with an outlook on some alternative process possibilities, my recommendations are given under the consideration of the initial project objective.

The results of the thesis, taking one example of biomass conversion, show that the utilisation of biomass in the production of chemicals by heterogeneous catalysis is promising from a technical point of view. But risks of market price excursions dominated by fossil based chemicals further set a criterion of a solid economic margin. Therefore, under market considerations other alternatives are to be investigated.

In addition to the technical conclusions it appears that a multi-disciplinary approach to process innovation is advantageous.

Resumé (in Danish)

I den samtidige debat om ressourceudnyttelse har anvendelsen af biomasse været diskuteret som en alternativ carbon-kilde til de fossile reserver med henblik på at reducere CO_2-emissionen til atmosfæren. Erstatningen eller supplementet til de oliebaserede transportbrændstoffer gennem konversion af biomasse er allerede etableret. Fremstilling af kemikalier fra biomasse har haft ringere bevågenhed.

Denne afhandling beskriver og evaluerer en søgen efter en alternativ konversionsrute, baseret på biomasseføde og under anvendelse af en heterogen katalysator, som er i stand til at omsætte føden til et merværdi-kemikalie. Projektarbejdet i denne forbindelse er udført med en tværfaglig tilgang omfattende fra fundamentale katalysatorundersøgelser, gennem eksperimenter, karakterisering og proces-evalueringer til markedsanalyse.

Rationalet herfor er søgt gennem aktiverne i den opnåede bæredygtige ressourceudnyttelse for sådan en proces og under hypotesen, at lønsomheden af processen, i sammenligning med de konventionelle teknologier, yderligere kan opnås gennem fordelen ved bevarelsen af kemiske C-C bindinger i biomasse-baserede føder. Med udgangspunkt i ethanol som eksempel på en biomasse-baseret føde, som har beholdt en C-C binding fra det oprindelige biomasse-udgangsstof, bliver aspekterne for at udnytte heterogen katalyse til dets omsætning til merværdi-kemikalier undeersøgt. Gennem en simpel analyse af kendte, men ikke-industraliserede procesruter, bliver ethanol til eddikesyre-ruten identificeret som én, der viser gode perspektiver.

Inkorporeringen af en nyttig katalysator i en effektiv proces er afgørende for potentialet af den overordnede procesinnovation. En gruppe Cu baserede katalysatorer, som viser sig aktive i pågældende konversion, bliver identificeret i en forundersøgelseseksperimentrække. Under hensynet til handlefriheden bliver endvidere procesudviklingsmuligheder afdækket, baseret på de opnåede eksperimentelle vidnesbyrd, teori og proceselementer beskrevet i litteraturen (fortrinsvis patent-). Der bliver søgt beskyttelse af de relaterede opfindelser gennem indlevering af tre patentansøgninger. Afhandlingens vigtigste bidrag er afspejlet i den endelige konklusion, at en ethanol til eddikesyreproces og tilhørende katalysator, begge genstande for videreudvikling, er identificeret.

Forståelsen af den katalytiske opførsel af udvalgte katalysatorer, Cu spinel ($CuAl_2O_4$) og Cu/SiO_2, bliver opnået gennem karakterisering heraf såvel som målinger af aktivitet, selektivitet og stabilitet bl.a. i formålsudviklede testopstillinger. Gennem adskillige karakteriseringsanalyser (XAFS, XRPD, SEM, TEM, TPR, carbon analysis etc.) kan det konkluderes, at den hurtige deaktivering af Cu spinel katalysatoren skyldes dannelsen af højmolekylære kulholdige stoffer som dækker katalysatoroverfladen, katalyseret af sure alumina sites, der opstår under katalysatoraktiveringen. Denne forklaring er i overensstemmelse med adskillige observerede fænomener for katalysatoren. Cu/SiO_2 - katalysatoren, som har en inert support, viser langt højere robusthed over for procesvariationer, men udviser umiddelbart en for lav katalytisk aktivitet set fra en industriel vinkel. Adskillige måder til forbedring af aktiviteten bliver belyst. F.eks. indikeres en aktivitetsafhængighed af Cu-krystalstørrelsen ved en sammenligning af aktivitet og XRPD analyser for nedknuste og hele katalysatorpiller. Der bliver udledt empiriske kinetiske modeller, i god overensstemmelse med de opnåede

eksperimentelle data for Cu/SiO_2-katalysatoren, for at understøtte etableringen af en forbedret økonomisk vurdering af den undersøgte proces. Ekstrapolation af de udledte modeller indikerer tilfredsstillende aktivitet i det industrielle trykområde. Cu/SiO_2-katalysatoren er endvidere i stand til at klare delvist oxidative dehydrogeneringsbetingelser, som tillader betydelige procesforbedringer.

Slutteligt bliver ethanol til eddikesyre processen sat i en større sammenhæng ved i et tilbageblik at revurdere de i arbejdet anvendte metoder, markedets indflydelse på processens chancer, konklusioner og forbedringsmuligheder for processen. Endeligt, i betragtning af nogle fremadrettede alternative procesmuligheder, gives mine konkluderende anbefalinger under hensynet til det oprindelige projektformål.

Afhandlingens resultater viser, med udgangspunkt i et enkelt eksempel på biomasse-konversion, at udnyttelsen af biomasse i produktionen af kemikalier er lovende fra et teknisk synspunkt. Men risikoen for markedsprisudsving, domineret af fossilt baserede kemikalier, stiller endvidere kriteriet om en pålidelig økonomisk margin. Derfor bør man under markedshensyn undersøge alternativer.

I tillæg til de tekniske konklusioner forekommer det, at en tvær-disciplinær tilgang til procesinnovation er fordelagtig.

Publications included in the appendices

1. Review Article (published): E. Taarning, C.M. Osmundsen, X. Yang, B. Voss, S. I. Andersen, C.H. Christensen, Zeolite-catalyzed biomass conversion to fuels and chemicals, Energy Environ. Sci., 4, 3, (2011), 793 – 804. (Enclosed in Appendix A.2).
2. Full paper (published): B. Voss, S.I. Andersen, E. Taarning, C.H. Christensen, C Factors Pinpoint Resource Utilization in Chemical Industrial Processes, ChemSusChem, 2 (2009) 1152-1162. (Enclosed in Appendix A.3).
3. Patent Application (published): B. Voss, N.C. Schjødt, Process for the conversion of ethanol to acetic acid, EP2192103 A1. (Enclosed in Appendix D.3).
4. Patent Application (published): C.H. Christensen, N.C. Schjødt, B. Voss, Process and reactor for the thermoneutral conversion of ethanol to acetic acid, EP2194036 A1. (Enclosed in Appendix D.4).
5. Patent Application (published): B. Voss, R. Mabrouk, C.H. Christensen, Process for the production of acetic acid, ethylene and vinyl acetate monomer, US 20110137074. (Enclosed in Appendix D.5).
6. Report (published): B. Voss, A. Puig-Molina, P. Beato, F. Morales Cano, J.-D. Grunwaldt, CuO/Al_2O_3 catalyst investigated by EXAFS, Photon Science 2009 (HASYLAB Annual Report) - online, http://hasylab.desy.de/annual_report/authors.php?letter=p&year=2009. (Enclosed in Appendix E.2)
7. Full paper (published): B. Voss, N.C. Schjødt, J.-D. Grunwaldt, S.I. Andersen, J.M. Woodley, Kinetics of Acetic acid Synthesis from Ethanol over a Cu/SiO_2 Catalyst, Appl. Catal. A, 402 (2011) 69-79. (Enclosed in Appendix F.1)

Miscellaneous publications

8. Conference proceedings and poster at The 15th National Conference of Catalysis of China held 28th November to 2nd December 2010 in Guangzhou: X. Yang, E. Taarning, B. Voss, F. Joensen, 'Haldor Topsøe's approach to catalytic conversion of biomass to energy and to transportation fuel and chemicals'.
9. Conference proceedings at DK2, DTU: B. Voss, J.-D. Grunwaldt, J. Woodley, S.I. Andersen, Chemicals from Biomass: Sustainability and Feasibility of a Cu-based Catalyst, Dansk KemiingeniørKonference 2010, Institut for Kemiteknik, Kgs. Lyngby, 2010, p.112-113

Notation

Abbreviation	Description
BASF®	Badische Anilin- und Soda-Fabrik
BuOH+	Butanol and higher alcohols, aldehydes, ketones and acids
C_i	Compounds having i carbon atom/s
DFT	Density functional theory
DI	Direct injection
EDS	Energy-dispersive X-ray spectroscopy
EOR	End of run
ETEM	*In situ* high resolution electron microscope
EtOH	Ethanol
EtOAc	Ethyl acetate
EXAFS	Extended X-ray absorption fine structure
GC	Gas chromatograph
GC-MS	Gas chromatograph with a mass spectrometer
HAc	Acetaldehyde
HOAc	Acetic acid
HOS	Hours on stream
HRTEM	High resolution transmission electron microscopy
IR	Infrared analysis
ISBL	Inside battery limits
LPG	Liquefied petroleum gas, propane and butane
MeOH	Methanol
MS	Mass spectrometer
MT	Metric ton
MTG	Methanol to gasoline
MTPY	Metric ton per year
MU	Make-up
NEB	Net Energy Balance
NWE	North West Europe
OH	Overhead
OSBL	Outside battery limits
PCT	Patent Cooperation Treaty
ROI	Return on investment
RT	Room temperature
Questimate®	Cost estimation program
QEXAFS	quick-scanning EXAFS
SS	Stainless steel
SOR	Start of run
TEM	Transmission Electron Microscopy
TGA	Thermogravimetric analysis
tOE	Ton of oil equivalent
TPR	Temperature programmed reduction
US	United States of America
USD	US dollar
VAM	Vinyl acetate monomer
XAFS	X-ray absorption fine structure
XANES	X-ray absorption near-edge structure
XRD	X-ray diffraction

XRPD	X-ray powder diffraction
*	Free site
I*	Component I adsorbed on surface site
$^{\theta}$ (superscript theta)	Standard conditions, °C and 1.013 bar

Expression	**Description**
$x_{i,m}/x_{u,m}$ i:u mixture	Liquid feed with mole ratios $x_{i,m}/x_{u,m}$ for components i and u.
Biomass I	Sugar or starch based biomass
Biomass II	Lignocellulosic biomass
Cu spinel-850	Copper aluminium spinel catalyst calcined at 850°C for 4 h.
Cu abc step site	Step site in the crystal plane with the Miller index [abc]
Cu(abc)	Cu plane with the Miller index [abc]
Depreciation	Investment/simple pay back time/production capacity.
Fixed cost	Yearly maintenance and salaries.
Gate price	The minimum selling price excl. ROI but incl. depreciation.
GIPS	General Integrated Programming System (modelling software)
Grand total investment	Total fixed investment + 25% (contingencies and professional services).
Karl Fischer	Analytical method for determining water content.
LECO	Combustion method for determining total carbon.
Make-up	The original feed to a synthesis section.
Return on investment	The percentage of profit annually of the capital invested.
(R+M)/P	Recycle and make-up to production weight ratio
Selectivity of i	Percentage of feed conversion to product i, to total conversion
Simple pay back time	The period over which the investment loan is paid down
Total fixed investment	ISBL+OSBL investment

Nomenclature	**Description**	**Unit**
[abc]	Crystal plane Miller index	-
a_{spec}	Specific Cu area	m^2/g catalyst
A_n	Pre-exponential factor in power law model	mol/(g·h·bar$^{\Sigma\gamma}$)
$A_{surf,ave}$	Surface area of a hemisphere w/ av. radius	m^2
d_h	Hydraulic diameter	m
D[abc]	Size of crystal plane w/ the Miller index [abc]	Å
E_{ads}	Adsorption energy	kJ/mol
E_n	Apparent activation energy	kJ/mol
E_{i*}	Energy of surface w/ adsorbed component i	kJ/mol
E_*	Energy of relaxed surface	kJ/mol
EtOHP	Ethanol feedstock price	USD/MT
F_i	Molar flow rate of component I	mol/h
G	Mass velocity/cross section area, empty tube	kg/(h·m^2)
ID	Inner diameter	m
K_n	Dimensionless equilibrium constant, step n	-
LHV	Lower heating value	J/kg
LHSV	Liquid hourly space velocity	ml/(g·h)
LWHSV	Liquid weight hourly space velocity	g/(g·h)
m_{cat}	Catalyst mass	g
M_i	Molar mass of component i	g/mol
n	Reaction step number	-

NGP	Natural gas price	USD/GJ
X	Molar part of ethanol converted oxidatively	-
x_i	Weight % of component I	%
$x_{i,m}$	Molar fraction of component i	-
p_i	Partial pressure of component i	bar
p^θ	Standard pressure, 1.013 bar	bar
p	Total operating pressure	bar
Q_n	Dimensionless reaction quotient, step n	
$Re_p=d_h\ G/\mu$	Particle Reynolds' Number	-
$STY_i=M_i\cdot(F_{i,\,out}-F_{i,\,in})/m_{cat}$	Space time yield for component i	g/(g·h)
SV	Space velocity	Nl/(g·h)
SV_m	Molar space velocity	mol/(g·h)
t	Temperature	°C
T	Absolute temperature	K
v_{spec}	Specific volume of Cu	m^3/g catalyst
V_{ave}	Volume of hemisphere with average radius	m^3
x_i	Weight fraction of component i	-
y_i	Mole % of component I in a mixture	%
$\beta_n=Q_n/K_n$	Approach to equilibrium for reaction step n	-
δ	Degree of reduction	-
γ_i	Kinetic coefficient for component i	-
μ	Viscosity	kg/(m·h)
θ	X-ray diffraction angle	°
θ_*	Coverage of free site	-
θ_i	Coverage of site with adsorbed component I	-
ρ	Density	kg/m^3

Chapter 1 Chemicals from Biomass

1.1 Introduction

The proper utilization of world resources is increasingly becoming an issue in light of the coming shortage of fossil fuel. Thus the interest of utilizing the bio-mass resource, being renewable, for the production of fuels and chemicals has been revived. Especially in a first round the major attention has been drawn to how the transportation fuel (which today primarily is produced from the refining of crude oil) can be replaced by renewable resources (*Institute for Environment and Sustainability*, 2007, *Thomsen et al., 2007*). The primary biofuels are ethanol produced by fermentation and the methyl esters produced by transesterification of triglyceride as substitutes for gasoline and diesel, respectively. But over the few past years, the interest in utilizing biomass for the production of chemicals of higher value from biomass via heterogeneous catalysis has grown too (*Corma et al., 2007, Christensen et al., 2008, Werpy et al., 2004*).

The well-known rationale behind the use of biomass as an alternative to fossil fuel is three-fold: The forecasted shortage of fossil sources, the desire for independence of fossil sources (*Cavallo, 2007*), and the arguments that the world climate suffers from the emission of vast amounts of CO_2 to the atmosphere, increasing thereby the green house effect, leading to global warming *(United Nations, Kyoto Protocol, 1998)*.

Biomass, being a renewable resource, offers a sustainability benefit over fossil fuel reserves, which are finite. But other sources covering some of our needs are renewable too, and biomass production is limited and must also cover our needs for food. Given that: How does the utilisation of biomass for the production of chemicals fit in terms of availability, suitability and feasibility? This chapter outlines the background for the subject, discusses the above mentioned aspects shortly and in conclusion presents the motivation, the scope and the structure of the thesis.

1.2 Sustainability: Needs covered on a long term basis

The most developed definitions of sustainability of for example a chemical and its production take into account the environmental, the economic, as well as the societal issues/influences (see Figure 1-1).

The global political focus on CO_2 emission, as one environmental aspect, signals that the climate impact of CO_2 is broadly accepted – or at least this is the common platform for the dialogue. Through CO_2 taxation policies and legislation the interest in CO_2 neutral alternatives to fossil fuels and feedstocks increases, because our societal needs for products must still be covered in an economically sustainable way – there is profit to gain in continuing doing so. Looking further into each of these sustainability categories many more details emerge for example on the borderline between the economic and societal aspects (the technologies should maintain the need for manpower), but the reduction of CO_2 emission is presently the leading factor in reviewing the sources available for the continued support of our needs.

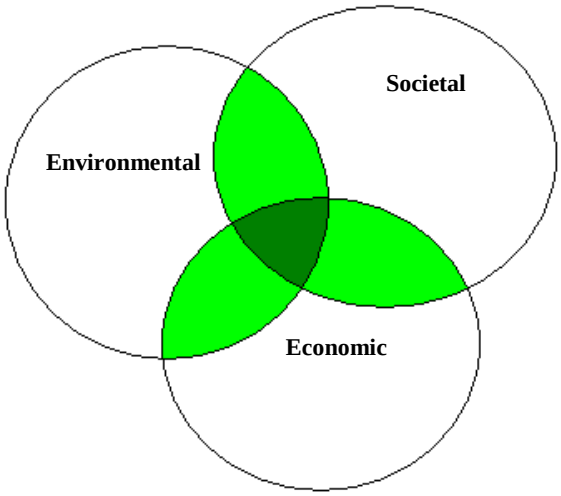

Figure 1-1: Sustainability must be obtained with respect to environmental, societal and economic aspects.

Human needs are many and diverse. But the ones related to sources are basically: We need food (and clean water) to keep our bodies going, we need materials and chemicals for medicine, clothes and building materials, and we need energy to produce these materials and chemicals, to keep us warm, to provide us with electricity for lighting our buildings, and to maintain the mobility of humans through efficient transportation. The needs are covered by utilizing different sources and these in combination. Depending on the current availability and price, the source patterns have changed over time and from place to place – sustainability now demands the forward-thinking, making sure that also a future solution to the future needs may be figured. Globally (*United Nations, Brundtland report*, 1987, *Azapagic, 2010)*.

1.3 The sources

The sources to cover the needs are also many, their nature and representation depending on the region they are consumed in. The sources comprise the fossil fuels, the biomass grown, the metals and minerals, and the water being recovered from the underground or desalted seawater. An important issue is whether they are seen as resources or as reserves. Logically reserves are limited and may not be used unrestrained and endlessly, if sustainability is the approach. Sources are in principle only *re*sources when being renewed or recreated at a speed comparable to their consumption.

The three groups of sources, most relevant to feedstock and fuel side for the chemical production, are discussed below: oil (and natural gas), coal and biomass.

1.3.1 Oil and natural gas

While initiated already in the middle of the 18th century, the production of oil really started expanding back in the 1950s and today the daily production of oil is higher than ever (*Mousdale*[a], 2008), about 30 billion barrels/year. Associated natural gas was

originally and is still to a large extent being burnt as an off-stream in the oil recovery; meanwhile, today there is an increased focus on its utilization in parallel to oil as a fuel and chemical feedstock rather than flaring it, in order to avoid CO_2 taxation. Stranded gas fields are also a source of natural gas, and these represent a quite substantial amount (36%) of the proven natural gas reserves (*Perego et al., 2009*). Crude oil may be refined into readily applicable diesels and gasoline fractions, whereas other fractions may be further hydrotreated, cracked or reformed to further obtain valuable products, for example ethylene which is an important monomer in the process of making plastic. Naphtha or natural gas may also be reformed into so-called synthesis gas (foremost hydrogen and carbon monoxide) from which chemicals such as methanol, formaldehyde, ammonia etc. are produced via (heterogeneous) catalysis. Historically, oil based technologies provided partly for the opportunity of man to establish an efficient worldwide infrastructure, and partly to exchange a number of biomass based chemical processes with more economic oil based ones, eventually erasing the biomass based industry in a lot of fields. The oil adventure will last only as long as new oil is found (*Goodstein, 2005*) – it is discussed these days for how long that is, and most experts agree that 30-50 years is a plausible time frame. Although it is believed by some clinging to the abiogenic hypotheses (reviewed by *Gold* in 1992) that the underground oil production is an ongoing process, it is widely accepted still that our present consumption rate is far higher than the production rate, rendering the oil a finite reserve.

1.3.2 Coal

Coal, also being a versatile feedstock, has a wider perspective in that the world consumption of fuel and feedstock seems to be covered for the next about >100 years (*World Coal Association, 2010)*. Presently the world consumption of coal is 7 billion MT per year. The mining of coal though has a great impact on the landscape, where coal is found, and in many places it implies unhealthy and risky working conditions for the people who are employed in the mines. It also sets requirements to the cleaning of effluents from the coal based power and chemical plants, as coal contains substantial amounts of mercury, arsenic and sulphur. If carefully mined and treated, coal has a great potential for taking over the role of oil for the supply of energy and chemicals to the world - for a period. The development of coal based technologies will also shift the power and influence from oil-producing countries to the ones with abundant coal reserves (China). Nevertheless, coal remains a reserve.

1.3.3 Biomass

The world only possesses a limited biomass growing capacity (*Jenkins, 2003*), even if the production rate is optimized by technological advances, in agriculture and in the conversion processes. Cellulose, the most abundant bio-compound, is produced at a level of 10^{10}-10^{11} MTPY (*Hutchens et al*., 2006). Biomass in this context includes all kind of living plant species: trees, agricultural, non-agricultural and aquatic plants, and the wide range of products arising from these, animal carbohydrate waste and parts of the municipal and industrial waste. Figure 1-2 shows how one example of a biomass type, trees, may go into an industrial or household use for example as a construction material, or may go directly to the energy supply and/or the production of chemicals. Likewise, waste material from the production of for example furniture or wooden floors may be used as a feedstock for biomass conversion. And eventually when the furniture or the floors are replaced by new ones the discarded material may also be used.

Herbaceous biomass is also very diverse and has different chemical composition. Figure 1-2 would look very much different taking for example corn or rape as an example.

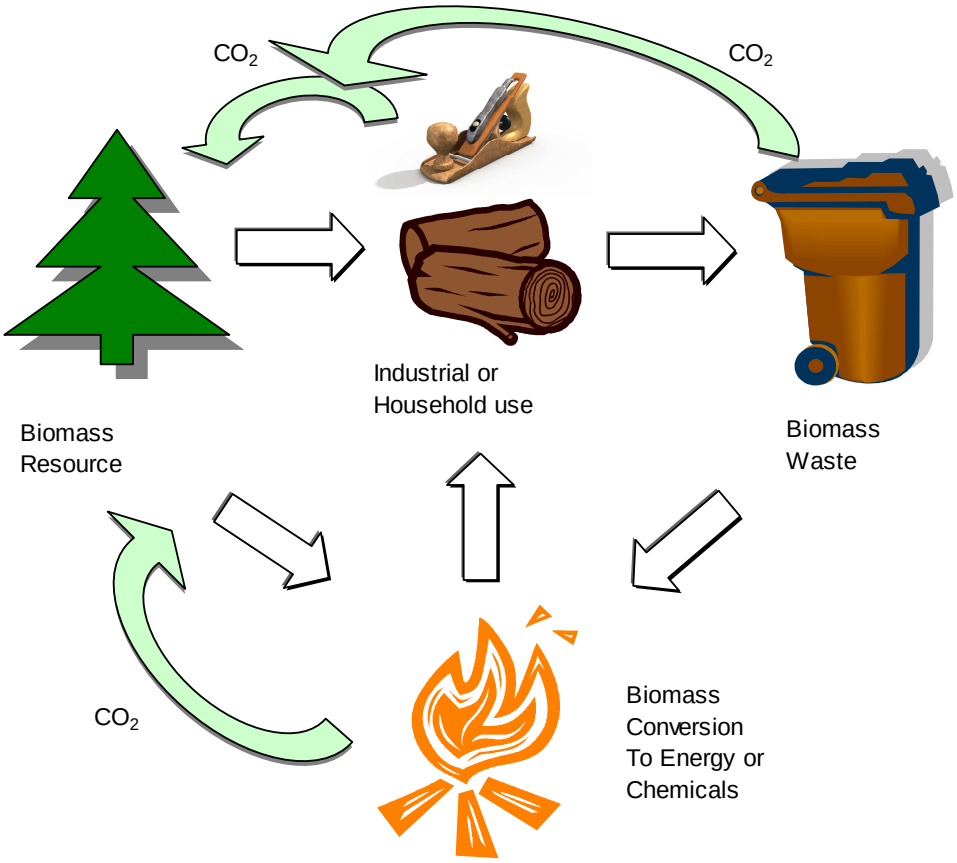

Figure 1-2: Biomass is available for conversion processes, either directly or as bio-waste from industrial or household use. Biomass conversion includes the production of materials, chemicals and heat. After ultimate conversion through combustion, C from spent biomass finally reverts to the atmosphere as CO_2.

As is well known biomass production depends highly on the growing conditions (fertility, arability, climate, diseases and animal competition). It has been studied, how crops may optimally be grown in combination, increasing the value of the crops harvested per acre and/or reducing the need for artificial fertilizers (*Sieling, 1997*). The kinds of crops grown in agriculture possess very different biomass characteristics. From plant to plant but also in the various parts of the plant the relative amounts of oils, carbohydrates, lignin, proteins, and waxes vary (*Clark et al.[a], 2008*). In order to reduce the special (low volume) chemicals production cost, research has been made in specializing the plants to achieve high concentrations of the desired components as a whole or in particular parts, for example the seeds.

The CO_2 neutrality of the biomass is a fact. However, whether the CO_2 concentration in the atmosphere is the main reason for the global warming, or not, is still being discussed. Other correlations associated with solar activity and its influence on the formation of clouds has been suggested (*Svensmark, 2007)*. Biomass is grown for the production of food, chemicals and energy. Biomass is a restricted and limited resource.

1.4 Prioritizing sources

Versatile as oil, natural gas and coal may be, they provide for chemicals and energy, but not for food; and they are reserves, not renewable. Nuclear power, wind power, water power and solar power are resources of energy, but neither of chemical feedstock or food. Biological waste is clearly a resource, while waste produced from fossil feed stock by its origin is a reserve but by its state is a resource. Waste of both types may be gasified and converted to synthesis gas, the chemical building blocks (intermediates) of today's natural gas/naphtha based chemical production, which may also be used for the power production in gas turbines. Biomass is literally the only long term carbon source (apart from CO_2 potentially sequestered from the atmosphere). Biomass based processes to chemicals and fuels also offer independence for the supply of fossil reserves, but it creates in turn a dependence of the green resource supply instead, which is limited, may fail (disease and insects) and may become insufficient. Figure 1-3 shows a simplified survey of how the needs for feedstock to the chemical production competes with other needs to be fulfilled and how the competing needs may be covered by alternative sources.

As one class of biomass to be mentioned, the annual crops, the most prominent are the ones having been optimized over generations for the provision of food, like wheat, corn, rape and potatoes. The competition between biomass for food and non-food uses is unavoidable, unless all food requirements are fulfilled before energy and chemical crops are grown, and only strictly non-food parts of the biomass is used for chemicals and energy production. The production of first generation ethanol for gasoline supplement might not compete with food production on a regional basis but may do so on a global basis.

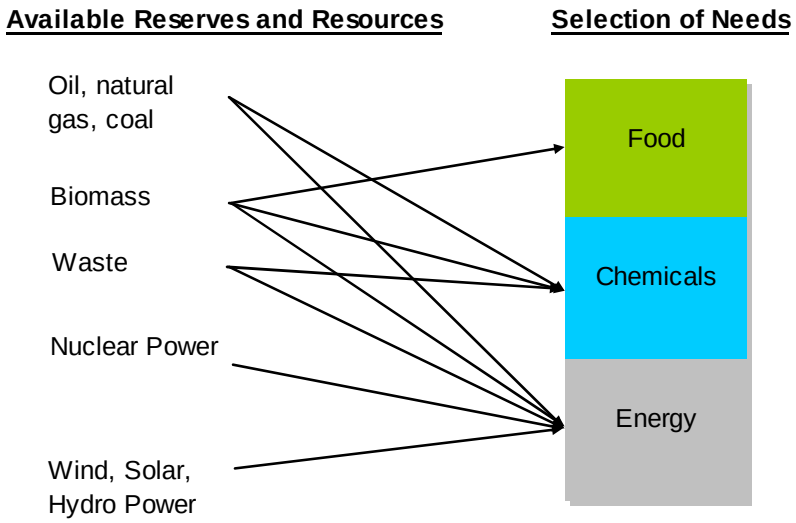

Figure 1-3: The coverage of needs from the available reserves and resources. Energy needs may be covered from all listed sources, but biomass is the only long term, sustainable carbon source providing for food and chemicals.

The *European Environment Agency* made a report in 2006 assessing the potentials in Europe for producing bio-energy without harming the environment and securing Europe a self sufficient food supply.

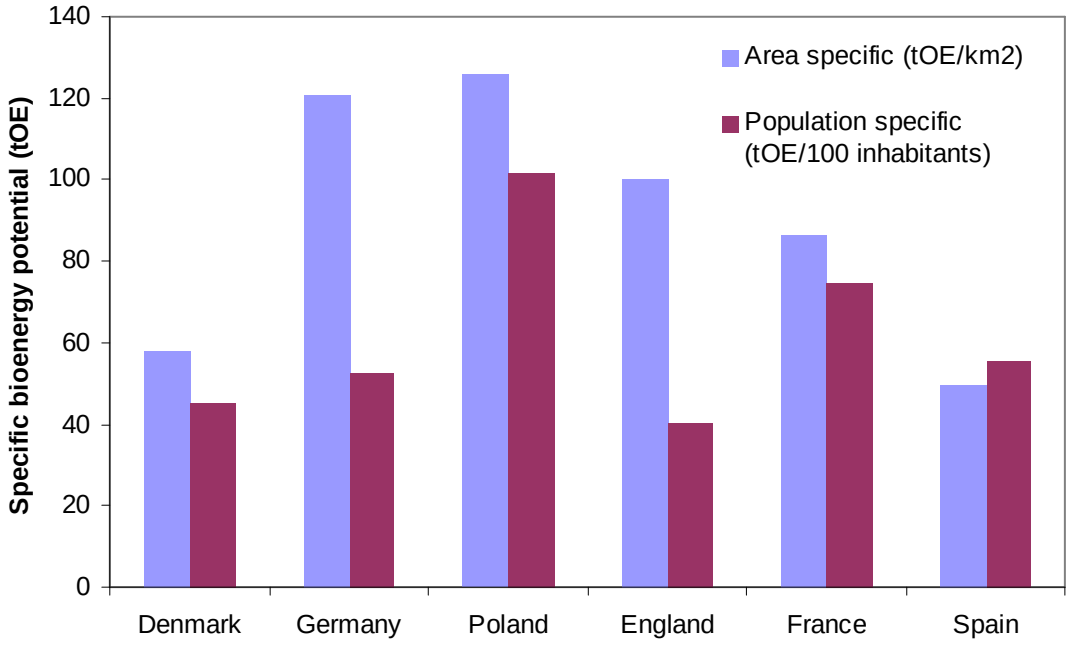

Figure 1-4: The 2030 specific annual bio-energy potential for different EU countries. The values forecast vary within Europe. The Danish annual consumption in 2007 was about 150 MT/100 inhabitants of oil alone, covering half the non-renewable energy consumption (*Danish Energy Agency, 2008*).

They conclude that significant amounts of biomass can technically be available, even if environmentally compatible (extensively cultivated areas maintained, low impact crops, protection of forests etc.) agricultural methods are applied. But the potentials of the different countries are very different, and one may imagine that on a world scale the figures are even more diverse. Figure 1-4 shows how the annual bio-energy potential 2030 varies in a number of European countries. With a present consumption of 300 tOE/100 inhabitants of fossil fuel annually in Denmark, we are not able to replace our fossil fuel supply with domestic bio energy production, unless the demand for energy is reduced drastically. The projection of the energy consumption in Denmark up to 2025 is that it will remain constant (*Danish Energy Agency, 2008*) - i.e. other supplementary energy sources are needed too.

In order to foresee enough food and the chemicals required from biomass, energy must come in third place in needs, being coverable by many sources. Encouragingly, the production of chemicals only takes up 5% of the consumption of the fossil feedstocks today (*Demirbas, 2008*), which judged from above is about 15 tOE/100 inhabitants per year, coverable in an environmentally sustainable manner as learned from the *European Environment Agency* (2006) report.

Furthermore, the economic potential in producing chemicals is normally higher than the economic potential in producing fuel, i.e. the unit prices of chemicals are higher than the feedstock of the most dominant route, owing to the simple relation that more process steps are added to a fuel platform in the course of conversion to the desired chemical. If a biomass feedstock allows for a shorter and smarter conversion route to the desired chemical, this alternative route may be economically attractive over the fossil based route.

Heterogeneous catalysis has been used in the conversion of fossil feedstock for a century now. In order for biomass based alternative routes to become competitive, catalysis may also offer the benefits of accelerating conversions of biomass feedstock at moderate operating conditions. Some biomass based processes may however only be viable based on subsidies, CO_2 taxation or legislation as a wind at the back.

1.5 Prerequisites to sustainable development

Realistically, the oil, natural gas and coal consumption can only be reduced drastically by the hand of politicians, empowered by the political and economic interests. Political interests may have roots in the wish for independence of fuel and feedstock supply, healthcare and sustainability driven legislation. For example, in the US new power plants must be prepared for the sequestration of CO_2 in order to get approved by the authorities; and the regional CO_2 quotas dictated and CO_2 taxes put on goods, in accordance with their respective energy consumption, are already influencing the mindset of the chemical industry (*Banholzer et al., 2008*). Another well known example is the subsidies paid to US bio-ethanol producers to increase the production capacity of fuel ethanol, reducing the domestic dependence on oil imports from the Middle East. Political interests may also be in areas such as high employment rates and competitiveness, sometimes conflicting with the energy saving and green politics.

On top of that, the chance for biomass based chemical processes to be commercialized depends on several other factors to become viable: the biomass based feedstock needed must be suitable and available in adequate amounts to feed the process, the biomass must be convertible to useful products, and the biomass based process must be competitive, directly or via subsidies, to conventional processes. The chance of obtaining subsidies or financial support for research and the green market pull is best obtained, if the environmental benefit over the conventional processes may be substantiated.

1.5.1 Bio-feed availability

The creation of a biomass platform has commenced through the growing interest in bio-ethanol for gasoline supplement, and transesterfication of rape seed oil for diesel replacement. Unlike the wide group of chemicals nowadays being produced predominantly from oil, gas or coal, ethanol production has maintained its roots in biomass. Less than 5% of the ethanol is synthesized from fossil resources (hydration of ethylene at 300°C on supported phosphoric acid). Alone in the US, the annual production capacity of ethanol has increased over the years 1980-2007, from about 1 to more than 30 million MT per year (*Mousdale*[c], 2008), and a total annual global production of 52 million MT of fuel ethanol (Figure 1-5) was reached in 2008 (*RFA, 2010*). The bio-diesel production in 2008 is estimated to have been 10.8 million MT (*Choi, 2008*). Since, in the production of bio-diesel, a product stream of aqueous glycerol (100 kg/MT bio-diesel produced) is co-produced, this gives an annual production of about 1 million MT of bio-glycerol. The price for most of the co-produced glycerol in bio-diesel production is low, and has even been negative. But the crude grade bio-glycerol is not readily applicable as a feedstock for the production of chemicals by catalysis, as it contains, apart from water and methanol, varying fractions of ash with many elements, for example calcium, magnesium, phosphorous and sulphur, and has varying pH (*Farm Energy Community, 2010*). Furthermore, the high

level, number and nature of impurities in crude bio-glycerol imply that its purification is very energy intensive. Pure glycerol has over 1500 different uses and may also be converted catalytically to for example 1,3-dihydroxyacetone, propylene glycol or acrolein (*Choi, 2008*). The price volatility of refined glycerol has been very high and unpredictable, with prices fluctuating between 400 USD/MT and 1800 USD/MT from 1970 until 2008. The impurity of the cheap crude and the price volatility of the refined product are two major obstacles that make glycerol a troublesome biomass based feedstock. Fermentative production of high value products from crude glycerol by means of specially developed strains seems a promising way of overcoming the purity drawback (*Choi, 2008*).

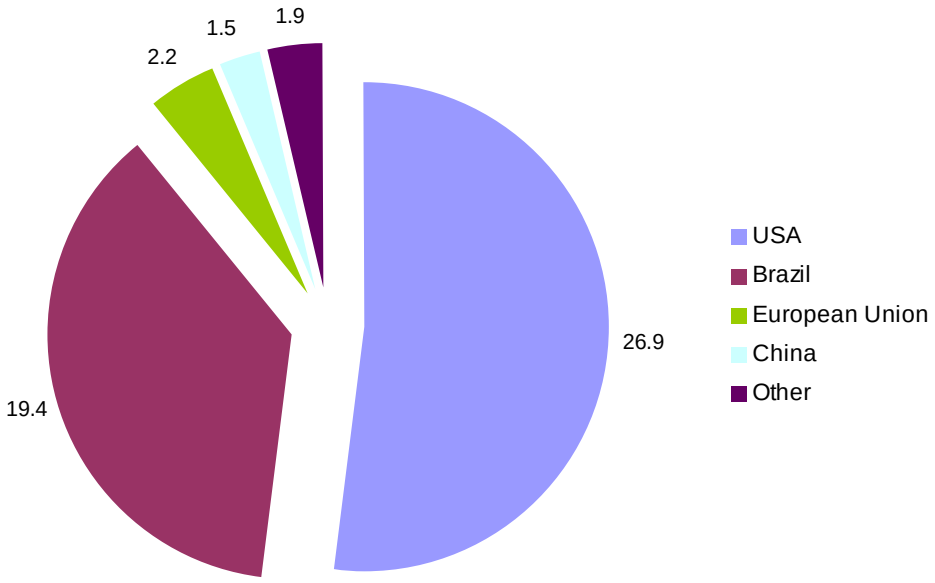

Figure 1-5: 2008 world wide production of fuel ethanol (52 million MT). USA has taken over the leading position as the world's largest ethanol producer.

Ethanol is today produced by fermentation of agricultural products such as sugar cane molasses, corn starch etc. (*Weissermel et al.*[b], *2003*), the world ethanol capacity is constantly expanding, especially in the US, Brazil, China and EU. Bio-ethanol comes with a lot of water. The ethanol concentration in the fermentation broth is 8-10 wt%, the broth containing apart from ethanol primarily water, CO_2, yeast and insolubles. By simple distillation in two columns a stream of up to 94wt% aqueous ethanol may be obtained. The dewatering of ethanol to make anhydrous ethanol for fuel additive is an extra expense in bio-ethanol economics (*Pfeffer et al., 2007*). The ethanol price paid to producers has fallen with accumulated installed production capacity indicative of an immature technology with technology improvements constantly underway (*Thomsen et al., 2007*).

Research has been made in the pre-treatment and hydrolysis of biomass waste by enzymes (*Viksø-Nielsen, 2009*) to attain an alternative feedstock for fermentation to ethanol. From lignocellulosic material (stover, stems etc.) both glucose and xylose, highly abundant but chemically bound as cellulose and hemicellulose, may be fermented into ethanol. Thus, in a future 2nd generation bio-ethanol process, the application of enzymes will make it possible to utilize the waste fraction, which does not

compete with the world production of food (see Appendix A.1 for details). Such a shift of technology toward a group of feedstocks (for example waste or wood) without food value will expand the capacity potential of bio-ethanol further. 2nd generation bio-ethanol warrants a future biomass based feedstock with a high availability, which does not compete with food production, and which has a low production cost. The ethanol fuel market will possibly expand, until a convincing biomass based fuel replacement successor outperforms ethanol as a fuel. And given the ethanol production capacity established already, the interface with developments in the motor industry and fuel infrastructure, quite a profit margin will have to be gained to make such a shift.

Overall, ethanol has as a feedstock more upsides than bio-glycerol has. A decision on whether bio-ethanol is not only suitable and available, but can also be said to support the other sustainability criteria, relies on the further discussion of these in below paragraphs.

1.5.2 Bio-ethanol suitability for chemical production

Distillates of ethanol with concentrations of 10-94 wt% primarily balanced by water may be withdrawn from the distillation based purification. Relatively high energy consumption is needed to remove the residual amount of water to obtain anhydrous ethanol (*Pfeffer et al., 2007*) sparking an immediate interest in the use of hydrous ethanol for the production of chemical.

Ethanol can be converted to a number of chemicals, which themselves are important precursors in further conversions or important end products (see Figure 1-6). Catalysis plays an important role in these conversion processes, serving to provide for conversions at low temperature and high selectivity.

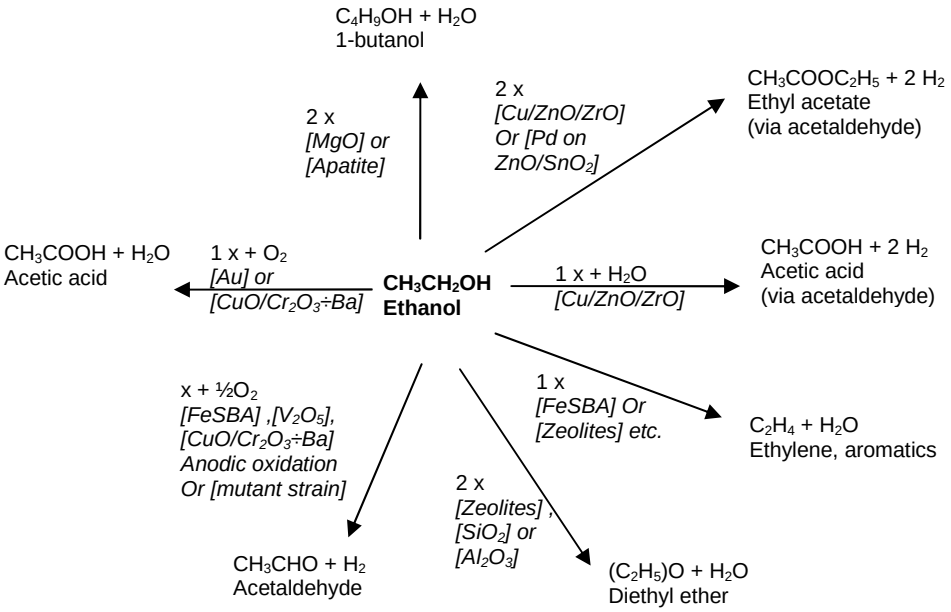

Figure 1-6: Ethanol is a versatile chemical that can be converted to a number of important end products or intermediates by heterogeneous catalysis.

Dehydration of ethanol to diethyl ether can be carried out, for example over acidic catalysts such as zeolites, alumina, silica alumina or aluminium silicate. These catalysts are also able to further convert diethyl ether to ethylene.

Zeolites fed with ethanol promote at temperatures over 400°C the formation of an aromatic co-catalyst compound in their cavities (parallel to the methanol induced hydrocarbon pool mechanism) capable of synthesizing aromatic products along with paraffins and olefins. The shape selectivity for zeolitic catalysts characteristically cuts off the conversion to products over a certain size, for example aromatics up to penta-methyl benzene are found as conversion product of methanol over H-ZSM5. The use of zeolites for the conversion of ethanol has many facets related to its dehydration and alkylation functionality. The conversion of bio-ethanol over zeolites is specifically discussed in Appendix A.2.

Cu/ZnO/ZrO_2 catalysts (*Inui et al., 2004)* have shown the ability to convert ethanol to ethyl acetate and acetic acid, where the water influences the product distribution on either product. The suggested mechanism goes through the dehydrogenation of ethanol to acetaldehyde, the reaction of acetaldehyde with one further mol of ethanol to hemiacetal and its further dehydrogenation to obtain ethyl acetate (see Scheme 1-1), which under aqueous conditions react to produce one mol of acetic acid and one mol of ethanol.

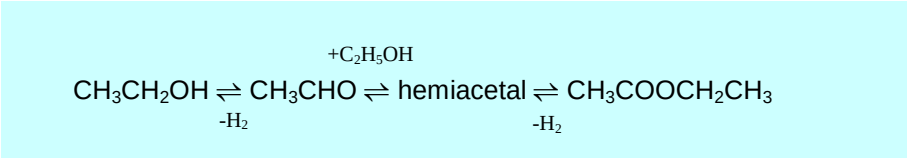

Scheme 1-1: Ethanol conversion to ethyl acetate via hemiacetal.

Pd on a mixed support of ZnO and SnO_2 has been shown to also promote the conversion of ethanol to ethyl acetate via acetaldehyde.

Acetaldehyde can be obtained from ethanol through the oxidative dehydrogenation over FeSBA (*Guan et al., 2007)*, V_2O_5 (*Kilos, 2010*) and barium free $CuOCr_2O_3$ (*Marcinkowsky et al., 1980*), all conducted at temperatures over 250°C, the mutant strain “Hansenula polymorpha” (*Moroz et al., 2000*), or alternatively through the anodic oxidation in a fuel cell with Pt anode material at modest temperatures <115°C (*Meshbesher, 1984*). Acetaldehyde is far more volatile than ethanol; thus ethanol conversion into acetaldehyde eases the downstream separation of biomass based product from excess water. On the other hand the market of acetaldehyde is shrinking.

Condensation products, such as butanols and derivatives, are obtained over basic solids such as MgO (*Ndou et al*., *2003*), where the conversion of ethanol was found to take place via the dimerisation of the alcohol, rather than via the self condensation of acetaldehyde.

Acetic acid is today mainly produced by means of carbonylation of methanol. However optimised, it seems that the Monsanto acetic acid process and its technological successors leave room for improvement due to hatches like its high investment demand and poisonous and carcinogenic co-catalyst, methyl iodide. The alternative route to acetic acid via acetaldehyde (primarily made from ethylene) has not been

competitive due to the high ethylene prices. It has also been reported that ethanol may be converted to acetic acid oxidatively, for example over a V_2O_5 catalyst (*Gubelmann-Bonneau, 1998*). Lately, it was also found that nano gold particles are active in this route (*Jørgensen et al*., *2007*). The non-oxidative dehydrogenation of ethanol to acetic acid was described to take place over especially copper catalysts in *Ullmann (1917)* and *Ullmann (1943)*, and late studies (*Marcinkowsky et al., 1980, Iwasa et al*., *1991*) confirm these early observations.

1.5.3 Economy for bio-ethanol

The first generation bio-ethanol technology has, despite its ancient roots, especially been developed and optimised over the years from 1980 to today. The optimisation of process conditions and economy of scale has brought about an ethanol price reduction by a factor of 5. It is reported by *Goldemberg et al. (2004)* that while the production of ethanol from sugar cane was originally subsidised in Brazil, the technological development of the first generation ethanol production has removed the need for subsidies. The high competition has caused the prices to move towards production costs. However, when the non-subsidised selling price of ethanol hit the gasoline selling price per LHV in 2002 (7USD/GJ or about 200 USD/MT), the ethanol price started following the Brazilian gasoline price, when it went up. According to *Mousdale*[b] (2008) the Brazilian ethanol selling price was not above 375USD/MT on an average-of-year basis 1998-2005. As mentioned before, US is now the world's leading producer of ethanol based on especially corn. The estimated variable production cost is about 0.26USD/l or 330 USD/MT ethanol (*Mousdale*[d], 2008) in 2006. This number was also reported in 2002 by *Shapouri et al. (2005)* and *Sklar (2008)*.

The 2nd generation ethanol production is not yet commercialised, and it takes far more expensive methods to release and ferment the C_6 and C_5 sugars in the lignocellulosic material (*Bohlmann, 2006*). According to *Thomsen et al. (2007)* about 3 t of wheat straw is required in order to produce 1 m^3 of ethanol, corresponding to almost 4 t of straw needed per MT of ethanol. In Appendix A.1 a rough process description and a simple mass and energy balance has been made for a 2nd generation ethanol plant based on corn stover. The contents of cellulose and hemicellulose in corn stover and wheat straw are largely the same, making the ethanol yields comparable. The calculated figure of 4.6 t of corn stover per MT of ethanol in Appendix A.1 of this work, assuming a modest hydrolysis yield, corresponds well to the above figure of 4 t wheat straw. The variable cost of 2nd generation ethanol depends less on the feedstock price as compared to the first generation ethanol.

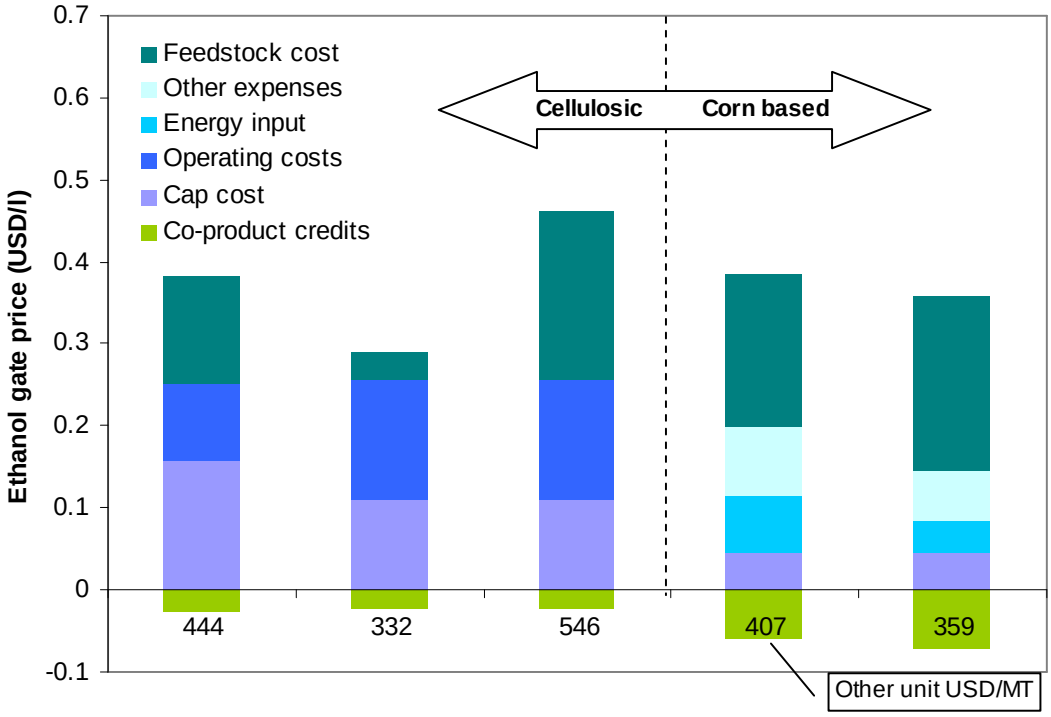

Figure 1-7: The gate price, total variables + depreciation, for 3 cellulosic and 2 corn based estimates (2006). The prices are based on the following references (from left): *Bioenergy Feedstock Information Network (2011), Bohlmann (2006) @ 10 USD/MT and @ 60 USD/MT biomass, respectively, Mousdale[d] (2008) and Shapouri et a (2005)l.*

Figure 1-7 compares the gate price estimates for three cellulosic and two corn based plants.

On top of the depreciation and the variable cost (total gate price) comes the return on investment (ROI). For a 2nd generation ethanol plant capacity of 150000 MTPY (or 50 million gallon/year) the ROI (25%) is estimated to 430USD/MT of ethanol (*Bohlmann, 2006*). Assuming a 30USD/MT feedstock price the total variable cost of a 2nd generation bio-ethanol is estimated to about 280USD/MT (hereof 90 USD/MT to feedstock), and when including a 140USD/MT depreciation, the total gate price becomes 420USD/MT.

To support furthermore an annual 25% ROI the total required selling price becomes 850 USD/MT. Meanwhile the recent breakthrough of improved enzymes hydrolysis is estimated to bring the variable cost down by almost 50% and the capital cost by 20% (*Viksø-Nielsen, 2009*). Repeating the above calculations the improved hydrolysis leads to the prediction of a short term selling price of about 630USD/MT 2nd generation ethanol (300 USD/MT total gate price).

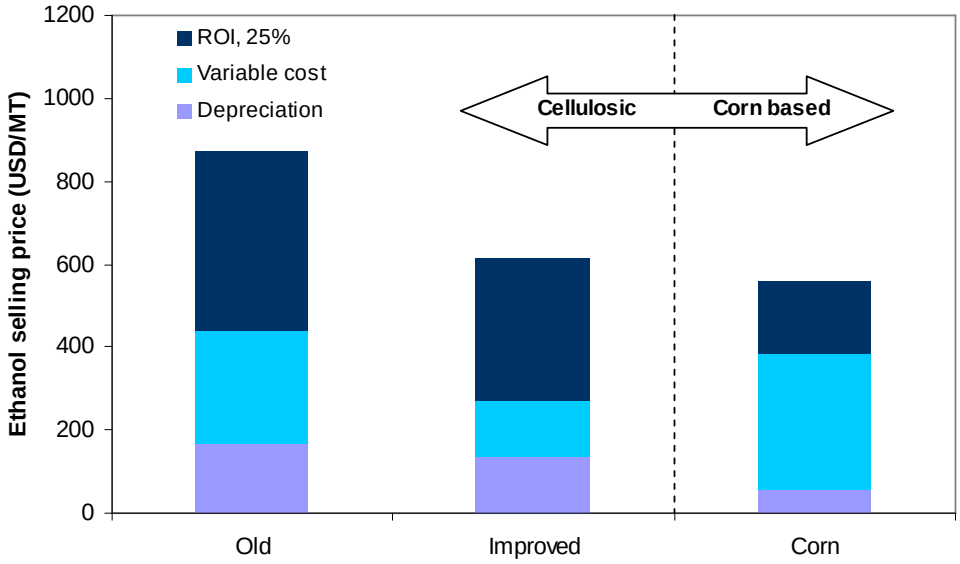

Figure 1-8: The required ethanol selling price for the old and the improved cellulosic ethanol production technology (*Viksø-Nielsen, 2009*) in comparison with the corn based.

Comparing only the corn based ethanol variable production price of 330USD/MT with the 140 USD/MT estimate of an improved 2nd generation ethanol the latter seems competitive. However, Figure 1-8 shows how the required selling price of 1st generation corn based and the improved 2nd generation cellulosic ethanol end up the same based on the individual contributions of variable cost, depreciation and ROI. This is in agreement with the forecast by *Viksø-Nielsen (2009)* that the improvements of the hydrolysis and fermentation processes in the cellulosic technology will shortly even out the difference. An estimate from 2006 on production price of 660 USD/MT for 2nd generation ethanol was reported by a Dutch research group (*Mousdale*[f], 2008); and their estimate of a long term lignocellulosic ethanol production price is that it will fall to about 330 USD/MT by 2030 primarily due to lower investment cost.

The ROIs on the matured first generation technology could be set lower, however, reflecting the lower risk taken when investing in this mature technology. This fact and government premiums paid to ethanol producers may explain the ethanol prices of around 500USD/MT which were found on the world market in 2008.

One point of orientation in 2008 of the ethanol price development forecast was that the 500USD/MT for 1st generation ethanol seen this year could potentially drop to about 330USD/MT over the next 20 years, if the production is replaced by 2nd generation ethanol, citing *Mousdale*[f] (2008). But the answer on how the ethanol selling price develops relies heavily on its coupling with the gasoline price in spite of the reduced production cost. If a surge in oil prices occurs, or legislation dictates that combustion based motors should be phased out, naturally the demand for gasoline drops; this may then allow the ethanol price to drop to close to production cost level.
The gasoline, and in turn the ethanol, price is the result of endless battles between diverging interests amongst oil producers, countries having surplus of bio-resources, motor industries, governments and global environmental organisations etc.

1.5.3.1 Gross margin analysis for bio-ethanol to chemicals

While many possibilities remain, a strategy could be to produce a chemical which today pays well off, where the market is expanding and large enough to absorb the extra capacity of new-coming technologies. Two of the above chemicals seem to especially fulfil those criteria, ethylene (>100 million MT per year, 2008, stable growth) and acetic acid (8-9 million MT per year, 2008, stable growth). Taking a simple look at the economic prospect (delta price analysis) for the conversion of ethanol to chemicals the most promising chemicals may be identified.

As most commodities, acetic acid has experienced large variations in the sales price over time. Furthermore, geographical variations connected to the cost of transport are seen as well. The price level of acetic acid in 2008 was on an average 850USD/MT (NWE), and the forecast was that the acetic acid market would keep growing on the back of Chinese economic growth and industrial activity.

Ethylene prices have largely followed the crude oil price, though it has been escalating from the oil price trend due to shortage of ethylene production capacity. In 2008 the ethylene price fell to 400USD/MT (NWE and US, *Plastemart.com, 2010*) back to its normal level in the period 1993-2003 (*Fishhaut, 2003*).

A rough expression on the feasibility of processes may basically be given as per Eq. 1-1:

$$\text{Delta P} = \text{Unit price}_{\text{product}}\ (100\%\text{yield, per kg feedstock}) - \text{Unit price}_{\text{feedstock}} \qquad \textbf{Eq. 1-1}$$

Table 1-1 shows the calculated results of inserting above 2008 chemicals prices with a yield set to 100%. The delta P values for acetic acid and ethylene from above Eq. 1-1 then become:

Table 1-1: The delta P number for two products, acetic acid and ethylene, from ethanol conversion (100% yield assumed).

Products	Delta P (USD/MT Ethanol)
Acetic Acid	609
Ethylene	-257

It appears that in 2008 the conversion of ethanol to ethylene is not favourable at all. Forecasting a halving of the ethanol price does not change the picture that acetic acid is superior to ethylene in the delta P analysis. Still, in India ethanol to ethylene production plants have been established as part of a glycol process.
Comparing the spot market ethylene and ethanol prices over time only leaves short periods where the production of ethylene is feasible.

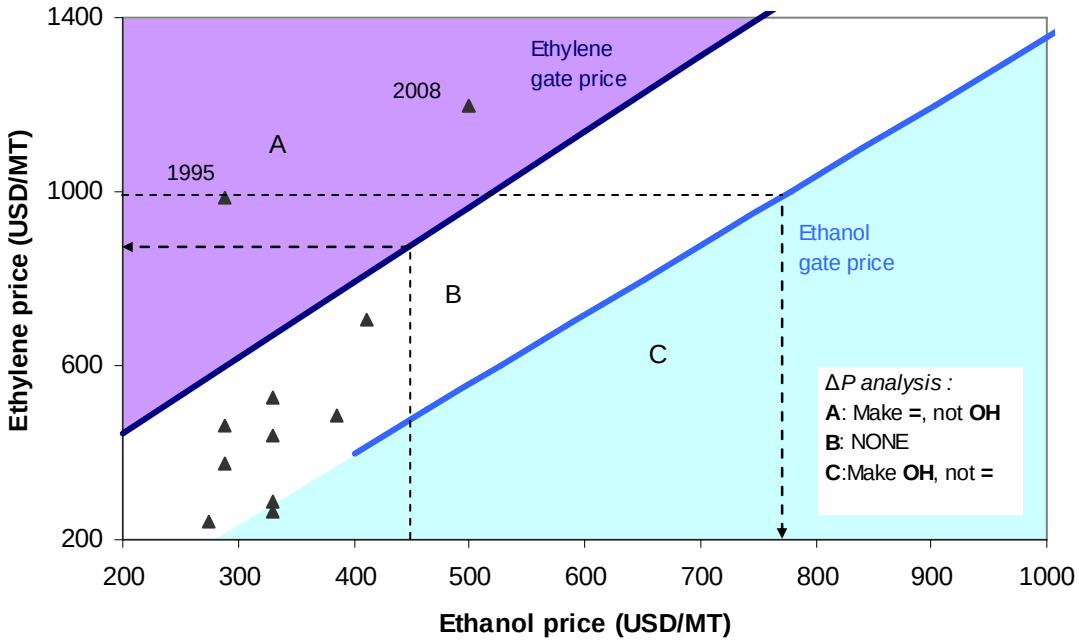

Figure 1-9: Depiction of estimates of ethylene production price from ethanol and vice versa together with actual ethylene and ethanol spot prices during Januaries 1994-2003. Only twice has it been feasible to produce ethylene from ethanol.

Figure 1-9 shows the actual spot prices of ethanol and ethylene and has an indication through the straight lines of in which areas the conversion of ethanol to ethylene and vice versa is feasible, assuming a total fixed cost and utilities cost of 100USD/MT for the conversion of ethanol to ethylene (dehydration, simple) and 150 USD/MT for the conversion of ethylene to ethanol (hydration, more complex). Only when a polyethylene plant is placed downstream of the ethylene plant do the overall economics seem favourable.

On the basis of the above preliminary analysis a decision was made to take a closer look at the viability of converting bio-ethanol to acetic acid.

1.5.4 The environmental substantiation

The answer to the greenness of a chemical process may be sought in the Green metrics.

The E-factor, being a well-known green metric, expresses how much waste is produced per kg of product. In a sustainability context this includes all the emissions (including auxiliaries, solvents and excess reagents) (*Clark et al.*[b], *2008*) without the discrimination between the environmental impacts of the individual emissions. In a simpler approach, the so-called C-factor (see Appendix A.3) only accounts for the amount of CO_2 being emitted during the production of 1 kg of a specific chemical (from "Well-to-tank"). Comparing the C-factor to the E-factor, the picture obtained for the E-factor, lumping all the emission together on a kg basis, does not justify the work that has to be put into studying each process in detail, unless the emissions are dominated by wastes other than CO_2. For example, some pharmaceutical processes are dominated by the use of solvents. With inaccurate definition of the E-factor, it leaves

open how many off-streams should be counted. Is treatable waste water a waste stream as such, or are only the compounds removed from such a waste stream the real waste? Rather, as by means of the C-factor tool, the level of CO_2 emission may be estimated with a fair accuracy for a lot of industrial processes, based on different conversion routes, giving a fast indication on the green- or blackness of the individual process.

Figure 1-10 shows that different reserves and resources may be converted to the desired chemicals via different routes. In aiming for sustainability, the reserves and resources should be spent intelligently to achieve the lowest possible emission of CO_2.

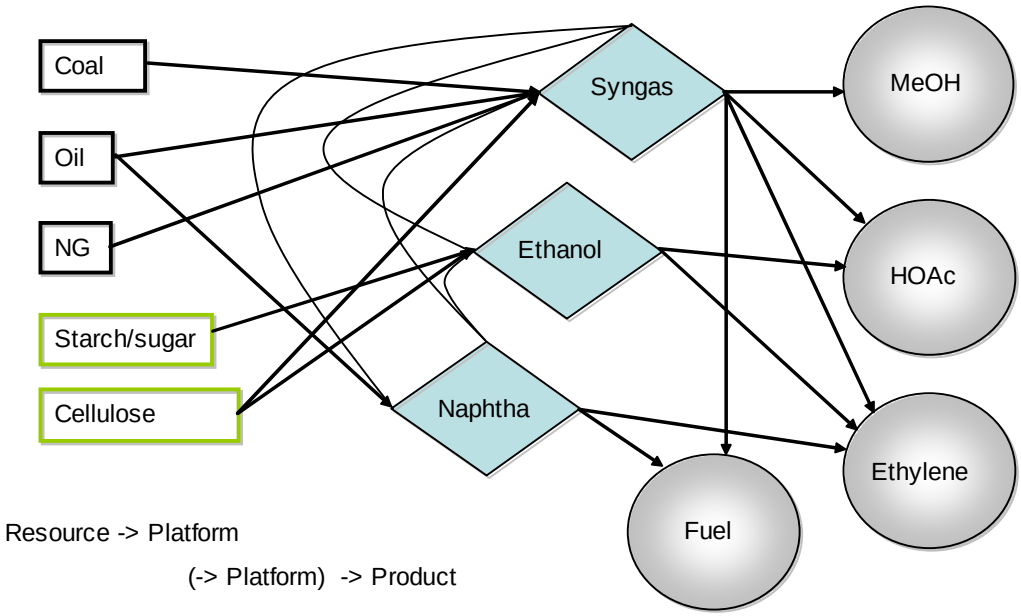

Figure 1-10: Chemicals may be reached via different platforms and different conversion routes.

For example, combining gasification of biomass or waste with reforming of natural gas provides for synthesis gas ideal for the production of synfuel with a resulting emission of CO_2 lower than the CO_2 emission originating from the refining of crude oil. In biochemical context (and especially related to the production of bio-ethanol as a gasoline substitute) the term net energy balance (NEB) has been introduced, expressing how much energy stored in the product comes out relatively to how much fossil energy was put into the process. Some of the figures found in the literature may also include the fuel energy input made from a renewable source. Below Eq. 1-2 expresses the NEB based on LHV of the energies.

$$NEB = Energy_{output} / (Energy_{input\ fossil}) \qquad \textbf{Eq. 1-2}$$

Confusion in using lower or higher heating values and the lack of differentiation of fuel inputs have made the discussions on the ethanol energy efficiency difficult. The majority of surveys arrive at a NEB, according to Eq. 1-2, above 1 (*Natural Resources Defense Council, 2006, Luo et al., 2009*). In Appendix A.1 the NEB has been estimated based on realistic assumptions (modest yields) on hydrolysis and fermentation recoveries and efficiencies for 2nd generation bio-ethanol production from corn stover. The calculated NEB of 4.4 has been used for the lignocellulosic biomass C-factor

calculation in Appendix A.3 in accordance with *Mousdale*[e] (2008). Based on this figure it may be calculated that if the vehicles are constructed to run on a 2nd generation ethanol, taking into account its lower energy intensity, the CO_2 emission per kilometre driven is less than half the value as compared to a kilometre driven on gasoline.

The screening with different carbon source alternatives in a number of bulk chemical productions show that lignocellulosic biomass (via 2nd generation fermentation or gasification) results in favourable low C-factors (See Figure 1-11), alone or in combination with another source natural gas (see Appendix A.3).

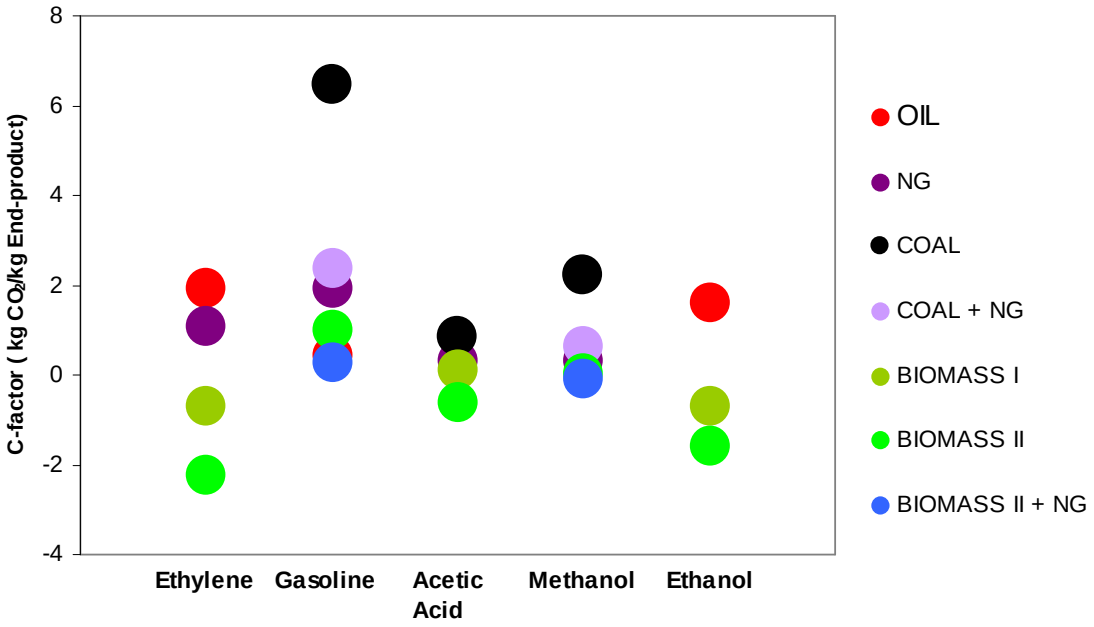

Figure 1-11: The C-factor of key chemicals produced from different sources. Biomass I designates starch or sugar based biomass. Biomass II designates lignocellulosic biomass.

A taxation of the production of chemicals dependent on their production route could be based on the C-factor, thereby promoting the chemical routes which are the most environmentally sustainable. In order to take effect, the taxes will have to be on a level per kg of CO_2 where the routes based on biomass start competing, i.e they could be based on the delta value according to Eq. 1-3:

$$\text{Tax pr kg product} = (\text{C-factor}_{actual} - \text{C-factor}_{sustainable}) * \text{Tax per kg } CO_2 \qquad \textbf{Eq. 1-3}$$

As may be gathered the ethanol to acetic acid process passes the environmental test, having a C-factor well below the conventional route. The C-factor not only tells which alternative route is preferred from a CO_2 emission point of view but, due to its simple approach, it also makes a comparison across a group of chemicals possible. Ethylene from biomass is from a C-factor perspective seen to have immediate benefits. But due to the fact that the gross margin of ethylene from ethanol is negative, the economic criterion is not fulfilled (see paragraph 1.5.3.1).

1.6 Motivation of the thesis

In our quest for a sustainable world, we also struggle with a lot of imbalances and conflicts of interests. On the international level we seem to agree though that the needs

for food should not compete with any other. The long term perspective of resource availability supports that chemicals should be produced from biomass, in a first round at least in part. The energy need to be fulfilled in competition with the need for chemicals may be covered by other sources.

In supporting this strategy, the biomass based technologies for chemical production need to be developed. It would be beneficial, if it is possible to find new processes based on biomass as a direct or indirect feedstock to produce chemicals. In striving for sustainability, we may benefit from the scientific and technical knowledge gained when we once developed the oil based technologies, for example on utilising heterogeneous catalysis for efficient and selective conversion. A stepwise revival of biomass based processes is thus possible whenever the following criteria: the availability, suitability and convertibility of feedstock, and the competitiveness to conventional process are fulfilled. The environmental friendliness of a biomass based process may accelerate its commercialization (legislation, taxation and subsidies), if its greenness is substantiated.

Ethanol is a good platform for the conversion to value-added chemicals, as its sustainable production and competitiveness to gasoline has already been established. Assuming a catalytic conversion of bio-ethanol, a high tolerance of water is beneficial in the process, and the operating conditions are favourably low pressure and low temperature, as these are the conditions of the bio-ethanol obtained after fermentation. Furthermore, any increase of pressure and temperature involves the investment of these services and the energy consumption that comes with the condition changes. An example of a promising product candidate for the conversion of ethanol has been identified as acetic acid, having a high delta P and exhibiting a negative CO_2 emission in its production route, as defined by the C-factor (see Figure 1-12).

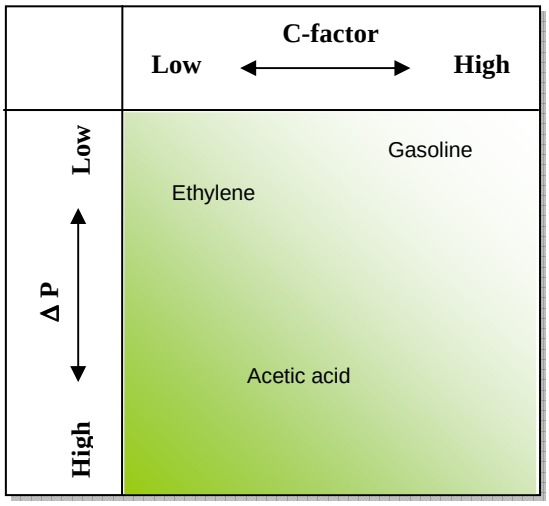

Figure 1-12: Product selection matrix. The C-factor must be low and the economic margin ΔP must be high to substantiate the two aspects of sustainability: the environmental and the economic.

It is beyond the scope of this thesis to discuss to what extent the world may be self sufficient in biomass production for all the purposes needed, alone or in combination with other resources and/or reserves. The rationale of this thesis is that the biomass feedstock to chemical production is advantageously converted in a manner, whereby it to some extent retains the chemical C-C bonds originally stored in the biological matter

provided by photosynthesis. The preferred conversion of ethanol in an aqueous solution would provide a further advantage, if the water present allows for a higher stability and selectivity of the catalyst through the prevention of uncontrolled side reactions.

It is the objective of the present work to find a heterogeneous catalyst capable of converting a biomass-based feed stream to a value added product with the required selectivity and activity to obtain a viable process alternative to the conventional.

1.7 Structure of the thesis

Project work of this nature, process innovation, involves a broad set of activities ranging from the fundamental research and analysis, process calculations to patents and commercial aspects such as feasibility study performed at an early stage to identify the perspective of the project. Inspiration for the project management methodology has been found in literature (*Wysocki et al., 2003, Ekvall, 1996)*. Figure 1-13 shows the INSPIRE model recommended for explorative projects *(Wysocki et al., 2003)*. In this project execution model an Initiation phase followed by an iteration over Speculate, Incubate and Review phases constitute the chronological project work phases; the Initiation phase being when the objective and the initial target are defined, the Speculate phase being when new investigations are specified, the Incubate phase when the activities set up in the Speculate phase are made, and the Review phase being when the results and the potential of the project continuation are evaluated. The latter three phases ideally involve the core project team.

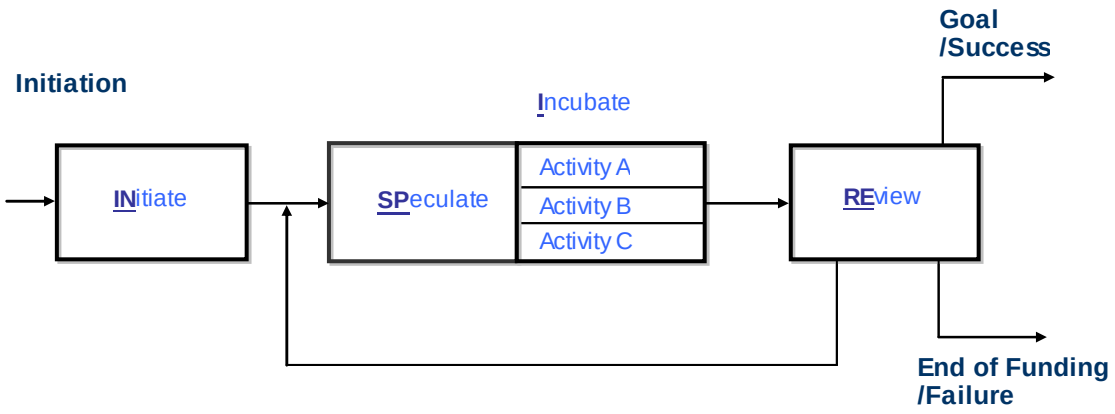

Figure 1-13: The INSPIRE model by Wysocki et al. describes the chronological work phases.

Best pace is obtained with short cycles – therefore the activities planned should be conducted by experts, if available. Accordingly, rather than aiming to attain all the competences myself, I have utilised the results of the specialized disciplines, conducted by in-house specialists, in combination with my own investigation results in order to set up new investigations to be made (Speculate). Meanwhile my instructions to assistants and my autonomous interpretation and understanding of the significance of the results have been crucial as to the progress of the investigation. I did all the initial screening work myself, and apart from the specialised analysis and characterisation work and the daily routines around the test set-ups, I have basically been taking care of all other kinds of activities comprising the design of test set-up, experimental planning, data analysis, modelling, specifications, patenting and

economic analysis. In Appendix A.4 the extent of my own and the expert contribution of the activities in the Incubate phases of the project are outlined.

Having selected bio-ethanol as one example of a bio-mass based feedstock and acetic acid as a sound product, the project was conducted with the target to provide a competitive bio-ethanol to acetic acid process based on heterogeneous catalysis, optimally with good integration to the prior fermentation and distillation steps. During the project, the review of the results of the planned process and catalyst investigations led to new guidelines for process and catalyst investigations.

Below I summarise the contents of following chapters (activities, major findings and conclusions) of this thesis in order to ease the understanding of its structure (see also Figure 1-14, showing the basic subjects behind the chapter titles).

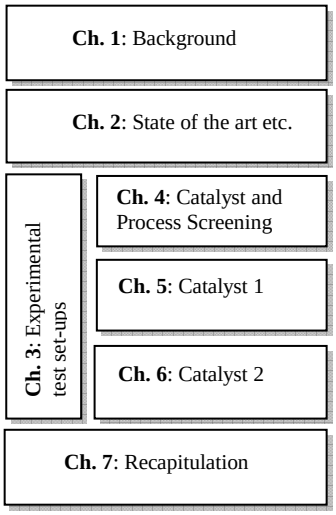

Figure 1-14: The overall structure and subjects of the thesis: After this background Chapter 1, Chapter 2 presents the state-of-the-art and known acetic acid technology. Chapter 3, describing the experimental test set-ups, is referred to in each of Chapters 4, 5 and 6 reporting on the catalyst and process screening, and the experimental results and discussions of two down-selected catalysts, respectively. Chapter 7 rounds off the thesis by stating a review and overall conclusion of the treated example and an outlook in a broader context.

In **Chapter 2** the conventional acetic acid technologies of today is assessed. Selecting the most dominant and competitive of these as a comparative example, the carbonylation of methanol, its benefits and drawbacks are presented, the gate acetic acid production price is estimated and its high load on investment discussed. The known, but not industrialised routes and catalysts for ethanol conversion to acetic acid, primarily from patent literature, are listed. In the literature, copper based catalysts have played a prominent role in the conversion of ethanol to acetic acid, but also Ag, Pt, V_2O_5 and Au based catalysts have been mentioned. Both a non-oxidative and an oxidative dehydrogenation route from ethanol to acetic acid are known. Experimental testing was required to identify catalyst candidates for further investigation.

In **Chapter 3** all the experimental test set-ups used are presented, as these have been used in turns and are frequently referred to. The need, purpose and the approach in putting together numerous test set-ups is outlined together with the principle of analysis. The screening test results are presented in Chapter 4. The experimental

results acquired from the investigation and the testing of the two types of catalyst in the test set-ups are presented in Chapters 5 and 6.

In **Chapter 4** the catalyst pre-screening program is presented, including the principles of preparation, eventually withdrawing the qualitative main results providing for the down-selection of a catalyst. Copper aluminium oxide (copper aluminium spinel, $CuAl_2O_4$) produced from CuO/Al_2O_3 precursors through calcination at 850°C (Cu spinel-850) shows, when reduced to Cu on Al_2O_3, the best characteristics, firstly due to its comparably high acetic acid activity and secondly its high mechanical stability. A quantification of heat consumption and mass flow rates in an industrial size non-oxidative ethanol to acetic acid plant is established through a process calculation based on experimental data. A second best catalyst candidate, Cu/SiO_2, having a lower activity but a higher selectivity, is identified too. Next, the process development possibilities, and the route and apparatus combination of the oxidative and non-oxidative dehydrogenation of ethanol to acetic acid into a new process are sketched. Furthermore the integration with neighbouring production units is discussed. Three patent applications have been filed to obtain intellectual property rights on some of these discoveries. The partly oxidative dehydrogenation process is found to be advantageous through its heat neutrality, but the non-oxidative dehydrogenation process is an attractive alternative under the concern of safety and a higher consumption of water.

In **Chapter 5** the observations on Cu spinel-850 of the tendency for rapid deactivation of the catalyst and the stability dependence of the reduction method is described. In the following many paragraphs, the search for the underlying reason through characterisation is described. Further, on the interesting characteristics around the partly oxidative dehydrogenation is reported that the Cu spinel-850 catalyst deactivates under the oxidative dehydrogenation conditions. The deactivation is attributed to carbonaceous compounds formed, possibly accelerated by alumina transformations. The short-comings of the catalyst seem hard to go around as they are indicatively related to *ab initia* characteristics.

In **Chapter 6** the characterisation and testing of the alternative catalyst candidate, Cu/SiO_2, is described and compared to the Cu spinel-850 catalyst. Cu on silica exhibits higher selectivity but lower activity, and no ethyl acetate side-product was found for the Cu on silica catalyst. Furthermore the carbonaceous compound formation is lower on this catalyst and its sensitivity to co-feeds of acetaldehyde and butanol is low. The support is suggested to influence the stability of the catalyst. Kinetics of the non-oxidative dehydrogenation route was derived in order to support the further process development. The rate expression of the oxidation of acetaldehyde with water to acetic acid and hydrogen revealed in this work is close to first order with respect to water and close to 0.5^{th} order with respect to acetaldehyde. The study on ethanol to acetic acid was halted.

In **Chapter 7** the work on acetic acid is rounded of under the concern of market developments. The main points of the study are recapitulated together with a review of the methods used. The product prices linking up to the oil price are less vulnerable to the recent ethanol feedstock price volatility. Another application of bio-ethanol conversion over Cu based catalysts is discussed, namely the production of higher

alcohols, enhanced in propanol selectivity by ethanol co-feeding. In order to improve the overall conversion efficiency further research may be put into direct catalytic conversion of mono-saccharides being the bio-ethanol precursor in fermentation. By direct conversion one may tentatively reduce the immense dilution of the biomass in water and avoid the loss of C through the CO_2 side-production, as compared to the fermentation conversion of sugars to for example ethanol.

Chapter 2 Acetic Acid as a Value-added Chemical

2.1 Introduction

The definition of value-added chemical herein is in principle any chemical which has a significantly higher economic value than its precursors, as established for acetic acid (**Table 1-1**).

The U.S. Department of Energy has reviewed a list of more than 300 biomass based chemicals based on the petrochemical model of building blocks, chemical and market data etc. in order to identify the top value-added chemicals (*Werpy et al*., 2004). These top value-added chemicals are identified as those among the building blocks or intermediates that can subsequently be converted to a number of high-value bio-based chemicals. Acetic acid was classified as a chemical with limited building block potential (as a reagent molecule adding C_2) and a large scale commodity from synthesis gas, and was therefore not chosen for the Top 30 list of value-added chemicals.

Acetic acid has today a broad use in the production of vinyl acetate, cellulose acetate and other esters used for plastics, fibres and paints; its salts are used for agents in the dying of textile and leather, and chloroacetic acid is used in pesticides and pharmaceuticals. Its yearly production capacity is 13 million MT (*Weissermel*[a], *2003*) of which most is produced by means of the carbonylation of methanol (Monsanto process, see paragraph 2.2.1).

2.2 Historical perspective, research and conventional production

Acetic acid, known since ancient times as a constituent of vinegar (from wine being exposed to air) was first isolated in 1789 by Tobias Lowitz (*Ullmann, 1917*). Later Johann Döbereiner discovered the catalytic conversion of ethanol to acetic acid over Pt (*Kauffman, 1999*) in 1821.

It has been known since early in the 20'th century that acetic acid may be produced by the heterogeneously catalysed oxygenation from a feed of ethanol and air over various catalysts, for example anthracitic coal and browncoal (1907), silver (1928), copper compounds (1920), vanadates (1924) and Fe_2O_3 (1929) (*Ullmann, 1943, Foerst, 1955*). In the patent literature, published during the early decades of the last century till today, problems around the stability and selectivity of especially copper based catalysts for the acetic acid synthesis from ethanol have been discussed.

According to the early Ullmann Encyclopedia (*Ullmann, 1917*) the industrial production of acetic acid around that time took place primarily via 2 routes.

1. The production of acetic acid by fermentation of aqueous ethanol, obtained from fermentation trickled over containers loaded with beach flakes holding a naturally occurring strain capable of oxidising ethanol to acetic acid.

2. Dry distillation of plant materials content of acetic acid.

It is also mentioned that acetic acid may be produced by the catalytic oxidation of ethanol via acetaldehyde with air in a two stage process. Ethanol is oxidised to acetaldehyde over zinc oxide or Pt, or acetaldehyde may be produced from acetylene. Also an electrochemical oxidation of ethanol to acetic acid is mentioned.

In the later version of the Ullmann Encyclopedia (*Ullmann, 1943*) it is described how acetic acid is now mainly produced by the oxidation of acetaldehyde with Mn acetate as a catalyst (a maximum yield of 75% of the theoretical is reported p. 651), the acetaldehyde either being produced from ethanol or acetylene, depending on the price of the feedstock. In addition the fermentation of xylose by means of *Lactobacillus pentoaceticus* from cheap (hemi)cellulosic material was discussed as a new research effort with potentials in those days.

Still in the 1955 Ullmann Encyclopedia (*Foerst, 1955*) the oxidation of acetaldehyde is the most important industrial process. Also the direct oxidation of ethanol to acetic acid is mentioned but is estimated to have little importance. Productions of acetic acid (in countries with a high production of cheap ethanol) go via acetaldehyde, obtained either through oxidation or dehydrogenation of ethanol. In this book the first advances in the carbonylation of cheap methanol with carbon monoxide are reported, the process hampered by the needs of high carbon monoxide surplus, a high operating pressure and exclusive materials resistant to the highly corrosive medium.

In the 1960s BASF commissioned its first carbonylation based plant involving a cobalt iodide catalyst, the process operated at 250°C and several hundred bars (*ICIS.com, 2010*). However, the technical problems around the carbonylation of methanol were solved, as we now know. The use of a modest surplus of 10% carbon monoxide, a moderate pressure of 25-40 bar and Hastelloy and Zirkonia materials have waved these objections away.

During many years of superior competitiveness from the carbonylation based process, the interest in the bio-based route diminished. The primary industrial biomass based acetic acid productions today is still the oxidation of acetaldehyde (produced from bio-ethanol) to acetic acid as conducted by for example small capacity plants in India. However, the predominant supply of acetaldehyde for oxidation to acetic acid comes from ethylene. The biomass based share of the acetic acid market was about 4% in 1994 (*Weissermel*[a], 2003).

2.2.1 The Monsanto acetic acid process and production economy

The original so-called Monsanto (later BP) catalyst discovered in the mid 1960es is a Rh based carbonyl complex, which together with its hydrogen iodide co-catalyst in the liquid phase promotes the carbonylation reaction between methanol and carbon monoxide.
Scheme 2-1 shows the overall conversion taking place in the BASF or Monsanto process, overlaying a catalytic cycle and several equilibriums:

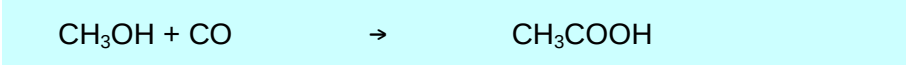

Scheme 2-1: Monsanto process: methanol carbonylation.

The carbonylation is typically conducted at a temperature of around 185°C and a carbon monoxide partial pressure of about 20 bar. The process is quite complex, involving a large number of equipment items made of expensive materials. On the other hand it is very selective, if fed with pure methanol. Today more than 60% of the world's capacity is produced by methanol carbonylation. Further details may be found in Appendix B.1 where the production price of acetic acid by carbonylation is estimated.

The estimates of the acetic acid gate price have been on three layouts (see Figure 2-1).

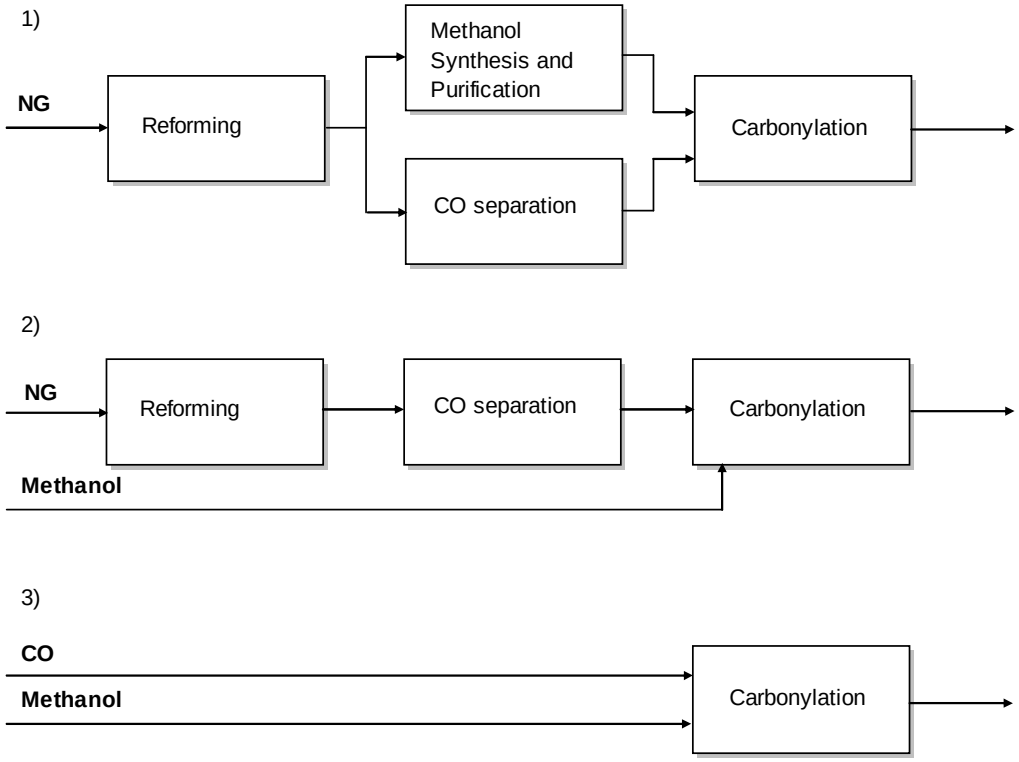

Figure 2-1: Three plant layouts for the carbonylation process are possible. 1) Production of methanol and CO from natural gas via synthesis gas + subsequent carbonylation; 2) production of CO from natural gas via synthesis gas + subsequent carbonylation with imported methanol; and 3) carbonylation of imported methanol and carbon monoxide. Layout 2 and 3 are the most typical.

1. One is where natural gas is converted to synthesis gas and part of the synthesis gas is used for methanol synthesis and another part is purified for the supply of carbon monoxide, together making up the feed stream for the acetic acid synthesis. This concept favours the economy of scale for the reforming part of the acetic acid plant.
2. Another is where carbon monoxide is produced from natural gas, and methanol is imported. This scheme offers the possibility of designing the reforming part of the plant as part of a dedicated CO plant with the potential savings associated herewith. Another benefit is that the total investment for a given capacity is lower. The draw back of this layout is that the plant economy depends on and is sensitive to the methanol market price.
3. A third layout is where both the carbon monoxide and the methanol are imported.

Of these three the second layout is the most common.

Rough cost estimates of the individual layouts, based on a 300,000 MTPY plant capacity, have been made on the basis of in-house information on reforming technologies, methanol technologies and carbonylation. In Appendix B.1 the numbers from the gate production price estimation are described in detail.

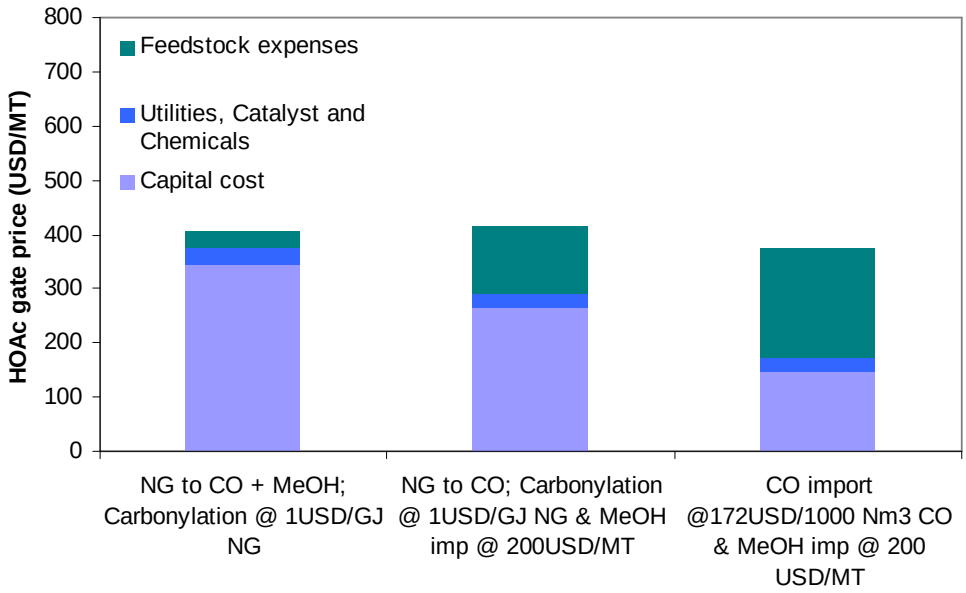

Figure 2-2: Gate production price of acetic acid based on carbonylation. The bars show the contributions of capital cost, utilities and feedstock expenses for three plant layouts: 1) On site production of CO and methanol, 2) on-site production of CO and import of methanol, and 3) import of both CO and methanol. Feedstock expenses count natural gas and methanol, if imported.

Very often, the acetic acid plants are situated where the natural gas is very cheap. Figure 2-2 shows the gate production price estimates of acetic acid via the routes presented above given a low natural gas price of 1 USD/GJ of natural gas, typical of remote locations. As can be seen, the contribution from the feedstock expenses varies very much, depending on the technology chosen, for example it is modest for the natural gas based plant. However, the total gate price of the acetic acid is meanwhile almost identical. In choosing between these technologies the security of CO supply (from neighbouring plants) may count as a decisive factor for choosing on site production of CO, while importing storable methanol is practicable, leading to this combination as the preferred. The dominance of the investment on the acetic acid gate price reflects the relatively complex process layout of the carbonylation based acetic acid plant. It was still found to be a tremendous step forward when the carbonylation process was invented as compared to the earlier oxidation of acetaldehyde.

2.3 Ethanol-to-acetic acid routes and process descriptions

The challenge is to identify a catalyst capable of converting ethanol to acetic acid at an adequate rate and with a selectivity which makes it possible to incorporate the conversion step in a feasible process context. Therefore more aspects have to be considered simultaneously. The known oxidative and non-oxidative dehydrogenation of ethanol to acetic acid are the immediate reaction route candidates as alternatives to

the conventional carbonylation of methanol route, if a bio-mass based route is being sought.
The respective reactions take place according to the following overall reaction schemes, Scheme 2-2 and Scheme 2-3:

$CH_3CH_2OH + O_2 \rightarrow CH_3COOH + H_2O$ ΔH^{θ}=-439 kJ/mol

Scheme 2-2: Oxidative dehydrogenation of ethanol.

$CH_3CH_2OH + H_2O \rightleftharpoons CH_3COOH + 2H_2$ ΔH^{θ}=43.9 kJ/mol

Scheme 2-3: Non-oxidative dehydrogenation of ethanol.

Whereas the oxidative route (Scheme 2-2) is exothermic, the non-oxidative (Scheme 2-3) is an endothermic (entropy driven) equilibrium reaction and goes via the intermediate acetaldehyde. Below the references found for the catalysts and processes related to the above reaction routes have been summarised and discussed.

2.3.1 Oxidative dehydrogenation

The catalysed oxidative dehydrogenation route has been suggested numerous times in the patent literature. US 4220803 (*Marcinkowsky et al., 1980*) mentions a Cu and Cr containing catalyst useful for oxidative dehydrogenation of ethanol to acetic acid at 285-325°C, prepared by impregnation of an alpha-alumina carrier, while in US 1911315 (*Haner et al., 1933*) a copper oxide wire or gauze is used as a catalyst for an oxidative dehydrogenation of ethanol at 320-340°C, where the activation of the catalyst takes place by means of reduction in ethanol vapour. Supported V_2O_5 optionally doped with Cu is suggested in US 5840971 (*Gubelmann-Bonneau, 1998*). Another recent patent (2005) on oxidative dehydrogenation of ethanol to acetic acid over a Pd based catalyst was granted to *Obana et al. (2005).* For both the V_2O_5 and Pd based catalysts is reported an activity of about 0.2 kg/(kg·h). Furthermore a gold catalyst has been found to catalyse the oxidative dehydrogenation (*Jørgensen et al., 2007*). *Li et al (2007)*, suggesting a supported Mo-V-Nb catalyst, obtained the highest conversion rate of about 1 kg/(kg·h).

The oxidative process route from ethanol to acetic acid has been commercialised, but not industrialised, by Wacker Industries. March 2008 Fridolin Stary, senior vice president of corporate innovations declared that Wacker Chemie was ready with the technology for the catalytic oxidation of ethanol to acetic acid, and that it was only a matter of when bio-ethanol becomes competitive in Europe and the US (*ICIS News, J. Chang, 2008*). In the corresponding patent description (*Rüdinger et al., 2008*) it may be found that the process is penalised by a large gas recycle in order to control the reactor bed temperature and in order to avoid operation within the explosion limits. In fact, a gas recycle to make-up ratio of about 30-60 is necessary. Their patent application (designated under PCT to more than 100 countries) has not been granted yet. If granted, the patent with the claimed process prevents other from conducting the oxidative dehydrogenation of ethanol over a catalyst comprising one or more oxides selected amongst TiO_2, ZrO_2, SnO_2 and Al_2O_3 in combination with V_2O_5 in a recirculation process wherein water is used for absorbing the raw product. Figure 2-3

shows the outline of the Wacker process for the oxidative dehydrogenation of ethanol, wherein the full oxidation of ethanol is the primary side-reaction (see Scheme 2-4).

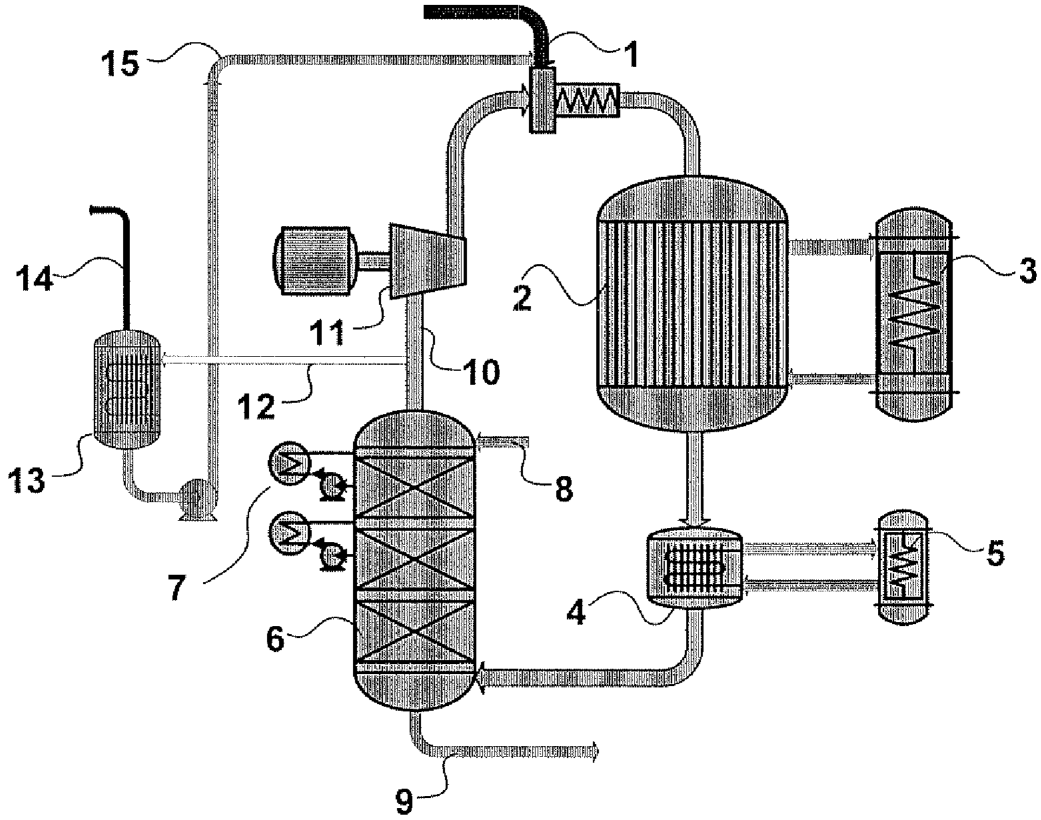

Figure 2-3: The Wacker process. In a mixing zone (1) feed streams containing oxygen and ethanol are mixed with the gas recycle stream (10) from downstream the process. The admixture is fed to a tubular reactor (2), where the ethanol and oxygen react to form acetic acid and water (Scheme 2-2) or alternatively CO_2 and water through full oxidation (Scheme 2-4). The reaction heat evolved during the exothermic process is removed by means of a circulating cooling medium on the outside of the tubes, in turn being cooled in an external cooler (3). The reactor effluent is cooled in a heat exchanger (4) by a cooling medium which is cooled in an external cooler (5) in a closed loop as well.

The cooled reactor effluent is passed to an absorber (6) furnished with external coolers (7) (installed in side draw pump-arounds) where the acid is absorbed in water (8) fed from the top of the absorber. From the bottom of the absorber is withdrawn a stream of acetic acid, water and side-products which must be rectified in order to obtain the purified acetic acid. The effluent gas freed of acid (10) is recirculated via recirculation compressor (11) to the mixing zone (1). In a split stream (12) a fraction of the recycle stream is purged in order to prevent the build-up of side-product gases, carbon dioxide, evolved through the full oxidation of ethanol as described above (*Rüdinger et al., 2008*).

Scheme 2-4: Full oxidation (combustion) of ethanol.

Rüdinger et al. (2008) mention their catalyst for the ethanol oxidation process being a mixed oxide catalyst containing vanadium oxide, for example $Ti_aV_bMo_cSb_dO_e$, where a=256, b=27, c=4, d=20 and e=611. The selectivity of the catalyst applied for oxidation is crucial. It is a classical problem in connection with the partial oxidation of a reactant that the parasitic full oxidation of the reactant to CO_2, being even more exothermic, is

conducted in competition with the desired (see Scheme 2-4). As normally also the selectivity toward the full oxidation increases with temperature, oxidation systems are in general penalised with the risk of a reactor temperature run-away. *Gubelmann-Bonneau (1998)* reports that the oxidative route in general suffers from selectivity problems due to the full oxidation of ethanol. The oxidative process route lacks the feature of the non-oxidative route of consuming i.e. removing water from the feed. Rather it produces water as a co-product.

2.3.2 Oxidative dehydrogenation by means of an oxygen carrier

GB 287064 (*Hale et al.,* 1929) describes a process where silver promoted Cu/CuO acts as an oxygen carrier in a circulating bed set-up. Ethanol is fed to the bottom of a moving bed column reactor containing a bed of Cu and CuO moving counter currently. The acetaldehyde and hydrogen produced (at about 280°C) over the Cu is subsequently further oxidised to acetic acid and water (at about 350°C) by reaction with lattice oxygen in CuO in the upper layer. Thus at the top of the column reactor the product stream containing mainly acetic acid and water is withdrawn whereas spent (reduced Cu) is withdrawn at the bottom of the column, then after introduction in a regenerator co-fed with air it re-oxidises and is recycled as CuO back to the top of the column reactor. Figure 2-4 shows the principle used in the 2-step process.

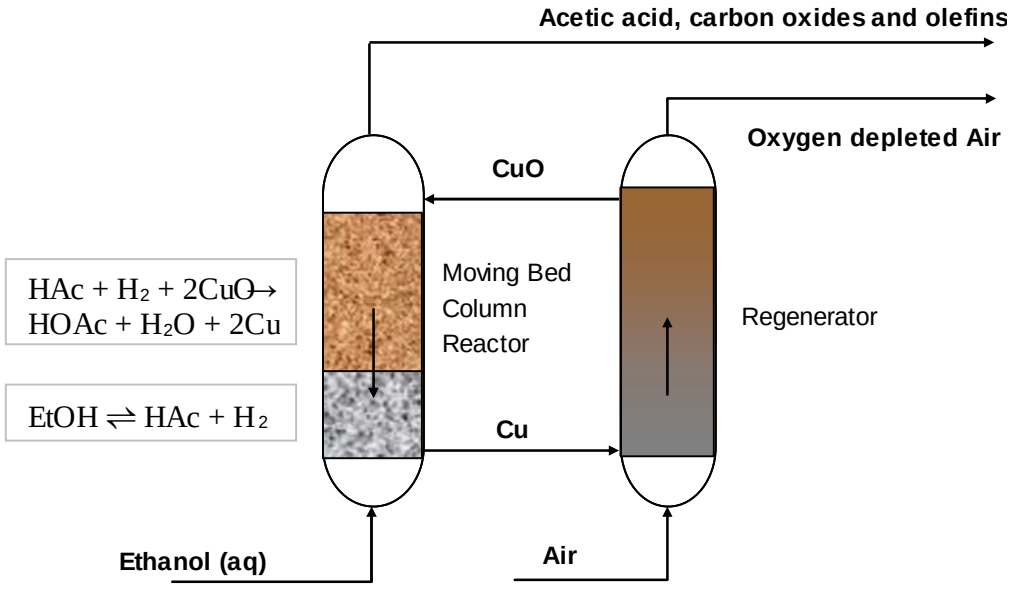

Figure 2-4: Oxidative dehydrogenation of ethanol in a moving bed reactor (GB 287064). Cu is used as an oxygen carrier being regenerated in a separate reactor (regenerator). The oxidative dehydrogenation takes place in two steps in the moving bed column reactor.

Adding the reaction schemes in the two steps results overall in Scheme 2-2. The circulation rate of the Cu/CuO must be carefully adjusted to correspond to the feed rate of ethanol. Handling large rates of solids in such a circulating bed set-up is always a challenge. Especially here, where the conversions over the 2 steps involve an endothermic dehydrogenation followed by an exothermic oxidation the heat management sets extra requirements. Furthermore the regeneration of the Cu to CuO probably requires quite a large excess of air in order to keep the delta T across the regenerator reasonably low. The process was never commercialised.

If at all operable one would today probably consider combining this reactor system, involving the co-production of a hot oxygen depleted air stream, with an application where an excess hot air stream is favourably used, for example as it would be in a gas turbine or in a convective reformer.

2.3.3 Non-oxidative dehydrogenation

In 1919 a patent application (*Legg et al., 1921*) was filed for a fused copper oxide as a catalyst for the catalytic oxidation of alcohols. A few years after a French patent (*Mailhe, 1921*) described a method for producing acetic acid by converting ethanol at about 270-280°C over a Cu based catalyst prepared from a tetra copper hydrate. According to US 6794331 (*Ostgard et al., 2003*) Raney copper has shown dehydrogenation activity of an alcohol to its corresponding organic acid at 80-200°C. JP 57102835 (*Tomaki et al., 1982*) lists the combination of Cu oxide with zinc oxide, chromium oxide and manganese oxide or Cu oxide supported on alumina or silica as a preferred dehydrogenation catalyst at 260-360°C.

The overall non-oxidative dehydrogenation of ethanol to acetic acid (see Scheme 2-3) is an endothermic reaction driven by entropy (ΔH^{θ}=43.9 kJ/mol, ΔG^{θ}=22.3 kJ/mol), thermodynamically favoured at low pressure. According to literature the route goes via acetaldehyde (*Inui et al., 2004, Iwasa et al., 1991*). Both acetic acid and ethyl acetate may be produced in the non-oxidative process. It has been discussed whether ethyl acetate is a co-product (*Iwasa et al., 1991*) catalysed in parallel over Cu based catalysts (Figure 2-5, Alt. 1, product of acetaldehyde and ethanol) or it is an intermediate (*Inui et al., 2004*) in the primary path to acetic acid (Figure 2-5, Alt. 2):

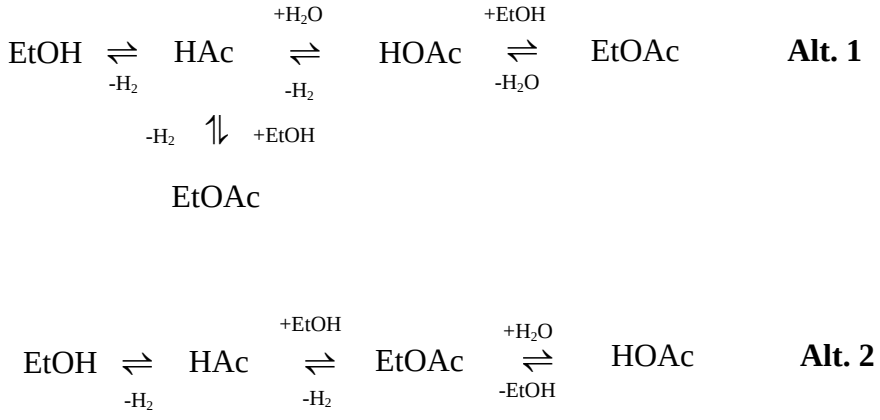

Figure 2-5: The suggested alternative pathways for non-oxidative dehydrogenation over Cu, Alt. 1 and Alt. 2, of ethanol to acetic acid via acetaldehyde, or via acetaldehyde and ethyl acetate. The pathways may be broken down into further elementary reaction steps.

Furthermore a certain amount of ethyl acetate may be produced through the acid catalysed esterification, as shown on the right in Figure 2-5, Alt. 1.

Thermodynamic calculations (ideal, by means of GIPS) made in this work on the reaction system starting from equimolar amounts of ethanol and water at atmospheric pressure, including the ethyl acetate intermediate or end product step as well, reveals

that under equilibrium conditions the acetic acid concentration increases with temperature (see Figure 2-6).

The concentration of acetic acid levels out at about 350°C. On the other hand the ethyl acetate concentration decreases with temperature. If the ester equilibrium is omitted, there is an optimum acetic acid concentration at about 260°C.

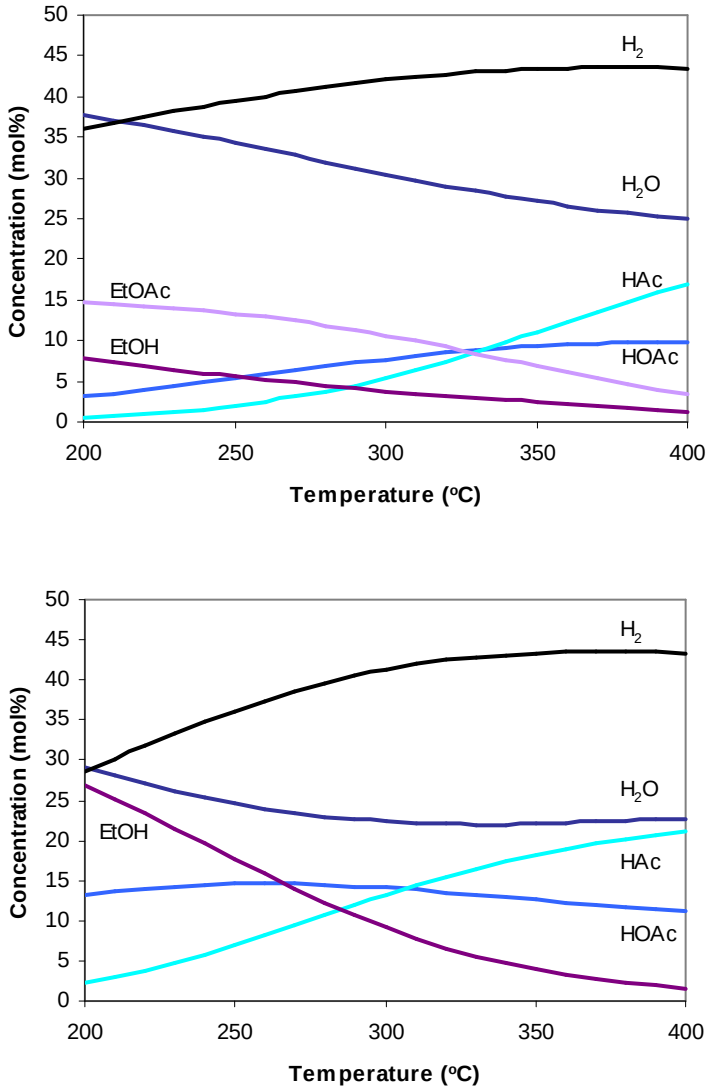

Figure 2-6: Thermodynamic equilibrium calculation (ideal) based on the reaction paths in Figure 2-5. Upper: calculation with ester equilibrium. Lower: calculation without ester in equilibrium. The predicted thermodynamic optimum depends hereon.

The upper temperature limit may practically be set by the selectivity and/or catalyst activity and stability. A parasitic reaction of the very reactive intermediate acetaldehyde to condensation products (by aldol condensation via 3-hydroxybutanal) is known to take place on metal oxide surfaces (*Inui et al., 2004, Iwasa et al., 1991*) at temperatures as low as 220°C. Furthermore, metallic Cu supported on a catalyst carrier is known to sinter at high temperature especially under the influence of water

(*Quincoces et al., 1997, Kamble et al., 1998, Sun et al., 1999*).Thus at temperatures adequately low, however high enough for suppressing the endothermic ester formation from the ethanol and the acetic acid, and for obtaining substantial catalytic activity, the optimal reaction system prevails.

In the above mentioned Japanese patent JP 57102835 (*Tomaki et al.,* 1982) a process for the non-oxidative dehydrogenation of ethanol to acetic acid is suggested. There is no mention of ethyl acetate. Reference is made to Figure 2-7.

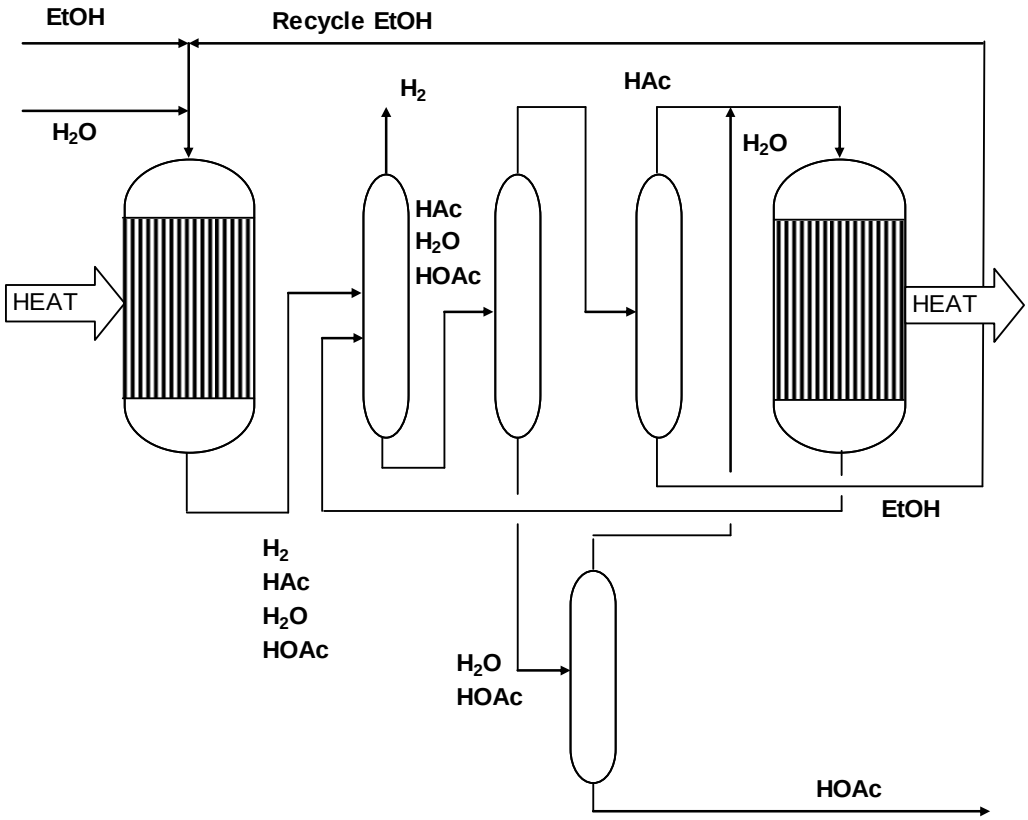

Figure 2-7: Process scheme for the most recent (1982) and advanced non-oxidative dehydrogenation process suggested in a Japanese patent (*Tomaki et al., 1982*) comprises 2 conversion steps and 4 separation steps. The ethanol feed is co-fed with a feed stream of water to a first dehydrogenation reactor together with a recycle stream of unconverted ethanol, the conversion taking place according to alternative 1 in Figure 2-5, excluding the ester equilibrium. The first product from the reactor, richer in acetic acid and hydrogen is passed to a first separation step, to which step also a downstream second product stream rich in acetaldehyde, water, acetic acid and hydrogen is passed. The hydrogen is separated from the product streams and fed to a second separation step, where acetic acid and water are withdrawn together and the remainder acetaldehyde and ethanol are fed to third separation step, where the unconverted ethanol is withdrawn and recycled to the first dehydrogenation reactor. The acetaldehyde withdrawn from the third separation is co-fed with a feed stream of water to a second dehydrogenation reactor, where acetaldehyde is dehydrogenated to acetic acid. The effluent from the second dehydrogenation reactor is recycled to the first separation step. Pure acetic acid may be attained through a distillation of the combined acetic acid and water stream from the second separation step. The water recovered from the acetic acid may be used as makeup water for the dehydrogenation of acetaldehyde.

The advantage of this layout is that the concentration of water in the combined acetic acid and water stream may be relatively low and that the dehydrogenation of acetaldehyde may be conducted under conditions ideal for this conversion solely; the

drawback is that many separation steps and two separate conversion steps, one being endothermic and one being exothermic, have to be involved, meaning that both heat supply and heat removal have to be considered setting extra requirements to the type of reactors employed.

In other patent descriptions related to oxidative and non-oxidative dehydrogenation of ethanol to acetic acid (*Haner et al., 1933, Mailhe, 1921*) a simple recycle of any unconverted intermediate or ethyl acetate is loosely suggested.

The non-oxidative dehydrogenation warrant the favourable utilisation of an aqueous ethanol feed, however it puts the restriction to the catalyst that it must be tolerant to water.

2.4 Conclusions

Both the catalytic oxidative and the non-oxidative dehydrogenation of ethanol to acetic acid routes are known and respective processes have been suggested. But none of these have been commercialised. The limited success may relate to the unrefined catalyst preparation methods of earlier times and the loss of motivation through the penetration of the carbonylation based process. There are process benefits and drawbacks connected to each of the process routes. The advantages for the non-oxidative process route is that water is consumed by the process making a good integration fit with hydrous bio-ethanol feedstock, there is no risk of temperature run-away and the process co-produces hydrogen which is also a valuable product, easily separated from the product stream, and that the IPR protections on catalysts have expired; the drawback is that energy has to be provided, however at a temperature level feasible for steam firing. The advantage for the oxidative dehydrogenation process is that it provides for its own preheating and heating needs; however the hatch in the oxidative dehydrogenation process is lower selectivity and a potential run-away problem (economic and safety issue), and the fact that water is produced rather than consumed. Furthermore two granted patents (assigned to Showa Denko and Rhodia) limit the freedom to operate an acetic acid process based on the oxidative dehydrogenation of ethanol over Pd and V_2O_5 based catalysts, and if granted so will the Wacker process patent.

The non-oxidative process immediately offers a majority of benefits over the oxidative route (see Table 2-1). The activities of the catalysts mentioned for the non-oxidative dehydrogenation of ethanol to acetic acid have not been reported.

Table 2-1: The non-oxidative dehydrogenation route bears more positive characteristics than the oxidative route does. The activities of the catalysts in the non-oxidative route are not known. Catalyst patents of the non-oxidative route have expired.

	Oxidative route	**Non-oxidative route**
Water consumption	÷	+
H_2 co-production	÷	+
Low recycle rate	÷	+
Self sufficient heat supply	+	÷
Avoidance t runaway	÷	+
High safety	÷	+
Selectivity	÷	(+)
Activity	(+)	(?)
Freedom to operate	÷ Pd, V_2O_5; + Cu, Au	+

Predominantly Cu based catalysts have been mentioned in relation to both routes, but Cu is however not amongst those mentioned for the effective patents, which leaves a freedom to operate and an opportunity to investigate, characterise and develop a catalyst type recently unattended by others.

The choice and development of the preferred route also relies on catalyst activity, selectivity and stability investigations, which will be described in Chapters 4, 5 and 6, the corresponding experiments being conducted in test set-ups described in the next Chapter 3.

Chapter 3 Experimental Test Set-ups

3.1 Introduction

During all the investigations of catalysts tested for their activity, selectivity and stability in the conversion of ethanol to acetic acid different experimental test set-ups have been used to gain the catalytic data. For easy reference, the description of all the test set-ups are collected in this chapter. The characterisation set-ups are described in connection with the individual characterisation results. The test set-ups were either existing but rebuilt to serve the actual purpose, or built from scratch (see Figure 3-1) in order to meet specific test objectives and criteria. From the basic thermodynamics it was clear that atmospheric testing would suffice in a first round. However, one existing test set-up, the stability test set-up, was already furnished with controls and shut-down system making it appropriate for testing at higher pressures, a feature which came in handy later.

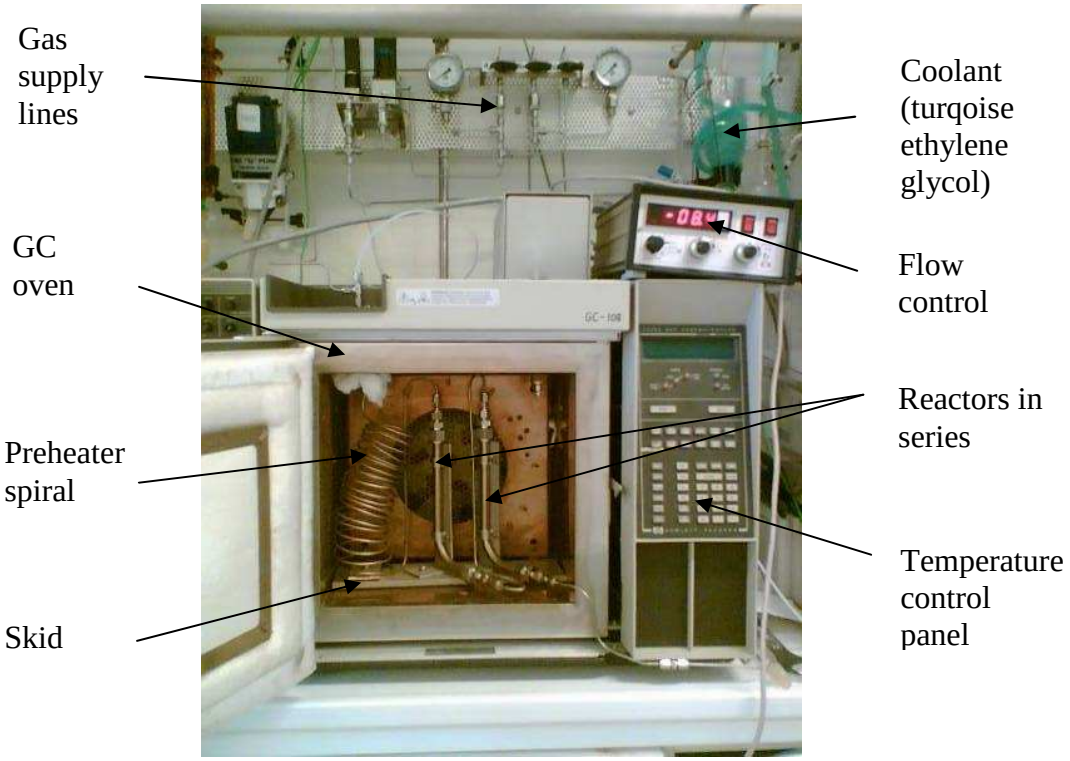

Figure 3-1: The kinetic test set-up. Different kinds of tests had to be conducted. Rebuilding an old GC oven provided a short-cut for establishing another test facility.

Firstly, a screening test set-up was needed to identify catalyst candidates for further investigation. The catalysts were tested in the temperature range 280-340°C, inspired by literature finding and optimum equilibrium conditions (see paragraphs under 2.3). This kind of tests does not require other than vaporisation of the feed and passing it over a bed at a temperature controlled reasonably accurately and collecting the product

for analysis. Good characteristics of the screening test set-up are simply that it is fast and easy to operate. Having selected one or few catalyst candidates a new test set-up was designed in order to better support optimum testing conditions (temperature and flow control, reactor geometry) and facilitate the oxidative experiments. In order to establish something fast the construction in glass equipment had to be foreseen. And in order to get a fast safety approval the set-up should be run at atmospheric pressure. The two restrictions are coherent in that glass equipment prescribes atmospheric operation. A hatch is that in spite of an improved (external) oven temperature control the heat conductivity in glass is not high, limiting the temperature control obtained in the reactor bed. As a next step, having reassured that the catalyst candidate indeed bears a snapshot potential of good activity and selectivity there remains a need for a test set-up which can be run continuously for many days/months in order to establish catalyst stability data. The automation of the stability test set-up as mentioned above also provided for continuous unmanned operation. Lastly, when a catalyst has proven itself active, selective and stable, kinetics must be investigated in order to optimise the operating conditions in the process of maturing the technology further. Isothermal operation during kinetic testing is optimal, but this is hard to obtain in fixed bed reactors at low heat conductivity conditions. Instead we made use of a reactor which may be modelled.

Running experiments in multiple reactor systems with each set of characteristics and problems take a lot of manning and may be hard to survey, however the pace of results also allows for a more condensed recording of results. Furthermore analysis principles for the smooth calculation of obtained conversions had to be created. The validation of the principle of analysis is substantiated through examples taken retrospectively from the kinetic experiments described in Chapter 6.

This chapter describes the individual test set-ups and analysis principles in further details, while the test results from the experiments are reported in Chapter 4 on screening and in Chapters 5 and 6 on the two types of catalysts dealt with. A survey of the test set-ups with main characteristics is included in the conclusion of this chapter.

3.2 Screening test set-up

The screening of catalyst was conducted in a glass set-up (see Figure 3-2) in a non-quantitative manner. The main sections of the setup comprise feed pumping, mixing with carrier gas, the passing of gas admixture through the reactor, and collection of condensable product downstream of the reactor. Collected condensates were analysed by GC-MS (Agilent 6890 Series GC system with Agilent 5973 Mass Selective Detector, polar method).

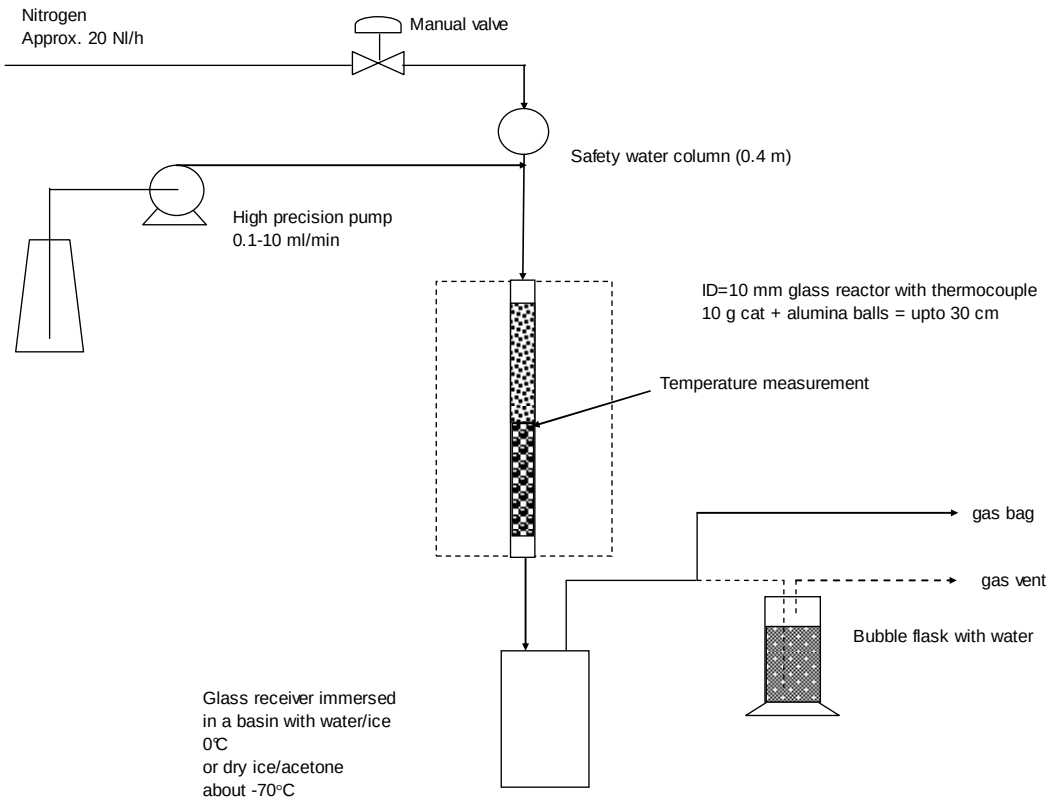

Figure 3-2: Sketch of the screening glass set-up.

In each case 10g of catalyst (pellets, extrudates or particles) was loaded into a glass reactor. A thermocouple was placed in the centre of the bed and small alumina balls serving to provide for evaporation of the liquid feed were put on top of the catalyst bed. The glass reactor (ID=10 mm) was installed in an atmospheric setup in a temperature controlled oven (mounted with ceramic electrically heated elements concentrically surrounding the glass reactor wall). The oven was calibrated comparing observed temperature vs. set point temperature at 300°C (see Figure 3-3).

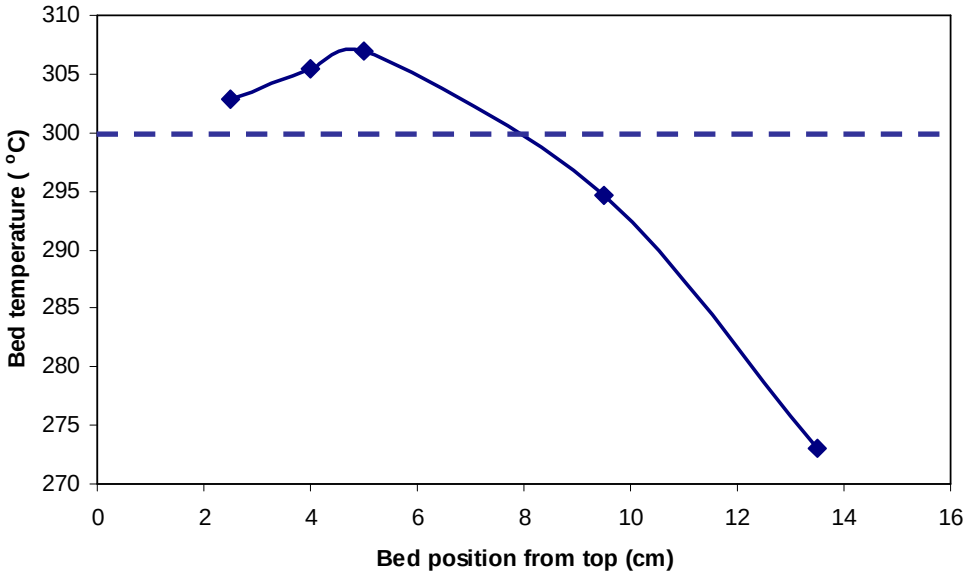

Figure 3-3: The temperature profile in axial direction through the temperature controlled oven, passing nitrogen through the reactor.

A large variation over the length profile existed, 30°C over 15 cm, in spite of insulation and exclusion of draught through the annulus between the reactor wall and the oven. During the experiments catalysts of different shape and density have been tested in the set-up. A poor flow distribution of the liquid feed was seen in the evaporation zone (alumina balls). This and the fact that the thermocouple could not be placed precisely in this set-up reduced the chance of keeping track of comparable operating conditions rendering the set-up unsuited for other than qualitative studies.

Nitrogen was flowing at an approximate rate of 250ml/min in all tests. The system was heated up to 250°C by switching on the temperature-controlled oven. Then the liquid feed was introduced from a high precision feed pump (HPLC pump, Knauer Pump 100, 0-10 ml/min). The catalyst was reduced (if required) by feeding ethanol at 250°C for half an hour. After reduction the temperature was typically raised to 320°C, hereafter the reactor was ready for operation. Typically a feed rate of 0.5 ml/min of ethanol or ethanol/water was used. Liquid product was accumulated in a glass receiver down stream of the glass reactor. The glass receiver was optionally cooled by indirect heat transfer to a medium in a basin underneath. In most cases no external cooling in the basin was provided, but for a selected number of experiments a mixture of solid CO_2 and acetone (saturated mixture boils at -77°C) was used in order to reveal more accurately the product composition of the condensables. Samples from the glass receiver was analysed in the GC-MS. In the cases where solids formed in the glass receiver due to freezing, the glass receiver was changed and plugged before being heated to ambient temperature, in order to obtain the total composition of condensables. The gas effluent (non-condensables) primarily containing acetaldehyde (especially if no cooling in the basin), nitrogen and product hydrogen was led through a bubble flask with demineralised water and vented in the fume hood.

Especially Cu based catalysts, but also other catalyst candidates were tested as to their activity. They comprise primarily Ag, Pt and Pd supported on for example TiO_2, silica or impregnated as a promoter on a Cu based catalyst. During the screening of each of the catalysts the water to the ethanol ratio of the feed was changed. This was done in order to investigate the influence of water on selectivity and activity.

Alternative constructions to the screening set-up were considered in order to ensure proper testing conditions. The advantages of the screening set-up were that it was easy to assemble/disassemble and operate, and the glass reactor had proportions which made the testing of many shapes possible. The glass reactor was furthermore well suited for the atmospheric operation which suffices in a first round, and provided for visual inspection. The screening set-up however suffered from more shortcomings: only nitrogen carrier gas could be fed as a gas stream in the feed system, the temperature characteristics of the reactor in the oven was poor, the reactor itself was non-optimally sized for the catalysts chosen for further investigation, the cooling of the condensate took place in a non-thermostated basin, the capacity for sampling of product was small, and the set-up could only be operated under constant surveillance.

3.3 New test set-up

As discussed above, the fastest way of obtaining a test set-up is by accepting glass as a construction material, as many special glass items, ready to connect with each other, are typically available. On the other hand, for attaining proper experimental data the

optimal reactor type is where isothermal conditions can be established. For an exothermic or endothermic reaction this is of course best secured by easing the heat conduction to/from the reaction zone by selecting materials with high heat conductivity and fluid conditions which give high heat transfer coefficients. In the light of this preference, glass equipment is definitely not ideal. Furthermore the heating source immediately available was a ceramic oven furnished with three temperature controlled heating zones providing heat to a cylindrical channel, i.e. when a cylindrical reactor tube is placed concentrically in the channel, the heat transferred from the oven to the reactor is provided via the annulus. This oven however offered a longer and more constant temperature profile than the screening set-up with only one heating zone. Figure 3-4 shows the temperature profile of the screening set-up when the oven was set on 300°C and the reactor loaded with alumina balls was flushed with 20Nl/h of nitrogen at atmospheric pressure. The temperature of the new glass set-up could be kept constant within ±2°C in a height span of 25 cm even at a set-point of 500°C. Due to the position of the thermo well placed in the reactor an actual bed height of about 15 cm could be achieved.

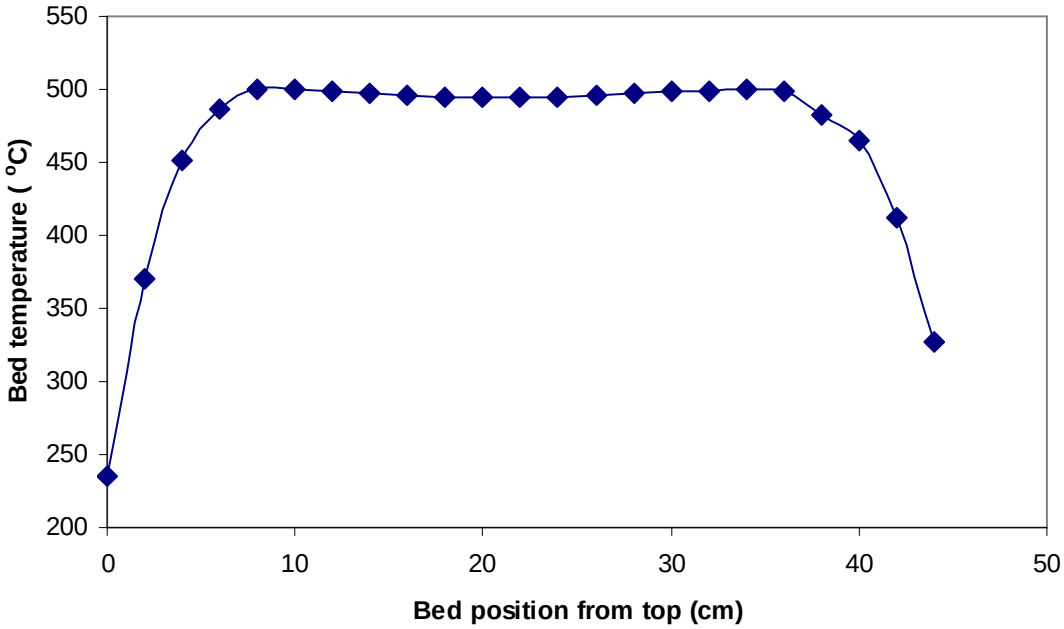

Figure 3-4: The temperature profile of the new glass set-up mounted with 8 mm glass reactor, loaded with inert alumina balls. .

3.3.1 Reactors in new test set-up

In the improved, though not ideal, experimental setup for the non-oxidative and partly oxidative dehydrogenation tests two kinds of glass reactors were designed, serving different purposes.

Reactor 1

One of the reactors was furnished with a central thermo well making it possible to position a thermocouple in different positions in the centre of a catalyst bed of pellets, thereby obtaining a temperature profile in the reactor bed during operation. This first reactor (ID=27 mm) was furnished with a glass catalyst grid in the bottom and a 4 mm glass thermo well penetrating at the top of the reactor. In this case about 50 g of

catalyst had to be loaded into the reactor (with alumina balls on the top) in order to obtain an adequate bed height. A conservative estimate says (assuming a reaction order of 1) that for moderate Re_p numbers (say Re_p=10-100) and degrees of conversion a bed height of 10 times the channel width must be obtained to avoid back-mixing and channelling (*Kapteijn et al., 1997*). The channel width in this context was judged to be the channel width from the central thermowell to the inside of the reactor wall, around 11 mm. Therefore, a catalyst bed height of 15 cm seems reasonable.

Reactor 2

The other reactor (mentioned above in the temperature profile measurement experiment) was (ID=8 mm) designed for the loading of 5-6 mm cylindrical pellets according to a single pellet string principle (see Figure 3-5) or for the loading of 1-1.4 mm sieve fraction of crushed catalyst. The single-pellet-string loading principle is well known to serve a laboratory reactor to best approach the radial gas distribution of a large industrial reactor, while allowing for the highest linear gas velocity securing the highest possible Reynolds number for the reactor (*Scott et al., 1974*). This second reactor had a thermo well penetrating from the bottom of the reactor, terminating at the catalyst grid.

In the case of the loading of crushed catalyst the bed was further supported on pyrex wool on the grid.

Figure 3-5: The single pellet string loading principle. Inert alumina or glass balls separate the individual catalyst pellets.

Either of the glass reactors was installed in the new test set-up (see Figure 3-6 showing the new test set-up with reactor 2 installed). The ethanol or other liquid feed was pumped by a high precision pump (LDC Analytical Consta Metric 3200) mixed with nitrogen as a carrier gas and air and evaporated in a 2 m stainless steel coil embedded in an electrically heated tracing element.

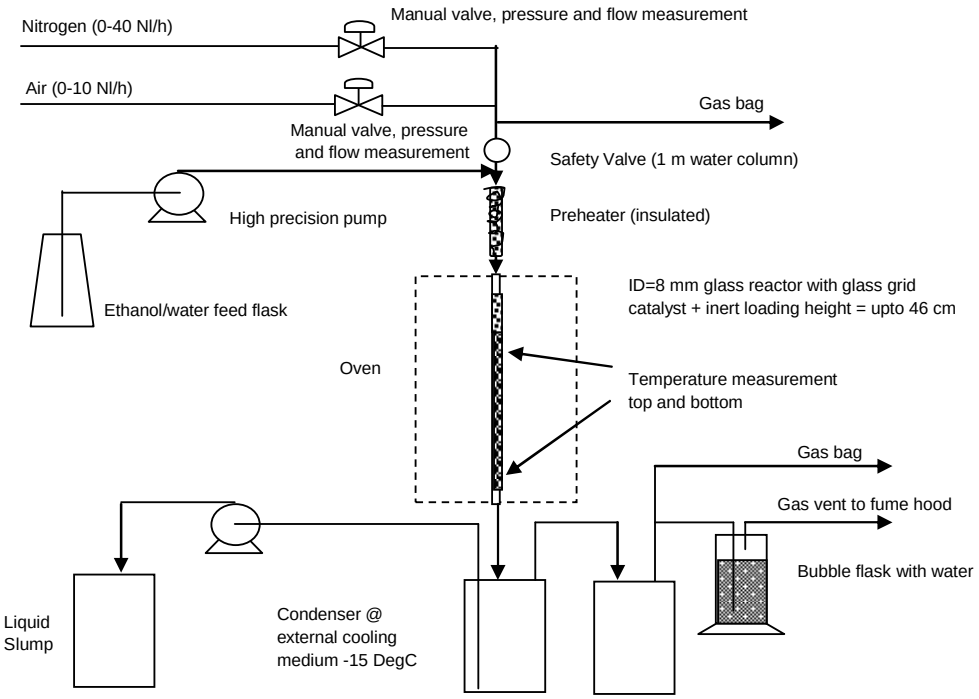

Figure 3-6: The new glass reactor set-up was designed to secure optimal practical, though not ideal, testing conditions.

Liquid product was accumulated in a double glass receiver system down stream of the glass reactor. The glass receiver was cooled by indirect heat transfer through a glass coil to a -15°C cooling medium (ethylene glycol) circulating in a closed circuit. The gas phase from the first condenser was connected to a secondary condenser in order to check the efficiency of the condenser in separating the phases. Samples from the glass receiver was analysed in the GC-MS for identification of components or by GC-FID (Agilent 7890A GC system, installed with a Flame Ionisation Detector). The gas effluent (non condensable) primarily containing acetaldehyde, nitrogen and product hydrogen was led through a bubble flask with demineralised water and vented. Gas analyses and gas flow rates were made on the gas line from the second condenser and before the bubble flask. The reactor set-up was safety approved for the manned run through day hours.

The new reactor set-up suffered from a low heat transfer from/to the reactor through the glass wall and the still air annulus. The new glass test set-up was also found to heat up relatively slowly and to reach steady state conditions (observed by the temperature and exit flow rate measurements) over a very long period, 3-4 h, meaning that only one/two sets of measurements could be achieved over a day. A marked temperature drop of 20°C under operation (inlet to outlet) was observed for the new test set-up, firstly reflecting the overall endothermic nature of the reactions, secondly indicating that isothermal operation in a fixed bed reactor type could not be obtained.

3.4 Stability test set-up

In order to break the limitation of running only during daytime, an existing automated test set-up constructed in steel was rebuilt as to its feeding system. The reactor

installed herein meanwhile had a large inner diameter of 17.5 mm, and its temperature profile (acquired similarly to the profile for the reactor in the new test set-up) revealed a valid bed height of only 50 mm, meaning that poor fluid dynamics prevailed with the catalyst amount loadable and the flow rates obtainable with a sensible degree of conversion (Re_p<10). However, for the purpose of continuously following the stability of the catalyst it was still an improvement. A sketch of the stability test set-up may be found in Appendix C.1.

The test set-up is furnished with an automation both of the feed flow rates and temperature set-points, and the liquid feed bottle (5 litres) is placed on a balance with data log which makes it possible to double check the consumption of liquid feed (g/h) against the pumping rate set-point (ml/min) giving a more accurate feed rate calculation. The pump is a high precision HPLC pump, Knauer Pump 100, 0-10 ml/min. Analysis of the condensate product was made by the GC-FID as described above (see paragraph 3.3.1). A few gas analyses for example in order to check side-product formation of CO_2 were made offline by means of gas bags.

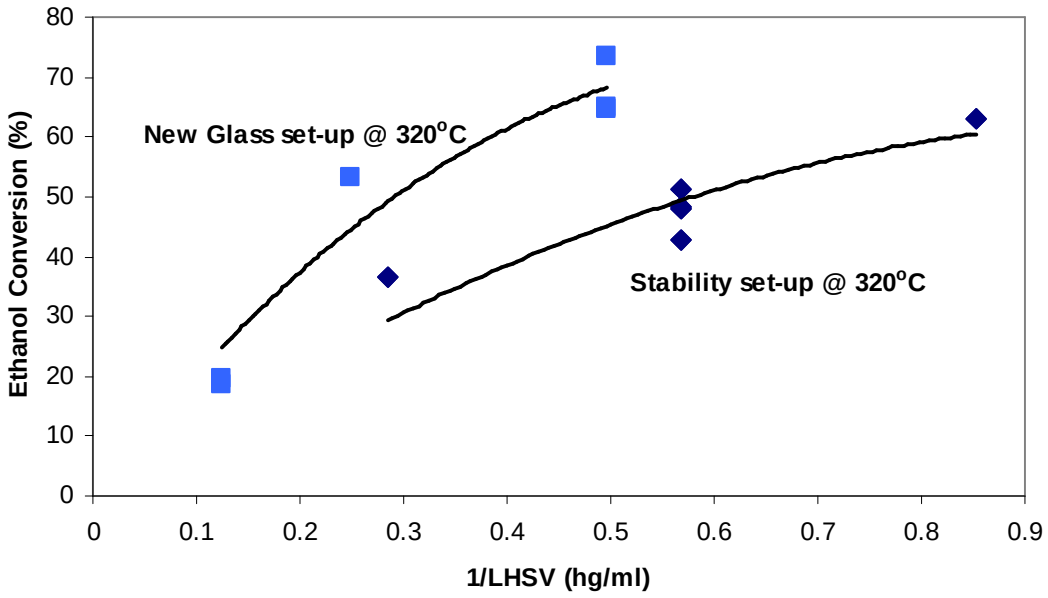

Figure 3-7: The conversion of ethanol:water feed (40/60) in the New glass set-up and the Stability set-up, respectively.

Comparing the data acquired for similar feed and operating conditions in the new glass set-up with the data from the stability set-up (see Figure 3-7) it appears that the poorer fluid dynamics of the stability set-up might cause a back-mixing of products, dampening the conversion of the ethanol.

3.5 Kinetic test set-up

If isothermal operation is not obtainable, as discussed for the new test set-up, the establishment of kinetic data set requirements to the ability of the reactor to be modelled. Sound modelling of a laboratory reactor is only obtained when both reasonable fluid dynamics (yielding plug flow conditions) and proper heat contact with a temperature controlled heat reservoir are present. The principle with single-pellet-string

as described above (paragraph 3.3.1) for one of the reactors in the new glass set-up was readopted while here, in the kinetic set-up, the heat transfer to/from the reactor was improved by exchanging glass with steel as the reactor wall construction material and providing for a close to uniform reactor wall temperature. Also the feeding system (lines and feed pump) and the condenser principle (external cooling circuit at -15°C) were adopted again. The two systems could be operated independently.

A rebuilding of a GC oven (with a defect GC but an operable oven) was seen as a possibility as it offered the features of being readily available, having a temperature program with ramping, and having a ventilated oven.

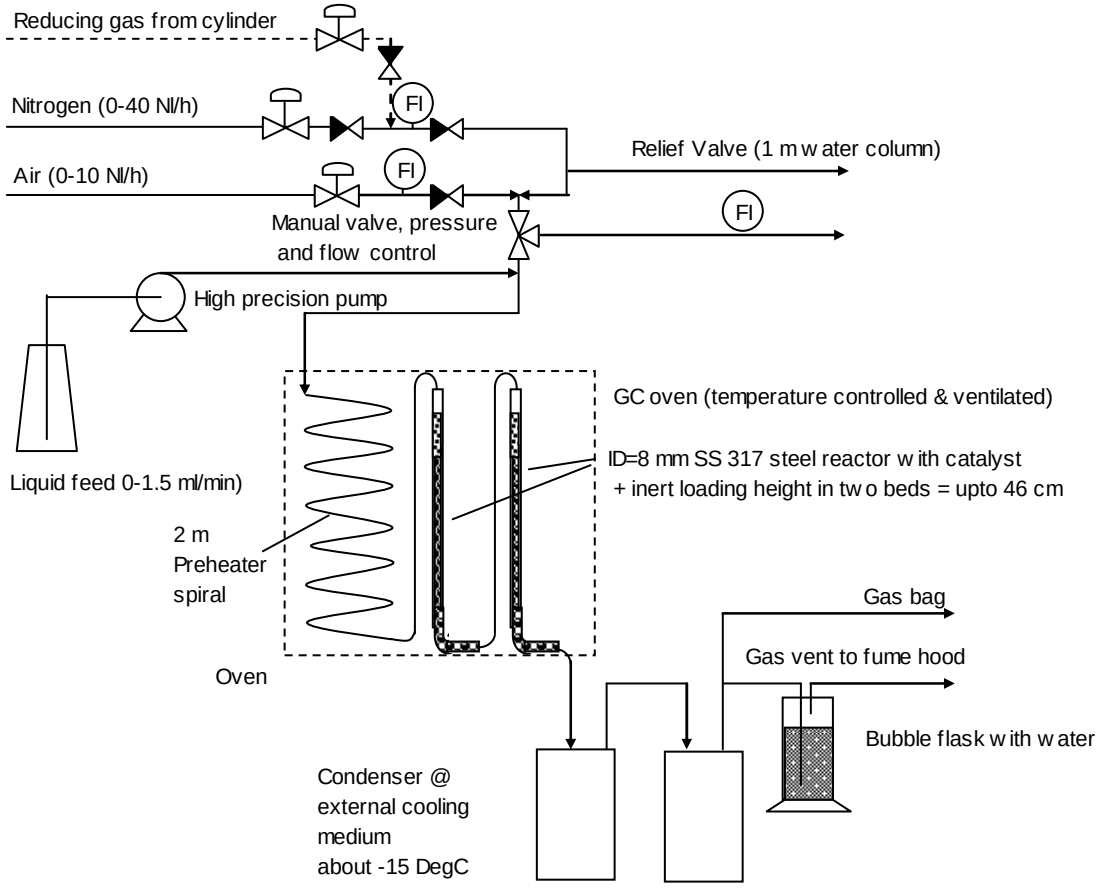

Figure 3-8: Sketch of the kinetic test set-up. It has the features of a fast response to changes, fast heating and good heat transfer characteristics. A pre-heater coil is incorporated into the GC oven upstream of the skid mounted reactors.

The oven height was limiting, but as the reactor was split into two in series a reasonable total bed height about 30 cm could be achieved. Accordingly a reactor system was sketched (see Figure 3-8) and a skid mounted with two reactors was ordered and constructed in the in-house workshop. The feeding system was laid out with a pre-heater incorporated into the GC oven. 2 m of SS tube was bended into a spiral and mounted on the feed line to the skid mounted reactors.

3.5.1 Steady state

The fast response to flow changes assumed was tested in an experiment. The experiment was conducted on 14 g of Cu spinel-850 and the LWHSV=3 g/(g·h), 40Nl/h

of nitrogen carrier gas and a temperature of 300°C. After 4 hours of initial operation, where the level of products stabilised, all the flow rates to the reactor were doubled.

In below graph (see Figure 3-9) the GC analyses of the condensate are depicted, demonstrating that stabilisation is obtained within 15 minutes or less. It is seen that the concentration of acetaldehyde and acetic acid decreases further after the flow doubling, however not more than could be ascribed to the general deactivation. The praxis adopted for the kinetic study, where the test conditions were frequently changed, was that at least 45 min had to pass before the steady state was considered to have been achieved. In comparison with the data in Figure 3-9 this is a conservative approach.

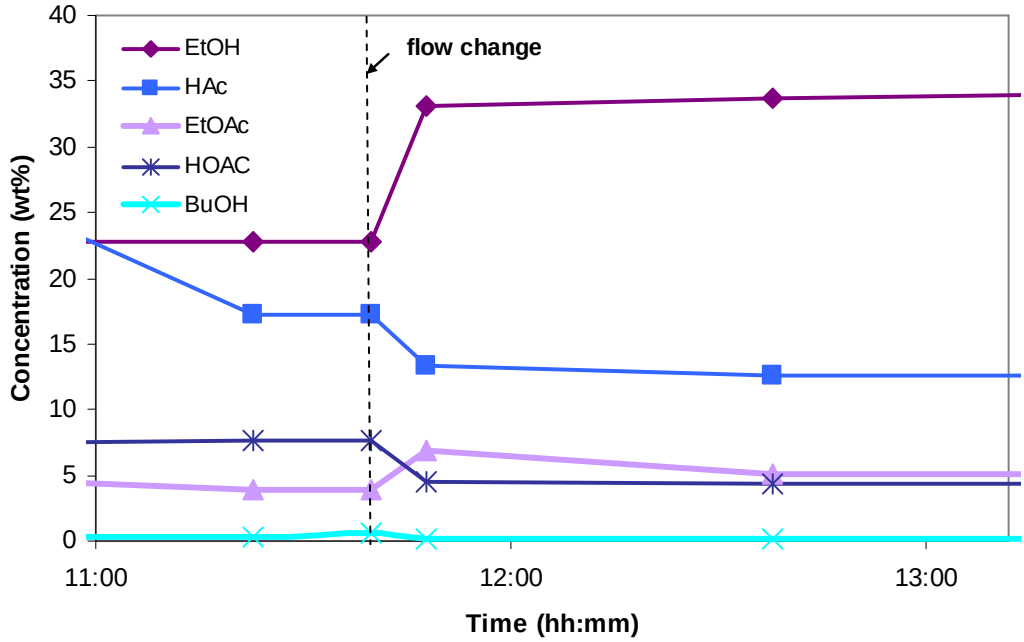

Figure 3-9: The response to flow change was measured by taking frequent samples around the point of change. The system stabilises adequately in less than 15 minutes.

3.5.2 Analysis principle

The calculation of the conversion of the feed over the reactor may be made if the total composition and the flow rate of the inlet and outlet streams are known. The total composition of the inlet stream may be calculated from the mass rate of the liquid feed and its composition (known from its preparation), the nitrogen flow rate and the air flow rate, if any.

The types of analyses available on the product side here, however, set limitations. No online GC of the total effluent could be achieved due to the risk of corrosion problems. Rather the condensate had to be sampled over a known time period in order to obtain the results of the condensate flow rate; and the amounts of acetaldehyde, ethyl acetate, diethoxy ethane, ethanol and side-product butanol in the sample was measured by means of injecting a portion of the liquid into the GC, while the content of organic acids (acetic + butanoic acid) was best determined by titration. The calibrations of response factors were not available from the start, and through the initial many experiments the activity level was expressed through the relative areas to the ethanol

area, i.e. a high area ratio represents a high conversion. The response factors were determined through a series of known standard mixtures as normal.

The concentration of water in the condensate was found as a balance to 100% of the other concentrations found by means of their respective response factors, and the acetic acid found by titration. The water concentration was double checked by means of Karl Fischer.

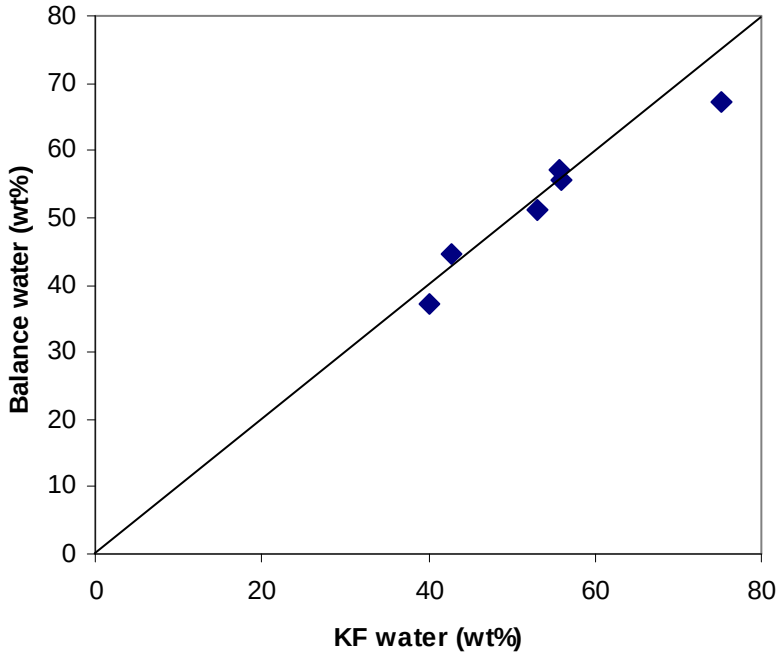

Figure 3-10: Parity plot of calculated water wt% vs. water determined by KF. The water is calculated from the balance to 100% of the other components. The values are compared regularly.

Figure 3-10 showing the relationship between the calculated and the measured water content of the condensate of some condensate samples indicates that this method is satisfactory. In order to calculate the total composition, a gas composition from the condenser system was in principle needed as well. Due to difficulties in getting access to online GC analyses of gas compositions the total mass balance had to be built on the basis of some assumptions. The first assumption is that the reactions can be described by means of the following four reaction equations in Scheme 3-1:

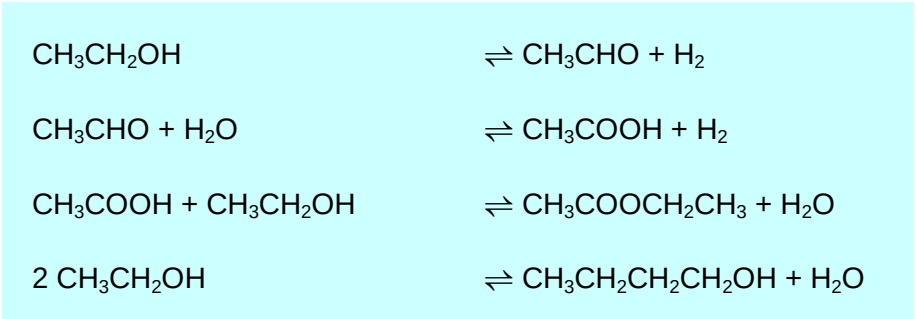

Scheme 3-1: Reactions accounted for in the mass balance.

The other assumption is that the only condensable present in the gas phase from the condenser is acetaldehyde. The mass balance describing such system including the above assumptions was created in a mass and heat balance calculation including a root search minimizing the error on the condensate composition. In order to ease the execution of the mass balance from experimental data entered into a spreadsheet and to recover resulting data in the same spreadsheet for the further elaboration an Excel-GIPS-Excel interface was created (GIPS is an in-house modelling software tool).

In order to reconfirm the validity of this method, the calculated condensate rate from the mass balance was compared to the condensate rate, as calculated from the amount of condensate sampled divided by the sampling time. Figure 3-11 shows the calculated condensate flow rate vs. the measured condensate flow rate based on the physical sample.

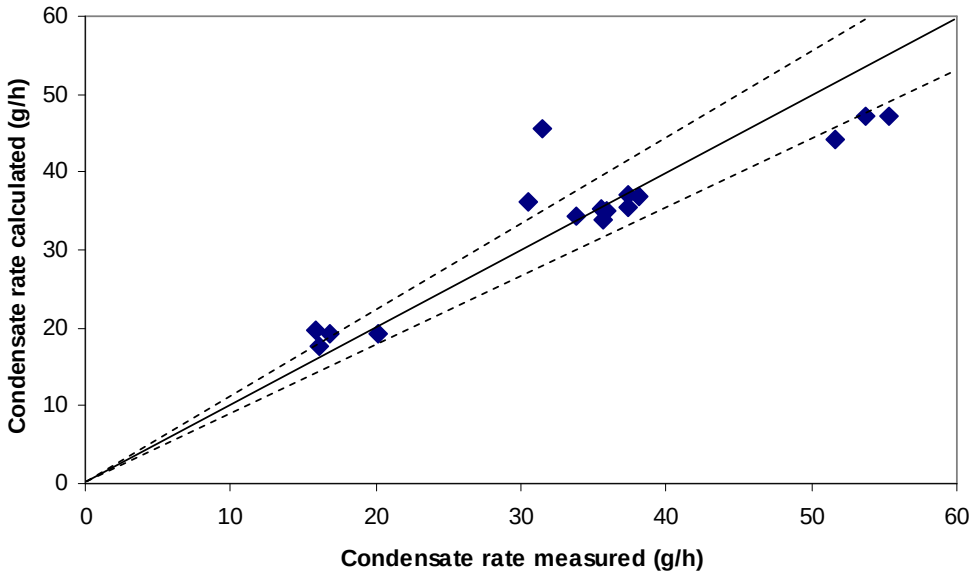

Figure 3-11: The calculated condensate flow rate vs. the measured. The stippled lines indicate a ±10% deviation.

It appeared, in general, that at high condensate flow rates, the calculated rate tended to be lower than the measured flow rate. The next most volatile compound to acetaldehyde is ethanol. A sensitivity analysis revealed that increasing the ethanol concentration of the actually measured composition, hereby simulating a composition of the condensate where the entrainment of ethanol had taken place, would increase the calculated amount of condensate. Thus entrainment may explain the deviation.

Furthermore, the acetic acid concentration as determined by titration was checked against the concentration as found by GC. Figure 3-12 shows the relationship between the measurements in one of the experiments. The measurement by titration was considered the most reliable and this value was used in the mass balance.

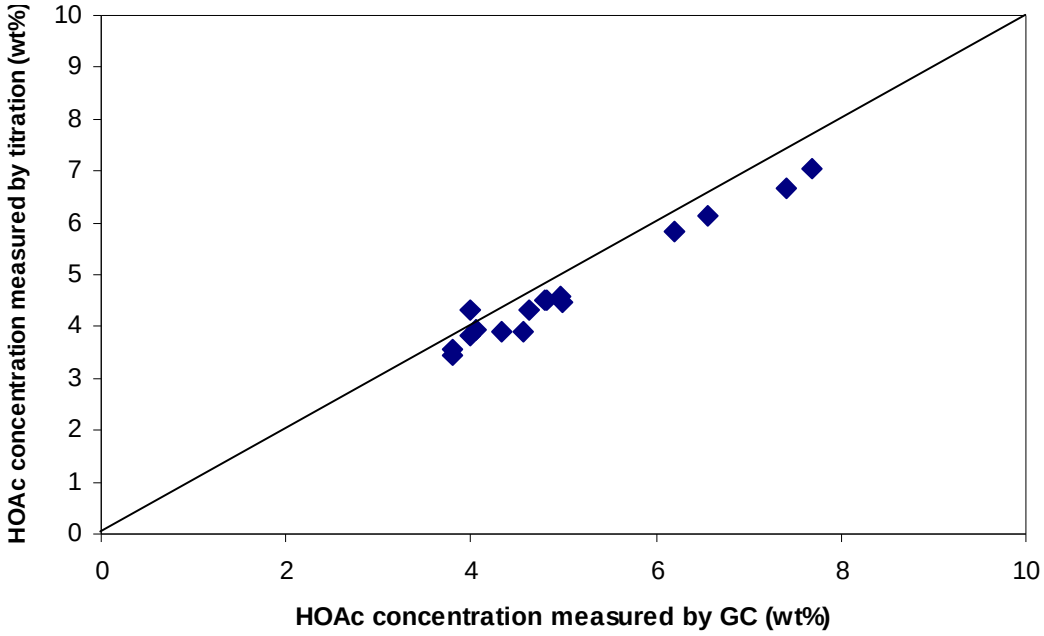

Figure 3-12: The concentration of acetic as obtained by titration and by GC analysis was compared.

3.6 Conclusion

Four test units were used in the investigation of the catalysts. The screening set-up was established based throughout on glass equipment, heated by a ceramic oven, having a very simple feeding, integrated preheating and non-steady condensate collection conditions. The new glass set-up was built with preheating means, better temperature profile, designed reactor dimensions, and a condenser with the ability to keep a constant condensation temperature. The two specially designed reactors made possible the measuring of a temperature profile and improved fluid dynamic conditions (higher Re numbers). Both of the test set-ups were run at atmospheric pressure. The rebuilt stability test set-up had the features of long term feed and sampling possibilities and process safety automation (no personnel needed continuously). Besides, being built throughout in steel the operating pressure could be raised (the total pressure in this work has been as high as 10 bar). The stability test set-up was however not very well suited for frequent catalyst re-loadings, changes of operating conditions or modelling (very low Re_p number<10). Last, the kinetic test set-up was designed in order to comply with the requirements to a kinetic testing program: reasonable fluid dynamics ($60<Re_p<200$) and proper heat transfer description (ventilated oven), making the modelling of reactor system reliable. The condenser system from the new set-up was copied. The response time to a 20°C temperature change was tested for the kinetic set-up and found to be about 5 minutes. The response to flow doubling was tested and an about 15 minute response time was measured. For obtaining a conservative approach 45 minutes from an actual process change to steady state was assumed for the experiments.

In below Table 3-1 a survey of selected characteristics of the individual test set-ups are shown.

Table 3-1: Survey of the individual test set-ups with listed advantages and disadvantages.

PrefixName of test set-up	Reactor material/ ID	Preheater/ condenser type	Isothermal height[a]	Pros	Cons
Screening	Glass/ 10 mm	(alumina balls)/ simple	0 cm	Visual[b] Easy	Not accurate Atmospheric
New	Glass/ 1:27mm w/4 mm thermowell and 2: 8 mm	Steel coil w/ heating tape/ 2 serial w/ external circuit[e]	15 cm	Visual[b] Good condenser SPS[c]	Poor heat transfer Slow response Atmospheric
Stability	Steel/ 17.5 mm	Electrical/ 1 w/external circuit[e]	5 cm	Automated 24-7 High pressure	Difficult reloading Very slow response Back-mixing
Kinetic	Steel/ 8 mm	Steel spiral in ventilated oven/ 2 serial w/ external circuit[e]	30 cm[d]	Fast response Good, well-defined heat transfer SPS[c] Good Re_p[d] Good condenser	Non visual[b] Atmospheric

a) During non-reaction conditions.

b) Visual. Visual inspection possible (for example in order to follow feed distribution in the screening set-up and colour changes during reduction).

c) SPS, single-pellet-string. Makes individual identification of spent catalyst pellets possible (characterisation).

d) The higher loading height provides for better fluid dynamic properties through higher feed rates, $60<Re_p<200$.

e) External cooling circuit w/ circulating ethylene glycol paasing through a thermostated cooler at -15°C.

The screening set-up was primarily used for the screening experiments described in Chapter 4 and a few mechanistic experiments described in Chapter 5. The new test set-up was used for the initial catalytic activity investigation and for acquiring a temperature profile in the partly oxidative dehydrogenation experiments described in Chapter 5 and 6.

The kinetic test set-up was used for attaining as reproducible results as possible. It was further used for the investigation of a catalyst series. For this set-up an analysis principle was established combining the analysis by GC, titration determination of acids, Karl Fischer determination of water, total mass balance calculation with minimisation of errors and double-checked by the physical measure of the condensate rates. Only data sets with good consistency between the measured vs. calculated parameters, being about half of the total sets, were used for the further data evaluation in the kinetic evaluation described in Chapter 6.

Chapter 4 Preliminary Investigations: Catalyst and Process Screening

4.1 Introduction

In order to closer investigate how ethanol may be converted to acetic acid in an economic way a catalyst must be identified and nested into a process. These investigations must go hand-in-hand in order to draw the first picture of the process and its innovation potential. Accordingly, the parallel activities comprise perusing the background information on catalysts and process suggestions, the screening of catalysts at hand, innovative process development, experimental substantiation, the identification of patent protections and novelty bars for future patent applications, and eventually the economic comparison to the conventional technology. At an early state many of these activities are inseparable, meaning a lot is on the plate. Later, the focus can change between the activities in turn, having become acquainted with the interactions from, and the influence of, new discoveries on other activity fields. However, then again far more details are to be dealt with in each area.

This chapter describes the literature findings, the down-selection of catalyst through screening, the initial process calculations and considerations based on the experimental data and an economic analysis of the gate production price of acetic acid made by the non-oxidative dehydrogenation of ethanol. The survey of 33 screened catalysts, the qualitative and semi-quantitative results and observations is enclosed in Appendix D.1. Especially Cu based catalysts were tested in a qualitative or semi-quantitative manner, but also other catalyst candidates were tested comprising V_2O_5 and the metals Ag, Pt and Pd supported on for example TiO_2, silica or impregnated as a promoter on a Cu based catalyst, inspired by the literature on ethanol dehydrogenation and oxidation described in Chapter 2.

4.2 Literature findings on Cu catalysts

Especially copper based catalysts have been mentioned to catalyse the dehydrogenation of ethanol to acetic acid, non-oxidatively and oxidatively (see paragraphs 2.3.1, 2.3.2 and 2.3.3). Cu catalysts ranging from fused CuO, Cu mesh, to supported Cu catalyst, optionally mixed with other metal oxide (especially Cr or Zn) and/or promoted with alkali metals have been mentioned. *Haner et al. (1933)* describes that it is difficult to continuously oxidise (dehydrogenate) an alcohol over silver and copper catalysts as a large amount of acetaldehyde and certain undesirable side-products are co-produced. Their solution is to run the process oxidatively over CuO activated by reduction in hot ethanol vapours.

Very closely related to the conversion of ethanol to acetic acid by dehydrogenation over Cu based catalysts is the dehydrogenation of ethanol to acetaldehyde (being the first dehydrogenation product given in Scheme 3-1) over similar Cu based catalysts. Therefore with only a few references on the dehydrogenation of ethanol to acetic acid one may learn from the challenges around stability described for the acetaldehyde

catalysts. The problems discussed relate to stability issues such as carbon formation and sintering. *MacLean* (1953) suggests a fluidised bed process for the production of aldehyde and ketones by oxidative dehydrogenation over a barium, chromium and cupric oxide catalyst in view of the need of easy regeneration with air. The reason for activity loss is said to be carbon deposits. *Knappsack-Griesheim Aktiengesellcschaft (1958*) advocates the importance of a low alkalinity in order to suppress secondary condensation reactions. A regenerable Cu based catalyst with 0.5-3wt% Cr_2O_3 is preferred. Alkali and alkaline earth metals have (*Knappsack-Griesheim Aktiengesellcschaft, 1959*) been used to improve the dehydrogenation activity of copper catalysts. They meanwhile prefer the use of catalysts with low alkalinity, which prevents aldol condensation. A regenerable catalyst prepared by decomposition of copper tetramine is proposed. The addition of stabilising agents such as magnesium oxide zinc or cobalt is cautioned due to their said favouring of side-product formation. The catalyst is reduced in hydrogen diluted with nitrogen in order to avoid sintering.

Hale et al. (1929) mention metallic Cu as the active catalyst form for the dehydrogenation of ethanol to acetaldehyde (first step in the ethanol to acetic acid dehydrogenation route, see Figure 2-5). Hot ethanol has been said to reduce the Cu oxides to Cu by *Haner et al*. *(1933).* The *Knappsack-Griesheim Aktiengesellcschaft (1959)* recommends reduction in diluted hydrogen in order to avoid sintering. It is well known that water constitutes a harsh component to supported copper catalysts by enhancing the sintering of the dispersed Cu crystals, reducing thereby their catalytic activity (*Quincoces, 1997, Kamble et al., 1998, Sun et al., 1999*). *Iwasa et al.* (1991) find that passing ethanol over unreduced Cu catalyst at 220°C (supported on SiO_2 or ZrO_2) shows no dehydrogenation activity, while after reduction in hydrogen (no dilution mentioned) the catalysts were very active. Subjecting a Cu based catalyst to a mixed feed containing ethanol and water at 280-320°C without prior reduction may then only potentially reduce the CuO of catalyst to Cu being the active form for the dehydrogenation of ethanol.

Furthermore it was learned from literature that the intermediate acetaldehyde is very reactive and the acetic acid product is corrosive. Thus it will be a challenge, in choosing a dehydrogenation route involving co-feeding of water, to identify and develop a Cu based catalyst with appropriate activity, selectivity and mechanical stability characteristics.

4.3 Catalyst screening

Taking into consideration the most favourable reaction conditions from a thermodynamic perspective (reference is made to 2.3.3) a screening of 33 catalyst candidates (Cu, Ag, Pt and Pd based and V_2O_5) for the production of acetic acid from ethanol via the non-oxidative dehydrogenation has been carried out in the screening test set-up (see paragraph 3.2). A few partly oxidative experiments were conducted too.

Cu based catalysts have been used for numerous other purposes, amongst other for the reforming of methanol and ethanol to synthesis gas and for the water gas shift reaction. It is well known from these applications that the aim for stability of the Cu based catalyst in aqueous media at high temperature is an ongoing struggle (*Quincoces et al., 1997, Kamble et al., 1998, Sun et al., 1999*). The Cu catalysts are of

individual characteristics due to the difference in the prevailing operating conditions and the different reactions involved in the syntheses. Optimisation of support types and use of promoters are made to adjust to these differences. As to stability for Cu catalysts there are some trends which may be valid universally. If the specific surface area of the catalyst correlates with the activity of the catalyst (*Ovesen et al., 1996, Askgaard et al., 1995*), common means may be applied to obtain activity and stability for a given catalyst. The attainment of a catalyst which is robust against the loss of Cu surface area is deeply connected to the preparation methods. Highly developed principles have been obtained over the year as an on-going process. Furthermore, another stability aspect, namely the mechanical aspect has been considered alongside. Making use of previously developed Cu based catalyst in the screening is therefore a step-up possibility.

The Cu based catalyst samples were reduced in approximately 50% ethanol in nitrogen at 250°C for 30 min before carrying out the screening test. For example the red Cu spinel catalyst (calcined at 850°C) turned black during this treatment as a visual indication of that the reduction took place. Typically feed ratios of 50/50 ethanol:water (mol/mol) have been used in the temperature range 280-320°C. Substantially higher temperatures have been tried, if no activity was found at these. All experiments were conducted at atmospheric pressure.

The condensates were sampled and analysed by GC-MS. No response factors were available during the screening, which means that the results were comparable only given the same test conditions and no quantitative compositions were attained. Side-product selectivities were evaluated based on the numbers of side-product peaks and their GC area%.

4.4 Catalyst preparations

As discussed above, some industrial Cu based methanol reforming and water gas shift catalysts were readily available. But further Cu catalyst variations were prepared by impregnation, precipitation according to new recipes or by simple means such as decomposing pellets of $CuCO_3$ powder (mixed with 4wt% graphite) *in situ*, cutting Cu thread etc.

A Raney Cu catalyst “hardware” was prepared by pouring and smearing a suspension of Raney Cu on a mat of pyrex wool manually felted, which was then rolled and loaded into the reactor, where it was allowed to dry in nitrogen gas at 150°C for one hour or more (until no droplets of condensing water appeared in the condenser system anymore).

4.4.1 Impregnation method

In some cases the promotion of existing catalysts with an additional metal, for example Ag or Pt, was found worthwhile pursuing and in some cases Cu was impregnated on a prepared carrier.

In all cases the impregnations took place according to the incipient wetness method, wherein the unpromoted catalyst or catalyst carrier, having a given and known absorption capacity (pore volume), is subjected to the absorption of a corresponding

volume of liquid, containing the desired amount of the catalytic or promoter metal, into its pores.

4.4.2 Precipitation method

For the later investigation of down-selected catalysts a series of Cu/Al_2O_3 with different Cu contents was produced and a series of new Cu/SiO_2 catalyst was prepared on the basis of several silica precursors after a switch of the catalyst support. All the catalysts prepared by means of precipitation methods were produced with the professional assistance from a technician skilled in such methods as this requires the knowledge of a specialist.

4.4.2.1 Cu/Al_2O_3 catalyst

The CuO/Al_2O_3 catalysts had been prepared by means of co-precipitation of $Cu(NO_3)_2$ with K_2CO_3 and $KAlO_2$ to form copper aluminiumhydroxycarbonate which when isolated as a powder upon heating produces CuO/Al_2O_3. The co-precipitation principle is well-known and widely described in more detail in literature for example by *Kumar et al. (2008), Slaa et al. (1992), and Gusi et al. (1986).* The CuO/Al_2O_3 catalyst was available as cylindrical pellets 6 mm x 6 mm, pre-calcined at 550°C.

Two further variations of the copper catalyst were obtained by calcining a portion of the CuO/Al_2O_3 pellets at two different temperatures, 850 and 1100°C for 4 h (2 h ramping +2 h holding time). By the calcining to 850 and 1100°C the colour of the catalyst changed to reddish brown, indicative of a degree of transition of the CuO and Al_2O_3 phases into $CuAl_2O_4$, or Cu(II) spinel (*Susnitzky et al., 1991)*. By means of XRPD the actual phases were established. Figure 4-1 shows the XRPD patterns of the catalysts with indication of the recognisable peaks characteristic of CuO and $CuAl_2O_4$ respectively.
Traces of spinel were found on the sample calcined at 550°C. Upon reduction of either CuO/Al_2O_3 or $CuAl_2O_4$ it is presumed that Cu/Al_2O_3 is obtained.

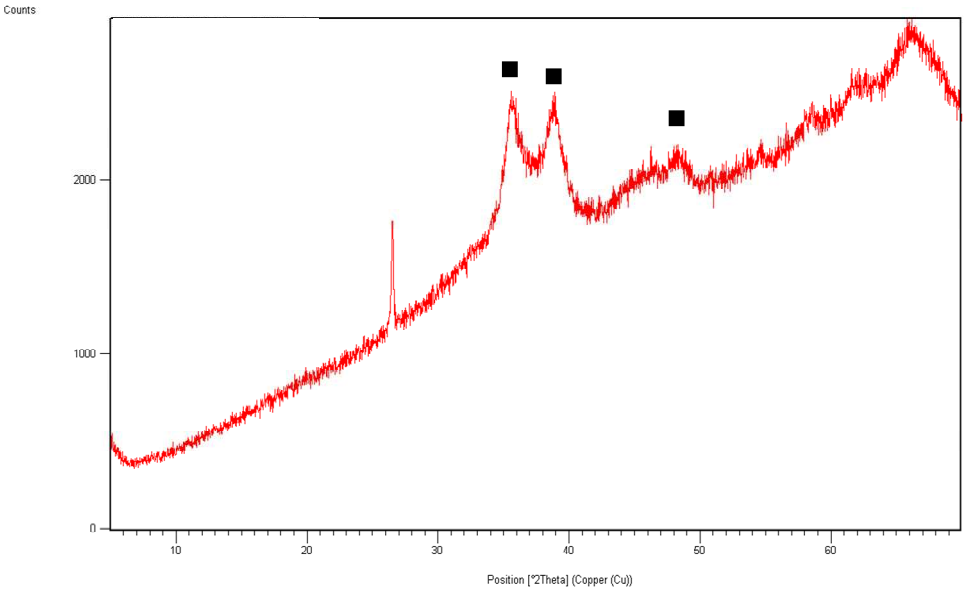

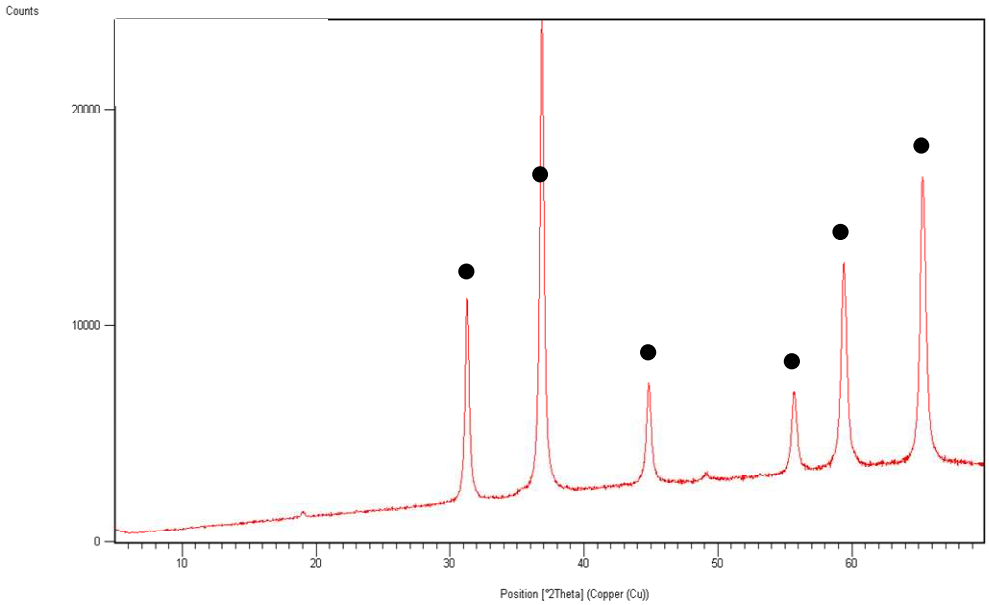

Figure 4-1: Powder X-ray diffraction patterns of the CuO/Al_2O_3 pellets. Upper: calcined at 550°C; lower: calcined at 850°C. Peak identification: (■) CuO, (●) $CuAl_2O_4$.

4.4.2.2 Cu/SiO_2 catalyst

The Cu/SiO_2 catalyst was prepared by precipitation of $Cu(NO_3)_2$ with K_2CO_3 in a suspension of high surface area silica (specific surface area= 348m^2/g) at pH 6.0. The precipitate was ripened at 60°C for one hour, then filtered and washed with hot water until the filtrate had conductivity less than 0.1 mS/cm, and finally it was dried at 80°C. The resulting catalyst powder was mixed with graphite and pelletised to obtain cylindrical pellets which were then calcined at 350°C, obtaining thereby so-called Cu/SiO_2 A catalyst. It was attempted to improve the volume based high surface area (HAS) silica based catalyst by adding water to the calcined catalyst powder before pelletising it (Cu/SiO_2 B catalyst). Indeed a higher density of the catalyst pellet was obtained for the B version (1.85 g/cm^3), but the activity of the pellet showed to be inferior to the previous preparation.

4.5 Results of catalyst screening

The catalysts tested may be divided into the following main groups: Cu, Cu based, Ag, Pt, Pd, V_2O_5 on supports, and supports without active metals. The exhaustive list may be found in Appendix D.1. For the broad group of Cu based catalyst tested, for example ZnO supported, it has been found that most of these lack either mechanical stability/strength or product selectivity toward the desired products. The mechanical stability was evaluated by visual inspection and by squeezing the pellets manually by a pincer after the test, during the screening phase.
The activities of the catalysts were compared semi-quantitatively by running the tests at as similar conditions as possible, i.e. as to amount of catalyst loaded and the operating temperature (see paragraph 3.2), and studying the area% of acetic acid obtained on

the respective GC-MS chromatogram and mass spectra. In short the main results for the Cu based catalysts are summarised in below Table 4-1.

For most of the Cu based catalysts both a dry ethanol and a 50/50 ethanol:water molar mixture was fed over the catalyst. In all cases it was found that the selectivity (qualitatively estimated through the number of side-product peaks identified by means of MS) to the desired products, including acetaldehyde and ethyl acetate, increased tremendously, when co-feeding water. The characteristics listed for the catalysts in Table 4-1 apply for the feeding of a 50/50 ethanol:water mixture at a LHSV of 3 ml/g·h.

Table 4-1: A survey of the acetic acid activity characteristics of a selection of the Cu catalysts tested. Only qualitative/semi-quantitative results were obtained during the screening, as GC response factors were not yet calibrated. Letting the highest activity be designated as high activity, medium activity was about half this value and low activity about 10-20% of the high activity acetic acid area%. High selectivity was judged when only a small peak of butanol appeared, good selectivity, when also butyric acid was seen, and reasonable selectivity, if more peaks emerged.

Cu formulation	Acetic acid activity, catalyst characteristics
Cu Chips	No acetic acid activity. Dehydrogenation at t>500°C
$CuCO_3$	Low acetic acid activity. High selectivity.
Raney Cu	Medium acetic acid activity. High selectivity.
Cu/ZnO	Medium-high acetic acid activity. Low mechanical stability. Reasonable selectivity
Cu/SiO_2	Medium-high acetic acid activity. High mechanical stability. High selectivity.
Cu/Cr_2O_3	Medium-high acetic acid activity. High mechanical stability. Good selectivity.
Cu/Al_2O_3 (Cu spinel)	High acetic acid activity. High mechanical stability. Good selectivity. Successful autothermal dehydrogenation experiment.

Remarkably, in the light of its rough principle of preparation the Raney Cu showed an impressive activity toward acetic acid, and the selectivity of acetic acid over C_{4+} components was very high – literally no side-product peaks were seen. Decomposed $CuCO_3$ (presumably almost pure Cu under operation) shows a low activity. *Iwasa et al. (1991)* ascribes the dehydrogenation activity of ethanol to metallic Cu, based on observations for a Cu/SiO_2 catalyst. We also find that pure Cu catalyses the dehydrogenation reaction with a significant activity.

The most promising catalysts, selected on the criteria of mechanical stability, selectivity and activity, for the production of acetic acid from ethanol/water have been found to be Cu/Al_2O_3, Cu/Cr_2O_3, Cu/ZnO and Cu/SiO_2, which remarkably all are Cu based catalysts. By means of these simple tests the mechanical stability of the ZnO

containing catalysts was found to be low. As to the Cu/Cr_2O_3 catalyst its risk of Cr (VI) contamination in the working and/or surrounding environment excludes this candidate under societal concerns. The best candidates remaining from this down-selection are Cu on alumina with an activity higher than Cu on silica.

4.6 Quantification of conversion over Cu on alumina

It was found that the Cu on alumina, calcined at 550, 850°C had similar activities, whereas the activity of the sample calcined at 1100°C had a significantly lower activity. The catalyst calcined at 850°C showed better selectivity as compared to the sample calcined at 550°C. The degrees of conversion of ethanol in a 50/50 ethanol:water mixture (ρ=0.857 g/ml, x_{EtOH}=71.8wt%) obtained for 10 g of the Cu on alumina catalyst calcined at 850°C (thence transformed to $CuAl_2O_4$) at LHSV=3ml/(g·h) were as follows: 55.8% to acetaldehyde, 4.1% to ethyl acetate, and 18.5% to acetic acid. In order to obtain the best possible mass balance the experiment was carried out with extra attention paid to avoiding leaks and with an acetone/dry ice mixture (t= -77°C) in the cooling basin, effectively cooling and actually freezing the condensate. Based on the above feeding rate and density the STY_{HOAc} was calculated to 0.35 kg/(kg·h). The calculation was made on the basis of the condensate composition found by iterative analysis of standard mixtures and the principle described in paragraph 3.5.2

The promotion of the $CuAl_2O_4$ with Ag and K which were mentioned in literature did not show any positive effect on neither the activity nor the selectivity of the Cu spinel catalyst calcined at 850°C.

4.7 Process route combination

Each of the oxidative and non-oxidative dehydrogenation of ethanol routes has draw-backs as mentioned above (see paragraph 2.4). Some of these draw-backs may be overcome if it is possible to combine the two reactions. Especially, if the need for heat input to conduct the non-oxidative reaction is outbalanced by the heat evolved through the oxidative dehydrogenation.

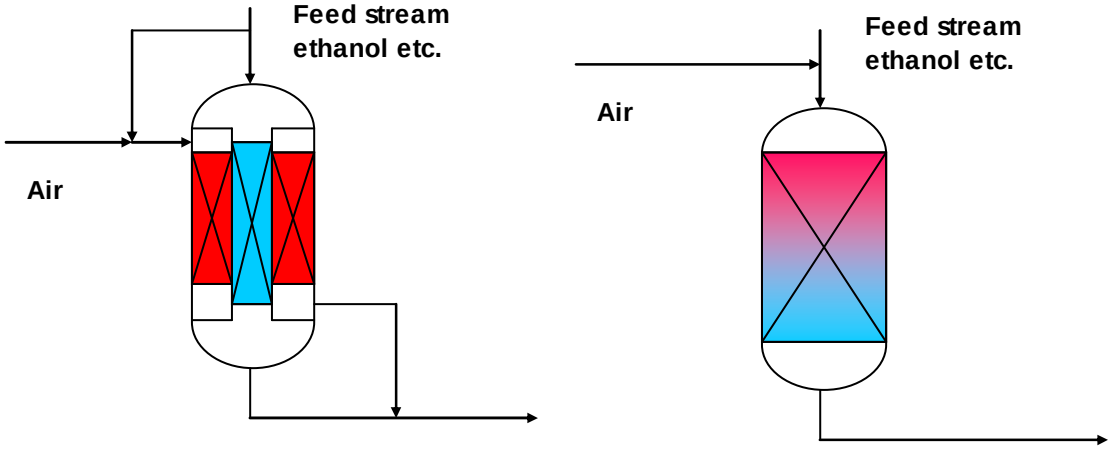

Figure 4-2: Sketches of the indirect and direct combination of oxidative (red) and non-oxidative (blue) dehydrogenation. For the direct combination the order of succession of the oxidative and non-oxidative synthesis is indicative.

This can be done indirectly by exchanging heat developed from the oxidative synthesis by whichever catalyst active in this reaction but it might also be combined directly by, if workable, oxidising product hydrogen from the non-oxidative dehydrogenation to water, also providing for a balanced overall heat of reaction (see Figure 4-2). If X designates the fraction of ethanol which is converted by the oxidative route, the relative overall reaction schemes of the reactions lead to the overall total in
Scheme 4-1:

$$(1\text{-}X)\ CH_3CH_2OH + (1\text{-}X)\ H_2O = (1\text{-}X)\ CH_3COOH + (2\text{-}2X)\ H_2$$
$$X\ CH_3CH_2OH + X\ O_2 = X\ CH_3COOH + X\ H_2O$$
$$CH_3CH_2OH + H_2O + X\ O_2 + 2X\ H_2 = CH_3COOH + 2\ H_2 + 2X\ H_2O$$

Scheme 4-1: Partly oxidative dehydrogenation of ethanol. Part of the ethanol is dehydrogenated oxidatively.

Or in a rearranged form it may be formulated as in below
Scheme 4-2 :

$$CH_3CH_2OH + H_2O = CH_3COOH + 2H_2$$
$$2X\ H_2 + X\ O_2 = 2X\ H_2O$$
$$CH_3CH_2OH + H_2O + X\ O_2 + 2X\ H_2 = CH_3COOH + 2\ H_2 + 2X\ H_2O$$

Scheme 4-2: Partly oxidative dehydrogenation of ethanol. Part of the hydrogen is combusted.

As can be seen from above reaction schemes the stoichiometric ratio of 1 mol ethanol needed to balance (1-2X) mol water in the feed increases, when increasing X.
Furthermore according to Scheme 4-2 combining the non-oxidative route with the oxidative one may be described as a non-oxidative dehydrogenation with the additional oxidation of a fraction of the hydrogen produced. The fraction $X= O_2/ CH_3CH_2OH_{total}$ is set by the relative amount of oxygen added. The catalytic oxidation of hydrogen takes place involving adsorbed atomic hydrogen indistinguishable from either set of elementary reactions of the oxidative or non-oxidative paths, implying that the oxidative dehydrogenation may be conducted in parallel on the surface of a non-oxidative dehydrogenation catalyst if hydrogen may be oxidised on the same surface at reaction conditions without deteriorating the catalyst.

It may be envisioned also that the oxygen or air co-fed is beneficially added in stages in the direct combination (see Figure 4-3). It may also be advantageous to introduce a second catalyst capable of oxidising hydrogen selectively.

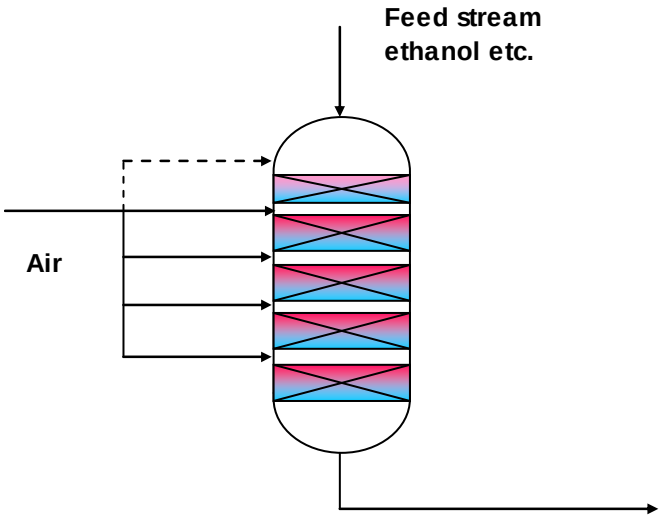

Figure 4-3: In the staged direct combination the individual catalyst beds may beneficially comprise a catalyst selective in the oxidation of hydrogen followed by a dehydrogenation catalyst.

4.7.1 Experimental evidence for route combination

A screening test employing Cu supported on alumina as catalyst confirmed the possible combination of the non-oxidative and the oxidative dehydrogenation reaction. The process aspects and the patentability are further discussed in paragraph 4.8.2.

As it appears, advantages may be obtained by conducting the dehydrogenation in an autothermal mode, for example the benefits of a thermoneutral process is that a cheaper reactor type may be applied, and that steam or another source of heat need not be provided for the firing of the reactor (as in the endothermic dehydrogenation process), while a certain amount of hydrogen co-production is maintained.

The potential of the Cu spinel catalyst as an autothermal catalyst was tested in the screening set-up (reference is made to 3.2). In this experiment special attention was paid to avoiding leakage in the junctions between the individual glass parts in order to be able to best possible establish a mass balance in a set-up which by nature is not well suited for mass balances.

10 g of Cu spinel-850 was loaded into the screening reactor (see paragraph 3.2), and the catalyst was reduced at 250°C for 30 min by means of ethanol (0.5 ml/min) diluted in a nitrogen carrier gas (300 ml/min). The temperature of the oven was set to 320°C and the condensate receiver was cooled with dry ice and acetone. A feed mixture containing 50/45/5 of ethanol:water:O_2 (the oxygen provided *in situ* by decomposing H_2O_2) was introduced to the reactor and the thermocouple reading was followed until steady operation was achieved. The feed composition corresponds to approximately 90% non-oxidative and 10% oxidative stoichiometry given full conversion of ethanol. After 20 min of steady operation the receiver was changed, and the gas bag valve was opened in order to allow the gas phase from the condenser to be collected. The starting time of sampling was noted. After 16 min of sampling the condenser was changed and plugged, the gas bag closed after 13 min of sampling. The mass of the condensate was calculated as the difference of the receiver with and without the

condensate sampled. The gas flow rate at the end of sampling time was measured. The flow rate varied somewhat.

The condensate from the receiver was analysed by GC-MS. At this time a calibration of the GC for the components in the sample was not made yet. Accordingly, in order to find the composition of the condensate iterative adjustments of standard solutions were made to match the GC area%s of the condensate obtained for acetaldehyde, ethyl acetate, ethanol, water, butanol and acetic acid,

Figure 4-4 shows the experimental set-up used for the mass balance experiment screening tests.

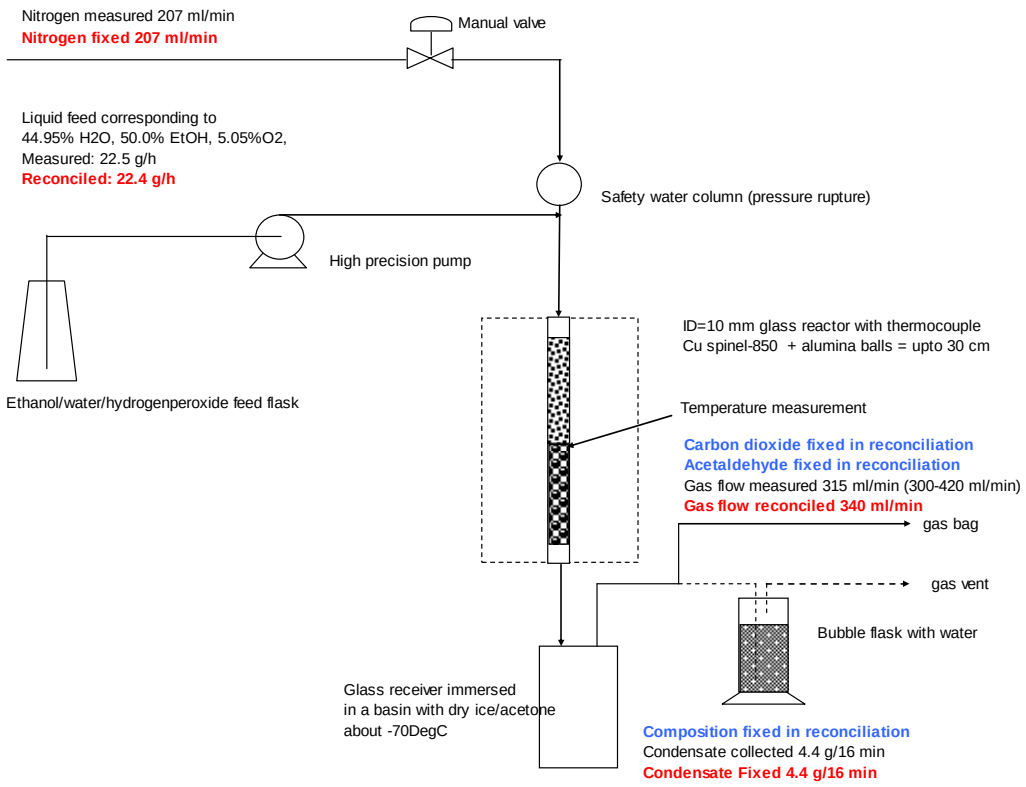

Figure 4-4: The experimental set-up used for the mass balance experiment on autothermal dehydrogenation of ethanol to acetic acid. A thermocouple was installed during loading of the catalyst, being placed in the lower half of the catalyst bed.

Based on the feed composition a simulation calculation was set up, reconciling the feed rate of the ethanol mixture and the total gas flow from the receiver, while fixing the condensate rate (precise) and the nitrogen flow rate (constant). The overall mass balance was 97% (out/in).

In the simulation calculation, a fraction of the ethanol was allowed to react according to the parasitic total oxidation reaction (see Scheme 2-4). Thus depending on the degree of the parasitic full oxidation taking place, different levels of CO_2 would be found in the gas phase.

Figure 4-5 shows the concentration of CO_2 that would be found in the gas phase taken that a certain fraction of the oxygen present is converted to CO_2 rather than dehydrogenating ethanol to acetic acid according to Scheme 4-1.

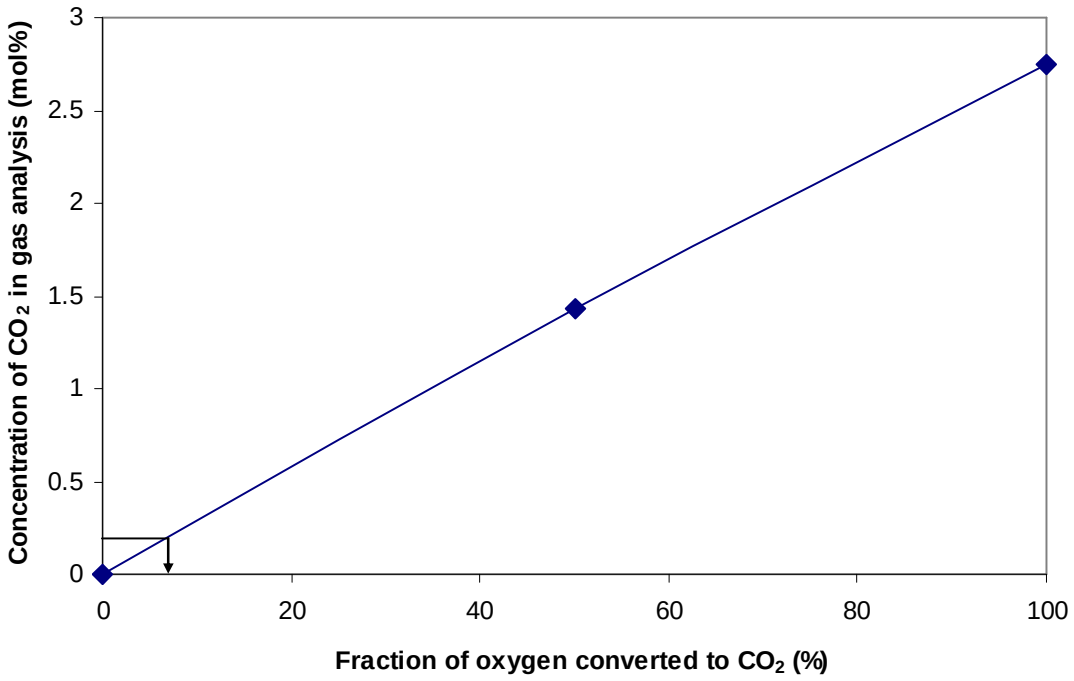

Figure 4-5: Calculated CO_2 in gas analysis assuming different degrees of parasitic full oxidation of ethanol. The degree is expressed as the fraction% of oxygen oxidising ethanol to CO_2.

By GC it was found that the CO_2 concentration in the gas phase from the receiver was about 0.25%. According to the graph above the corresponding fraction of oxygen converted to CO_2 is less than 10%. As to parasitic ethanol consumption, only about 10% of the ethanol conversion takes place via an oxidative route, and with the stoichiometry of oxygen to ethanol given for the full oxidation, less than 0.3% of the ethanol is lost via full oxidation reaction in this example, which was an encouraging result. Apart from this important selectivity result the degree of ethanol conversion to acetaldehyde, acetic acid, ethyl acetate and butanol were similar (but higher) than the conversions calculated for the non-oxidative conversion of ethanol over Cu spinel-850 (see paragraph 4.6).

4.8 Process layouts based on experiments

In the light of the above finding, several process schemes have been developed. In below paragraphs the initial process considerations in connection with the experimental screening results are presented.

4.8.1 Non-oxidative dehydrogenation

In the first round it was anticipated that the separation of unconverted intermediates from acetic acid may be conducted by simple distillation. Figure 4-6 shows this first approach for a bio-ethanol based process scheme. A preliminary GIPS mass and heat balance calculation was set up for a 300,000 MTPY acetic acid plant based on this assumption. The individual conversion approaches for the reactions in Scheme 3-1

found experimentally for Cu spinel-850 (paragraph 4.6) were used, lumping the side-products in the butanol equation.

The process flow diagram corresponding to this calculation may be found in Appendix D.2.

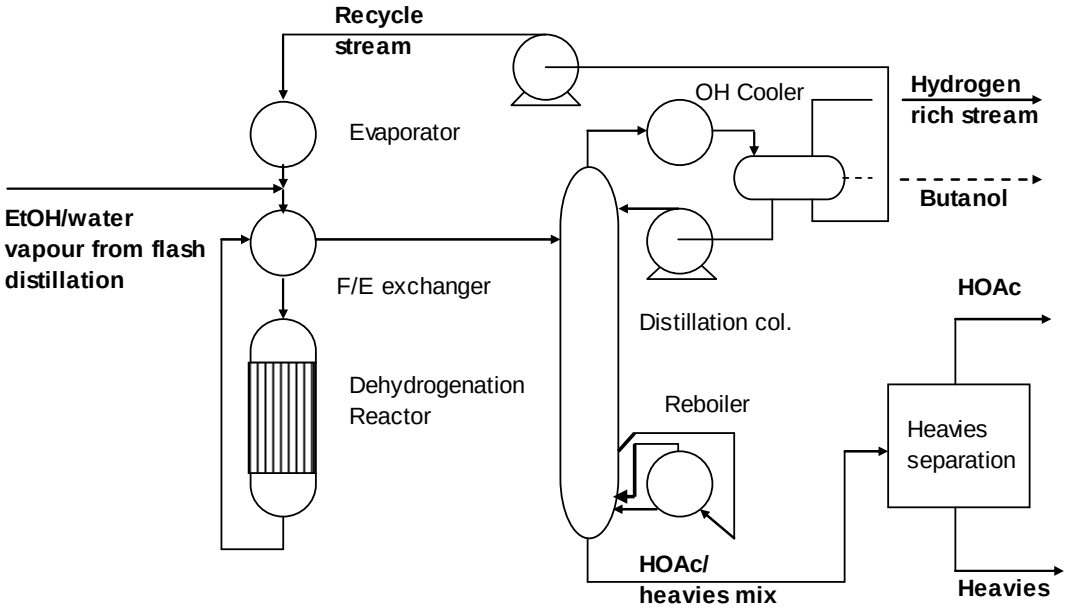

Figure 4-6: An acetic acid process based on import of aqueous ethanol being dehydrogenated non-oxidatively in a heated reactor. The unconverted ethanol and intermediate components are recycled to the reactor, while butanol is removed somehow in a side draw. Heavies are removed from acetic acid in a second distillation column.

As it became clear during the closing of the recycle balance, the level of the water concentration in the feed + recycle stream to the reactor may be set different from but not independently of the feed. During the operation of the acetic acid plant the ethanol to water ratio in the feed stream may be varied either by the extra addition of MU water or the use of multiple side draws from the ethanol distillation. In a process where the consumption of water depends on the degree of conversion of ethanol to side-products, and where water may be extracted in side-product removal the water to ethanol feed ratio must be adjusted too. The control of a constant water balance can be achieved by measuring the water concentration in the recycle stream and adjusting the ethanol to water ratio in the make-up stream.

A patent application has been filed for the control of the water concentration in the reaction zone by measuring the water concentration in the recycle stream and adjusting the ethanol to water ratio in the feed stream accordingly. The application filed may be found in Appendix D.3. An economic evaluation of the corresponding process flow diagram of this process scheme was made, see paragraph 4.11.

4.8.2 Partly oxidative dehydrogenation

In a next version of a process scheme, the partly oxidative dehydrogenation (reference is made to paragraph 4.7, Figure 4-3) was presented based on the overall reaction equation according to Scheme 4-2. A GIPS mass balance calculation was established

in line with the previous. While maintaining the previous approaches to equilibrium for the non-oxidative dehydrogenation (confer paragraph 4.7.1), the degree of the oxidative dehydrogenation was adjusted to meet an adiabatic temperature rise of 15°C. Accordingly, the X was found to be 0.11 (see Scheme 4-2). The small but still significant temperature rise was targeted in order to make cheaper heat integration in the form of a feed/effluent heat exchanger taking the feed + recycle right to the inlet temperature of 300°C by cooling the 315°C reactor effluent. The specific point of oxygen or air addition was not reflected in the calculation, but a staged addition of oxygen/air is the precautious solution, precluding that a fast kinetic for the oxidative reaction as compared to the non-oxidative will lead to a rapid escalation of the temperature in the top of the reactor followed by a temperature decrease (see Figure 4-7).

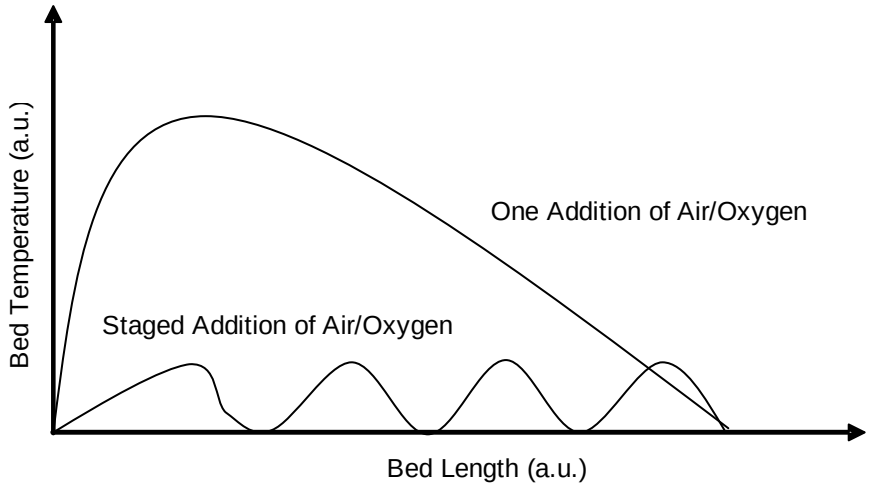

Figure 4-7: One addition of air/oxygen could lead to the temperature excursion (with a risk of catalyst deactivation) whereas the staged addition has a more moderate temperature rise per addition.

Figure 4-8 shows the process scheme for the partly oxidative dehydrogenation of ethanol to acetic acid. Comparing the characteristics of the partly oxidative dehydrogenation process with those of the oxidative and the non-oxidative dehydrogenation routes listed in Table 2-1, the partly oxidative dehydrogenation immediately may help overcome the few drawbacks of the non-oxidative dehydrogenation route.

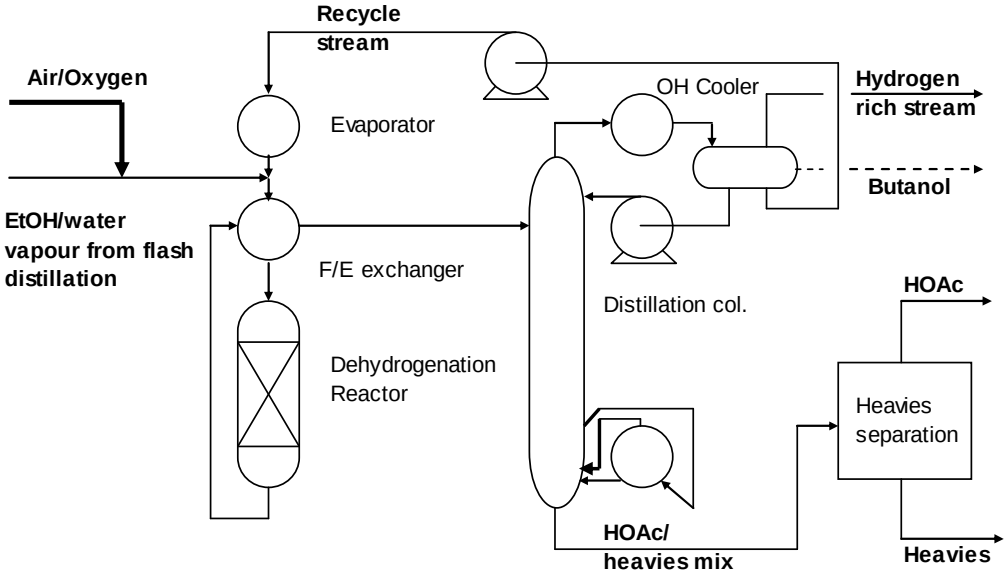

Figure 4-8: The partly oxidative dehydrogenation of ethanol to acetic acid. The amount of oxygen fed to the process is adjusted to obtain a moderate but positive temperature increase over an adiabatic reactor. The separation takes place like in Figure 4-6.

Considering the patentability of the partly oxidative dehydrogenation process, having the characteristics of a close to thermoneutral conversion, with the closest prior art, the oxidative processes described by *Marcinkowsky* (1980) and *Haner (1933)* are the most relevant. However, in the patent to *Marcinkowsky* (1980) the oxygen:ethanol molar ratio mentioned is 0.1 to 0.5. Further, a water content in the ethanol feed of 8.29 wt% is mentioned corresponding to 18.8 mol%. In case a feed of 81.2/18.8 ethanol:water is co-fed with 0.1-0.5 mol O_2 per mol ethanol, the feed mixture will be deficient in water in the O_2 to ethanol molar ratio range 0.1-0.25, relevant to the thermoneutral process, owing to the overall reaction Scheme 4-2. In the patent granted to *Haner (1933)* it is suggested to add an amount of water equalling in weight the ethanol vapour corresponding to 28.2/71.8 ethanol:water, and further to add air in an amount corresponding to 0.73 mol O_2 per mol ethanol. By feeding such a high ratio of oxygen to ethanol, surely the process is far from thermoneutral. It may also be gathered from patent description that in order to maintain the operating temperature at 325°C the activated copper oxide catalyst is loaded into a bath of liquid sodium and potassium nitrate. Therefore the patent by *Haner (1933)* does not describe a thermoneutral process for the conversion of ethanol to acetic acid.

A patent application has been filed (see Appendix D.4) on the found assets of the partly oxidative dehydrogenation.

4.8.3 Butanol side-product

Butanol and other side-products were during screening produced with a yield of about 1%. The challenge of 1-butanol as a side-product is that it boils very closely to acetic acid and they form an azeotrope. The possibilities to circumvent this problem are to either develop a catalyst which does not produce butanol or to be able to remove it. In order to obtain an acetic acid (99.85% which is the technical grade) of adequate purity the need for the removal of butanol must be foreseen. The possibility of a membrane separation of butanol was looked for. In fact the selective removal of butanol by pervaporation from a ternary mixture of butanol, water, butyl acetate was found by *Liu*

et al. (2005). However, it was estimated that the technology is too immature for its application in a close future industrial scenario.

Another method of removing the butanol was searched for via the reaction of butanol with acetic acid to butyl acetate, as this compound is considerably higher-boiling than water, and does not form an azeotrope with acetic acid. It was found that passing a 5% butanol in 95% acetic acid feed mixture at a LWHSV=3g/(g·h) over HZSM-5 as a catalyst (120°C, atmospheric pressure) in the screening set-up literally removed the butanol. The conversion to butyl acetate was quantitative according to GCMS. The removal of butanol by means of its conversion to butyl acetate is efficiently achieved in compositions where water is not present in large concentration, due to the *in situ* removal of product water in the distillation column. Water is co-produced according to the ester equilibrium as shown in Scheme 4-3:

$$C_4H_9OH + CH_3COOH \rightleftharpoons CH_3COOC_4H_9 + H_2O$$

Scheme 4-3: Butyl acetate formation from butanol and acetic acid.

The best placement of an efficient conversion of butanol with acetic acid would be in the bottom part of the distillation column, separating the acetic acid and heavy compounds from the recycle compounds (see Figure 4-9).

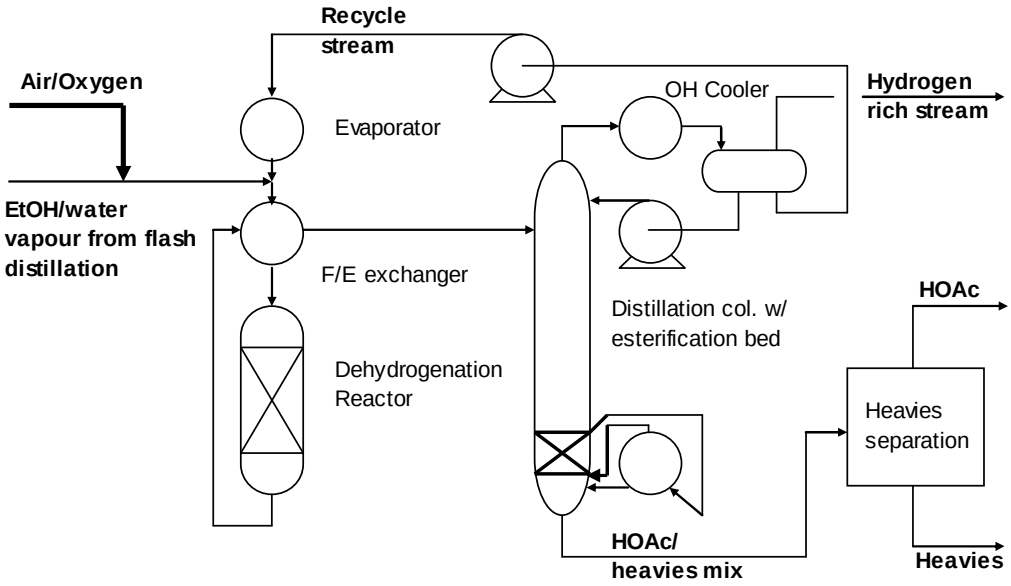

Figure 4-9: The butanol side-product of the partly oxidative dehydrogenation of ethanol to acetic acid is converted in a reactive distillation bed, converting butanol to butyl acetate.

The product water is removed from the reaction zone to the stages above, as it boils at a lower temperature than acetic acid and butyl acetate.

4.9 Hydrogen co-product

Clearly, the separation of co-product hydrogen concurrently with the recovery of the recycle compounds highly increases the diameter of the distillation column. Removal prior to the distillation column could be managed by means of a membrane (above the dew point).

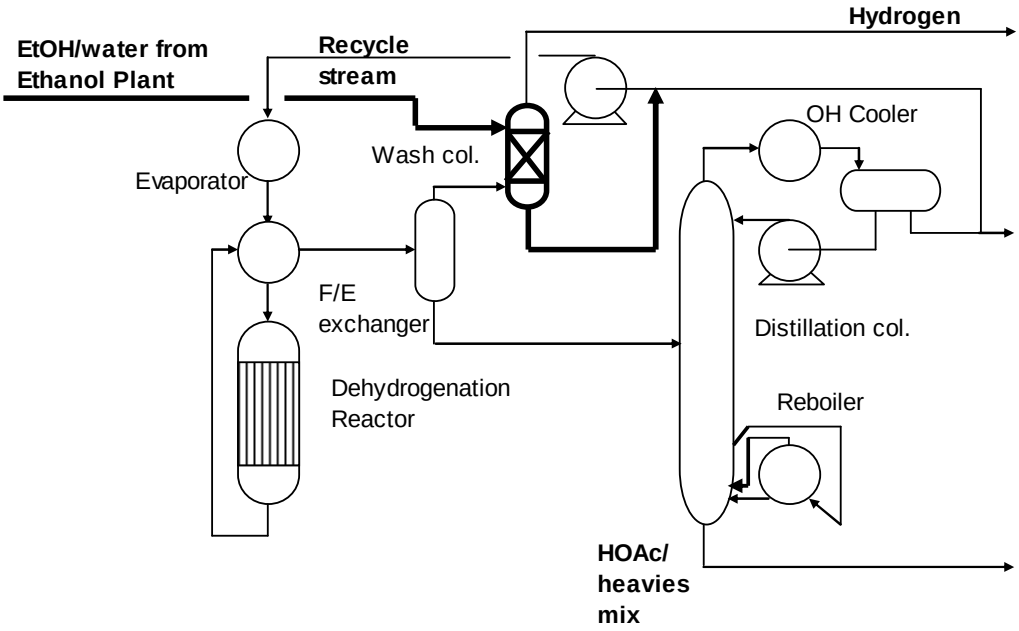

Figure 4-10: The non-oxidative dehydrogenation process with a separation of hydrogen prior to the distillation. The ethanol feed is used as solvent for the absorption of acetaldehyde otherwise lost in the hydrogen.

However, a simpler solution may be to separate the hydrogen from the reactor effluent in a liquid and gas phase separator. The gas phase contains apart from hydrogen a lot of highly volatile acetaldehyde, which as a product precursor must be recovered. This may be achieved in a wash column, where the ethanol/water feed stream from the ethanol plant is used as absorbent. Figure 4-10 shows how the co-product hydrogen may be recovered from the reactor effluent prior to the first distillation column. If the hydrogen is regarded as a co-product (whose value has to materialise) it may be required to further purify this stream. Hydrogen is a versatile product which may be used for hydrogenation of various compounds, for example as a fuel for fuel cells, for the selective removal of impurities such as acids and aldehydes, in hydrocracking, or for the adjustment of synthesis gas compositions. Thinking the ethanol plant and the acetic acid plant add-on into a larger complex, there could be numerous uses for the hydrogen.

4.10 Process integration with VAM

Production of vinyl acetate monomer (VAM) is one of the major uses for acetic acid. VAM is being produced industrially by oxidising acetic acid with ethylene in the presence of oxygen. Being put into a broader perspective the ethanol to acetic acid process may be integrated with a process converting ethanol to ethylene, in common providing the feedstocks for a VAM synthesis. The possibilities of making integrations of units, heat or compositions were investigated. Characteristics of the state-of-the-art VAM production are that it takes place over a Pt based catalyst at a relatively low temperature (<200°C). Due to the relatively low operating temperature the heat evolved during the synthesis may not be fully utilised in the recovery section of the VAM plant, leaving a need for import of steam at higher temperature, while at the same time exporting low value steam. By combining the VAM plant with the plant units of acetic acid conducted with a balanced degree of oxidation and an ethanol dehydration plant

for the provision of ethylene for the VAM process, an optimal exchange of heat may be obtained (see Figure 4-11).

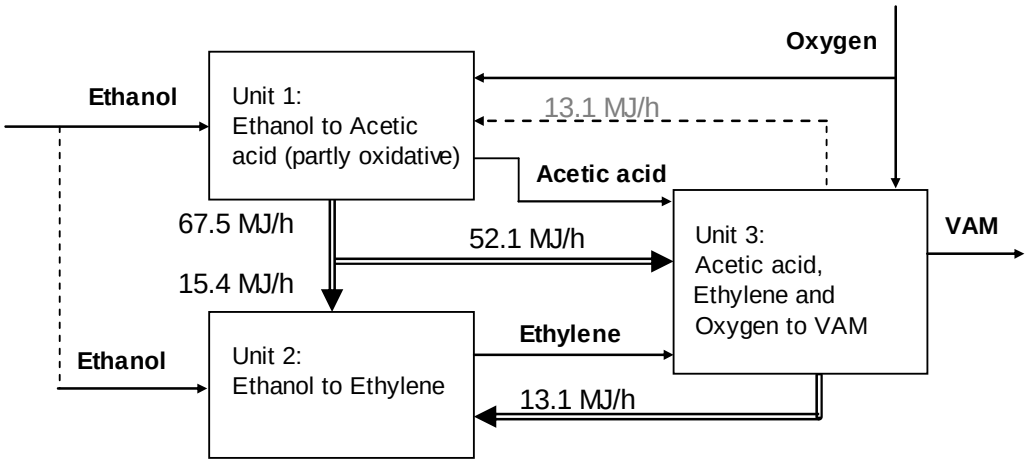

Figure 4-11: Favourable heat integration may be obtained when integrating the partly oxidative acetic acid process (Unit 1) with the ethylene process (Unit 2) and the VAM process (Unit 3).

A patent application has been filed to protect this invention. Further details as to how the integration is foreseen may be found in Appendix D.5 in the patent application concerning this invention.

4.11 Production price comparison

In order to assess the competitiveness of the ethanol to acetic acid route an economic analysis of the acetic acid production price is needed comparing it to the conventional route. The approach is to compare a best-case conventional route with a non-optimistic bio-route. Accordingly the most robust version of the ethanol routes, namely the non-oxidative, was selected for further evaluation and comparison to the conventional.

Based on the GIPS heat and mass balance program simulation of the non-oxidative dehydrogenation of ethanol to acetic acid, including a simplified distillation calculation, a process flow diagram with a capacity of 300,000 MTPY HOAc was prepared (see Appendix D.2). Hereby the energy consumptions and cooling water consumptions of the non-oxidative dehydrogenation process were estimated. As a conservative approach the yield of acetic acid from ethanol was set to 95%, and furthermore a STY_{HOAc}=0.5 kg/(kg·h) as found for the Cu spinel catalyst (see Figure 6-6). In Appendix D.6 a process description of the process shown in Appendix D.2 and the corresponding key figures are presented. The key figures summarise the combined feed and utility consumption figures and the investment cost estimated for the calculation of the acetic acid production price. A credit for the hydrogen co-produced has not been assumed as a conservative approach.

The corn based ethanol market price is presently at 500USD/MT, and the required selling price for the 2nd generation ethanol may be foreseen to approach this value soon, making the 2nd generation ethanol competitive.

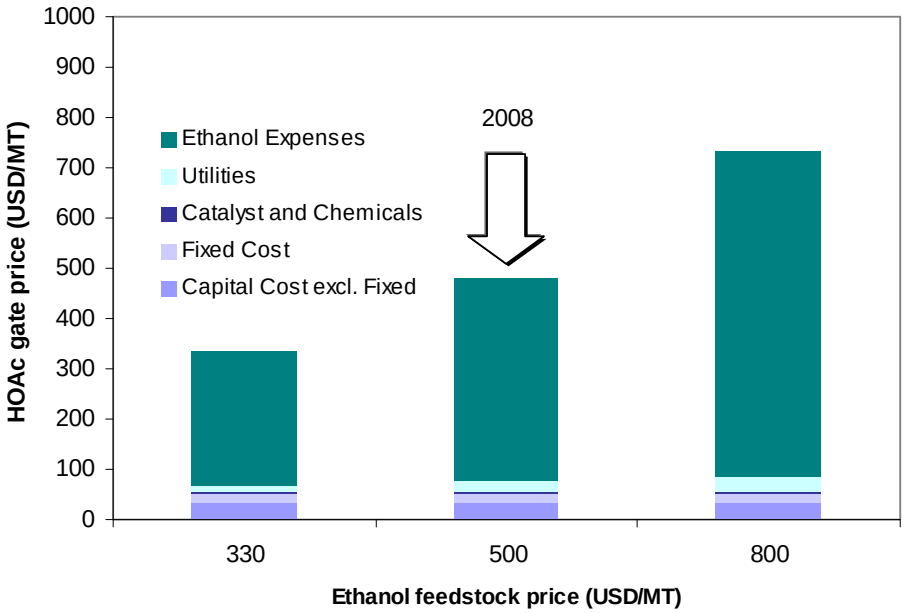

Figure 4-12: Acetic acid gate price at 3 ethanol feedstock prices, assuming 95% yield. The acetic acid gate price highly depends on the ethanol feedstock price. The natural gas for fuel is assumed available at a low price, 1 USD/GJ.

Figure 4-12 shows the calculated gate acetic acid price based on the long term optimistic ethanol market price estimate of 330 USD/MT, the present being 500 USD/MT and one of 800 USD/MT, representing a sensitivity scenario of increasing ethanol prices on the back of oil price increments. For comparison to the carbonylation route based acetic acid production price reference is made to paragraph 2.2.1 and Appendix B.1 showing the details of the production price estimation of acetic acid according to the conventional carbonylation route. Both acetic acid production price estimates have been based on a yearly capacity of 300,000 MT, which is 2/3 of the typical current capacity of a conventional acetic acid plant but represents a large plant if based on the bio-ethanol plant capacities of today.

External experts were asked to look closer into the thermodynamics of the distillation section of the process flow diagram of the non-oxidative dehydrogenation route. They evaluated that the thermodynamics of this system is not straight-forward and its elaboration should be halted until the eventual concentrations are known. The butanol may be separated from the product, but the concentrations of acetic acid and butanol in the distillation feed have a high impact on the distillation section layout and the energy consumption. The process flow diagram, but especially the distillation section hereof, is only representing a first version, subject to development.

From the preliminary process flow diagram, the fired energy input is estimated to be 6.3 GJ/MT per MT of acetic acid produced via dehydrogenation of ethanol. With an assumed thermal efficiency of 80% in the steam generation section the total energy input is 7.9 GJ/MT. For comparison the energy input in terms of LHV of natural gas in a stand alone carbonylation based integrated plant totals 7.5 Gcal/MT. The main share of the energy consumption relates to the magnitude of the recycle ratio in the process. A larger degree of conversion per pass in the ethanol-to-acetic acid obviously would improve the specific energy consumption number.

Furthermore, during the specification of the equipment items, the STY has been assumed equal to the start-of-run (SOR) value found for the Cu spinel catalyst. This assumption is preliminary as well firstly because rather an end-of-run (EOR) value should be used for design purposes, but secondly because this value is a premature activity value not having been validated through long term testing. The sensitivity of the acetic acid production price of a doubling of the energy need and a 5 times lower STY_{HOAc} has been investigated, in order to evaluate the risk of basing ourselves on preliminary energy consumption and activity values (see Figure 4-13).

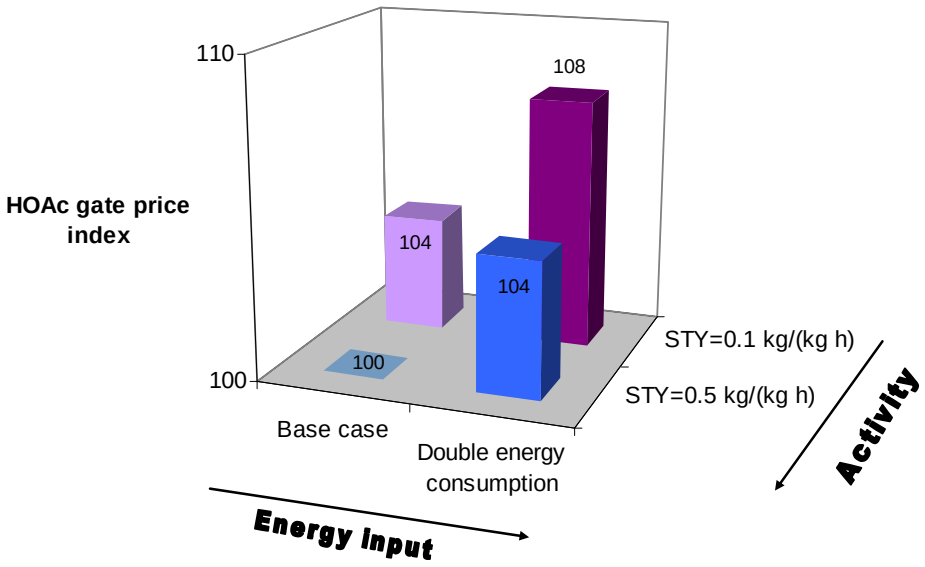

Figure 4-13: Sensitivity of the HOAc gate price index for the non-oxidative dehydrogenation of ethanol to acetic acid with a) a doubling of the energy input, b) an catalyst activity expressed through a STY_{HOAc}=1/5 of the base case STY_{HOAc} , and the combination of a) and b).

It seems the HOAc gate price is rather insensitive to the assumptions on energy and STY made. However, the STY assumed may encounter other constraints related to sound reactor design. Taking 300,000 MTPY as an example and assuming one cylindrical fixed bed reactor as an approximation, an operating pressure of 4 bar, a (R+M)/P=4, a fluid viscosity=0.08 kg/(m·h), a catalyst filling density=1000 kg/m^3 and a pellet size of 5 mm, the following estimation of main reactor dimensions has been made for different STY_{HOAc}s (see Table 4-2).

Table 4-2: Estimate of reactor dimensions. Capacity=300,000 MTPY, 8000 run hours per year, p=4 bar, catalyst filling density=1000 kg/m^3, d_h=5mm.

Calculation value	STY=0.1 kg/(kg·h)	STY=0.2 kg/(kg·h)	STY=0.5 kg/(kg·h)
Reactor diameter (m)	6.9	4.9	4
Reactor height (m)	10	10	6
Re_p	251	499	746
-Δp (bar)	0.2	0.6	1.5

As may be seen a STY_{HOAc}=0.1 kg/(kg·h) results in a Re_p which is far down in the laminar flow regime. But the higher the STY, the higher a Re_p is obtained, being desirable for approaching turbulent fluid properties (Re_p > 1500) in plug flow reactors. Here, the diameter has to be increased for the STY=0.5 kg/(kg·h) in order not to get a too high pressure drop. This sets a limit for the Reynolds number obtainable with a given catalyst shape. For the low catalyst activities corresponding to STY=0.1 and 0.2 kg/(kg·h), a maximum practical bed height of 10m is also limiting. The above calculation is a rough estimate built on assumptions. But it may serve as a guidance as to which level of catalyst activity is acceptable. Herein, and based on the above, the rule-of-thumb applied is that a STY_{HOAc} >0.3 kg/(kg·h) as an SOR catalyst activity, anticipating a EOR activity of 0.2 kg/(kg·h) must be obtained for a catalyst to properly support the conversion of ethanol to acetic acid in an industrial size plant (300,000 MTPY).

Furthermore, a high energy consumption off-sets the low C-factor obtained by utilising a biomass based feedstock. Therefore, irrespective of the low influence of the energy consumption on the gate price of acetic acid a low energy consumption should be aimed at in order to attain highest possible sustainability. Process layouts with higher conversions per pass (as discussed above) could classically be obtained by means of interstage or in situ product removal. Applying the partly oxidative dehydrogenation rather than the mere non-oxidative is also helping increase the conversion, in that the oxidative part of the dehydrogenation is unlimited by equilibrium.

Reverting to the process economy, the 2008 acetic acid market price was 850 USD/MT (see paragraph 1.5.3.1).
As may be seen from the above Figure 4-12, the investment load on the acetic acid production from ethanol is very low. Comparing the acetic acid gate price of the conventional of about 400 USD/MT (see Figure 2-2) with the alternative acetic acid gate price of about 500 USD/MT based on an ethanol unit price of 500USD/MT, the latter immediately seems less attractive. However, the profit margin of 350 USD/MT acetic acid (based on the 2008 market price) is quite high, and due to the far lower investment load for the dehydrogenation route, the ROI becomes much higher for the ethanol-to-acetic acid route over the two most conventional carbonylation processes (reference is made to Figure 2-2). Assuming a long term ethanol price of 330USD/MT the acetic acid gate production price becomes 330 USD/MT, giving a very high ROI. Assuming the ethanol market price increases to 800 USD/MT the economic incentive for making acetic acid from ethanol vanishes.

It may be argued that the production price for aqueous ethanol is lower than the production price for anhydrous ethanol of 500USD/MT, i.e. the above comparison is too conservative. The distillate recovered in a side-stream at the top of the beer column, having an ethanol concentration of 40-45wt% or up to about 24 mol%, is not so far from what may be used in a dehydrogenation process, see Appendix D.2. Due to the heat integration between the pre-heater of the rectifying column producing 94 wt% ethanol and the beer column the net energy saving only approximately corresponds to the rectifying column reboiler and heat inputs minus the condenser and cooler heat output, namely 1.15 GJ/MT ethanol, based on the analysis by *Pfeffer et al. (2007*). As

compared to the total net heat consumption outlined for bio-ethanol production by fermentation and purification the saving of the final rectification and dehydration of ethanol as conducted for the anhydrous motor fuel grade ethanol amounts to less than 15% of the total heat demand in a 2nd generation ethanol plant. Accordingly, it may be estimated that the production price for a 50/50 ethanol:water (mol/mol) 2nd generation bio-ethanol is only 1-4 USD/MT lower than the production price for a 2nd generation anhydrous bio-ethanol if a biomass fuel price of 0.5-3.5 USD/GJ fuel is assumed. The energy consumption in the final drying up to 99.9wt% ethanol is also estimated to be around 1GJ/MT (*Knight et al.*) The savings in energy expenses in production cost by producing hydrous ethanol is thus low, around 1% of the ethanol market price. When, however, anhydrous ethanol is said to be considerably more expensive (*Thomsen et al*., 2007), it may reflect the relatively high investment for drying and feedstock load as compared to operating cost on the ethanol gate and selling prices (see paragraph 1.5.3). For keeping a conservative approach the price of anhydrous ethanol was applied in this study.

The comparison of the gate prices of the conventional route and the ethanol dehydrogenation route is most relevant in the present expanding acetic acid market creating constant need for new acetic acid plants. The comparison will not be pertinent in a stagnant or soft market where the overcapacity of acetic acid production leads to closing down of acetic acid plants and where a large fraction of the plants running are old enough to have been paid down. In this case the production price of the new-comer technology should more or less compete with the production price of the existing technology without the depreciation counted in, and temporarily the ROI could even be reduced to a minimum in order to prevent penetrations of new technology. In this latter case only the ethanol-to-acetic acid technology based on the long-term ethanol price of 330 USD/MT competes with carbonylation plants where both CO and methanol are imported.

4.12 Conclusion

Cu catalysts have been mentioned in literature on ethanol dehydrogenation, both in connection with non-oxidative, oxidative dehydrogenation and in regenerative oxidation. Pure copper (Raney copper and decomposed $CuCO_3$) showed to be active in the dehydrogenation reaction with a high selectivity. A substantial activity in dehydrogenation of ethanol on Cu based catalysts is ascribed to the metallic Cu surface.

After screening a selection of Cu, Ag, Pd, Pt based catalysts under non-oxidative and some under partly oxidative conditions two catalyst candidates for further investigation were found: The Cu/Al_2O_3 catalyst prepared by calcining a co-precipitated mixture of CuO/Al_2O_3 at 850°C for 4 h, and Cu/SiO_2 which however showed a low activity.

Three patent applications were filed to attain intellectual property right over the discoveries that 1) the water concentration in the dehydrogenation process may be controlled in a simple manner by measurement of the recycle stream, 2) the oxidative and the non-oxidative dehydrogenation may be combined in a single partly oxidative conversion step, and 3) the process unit of the partly oxidative dehydrogenation of ethanol to acetic acid, the dehydration of ethanol to ethylene and the conversion of acetic acid with ethylene and oxygen to vinyl acetate monomer may be heat integrated.

Selecting the non-oxidative route as a non-optimistic example of a bio-ethanol to acetic acid process, a preliminary process flow diagram was established and a ±30% cost estimate of a 300,000 MTPY acetic acid plant was prepared. Based on this, the feedstock and utility consumption the estimated present gate price of acetic acid was calculated for varying ethanol feedstock prices (not crediting the value of hydrogen co-produced). Using the 500 USD/MT ethanol price in 2008 the calculated acetic acid gate price of about 500 USD/MT features a good profit as compared to the present acetic acid selling price of 850USD/MT. The present presumably conservative gate price is only marginally higher than when produced from carbonylation of methanol. However, due to the low investments in the ethanol based acetic acid plant the ROI is much higher than in the carbonylation based process.

Largely speaking, the gate price for acetic acid produced from ethanol equals the ethanol feedstock price. Depending on how the ethanol selling price connects to the gasoline price the ethanol based acetic acid gate production price may drop to 330 USD/MT, if an acetic acid plant is built as an add-on. In such case new ethanol based acetic acid plants may even be found to compete with old paid down carbonylation plants. Thus the prospects for ethanol-to-acetic acid plants are favourable on a short term if the market is tight and even more promising on a longer term if the production of 2^{nd} generation ethanol takes the leading role in the transportation fuel market.

Recapitulating, the production of acetic acid from ethanol via the non-oxidative route seems more favourable than the oxidative (see Table 2-1). However, yet more favourable seems the partly oxidative process, allowing for the benefits of an autothermal (slightly exothermic) reactor and the benefits of its possible heat integration with the VAM process. The ideal catalyst for this layout accordingly should be able to withstand such conditions. The Cu on alumina was selected as the primary candidate for the further thorough investigations under the consideration that its lower selectivity may be sought remedied through support adjustments or through process development. In the screening study it showed good conversion under the partly oxidative reaction conditions. Thus experiments investigating catalyst activity, selectivity and stability must comprise operation under partly oxidative conditions in order to seek the full potential of the catalyst from a process angle.

The results of the study on Cu on alumina, including characterisation and catalytic testing, are reported in the next Chapter 5 but also in Chapter 6, where its performance is compared to the secondary catalyst candidate Cu/SiO_2.

Chapter 5 Results for Cu Spinel Catalyst – characterisation and tests

5.1 Introduction

The Cu(II) spinel ($CuAl_2O_4$) catalyst obtained by calcining pellets of CuO/Al_2O_3 for 4 h at 850°C (see paragraph 4.4.2.1), hereinafter the Cu spinel catalyst, had been selected from the ongoing screening experiments as the preferred catalyst for the dehydrogenation of ethanol to acetic acid in the presence of water. The known composition obtained in the batch for the Cu spinel catalyst was close to stoichiometric spinel, with a small excess of alumina: 30.9wt% Cu, 25.3 wt% Al, 0.094 wt% K, balanced by oxygen. The Cu spinel catalyst was tested either as whole pellets being cylinders with the geometry d=h=5 mm or as crushed down catalyst pellets in the 1-1.4 mm sieve fraction.

Subsequent to its identification in the screening set-up, the preferred catalyst was investigated closer under more controlled conditions. Despite its superior activity, a number of problems related to the catalyst arose calling for thorough characterisation and understanding. By nature characterisation techniques often only provide a single piece of information, and complementary techniques are needed in order to support a theory or discard it. In this particular case deactivation was observed for the catalyst under numerous conditions. The causes of the problems were pursued through many different analyses in combination with activity tests, not all conclusive and in agreement. Comparison with literature findings was needed to settle some indicative results. The contents of this chapter reflect this puzzling of information through its many paragraphs. Validation of the partly oxidative dehydrogenation route identified in the previous chapter was sought through closer investigations. The characterisation results have to a large extent been obtained through the co-operation with different experts within the field of characterisation.

The experimental results described and discussed in this chapter have been obtained from the runs in the so-called new test set-up and the stability test set-up (reference is made to 3.3 and 3.4).

5.2 Mechanistic pre-investigations

For the understanding of the reaction path for ethanol conversion to acetic acid (reference is made to Figure 2-5), it was investigated whether acetaldehyde and water as a feed would produce acetic acid over the catalyst. By only feeding acetaldehyde and water, thereby not allowing acetaldehyde to react with ethanol to ethyl acetate (alternative 2), a substantial production of acetic acid will show that the redox reaction between acetaldehyde and water (alternative 1) is a significant route.

The screening set-up (see paragraph 3.2) was used and a 1:1 feed mixture of acetaldehyde and water was fed at a rate of 1 ml/min at 320°C. It was found that the

formation of acetic acid was faster when starting from acetaldehyde and water than when starting from ethanol and water, while no ethyl acetate was formed (as expected). The higher rate of acetic acid formation may be due to the lower acetaldehyde partial pressure under the conditions where ethanol and water is fed. The fact that a high productivity to acetic acid is obtained while no ethyl acetate is formed in the product indicates that the redox reaction between acetaldehyde and water is the predominant route and that the rate determining step has a positive reaction order with respect to acetaldehyde.

5.3 Reduction methods

During the screening experiments the Cu based catalysts were in general reduced by means of feeding ethanol at 250°C for half an hour. From earlier in-house experience it was known that the Cu spinel catalyst was completely reduced when exposed to diluted hydrogen gas (2-5%) during a temperature ramping up to 380°C.

When introducing the improved experimental set-ups, the new test set-up and the stability test set-up, only the stability set-up was on beforehand equipped with the supply of hydrogen. Therefore in a short period the Cu spinel catalyst was reduced either with hydrogen or ethanol, without discriminating between these methods. The hydrogen reduction was standardised by calculating the minimum flow rate of the hydrogen containing reducing gas needed for the reduction of a given amount of catalyst. The basis for the calculation is that Cu is present as CuO before reduction that the reduction starts at temperatures above 150°C, and that a flow rate of 4 times the theoretically needed is calculated and used as the actual reducing gas flow rate.

Assuming that only the phases Al_2O_3 and $CuAl_2O_4$ are present in the unreduced Cu spinel catalyst its composition corresponds to a mixture of 11.8 wt% Al_2O_3 and 88.2 wt% $CuAl_2O_4$ spinel. By XRD it may be seen that apart from the crystalline alumina phase the only other crystalline phase present in the Cu spinel catalyst is a $CuAl_2O_4$ phase (see Figure 4-1). Based on this it may be calculated that a 7.77 % weight loss of the Cu spinel catalyst may be obtained if full reduction occurs.

5.4 Observation of deactivation

The deactivation rate of the catalyst must be low in order to comply with process feasibility. Deactivation may relate to the physical change of the catalyst either in structure or the accessibility of the reactants to the catalyst surface, for example through the plugging of its pore system. More causes of deactivation were observed for the Cu spinel catalyst in the acetic acid synthesis.

5.4.1 Reduction and idle operation

It was soon observed that when shifting from the screening set-up, which was typically operated for 2 h, to the new glass set-up, where operation could be continued for 5-6 hours, the catalyst started to make condensation products determined by GC-MS (accompanied by a yellowing of the condensate) after approximately 5 hours, and after a few days (of 5 hour runs each) the Cu spinel catalyst completely lost its activity. An initial explanation to this behaviour was sought in insufficient preheating or the contamination of the reactor feed. In a first round the inclusion of a steel preheater (steel coil surrounded by heating tape) was tried, which in the next attempt was

replaced by a glass container with alumina balls surrounded by electrical heating tape. But a few experiments with above mentioned modifications had little effect on the fate of the catalyst, which deactivated again within 5 days.

It was furthermore speculated, whether the size of the catalyst had an influence on the reducibility of the catalyst. A crushed 1-1.4mm sieved fraction of catalyst was reduced with ethanol. This also had a beneficial but limited effect on the life time of the catalyst, which increased by 2 days to 7 days of operation before a yellow condensate was observed.

Perusing the relevant literature (see paragraph 4.2) brought the attention to the reduction step. As mentioned above, on the basis of the screening experiments it was planned to reduce the Cu spinel catalyst with ethanol. Meanwhile more often hydrogen had been mentioned as reducing agent in literature.

Therefore the new glass test set-up was furnished with a feeding line for reduction gas (3% H_2 in nitrogen). It was found that the reduction with hydrogen made it possible to continue the experiments for more days.

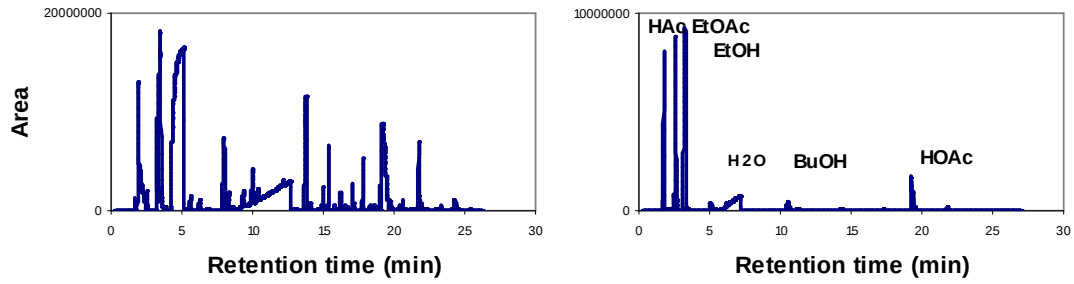

Figure 5-1: Left: GC diagram for condensate of 40/60 ethanol:water feed reduced in 99.9% ethanol. Right: GC diagram for condensate of 40/60 ethanol:water feed reduced in 3% hydrogen in nitrogen.

Figure 5-1 shows the GC diagram obtained for the condensate sampled for the conversion of a 40/60 ethanol:water feed at a LHSV=3 ml/(g·h) over Cu spinel pellets at 320°C. It is clear that the charge reduced with hydrogen shows far higher selectivity. On this basis it was decided to reduce the catalyst installed for the stability test with hydrogen.

Leaving the reactor at hot conditions (reaction temperature: 280-340°C) overnight, just shutting the ethanol feed off while maintaining the nitrogen flow, had a detrimental influence on the activity of the catalyst. This is believed to be related to the side-production of detrimental compounds adsorbed on the catalyst surface. On this basis it was decided to keep the liquid feed going until a temperature below 150°C was achieved during shut-down of the reactors.

5.4.2 High temperature limitation

As mentioned before (reference is made to 3.4) the stability test set-up has really poor fluid dynamics properties (Re_p<10) and a pellet bed height of only10 pellets (50 mm). Meanwhile it featured a continuous run for several weeks if it was supplied with fresh feed as needed and the condensate collector was emptied.

A stability run was started on the stability test set-up, loaded with 17g Cu spinel catalyst, reduced with 3% hydrogen diluted with nitrogen supplied from a gas bottle. A feed of 40/60 ethanol:water was fed by the pump at varied liquid weight hourly space velocities and at 300°C through most of the experiment.

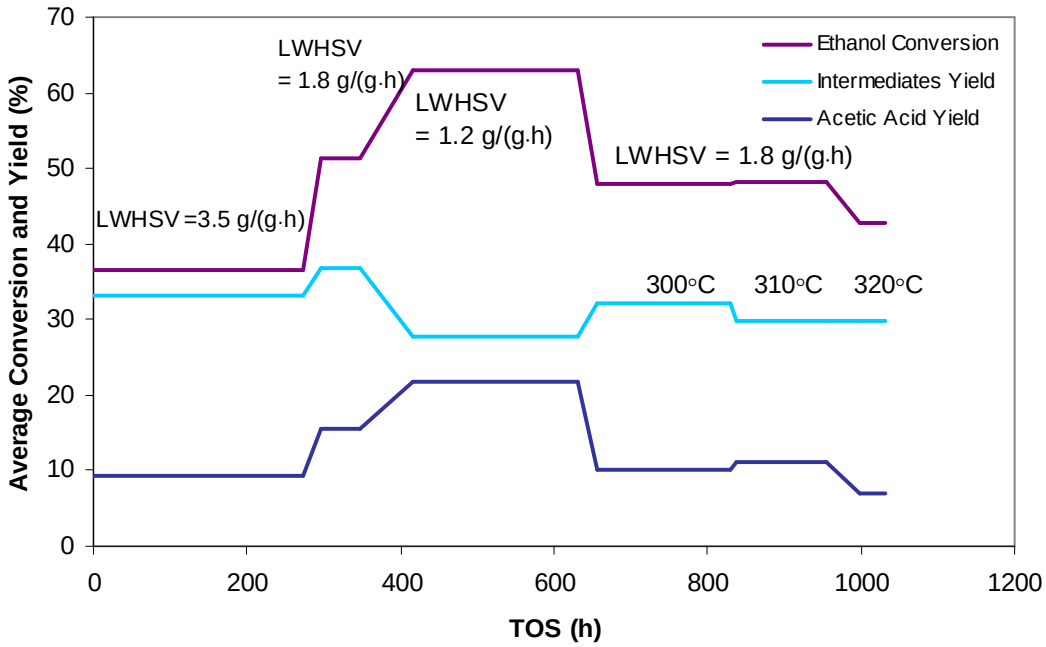

Figure 5-2: The estimated average ethanol conversion (± 10%) and yields vs. run hours in the stability set-up. The numbers are estimated based on GC areas.

The LWHSV was varied over time while keeping the nitrogen flow rate constant at 20 Nl/h. As may be seen the reduction of the conversion degree of ethanol and the acetic acid yield increases with decreasing space velocity and vice versa. The temperature variations in the end are indicated on the graph in Figure 5-2. After a rather short time running at 320°C the catalyst looses all its activity. The loss of activity may be linked to the increase of the temperature.

5.4.3 Co-feeding with recycle mixture

In either of the suggested process layout (see paragraph 4.8) it is foreseen that unconverted acetaldehyde is recycled to the dehydrogenation reactor. Therefore the catalyst must show tolerance to a high acetaldehyde concentration.

In an experiment run in the stability set-up the degree of acetaldehyde co-feeding was increased stepwise.

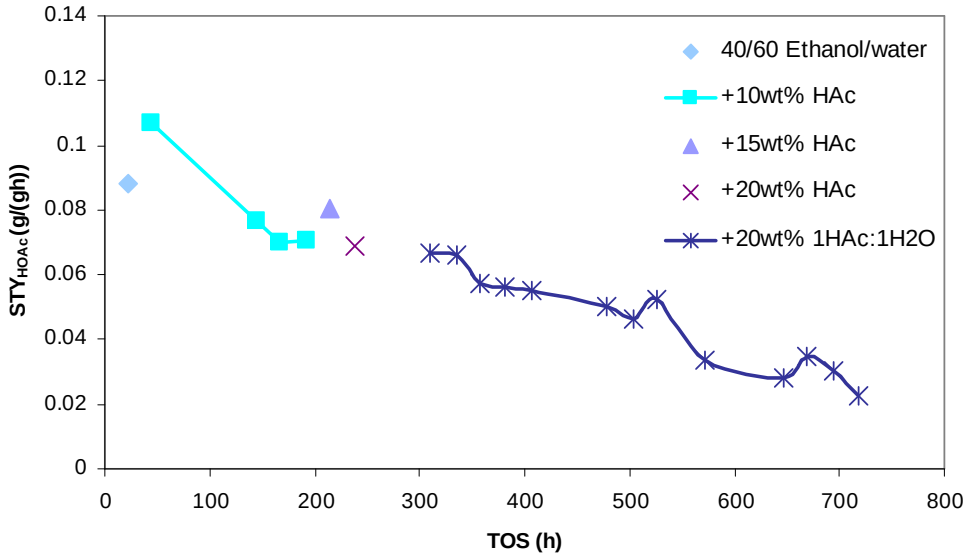

Figure 5-3: The STY of acetic acid as a function of time on stream at LWHSV=1 g/(g·h). The addition of acetaldehyde co-feed is increased stepwise.

Figure 5-3 shows the STY of acetic acid vs. time on stream. The addition of acetaldehyde reduces the activity strongly, but the butanol and butanoic acid side-products do not increase.

Furthermore in case the butanol which is co-produced is not quantitatively separated a co-feed of minute amounts of butanol must also be tolerated without detrimental catalytic effect.

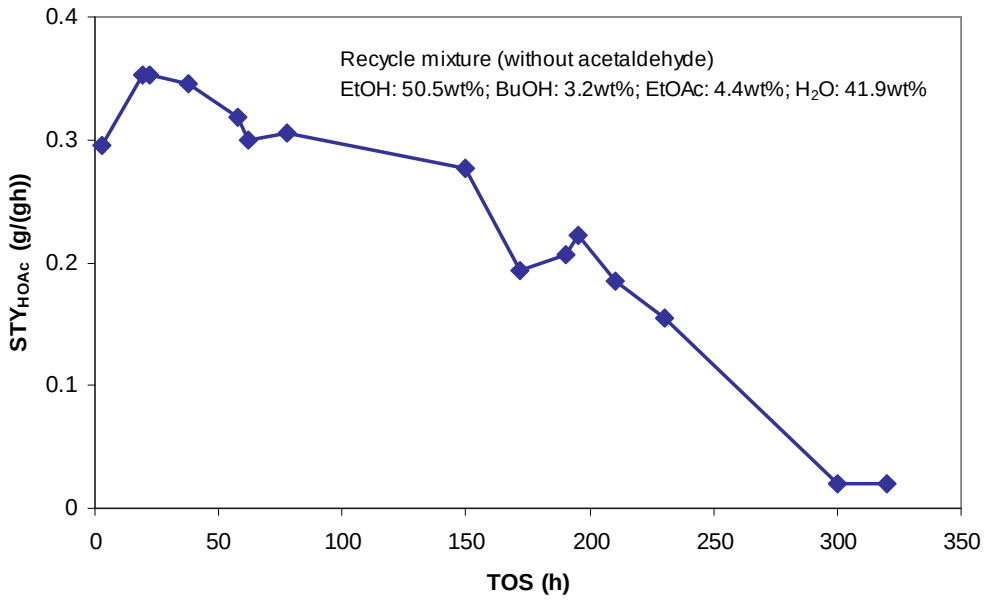

Figure 5-4: The STY of acetic acid as a function of time on stream when a recycle mixture without acetaldehyde but with butanol is used.

Figure 5-4 shows how the STY of acetic acid over time is influenced by the feeding of a simulated recycle mixture without acetaldehyde but with butanol. The deactivation is much faster. After 325 h the catalyst is completely deactivated. An increased level of butyric acid was observed too. As at the time of operation the analytical principle and calibration was not in place the 'STY' calculated is an arbitrary value based on the feed flow rate and the GC area% of acetic acid.

5.5 Regeneration with oxygen

According to literature (*Knapsack-Griesheim Aktiengesellschaft, 1958 and 1959, Dreyfus, 1933*) Cu catalysts, for example copper oxide or Cu/Cr_2O_3, used for dehydrogenation of ethanol to acetaldehyde (and acetic acid) were successfully regenerated by heating these up under exposure to a few percent of oxygen at 350-400°C.

Heating up the Cu spinel catalyst to 400°C after deactivation and exposure to 2% oxygen (as reported) was meanwhile not found to recover any activity under normal operating conditions after re-reduction. However, if the catalyst was heated up to 850°C in air for a couple of hours, cooled down and re-reduced some activity was regained. The latter treatment may correspond to the re-spinelisation of the Cu on Al_2O_3 as originally conducted during the calcination (indicated by the colour change from black to reddish brown and the fact that CuO/Al_2O_3 is not stable under these conditions, *Susnitzky et al., 1991*). It would however be cumbersome to perform high temperature calcination on a regular basis in an industrial plant.

5.6 Investigation of deactivation

With reference to above paragraph 5.4.1 the reduction plays a role for the stability and selectivity of the catalyst. Furthermore from the stability run (paragraph 5.4.2) no known changes but increasing the temperature disrupted the activity of the catalyst; and deactivation connected to the cutting of feed at operating temperature and introduction of side-products (acetaldehyde and butanol) in the feed was puzzling.

Two primary tracks were followed to pursue the observed deactivation phenomena: 1) the characteristics of the catalyst and its reduction and 2) its fate during operation (spent catalyst). Accordingly parts of the explanation to this crucial asset were sought in a characterisation and reduction study of the fresh catalyst all while the testing of the catalyst under various conditions went on. Some of the spent samples that had been subject to rapid deactivation were sent to special analysis: C elemental, TEM, SEM, Cu surface area and pore volume. In the following paragraphs the tracking of the cause for the observed deactivation is reported.

5.7 Characterisation and reduction of the Cu spinel catalyst

In summary the observations made for the Cu spinel catalyst was that means and method of reduction of the catalyst has strong impact on the catalyst activity. It was speculated whether the degree of reduction obtained by the two methods was the source of the deactivation behaviour. It was also considered whether the catalyst reduction progressed differently under the influence of the two reduction media. Furthermore the effect of the ratio of Cu to its alumina support, and the alumina support influence, was studied.

5.7.1 XAFS *in situ* reduction and operation

Samples were prepared for an X-ray Absorption Fine Structure (XAFS) study. The investigations were carried out at MAX-lab in Lund and HASYLAB in Hamburg, two facilities comprising positron/electron storage rings providing photons in beam-lines for experimental investigations.

The experimental set-up in Lund used on the I811 beam-line experimental station for the XAFS comprised a gas supply with mass flow controllers connected to an about 1 mm quartz glass tube (capillary) for containing the catalyst installed in an x/y adjustable rig for optimizing the position of the sample in the photon beam. The glass tube was heated by a hot air jet. The effluents from the reactor were emitted to an emission gas line. Accordingly 100-200 micron sieve fractions of the Cu spinel (30.9wt% Cu) catalyst was prepared and mixed with high purity alumina of the same size in a weight ratio 1:5.

In parallel a sample of a model catalyst was prepared containing 2.5wt% Cu on alumina. The reason for the preparation of a model catalyst was to ease the recording of the reduction progress without having the signal from the bulk spinel crystal Cu overshadow the emerging reduced Cu. A drawback is that the predominance of alumina in the model sample may affect the Cu to actually behave differently in the Cu-Al-O framework. The model catalyst was prepared by impregnation of high surface area gamma-alumina 1/25" trilobe extrudates with copper acetate dissolved in water to incipient wetness. The sample was dried at 100°C over night and calcined at 850°C for 2 hours to bring the Cu into its spinel structure (which was confirmed later by means of EXAFS analysis, see Figure 5-11).

In a first experiment with *in situ* reduction of the catalyst in MAXLAB in Lund only proper XANES (as opposed to EXAFS) data were obtained due to the fact that only a Si(311) had been installed (and not on the preferred Si(111)). Reference data (energy calibration) for the setup were obtained by concurrent measurements on a Cu foil.

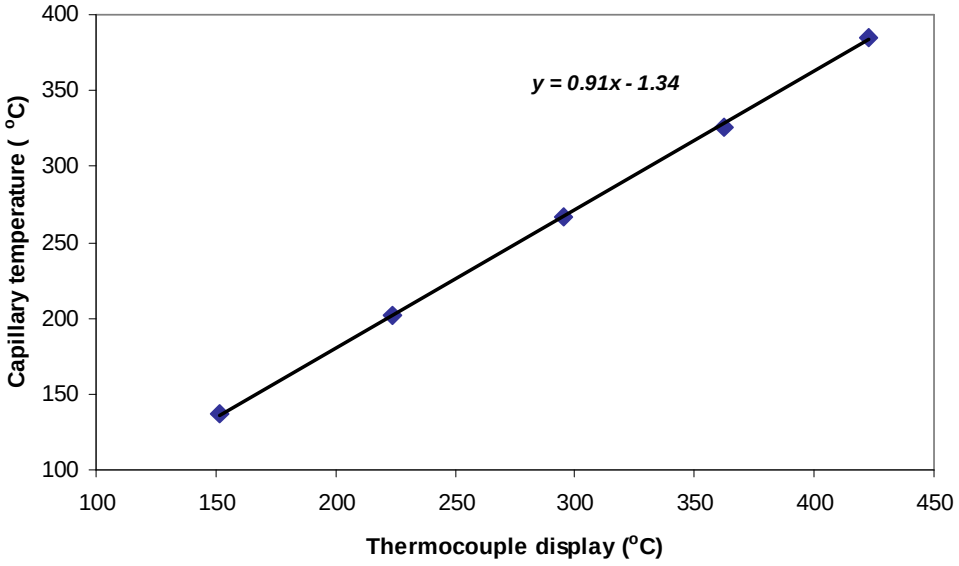

Figure 5-5:The relationship between the capillary and the displayed oven temperatures was linear.

The temperature was increased with approximately 5°C/min while recording XAFS data. The relationship between the set-point of the oven and the temperature measured in the jet stream was established (see Figure 5-5). First, spectra were recorded at RT, then at 180°C, wherefrom the temperature was increased with recording intervals of 40-60°C terminating at 380°C. The Cu spinel catalyst was reduced both in 5% hydrogen with a SV of 10 Nl/(min·g) and ethanol saturated at room temperature in helium (6.6%). These flow rates are so high that the stoichiometric amount of reduction medium is fed within few seconds.

In Figure 5-6 is shown how the spectra recorded for the two samples look at the start of reduction (180°C) and the end of reduction (380°C) at largely comparable temperatures. The model catalyst was reduced both in hydrogen and ethanol.

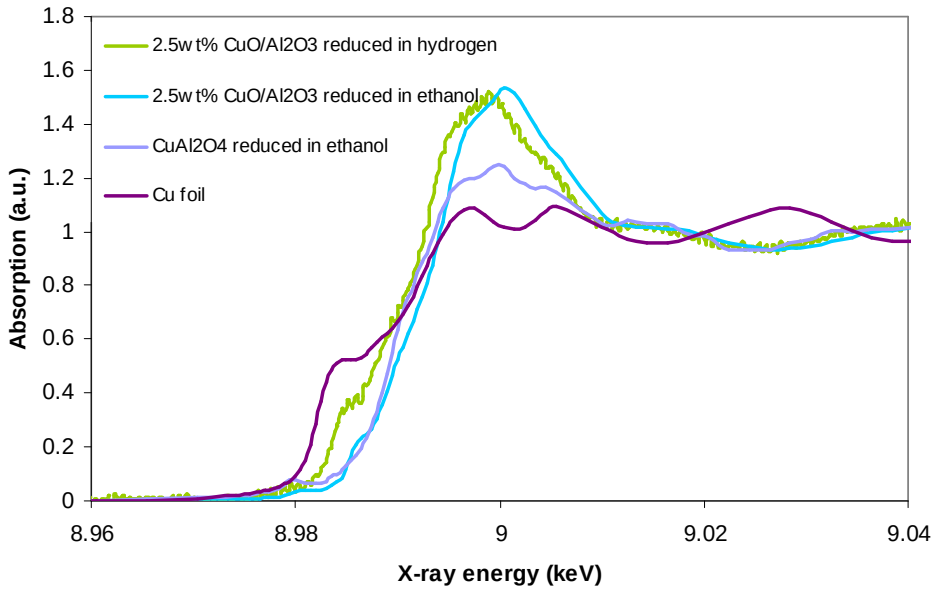

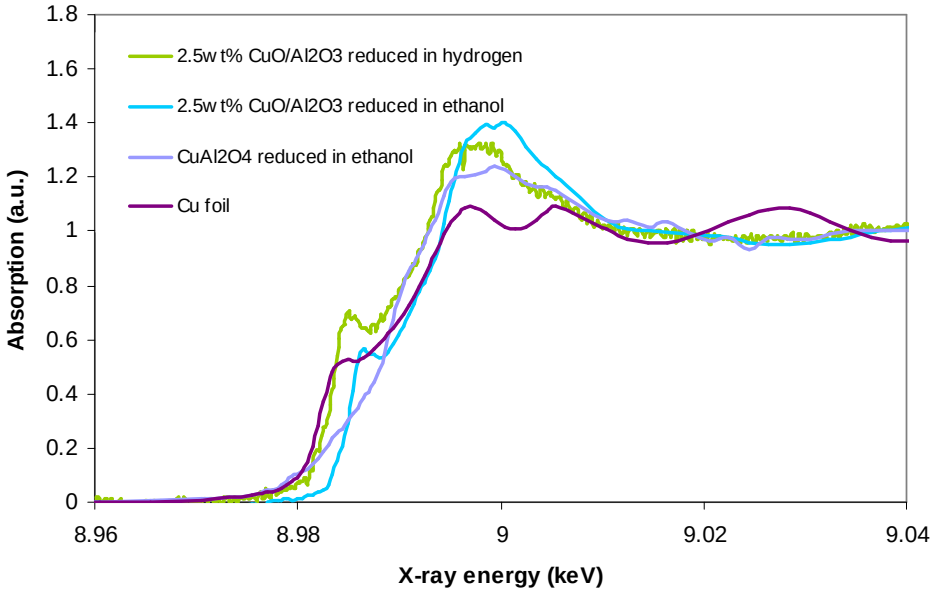

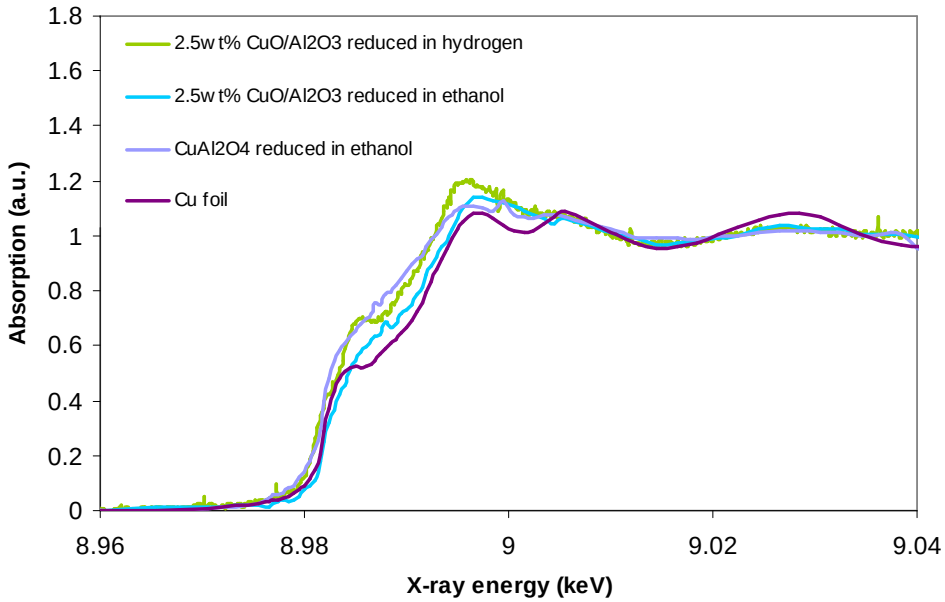

Figure 5-6: The XAFS absorption spectra recorded at two reduction temperatures. Upper: 181-209°C. Middle: 250-260°C. Lower: 358-383°C. The Cu foil absorption represents Cu(0) absorption spectrum. Full reduction was not obtained in either of the reduction experiments.

The RT scans and another set of intermediate scans are enclosed in Appendix E.1. It is seen from Figure 5-6 (middle) that while for the 2.5 wt% Cu/Al_2O_3 sample a XANES peak characteristic of Cu(I) appears temporarily at an X-ray energy of 8.982 keV and disappears gradually, the XANES analysis does not show any interim Cu(I) for the Cu spinel catalyst. Neither of the spectra of the 2.5 wt% Cu/Al_2O_3 nor of the Cu spinel catalyst coincides entirely with the spectrum of the Cu foil, indicative of an uncompleted reduction.

The conclusions drawn from these first experiments are that

- Not all Cu is reduced at 380°C (or lower) and the degree of reduction increases until this end temperature.
- Cu(II) in $CuAl_2O_4$ is reduced straight to Cu(0)
- Similar degrees of reduction is obtained with hydrogen and ethanol at a given temperature for the model catalyst
- The model catalyst reduces via Cu(I)

The *in situ* reduction study was extended with an experiment under operating conditions at HASYLAB (XAFS experiments at the Cu K edge as earlier in Lund), where also more details on the reduction part were found by performing an EXAFS analysis. The scans were made by means of the preferred Si(111) crystal for the reflection of the photon beam providing for both XANES and EXAFS data.

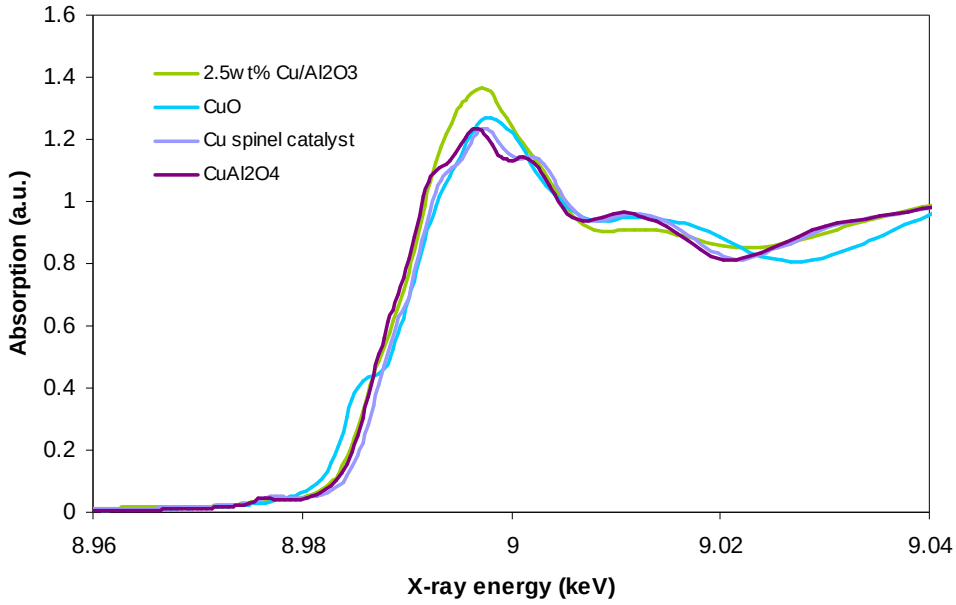

Figure 5-7: RT EXAFS spectra of the as prepared samples (before reduction), Cu spinel catalyst and 2.5 wt% Cu/Al_2O_3. Cu spinel exhibits clear $CuAl_2O_4$ characteristics, while the 2.5% Cu/Al_2O_3 model catalyst deviates from both the $CuAl_2O_4$ and the CuO sample.

For reference RT scans of a pure $CuAl_2O_4$ sample as well as of the samples were initially made. Figure 5-7 shows that the unreduced Cu spinel catalyst is indeed recognised as $CuAl_2O_4$, while the 2.5% Cu/Al_2O_3 model catalyst has fewer apparent similarities. However, an EXAFS analysis above the K-edge revealed though that the Cu in the model catalyst was coordinated as spinel (see Figure 5-11).

The ramping was conducted in the same manner, while the reactor was here made of kanthal embedded in alumina (like a bell) providing heat. The reactor (containing 50 mg of the crushed and sieved 100-150 micron sample in between graphite sheets) is made of stainless steel connected to the feeding system and the outlet. The reduction ethanol was here introduced via a high precision Isco syringe pump at a rate of 52 µl/min, evaporated and mixed with nitrogen carrier gas flow of 20 Nml/min to obtain a 50/50 ethanol:N_2 mixture. When reaching 380°C the feed was switched to nitrogen and the temperature was lowered to 300°C before a feed of ethanol/water was introduced. The Cu spinel catalyst, again diluted by means of alumina, was reduced in 5% hydrogen in nitrogen whereas the *in situ* reduction of the 2.5 wt% model catalyst in both hydrogen and ethanol was obtained.

Cu spinel catalyst

The spectra acquired during the reduction show (see Figure 5-8) that the main part of the reduction takes place in the temperature range 300-380°C. Again here the SV of the gas was high enough to stoichiometrically reduce the catalyst in less than a minute.

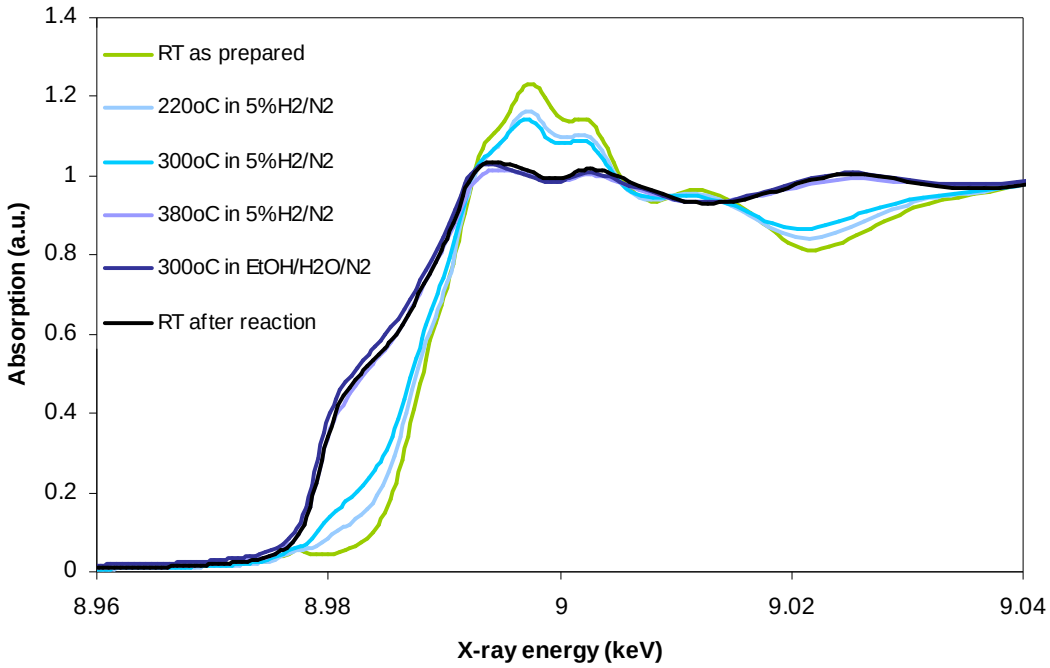

Figure 5-8: Reduction of Cu spinel catalyst in 5% hydrogen. The main reduction of Cu spinel takes place between 300 (turquoise) and 380°C (lilac). The Cu state is conserved during reaction conditions (indigo).

Model catalyst 2.5wt% Cu/Al_2O_3

While the Cu spinel catalyst was the sample of original interest it was hoped that the model catalyst with a lower Cu load (2.5wt% vs. 31wt%) might provide further details on how the Cu state initiates its change. The model catalyst was subjected to reduction in hydrogen identically to the reduction of the Cu spinel catalyst. Figure 5-9 shows the scans recorded for the reduction of the model catalyst in 5% hydrogen. Noteworthy is that the Cu is reduced via the Cu(I) state, perhaps via $CuAlO_2$ or Cu_2O but ends up also as Cu(0) at the final reduction temperature at 380°C.

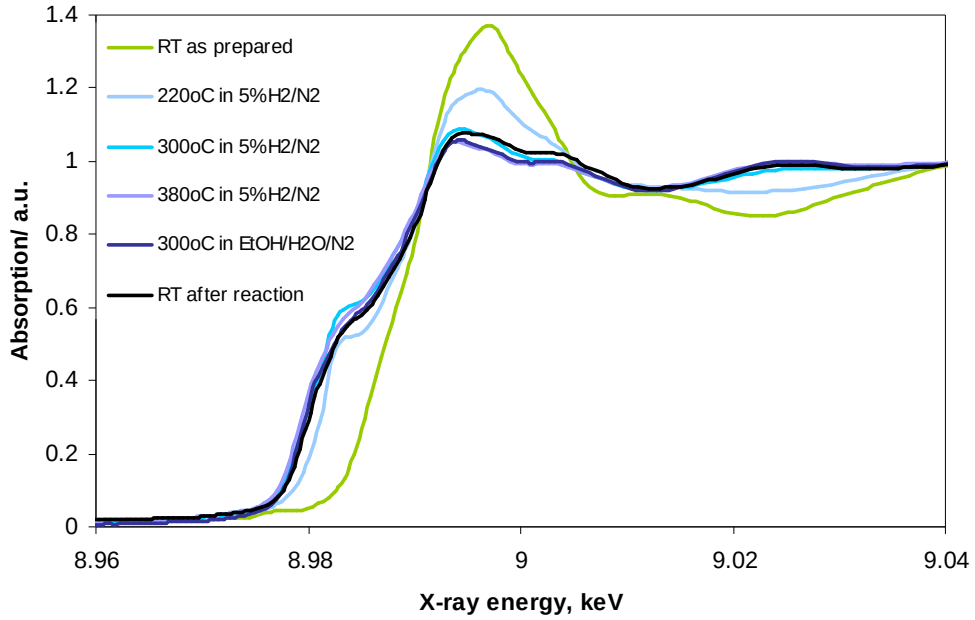

Figure 5-9: Reduction of 2.5wt%Cu/Al_2O_3 in 5% hydrogen. The XAFS spectra shows that reduction of Cu(II) takes place via the Cu(I) state (peaks around 8.982 keV) already at 220°C (light blue), develops at 300°C (turquoise) while nearly full reduction is obtained at 380°C (lilac).

Also here the Cu state remains unchanged after the switching to operating conditions (300°C in EtOH/H_2O/N_2). In addition to the reduction experiment was conducted using ethanol as the reducing agent (see Figure 5-10).

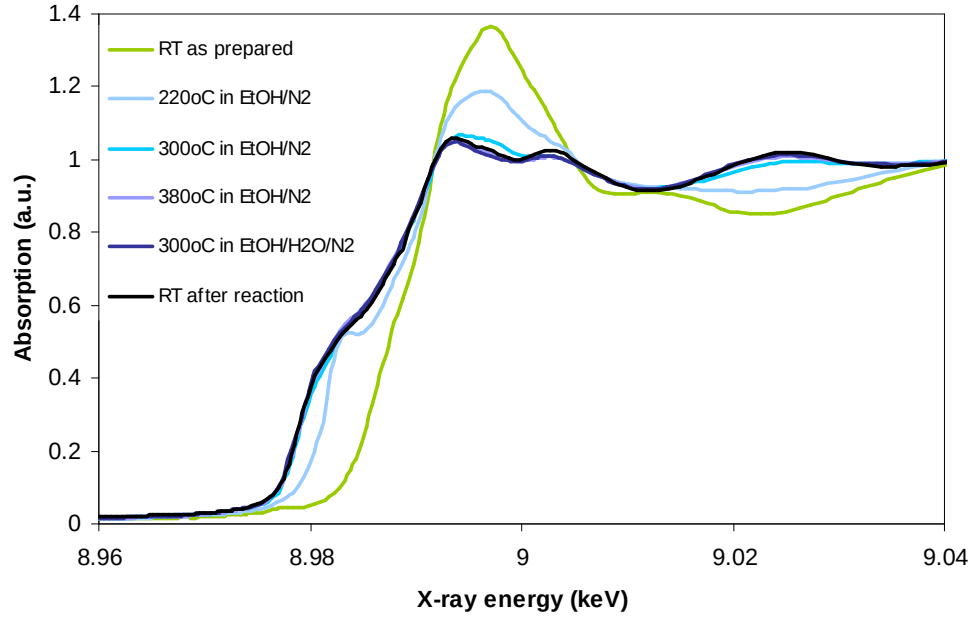

Figure 5-10: Reduction of 2.5wt%Cu/Al_2O_3 in about 50% ethanol in nitrogen. The acquired XAFS spectra for the 2.5wt% Cu model catalyst.

By comparing the XAFS spectra for the model catalyst reduced by the two methods (Figure 5-9 and Figure 5-10) it can be seen that the progression of reduction vs. temperature is similar in the two cases. And again the Cu(II) reduces to Cu(0) via Cu(I).

Furthermore an EXAFS analysis was made on the spectra. The Fourier transformed EXAFS are shown in Figure 5-11. It shows that the Cu of both the as prepared (unreduced) Cu spinel and model catalyst were surrounded by oxygen atoms in a $CuAl_2O_4$ like structure (same spectra as the $CuAl_2O_4$ spectrum). Strong indications are here that actually a copper spinel was obtained for the model catalyst although the colour of the model catalyst was greenish/turquoise while the Cu spinel was dark orange brownish (as $CuAl_2O_4$ is known to be). The Cu state of Cu spinel and the model catalyst after reduction and exposure to reaction feed is metallic, and indications are that the Cu crystals are larger for the model catalyst reduced in ethanol/nitrogen.

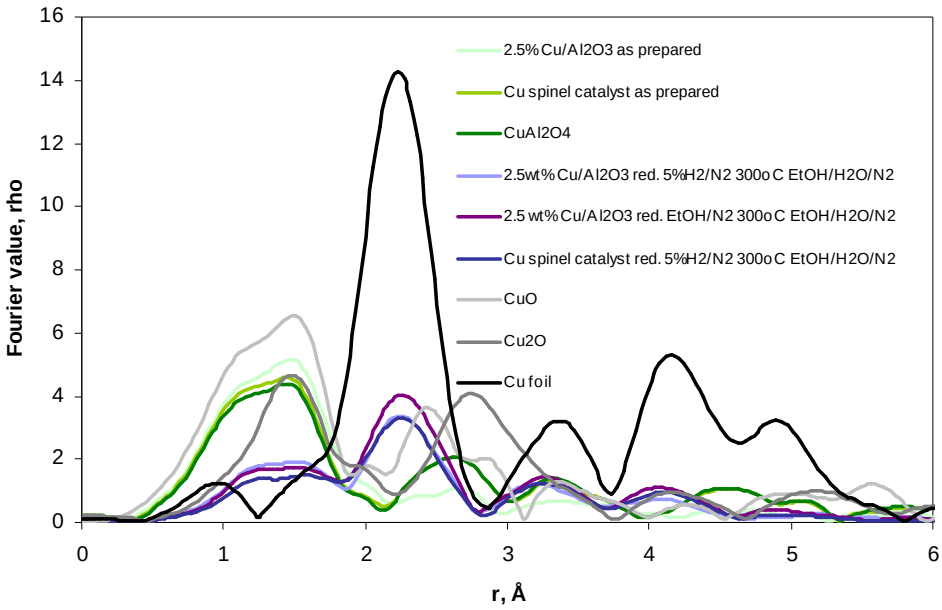

Figure 5-11: The Fourier analysis of the interference of photons show that both Cu spinel and the model catalyst bear the characteristics of a $CuAl_2O_4$ structure before reduction, while after reduction the Cu is metallic.

By means of the Cu-Cu coordination number (6.9-8.2) it was estimated that the average size of the Cu particles in the reduced samples was about 10-16Å, with a tendency of larger Cu particles in the sample reduced with ethanol and in both samples after having been exposed to operating conditions. Next to the Cu-Cu interference, a small contribution of oxygen is observed by EXAFS with a Cu-O bond distance of 1.96-1.98Å, which could be due to the presence of unreduced Cu(I), a Cu support interaction or a thin oxygen layer covering the Cu particles.

A selection of the results of the *in situ* EXAFS study was reported in a HASYLAB year report enclosed in Appendix E.2.

5.7.2 XRPD *in situ* reduction and operation

In order to support the findings from the XANES/XAFS reduction experiments and to study how the phases are influenced by the operating conditions a parallel reduction

experiment was set up making use of *in situ* X-ray Powder Diffraction (XRPD) technique. The source of X-ray is emitting Kα1–radiation (photon energy 8.045 keV) originating from Cu being bombarded by electrons. Diffractions are measured by means of a PW3011 detector and data analysed by means of Philips PC-APD software. Thus the above procedures were repeated for fresh 100 mg loads of (crushed and sieved, 100-150 micron) Cu spinel in an XRPD set-up, only here the temperature of the reactor was held constant for half an hour for every 20°C in the temperature range 140-380°C in order to conduct the XRPD at constant temperature. The Cu spinel sample was after reduction cooled to 300°C and then run at operating conditions (normal feed composition i.e. a 40/60 ethanol:water mixture, 300°C and atmospheric pressure) for about 26 h period. After running under reaction conditions the feed was switched to nitrogen and the sample cooled down to room temperature and passivated. The crystal sizes estimated by XRPD are based on the Scherrer equation, corrected for instrumental line broadening.

Ideally the catalyst ought to be unloaded and analysed after use without being exposed to oxygen in order not to reoxidise, thereby changing the at least the Cu state, but this is not practical. However, if the catalyst is exposed to very low concentration of oxygen, for example 1%, at room temperature a thin layer of CuO evolves on the surface of the Cu crystals through a controlled and slow oxidation which passivates the bulk part of the Cu from complete oxidation. In order to test whether the passivation with 1% of oxygen passed over the catalyst at room temperature for a couple of hours suffice in protecting it against phase changes, an ex situ XRPD analysis was repeated on such passivated sample numerous times in a period over 2 weeks. The diffractograms showed that the crystal phases and their quantitative representation found in the analysis conducted shortly after passivation was literally identical to the phases in the analysis made 2 weeks after the passivation of the catalyst. Therefore based on this indication the method of subjecting the catalyst to 1%O_2 in nitrogen at atmospheric pressure and room temperature for 2.5 h was considered to successfully passivate the catalyst.

In one part of the reduction experiment 3%H_2 in nitrogen was used for reduction of Cu spinel. The results of the Cu crystal size calculations for the planes [111] and [200] from the XRPD *in situ* reduction experiment is shown in Figure 5-12.

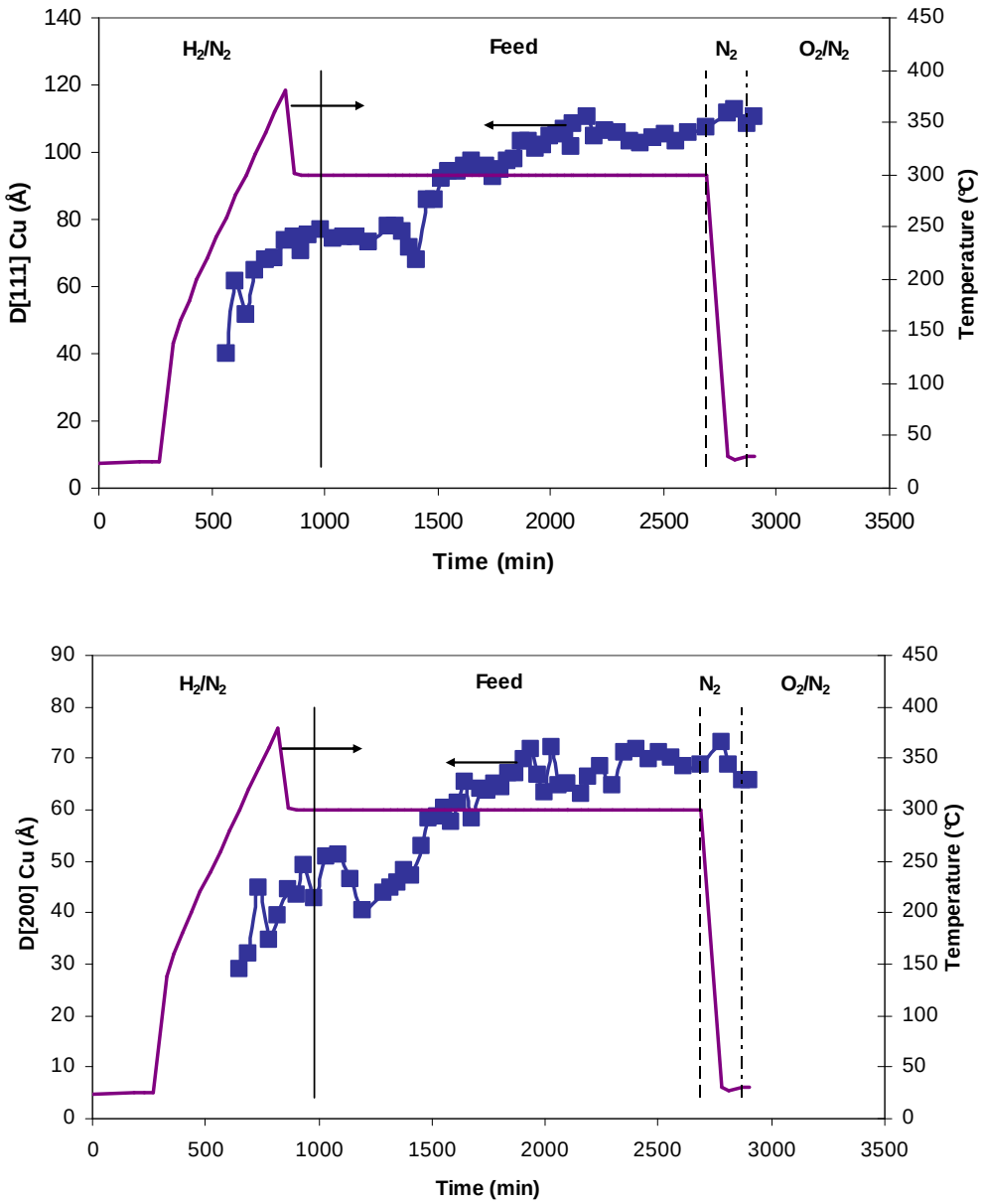

Figure 5-12: *In situ* XRPD reduction. Upper: Growth of Cu(111) plane during reduction in 3% H_2 and exposure to EtOH/H_2O. Lower: Growth of Cu(200) plane during reduction in 3% H_2 and exposure to EtOH/H_2O.

Figure 5-12 shows that the Cu crystals grow in the Cu(111) direction and level out at 50-70 Å during reduction up to 380°C, then resume growing (with time delay) under reaction conditions (EtOH/H_2O) and level out at 70-110Å. The same trend is seen for the Cu(200) plane, however having a lower size.

The analysis of the amount of crystalline phases was conducted in parallel (Rietveld). The estimates of the relative amounts are not very accurate due to the instrumental line broadening induced by *in situ* equipment.

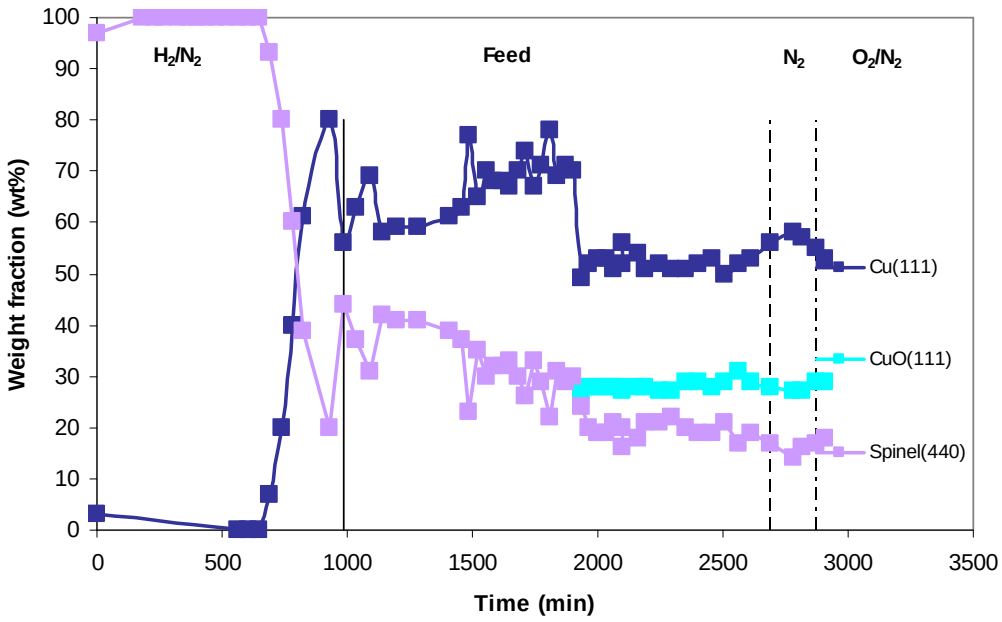

Figure 5-13: *In situ* XRPD reduction in 3%H_2. The relative amounts of spinel ($CuAl_2O_4$ and eta-Al_2O_3), Cu and CuO during reduction with hydrogen and exposure to EtOH/H_2O.

The Cu spinel sample subjected to 3%H_2 in N_2 showed the appearance of significant amounts of Cu at around 285°C (see Figure 5-13). The relative amount of Cu to spinel does not level out during reduction until the reduction end temperature (380°C) is reached. Both $CuAl_2O_4$ and eta- or gamma-Al_2O_3 are identified as spinel in XRD analyses, the Cu spinel distinguishable by its slightly higher unit cell parameter, 8.08Å vs. 7.91Å for alumina. Eta and gamma alumina are hardly distinguishable (*Maciver et al.,1963*), but it is estimated that eta- rather than gamma-alumina emerges during the reduction of $CuAl_2O_4$, as it contains more defects. Both alumina types are catalytically active.

The reduction stage was followed by exposure to EtOH/H_2O (40:60) for 26 h. It was further found for the sample reduced in hydrogen that after changing to operating conditions a sudden CuO signal emerged after 13 h. Besides it seems that amorphous alumina forms as a part of the alumina. The theoretical weight fraction of Cu, taken that all $CuAl_2O_4$ reduces into Cu/Al_2O_3, approaches 34%. In present analysis the Cu wt% gets almost double, indicating that part of the Cu vacant alumina framework probably ends up as an amorphous alumina (not accounted for), while another part ends up as crystalline eta-alumina, which is also seen as a spinel phase in the XRPD analysis, as mentioned.

The XRD reduction experiment was repeated, only here the medium of reduction was ethanol (in carrier gas). With a sample of 100mg of catalyst powder loaded into the reactor a carrier gas flow of 5.2Nml/min was fed and mixed with ethanol dosed from an Isco syringe pump at 0.624g/h (0.78 ml/h), corresponding to a 50% ethanol/50% nitrogen mixture.

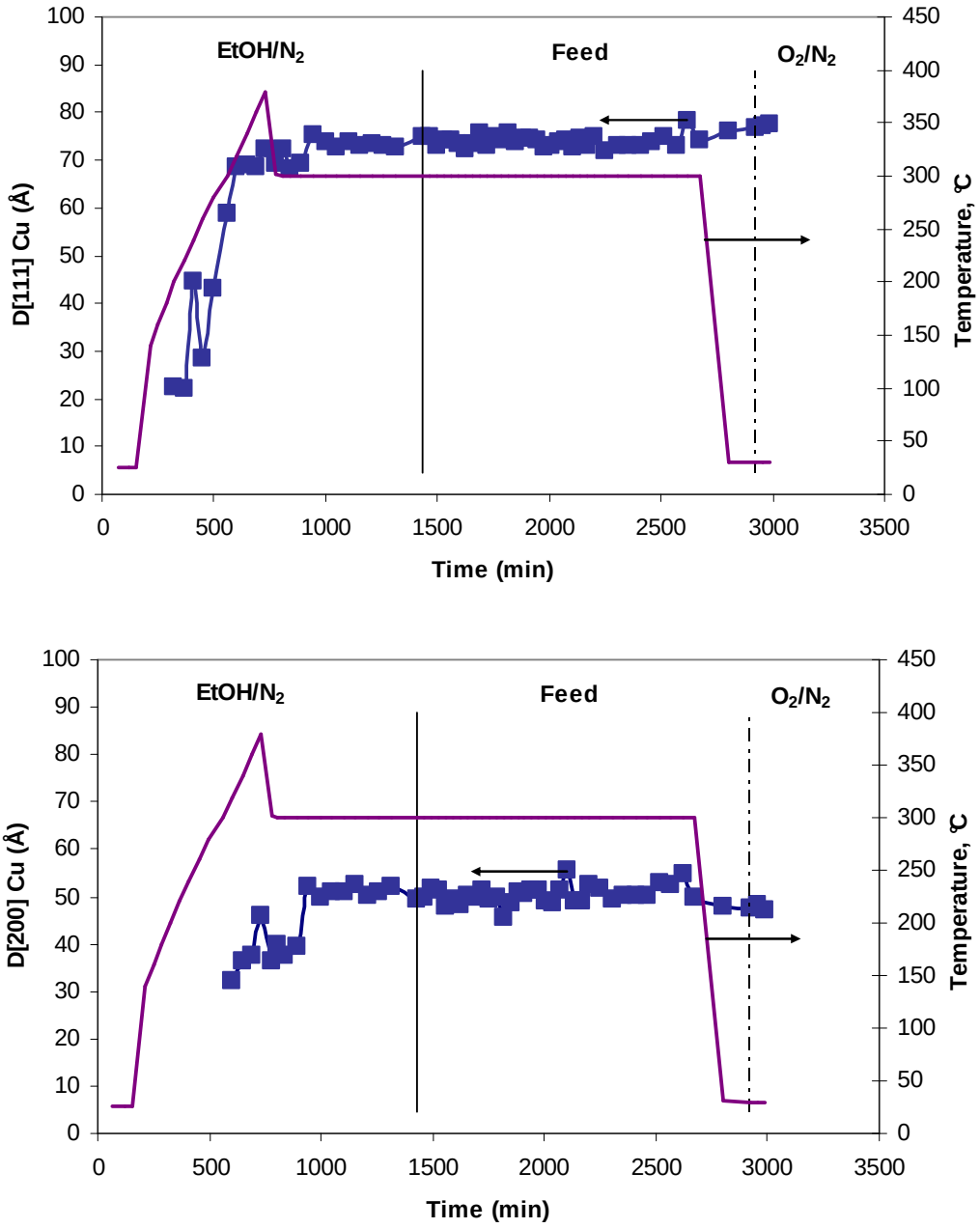

Figure 5-14: *In situ* reduction. Upper: Growth of Cu(111) plane during reduction in 50% ethanol and exposure to EtOH/H_2O. Lower: Growth of Cu(200) plane during reduction in 50% ethanol and exposure to EtOH/H_2O.

Figure 5-14 shows a growth of Cu crystals to a constant size of 70 and 50Å, respectively, derived for the Cu(111) and Cu(200) reflections. The (440) peak for spinel (Figure 5-15, lower) shifts to a higher angle position during the temperature ramping under reduction, where also Cu is formed, corresponding to a reduction of the distance between the (440) planes (Bragg's law) as is the case when going from Cu spinel (8.08Å) to eta- or gamma alumina (7.91Å).

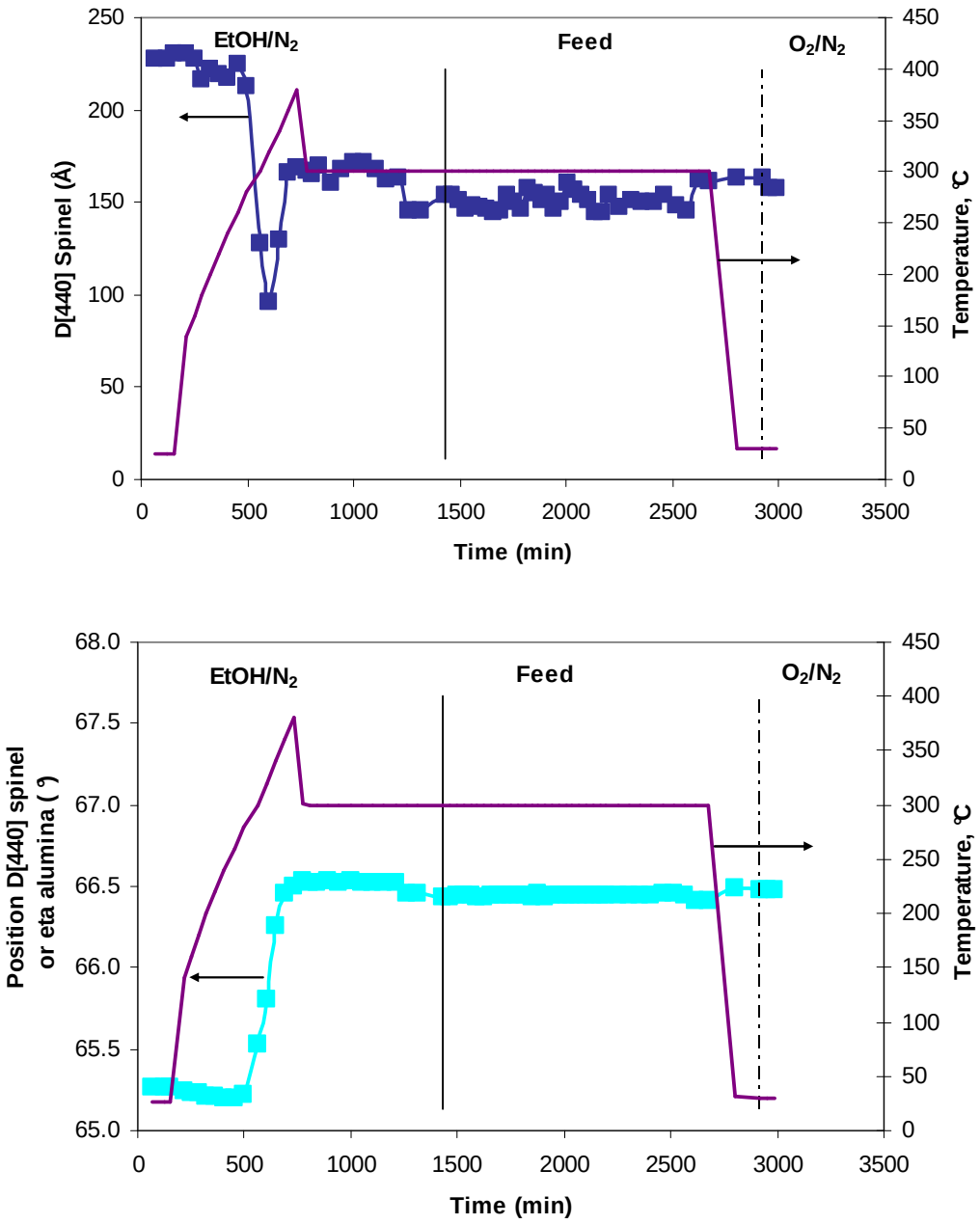

Figure 5-15: In situ reduction in 50% ethanol. Upper: The (440) spinel crystal size reduces during the reduction. Lower: The (440) spinel 2θ position changes concurrently from 65.3 to 66.5° indicative of a spinel phase shift.

Thus the simultaneous shift of the (440) spinel 2θ position and the forming of Cu crystals indicate the transformation of spinel $CuAl_2O_4$ to Cu and spinel Al_2O_3 during reduction.

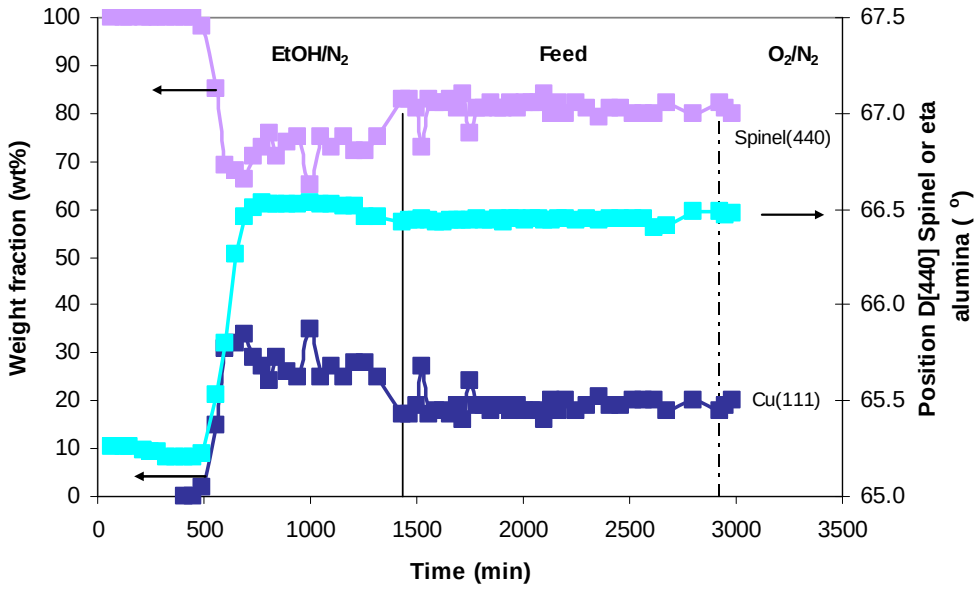

Figure 5-16: The relative amounts of spinel ($CuAl_2O_4$ and eta-Al_2O_3), Cu and CuO during reduction with ethanol and exposure to EtOH/H_2O.

The shift of the spinel structure is finalised at 360°C, while the amount of Cu has reached its final maximum level relative to spinel already at 340°C (see Figure 5-16), whereas for the reduction in hydrogen the levelling out was found at 380°C.

5.7.3 TPR *in situ* reduction

In order to establish which reaction products occur on Cu spinel over the reduction period with reducing gases containing 3% hydrogen and 1.6% ethanol respectively as reducing agents a TPR experiment was set up. A stream of reducing gas was passed over the sample of Cu spinel (crushed, sieved 100-150 micron) which was heated linearly (2°C/min) with time. The concentrations of various components in the stream were measured by a Balzers GAM400 mass spectrometer (MS) with Quadstar software while increasing the sample temperature. The mass spectra from the reactor effluent were acquired for both of the two reduction methods.

As for the reduction with ethanol a closer study of the components characteristic spectra (see Figure 5-17) reveals that ethanol (with dominant peaks at 27, 29, 31 and 45) is converted at about 200°C to acetaldehyde (with dominant peaks in 15, 29, 43 and 44) and hydrogen (peak 2, see Figure 5-18, right), whereas from about 350°C ethylene (with dominant peaks at 26, 27 and 28) is made through dehydration of ethanol.

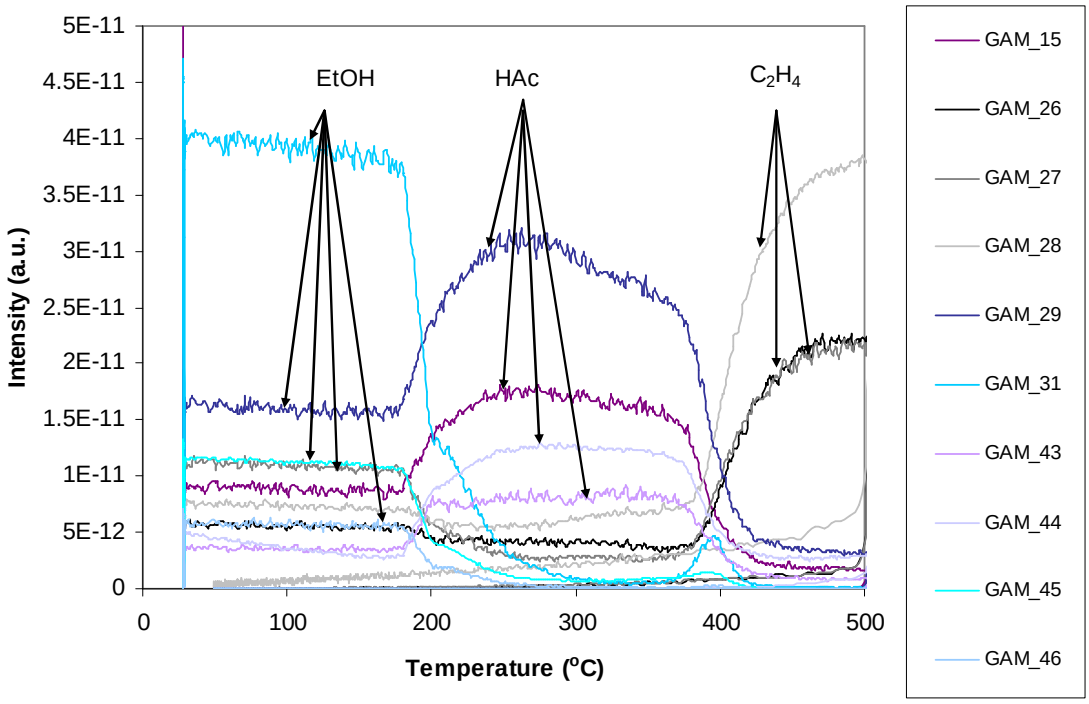

Figure 5-17: TPR reduction with ethanol. The mass signal intensities (Amperes) for selected components in the effluent from the reduction reactor during reduction with ethanol are plotted as function of temperature.

Comparing the occurrence of hydrogen and water during the progress of reduction (see Figure 5-18) it is found that the water content of the reduction medium becomes much higher for the sample being reduced with ethanol above 350°C due to the production of ethylene.

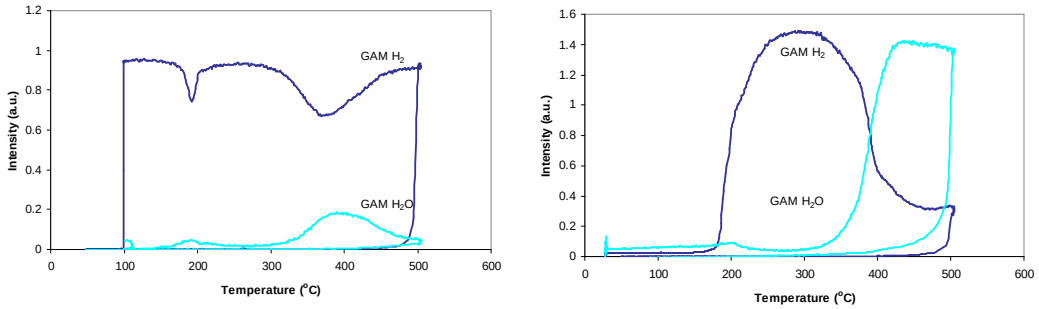

Figure 5-18: The hydrogen and water signals during the reduction of Cu spinel in hydrogen (left) and ethanol (right). The water content of the reduction medium is higher for the sample reduced with ethanol above about 350°C due to ethylene formation. The y-axis units are arbitrary.

The water partial pressure is higher for the sample reduced in ethanol above 350°C. This may influence the tendency of forming eta-alumina over amorphous alumina, when reducing $CuAl_2O_4$ to Cu and Al_2O_3. However, the reduction temperature used (340°C) in the activity test is below the off-set temperature for the dehydration of ethanol to ethylene and water. In both cases therefore, using hydrogen or ethanol, the reduction water product is the only water present during reduction.

Notably, acetaldehyde is present during the reduction of the Cu spinel catalyst in ethanol.

5.7.4 HRTEM *in situ* reduction

One of the visual methods available for inspecting crystal growth *in situ* is high-resolution Transmission Electron Microscopy (HRTEM). This technique was made use of in order to shed light on the structural changes under reduction and better interpret the results obtained from XAFS and XRD. The sample was imaged at room temperature (RT) in the vacuum *in situ* mode or *in situ* during exposure to 1-10 mbar H_2 at 300-400^{o}C in a Titan ETEM apparatus. Figure 5-19 shows the HRTEM images of the fresh state of the Cu spinel catalyst powder, and that these oxide particles have facetted shape and uniform contrast.

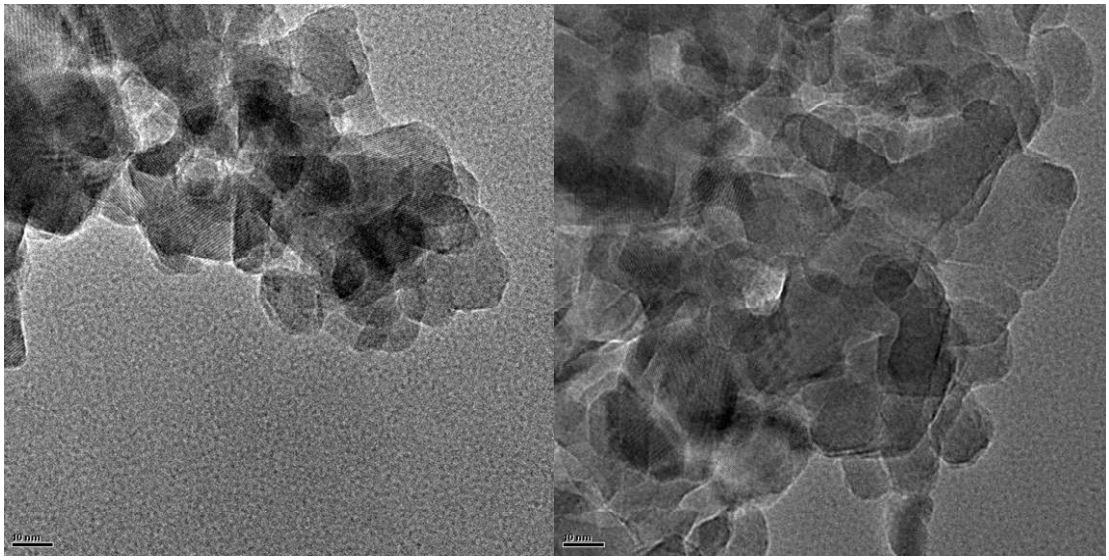

Figure 5-19: HRTEM images of the fresh Cu spinel ($CuAl_2O_4$) powder at RT in vacuum.

The sample was then heated in ca. 1mbar H_2 to 357^{o}C for 45 min and 407^{o}C for 50 min and, subsequently in ca. 10 mbar at 407^{o}C. During this heating sequence HRTEM images were collected under isothermal conditions. Finally, after cooling to room temperature and pumping the H_2 out of the environmental cell, reference HRTEM images were obtained from a window area that had remained unexposed to the electron beam during the heating sequence, and hereby not influenced by changes induced by the electron beam, for example sintering or even sublimation caused by local heating.

Figure 5-20 shows that H_2 exposure at elevated temperature induces structural changes of the oxide nano particles. The spherically shaped particles with a uniform dark contrast formed are presumably metallic Cu particles. More irregularly shaped particles with brighter contrast are attributed to the oxide framework. Specifically it is noted that a bright, speckled contrast has appeared which could indicate a porous structure induced for instance by agglomeration of mobile Cu vacancies. Moreover, some oxide particles appear not to have changed during this experiment. These could be the surplus of Al_2O_3 in the Cu spinel catalyst, or it could be a sign of incomplete reduction.

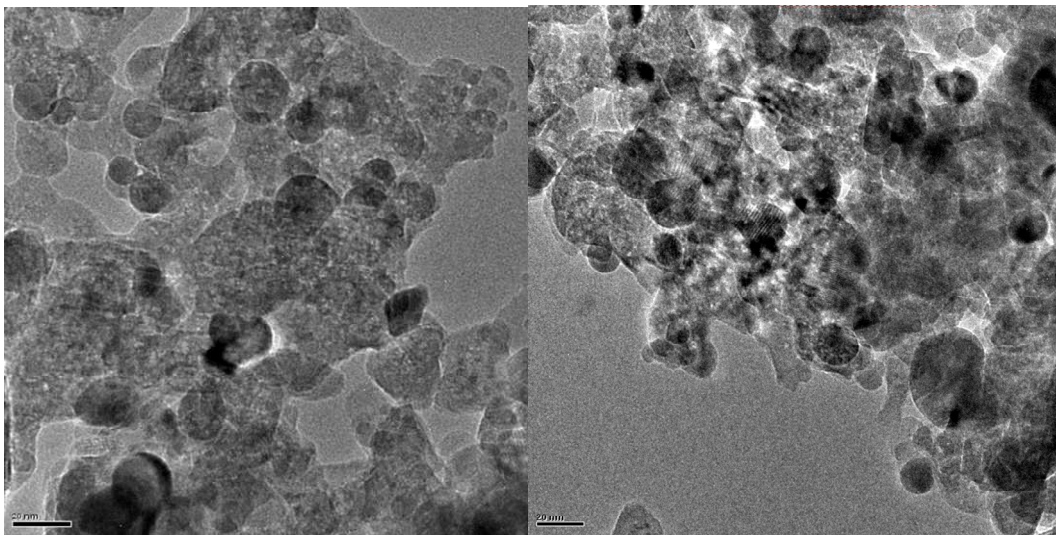

Figure 5-20: HRTEM images of the reduced Cu spinel catalyst powder at RT in vacuum. A speckled contrast appears indicating for example agglomeration of Cu vacancies.

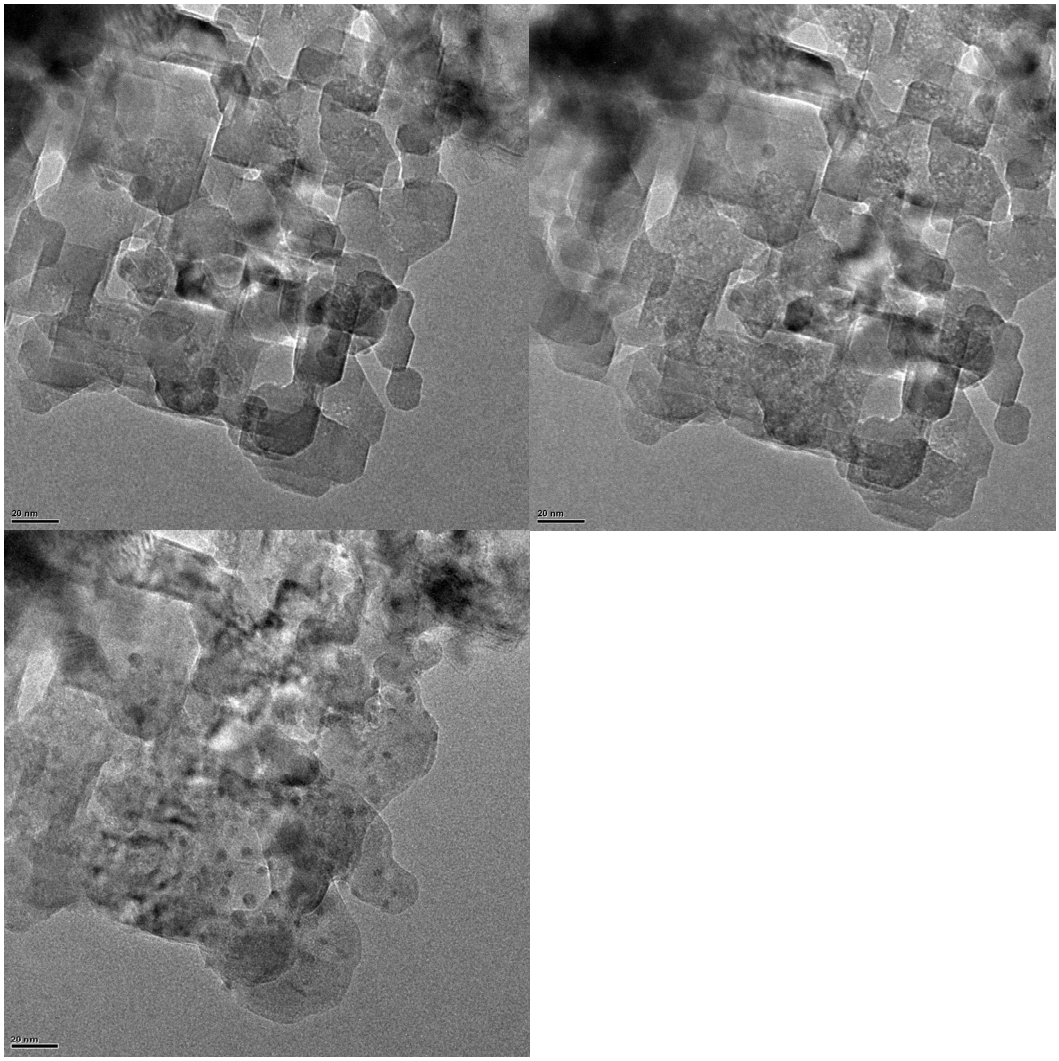

Figure 5-21: HRTEM images obtained *in situ* during exposure to ca. 10 mbar H_2 at 407^{o}C. (Between the second and third image the specimen was cooled to RT for a few min. to study beam effects at a separate area).

Figure 5-21 shows three HRTEM images obtained *in situ* at ca. 10mbar and 407°C. The images show how the speckled contrast develops and Cu particles eventually appear. The effect of the beam is still rather unexplored. With too intense a beam an almost instantaneous sublimation of Cu was observed. This phenomenon may have influenced the series shown in Figure 5-21 above.

In situ HRTEM of Cu spinel during H_2 reduction shows that 20-50 Å Cu particles form and that the oxide particles obtain more irregular shapes with a contrast pattern indicating that a more porous structure forms.

5.7.5 Optimisation of reduction t by activity measurements

The results from the above XANES and XRD reduction experiments immediately point to that the reduction should take place up to at least 380°C in order to reach nearly full reduction of Cu anticipating that the catalyst activity may be connected to the Cu mass available on the alumina surface.

However, it is well known from other Cu based catalyst systems that Cu particles tend to sinter. As the temperature of the catalyst rises, the particles start to become mobile and sinter (coalesce). This phenomenon becomes substantial as the Cu approaches its Tammann temperature (405°C, half the material's melting point on the absolute temperature scale) (*Satterfield, 1996*). Another sintering mechanism is the Ostwald ripening. Sintering means a loss of surface area available for reactants. It may therefore be that the optimum reduction temperature is lower than 380°C in spite of the lower degree of reduction obtained.

A series of experiments were set up at an early point where the full procedure for proper analysis was not available, thus only GC areas were available as a measure of productivity. The experiments were conducted in the new glass test set-up in reactor 2 (reference is made to paragraph 3.3 and Figure 3-6). During reduction the catalyst loaded was heated up while 3% hydrogen was led over the catalyst at a SV of 4 Nl/(g·h) for 5 hours. The terminal reduction temperature was 300, 320, 340 and 380°C, respectively. After reduction the hydrogen was switched off and nitrogen was put on while the reactor cooled off. The introduction of feed typically took place the day after the reduction had been carried out. The catalyst was fed with ethanol:water in a ratio 40/60 (molar basis), 20/80 and a so-called recycle mixture (23.5/49.9/24.6/1/1 ethanol:water:acetaldehyde:ethyl acetate:1-butanol) simulating how a fresh feed of ethanol in combination with a recovered stream of intermediates and unconverted feed components may be composed in a closed process loop layout. The LWHSV of the feed was 2.4 g/(g·h) in all cases and the temperature was approximately 320°C.

a)

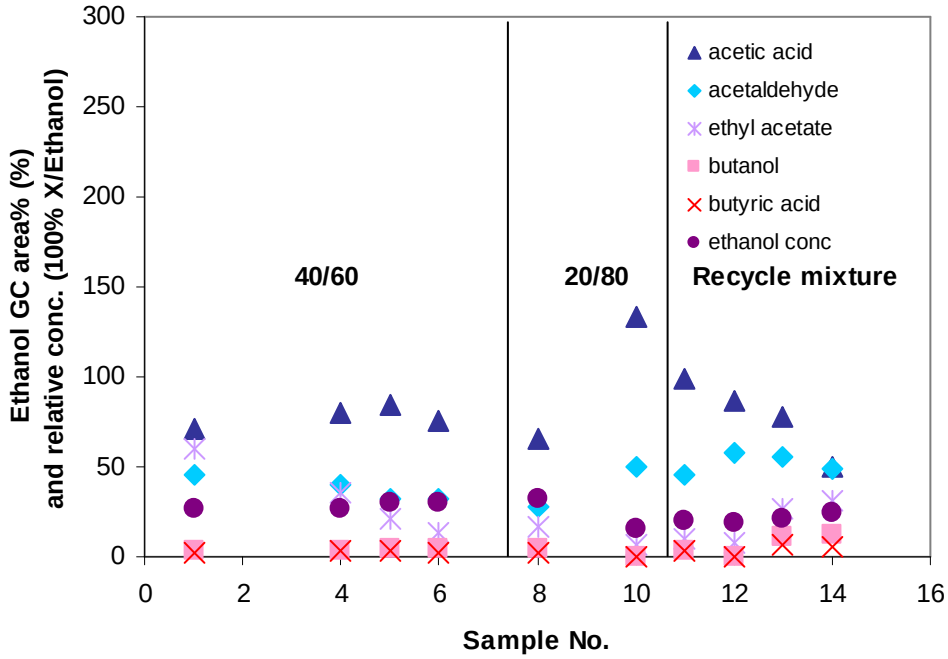
Ethanol GC area% (%)
and relative conc. (100% X/Ethanol)
300
250
200
150
100
50
0
0
2
4
6
8
10
12
14
16
Sample No.
40/60
20/80
Recycle mixture
acetic acid
acetaldehyde
ethyl acetate
butanol
butyric acid
ethanol conc

b)

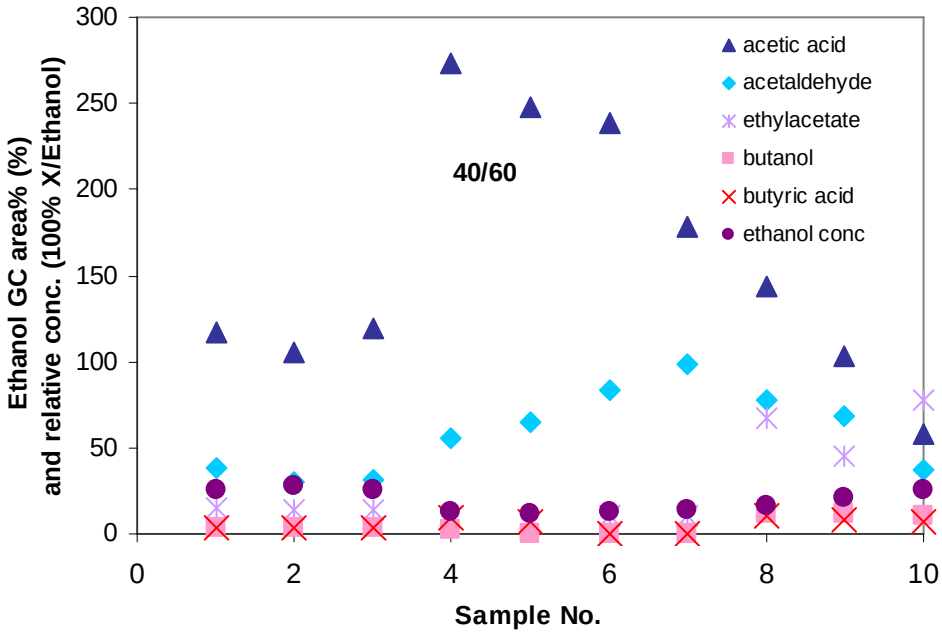
Ethanol GC area% (%)
and relative conc. (100% X/Ethanol)
300
250
200
150
100
50
0
0
2
4
6
8
10
Sample No.
40/60
acetic acid
acetaldehyde
ethylacetate
butanol
butyric acid
ethanol conc

c)

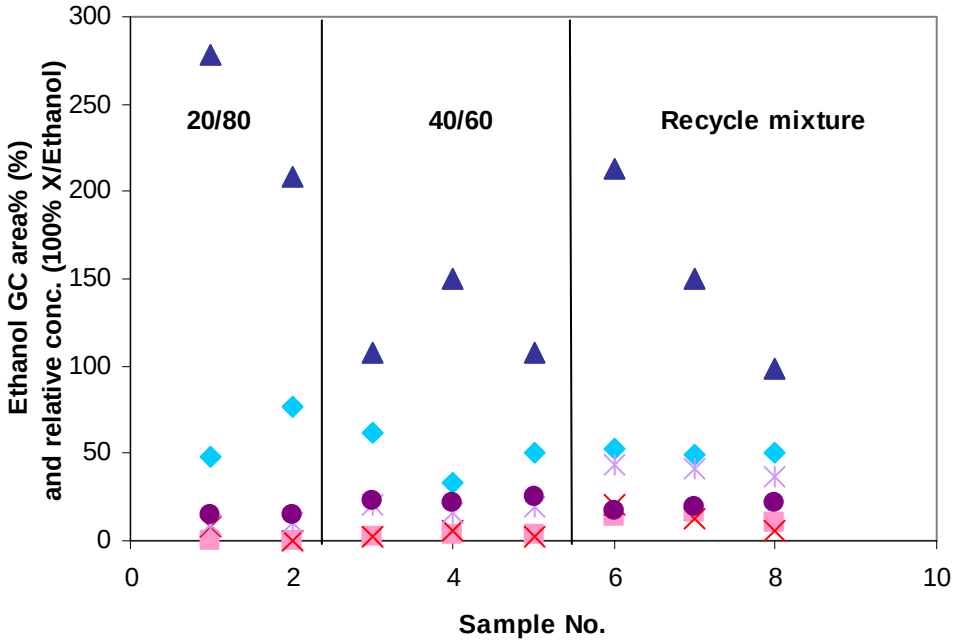

d)

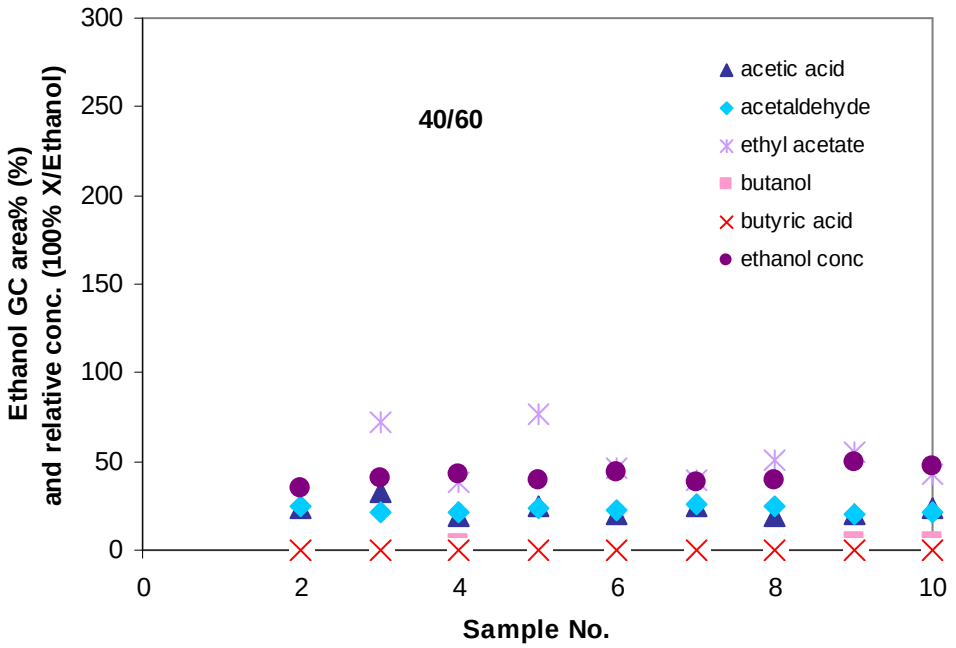

Figure 5-22: The ethanol concentration and relative concentrations of effluent components for the conversion of 20/80, 40/60 molar ratios of ethanol:water and a recycle mixture fed at a LWHSV=2.4 g/(g·h) and 320°C, converted over spinel catalyst reduced at a) 300°C, b) 320°C, c) 340°C, d) 380°C.

Figure 5-22 a) b) c) and d) show the relative GC areas of the components in the condensate. The GC area% of ethanol is set to 100%, and the remaining concentrations are given relative to this. It may be gathered that the activities of the catalysts reduced at 320°C and 340°C respectively are similar, however with a better performance of the catalyst reduced at 340°C on the recycle mixture.

This may indicate that indeed a Cu sintering phenomenon overlays the degree of Cu reduction.

5.7.6 Complementary reduction t optimisation: TGA, chemisorption, TPD

In order to fine-tune the Cu area measurements (under the previous presumption of a connection between activity and Cu surface area) a reduction series was performed in a TGA (Termogravimetric Analysis, Mettler TGA/DSC1). Samples were placed in 100 µl alumina pans for the measurements. The reductions were followed by flushing and titration with CO as the probe molecule and NH_3 for obtaining information of acidity of the Cu spinel catalyst.

Reduction by heating from RT to 500 ℃ at 4 heating rates in 3% hydrogen showed two reduction reactions. A low temperature autocatalytic reaction starting around 150℃ accounting for 10% of the weight loss and a more dominant reaction at higher temperature (>225-450℃) accounting for 80% of the weight loss. This qualitatively corresponds well with what was seen for XAFS (see Figure 5-6). Both reactions were exothermic with approximately 67 kJ/mol heat of reaction. A hypothesis is that the low temperature mass loss may be caused by the reduction of CuO or some easily reducible Cu-species, like surface Cu in the spinel phase. The low temperature reaction is an exothermic (40 J/g cat = 4.3 kJ/g weight loss = 68.6 kJ/mol O) and autocatalytic reaction. The autocatalytic nature of this first reduction can be seen from the crossing curves in Figure 5-23 between 2 and 2.4 1000K/T. The black lines are indicating iso relative actual-to-maximum weight loss, for example 0.02 corresponds to a weight loss of 2% of the maximum theoretical weight loss possible, assuming that one oxygen atom may be lost per Cu atom and based on the known composition.

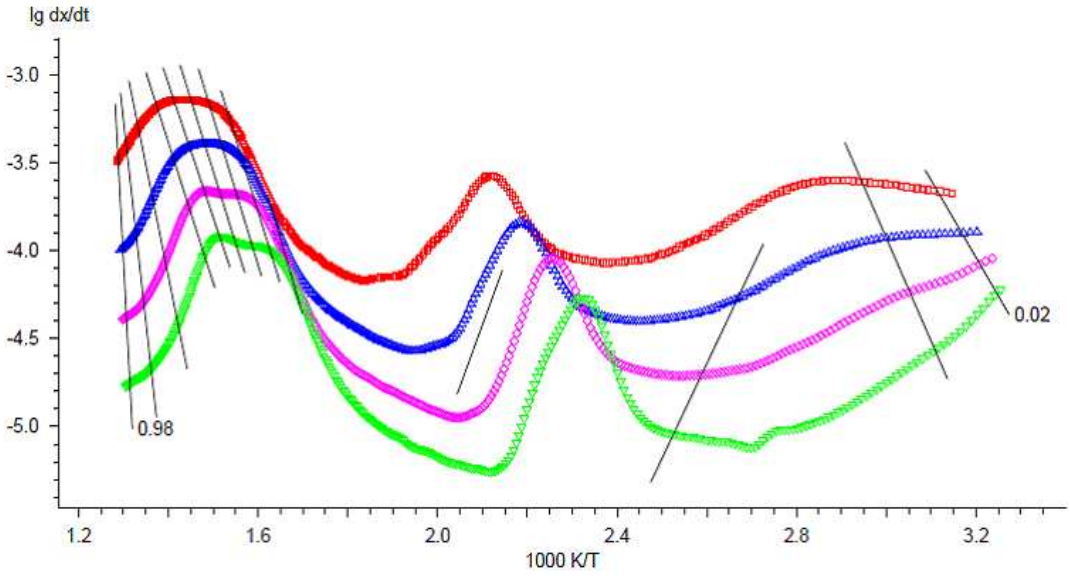

Figure 5-23: Arrhenius plot of the copper catalyst weight data obtained during reduction at 4 heating rates from RT to 500°C. Red: 8.2°C/min, blue: 4.1°C/min, pink: 2.0°C/min, green: 1.0 °C/min.

The relative active surface areas were analysed by gravimetric CO chemisorption measurements after reduction for 5 and 10 hours by hydrogen gas at temperatures between 320 and 380 ℃. The CO exposure caused a rapid weight increase (due to chemisorption and physisorption) followed by a reduction in weight during flushing, but

after some time the samples resumed the weight gain. This opens for two possible evaluations of the CO adsorption: Horizontal step and tangential step. Horizontal step adsorption is measured from the minimum weight measured during flushing subtracted the weight before CO adsorption, while tangential is measured as the vertical distance between the intersection of the two tangents from the weight curve before and after the adsorption at the tangent of the curve at highest curvature. The results from the TGA measurements are shown in below Table 5-1.

Table 5-1: Adsorption data for CO and NH_3 at different temperatures. Theoretically a weight loss of 7.8% is expected with a copper spinel catalyst containing 30.9% Cu.

Reduction temperature and time	Weight loss by reduction (%)	Tangential step CO adsorption (%)	Horizontal step CO adsorption (%)	NH_3 adsorption (mmol NH_3/g)
320℃, 5h	5.39	0.094	0.151	0.15
340℃, 5h	6.77	0.115	0.169	0.11
360℃, 5h	7.01	0.101	0.161	0.14
380℃, 5h	7.39	0.086	0.138	0.15
320℃, 10h	7.02	0.100	0.160	0.15
340℃, 10h	6.44	0.107	0.167	0.16

The CO adsorption value goes through a maximum around 340 ℃. This indicates the largest metallic (active) Cu surface is present after reduction at this temperature. As compared to the activity data obtained (see paragraph 5.7.5) the mere Cu area seems to have a rather flat optimum which in itself cannot explain the difference of activity by minimum a factor 2. Especially at high reduction temperature (380°C), the Cu area as determined by TGA can not explain the severe decrease of activity for Cu spinel. The reduction at 320 and 340°C were repeated in experiments lasting 10 h. The adsorption values found after 10 h reduction largely match these figures, meaning that further reduction time does not change the position of the optimum temperature. The lower weight loss recorded after 10h at 340°C than after 5 h expresses the inhomogeneity of the sample.

As compared to the theoretical weight loss of 7.8% obtainable with a Cu spinel containing 30.9% Cu (a little surplus of Al_2O_3 is present) the reduction is found to be almost complete at 380°C (degree of reduction=95%) while at 340°C the reduction has only progressed 87%. The 5% missing to be reduced at 380°C may explain the Cu-O signal found in the EXAFS analysis (presence of unreduced $Cu_2Al_2O_4$), especially in the light that the EXAFS reduction were conducted over a shorter period of time. The reduced samples were also tested for their acidity by exposure to ammonia. These results (see Table 5-1) showed a minimum in acidity for samples reduced at around 340 ℃.

The data was further normalized to the amount of metallic Cu calculated from weight loss during reduction. These results are plotted versus reduction temperature in Figure 5-24. It can be seen that the amount of CO adsorbed relative to the amount of metallic Cu decreases with an increasing reduction temperature. Longer reduction time also reduces the amount of CO adsorbed relative to the amount of metallic Cu. This behaviour is consistent with a decrease specific surface area of the copper with increasing reduction temperature and increasing reduction time, which again is consistent with sintering of the copper particles into larger.

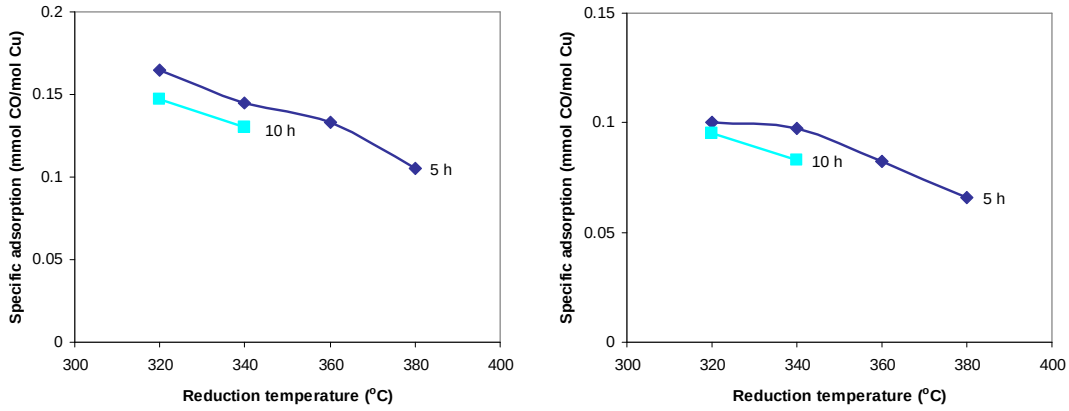

Figure 5-24: CO desorption normalised to the amount of metallic Cu using the Horizontal step (left) and the Tangential step (right) for 5 and 10 h of reduction.

The measured CO adsorption is so low that complete coverage is unlikely, which is also to be expected due to the high adsorption temperature (30℃). Results are consequently only relative and not suited to provide quantitative information on crystal size.

In supplement to the TGA experiments a standard H_2 TPD was made in order to possibly confirm the optimum Cu area found and partly in order to more precisely find the absolute Cu surface area and thereby help estimate the size of the Cu crystal. Prior to the TPD examination 5 samples of 0.2g (crushed and sieved 100-150 micron) Cu spinel were reduced by ramping up to 5 different temperatures: 300, 320, 340, 360 and 380°C, respectively at a heating rate of 2°C/min and a SV=12 Nl/(g·h) and 1% H_2 for a total of 5 hours. Then a hydrogen gas stream was passed over the sample (indirectly cooled by nitrogen boiling at -196°C) allowing some of the molecules in the stream to adsorb at the surface of the sample until saturation.

Hereafter the flow was changed to He, and the sample was heated linearly with time while monitoring the concentration of the hydrogen molecules desorbing from the sample surface by a mass spectrometer.
Examples of the data acquired by means of this method are shown in below Figure 5-25 and Figure 5-26.

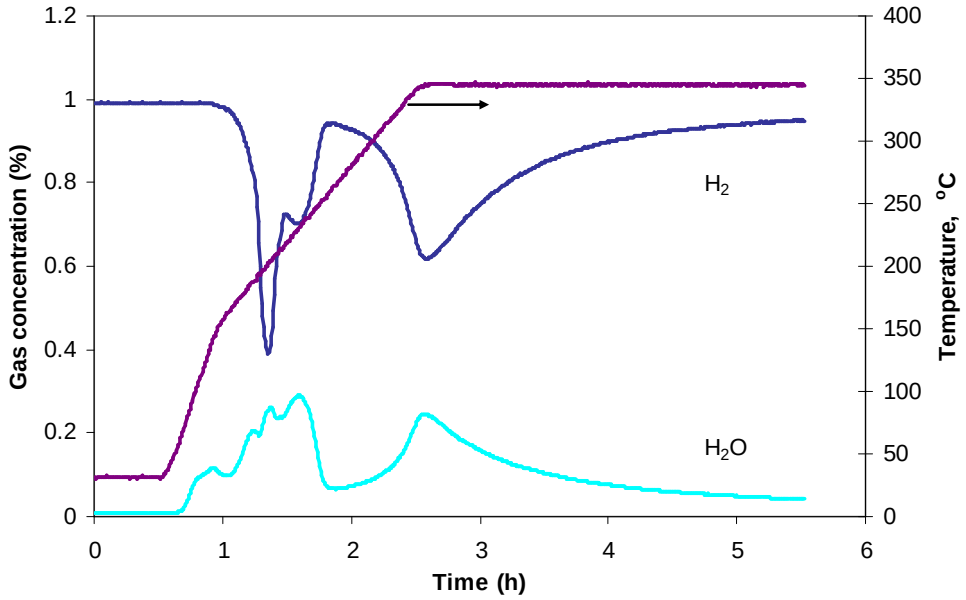

Figure 5-25: The concentrations of hydrogen and water in the effluent from the TPD reactor being exposed to 1% hydrogen reducing gas, reduced during temperature ramping up to 340°C.

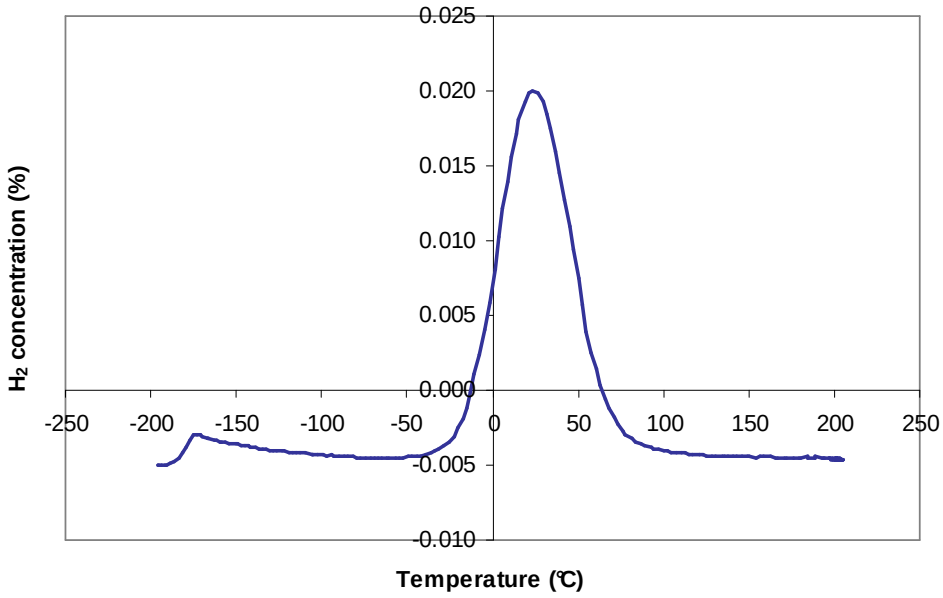

Figure 5-26: Desorption of hydrogen from Cu spinel during TPD heating from -196°C to 200°C after reduction terminating at 340°C.

The results from the measurements are presented in below Table 5-2. The values of the mass specific Cu surface area are calculated on the basis of the unreduced catalyst mass.

Table 5-2: The Cu surface area as a function of reduction temperature.

Reduction temperature (°C)	Cu surface area (m^2/g cat)
300	9.33
320	9.48
340	9.15
360	8.48
380	7.79

Making a rough assumption of equally sized hemispherical crystals of copper distributed on the alumina surface, all accessible by hydrogen via the pore system, an estimate of the average crystal radius may be calculated according to Eq. 5-1:

$$\bar{r} = \frac{3 \cdot V_{ave}}{A_{surf,ave}} = \frac{3 \cdot v_{spec}}{a_{spec}} = \frac{3 \cdot \delta \cdot x_{Cu}}{\rho_{Cu} \cdot a_{spec}} = \frac{3 \cdot 0.87 \cdot 0.309 (gCu/gCat) \cdot 10^8 (Å/cm)}{8.78 (gCu/cm^3) \cdot 9.15 \cdot 10^4 (cm^2/gCat)} \approx 100 Å \qquad \textbf{Eq. 5-1}$$

where V_{ave} is the volume of the hemisphere with the average radius and $A_{surf,ave}$ is the surface area of the hemisphere with the average radius, their ratio being equal to the ratio of the mass specific Cu volume and surface area, v_{spec} (m^3/g) and a_{spec} (m^2/g), as well, each proportional by the number of average sized crystals per mass unit. Further v_{spec} may be calculated from the degree of reduction, δ, the content of Cu in the unreduced catalyst, x_{Cu}, and the density of Cu at 340°C, ρ_{Cu} (gCu/cm^3). The density of Cu at 340°C $\rho_{Cu,\ 340°C}$ = 8.78 g/cm^3 based on a linear expansion coefficient of $16.5 \cdot 10^{-6}$ K^{-1} and $\rho_{Cu,\ RT}$ = 8.92 g/cm^3. The degree of reduction was found by TGA analysis (see paragraph 5.7.6), and the mass specific Cu surface area was found by TPD (see Table 5-2, above).

An average crystal "size" estimate would then be in between this radius and its double (see Figure 5-27).

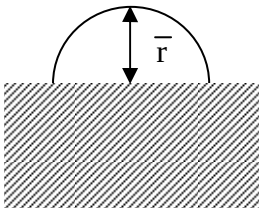

Figure 5-27: Cu crystal sketched as a hemisphere on an alumina surface. The 'size' of the crystal is between the radius and the diameter.

In reality the Cu particles on the alumina surface are shaped angular (*Hansen et al., 2002*). Assuming a Cu surface density of $1.47 \cdot 10^{19}$ Cu atoms/m^2, the metallic Cu dispersion (actual Cu surface area/theoretical Cu surface area) may be calculated to 5.3%.

5.7.7 Alumina support activity

The catalytic activity of the support alone was investigated by loading 10 g of high surface area gamma-alumina support into the screening reactor. When subjecting it to pure ethanol and an 50/50 ethanol:water mixture in nitrogen carrier gas at 300°C condensation products were found to have formed apart from a little ethyl acetate. A dark brown top phase rich in condensation products built in the receiver and more than 100 peaks emerged on the GC-MS spectrum. The water rich phase below contained mainly acetaldehyde, ethyl acetate and ethanol and very little acetic acid (3 orders of magnitude lower than the ethyl acetate).

Water has an inhibiting effect on the alumina support activity in the formation of condensation products. This corresponds well with the lower side-product level found for aqueous ethanol in the screening tests.

5.7.8 Cu/Al ratio

The Cu/Al ratio of the catalyst was studied in order to find the optimum Cu load for the catalyst, thereby obtaining the highest weight or volume based activity for the catalyst.

A series of Cu/Al_2O_3 catalyst were prepared (co-precipitation, see paragraph 4.4) having contents of Cu of 2, 8, 14, 20, 26 and 33% of Cu to Cu+Al (metal%), where the latter corresponds to stoichiometric copper spinel similar to the Cu spinel catalyst normally tested. The Cu series samples were all calcined at 850°C.

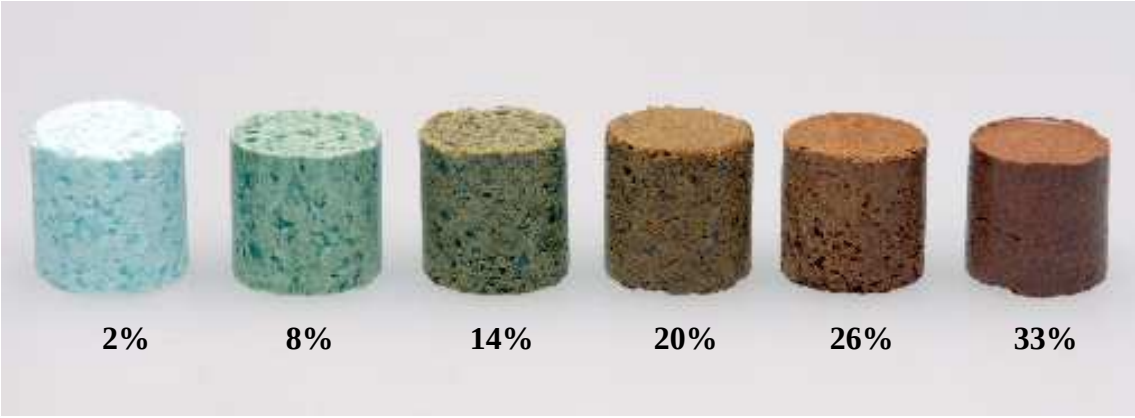

Figure 5-28: Picture of a pellet from each of the preparations in the Cu series. The figures indicate the Cu content of metals (Cu + Al).

Figure 5-28 shows how the Cu content of the catalyst influences the colour of the final calcined preparation. All the samples except for the 2% sample was analysed in the kinetic set-up.

The activity tests were conducted in the kinetic test set-up (see paragraph 3.5) by feeding a 40/60 ethanol:water mixture, diluted with nitrogen over 10g of catalyst loaded in a single-pellet-string bed configuration at atmospheric pressure and a temperature of 300°C. SV_m variations (at constant initial ethanol and water partial pressures) were made in order to create conversion profiles.

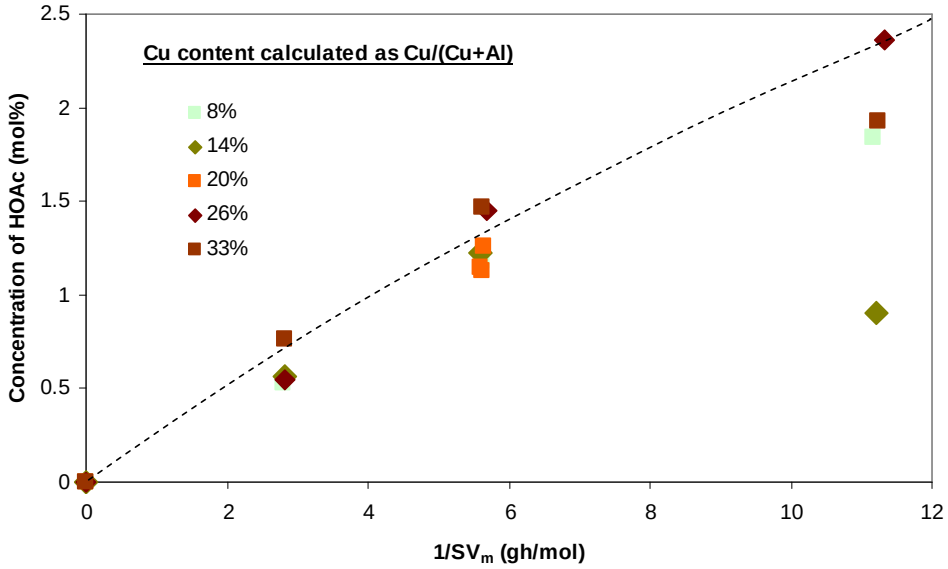

Figure 5-29: The conversion profiles of Cu/Al_2O_3 catalysts with Cu metal% 8-33% fed with a 40/60 ethanol:water mixture at a temperature of 300°C and atmospheric pressure.

Figure 5-29 shows the conversion profiles found for the Cu/Al_2O_3 catalysts with the different Cu loadings. As may be seen, disregarding a single point for the lowest SV_m in the 14% Cu profile, there was not found any major difference in the degree of conversion for the catalyst with the different Cu loadings. By mistake the SV_m for the 20% Cu sample was not varied according to the plan, but the three orange points on top of each other ($1/SV_m$=5.6 (g·h)/mol) align with the other profiles. However, the side-product formation of the condensation products on the catalyst increased drastically with decreasing Cu content, indicating that the activity of the alumina support shows more dominance as the Cu content decreases. The experiment with the 2% Cu sample was given up due to too high side-product level.

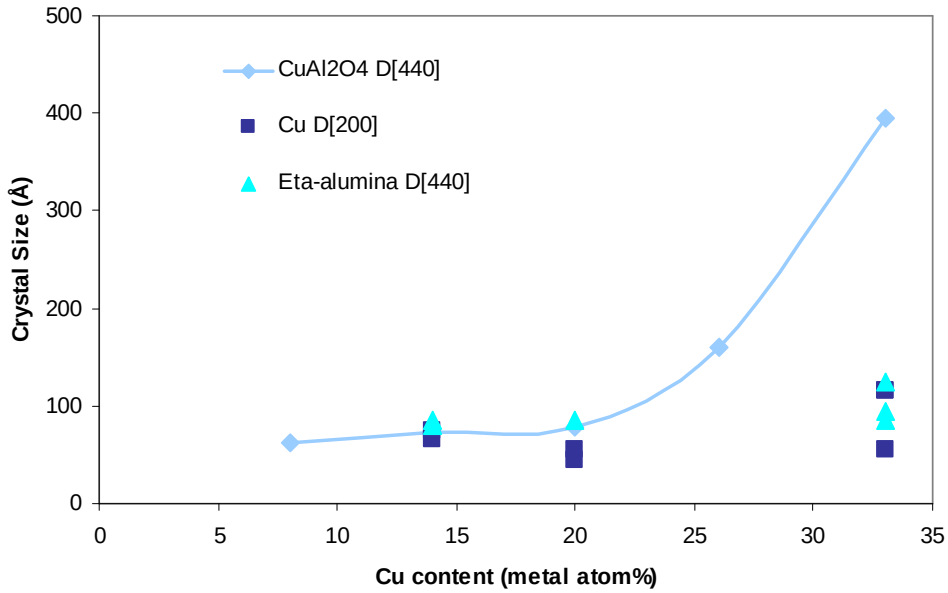

Figure 5-30: The crystal size of the spinel and the Cu crystals respectively as a function of the Cu content of the fresh calcined CuO/Al_2O_3 catalyst and the spent, passivated (see paragraph 5.7.2) Cu/Al_2O_3.

XRPD analyses made *ex situ* on the spent catalysts (see Figure 5-30) show that even if the Cu content of the CuO/Al_2O_3 highly affects the size of the Cu spinel crystals ($CuAl_2O_4$) formed during its calcination, the Cu crystals and the alumina spinel crystals resulting from the decomposition of the Cu spinel crystal structure during reduction is more or less of the same size independently of the Cu content.

5.8 Spent catalyst analyses

All while the characterisation of the Cu spinel catalyst was carried out experiments were carried out on the Cu spinel catalyst varying the feed composition, for example the ethanol to water molar ratio and more or less of unconverted intermediates and side-products. The catalyst samples unloaded after the non-oxidative dehydrogenation experiments were rather strong mechanically and had a steady blackish appearance on the outside, while when halved a vaguely red shading of the black cylindrical pellet appeared closer to the centre.

5.8.1 Cu crystal size, XRD

XRD was routinely used in order to follow how the catalyst phases and especially crystal size were affected by the reaction conditions. By plotting the Cu D[200] versus time on stream it could be found that the Cu crystals on the Cu/Al_2O_3 catalyst stabilised on a level of about 150Å (see Figure 5-31).

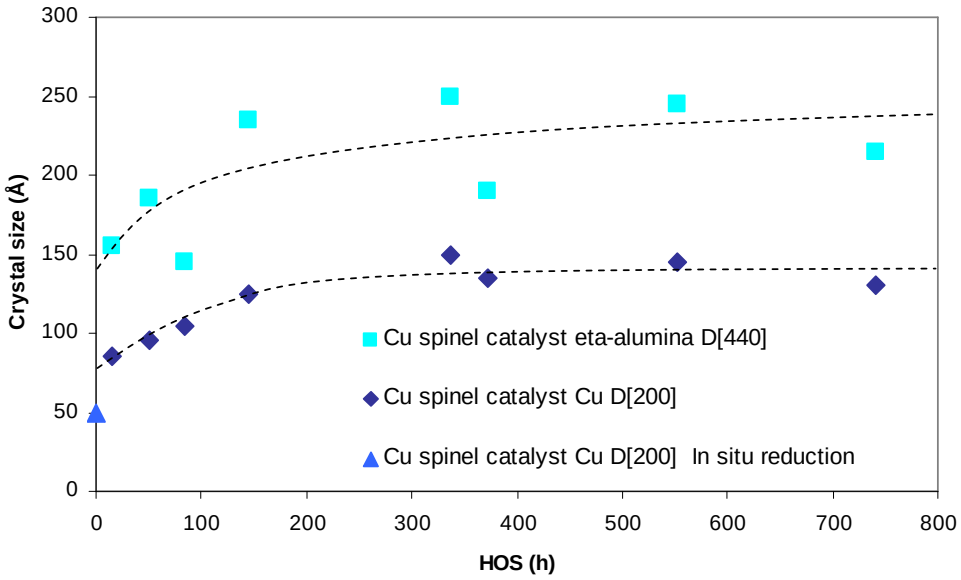

Figure 5-31: A plot of the Cu D[200] crystal and η-alumina D[440] crystal size as a function of hours on stream.

The graph represents both partly and totally deactivated catalyst samples. The sintering of Cu on the catalyst surface is an explanation to the moderate decrease of activity but not to the detrimental complete deactivation of the catalyst. It may be remarked that the sample reduced *in situ* (crushed) has an initial D[200] which is 50Å and which over 10 hours stabilises at 70Å.

5.8.2 Cu crystal size, XAFS

A sample of the deactivated Cu spinel catalyst unloaded from the experiment described in 5.6 (subjected to increasing degree of acetaldehyde co-feeding) was sent to XAFS analysis in order to study the longer term impact on the Cu crystal size.

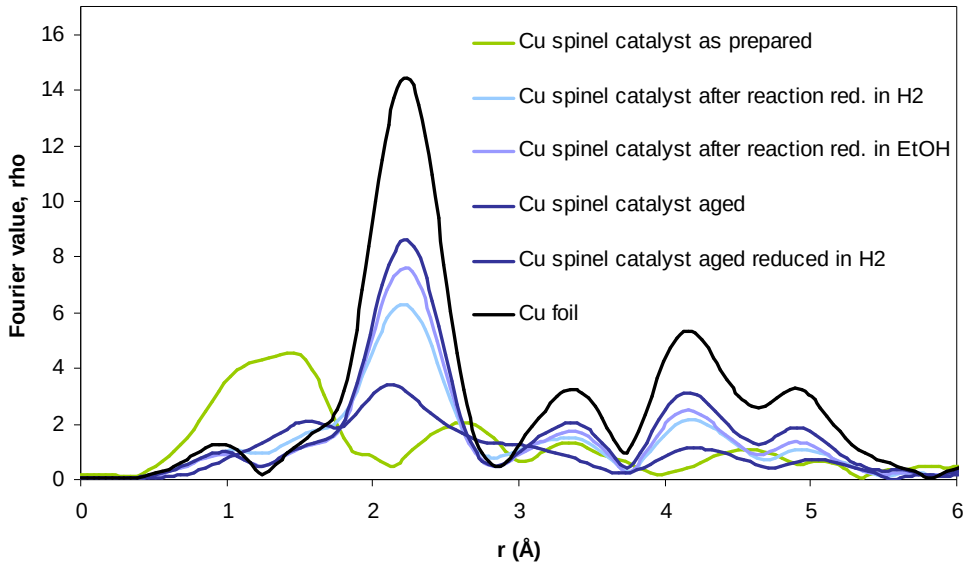

Figure 5-32: The Fourier transformed EXAFS spectra of the aged Cu spinel in comparison with the fresh (as prepared).

The Cu coordination numbers obtained from the Fourier transformed EXAFS spectra (see Figure 5-32) shows that the Cu particle size has only grown modestly from the state estimated for the sample shortly exposed to reaction conditions and to the state of the sample coming from the deactivated catalyst, passivated (see paragraph 5.7.2) and unloaded after 740 h of operation. It was found that the Cu crystal size seemed to be only slightly effected by the long term run, and the deactivation could not be explained by crystal growth or sintering.

5.8.3 Surface area, pore volume and mean pore radius

A sample of the Cu spinel catalyst having suffered from the complete deactivation after exposure to a 32/52/10 ethanol:water:acetaldehyde feed in 51 h was sent for surface area analysis. A fresh catalyst sample (reduced and passivated, see paragraph 5.7.2) was sent for analysis too. The pore volume or its distribution as to the pore size had not changed remarkably, though a small decrease on both values was found. Table 5-3 shows the surface area and the mean pore radius as found by Hg porosimetry.

Table 5-3: The surface area and the mean pore radius of the fresh and the spent catalyst.

Catalyst sample	Surface Area (m^2/g)	Mean pore radius (Å)
Fresh	27.5	245
Spent	23.6	224

5.8.4 Carbon analysis

Samples of unused and spent Cu spinel catalyst from the non-oxidative dehydrogenation experiments were sent for carbon analysis. The unused Cu spinel catalyst had a carbon content <0.1 wt%; the few wt% graphite originally mixed with catalyst powder prior to pelletising as lubricant is apparently virtually removed during the calcination of the catalyst at 850°C (presumably due to oxidation). For the group of deactivated catalyst samples a significant increase of the carbon concentration, 1.6-6 wt% of C, of the catalyst was measured (LECO combustion analysis method, see paragraph 6.5). Cu spinel catalysts which were active until unloading had carbon levels of 0.7-0.9 wt%, i.e. much lower amounts of carbonaceous compounds had formed. This seemed like the most marked difference between freshly reduced and spent samples.

Further investigations to pursue the origin and the kind of carbonaceous compounds deposited were made through an ex situ TEM analysis on deactivated samples from both non-oxidative and partly oxidative dehydrogenation experiments. The TEM results are described in paragraph 5.1.

5.9 Partly oxidative dehydrogenation

In order to expand the experience on the partly oxidative dehydrogenation and to better follow the temperature profile under these operating conditions a number of experiments were conducted in the new set-up, where such temperature measurements are possible. The concentration of oxygen was gradually increased by changing the air flow in order to follow the response by the reactor system.

5.9.1 Crushed catalyst

In an earlier test whole Cu spinel catalyst pellets underwent rapid deactivation after a few hours of operation, whereas the crushed catalyst showed better stability. In order to pursue the possibility of conducting the autothermal dehydrogenation of ethanol with a special catalyst formulation (for example as a catalysed hardware on monoliths) a sample of crushed pellets reduced in ethanol at 250°C was studied. The test was conducted in the small reactor 2 (reference is made to 3.3.1).

Two thermocouples were installed in the annulus between the reactor and the ceramic oven adjacent to the bed top and the middle to give indicative bed temperatures and furthermore a thermocouple was installed in the thermo well measuring the temperature in the bottom of the bed, in order to follow the course of the exothermic/endothermic behaviour of the reaction (see Figure 5-33). The temperature measurements in the top and middle position indicate a kind of average temperature of the catalyst bed and the oven. This is not optimal, as preferably the thermocouples should be installed in the bed itself, if possible.

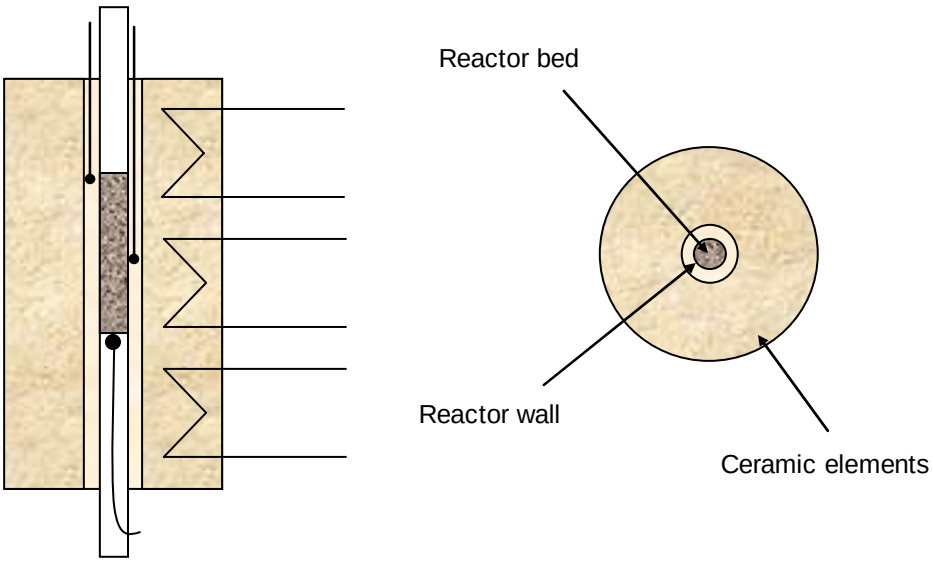

Figure 5-33: Side cross sectional view and top view of reactor alignment in the ceramic oven. Two thermocouples were installed in the annulus corresponding to the bed top and the bed middle. A further thermocouple was installed in the thermo well in contact with the catalyst support.

It was estimated beforehand how much oxygen would suffice to obtain autothermal or rather slightly exothermal conditions, aiming for a temperature of 300°C and the degree of conversion as observed for the screening experiment, by means of a GIPS mass and heat balance calculation (not enclosed). As may be seen in Figure 5-34 the fraction of oxygen in the total composition is a little more than 6%. In this calculation the constant concentration of ethanol was secured by adjusting the nitrogen flow rate in accordance with the air flow rate. Apart from the basic principle of changing only one parameter while keeping the other constant this secured also that the explosion limits were not surpassed.

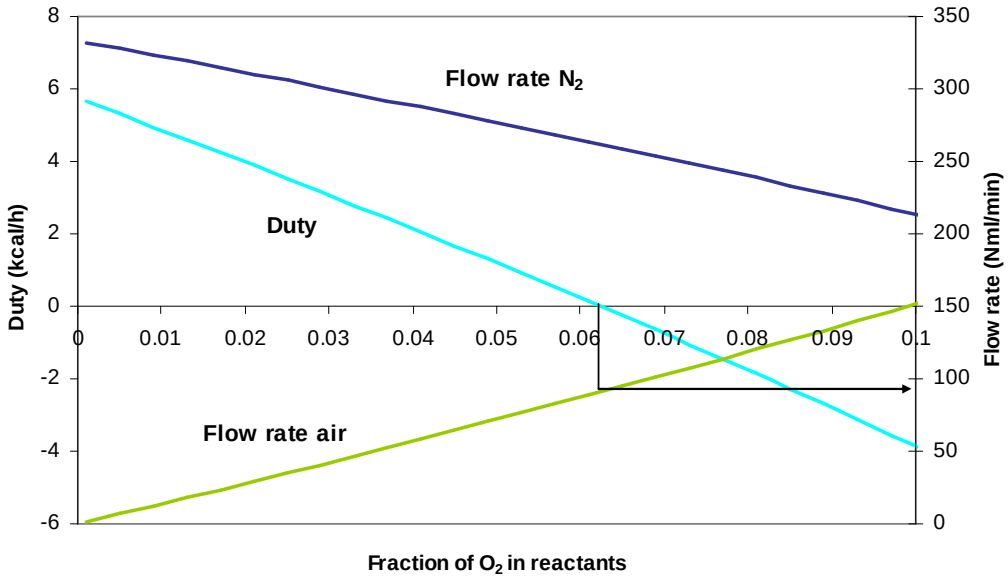

Figure 5-34: Calculated reactor duty as function of the air flow rate and corresponding nitrogen flow rate for the partly oxidative experiment, assuming the degree of conversion equal to the previous from the mass balance experiment. Feed is 60/40 ethanol:water at a rate of 0.5 ml/min, nitrogen flow rate is constant (325 Nml/min).

From this calculation it was predicted that at least 70 Nml/min of air had to be added in order to obtain the reaction conditions corresponding to autothermal synthesis of acetic acid in an industrial reactor on a 60/40 ethanol:water feed.

6.75 g of a 1-1.4 mm sieve fraction of the Cu spinel catalyst was loaded into the reactor. The catalyst was reduced in 99.9% ethanol at 250°C (0.5 ml/min). Then the oven was set on 300°C, the liquid feed was changed to a 60:40 (ethanol/water) mixture being pumped at a rate of 0.5 ml/min, the nitrogen flow rate was 325 Nml/min and the initial air flow rate was 0. After the stabilisation of the system a first condensate sample was acquired and the air flow was changed to 10Nml/min and the temperature profile was recorded. On the air step-ups a prompt temperature response of 10-15°C increase of the exit temperature was seen followed by a decrease to about the same temperature as before the step.

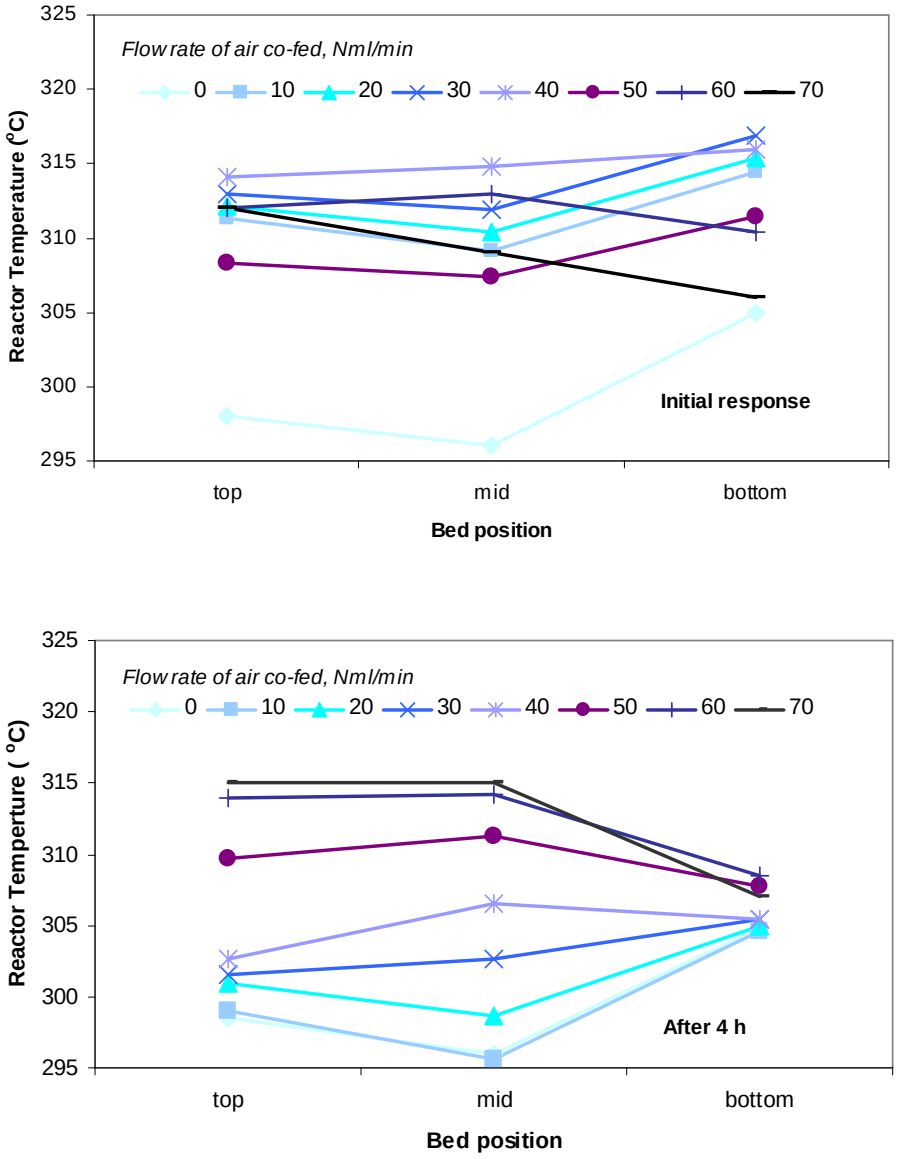

Figure 5-35: Reactor temperature profile at 300°C with a 60/40 ethanol:water feed. Upper: Initial effect of adding 10-70 Nml/min of air. Lower: The 'steady state' effect (4h) of adding 10-70Nml/min of air.

The temperature mainly stabilised over 1 h, but the complete stabilisation was first obtained after about 4 h, and the temperature profile was recorded again. Then the air flow rate was raised by another 10Nml/min to 20 Nml/min. These steps were repeated until a flow rate of 70 Nml/min was obtained. Keeping in mind that the top and the middle temperatures are dampened the temperature 'profiles', initially and after 4 h, of the catalyst bed at the different air flow rates are shown in Figure 5-35.

By comparing the individual temperature profiles with the temperature profile with 0 Nml/min addition of air, it is indicated that the exothermic part of the reaction primarily takes place in the top of the catalyst bed. Response factors for the individual components were not available at that time but the relative concentrations of the individual components to ethanol were calculated. It is seen in Figure 5-36 that the activity drops off when the catalyst is exposed to 40 Nml/min of air (3% oxygen) which is about half the required amount to obtain autothermal conditions. This deactivation coincides with the shape change of the steady state temperature profile in Figure 5-35, bottom.

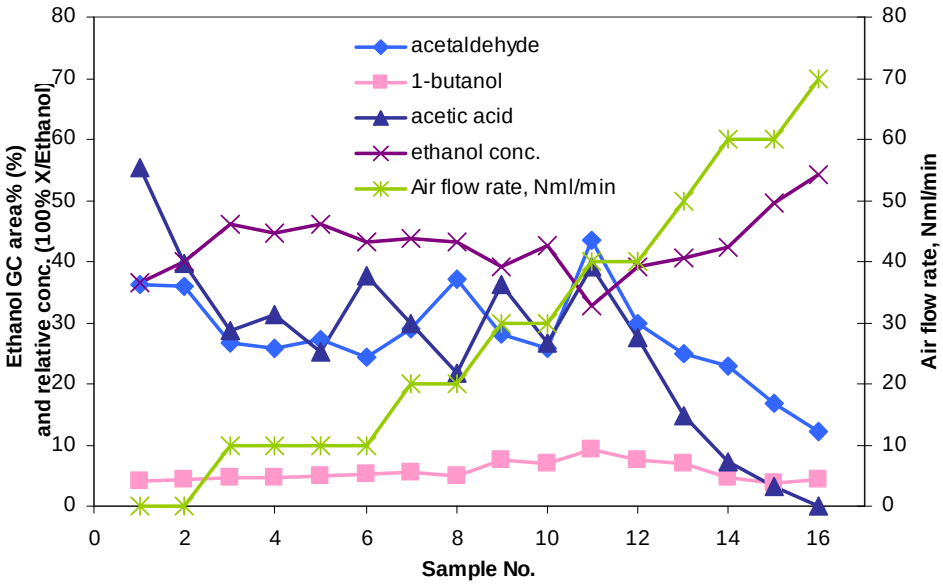

Figure 5-36: The ethanol concentration and the relative concentrations of effluent components with increasing air flow rate. Feed is 60/40 ethanol:water at a rate of 0.5 ml/min

A further increase of the air flow rate further decreased the activity while further lifting the bed top temperature indicative of an exothermic reaction taking place. Notably, the exit temperature was maintained in any case indicating that the oxidative conversion of 6% of the ethanol (which may take place according to stoichiometry) is managed over the catalyst bed, until the catalyst dies and no acetaldehyde is available for oxidation. Accordingly, it seems that the catalyst activity of the oxidation reaction maintains at a higher level than the dehydrogenation reaction does when increasing the air flow rate. The deactivation as found by GC took place in parallel to the observation of an increasingly yellow coloration of the condensate during the increasing flow rates indicative of condensation products increasingly being formed. This was confirmed by GC-MS showing an increasing number of peaks of higher alcohols, aldehydes and acids. And soon after the operation on 70 Nml/min of air the catalysts deactivated abruptly and became totally inactive.

5.9.2 Whole catalyst pellets

It was found in the reduction study that whole pellets exhibited greatly improved stability when reduced in hydrogen as compared to reduction in ethanol. As previously established the reduction in hydrogen was preferred over reduction in ethanol for obtaining a stable catalyst. A single-pellet string experiment was conducted in the new test set-up in reactor 2 in order to study the activity of the Cu spinel catalyst reduced in hydrogen. A further purpose of the experiment was to study the response to the introduction of a feed composition reflecting the feed and recycle admixture stream of an industrial plant.

The catalyst was reduced in 3% H_2 in Ar ramping up to 340°C with 1°C/min (100 Nml/min) for 5 hours. The oven was the set on 320°C, the initial feed introduced was a 40/60 ethanol:water mixture, the nitrogen flow rate was 330 Nml/min and the initial air flow rate was 0. Sampling was made after approximately one hour of operation whereafter the liquid feed was changed to a mixture of 80wt% 60/40 ethanol:water + 20wt% 50/50 acetaldehyde:water being pumped at a rate of 0.5 ml/min. After another stabilisation a sampling was made. While maintaining the liquid feed the air flow rate was increased to 50 Nml/min, corresponding to autothermal conditions. After the stabilisation of the system a third condensate sample was acquired while the air flow was unchanged. Several more samples were acquired the same day. It was observed that the condensate from one sample to the next became more yellow, indicative of an increasing level of condensation side-products, after the introduction of air. The experiment was resumed the next day and went on for the next day too, but still more yellow and less acetic acid containing condensate was achieved (see Figure 5-37). The experiment was stopped due to the deactivation. The catalyst sample was passivated (see paragraph 5.7.2).

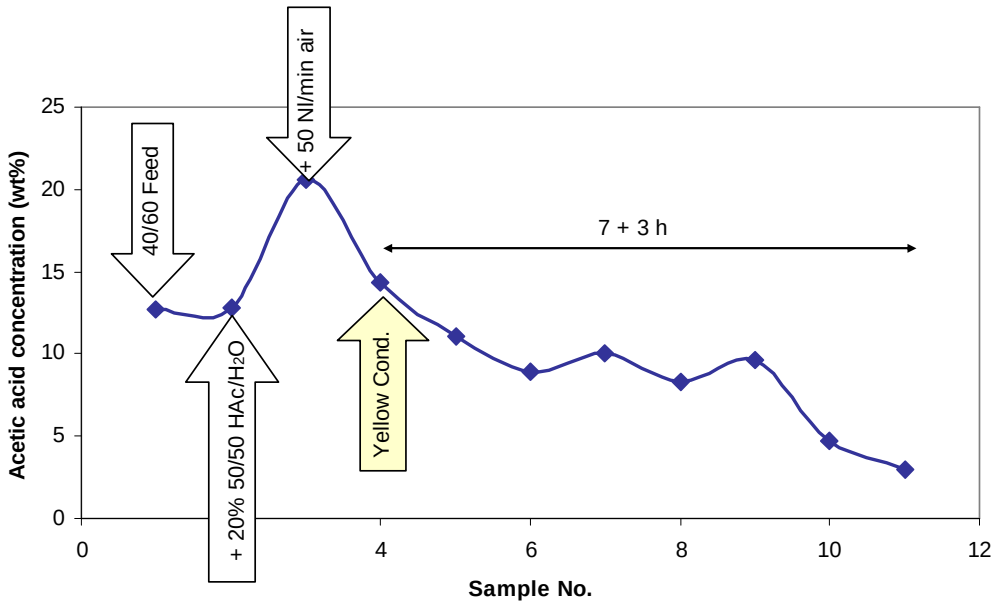

Figure 5-37: The acetic acid concentration in the condensate from the new set-up during exposure to 50 Nl/min air. Samples 1-2 are prior to air addition.

It seemed, however, that the addition of air immediately leads to an initial increased production of acetic acid. This may be due to the temperature increase in connection with air addition as observed in the earlier experiment.

5.9.2.1 SEM analysis

By visual inspection it was evident that the operation under the partly oxidative conditions had changed the structure of the catalyst non-uniformly. The outer surface of the uppermost catalyst pellet was orange/green dappled, while the lowermost was mostly greenish. When parted, the inner part of the catalyst cylinders revealed numerous shifts of colour indicative of structural changes. Both the uppermost and the lowermost pellet had a dominant, mechanically weak blackish core. These samples were sent to SEM for combined C analysis and analysis for structural changes.

The purpose of the structural analysis was to study how it changes over the radius of the pellets, as apparently a centre-symmetrical colouring of the pellets had taken place as a result of the partly oxidative operation (see Figure 5-38) on the circular cross section of the cylinder.

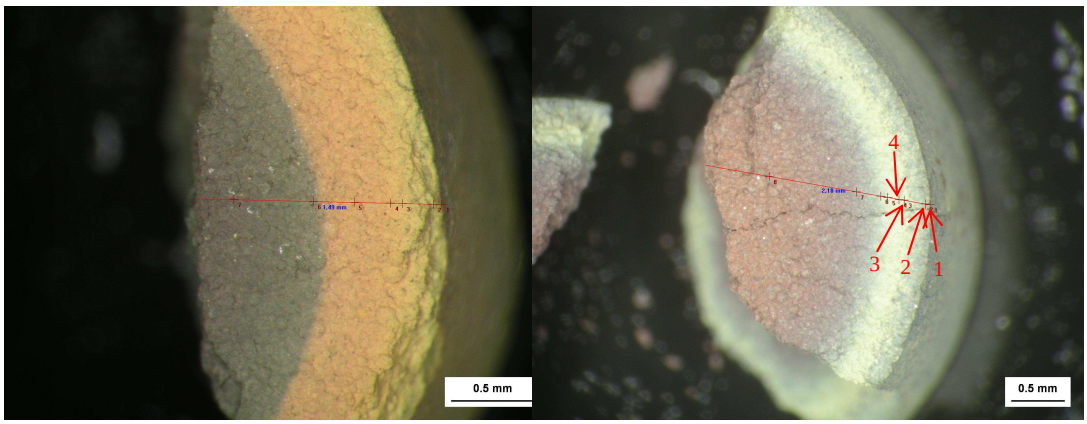

Figure 5-38: SEM analysis. Left: The multi-coloured shell of the uppermost pellet (Cu spinel) in the partly oxidative dehydrogenation of ethanol. Right: The multi-coloured shell of the lowermost pellet in the partly oxidative dehydrogenation of ethanol. The greenish/yellow ribbon (outermost shell) are represented by points 1-4.

For each of the 2 pellets 2 samples were mounted on an Al support with double-adhesive tape without Ag paint.

The structures in the transitions between the coloured layers of the outer part of the shell were carefully studied with Quanta-SEM (high vacuum, 5kV). Concurrently, the carbon content over the radius was estimated (low vacuum (0.8 mbar), 15 kV; EDS, lower detection limit 1 wt%).

Some big crystals are seen in the reddish phase of the uppermost pellet, which are not seen in the lowermost pellet (see Figure 5-39). Large crystals could be indicative of a high temperature.

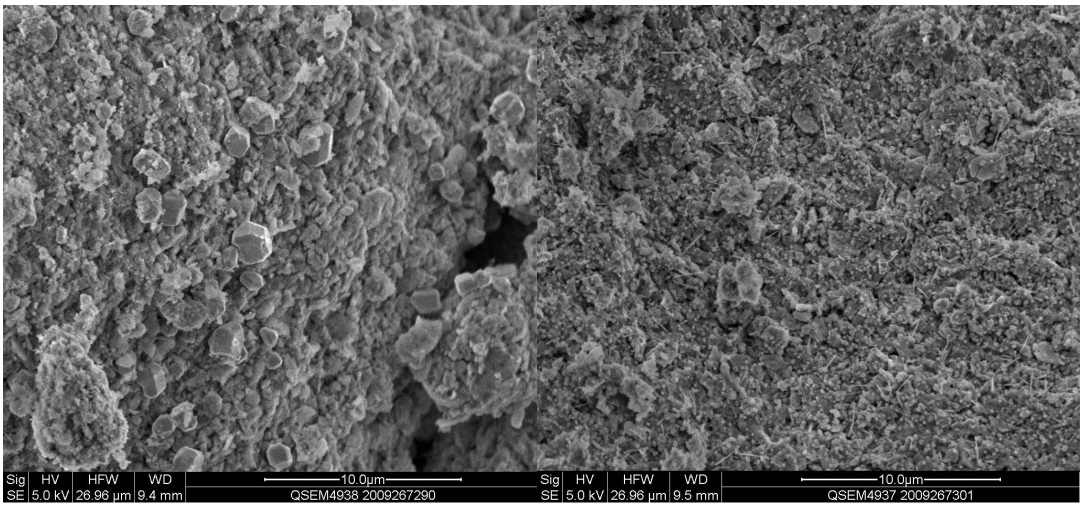

Figure 5-39: Left: QSEM picture of the black/reddish structure of the uppermost pellet 500microns from the periphery. Right: QSEM picture from the blackish structure 500 microns from the periphery.

On the other hand, the lowermost pellet seems to have more structural transitions than the uppermost. Besides, the lowermost pellet contains needle shaped particles in the centre of the pellet (see Figure 5-40), while no “needles” were found in the greenish/yellow ribbon (points 1-4 in right picture, Figure 5-38).

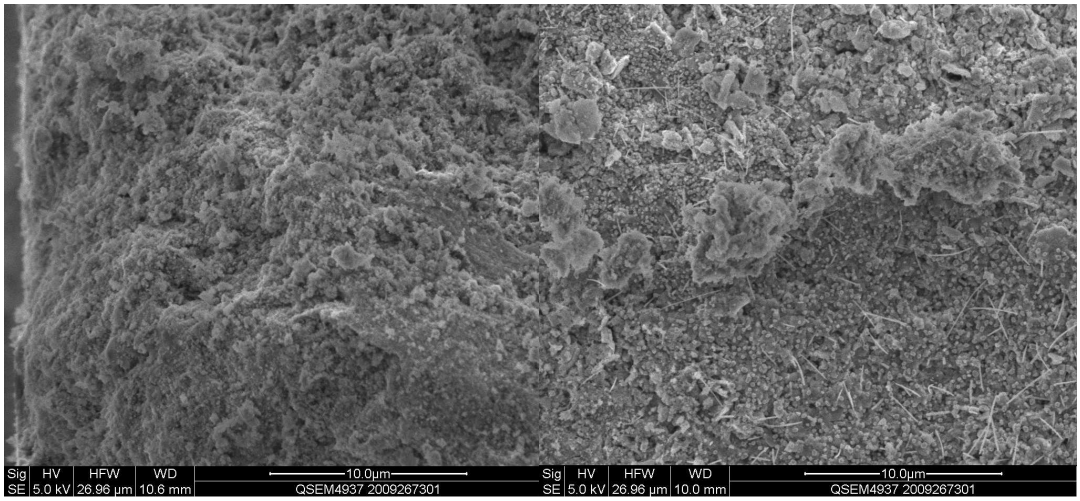

Figure 5-40: Left: QSEM picture of outer surface of lowermost pellet. Right: 500 micron from periphery of pellet. “Needle” shaped crystals are found inside the yellow ribbon, Figure 5-38.

Needles are a significant indication of a phase change which has been observed in systems with alumina before.

The simultaneous EDS analyses indicate that the carbon level is higher at the outer surface of the pellet as compared to the inner pellet. Figure 5-41 shows the C-profile through the samples from the uppermost pellet (TOP) and the lowermost pellet (BOTTOM) exposed to partly oxidative reaction conditions.

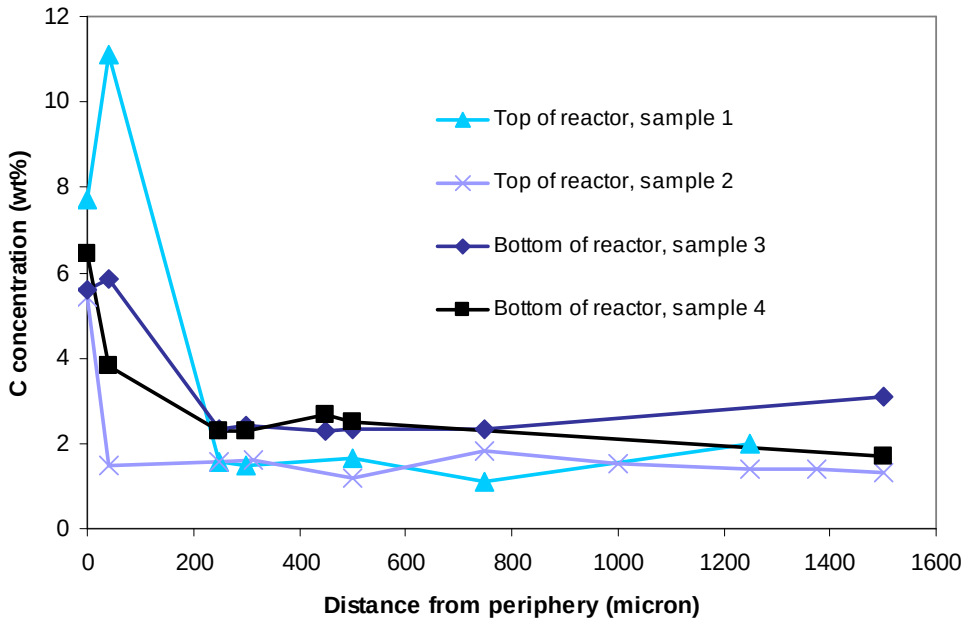

Figure 5-41: The C profile (inclusive graphite) through the spent pellets unloaded from the top and bottom of the reactor after the run under partly oxidative conditions.

The EDS analyses indicate that more carbonaceous material is present at the outer surface of the catalyst, both at the top and at the bottom of the reactor. However, with measurements close to the outer surface there is a risk that the analysis is influenced by the presence of carbon tape. Looking only at the inner parts of the catalyst pellets it appears that the catalyst pellet unloaded from the bottom of the reactor has a slightly higher level of carbon as compared to the pellet unloaded from the top (2.5-3 wt% vs. 1.5-2 wt%). In comparison with the C content of the unused Cu spinel catalyst of <0.1 wt% the carbon level (5.8.4) had increased during the partly oxidative operation.

5.10 TEM: Coke or wax?

From the carbon analysis there seemed to be a correlation between the formations of carbonaceous compounds and deactivation. Indications were that the deactivation took place according to the same pattern, however more or less accelerated by the operating conditions (increasing level of condensation products and sudden deactivation). In order to understand what could be the cause of the formation of carbonaceous compounds, it would be useful to know which kind of carbonaceous compounds had formed, in turn in order to counteract the mechanism behind. Furthermore the physical appearance and the mechanical strength of the spent catalyst from the non-oxidative and the partly oxidative dehydrogenation, respectively, were very different as described.

A TEM analysis was made in order to shed light on these unknowns and differences. Four samples of catalyst were sent for TEM analysis, two from a non-oxidative experiment (top and bottom, 4.8wt% C and 1.6wt% C found by C analysis) and two from a partly oxidative experiment (top and bottom) in which the catalyst loadings deactivated. The samples for analysis were taken both from the outer surface and the

centre of the pellets, respectively. The material for analysis was ultrasound treated in ethanol and a droplet was transferred to a Cu grid with lacey carbon film. The carbon content of the samples was investigated by TEM recording on CM200.

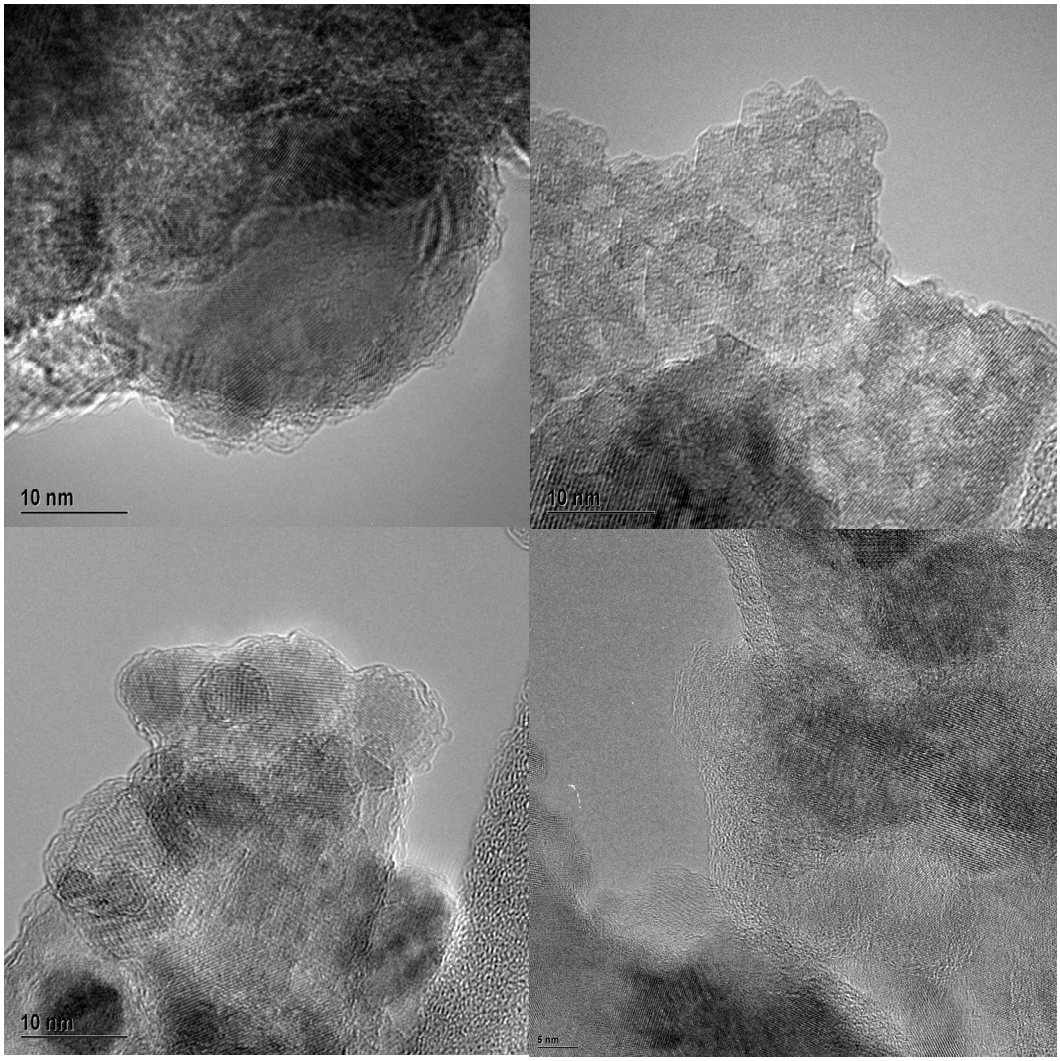

Figure 5-42: TEM pictures of analysed samples acquired in order to find the nature of carbon. Upper left: Cu spinel pellet with 4.6% C unloaded after non-oxidative dehydrogenation. Upper right: Cu spinel pellet with 1.6% C unloaded after non-oxidative dehydrogenation. Lower left: Cu spinel pellet unloaded from top of bed after partly oxidative dehydrogenation. Lower right: Cu spinel pellet unloaded from bottom of bed after partly oxidative dehydrogenation.

In TEM microscopy carbon is seen either as whiskers, gum, or other kinds of carbonaceous structure (for example amorphous).

The analyses of the 4 samples from the outer surface showed no C. But carbon was found in the centre of all samples. Figure 5-42 shows the resulting TEM pictures from the 4 analyses of the samples taken from the centre of the catalyst pellets. The non-quantitative content of carbonaceous structures was estimated to be low in both of the samples from the non-oxidative experiment. The highest carbon content was found in the top pellet from the partly oxidative experiment.

The TEM pictures show that no whiskers are formed (easily recognisable bulky nanotube feathers and spirals). Rather, there was found graphitic carbon or another

kind of a spine layered structure smearing out on both the Cu crystals and the support surface (recognised as ‘woven’ ribbons of strings). This carbonaceous material may comprise graphite originally mixed with the catalyst powder before pelletising. Judged by the distance between the individual carbon layers more different structures are dealt with. The carbon spines in question apparently have a content of hydrogen, as for example waxes, which results in a larger distance between the carbon spine planes than the pure graphitic does (4.9Å observed vs. normally 3.4Å for graphite).

5.11 Discussion

The Cu spinel catalyst has shown satisfactory initial activity. As compared to for example a Cu based catalyst applied in methanol synthesis having a typical STY EOR of 1 kg/(kg·h) at 80 bar, an acetic acid activity of 0.35-0.5 kg/(kg·h) (see paragraph 4.6 and Figure 6-6) is not ‘unreasonable’ and it meets the target set under process design considerations (see paragraph 4.11). The major problem with the Cu spinel catalyst is that it deactivates for various reasons of which some were identified and some still have to be elucidated. The physical changes induced upon the catalyst being responsible for the deactivation were pursued.

5.11.1 Calcination

The Cu spinel catalyst is produced by the co-precipitation method (see paragraph 4.4) yielding in the first round $CuAl_2(OH)_x(CO_3)_y$. During a first calcination of the catalyst powder up to 400°C the CO_2 is sublimated and catalyst is oxidised into CuO/Al_2O_3. The pre-calcined powder is then pelletised and may be post-calcined to a higher temperature, if desired. Higher temperature calcination of the Cu spinel may provide for a higher mechanical stability, but furthermore structural changes may also occur. *Susnitzky et al. (1991)* present a phase diagram of Cu_2O/CuO/alumina, where Al_2O_3 and CuO are the only stable phases below 620°C whereas above this temperature and up to 1000°C $CuAl_2O_4$ becomes stable (in combination with either Al_2O_3 or CuO, depending on the Cu to Al ratio). The rate of solid reaction $CuO + Al_2O_3 \rightarrow CuAl_2O_4$ is found to be a function of the calcination temperature and time. By post-calcining a catalyst already post-calcined at 550°C further at 850 and 1100°C a series of CuO/Al_2O_3 catalysts was prepared. An XRPD analysis of the 550°C calcined catalyst confirms that mainly CuO/Al_2O_3 and only traces of Cu spinel is found, while the XRPD analysis of a fresh sample post-calcined at 850°C for 2 h (4 hours including ramping) we only find $CuAl_2O_4$ (260Å, *ex situ* XRD). The sample calcined at 1100°C also only shows $CuAl_2O_4$ but with a crystal size of more than 1000Å.

In the screening study of this work it was found that the catalyst post-calcined at 850°C had the optimum activity and a better selectivity compared to the others, calcined at 550 and 1100°C. *Patrick et al. (1990)* found by investigation of CuO/Al_2O_3 calcinations that the formation of $CuAl_2O_4$ was limited by solid-state diffusion and being retarded in the upper temperature region by diffusion through a growing layer of sintered Cu aluminium oxide. A graphical plot (see Figure 5-43) of their results shows that the non-stoichiometric compositions, both above and below the stoichiometric spinel ratio, in fact yield lower fractions of $CuAl_2O_4$ even at much longer duration of the calcinations process. All yielded fractions of $CuAl_2O_4$ for the non-stoichiometric samples are significantly below their maximum theoretically achievable value.

The observations made in this work fit into these results and so do largely the individual results of the studies on stoichiometric compositions by *Kumar et al. (2008), Barrosso et al., 2006, and Faungnawakij et al. (2008)*: the conversion of stoichiometric CuO/Al_2O_3 to $CuAl_2O_4$ increases with time and calcination temperature.

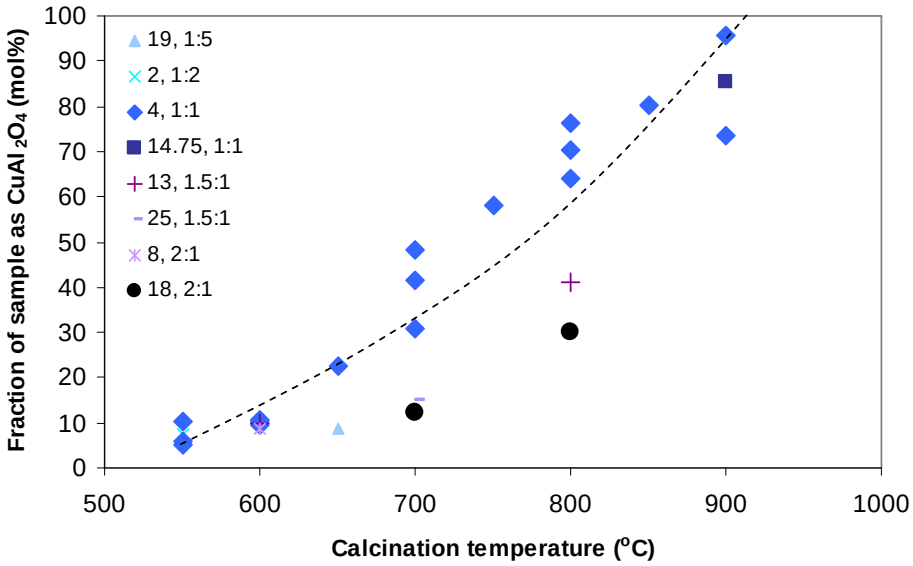

Figure 5-43: Graphical presentation of data from *Patrick et al.(1990)* of CuO/Al_2O_3 samples conversion to $CuAl_2O_4$ during calcination. Legend values are calcinations duration and $CuO:Al_2O_3$ molar ratio. The formation rate of $CuAl_2O_4$ is optimal for the stoichiometric ratio of $CuO:Al_2O_3$.

In accordance with the results in Figure 5-43 *Kim et al. (2001)* finds that the calcining of a 10wt% CuO/Al_2O_3 at 700°C for 10 h almost did not transform any CuO to spinel. However, in contradiction to this, *Fernadez-Garcia et al.* find that calcining at 650°C for 2 h is enough for the transformation of 5wt% loadings of Cu on alumina. It was found by XAFS that the copper in the model catalyst (with 2.5wt% Cu on alumina) calcined at 850°C for 4 h is in a spinel structure. In the work by *Alejandre et al. (1999)* a Cu-Al series was studied with Cu:Al of 0.5 (stoichiometric to spinel), 2 and 3. The samples were calcined to 400, 600, 650, 800 and 1000°C. They found that the rate of formation of copper aluminate depends inversely on the Cu content of the samples above the stoichiometric ratio of $CuO:Al_2O_3$.

It overall seems that at lower or higher Cu loadings of CuO on alumina than stoichiometric the transition of CuO into spinel becomes harder or slower, i.e. it requires higher calcination temperature and/or longer calcination time, which can be attributed to the kinetics associated with the solid state formation of spinel. The scattering of results may indicate a dependency on the preparation methods used.
In this work there is characterisation evidence for the full transition of CuO/Al_2O_3 to $CuAl_2O_4$ on both the stoichiometric precursor (prepared by co-precipitation) by *ex situ* XRPD (see paragraph 4.4.2.1) and the sample with low Cu loading (prepared by impregnation) by EXAFS analysis (see paragraph 5.7.1) when calcining these at 850°C for 4 h.

5.11.2 Reduction

The Cu spinel catalyst, calcined at 850°C, was reduced primarily in two steps during TPR with a small peak around 230°C and in a large, broad reduction peak around 400°C in agreement with *Tanaka et al. (2003)* studying a similarly prepared $CuAl_2O_4$ catalyst.
Barroso et al. (2006) found good evidence for the low temperature TPR peak being ascribed to the reduction of residual CuO, as observed by XRD. The *ex situ* XRD studies by *Patrick et al. (1990*) also support that most of the CuO is reduced more easily than $CuAl_2O_4$, but not all due to the retardation induced by sintering of CuO or Cu, isolation of CuO by the building of a $CuAl_2O_4$ shell, or strong interaction of CuO with Al_2O_3. It was further found that an excess of alumina retards the reduction. Intermediate $CuAlO_2$ and Cu_2O were observed during reduction of a stoichiometric spinel to Cu(0). XANES in this work shows that the reduction only goes via Cu(I) for the model catalyst, not for the spinel catalyst. *Kumar et al. (2008)* observed a single peak at about 250°C in a TPR experiment reducing a close-to stoichiometric sample having only CuO phases due to insufficient calcination. *Fernandez-Garcìa et al. (1998)* also find a low temperature reduction peak which they attribute to the reduction of amorphous CuO. In correspondence herewith TPR analyses by *Alejandre et al. (1999)* showed one reduction peak at 250°C for the sample calcined at 600°C, a small reduction peak at 250°C and two further peaks around 400°C and 480°C and for the sample calcined at 1000°C (almost pure copper aluminate) no reduction peak showed at 250°C, a small peak showed at around 400°C and the highest temperature peak grew and broadened.

A further important finding by *Alejandre et al. (1999)* for the stoichiometric to high loadings of Cu on alumina is that for the samples calcined at above 700°C the degree of reduction is adversely affected by a high calcination temperature but increases with the Cu loading. On the other hand the CuO and $CuAl_2O_4$ particles obtained after calcination are larger for samples with a high Cu loading, which may in turn adversely affect the Cu surface area of the reduced sample. It was however found in this work in the series of Cu variation, that even if the spinel crystal size is increasing with the Cu load the size of the Cu crystals resulting from the reduction is independent hereof.

Based on the above, our Cu spinel catalyst, having been calcined at a temperature around 850°C and having had CuO detected by *ex situ* XRD, the low temperature peak may likely be ascribed to the reduction of small amounts of bulk CuO, which is reduced reasonably fast already at temperatures 150-225°C (*Gusi et al., 1986*) and easier than strongly alumina associated CuO (*Alejandre et al., 1999*). Present works analysis by XAFS shows almost full reduction at 380°C and by TGA measurements the degree of reduction at 380°C was determined to be about 95%.

Amano et al. (2006) furthermore found that the reduction temperature (max. hydrogen consumption) increases with decreasing Cu loading in the Cu load range 0.5-5wt%, and that the TPR peaks broaden with decreasing Cu loading. Their 3wt% Cu on alumina yields 0.84 H_2/Cu up-take up to 500°C whereas on the 0.5% Cu on alumina sample the hydrogen uptake was 0.34, showing the part wise lesser reduction to metallic Cu for the lower loading. It is argued this may be due to the more isolated nature of the Cu(II) for the low Cu loadings on the alumina surface. This was confirmed by *ex situ* XANES and XAFS analyses on the reduced samples, where the 0.5wt% Cu

sample had a Cu(I) peak and the 3wt% Cu on alumina showed the characteristic spectrum of Cu foil; and an EXAFS Fourier transformation revealed low coordinated Cu for the 0.5wt% Cu load. In this work the reduction temperature for the 2.5wt% model catalyst was not observed to be higher than for the Cu spinel catalyst in the XAFS analysis, i.e. the sample was found to be reduced to the same degree at 380°C as was also the stoichiometric spinel catalyst. However, it was observed in present work by XANES and TGA characterization analyses, that by subjecting $CuAl_2O_4$ to the reducing agents hydrogen and ethanol, respectively, an only near to full reduction of framework Cu(II) to metallic Cu(0) may be obtained with adequate amounts of reducing agent. According to XANES analysis also the progression of the Cu reduction is similar whether the reducing agent is hydrogen or ethanol. It relies perhaps on the fact that the ethanol reducing agent oxidizes to acetaldehyde in contact with the catalyst (as established by TPR, see paragraph 5.7.3) thereby producing hydrogen throughout the temperature range of reduction, such that in reality in both cases it is hydrogen that reduces the Cu in the $CuAl_2O_4$ framework to metallic Cu particles. The progression of reduction in the two cases is meanwhile not identical according to the measurements obtained by XRPD. Here, significant amounts of Cu crystallites emerge at around 285°C and level out at 380°C in hydrogen (see Figure 5-13), while when reduced in ethanol significant amounts of Cu crystallites emerge already at about 260°C, levelling out at 300°C (see Figure 5-16). The hydrogen reduction fits also with the TPR results.

5.11.2.1 Cu states

Looking into the Cu states for $CuO:Al_2O_3$ catalysts observed during the course of reduction it seems that not only the nature, the bulk CuO, $CuAl_2O_4$ or CuO closely associated with the alumina, but also the loading of the Cu(II) species present in the sample is decisive.

At low (3-5wt%) Cu loadings it is observed (*Fernandez-Garcìa et al., 1998*) how Cu in the spinel reduces to Cu(I) in a two step mechanism via $CuAlO_2/Cu_2Al_2O_4$, subsequently migrates as Cu+ to the surface and then reduces to Cu(0). If a hardly reducible CuO-like phase is present (due to insufficient calcination) it reduces straight to Cu. In the study by *Patrick et al. (1990)* it was found that for low Cu loadings the amount of CuO closely associated with alumina decreases with calcination temperature. In reduction experiments of Cu(II) investigated with quick-scanning XANES and EXAFS (*Stötzel et al., 2009*) no Cu(0) was found in the sample with the lowermost Cu content (shorter impregnation time), whereas the sample with the higher Cu loading reduced via Cu(I) to Cu(0). It is discussed herein that the reduction behaviour of Cu has to do with its stabilisation in the alumina matrix. In a surplus of alumina (low $CuO:Al_2O_3$) the Cu seemingly increases its ability to stabilise in its oxidation state 1, for example as $CuAlO_2$. This may be affected by a lesser tendency for low loadings of Cu(I) to disproportionate through the reactions 2 $CuAlO_2$ -> $Cu_2Al_2O_4$ -> Cu + $CuAl_2O_4$ (ΔG is around -80 kJ/mol) which is thermodynamically highly attractive in a very broad temperature range (0-1000°C). If at low Cu loading the CuO/Al_2O_3 catalyst is not calcined at a temperature high enough to form spinel, the CuO of the fresh calcined sample reduces partly to Cu(I) and partly to Cu(0), depending on the Cu loading (*Amano et al., 2006*), analysed by TPR and XANES.

Barrosso et al. (2006) found only metallic Cu and $CuAl_2O_4$ after the first TPR peak during the reduction of stoichiometric spinel (calcined at 700°C, with traces of CuO).

This may also indicate that the reduction of Cu does not take place via Cu(I) for stoichoimetric catalysts as opposed to the lower Cu loading catalysts described above. In disagreement herewith *Patrick et al. (1990)* a stoichiometric sample calcined at 900°C (96% $CuAl_2O_4$) was reduced by TPR and analysed with XRD in combination, revealing the presence of $CuAlO_2$ during reduction, indicating that at least part of the reduction of Cu(II) spinel goes via the Cu(I) spinel to Cu(0).

The 2.5wt% Cu model catalyst of this work ($CuAl_2O_4$ spinel/alumina, calcined at 850°C) also reduces via Cu(I) to Cu(0) according to the XANES observations made, consistent with numerous literature observations, whereas the Cu(II) in the stoichiometric $CuAl_2O_4$ Cu spinel catalyst was observed to reduce straight to Cu(0) in agreement with *Barrosso et al (2006).*

5.11.3 Cu crystal size

The sizes of the Cu crystals grown under reduction in ethanol and 3% hydrogen *in situ* XRPD are about the same (50-80Å), while it is estimated that larger crystals are obtained with ethanol as reducing agent in the EXAFS experiments made at HASYLAB. The Cu particles after in situ XRPD reduction in 3% hydrogen reduction were found to grow further to 120Å after shifting to operating conditions at 300°C and feeding the reactor with 40/60 ethanol:water, whereas according to EXAFS much smaller 10-16Å Cu particles are estimated after reduction in 5% hydrogen.

The *in situ* HRTEM reduction conducted at a few mbar hydrogen partial pressure visually establishes how Cu evacuates from the $CuAl_2O_4$ framework and diffuses to the surface of the Cu depleted alumina framework where they build almost equally sized and distanced particles. The Cu leaves vacancies in the alumina framework which agglomerate into larger vacancies in turn fading, leaving a more open porous alumina structure. The reduction conditions in the *in situ* HRTEM of 10 mbar H_2 is far from similar to the normal reduction conditions. The immediate estimate of crystal sizes from the HRTEM analysis is 20-50Å. Both the XRPD and the XAFS reduction in diluted hydrogen were conducted *in situ*, similar to normal reduction conditions, making them comparable. Extrapolating the estimated crystal sizes of Cu D[200] in the spent sample (see paragraph 5.8.1), analysed by *ex situ* XRPD, back to 0 h (SOR) gives a Cu(200) crystal size of about 80Å. Taking into account the higher value of Cu D[111] found under *in situ* reduction (compare for example D[111] with D[200] depicted in the upper and lower graph in Figure 5-12) the initial Cu crystal size after exposure to 50 mbar of hydrogen under reduction is about 80-130Å.

Reduction at higher hydrogen partial pressures is likely to form larger Cu particles as the reduction is an exothermic process, and larger Cu crystals tend to form at higher temperatures as found in the TGA analysis. *Faungnawakij et al.* (2008) found by XRD (Scherrer equation) analysis that a stoichiometric CuO/Al_2O_3 calcined at 900°C (and therefore transformed into spinel) had Cu crystallites of the average size 316 Å after reduction at 350°C in a 10%H_2/N_2 and which grew to 389Å after exposure to reaction conditions.

Due to the autocatalytic nature of reduction (see paragraph 5.7.6), and the temperature dependency on sintering, a relation between Cu particle size and hydrogen partial pressure during reduction may be suggested. The finding of 20-50Å Cu particles for

reduction in10 mbar H_2 (HRTEM), about 50-80 Å Cu particles for reduction in 30 mbar H_2 (XRD and TGA) and about 80-130 Å Cu particles for reduction in 50 mbar H_2 (reduced, 15 h run, passivated sample (see paragraph 5.7.2), D[111] estimated) seems consistent with the findings of about 300Å Cu particles for a sample reduced in 100 mbar H_2 (*Faungnawakij et al., 2008*). *Quincoces et al.* (1997) also find that a high hydrogen partial pressure enhances sintering of Cu crystals.

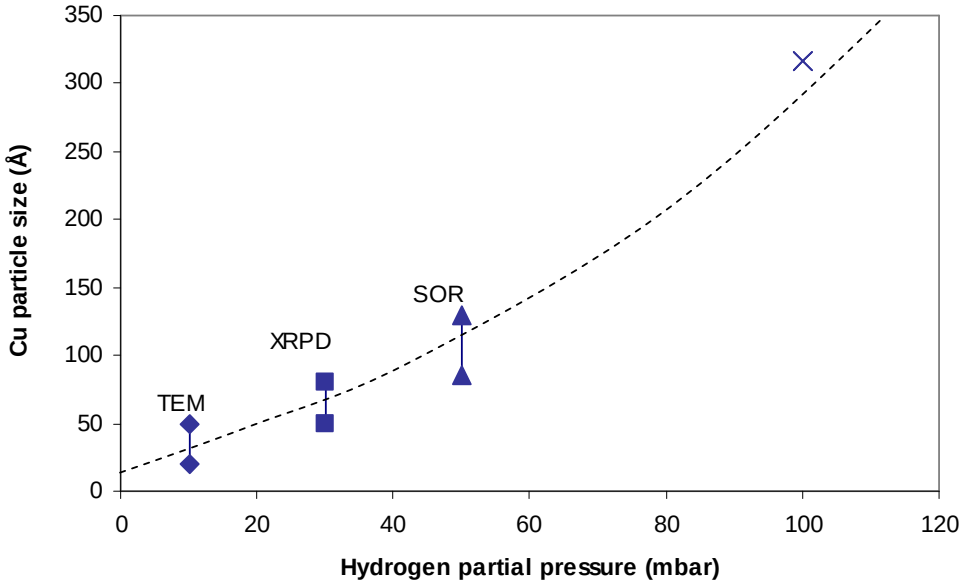

Figure 5-44: The Cu particle size of stoichiometric $CuAl_2O_4$ after exposure to hydrogen at 340°C for 3 h. Diamonds: HRTEM, squares: *in situ* XRPD, triangles: *ex situ* XRPD, experiment SOR, cross: (*Faungnawakij et al., 2008*).The reference sample reduced in 100 mbar hydrogen was reduced at 350°C for 3 h.

Figure 5-44 shows the approximate relationship between the resulting Cu particle size after reduction of stoichiometric spinel and the hydrogen partial pressure found by the various analytical methods, as mentioned above. The reference sample was treated at a moderately higher bulk temperature, which is considered of minor importance.

The only method which falls outside this relationship is the XAFS, where 10-16 Å Cu particles were found for a stoichiometric $CuAl_2O_4$ sample being exposed to a hydrogen partial pressure of 50 mbar. 10-16 Å Cu particles are only a 4-5 atoms broad (based on a Cu lattice constant of 3.6Å). Such a high dispersion of Cu (>50%) is not very likely.

From the *in situ* XRPD analysis Figure 5-16 it seems that the introduction of the ethanol/water feed instantly reduces the amount of Cu relative to the spinel. Such shift is maybe linked to a formation of crystalline alumina from a non-crystalline alumina precursor under the influence of water (*Sato, 2004, Murray et al., 1962, Glazoff et al., 2010*). It is seen on the corresponding curve (Figure 5-13) for the sample reduced with hydrogen that a gradual decrease of the spinel fraction is abruptly and without any external influence changed to a drastic drop (while a CuO phase apparently emerges). HRTEM analysis of this work indicates that presumably the Cu depleted alumina initially retains its original spinel framework around the Cu vacancy. Then structural changes seemingly happen spontaneously allowing the alumina vacancies to agglomerate, finally creating a porous structure. The structural alumina changes

observed in HRTEM supports the above suggested transformation of amorphous alumina into crystalline alumina.

Comparing XRD Figure 5-13 (hydrogen reduction) and Figure 5-16 (ethanol reduction) it appears that the building of alumina crystal structure has been promoted in the case where ethanol is used as the reducing agent, as the analysed Cu content is closer to the theoretical. Tentatively, this might be due to a higher water partial pressure arising if ethanol dehydrates to ethylene over the alumina surface under reducing conditions. However, by means of *in situ* TPR study it was established that no ethylene was formed below 340°C in a sample reduced in ethanol.

The optimum Cu area was found at a catalyst reduction temperature about 340°C by the TGA analysis. A calculation of the relative area to the amount of Cu reduced indicates that larger Cu crystals are grown at higher reducing temperature. As meanwhile also a larger fraction of Cu is reduced at higher reduction temperatures this ends up in an optimum Cu surface area estimate which was confirmed by H_2 TPD indicating an optimum at around 320°C. Without having a firm link between the Cu surface area and the catalyst activity on ethanol dehydrogenation to acetic acid the optimum activity of the catalyst was also found in this range, 320-340°C. Experimentally it was found that very little acetic acid or derivatives is formed over pure alumina, while with a Cu on Al_2O_3 loading between 8 and 33% of Cu (metal%) the Cu/Al_2O_3 catalysts exhibited the same conversion rate of an ethanol and water feed. Thus the main activity for acetic acid formation may be attributed to the Cu. But at the same time it was found by XRPD that the Cu crystal size was almost independent of the Cu loading. While this supposedly would give an increasing activity with Cu loading the activity test and the XRPD results together surprisingly indicate that the specific activity with respect to Cu area is reduced with an increase of the Cu loading. In another study (*Iwasa et al*., 1991) the ethyl acetate product selectivity at constant ethanol conversion of a Cu based catalyst (Cu/SiO_2) increased very little with the Cu loading. Without having straight similarities the NO reduction activity of a Cu based catalyst was found to depend on the Cu content, when the Cu content was varied between 0.25 and 3.5 wt% (*Janas et al., 2009*).

5.11.4 Deactivation and alumina behaviour

The reason for the deactivation encountered after reduction in ethanol and the subject to increased feed concentration of acetaldehyde was sought through the many characterisation exercises. As established by XRD and XAFS the reduction with ethanol appears to give about the same size of Cu crystals as hydrogen does. The small changes of Cu crystal size, Cu area and pore size and pore volume could not explain the complete deactivation of the catalyst. Cu in itself (tested as Raney Cu and decomposed $CuCO_3$) showed an extremely high selectivity to acetaldehyde, acetic acid and ethyl acetate. The compounds found in the effluent at the break of deactivation are increasing formation of condensation products such as butanol, butanoic acid and other higher alcohols, acids, aldehydes and aromatics. Especially the increased level of butanol in the reactor effluent is an early indication of the catalyst approaching complete deactivation.

The most substantial differences between the samples reduced with hydrogen and ethanol respectively are 1) the immediate level of amorphous alumina indicated by the

XRPD analysis and 2) the condensation precursor acetaldehyde occurs during the reduction with ethanol. Crystalline eta- and gamma-alumina is known to catalyse the condensation of acetaldehyde (*Sokolskii et al., 1976*), supported by our own investigations (see paragraph 5.7.7). Alumina surfaces possess both basic and acidic sites. *Iwasa et al. (1991)* succeeded in reducing the side-product activity of Cu/Al_2O_3 catalyst by doping 1%K on the catalyst, suggested to eliminate acid sites. But we did not obtain that effect when adding 2%K to the Cu spinel catalyst during the screening study, resulting both in a lower activity and lower selectivity (see Appendix D.1).

According to *Santacesaria et al. (1977)* water treatment of alumina surfaces gives weak Brønsted acid sites rather than strong Lewis acid sites in turn affecting the strength of the basic sites. *Fu et al.* (2005) observed for the acid catalysed dehydration of methanol to DME that γ-Al_2O_3 possessing strong Lewis acidity deactivated due to water poisoning. We observed a marked lower side-product formation when co-feeding water. As the condensation of acetaldehyde is known to take place on both acid and basic sites, using two adjacent sites, both the preferred adsorption on water on the sites and the dampening of the site strengths will suppress the condensation activity of the alumina support in consistence with our observations. We also observed certain, however low, dehydrogenation activity of ethanol on the alumina support. In consistence herewith *Sanchez-Sanchez et al. (2010)* suggest that surface acetates are formed from acetaldehyde over an alumina surface. The dehydrogenation activity of the support may help explain the activity insensitivity of the Cu loading. However, a highly selective significant dehydrogenation activity on pure Cu surfaces was observed (Cu pellets, obtained as a decomposition product of pelletised $CuCO_3$ powder, and Raney copper). These observations and literature findings together lead to the picture that the alumina surface, its state and activity impacted by the presence of water, is responsible for the side-product formations of acetaldehyde and in turn longer chain condensation products.

The concentration of C deposits was found to be higher on the deactivated samples 1.6-6wt% vs. up to 0.9wt% for the active samples. The nature of the carbon, as determined by TEM, was probably long chained wax-like compounds and not coke. *Luo et al. (2009)* reports that acetaldehyde undergoes continued aldol condensation on TiO_2 to high molecular weight compounds. The finding of wax-like carbonaceous material in the centre of the deactivated catalysts supports that condensation of the reactive acetaldehyde has taken place. In agreement herewith sudden deactivation occurred in the runs shortly after acetaldehyde and butanol were co-fed over the Cu spinel catalyst.
The position of C inside the catalyst pellet rather than on the outside shell could be due to thermal conductivity or diffusion limitations in the pellet. According to the SEM analysis C primarily deposits in the outer shell, however the SEM analysis was made on carbon tape which could have disturbed the results.

5.11.5 Partly oxidative dehydrogenation

The process-wise advantage associated with the partly oxidative dehydrogenation alternative is its thermoneutral or slightly exothermic nature, decreasing the need for steam consumption and potentially reducing the cost of the reactor. The negative aspects around the partly oxidative dehydrogenation naturally count the risk of

explosive mixtures with ethanol, the risk of a reactor temperature runaway and complex feed control. The latter obstacles may be handled if attended to. Furthermore if nitrogen can not be accepted in the hydrogen co-product, oxygen would be required for the process, for example provided by air separation (distillation or membrane).

If at adequate oxygen concentration, the adsorbed acetaldehyde reacts with adsorbed atomic oxygen, directly or as ethoxy as shown in Scheme 5-1,

$CH_3CHO^* + O^* = CH_3HCOO^* + *$

$CH_3HCOO^* + * = CH_3COO^* + H^*$

Or

$CH_3CHO^* + * = CH_3CO\ ^* + H^*$

$CH_3CO^* + O^* = CH_3COO^* + *$

Scheme 5-1: Cu surface reactions: acetaldehyde oxidation or acetyl oxidation.

one may imagine that the disproportionation reaction of molecular oxygen into atomic adsorbed oxygen is fast and makes a shortcut for the slower disproportionation of water (see Scheme 5-2) on the catalyst surface as described in the article by *Ovesen et al. (1996)*, potentially making way for a mechanistic shift, if the abundance of adsorbed atomic oxygen is increased.

$H_2O + * = H_2O^*$

$H_2O^* + * = OH^* + H^*$ (comparably slow)

$OH^* + OH^* = H_2O^* + O^*$

Scheme 5-2: Cu surface reactions: Water dissociation reactions.

The initial temperature leap may be explained by a wipe-off of adsorbed hydrogen with oxygen from the catalyst surface. However, the duration of the stabilisation period tends to indicate that an actual deactivation caused by the temperature rise overlays this phenomenon. This hypothesis is further supported by the decreasing acetic acid concentration in the condensate over time after the introduction of air.

The finding of a higher C deposit in the spent catalyst of the partly oxidative dehydrogenation experiment in comparison with the non-oxidative dehydrogenation experiment indicates that running the dehydrogenation in the partly oxidative mode increases the severity of the catalyst operating conditions.

In the light of the above the trends for the partly oxidative dehydrogenation are negative.

5.12 Conclusion

During the early investigations of the Cu spinel catalyst it was found that several factors could lead to its deactivation. In the attempt to circumvent the deactivation of this catalyst which exhibited a high initial activity a thorough catalyst characterisation study was made including *in situ* reduction.

According to literature the rate of $CuAl_2O_4$ formation is optimum for the stoichiometric $CuO:Al_2O_3$ ratio. More importantly it is found that the degree of reduction obtainable from a calcined $CuO:Al_2O_3$ decreases with calcination temperature and increase with the Cu loading; but that the resulting crystal size of the excess CuO of the calcined high Cu loading samples is much higher than for the stoichiometric sample, leading probably to a lower surface area/Cu loading. Catalysts lower in Cu than the stoichiometric spinel exhibit as high activity to acetic acid as the stoichiometric catalyst but the side-production of condensation products increases. Thus a stoichiometric composition $CuO:Al_2O_3$ being calcined at a temperature high enough to within a reasonable time obtain the almost full transition of $CuO:Al_2O_3$ to $CuAl_2O_4$ seems optimum.

By HRTEM on Cu spinel catalyst it was found, that under reduction Cu atoms leave the $CuAl_2O_4$ framework to gather in equally sized, at least locally equally distanced, crystals. By *in situ* XAFS technique it is observed that Cu(II) in Cu spinel catalyst reduces directly to metallic Cu(0), while at low Cu loadings it reduces via Cu(I) (paper enclosed in Appendix E.2). The size of the Cu crystals is estimated by ex situ XRD to be 80-130Å after reduction in 5% hydrogen applied in the experiments. These Cu particles further grow under reaction conditions. *Ex situ* XRPD analyses of spent catalyst reveal crystal sizes of 200-250Å Cu particles. The optimum reduction temperature is about 320-340°C according to activity tests. The underlying explanation of an optimum Cu surface area resulting from the balancing of the fraction of Cu reduced and the size of the Cu particles obtained during reduction is supported by an optimum Cu surface area found. No remarkable changes in the Cu crystal phase in the Cu spinel catalyst was seen by means of XRD and XAFS under the introduction of the feed after reduction, neither after having been under operation nor after deactivation.

The Cu spinel catalyst showed an initial satisfactory activity ($STY_{HOAc} \approx 0.5$ g/(g·h)). Meanwhile it suffered from a number of sudden rapid deactivations. For example the idle operation at temperatures above 150°C, and the reduction in ethanol should be avoided as it caused deactivation. Furthermore, in a stability test lasting for more than 1000 h, despite several interruptions (which could have be damaging to the catalyst, as established) the Cu spinel-850 catalyst suddenly deactivated after a short term exposure to a higher operating temperature, 320°C. Also the increased levels of acetaldehyde (10%) and even 1-2% butanol co-fed with the ethanol/water feed lead to rapid deactivation. The distinct deactivation caused by increasing the operating temperature is consistent with the finding of the highest level of C found in the top pellet, having the highest operating temperature. The gradual deactivation was accompanied by a yellow colouring of the dehydrogenation product and the increasing level of condensation side-products, primarily C_{4+2n} aldehydes, acids and alcohols, but also cyclic products.

The observed deactivation of the Cu spinel catalyst most probably relates to formation of wax on the alumina structure resulting from the reduction, the wax smearing out on both the Cu and the alumina surface. The increasing selectivity of condensation products during deactivation points to an acceleration of the condensation reactions over the dehydrogenation and oxidation reactions, i.e. the initial predominant deactivation of the Cu activity, in turn followed by the complete loss of activity.
Running the partly oxidative dehydrogenation over the Cu spinel catalyst accelerates the deactivation. The highest level of C was found in the top pellet from the partly oxidative dehydrogenation experiment.

The proneness of the Cu spinel catalyst activity to co-feeds of butanol, acetaldehyde and to slightly elevated temperature were not encouraging as in a process context the catalyst needs stability. Further in a process context the side-production of butanol leads to an increased energy consumption. In spite of the disappointing results in particular for the partly oxidative dehydrogenation the original non-oxidative ethanol-to-acetic acid process retains attractiveness over the conventional carbonylation process, if the right catalyst may be identified.

Hence, when aiming for a Cu catalyst improvement a less acidic/basic support would seem beneficial. During the screening for catalysts a Cu/SiO_2 catalyst was identified as the second best candidate having a higher selectivity and medium activity. This catalyst was further activity and stability tested and compared to the Cu spinel catalyst. The characterisation of the Cu/SiO_2 catalyst, its comparison to the Cu spinel catalyst and further related studies are described in Chapter 6.

Chapter 6 Results for Cu/SiO_2 catalyst – comparison & kinetics

6.1 Introduction

The instability of the Cu spinel catalyst described in Chapter 5 which was suspected to be related to its tendency of producing condensation and dehydration products was, accordingly, in turn related to the basicity and acidity of the alumina carrier of the catalyst (*Santacesaria et al., 1977*). In order to circumvent the dehydration and condensation activity of ethanol to ethylene and the condensation of acetaldehyde the next down-selection of a Cu based catalyst was made to a type showing about half the activity, i.e. STY_{HOAc}=0.15-0.25 g/(g·h) in comparison with the previous Cu spinel catalyst. Cu on silica was pointed out as second best in the screening of catalysts based on the few criteria set up, having the highest emphasis on activity. It was not as active as the Cu spinel catalyst, but it was more selective due to its more neutral (*Tu et al.*, 2001, *Daniell et al., 2000, Liu, L. et al., 2006, Venezia et al., 2004*) carrier. Further during the screening experiments catalysts such as pure copper, Raney copper and Cu obtained from heating of $CuCO_3$ pellets, were found to catalyse the dehydrogenation of ethanol to acetic acid literally without any side-product formation such as butanal, butanon, butanol and butanoic acid, but these exhibited a low activity, STY_{HOAc}=0.05-0.1 g/(g·h) or lower.

In acquiring the initial knowledge on the Cu/SiO_2 catalyst during the screenings only few comparisons were made to the Cu spinel catalyst. In this chapter the further comparison between the down-selected Cu/SiO_2 over the Cu spinel catalyst are made, identifying thereby analogies and differences of these helping to understand their different catalytic behaviour.

In particular, having a high stability and robustness to process variations, the Cu/SiO_2 catalyst was further investigated in a kinetic study, allowing in turn a further maturing of the process. Two preparations of the Cu/SiO_2 were made – one with the purpose of screening (A) and one (B) made in an attempt to reproduce the first preparation, which however exhibited lower initial activity. The Cu/SiO_2 catalysts were tested either as whole pellets being cylinders with the dimensions d x h = 5 x 5.5 mm or as crushed down catalyst pellets in the 1-1.4 mm sieve fraction.

In this chapter the kinetic testing and modelling results of the Cu/SiO_2 B catalyst have been described and discussed against literature findings on the elementary surface reactions.

6.2 Characterisation

The compositions of the Cu/SiO_2 catalyst powder obtained (preparation as in paragraph 4.4.2.2) was for the preparation A: 44.4wt% Cu, 15.5wt% Si and 0.27Wt% K balanced by oxygen. Preparation B: 45.7wt% Cu, 15.3wt% Si, 0.24wt% K, balanced by

oxygen was made in supplement to preparation A, because the amount of catalyst pellets attained in preparation A was not sufficient for all the further tests to be conducted. The catalysts made from the preparation A and B catalyst powder will be referred to as the Cu/SiO_2 catalyst, with the suffix A and B, hereinafter. The catalyst pellets were made by compressing a mixture of the obtained catalyst powder and 3.3wt% graphite as lubricant. Although the preparation recipe was repeated, the resulting activity levels were not the same. The reason for the activity change was not pursued in detail in this first round of investigation, but it may be the result of a different procedure adopted for the pelletising. The Cu/SiO_2 A catalyst has been used for screening and initial activity and stability study. The Cu/SiO_2 B catalyst has been used for the promoter study, the kinetic study and stability study on butanol and elevated operating pressure.

Furthermore the addition of specific promoters was presumed to enhance the activity, and especially the water cleavage rate, on the Cu surface. Inspired by the promoters known from water gas shift catalysts, where water cleavage is believed to be rate limiting under low water conditions (*Ovesen et al., 1996*), a series of promoted Cu/SiO_2 catalyst was prepared based on the Cu/SiO_2 B catalyst. Especially Cs and Ga have been mentioned as water cleavage promoters (*Klier et al., 1986, Campbell et al., 1992, Lachowska et al*., 2004, and *Kunkes et al., 2011*). Furthermore the addition of oxidation promoters such as Pt and Pd may shift the coverage of species on the sites, leaving room for the desired reactions to take place. Pd has been found to promote methanol formation activity on Cu based catalysts (*Ma et al., 1999, Wainwright, 1978*). Impregnations of Cu/SiO_2 B with 0.1 and 1 wt% Pt, Pd, Cs and Ga were made (see paragraph 4.4.1).

6.2.1 The Cu crystal size found by TEM, Cu/SiO_2 A catalyst

In order to support the picture that upon reduction the Cu particles on a SiO_2 surface have similarities with Cu particles on an alumina surface a HRTEM *in situ* reduction of Cu on SiO_2 was conducted. The catalyst powder was crushed with pestle in a mortar and ultrasonically dispersed in 99.99% ethanol. A droplet was added to a hotplate (TN1429 w4 no 2) on the trough side and dried in ambient. A Titan ETEM was used for the *in situ* experiment, operated at 300kV and tuned to a flat information transfer out to 20mrad using the supporting SiN membrane window as preparation.

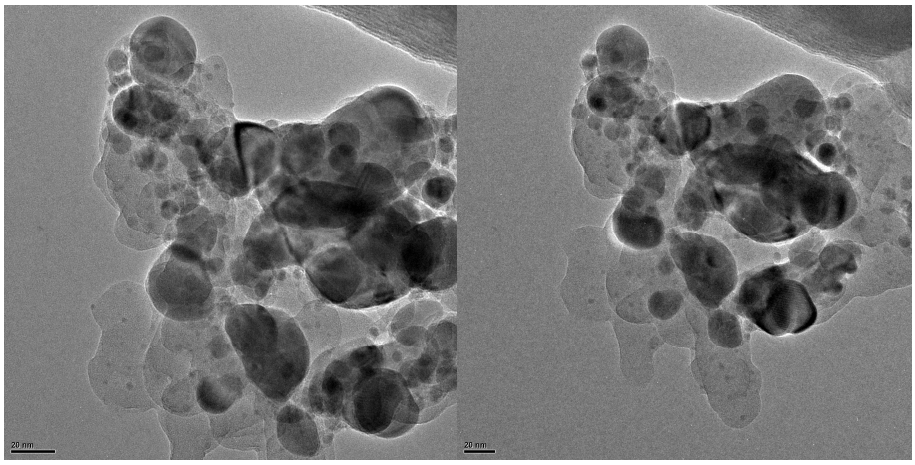

Figure 6-1: TEM images of TEM3495 at conditions: Left: 335^{o}C, 10.5mbar H_2. Right: 385^{o}C, 10.5mbar H_2.

The hydrogen source was Alphagas H_2. Figure 6-1 shows TEM images recorded of an agglomerate during exposure to ca 10mbar H_2 at 335 and 385^o.

The image series reveal the initial CuO state and reduction of CuO to Cu. It appears that CuO is at room temperature initially distributed in domains that are smeared out over the silica support, but upon reduction to Cu agglomerate into particles with diameters > 100Å.The Cu particles seem steady in the temperature range 335-385°C.

6.2.2 Reduction of the Cu/SiO_2 catalyst B

By means of an *in situ* reduction EXAFS study it was investigated at which temperature the Cu on the CuO/SiO_2 reduces to Cu/SiO_2.

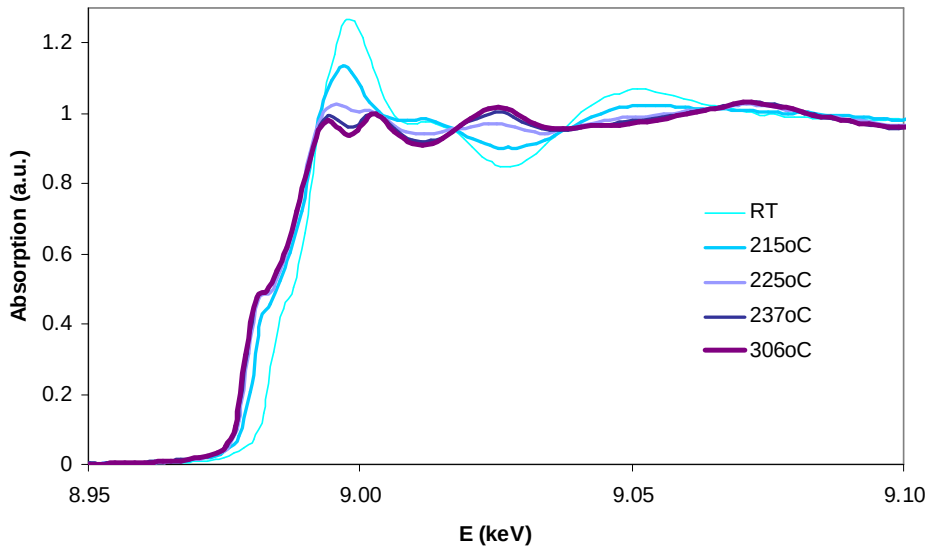

Figure 6-2: XAFS spectra of the reduction of the Cu/SiO_2 catalyst in 5% hydrogen at SV=10 Nl/(min g). The catalyst reduces rapidly between 225 and 237°C.

QEXAFS scans were recorded using a Si(111) double-crystal monochromator in continuous screening mode between 8.5 and 9.7 keV, similarly to the reduction of the Cu spinel catalyst in hydrogen (see paragraph 5.7.1). The background and data fitting were conducted with the Win XAS software. Figure 6-2 shows 5 selected EXAFS scans from the study, at room temperature, 215, 225, 237 and 306°C. Already at 225°C the Cu(II) reduced very rapidly to Cu(0).

In order to minimise sintering, the standard reduction temperature prior to all experiments on the Cu/SiO_2 catalyst was set to 250°C. The amount reducing gas used corresponding to 4 times the stoichiometric amount of hydrogen needed.

6.2.3 Silica support activity

In spite of the immediate reason for picking SiO_2 as a support, being its neutral character (*Tu et al*., 2001), a support activity experiment was carried out.

Samples of high surface area silica being used as a precursor for silica based Cu catalyst was calcined at 350 and 800°C (high and low surface area) and subjected to a feed of 50/50 acetaldehyde:ethanol and a 50/50 acetaldehyde:water feed at a LHSV of

3 ml/(g·h) at 300°C and atmospheric pressure. As established by a condensate analysis on the GC-MS it was found that silica was literally inert to either of the two feeds.

6.3 Stability, Cu/SiO_2 A catalyst

In the screening test the Cu/SiO_2 showed similar or lower tendency of side-product formation. Remarkably, it was also found that ethyl acetate was not catalysed on the Cu/SiO_2 catalyst, whereas a new peak on the MS showed to be diethoxy ethane, established by the analysis of the MS radicals. Upon heating, the condensate diethoxy ethane was found to disintegrate into acetaldehyde, ethanol and water.

As in the earlier study on Cu spinel catalyst, the co-feeding of some of the products together with the ethanol/water feed was studied. This co-feeding demonstrates the effect of recycling the acetic acid lean stream from the separation step to the reactor, containing primarily acetaldehyde, water, potentially diethoxy ethane and minute amounts of butanol.

In an experiment in the new test set-up the Cu/SiO_2 A catalyst was first subjected to co-feeding of a 50/50 acetaldehyde:water mixture, i.e. the total feed admixture being a mixture of 80wt% of 40/60 ethanol:water and 20wt% of 50/50 acetaldehyde:water. In a next round the catalyst was subjected to a 5wt% addition of diethoxyethane to the total admixture described above. In below graph is shown the effects of the addition of acetaldehyde and diethoxyethane.

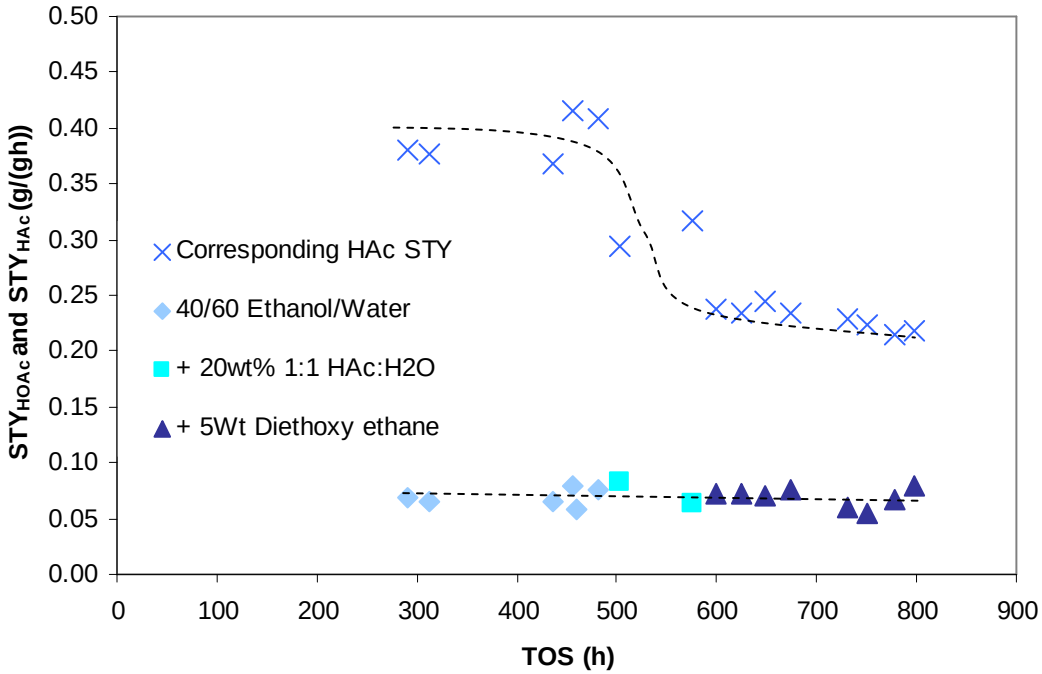

Figure 6-3: The acetic acid space time yield (STY) as function of time on stream (TOS, h) at 1/LWHSV=0.8 (g·h)/g shows the effect of co-feeding 20wt% 50/50 acetaldehyde:water and additional 5wt% diethoxyethane respectively, keeping the LWHSV constant. The corresponding acetaldehyde STY is plotted as well.

It may be noted in Figure 6-3 that the acetic acid activity at atmospheric pressure seems to be unaffected by the addition of acetaldehyde or diethoxy ethane. On the

other hand the acetaldehyde STY is strongly affected by the addition of a 50/50 acetaldehyde:water mixture, and further by the addition of diethoxy ethane. Almost no deactivation of the catalyst (run at 300°C) was observed over 800 h.

6.4 Promoter study and butanol and pressure stability, Cu/SiO_2 B catalyst

When investigating the selection of promoters only the addition of 1% Ga seemed to have a slight, if any, effect on the activity. The other promoters showed a negative effect under the non-oxidative dehydrogenation test.

Pressure study, Cu/SiO_2 B catalyst

Immediately the increase of the operating pressure is not beneficial in volume expanding processes such as dehydrogenation. However, kinetically there may be a gain in increasing the pressure, as it is well known that the reactivity of a catalytic system often relates to the partial pressure of the reactants.

The only experimental set-up suited for higher than atmospheric operation was the stability set-up. The reactor in the stability test set-up (see paragraph 3.4) was loaded with 4 g of the Cu/SiO_2 catalyst and reduced at 250°C. A 40/60 ethanol:water feed was pumped at a LWHSV of 5 g/(g·h) and the pressure was raised to 10 bar. It was found by calculation that the STY for acetic acid (see Figure 6-4) increased vaguely at the high pressure.

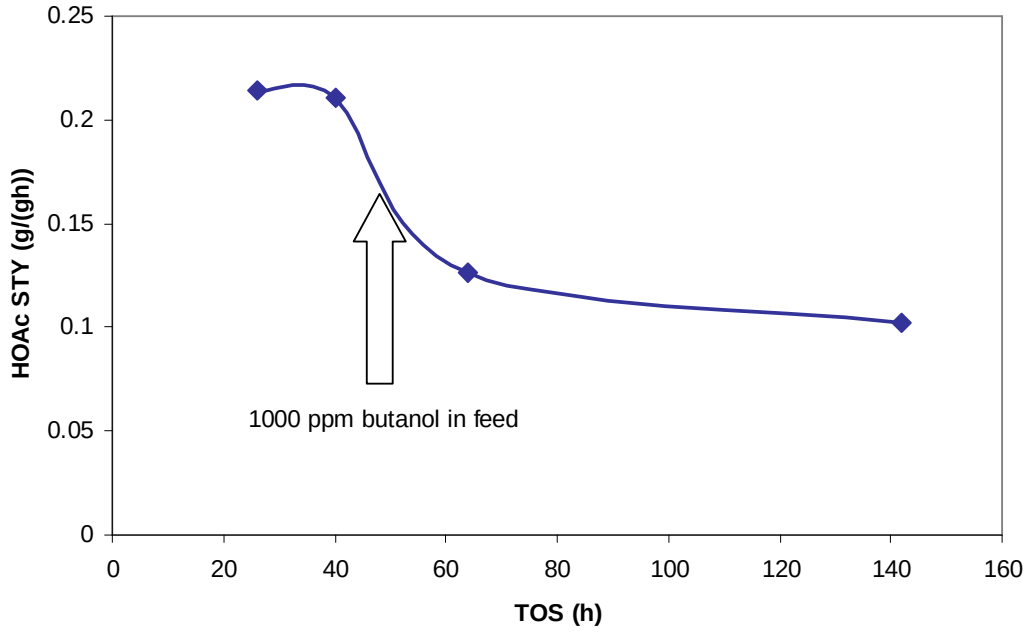

Figure 6-4: The effect of butanol addition on acetic acid STY at high pressure. The activity abruptly reduces irreversibly.

Specifically, the acetic acid over the acetaldehyde ratio increased when the pressure was increased. However, some negative effects were found as well. The condensate which used to be colourless and clear became red. And the activity was lost. It was suspected this could relate to the leaching of Cu from the catalyst. Two pellets of the spent catalyst were sent for XRPD. The Cu crystal size was >1000Å, indicating that pronounced sintering of the Cu crystals had taken place. As the distinction between the

two influences, the high pressure and the addition of butanol, was impossible another experiment was run where only the operating pressure was increased.

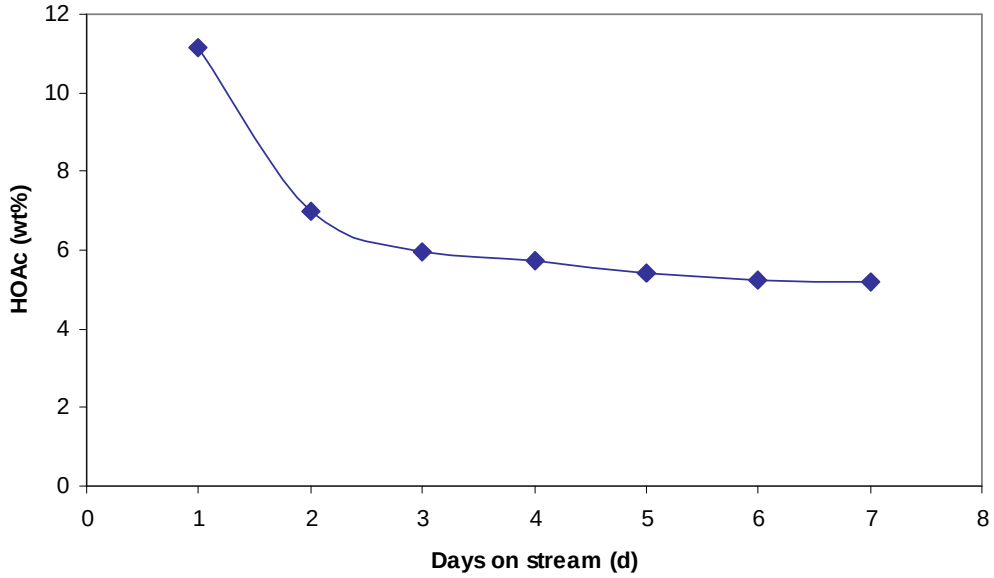

Figure 6-5: Stabilisation of activity is obtained at an operating pressure of 7.5 bar.

This time no butanol was added, but furthermore the pressure was reduced in order to see whether the catalyst would attain stabilisation at a more modest, still elevated pressure. The titrations of the condensate obtained under these tests show how the acetic acid concentration stabilises over 7 days (see Figure 6-5). The experiment was stopped due to a power cut, under which the catalyst had suffered from flooding under the cooling process. The catalyst was deteriorated.

6.4.1 Activity comparison of Cu/SiO_2 catalysts to Cu spinel catalyst

As an illustration of the different activities found for the two types of catalysts, their individual STY of acetic acid vs. time have been depicted in Figure 6-6. The data were recorded at LWHSV=0.4-0.5 g/(g·h) and temperatures 290-300°C. It should be noted that the activity data for the Cu/SiO_2 A catalyst was acquired from the stability test set-up, having poorer plug flow characteristic than the new test set-up where the Cu spinel catalyst was tested, and the kinetic test set-up where the Cu/SiO_2 B catalyst was tested, i.e the activity data for Cu/SiO_2 A catalyst may be a little underestimated. Further it should be noted that that isothermal conditions were not attained (see Appendix F.1). For the Cu/SiO_2 A and B catalysts the activity numbers are based on a 60/40 ethanol:water liquid feed composition. The feed composition for the Cu spinel catalyst was 80wt% 60/40 ethanol:water + 20wt% 50/50 HAc:water – as seen on Figure 6-3 the adding 20wt% 50/50 HAc:water slightly increased the HOAc STY for the Cu/SiO_2 A catalyst. As Figure 6-6 shows, the activity is initially much higher for the Cu spinel catalyst.

However, the stability of the Cu/SiO_2 catalysts is superior. The activity of Cu/SiO_2 B catalyst is about half the activity of the Cu/SiO_2 A catalyst.

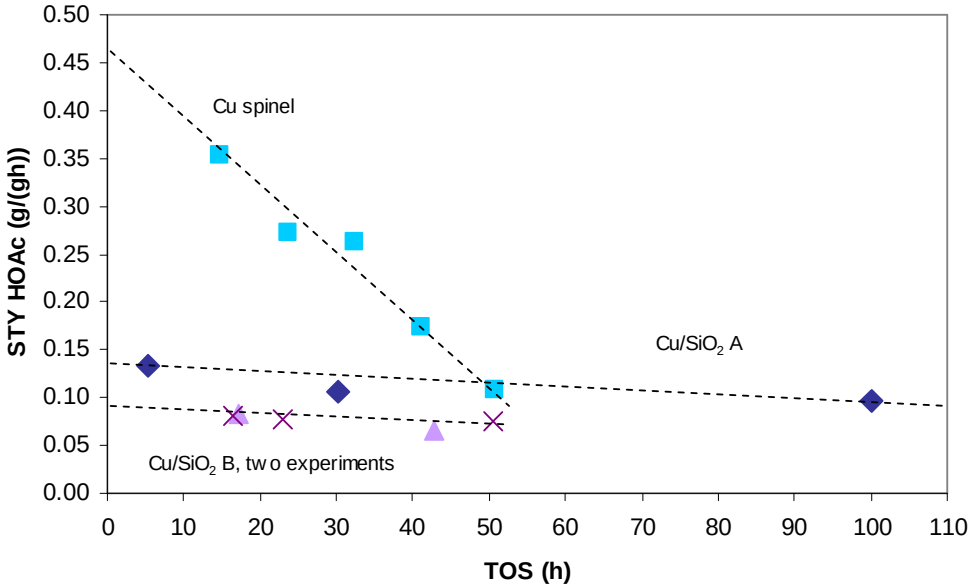

Figure 6-6: STY HOAc for the Cu spinel (new test set-up, reactor 2), the Cu/SiO_2 catalyst A (stability test set-up) and the Cu/SiO_2 catalyst B in two experiments (kinetic test set-up), at LWHSV=0.4-0.5 g/(g·h) and t_{bed}=290-300°C. The feed converted over the Cu/SiO_2 catalysts was a 40/60 ethanol:water mixture; the feed converted over the Cu spinel was 80wt% 40/60 ethanol:water mixed with 20wt% 50/50 HAc:water.

The activity experiment on Cu/SiO_2 catalyst B was repeated. As may be seen a fairly good reproducibility of the activity was obtained for Cu/SiO_2 B catalyst. The selectivities to the products also change over time. Here calculated as the relative ethanol conversion to the individual product over the total ethanol conversion, as C%.

a)

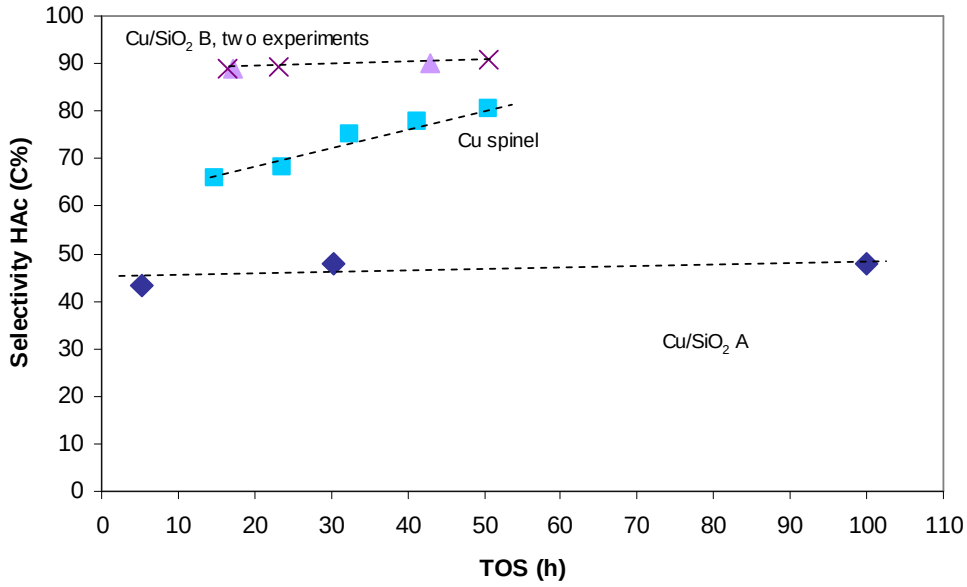

b)

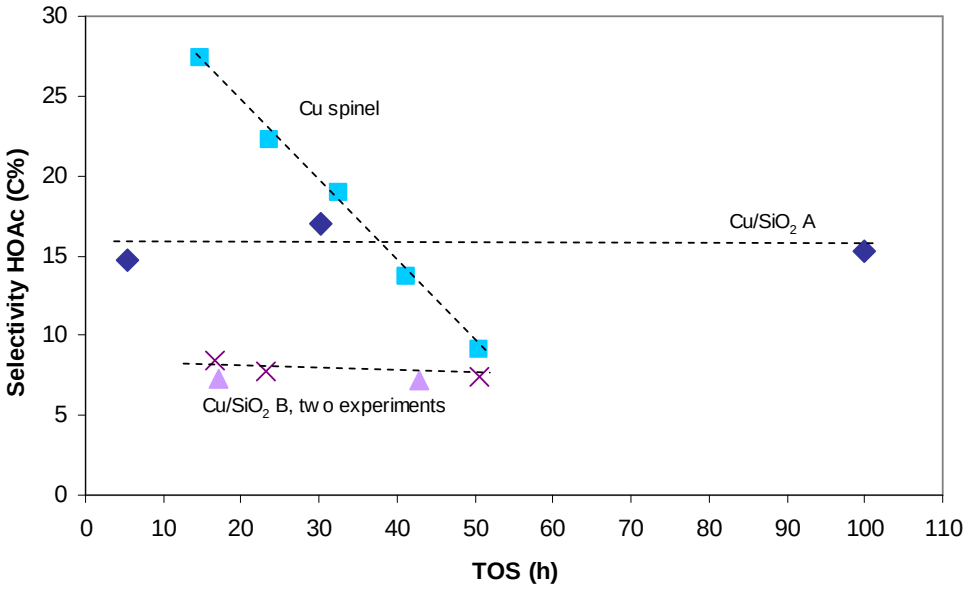
Selectivity HOAc (C%)
TOS (h)
Cu spinel
Cu/SiO2 A
Cu/SiO2 B, two experiments

c)

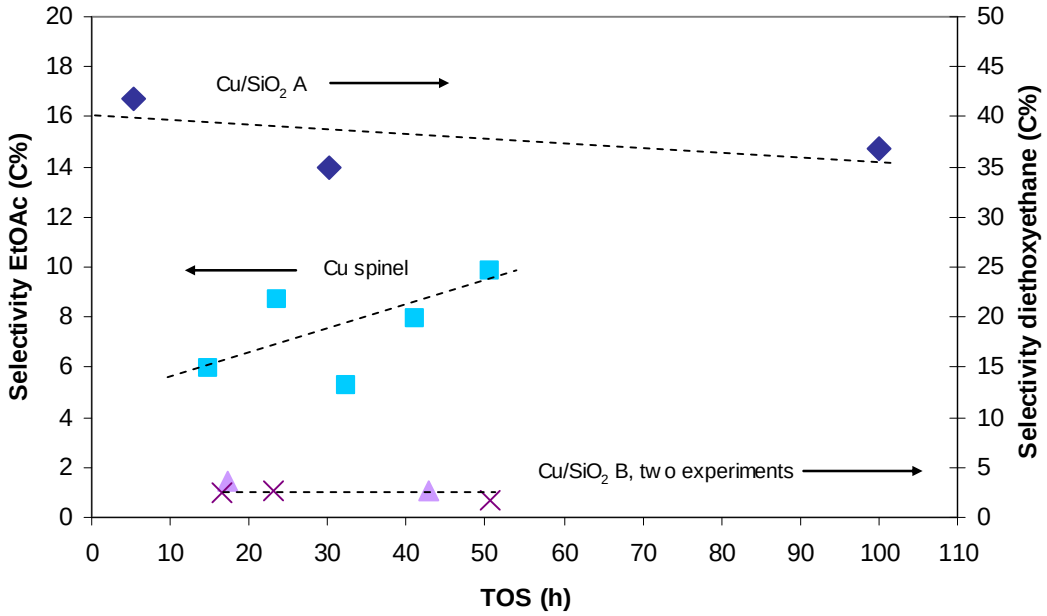
Selectivity EtOAc (C%)
Selectivity diethoxyethane (C%)
TOS (h)
Cu/SiO2 A
Cu spinel
Cu/SiO2 B, two experiments

d)

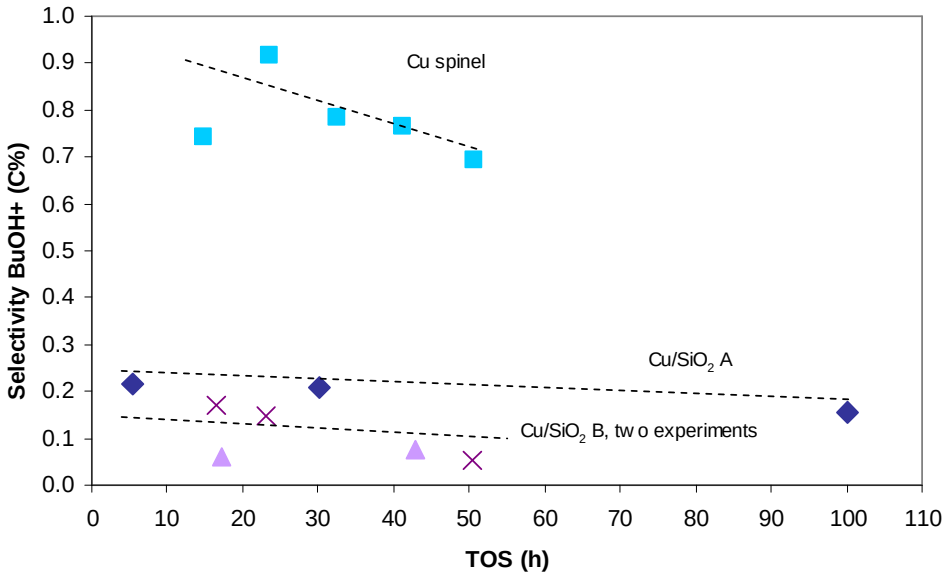

Figure 6-7: Selectivities vs. TOS for the three catalysts Cu spinel, $CuSiO_2$ A and B: a) acetaldehyde; b) acetic acid; c) ethyl acetate and diethoxyethane; d) BuOH and heavier products.

Figure 6-7 shows the product selectivities of the three catalysts tested. Whereas for the spinel catalyst the selectivities to acetaldehyde and ethyl acetate increase over time at the expense of the acetic acid selectivity, the product selectivities change much less over time for the Cu/SiO_2 catalysts, especially for the Cu/SiO_2 B.

6.5 Spent catalyst analyses: Cu/SiO_2 catalyst A vs. Cu spinel catalyst

The analogies and differences of the two Cu based catalyst pellets were also pursued through individual analyses on the fresh and spent catalyst samples.

Table 6-1: Characterisation parameters analysed for the Cu spinel and Cu/SiO_2 A catalysts.

Characterising Parameter	**Cu spinel (31wt% Cu)**		**Cu/SiO_2 (44wt% Cu)**	
	Fresh	**Spent**	**Fresh**	**Spent**
HOS (h)	0	336	0	994
Pore volume (cm^3/g)	0.337	0.264	0.280	0.310
SPSA (m^2/g)	27.5	23.6[f]	153	97.2
Average pore diameter (Å)	110/550[a]	95/500[af]	72.5	125
Carbon[d] (wt%)	<0.1	4.8[b]	3.4[c]	4.7
Cu D[200] (Å) at HOS=300 h	80	150	160	400[e]
Cu Surface Area (m^2/g)	9.5	1.55[b]	12.9	N/A

a) The pore distribution is bimodal with an optimum around the two pore diameters.

b) The sample deactivated abruptly.
c) The Cu/SiO_2 catalyst is mixed with graphite before pelletising.
d) Incl. graphite.
e) Estimated by interpolation
f) Analysis made for a sample which was deactivated after 51h.

The pore volume, the specific surface area (SPSA) and the average pore diameters were found by HBET, whereas the carbonaceous material was found by the LECO method (mixed with pure iron and heated by induction to 1600 ℃ in pure oxygen; the carbon dioxide determined by IR-absorption) while the Cu surface area was determined by H_2 TPD by the method as described earlier (see paragraph 5.7.6). In Table 6-1 is shown the characteristics for each of the two catalysts which were both tested at atmospheric pressure under non-oxidative dehydrogenation conditions, fed with 40/60 ethanol:water.

The carbon content in the fresh Cu spinel and Cu/SiO_2 catalyst represents the graphite added as a lubricant.

6.6 Partly oxidative dehydrogenation, Cu/SiO_2 catalyst B 1wt% Pt

It was believed that a Cu/SiO_2 catalyst would have a higher resistance against the deactivation by deposition of carbonaceous compounds as compared to the Cu spinel catalyst: If in particular the deactivation under partly oxidative conditions could be ascribed to the tendency of Cu spinel to form carbonaceous deposits, then a Cu/SiO_2 would be predicted to have better chances as an autothermal catalyst, as SiO_2 has little/no activity for ethylene formation (no co-product water in condensate, see paragraph 6.2.3).

A 1% Pt promoted Cu/SiO_2 catalyst was prepared by impregnation of the Cu/SiO_2 catalyst B by means of the incipient wetness method (see paragraph 4.4.1), using $Pt(NH_3)_4(HCO_3)_2$ as a Pt source. Like with the previous autothermal experiment (see paragraph 5.9.2) a single-pellet string reactor was loaded with 3mm glass spheres in between the individual catalyst pellets. 5.24 g was loaded corresponding to 15 cm. A LHSV of 3 ml/(g·h) of a 40/60 ethanol:water feed was fed. The air flow rate was raised stepwise while the nitrogen flow rate was reduced in order to maintain a constant ethanol concentration over the entire experiment, as previously described. The oven set point was 300°C.

Figure 6-8 shows the concentration in wt% of acetic acid found in the condensate and the amount of air added.

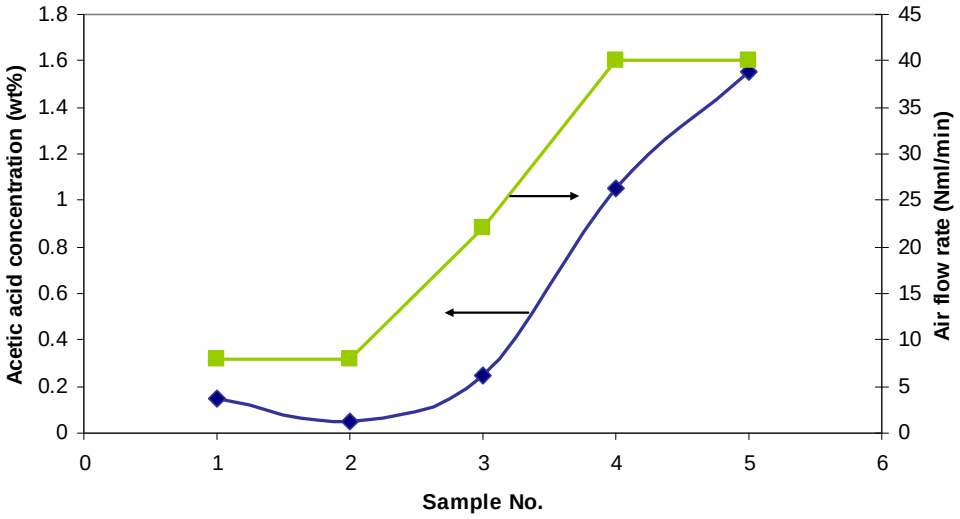

Figure 6-8: The acetic acid % (determined by titration) in the condensate and the air flow rate respectively vs. sample no.

It may be observed that the activity of the catalyst is very modest. On the other hand it may also be observed how the acetic acid level raises concurrently with the air flow rate. This behaviour was unlike the whole Cu spinel catalysts, which immediately started deactivation after exposure to air.

The unpromoted catalyst Cu/SiO_2 was also tested on a 40/60 ethanol:water feed at LHSV of 3 ml/(g·h) at 300°C in the kinetic set-up (see paragraph 3.5). For comparison the acetic acid concentrations of the condensate were found to be 10-13wt% acetic acid.

6.7 Kinetic results for Cu/SiO_2 catalyst B

For unexplained reasons the catalyst in the partly oxidative dehydrogenation test on Cu/SiO_2 described above (see paragraph 6.6) suffered from a low initial activity. Though the reasons could have been pursued, external factors of which will be learned in the next chapter made a downturn on the general effort within the conversion of ethanol to acetic acid. Emphasis was put on delivering a research technology package with high robustness in case the maturing of the process becomes relevant. It was assessed that the highest catalytic robustness had been found for the non-oxidative dehydrogenation on Cu/SiO_2.

Important to the maturing of a chemical process is that a proper reactor design must take place. When a catalytic reactor is involved one must be able to describe and predict the reaction rate of the catalysed process in mathematical terms, i.e. the kinetics of the system must be investigated.

Kinetics may be produced at different levels (*Levenspiel, 1972*). Basing the kinetics on the elementary reactions taking place on the catalytic surface (for example as confirmed by IR studies), combined by a model describing the change or development of the catalytic surface over time (as found by XRD, TEM and pore volume distribution), is the most detailed type of kinetic model. However, it represents an overwhelming

amount of work. Quite often less will do. Furthermore present kinetic study does not comprise IR-studies and the experimental set-up, the principle of analysis and catalyst behaviour does not provide for accurate data which are required for microkinetic models.

Systematic variations of feed composition, space velocity and temperature uncover the systems response to these changes from a macroscopic angle. The macroscopic model eventually expresses the apparent reaction orders and activation energy being weighted and summed from the bottleneck (rate limiting) microkinetic equations. Therefore, in the end the validity of the empirical model may be compared against microkinetic models. By comparison the found reaction orders may suggest the most likely rate determining steps.

A kinetic study was undertaken on the non-oxidative dehydrogenation of ethanol to acetic acid on the Cu/SiO_2 catalyst in the kinetic test set-up (see paragraph 3.5). The experimental including catalyst preparation, characterisation and testing, the methods used for data analysis and the results have been described thoroughly in an article submitted to the journal Applied Catalysis A: General. The submitted text is enclosed in Appendix F.1. Furthermore the found values are discussed against microkinetic models derived on the basis of suggested pathways.

The operating temperature was varied within the operating range relevant for industrial operation, 5 strategically chosen different feed ratios of ethanol:water and LWHSV was changed to obtain integral analysis at different degrees of conversion. The reactors were loaded in the single-pellet-string configuration (see paragraph 3.3.1) in order to obtain test result with best possible modelling ability. All the kinetic experiments in this set-up were run at atmospheric pressure (0-0.05 bar g). Repeated reversion to identical (standard) conditions over time was made to keep track on the deactivation. In the next paragraph the main results from the kinetic study are summarised with reference made to the submitted article.

6.7.1 Summary of results and discussion

In below paragraphs are shown the experimental results and conclusions made in the above mentioned article (see Appendix F.1) on acetic acid kinetics.

6.7.1.1 Characterisation

All the spent catalyst samples from the kinetic experiments were sent for XRPD analysis together with a fresh catalyst sample only being reduced and passivated (see paragraph 5.7.2). In a XRPD survey the Cu D[200] of spent catalyst was plotted against the time on stream.

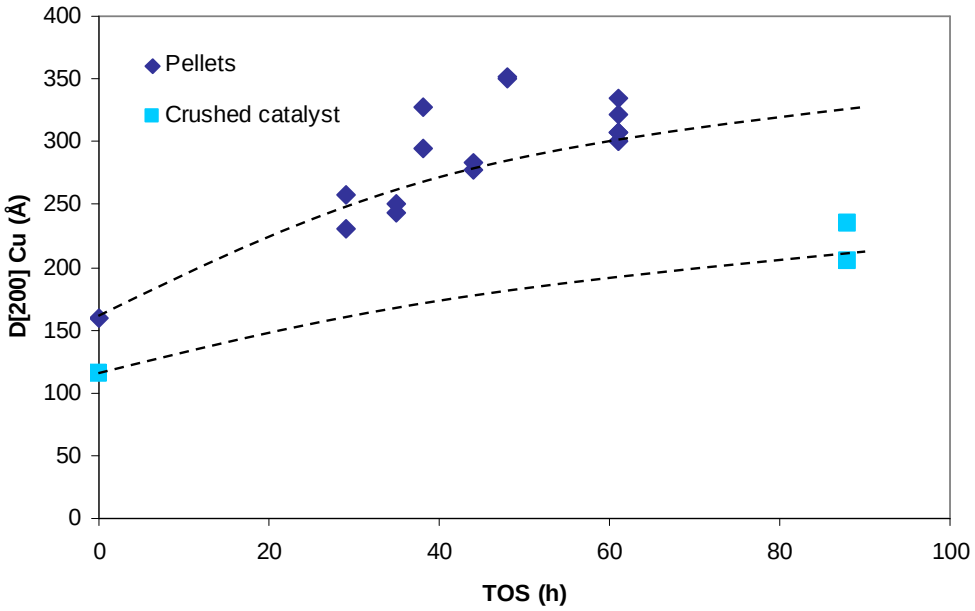

Figure 6-9: Plot of the XRPD Cu D[200] sizes from spent Cu/SiO_2 catalyst.

Figure 6-9 shows the plot of Cu D[200] sizes vs. hours on stream found by XRPD analyses on spent catalyst used in the short runs. From the information acquired from the TEM images the initial crystal size is about twice the crystal size of Cu spinel. XRPD analysis, made on reduced and passivated (see paragraph 5.7.2) samples of whole pellets and crushed pellets, confirms this doubling (see initial Cu D[200] of Cu spinel catalyst in Figure 5-31). The initial Cu D[200] for the crushed Cu/SiO_2 catalyst was about 115Å (the Cu crystal size estimated from TPD is around 100-150Å) whereas the whole pellets had a Cu D[200] of 160Å. From above Figure 6-9 it appears that under operation the Cu D[200] size increases for the crushed catalyst as well but it stabilises at a lower value. The Cu crystal size at for example at HOS=40 h is estimated to be almost double for the pellets.

6.7.1.2 Theoretical calculation

The water adsorption and dissociation on different Cu surfaces have been studied theoretically by means of DFT calculations.

Below is reported the main results from the DFT calculations on the adsorption of water on two different crystal surface planes, (211) and (111), providing information on preferred water adsorption sites and the activation energy for dissociation of water.

The calculations were done on a three-layer thick copper slab, with a 2 x 3 unit cell. Both copper (211) and (111) crystal surfaces were tested. Electronic structure calculations were performed within the DFT framework using a Dacapo calculator. The top layer was relaxed in all of the calculations and the bottom 2 layers were fixed during the transition state calculations. The starting positions for the water molecule were approximately 1.9 Å above the surface copper atom. The DFT calculations give the total energy of a relaxed Cu structure with and without adsorbed molecules. The water adsorption (binding) energy, E_{ads} may be calculated by means of Eq. 6-1:

$$E_{Ads} = E_{H_2O/OH^*} - E_* - E_{H_2O} \qquad \textbf{Eq. 6-1}$$

where E_{H_2O/OH^*} is the energy of the copper structure with the adsorbed water species on the surface, E_* is the energy of relaxed copper slab, and E_{H_2O} is the energy of relaxed water molecule in the gas phase. The lowest adsorption energy, thus where the strongest adsorption was found, were found for slabs where water is attached to one copper atom at the top of a step site.

The activation energy of water dissociation is found by calculating the total energy at different distances between the oxygen in the OH group and the dissociated hydrogen. The energy barrier height corresponds to the activation energy needed for the water dissociation reaction to occur.

The overall results from the DFT calculations are that water adsorbs much stronger to the Cu (211) surface than to the Cu (111) surface. Actually the water molecule preferred to stay in the gas phase for all of the Cu (111) surface calculations. Figure 6-10 shows a schematic figure of a dissociated water molecule on a Cu 211 step site.

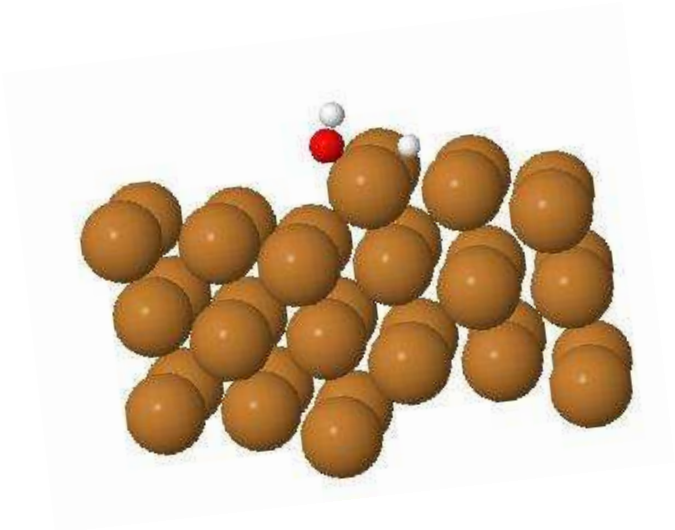

Figure 6-10: Representation of Cu 211 with dissociated water on the surface step site.

The Cu (211) surface calculations give the water dissociation activation energy of 1.3 eV (or 125kJ/mol) with a bond distance between OH group and hydrogen at around 1.7 Å.

6.7.1.3 Experiments, modelling and pathway

In order to simplify the problem only the description of the main reactions were aimed at. Thus in the case of Cu/SiO_2 B catalyst the major reactions are the dehydrogenation of ethanol to acetaldehyde and the oxidation of acetaldehyde with water to acetic acid and hydrogen. A minor conversion of acetaldehyde to diethoxy ethane took place as well, but this was only minor. And the side-product formation of butanol was negligible. The results from the experiments were treated in the mass balance program as described earlier (see paragraph 3.5.2).

Thus the ambition was to test the kinetic data in power law models, one model set up for the dehydrogenation of ethanol to acetaldehyde and one for the dehydrogenation of

acetaldehyde with water to acetic acid and hydrogen, the two first conversion steps in Scheme 3-1, p.45. For easy reference Scheme 6-1 and Scheme 6-2 show the two steps investigated.

$CH_3CH_2OH \rightleftharpoons CH_3CHO + H_2$ ΔH^{θ}=68.7 kJ/mol

Scheme 6-1: Step 1. Ethanol dehydrogenation to acetaldehyde.

$CH_3CHO + H_2O \rightleftharpoons CH_3COOH + H_2$ ΔH^{θ}=-24.8 kJ/mol

Scheme 6-2: Step 2. Acetaldehyde dehydrogenation to acetic acid.

The experimental data for Cu/SiO_2 B catalyst showed about 10 times faster conversion of ethanol to acetaldehyde as compared to conversion to acetic acid (see Figure 6-7, Figure 6-11 and Figure 6-13).

The kinetic reaction order of the first reaction step (Scheme 6-1) was known from the literature (*Tu et al., 2004*). Therefore, emphasis was put on finding the kinetic expression for the second conversion step (Scheme 6-2). However, for the reconfirmation of the reaction order found by Tu et al. and for the proper modelling of the conversions in the kinetic experiments the equilibrium had to be known for the ethanol dehydrogenation reaction (Scheme 6-1). Running an experiment at a low LWHSV provided for trustworthy equilibrium data, wherefrom a dimensionless equilibrium constant, K, of 0.7 could be determined, taken as being approximately equal to the reaction quotient at very low LWHSV according to Eq. 6-2:

$$K \approx Q_{appr} = \frac{p_{H_2} \cdot p_{CH_3CHO}}{p_{CH_3CH_2OH} \cdot p^{\theta}} = \frac{y_{H_2} \cdot y_{CH_3CHO} \cdot p}{y_{CH_3CH_2OH} \cdot p^{\theta}} = \frac{0.188 \cdot 0.085 \cdot 1.05 bar}{0.025 \cdot 1.013 bar} = 0.7 \qquad \textbf{Eq. 6-2}$$

This equilibrium constant value was found to be in proper agreement with the calculated equilibrium constant at 315°C of 0.8 found in literature based on thermochemical data reported by *Stull et al. (1969)* and with the calculated equilibrium constant of 0.6 based on an extrapolation of the experimental data by *Happel et al. (1974)* The standard entropy 264.2 J/(mol K) and formation enthalpy -166.4 kJ/mol values for acetaldehyde reported by *Stull et al. (1969)* were used in the further data evaluation.

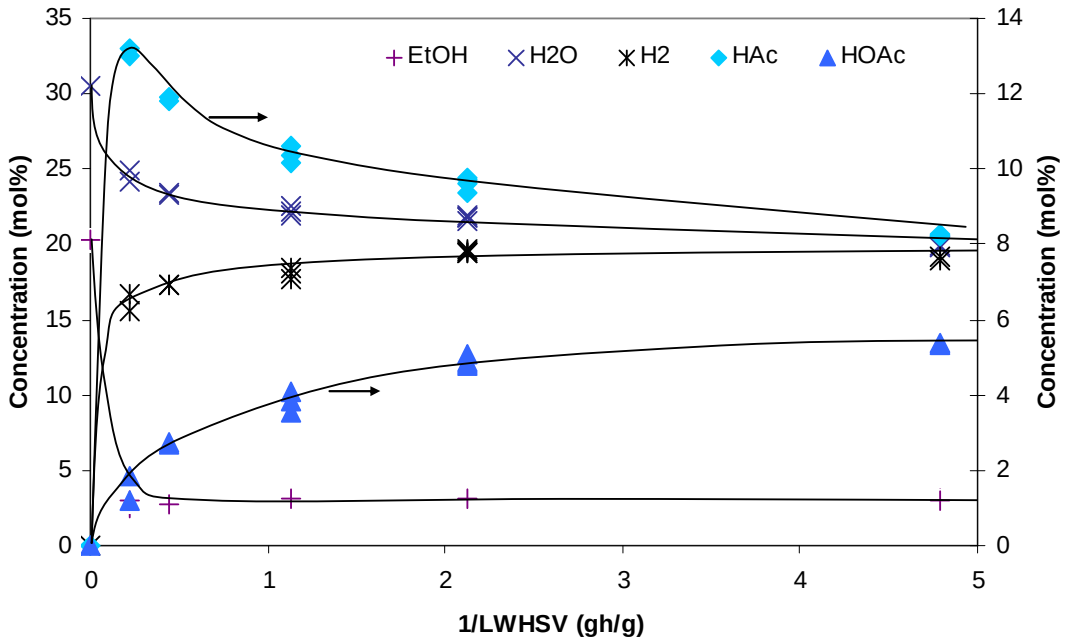

Figure 6-11: The conversion profile of a 40/60 (mol/mol) ethanol:water feed over crushed Cu/SiO_2 catalyst at low to very high contact time.

Figure 6-11 shows the conversion profile recorded during the equilibrium experiments. As it can be seen from the graph, acetaldehyde exhibits the behaviour of a typical intermediate, going through a maximum and being consumed at high contact times. The concentration of acetic acid was far below equilibrium in all the experiments.

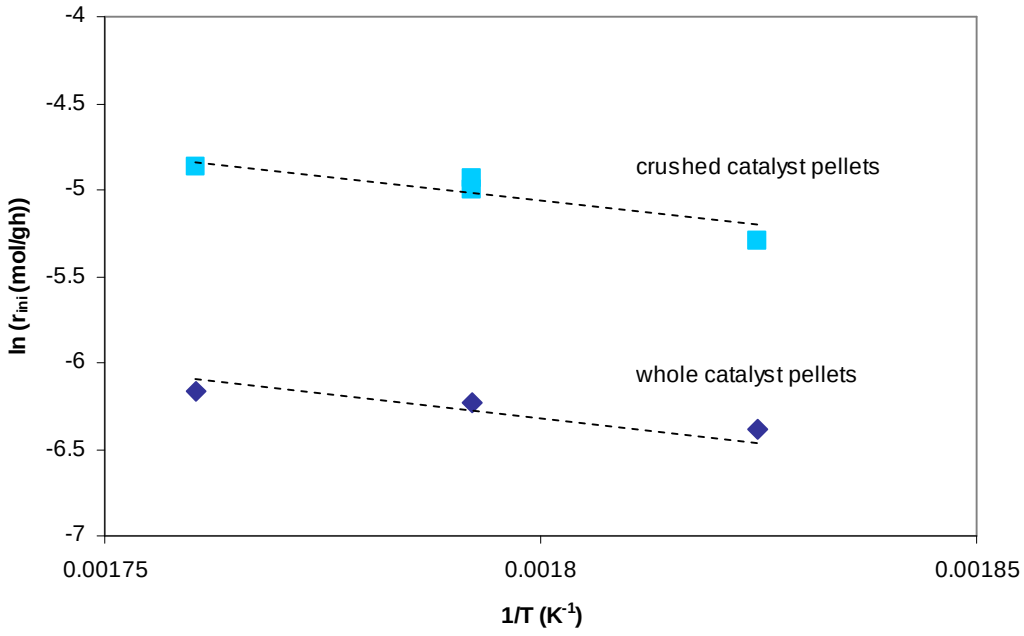

Figure 6-12: Arrhenius type plot of the initial acetic acid formation rates observed for crushed and whole catalyst pellets. The initial rates (mol/(g·h)) are estimated from the slope of the reaction profiles, y (mol%) vs. $1/SV_m$ ((g·h)/mol), established by SV_m variations under the assumption of isothermal conversion. $P_{CH3CH2OH}$=0.2 bar.

Comparing initial reaction rates obtained for crushed Cu/SiO_2 catalyst pellets and whole catalyst pellets run on an 40/60 ethanol:water feed at 275-295°C (approximate average bed temperature, in-out) revealed that 3-4 times as high reaction rates were obtained for the crushed catalyst.

On the other hand (as seen in Figure 6-12) by rough estimation the activation energy for the two systems seemed similar. As discussed in Appendix F.1 the most likely explanation to this was found in the influence of the catalyst particle size on the resulting Cu crystal size after reduction (see paragraph 6.7.1.1 and Figure 6-9).

A concluding modelling of a kinetic experiment based on whole pellets retrospectively confirmed that the experiments could not be assumed to take place isothermally. However, by making approximate differential analysis on crushed catalyst (1-1.4 mm sieve fraction) data a kinetic order with respect to ethanol of about 0.8 in the ethanol dehydrogenation step (Scheme 6-1) and a reaction order of about 1 with respect to water in the dehydrogenation of acetaldehyde step (Scheme 6-2) could be established (see Appendix F.1, Figure 5). Based on literature findings (*Tu et al., 2004*), it was assumed that the dehydrogenation of ethanol to acetaldehyde is a 1st order reaction in ethanol.

All the proper data sets (71 sets) were corrected for deactivation by anticipating an exponential decrease of activity as shown in Eq. 6-3. A good fit of the relative activity to the smoothed deactivation line was obtained hereby.

$$TF = TF_0 \cdot \exp(-k_{decay} \cdot HOS) \qquad \textbf{Eq. 6-3}$$

The relative initial activity TF_0=1, and the deactivation constant, k_{decay} (h^{-1}), was determined as the smoothed value of the depiction of standard condition activities vs. HOS (h). The correction factor to the observed reaction rates, TF, was calculated for each set of data. The TF, the oven temperature, the total feed composition incl. carrier gas was then stored in a data file together with the resulting concentrations of acetaldehyde and acetic acid. By using the reaction orders as found by the approximate differential analysis as starting points for the empirical power law models the experimental data were fitted into the following rate equations Eq. 6-4 and Eq. 6-5 for the equilibrium reactions in Scheme 6-1 and Scheme 6-2, respectively:

$$-r_{CH_3CH_2OH} = TF \cdot A_1 \cdot \exp(-E_1/RT) \cdot p_{CH_3CH_2OH} \cdot (1-\beta_1) \qquad \textbf{Eq. 6-4}$$

where A_1 is the pre-exponential factor in mol/(g·h·bar), E_1 is the apparent activation energy in kJ/mol, $p_{CH3CH2OH}$ is the partial pressure of ethanol in bar, and β_1 is the observed reaction quotient divided by the equilibrium constant for the reaction in Scheme 6-1; and

$$-r_{CH_3CHO} = TF \cdot A_2 \cdot \exp(-E_2/RT) \cdot p_{CH_3CHO}{}^{\gamma_{CH_3CHO}} \cdot p_{H_2O}{}^{\gamma_{H_2O}} \cdot (1-\beta_2) \qquad \textbf{Eq. 6-5}$$

where A_2 is the pre-exponential factor in mol/(g·h·bar$^{\Sigma\gamma}$), E_2 is the apparent activation energy in kJ/mol, p_{CH3CHO} is the partial pressure of acetaldehyde in bar, p_{H2O} is the partial pressure of water in bar, γ_{CH3CHO} and γ_{H2O} are the apparent reaction orders with respect to acetaldehyde and water, and β_2 is the observed reaction quotient divided by the equilibrium constant for the reaction in Scheme 6-2. Table 6-2 shows the constants found by minimisation of error between measured and calculated data. The values for step 1 represent pellet kinetics for the tested catalyst geometry and pore volume distribution, derived to facilitate the establishment of a kinetic model for step 2. The

step 2 values are close to intrinsic, judged by the reaction rate. In both cases the models are empirical power law expressions only and the range of validity only covers the ranges building the basis of these, i.e. temperatures 280-320°C, p_{EtOH}= 0.11-0.26bar, p_{HAc}=0-0.2bar, p_{H2O}=0.18-0.44 bar.

Table 6-2: The kinetic constants found by minimisation of the error between measured and calculated data.

	Pre-exponential factor	Optimised Reaction order		Apparent Activation Energy
Eq. 6-4, step 1	A_1= 3.53E3 mol/(g·h·bar)			E_1=43.7 kJ/mol
Eq. 6-5, step 2	A_2= 20.4 mol/(g·h·bar$^{1.34}$)	γ_{CH3CHO}=0.45	γ_{H2O}=0.89	E_2=33.8 kJ/mol

The parity plots produced accordingly, comparing the modelled concentration of acetic acid and acetaldehyde vs. the measured values, are shown in below Figure 6-13.

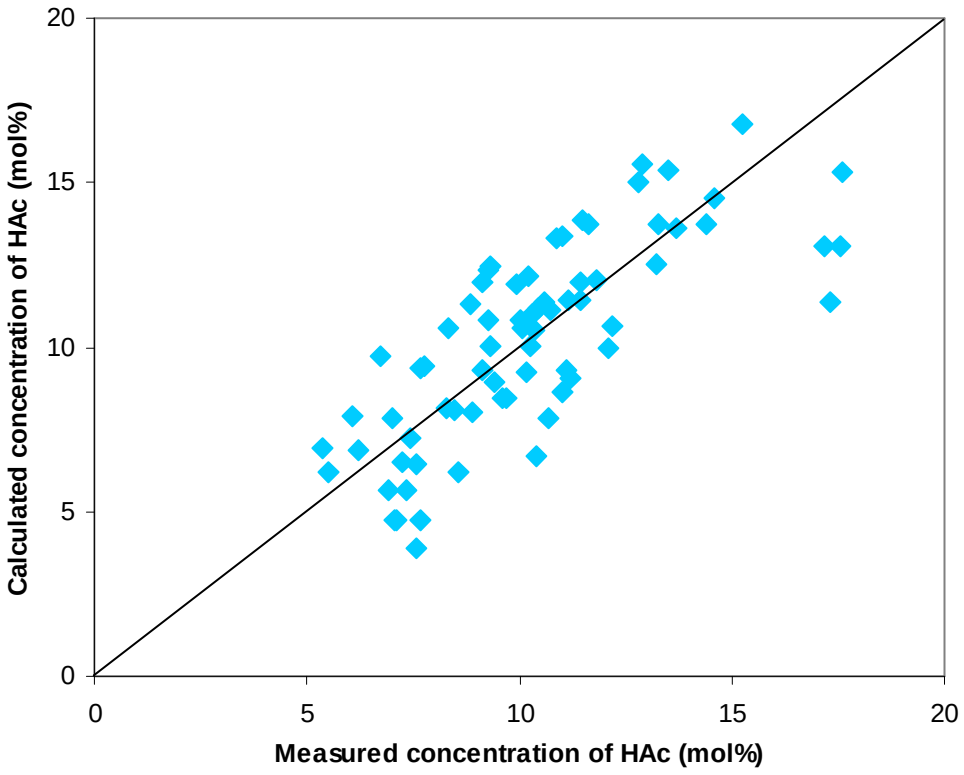

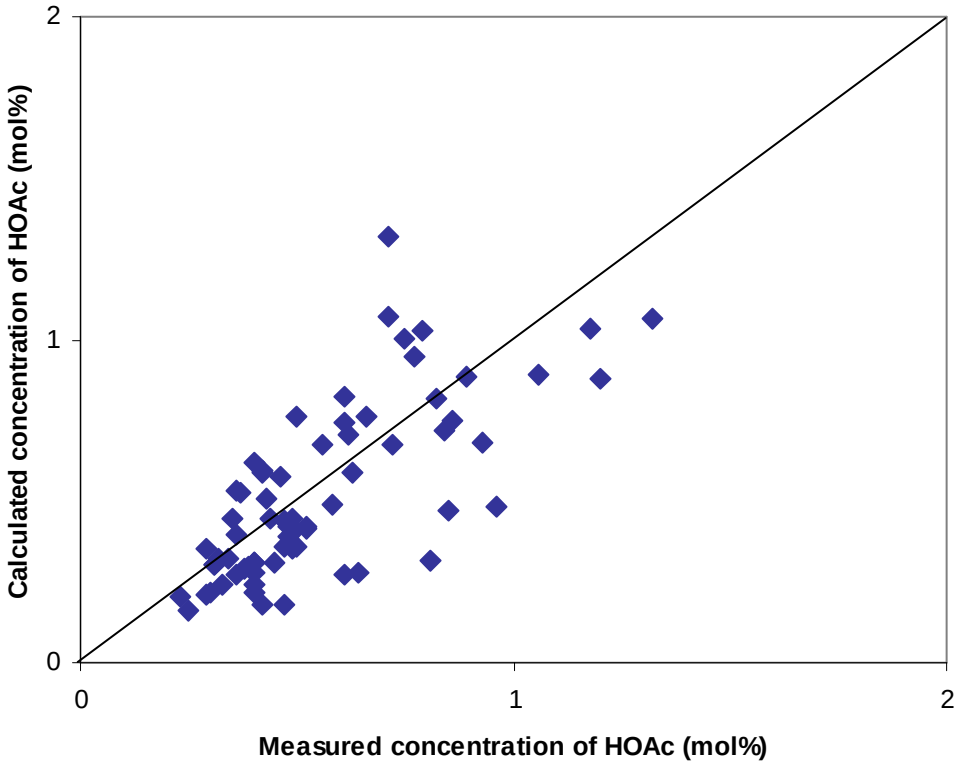

Figure 6-13: Parity plots of the calculated vs. the measured acetaldehyde and acetic acid concentrations in the reactor effluent. Upper: acetaldehyde. Lower: acetic acid.

Mechanistic and surface studies have been conducted for ethanol on Cu surfaces by *Iwasa et al. (1991), Chung et al., (1993), Inui et al. (2004), Shimada et al. (2005),* and *Colley et al. (2005)*, while others have studied the reactions related to methanol synthesis (and reforming) and the water gas shift reactions (*Askgaard et al., 1995, Ovesen et al., 1996, Shustorovich et al*., 1991). Mechanistic parallels may be drawn between the ethanol reforming and methanol reforming reactions according to *Iwasa et al. (1991), Chung et al. (1993)* and *Shimada et al*. *(2005)*. Reference is further made to study results on water dissociation made by *Guan et al. (2009), Phatak et al. (2009)* and *Chen et al. (2010).* These are discussed in more detail in the article submission enclosed in Appendix F.1. The elementary reactions are shown in Table 6-3, accordingly.

The elementary reactions indicated by red font are not considered likely based on the surface concentration of adsorbed atomic oxygen (*Phatak et al., 2009, Chen et al., 2010*). The elementary reactions indicated by blue font are considered less dominant due to the high concentration of acetaldehyde observed in this study compared to the known low activation energy for hydrogen abstraction to acetyl (*Colley et al., 2005*).

Table 6-3: The elementary reactions suggested based on literature. An asterisk signifies a free surface site.

	Elementary surface reaction	Type	Reference
I	CH3CH2OH(g) + * = CH3CH2OH*	Ethanol adsorption	a, b
II	CH3CH2OH* + * = CH3CH2O* + H*	Hydroxyl hydrogen abstraction	a, b
III	CH3CH2O* + * = CH3CHO* + H*	Ethoxy α-hydrogen abstraction	a, b
IV	CH3CHO* = CH3CHO(g) + *	Acetaldehyde desorption	a, b, c, d
V	CH3CHO* + * = CH3CO* + H*	Acetaldehyde α-hydrogen abstraction	b
VI	CH3CO* + OH* = CH3COOH* + *	Acetyl hydroxyl oxidation	(b)
VII	CH3CH2O* + O* = CH3CHOO* + H*	Ethoxy oxidation	e
VIII	CH3CHO* + O* = CH3CHOO* + *	Acetaldehyde oxidation	e
IX	CH3CHO* + OH* = CH3CHOO* + H*	Acetaldehyde hydroxyl oxidation	e
X	CH3CHOO* + * = CH3COO* + H*	Acetate formation	e
XI	CH3COO* + H* = CH3COOH* + *	Acetic acid formation	e
XII	CH3COOH* = CH3COOH(g) + *	Acetic acid desorption	c, d, e
XIII	H2O(g) + * = H2O*	Water adsorption	c, e, f
XIV	H2O* + * = OH* + H*	Water dissociation	c, e, f
XV	2OH* = H2O* + O*	Hydroxyl disproportionation	c, e, f
XVI	OH* + * = O* + H*	Hydroxyl dissociation	c, e, f
XVII	2H* = H2(g) + 2*	Dihydrogen formation	c, d, e, f

a) *Chung et al. (1993)*
b) *Colley et al. (2005)*
c) *Iwasa et al. (1991)*
d) This work
e) *Askgaard et al. (1995)*
f) *Chen et al. (2010), Phatak et al. (2009)*

The rate determining step could potentially be the hydroxyl disproportionation, step XV, which is known to be slow (*Ovesen et al., 1996*), but the calculated activation barrier (see paragraph 6.7.1.2) calculated by DFT is in disagreement with the observed activation energy of the empirical expression (see Table 6-2).

A microkinetic reaction rate model may be set up based on the above elementary reactions, anticipating that the oxidation of surface acetaldehyde, step IX, is the rate determining step. Assuming equilibrium of steps I-IV and XIII, XIV and XVII the following equilibrium equations may be formulated, where θ_* designates the coverage of free sites, θ_i designates the coverage of a site occupied by a component i, and K_i designates the equilibrium constant of the adsorption of a component i on a free site (i + * = i*):

$$K_{CH_3CHO} = \frac{\theta_{CH_3CHO}}{p_{CH_3CHO} \cdot \theta_*} \quad \textbf{Eq. 6-6}$$

$$K_{H_2O} = \frac{\theta_H \cdot \theta_{OH}}{p_{H_2O} \cdot \theta_*^2} \quad \textbf{Eq. 6-7}$$

$$K_{H_2} = \frac{\theta_H^2}{p_{H_2} \cdot \theta_*^2} \quad \textbf{Eq. 6-8}$$

$$1 = \theta_* + \sum \theta_{ads} = \theta_* \cdot \left(1 + \sum K_{ads} \cdot p_{ads}\right) \quad \textbf{Eq. 6-9}$$

Insertion into the microkinetic rate expression reduces to:

$$r_{rds} = k \cdot \theta_{CH_3CHO} \cdot \theta_{OH} = k \cdot K_{CH_3CHO} \cdot p_{CH_3CHO} \cdot \theta_* \cdot \frac{K_{H_2O} \cdot p_{H_2O} \cdot \theta^2}{\theta_H} = k \cdot K_{CH_3CHO} \cdot p_{CH_3CHO} \cdot \theta_* \cdot \frac{K_{H_2O} \cdot p_{H_2O} \cdot \theta_*^2}{K_{H_2}^{½} \cdot p_{H_2}^{½} \theta_*}$$

$$= k' \cdot \frac{p_{CH_3CHO} \cdot p_{H_2O} \cdot \theta_*^2}{p_{H_2}^{½}} = k' \cdot \frac{\frac{p_{CH_3CHO} \cdot p_{H_2O}}{p_{H_2}^{½}}}{(1 + \sum K_{ads} \cdot p_{ads})^2} \quad \textbf{Eq. 6-10}$$

The denominator in Eq. 6-10 is assumed to be close to unity, due to the high coverage of free sites on Cu surface at the reaction conditions (*Askgaard et al., 1995*). As the hydrogen co-produced is produced in equimolar amounts to acetaldehyde and this is the predominant product (intermediate) during the kinetic study, the partial pressures of these are correlating and indistinguishable in an optimisation of the model parameters to the experimental data. Finding therefore by optimisation (minimisation of error) a close to 1st order dependence in water and a close to ½th apparent order in acetaldehyde in the empirical rate expression (see Eq. 6-5 and Table 6-2) is consistent with the orders of above microkinetic rate equation, Eq. 6-10.

A similar derivation of the microkinetic expression based on the assumption that step VI (followed by step VII) is rate determining leads to a rate expression without any apparent acetaldehyde dependence which does not comply with the experimental findings.

The reaction orders found for the experimental data are best consistent with a reaction pathway where the elementary oxidation of surface acetaldehyde with hydroxyl takes place as the rate determining step. The pathway is rendered most probable based on the consistence of the reaction orders, above considerations on similarity to the methanol reforming reactions, the low abundance of surface atomic oxygen (Chen, C.-S., et al., 2010) and the high concentration of acetaldehyde in the product.

6.8 Discussion

The pre-investigations and characterisations of the Cu spinel catalyst drew the picture that under reaction conditions the Cu crystals are present as small crystals <100Å on the surface of alumina particles, their surface making up the inner Cu surface area of the catalyst pellet. Furthermore, the catalytic activity of ethanol conversion to acetic acid was found to be rather independent on the Cu loading from 5-33 % (Cu/(Cu+Al)) whereas the selectivity to condensation products depend much on the Cu loading, i.e. at low Cu loading the number of side-products increases. The Cu crystal size was not

found to depend on the Cu loading. The Cu particles of the size 150 Å obtained after reduction of Cu on silica are twice as big as the Cu crystals on alumina after reduction, but in both cases equally sized and spread on the support surface.

The activity level in terms of a STY_{HOAc}= 0.07 g/(g·h) found for the Cu/SiO_2 B catalyst and STY_{HOAc}= 0.15 g/(g·h) found for the Cu/SiO_2 A catalyst in non-oxidative dehydrogenation route is immediately too low to serve in an industrial size plant (see paragraph 4.11), especially seen in the light that indirect heat has to be supplied to the non-oxidative process. And the attempt to increase the activity of catalyst B by promoting with Pd, Pt, Cs and Ga showed (almost) no or negative effect on the activity. If for example promoters amend the defect Cu sites, the step sites, the preferential water adsorption and dissociation on this type of Cu sites hereby is reduced, reducing also the formation rate of acetic acid.

Meanwhile, one should keep in mind that the STY_{HOAc} calculated for the experiments are acquired under diluted conditions, where about 50% of the reaction medium is nitrogen. Anticipating that the kinetic reaction model of this work is valid also at slightly elevated pressure, say 3-4 bar, a GIPS modelling calculation of the STY in an adiabatic reactor with an inlet temperature = 300°C was made based on the derived models (see Table 6-2) using the SOR activity and the feed gas composition in the process flow diagram in Appendix D.2.

Table 6-4: Estimated STY_{HOAc} for the full conversion (T_{app}<20°C for the acetaldehyde oxidation to acetic acid) in an adiabatic industrial reactor assuming the validity of the kinetic model in this range.

	P= 3 bar	**P=4 bar**
STY_{HOAc} (kg/(kg·h))	0.30	0.43

In preparing the kinetic model for the dehydrogenation of ethanol to acetic acid experiments the composition of the feed, the feed rate, the carrier gas rate and the temperature were varied but not the pressure. However, as earlier established the activity seemed to stabilise at a higher activity even at operating pressures as high as 7.5 bar (see Figure 6-5). This stabilisation was found in the less trustworthy stabilisation test set-up. Further experiments will be needed to be conducted under conditions which may be reproduced and modelled, for example in a reconstructed kinetic test set-up, having been modified to allow the elevation of the operating pressure. Under the assumption of the model validity the STY_{HOAc} obtained under industrial conditions is above 0.3 kg/(kg·h)

The above modelling calculations also indicate that adiabatic reactors may be adequate for the non-oxidative dehydrogenation process. The temperature profile calculated for the conversion at 4 bar is presented in below Figure 6-14. It shows a drastic drop of the temperature at the inlet, reflecting the fast dehydrogenation reaction of ethanol to acetaldehyde down to 268°C, but it is followed by a temperature increase to 293°C induced by the exothermic acetaldehyde oxidation with water to acetic acid and hydrogen, allowing further acetaldehyde conversion. If this GIPS modelling of an industrial reactor holds, savings in the plant investment may be obtained by

exchanging the cooled reactor assumed in the process flow diagram with a trim preheater followed by an adiabatic reactor (see Figure 6-14).

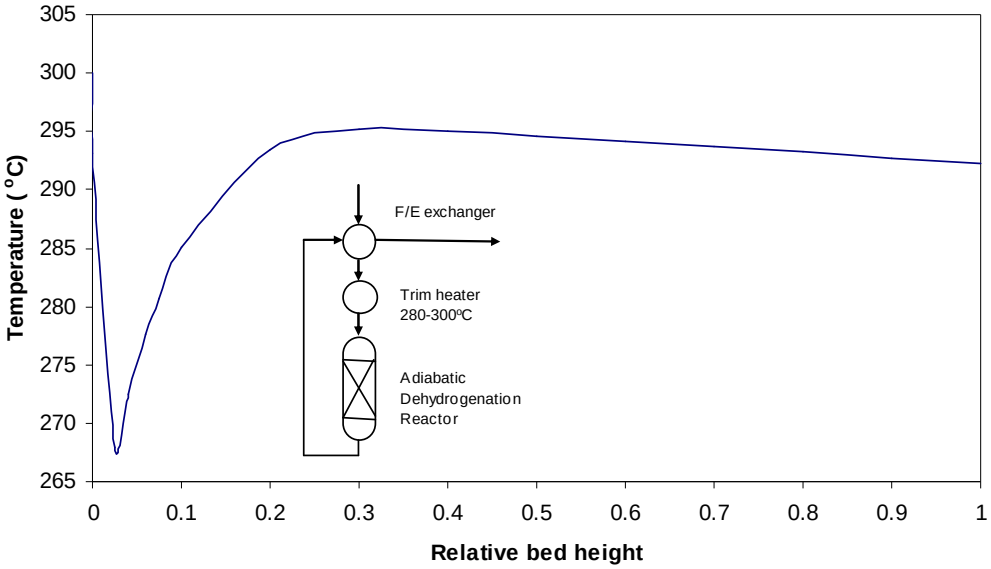

Figure 6-14: Calculated temperature profile in a modelled industrial adiabatic reactor with an inlet temperature of 300°C, anticipating the validity of the derived kinetic model at elevated pressure= 4 bar.

In the above calculations ideal thermodynamics were assumed. This is a good approximation for the ethanol dehydrogenation to acetaldehyde step. But knowing that carboxylic acids dimerise, ideal thermodynamics is not accurate for the acetaldehyde oxidation to acetic acid, however conservative. In order to make a next generation process development and process flow diagrams representing these, the equilibrium constant of the acetaldehyde oxidation to acetic acid in Scheme 6-2 should be acquired.

There are furthermore indications that the activity may be increased substantially by modifications of the preparation procedure (for example the ripening time and temperature) as the Cu/SiO_2 A catalyst powder had been prepared from the same recipe as Cu/SiO_2 B catalyst, but the calcined pellets of the A version exhibited about the double activity. The influence of the silica source, the calcination temperature, the reduction conditions etc. may determine the pore volume and the Cu dispersion obtained in the catalyst pellet. One promising way of increasing the catalyst activity for Cu/SiO_2 catalyst is to increase its dispersion of Cu. New methods for the production of highly dispersed Cu/SiO_2 catalysts have been investigated by *Chen (L.-F.) et al. (2008).*Stabilising promoters may help to reduce the deactivation rate (*Tu et al.*, 2001). Further with an increased activity the operating temperature may be reduced, reducing thereby the sintering of the Cu on the SiO_2. These are just mentioned as some catalyst development options. Alternative catalyst shapes may also be taken into consideration should the optimisation of the Cu dispersion offset the pore volume. But also other neutral type carriers may be tried. The unsupported Raney copper exhibited a surprisingly high activity and a high selectivity, especially when keeping in mind the careless preparation of it.

If the activity under the non-oxidative dehydrogenation conditions can not be increased considerably by catalyst improvements, say to a STY_{HOAc} of about 0.3 kg/(kg·h) or higher, one may further want to reinvestigate the partly oxidative dehydrogenation, as some good prospects were seen for the Cu/SiO_2 catalyst under these conditions. For example it was seen that the acetic acid formation activity increased by a factor of 8 (from a low level), when the Cu/SiO_2 B catalyst with 1wt% Pt was run under partly oxidative dehydrogenation. Or one may look for other Cu based catalyst on neutral and inactive carriers. Turning the focus back to the partly oxidative dehydrogenation obviously resolves the process related problem around transferring heat an endothermic dehydrogenation taking place in large volume catalyst bed. The superficial investigation on the partly oxidative dehydrogenation made was just a first shot, and more investigations are needed to support this route. Many possibilities remain for the layout of the addition of the oxygen source, and the catalytic behaviour of the catalyst must be understood before a preferred reactor type may be identified.

Therefore, despite the lower activity of the Cu/SiO_2 catalyst compared to the Cu on alumina, many possibilities for activity improvements for the Cu/SiO_2 catalyst are yet untried. With this outlook and the higher selectivity of Cu/SiO_2 already shown, a higher technical feasibility of the non-oxidative dehydrogenation process based on the Cu/SiO_2 catalyst, as compared to the conventional based on carbonylation, would be attained, if better catalyst robustness was obtained too.

It was previously observed how the co-feeding of butanol and possibly acetaldehyde caused detrimental deactivation of the Cu spinel catalyst. By changing the support to another type, here SiO_2 being more neutral (*Tu et al.*, 2001, *Daniell et al., 2000, Liu, L. et al., 2006, Venezia et al., 2004*), one may expect that certain characteristics related to the Cu particles and the reactants behaviours on these remain while the behaviour of Cu in relation to the support (interaction), and the effects induced by the support itself change. Indeed the Cu/SiO_2 exhibited much higher tolerance to process variations (see Figure 6-3 and Figure 6-4), for example co-feeding of acetaldehyde and diethoxy ethane, and the side-production of butanol was strongly reduced. The change of support from acidic to neutral apparently cut off the ethanol esterification with acetic acid the dehydrogenation reaction of ethanol with acetaldehyde to form ethyl acetate and hydrogen (see Figure 2-5). The change of side-product ethyl acetate to diethoxy ethane does not immediately change the feasibility of the process. The removal of diethoxy ethane most probably takes place spontaneously during distillation (see paragraph 6.3). Importantly, the stabilisation of the acetic acid activity on Cu/SiO_2 was obtained at an increased pressure of 7 bar (see Figure 6-5).

Comparing the characteristics of the fresh and the spent catalyst of either the Cu spinel or the Cu/SiO_2 catalyst three parameters stand out (see Table 6-1): the specific surface area measured by HBET, the delta carbon content (fresh-spent catalyst) and the Cu crystal size. The other parameters do not change that much, and are alike or their differences relate to the above factors. While the pore volume is the same in the compared samples, the specific surface area is substantially higher for the Cu/SiO_2 catalyst, presumably due to the larger pores in the Cu spinel catalyst. The accessible Cu surface area is higher in the Cu/SiO_2 catalyst, proportional to the Cu content as compared to the Cu spinel catalyst. The increase of the C content, comparing the fresh and the spent catalyst, expresses the amount of carbonaceous compounds trapped

inside the catalyst during the run hours. The lower delta carbon (wt%) for the Cu/SiO_2 catalyst of 1.3 wt%, as compared to the delta carbon of >4.7 wt% for the Cu spinel catalyst, developed over three times as long exposure time shows its far lower tendency to form carbonaceous compounds. The neutrality and inert carrier characteristics of silica were already indicated by the support study results (see paragraph 6.2.3) and by literature findings (*Tu et al.*, 2001, *Daniell et al., 2000, Liu, L. et al., 2006, Venezia et al., 2004*). The reduction of the acidity of the catalyst support apparently reduced the acid catalysed side-production of high molecular aldol condensation products (*Luo et al., 2009*) found by TEM in this work. *Luo et al. (2009)* also suggest that the high molecular products are responsible for the deactivation encountered for their alumina supported catalyst.

Another outstanding difference of the Cu spinel catalyst and the Cu/SiO_2 catalyst is the size of the Cu crystals obtained after reduction. For the Cu spinel catalyst the Cu crystal size was independent of the Cu loading and the size of the Cu spinel crystals prior to reduction (see Figure 5-30) it grew at higher reduction temperature (see Figure 5-24) and over time on stream during operation (see Figure 5-31). Furthermore the size of the Cu crystals is suggested to depend on the hydrogen partial pressure, supported by literature findings (*Quincoces et al., 1997*). For the Cu on SiO_2 the Cu crystal size resulting from reduction was found to be dependent on the size of the catalyst particle reduced and time on stream (see Figure 6-9). Water is known to increase the tendency of sintering the Cu crystals on catalyst surfaces (*Quincoces et al., 1997, Kamble et al., 1998, Sun et al., 1999*). The lower initial crystal size for the crushed catalyst may be explained by a lower reduction water concentration in the pores. Due to the autocatalytic nature of the reduction (see Figure 5-23) a temperature and a hydrogen partial pressure dependency could also be foreseen for the Cu/SiO_2 catalyst.

Under partly oxidative dehydrogenation conditions the acetic acid reaction rate on the Pt promoted Cu/SiO_2 increased with the air flow rate, i.e. the concentration of oxygen, without showing signs of deactivation through an increased level of condensation products in the condensate. In the partly oxidative dehydrogenation experiments on whole Cu spinel catalyst the addition of air led to the forming of condensation products and rapid deactivation (see Figure 5-37). Apparently the Cu/SiO_2 catalyst is less prone to the partly oxidative conditions, which give good prospect for a reinvestigation.

6.8.1 Kinetics

The empirical kinetic model (see Eq. 6-4) derived for the dehydrogenation of ethanol (Scheme 6-1) based on *Tu et al, 2004*. had a reasonable fit with experimental data and the apparent activation energies were in good accordance. The effect of pore diffusion was assessed by means of the effective diffusivities as evaluated from the pore volume distribution and calculating the effectiveness factor under actual reaction conditions (*Bischoff et al.*). With the cylindrical pellet size of d x h=5 x 5.5 mm an effectiveness factor between 50% and 90% was estimated by means of the generalised Thiele modulus, ϕ, and the relation according to Eq. 6-11 (approximation: as spheres):

$$\eta = \frac{1}{\phi} \cdot \left[\frac{1}{\tanh(3\phi\ )} - \frac{1}{3\phi} \right] \qquad \textbf{Eq. 6-11}$$

where $\phi=R/3\ (k/D_e)^{½}$.
No external limitation was estimated for the first conversion step over the Cu/SiO_2 catalyst as per the Mears criterion. With low effectiveness factors, i.e. strong pore diffusion limitations, one would observe a pronounced deviation for the apparent activation energy as compared to the intrinsic. Here, we do not obtain an apparent activation energy in the empirical model (44 kJ/mol) significantly different from the intrinsic value reported by *Tu et al, 2004* (50 kJ/mol).

The empirical kinetic model (see Eq. 6-5) derived for the second conversion step (Scheme 6-2) is most consistent with the microkinetic model for the hydroxyl oxidation of acetaldehyde being the rate determining step. Judged by the quality of the parity of the kinetic data versus modelled data, the empirical model can not serve as a proof of evidence of the pathway or the rate determining step, though.

Assuming that the Cu surface area relates inversely to the Cu crystal size for a constant Cu loading (based again on Cu crystals being hemispheres), the specific Cu area was 1.4 times as high for the crushed catalyst as compared to the specific Cu area of the whole pellets. Furthermore, the density of Cu step sites on a Cu surface presumably depends inversely on the Cu crystal size as do Au steps sites on Au crystals (*Guan et al., 2009*) implying a catalyst mass specific number of steps sites increasing inverse proportionally to the square of the Cu crystal size for a constant Cu loading. Therefore, as discussed in the article on kinetics enclosed in Appendix F.1, the 3-4 times higher activity observed for the crushed catalyst, giving the activity dependency an order with respect to the Cu crystal size higher than one, may point to that the rate determining step preferentially takes place on the step sites (for example steps in the Cu 211 plane) of the catalyst. In close accordance with above suggested elementary reaction pathway, water indeed does preferentially dissociate into hydroxyl on the step sites according to the DFT calculations, producing thereby the oxidant required for the elementary oxidation of surface acetaldehyde.

The mechanism and kinetics of the dehydrogenation of ethanol to ethyl ethanoate over a Cu/Cr_2O_3 was studied by *Colley et al. (2005).* They found that ethoxy further dehydrogenate to form adsorbed acetyl which in the suggested rate determining step combine with another ethoxy to form adsorbed ethyl ethanoate, having an apparent activation energy of 92 kJ/mol. Our apparent activation energy is less than half (33.8 kJ/mol) suggesting another rate determining step prevails than the parallel acetyl oxidation with hydroxyl.

On the basis of above assumption it is striking that whereas the activity remained constant for the Cu spinel catalyst with increasing specific Cu surface area (increasing the Cu loading without increasing the Cu crystal size, see Figure 5-29 and Figure 5-30), the activity increased with a factor of 3 for the Cu/SiO_2 catalyst when doubling the specific Cu surface area (by halving the size of the Cu crystals at constant Cu loading). The activity independence of the Cu loading for the Cu/Al_2O_3 catalyst may point to a strong support influence. *Chang et al*. (2003) also found a low dependence on copper loading for the dehydrogenation of ethanol over Cu supported on rice husk ash, comparing it to a Cu/SiO_2 catalyst.

Both kinetic models describe in principle pellet kinetic and are therefore geometry specific and with the limitation that they are only valid within the process ranges they were built on. The kinetic expression for the second step is however not limited by diffusion and may be used as an intrinsic kinetic model, making the prediction of other catalyst geometries possible.

6.9 Conclusion

Cu/SiO_2 was found to be a much more selective and stable, however less active catalyst than Cu spinel catalyst. The higher selectivity and stability of the Cu/SiO2 catalyst may be attributed to its more neutral SiO_2 carrier in comparison with the γ- and η-alumina support of the Cu spinel catalyst. Contrary to the Cu spinel catalyst the activity of the Cu/SiO_2 catalyst indicatively increases with the specific Cu surface area and it is estimated to increase approximately proportionally to the estimated catalyst mass specific abundance of step sites.

An empirical intrinsic kinetic expression was derived for the dehydrogenation of acetaldehyde to acetic acid step by fitting to 71 experimental data sets obtained. By comparing the surface study results found in literature, in turn suggesting microkinetic models, with the derived empirical kinetic expression, the elementary pathway going via the oxidation of surface acetaldehyde with surface hydroxyl, as the rate determining step, was most consistent. Furthermore, the above mentioned activity dependence points to a rate determining step which takes place on a step site. DFT calculations show the preferential water dissociation at Cu step sites (activation energy of 125kJ/mol), being consistent with the proposed mechanism, as hydroxyl, being a reactant, is primarily present on step sites.

The kinetic models found may be used to improve the process modelling. However, in order to make further proper process development, knowledge of the equilibrium constant for the acetaldehyde to acetic acid reaction should be established. As a preliminary activity value a STY_{HOAc}=0.07-0.15 kg/(kg·h) may roughly and conservatively be assumed as an EOR activity. This value is immediately inferior to a minimum sound activity 0.3 kg/(kg·h) for obtaining proper reactor design (see paragraph 4.11). Extrapolation under the assumption of the model validity at 3-4 bar indicates that the catalyst activity is >0.3 kg/(kg·h) under industrial conditions.

Otherwise, the activity of the Cu/SiO_2 catalyst has to be improved to comply with industrial preferences of STY of products >0.3 kg/(kg·h). The Cu/SiO_2 catalyst has not been optimised yet, nor has it been investigated in detail as to reduction, butanol co-feeding and idle operation. The optimisation of the specific Cu area may help increase the catalyst activity, but also the optimisation of the catalyst pore structure may contribute. The silica source, the calcination and reduction of Cu/SiO_2 and promoters are amongst other parameters that could be looked into in that respect. With a successful catalyst improvement and under the initial price conditions given, the further improved Cu/SiO_2 catalyst, having a STY_{HOAc} of at least 0.3 kg/(kg·h), could be embedded in the preliminary non-oxidative ethanol to acetic acid process scheme at realistic conditions, which according to the conservative estimate made in Chapter 4, Appendix D.2 and D.6 of the corresponding acetic acid gate production price and the ROI, is feasible and competitive over the conventional carbonylation process described in Chapter 2 and appendix B.

Indicatively, previous investigation on the Cu spinel catalyst under partly oxidative dehydrogenation showed increased severity of the operating conditions. Cu/SiO_2 on the other hand showed better behaviour during the exposure to oxygen. As a more ambitious approach the partly oxidative dehydrogenation alternative (slightly exothermic) could be investigated further and another process flow diagram developed accordingly, with special emphasis on the reactor type applied (see paragraph 4.8.2).

The investigation of the conversion of ethanol to acetic acid was halted. In the last Chapter 7 (next) the reason for the weakening of the process basis will be discussed, and alternatives measures of utilising biomass feeds for the production of value-added chemicals are suggested.

Chapter 7 Status, Review, Outlook and Recommendations

7.1 Introduction

In this thesis the investigation of a bio-ethanol to acetic acid process was undertaken, based on literature study, catalyst investigations, process calculations, economic evaluations etc. Envisioning the present project as an example of a process innovation effort, a relevant project methodology has been aimed at. According to the INSPIRE model (see Figure 1-13, *Wysocki et al., 2003*) suggested for explorative projects, repeated reviews must decide for their destiny. The day-to-day project life must have a certain degree of isolation from the outside world, but reviews may occasionally need to be expanded to involve quite important external factors, which may redefine the project scope. Using the INSPIRE model terms the target in this project will then have changed. The objective '*to find a heterogeneous catalyst capable of converting a biomass-based feed stream to a value-added product, with the required activity and selectivity, in order to obtain a viable process alternative to the conventional*' has however remained.

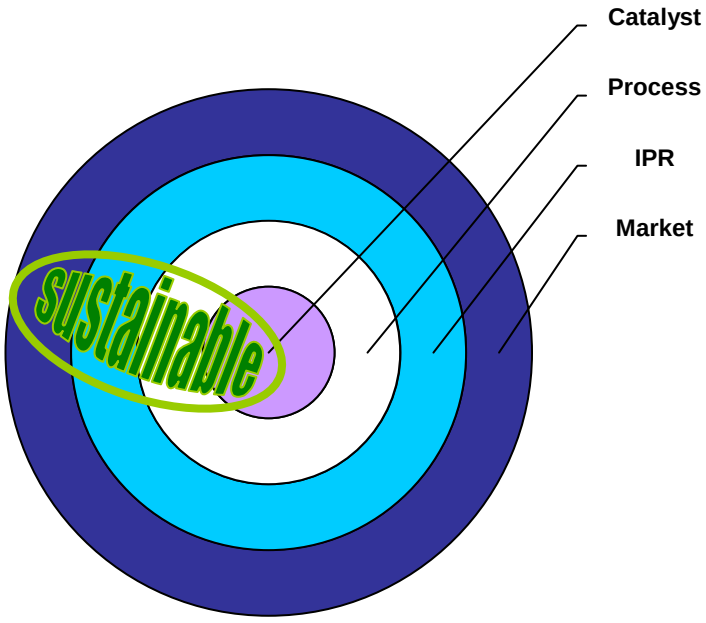

Figure 7-1: Once the sustainability aspects had been sorted, the main focus in the day-to-day project life has been the catalysts, their characterisation, catalytic behaviour and process implications. IPR has been tended to with respect to freedom to operate and for the protection of discoveries. Market issues were dealt with initially, but received less attention routinely.

This final chapter presents the status of the project, making a short summary of the essence of the activities conducted. Further in a review of the methods used, the basis for the analysis and the interpretation of the results achieved are treated. Some external factors, which have been less attended to during the catalyst and the process investigations, and which bear the potential of changing the project scope, will be discussed. The conclusions related to the original project and in view of these factors will be given. In the continuation hereof an outlook for the prospects of resuming the original project scope, changing the target product or more radically changing the feedstock state, are considered.

This chapter is concluded with my overall recommendations on the conversion of biomass based feedstocks in the light of these discussions and conclusions.

7.2 Status of the acetic acid process

The investigation of the conversion of ethanol to acetic acid was taken as an example of converting a biomass based feedstock to a value-added chemical. The use of biomass as an alternative feedstock to fossil based for chemicals production was reasoned. Ethanol was pointed out as a sensible biomass platform, and acetic acid as a product was selected by means of a gross margin analysis. From the literature the ethanol dehydrogenation to acetic acid, non-oxidative or oxidative, was found to be catalysed by a number of catalysts, comprising Cu based. Stability problems for Cu catalysts had been discussed in the patent literature. No commercialisation of the direct non-oxidative dehydrogenation, bearing the highest number of process advantages, had been obtained.

A screening of a selection of 33 different kinds of catalysts, inspired by literature findings, supported and unsupported, was made with the focus on activity, mechanical stability and selectivity for the conversion of a feed of ethanol, optionally with water, to acetic acid. The most selective catalysts found were the Raney Cu and Cu catalyst produced by the heating of $CuCO_3$. However, with the highest priority on activity and mechanical stability the first choice was a Cu spinel catalyst obtained after calcination of CuO/Al_2O_4 at 850°C. A second best candidate which was pointed out was a Cu/SiO_2 catalyst having medium activity, high mechanical stability, but with a higher selectivity than the Cu spinel catalyst. The highest product selectivity was in general found when co-feeding ethanol and water over the catalysts.

The main equilibrium limited reactions in the above non-oxidative dehydrogenation of ethanol-to-acetic acid process are shown in Scheme 7-1 below:

$CH_3CH_2OH \rightleftharpoons CH_3CHO + H_2$ $\quad\quad \Delta H^{\theta}=68.7$ kJ/mol

$CH_3CHO + H_2O \rightleftharpoons CH_3COOH + H_2$ $\quad\quad \Delta H^{\theta}=-24.8$ kJ/mol

Scheme 7-1: The two main reactions in the one stage non-oxidative dehydrogenation of ethanol to acetic acid. The relevant industrial operating conditions are 280-320°C and a pressure slightly elevated above atmospheric.

But also side-product formation of ethyl acetate, diethoxy ethane, butanol, and minute amounts of butyric acid was found for the catalysts investigated in present work.

An actual set of conversion degrees found by experiment was specified in a process calculation, comprising a conversion step followed by a separation step (see Figure 7-2).

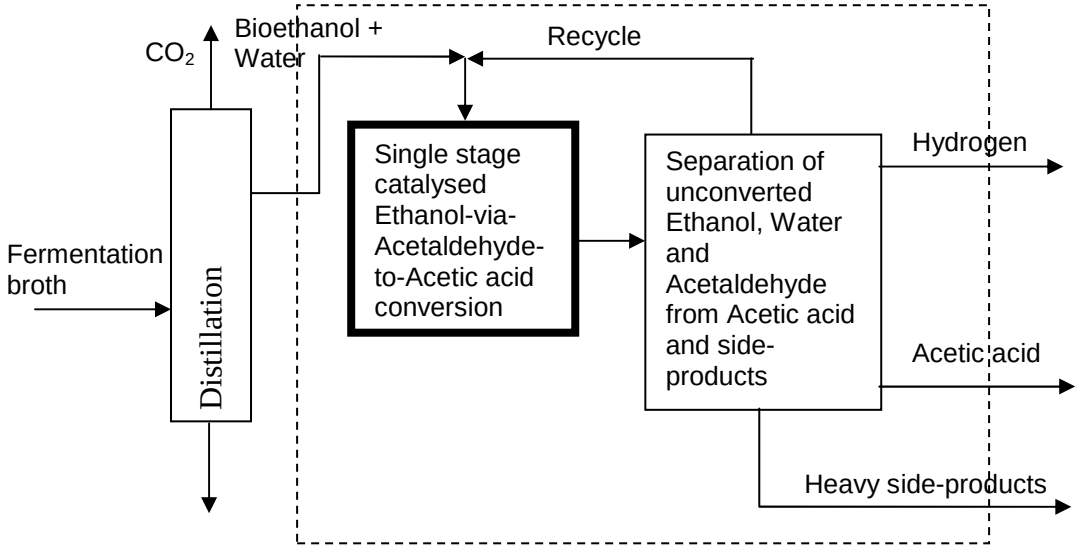

Figure 7-2: Simplified schematic representation of the non-oxidative dehydrogenation of ethanol-to-acetic acid process (dashed line box) fed with a distillate from bioethanol production (by fermentation). The recycle stream consists of ethanol, water, acetaldehyde, (ethyl acetate). The main focus of this work was related to the catalytic conversion step and the process aspects.

Hereby a recycle of the unconverted ethanol and intermediates was illustrated. The separation of acetic acid from side-products, intermediates and unconverted ethanol and water was assumed possible. By up-scaling the process calculation to a bioethanol-to-acetic acid plant production capacity of 300,000 MTPY of acetic acid, the mass flow rates and heat exchanger duties etc. could be presented in a process flow diagram. One-line specifications were prepared based on the figures of the process flow diagram and the plant investment was in turn estimated. The ±30% investment estimate made from these specifications showed to be encouragingly low.
The overall bioethanol-to-acetic acid gate price (conservatively disregarding a potential credit of the hydrogen co-product, and showing little sensitivity on catalyst activity and energy consumption) was compared to the estimate of a conventional 300,000 MTPY acetic acid plant. The competitiveness of the bio-route vs. the conventional and the comfortable margin between the market price and the gate price allowed for a continued investigation. Furthermore, the bioethanol-to-acetic acid process suggested is fed by an aqueous ethanol make-up stream in compliance with the desire of converting a biomass derived feed stream without prior water removal.

In spite of encouraging activity results obtained during the screening of catalysts, the Cu spinel catalyst was rejected after thorough characterisation establishing that its fast deactivation and decreasing selectivity was related to its support acidity and basicity. The alternative Cu catalyst on an inert SiO_2 carrier on the other hand was capable of converting ethanol to acetic acid via non-oxidative dehydrogenation at a temperature of 280-320°C and atmospheric pressure with a high selectivity.

An industrial operating pressure higher than atmospheric must be foreseen to secure a driving force in the downstream cooling train and separation section. An operating pressure of 10 bar g and small additions of butanol was found to deteriorate the catalyst, while a stabilisation of the activity was seen for a moderate elevation of the operating pressure to 7.5 bar g without butanol additions.

A further, important feature indicated by experiments was that the Cu/SiO_2 catalyst has the ability of converting ethanol to acetic acid under so-called partly oxidative dehydrogenation conditions, which is a discovery done in present work, providing several process advantages. Partly oxidative dehydrogenation is obtained by co-feeding a source of oxygen, oxidising part of the hydrogen co-produced in the non-oxidative dehydrogenation process. The partly oxidative dehydrogenation allows for a controlled removal of heat from the synthesis. The advantageous process heat integration of 1) the partly oxidative bioethanol conversion to acetic acid, 2) the conversion of bioethanol to ethylene in combination with 3) the production of vinyl acetate monomer from acetic acid, ethylene and oxygen was discovered.

Three patent applications have been filed in order to obtain IPR protection: a process control obtained by controlling the water content of the recycle stream, the partly oxidative dehydrogenation and the process integration with VAM.

Summarising pros and cons, the non-oxidative process provided more robustness than the partly oxidative dehydrogenation. Empirical kinetic expressions were derived for the two reaction steps making up the non-oxidative dehydrogenation route from ethanol to acetic acid.

The SOR activity of 0.07-0.15 kg/(kg·h) found for the Cu/SiO_2 catalyst was immediately inferior to the requested activity level for industrial catalysts as of 0.3 kg/(kg·h) set by basic reactor design constraints. Extrapolation of the derived model to an industrial pressure however indicates an activity $\geq$ 0.3 kg/(kg·h). Furthermore, under these assumptions the possible application of an adiabatic reactor is indicated reducing the assumed investment. The Cu/SiO_2 catalyst has still not been optimised neither have the calcination and reduction procedures during its activation, leaving improvements potentials open.

If defining competitiveness as conditions where the ROI is higher and adequate than those of a comparative example, and the activity of the Cu/SiO_2, or an alternative catalyst with high selectivity and robustness to acetaldehyde, may be confirmed or increased to comply with an industrial value>0.3 kg/(kg·h) the non-oxidative dehydrogenation process remains competitive over the conventional carbonylation process. Such improvement is believed to be within the reach of catalyst development. The process and investment implications of introducing a partly oxidative dehydrogenation have not been pursued yet.

7.3 Review

As a basis for the study, bio-ethanol was quickly selected over bio-glycerol as the most promising biomass based feedstock among these two most relevant feedstocks. Ethanol remains a sensible choice for studying catalytic conversion to value-added chemicals based on the sustainability criteria initially considered.

The number, nature and quality of the analyses to evaluate the project state were continually refined throughout the progression of the project in several aspects: catalyst characterisation, test facility and product analysis, modelling tools, process considerations, competitiveness and intellectual property rights. Very rough prediction and anticipations were made initially on all aspects (see Figure 7-3).

	Progression of project →			
Market	Gross margin analysis	Gate price analysis		Price development
IPR	Freedom to operate	2 patent applications	1 patent application	
Process	Degree of conversions	Process development	Activity, selectivity review	Equilibrium review
Modelling	Root search on condensate analysis		Mass balance tool	Parameter estimation
Experimental test set-up	Screening	New + Stability	Kinetic	
Catalyst activity	Non-quantitative	Quantitative condensate	True activity	Kinetic expressions
Catalyst characterisation	XRPD	In situ EXAFS, XRD, TPR, chemisorption, TEM		Elementary reactions

Figure 7-3: The parallel activities on aspects related to process innovation. During the progression of the project (left to right) the focus has been shifting between the parallel disciplines, and the methods and equipment adopted in these have continuously been refined.

As an example of the progression during the project the number and types of experimental test set-ups expanded in order to overcome shortcomings of the initial screening test set-up (see Chapter 3) to further comprise a new (improved), a stability (high pressure, automated) and a kinetic test set-up. But also here compromises were made. For example the reactor type in the stability test set-up was given a low priority for the mere availability of an automated test set-up. A kinetic test set-up was designed and built into a GC oven, aiming to secure as good heat transfer conditions as possible, while at the same time securing proper fluid dynamics (in an appropriate Re_p range) in a single-pellet-string arrangement of the catalyst bed. Meanwhile reactor modelling using the derived kinetics revealed that the reactor was not operated isothermally. Preferably a back-mix type of reactor should have been used for the kinetic experiments, enabling superior to isothermal conditions.

The greatest source of error or imprecise analysis on the catalyst activity aspect level was that corrosion problems prevented us from making online total composition measurements. In addition, the modelling shortcomings of the reactor in the kinetic test set-up were a source of inaccurate measurements.

Further suggested investigations and developments to support process innovation are listed below.

Experiments run on crushed catalyst in supplement indicated the reaction orders of ethanol and water respectively by approximating the initial reaction rate to calculated STY values. These results were only used as a starting point for the integration analysis based on a computer aided reactor model. Principally the parameter fitting of two consecutive reaction steps, of which the first is close to equilibrium, decreases the certainty of the obtained values for the second reaction. Very precise experimental data is required. The quality of the data may have been improved by developing better methods for co-feeding acetaldehyde under reliable conditions.

The significance of the Cu loading is unknown. In spite of the low Cu loading dependence found for the Cu on alumina system, the indications were that a lower

support interaction could be expected in the Cu on silica catalyst system. This point should be pursued too.

Indications of successful partly oxidative dehydrogenation were observed. The experiment on the partly oxidative dehydrogenation on Cu/SiO_2 should be repeated. The co-feeding influence of hydrogen with regard to stability and activity should be investigated in this respect.

As discussed before, water constitutes a source of deactivation through sintering. On the other hand it enhances the process kinetics. In a future study the optimal water to ethanol ratio should be found.

Most of the experiments were conducted at atmospheric pressure. The operating pressure is preferably raised to at least 3 bar in order to provide a physical driving force in the process industrially, overcoming the pressure drops in the flow units. It seems the catalyst is prone to increased operating pressure (10 bar is too high). It should be established how much butanol may be added at 3-4 bar pressure (industrial relevant pressure), observing the deposition of carbonaceous material on the catalyst, and the growth of the copper crystal size under these conditions.

All the kinetic experiments were run far from the acetaldehyde oxidation equilibrium. Furthermore, it should be pursued how to increase the conversion per pass in order to reduce the energy consumption. The equilibrium of the acetaldehyde oxidation with water to acetic acid and hydrogen (see Scheme 6-2) has to be established before the process development challenging this equilibrium may materialise. Until then only experimentally based diagrams may be drafted.

The process diagram representing the non-oxidative bio-ethanol to acetic acid route is only preliminary. The evaluation of the process is therefore also made on a preliminary level. More detailed thermodynamics must shed light on the layout and the energy consumption of the separation section. Especially, the means of butanol removal should be looked further into. The equipment specifications were made as one-line specs and the columns in the distillation section were specified based on a simple internal PRO-II design tool. Significant incremental investment could be needed to fulfil the requirements for the acetic acid purification to meet the market specifications. Therefore in order to make a more solid economic comparison a detailed mass balance calculation must be established simulating the separation section based on a sound thermodynamic model. Furthermore, a new set of specifications must be prepared based on this improved flow diagram. Meanwhile the investment load on the acetic acid gate price is much lower than for the carbonylation based plant.

7.4 External factors

While conducting the project with the main focus on the catalyst and the related process, presuming continued sustainability fulfilment, only a lazy eye was kept on the external factors. One of the essential aspects around sustainability as mentioned before (see paragraph 1.2) is the economy. This aspect holds universally: in order for a process to be matured and realised, it must be feasible.

7.4.1 Market price development

In present case the acetic acid price development has suffered from a high volatility. Due to the few technology suppliers on the acetic acid market the acetic acid price has been at a relatively high level through the 1990's until 2008, when suddenly all commodities were lamed due to the international financial crisis, dampening the general activity level and leading to an overcapacity of products in the world market (*Ravinchandran, 2009*). Figure 7-4 shows how the European acetic acid spot price first experienced a steady upturn during 2003-2007 while the demand for most chemicals rose; following further up when the oil price went from 60-70 to 140 USD/bbl. The high commodity prices could not be sustained due to the international financial crisis, leading to a general activity down-turn. They fell during the second quarter 2008 reducing the producers' margin, and continued falling with the downturn in oil prices from 140 to 40USD/bbl in the third quarter of 2008 (see Figure 7-4).

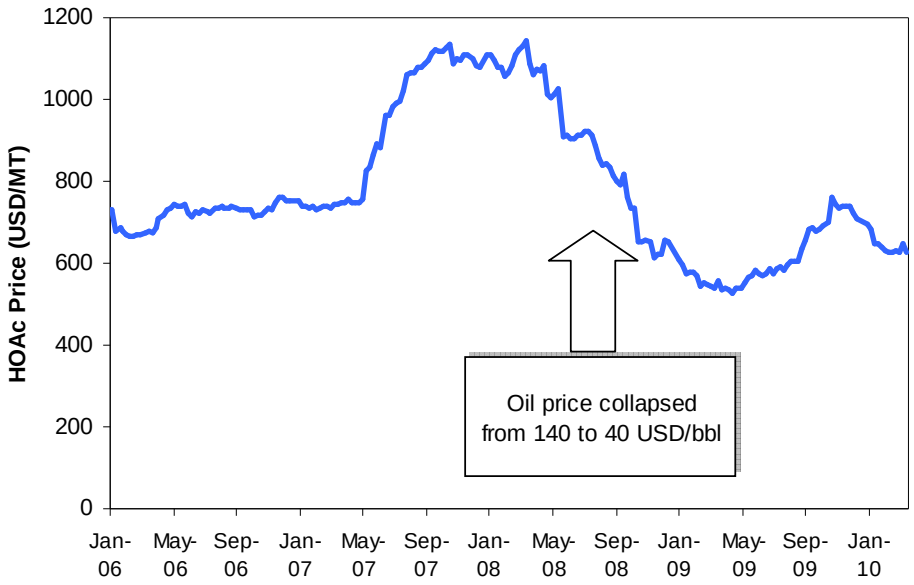

Figure 7-4: Acetic spot price NWE average 2006-2010 (*ICIS, ICIS Price Report, 2010)*. The international acetic acid spot price has been fluctuating between a low of 350 and a high of 800 USD/MT during the past decade (*Ravinchandran, 2009*).

According to ICRA Rating Services (*Ravinchandran, 2009*) the overall ethanol-to-acetaldehyde-to-acetic acid route is only profitable during periods of high acetic acid prices.

During the 2006-2009 the ethanol market price was only vaguely influenced by the oil price development. But in 2010 the ethanol price went up, gradually reducing the economic margin of the ethanol-to-acetic acid route to an unfeasible level. Figure 7-5 shows the price development for ethanol during 2006-2010.

Comparing the carbonylation based acetic acid gate production price of 400 USD/MT (see paragraph 2.2.1) with the acetic acid selling price during the crisis of down to 350-400USD/MT in some regions, the profit has been zero or negative for the newly established carbonylation based acetic acid plants. This estimate is confirmed by the market observer statement by *Lee, ICIS pricing (2010)* that small acetic acid plants were still bleeding when the market price was in the neighbourhood of 500USD/MT.

Acceptable profitability may have been maintained for the down paid carbonylation based plants, as the methanol spot prices followed down to 200USD/MT, when the oil price fell.

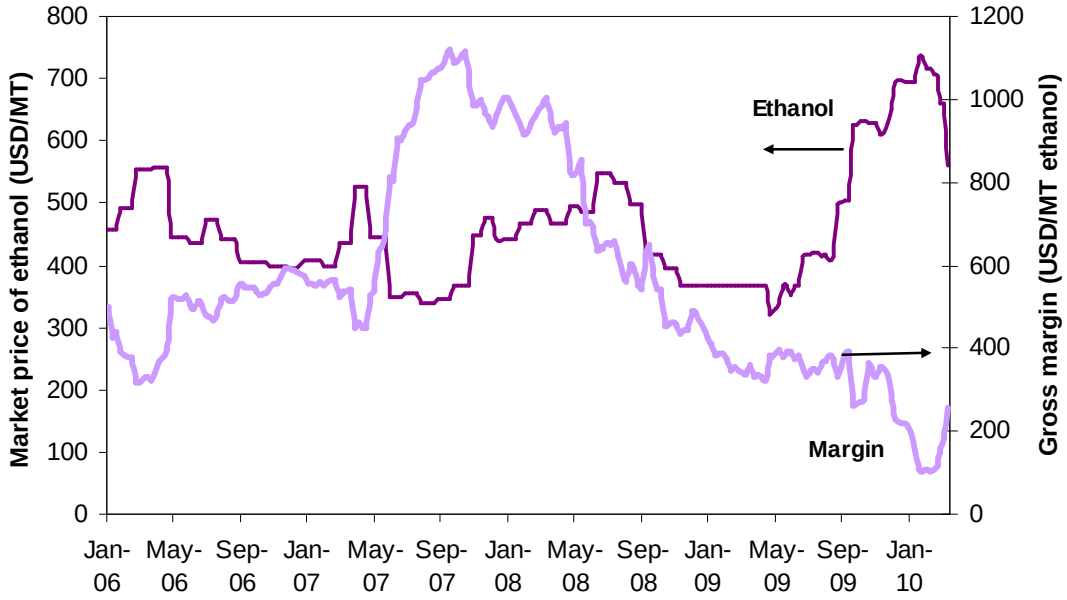

Figure 7-5: Ethanol market price (FCA Brazil) development during 2006-2010 (purple, solid line) (*ICIS, ICIS Price Report, 2010*). The gross margin (black, stapled) of the ethanol to acetic acid route (calculated according to Eq. 1.1) reduces to 100-200USD/MT ethanol.

The initial economic basis for making acetic acid from ethanol seemed promising. Then the crisis came revolting the demand and supply balance, erasing the price gain between fuel and bulk chemical value, thereby in effect making any introduction of new chemical technology troublesome. The acetic acid price is slowly on its way up again, but the market is soft. When the market tightens the demand to supply ratio is controlled by the two major players, BP (UK) and Celanese (US) by allowing only capacity additions in a measured way (*Ravinchandran, 2009*). The outlook is that a rise from the present 650USD/MT will be tempered by the temporary surplus capacity. However, as the demand-supply balance restores and the market expands the acetic acid selling price will rise to a level allowing a satisfactory profit margin, also for newcomers.

7.4.2 Green pricing

While the power of ruling the energy prices is pulling one end of the rope, the customers are the determining the pull in the other end (see Figure 7-6). The business-to-business segment has not to a great extent paved the way for introducing green premiums in business, because the commercial advantage of a green alternative in the business to customer segment has only been realised sporadically. With very few exceptions people are not willing to pay more for sustainable goods (*Alapekkala, 2010*). And the goods where sustainability is highly prioritized amongst customers are primarily the least prepared, for example food, whereas less attention has been paid to

for example packaging etc. Acetic acid is an example of such a product used in the business-to-business segment. Most of the acetic acid production is absorbed by VAM production, thus it typically ends up in plastic.

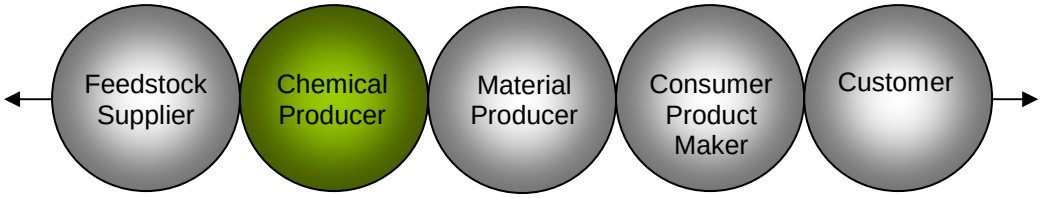

Figure 7-6: Supply chain. The activities conducted in the business-to-business segments are ultimately determined by the feedstock supplier in one end and the customer in the other.

The green awareness of end-customers may theoretically increase to such an extent that they are loyally willing to pay more for 'green' goods, creating a market pull and providing for a market premium on 'green' products. However, this is not likely to happen according to the present market knowledge (*Alapekkala, 2010*).

So the share of the 'green' products must be foreseen to drop, if the buying power of the end-users is decreasing, making the investment in such alternative technology risky. Especially the business-to-business segment 'green' products, for example materials for use in combination with other components, are sensitive as they enjoy less attention. Today the green technology pioneers have to be truly competitive (except from those serving national interests, for example where oil independence is at stake). The 'green' investments which do not readily pay off fast, depend on governmental CO_2 taxation of fossil based technologies or subsidies paid to the producers of sustainable chemical.

7.5 Conclusions and future work

In this work the catalytic conversion of bioethanol to acetic acid was selected as an example of a process converting a biomass based feed to a value added chemical under the consideration of availability, suitability of the feedstock and classic sustainability criteria. The most central conclusions attained during these investigations are repeated here below.

The dominant conventional acetic acid technology, the carbonylation of methanol, is characterised through its numerous conversion and purification steps and the complexity of the carbonylation. Furthermore, expensive construction materials (for example Zirconia) are required in order to withstand the strongly corrosive conditions induced by its homogeneous catalytic system, comprising HI. On the other hand it can be fed by cheap natural gas in an integrated layout. The high investment load for the carbonylation technology leaves room for improvement of the product gate production price. Through the preliminary development of a 300000 MTPY acetic acid plant based on the catalytic conversion of bio-ethanol, represented in a process flow diagram, a comparatively low investment conversion route to acetic acid has been obtained. The benefits of conserving part of the chemical C-C bonds of the original biomass are reflected through fewer conversion and purification steps than in the carbonylation based process.

In the initial catalyst screenings Cu proved to be a significant dehydrogenation catalyst, and pure metallic Cu was identified as a prominent catalytic phase. Water co-fed with ethanol advantageously increased the product selectivity dramatically. Thus both the up-stream and downstream process steps can profit from need of the water reactant by demanding a lower degree of water removal in the prior ethanol distillation and by easing the downstream separation of side-products from acetic acid.

A first catalyst candidate found by screening, a Cu spinel catalyst calcined at 850°C ($CuAl_2O_4$) having a relatively high initial activity and good mechanical stability, was investigated by means of *in situ* reduction techniques and several other complementary characterisation techniques. By means of these, and with support from literature, it was established that the Cu spinel during activation (reduction) transforms into highly dispersed Cu crystals, equally sized about 100 Å, on a Cu depleted η- or γ-alumina phase, Cu/Al_2O_3. The Cu/Al_2O_3 showed to be prone to deactivation under several influences, i.e. it lacked stability. The deactivation is suggested to be related to the acid sites of the alumina support catalysing the conversion of intermediate acetaldehyde to high molecular condensation products, smearing out on the inner surface of the catalyst. For this reason the industrial application of the Cu spinel catalyst was disregarded in the further investigations.

Based on the above understanding gained on the significance of the catalyst support the down-selection to an alternative catalyst candidate, the Cu/SiO_2 catalyst was made. In line with the Cu spinel catalyst the Cu crystals were dispersed on the SiO_2 surface as about 200Å Cu crystals as found by *in situ* HRTEM and *ex situ* XRPD technique. The activity for the alternative highly selective and stable Cu/SiO_2 catalyst was found to be only 0.05-0.15 kg/(kg·h) at low conversion degrees. Through the comparison of Cu crystal size estimated by XRPD spectra of spent catalysts vs. catalyst activity, it appears that the activity depends on the Cu area. Empirical kinetic models were derived for the two main equilibrium limited reactions catalysed over the Cu/SiO_2 catalyst in the conversion of ethanol to acetic acid. Good agreement with the experimental data, recorded with industrially relevant compositions, was obtained.

Anticipating, that an acetic acid formation activity of at least 0.3 kg/(kg·h) may be obtained for the Cu/SiO_2 catalyst over the entire conversion range in an industrial reactor, established through the kinetic model validation at industrial pressure or by further catalyst development, this catalyst shows good characteristics, for example high stability and selectivity, for a non-oxidative dehydrogenation process. Under the initial price conditions given, the further improved Cu/SiO_2 catalyst, having a STY_{HOAc} of at least 0.3 kg/(kg·h) could be embedded in the preliminary ethanol to acetic acid process scheme at realistic conditions, which according to a conservative estimate of the gate production price and the ROI, is feasible and competitive over the conventional carbonylation process.

An equilibrium constant was determined for the first reaction in order to improve the determination of the kinetic parameters in the second step. By studying the elementary reactions it was found that the anticipation of the addition of adsorbed hydroxyl and acetaldehyde as the rate determining step is most consistent with the derived models, and the dependency of activity on the Cu crystal size. By DFT calculation water was found to dissociate primarily on Cu step sites being consistent with the >1^{st} order of the

activity dependency on the Cu crystal size. The activation barrier for water dissociation on Cu(211) was calculated as 125kJ/mol.

The energy consumption of the preliminary bioethanol-to-acetic acid process is 6.3 GJ/MT acetic acid. This figure is preliminary and is estimated to depend especially on the side-product level and the degree of conversion to acetic acid. An incentive for the further development of the bioethanol-to-acetic acid process is thus identified. Further it was indicated that the Cu/SiO_2 catalyst is able to convert bio-ethanol to acetic acid under partly oxidative dehydrogenation conditions. Such further development could involve the partly oxidative dehydrogenation, which is advantageous over the non-oxidative dehydrogenation. As a further development option the improved Cu/SiO_2 catalyst may be applied in a partly oxidative dehydrogenation making way for a reduced investment and a lower energy consumption.

Three patent applications have been filed in order to protect the IPR on the discoveries made, counting a method of controlling process water, the partly oxidative dehydrogenation, being slightly exothermic and the process integration with ethylene and VAM production units.

If further thermodynamic knowledge is gained for the second reaction step, i.e. the dehydrogenation of acetaldehyde, allowing process development based on equilibrium calculations, new suggestion on process layouts may be better substantiated *in silico*. In a future study a catalyst, e.g Cu/SiO_2 based and improved in activity, is therefore preferably developed and a next generation process flow diagram must be prepared making use of further thermodynamic information, which must be established beforehand.

But the increasing ethanol feedstock price and the decreasing acetic acid product price development have erased the overall economic advantages of converting ethanol to acetic acid, removing thereby the economic sustainability incentive.

7.6 Outlook

It is not necessarily rendered wrong to pursue processes technically which loose their economic incentive – the right time may be just around the corner, and then you will be ready to launch your process without the competition from those who gave up earlier. But time may be spent better by drawing the essence of the findings in such processes, mothballing these and starting to identify a new possible product, advantageously using the learnings obtained from the previous study. The downturn of the gross margin for the ethanol to acetic acid route was imposed by a combination of recession and up-going oil prices may come to an end. This may inspire further research into an alternative ethanol conversion process, producing a chemical, whose profitability is not so dependent on oil price fluctuations.

If the ethanol price links up with the gasoline price, which in turn links up with the oil price, the most stable delta P (see paragraph 1.5.3.1) is secured by making a product from ethanol which itself is linked closely to the oil price. In spite of a narrow margin a stable delta P ahead eases a successful introduction of an alternative production route, especially because the volatility of the oil price is high. And in the long-term perspective the oil prices presumably will spiral up.

Transition from fossil based to biomass based technology in the chemical production can be imagined to take place via combinations of fossil and biomass feedstocks, and old and new technology. Today the blending of ethanol into gasoline is one example of how also a product can be a direct combination of fossil and bio-based products.

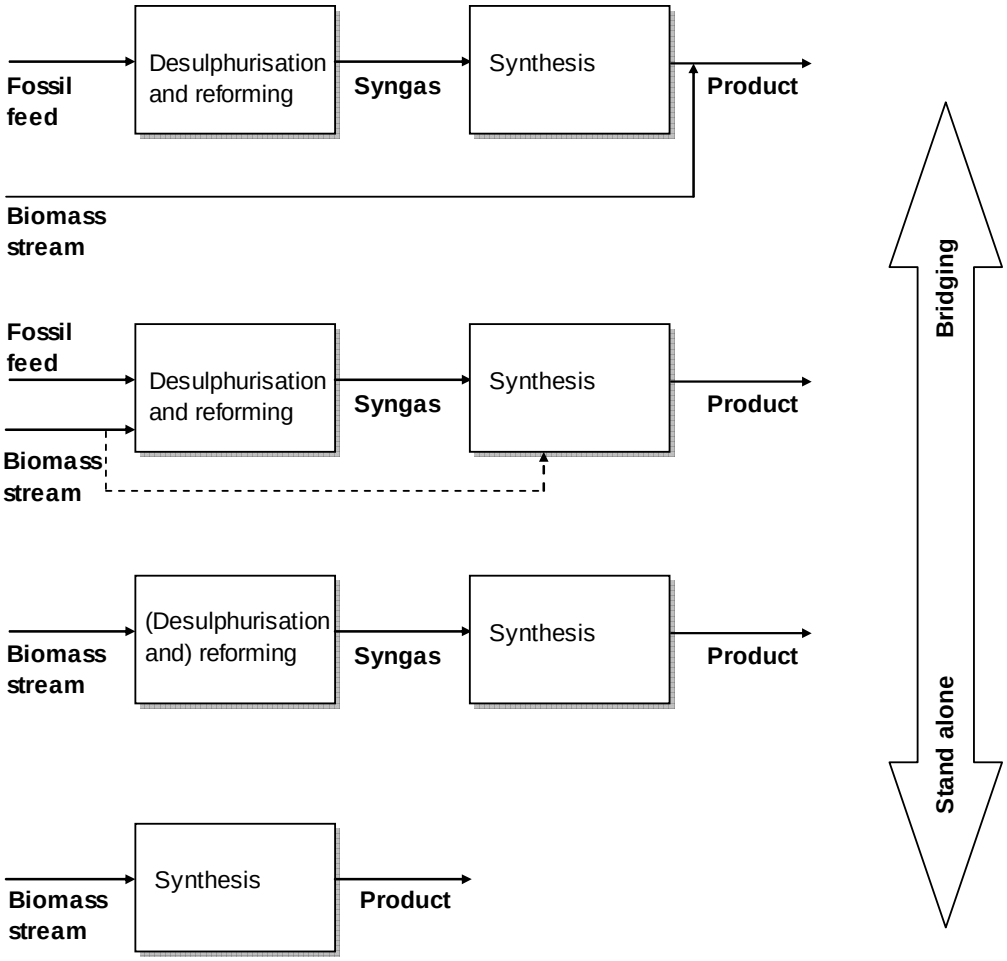

Figure 7-7: The transition between fossil and biobased feed may take place through steps from bridging to stand-alone technologies. The blending of ethanol into gasoline is an example of the simplest approach. In the so-called Hynol process, producing methanol, biomass and natural gas is co-fed to the reforming section. Biomass streams may also be co-fed to the synthesis section, for example as in the integrated gasoline process co-fed with bio-oil (*Joensen et al., 2010*). The non-oxidative dehydrogenation is an example of a stand-alone biomass based plant.

Fuel additives lie on the border between chemicals and fuel products. Certainly their value is closely connected to the price of the dominant fuel origin, so far being oil.

7.6.1 Alternative product: Higher alcohols

Higher alcohols are used as fuel additives (*Beretta et al., 1998, Burcham et al., 1998, Mahdavi et al., 2005*). Previous experiments conducted in-house at Haldor Topsøe A/S on ethanol co-feeding to a higher alcohols synthesis show the potential of ethanol co-feeding in an increased selectivity of propanol over other higher alcohols. The ethanol is converted together with synthesis gas via methanol synthesis and condensation reactions (see Scheme 7-2). By applying bio-ethanol part of the chemical C-C bonds of the original biomass source used in the fermentation has been conserved. Propanol is

today produced primarily through oil based production, namely the hydroformylation of ethylene to propanal and its further hydrogenation.

$Cu/ZnO/Al_2O_3$ catalysts (*Beretta et al., 1998, Mahdavi et al., 2005*) are one group of catalysts which may be used for the production of higher alcohols from synthesis gas. By optimising the catalyst composition the selectivity of the highly desired alcohols over others may be changed in order to maximise the overall feasibility of the process. Especially the optimum product selectivity while co-feeding bio-ethanol may be quested. The ethanol feed co-fed may be aqueous, as the water gas shift reaction is capable of removing the water. Thereby the ethanol feedstock may easily be provided from a bio-ethanol plant. The synthesis gas may also be generated from biomass, making the higher alcohols production plant 100% biomass based.

The development of a Cu based catalyst capable of featuring the co-feeding of ethanol with enhanced process economics seems a vital way of utilising the knowledge built on Cu based catalysts while accelerating the introduction of biomass as an alternative feedstock.

The production of higher alcohols from synthesis gas is a well-known synthesis (*Beretta et al., 1998, Burcham et al., 1998*). Higher alcohols mixtures have caught interest as a gasoline octane booster as they may be produced from a cheap gasification feedstock and be sold at a price considerably higher than the gasoline price. Besides, the modest addition of higher alcohols to methanol as a gasoline supplement will increase the methanol miscibility with gasoline. A price estimate of a higher alcohol mixture for gasoline boosting may conservatively be set equal to 80% of the gasoline retail price (being the gasoline gate price), resulting in around 900 USD/MT presently (*U.S. Energy Administration Information, 2011*). Increasing the productivity of a few, selected alcohols over the broad range of C_1-C_8 alcohols may provide for an even more economic production. Some experiments involving co-feeding of ethanol in a higher alcohol synthesis have already taken place in-house. For example it has been established that co-feeding of ethanol, for example bio-ethanol, to the higher alcohol synthesis increases the propanol yield. But the catalyst composition influence on the effects of ethanol co-feeding in a higher alcohol synthesis has not been elucidated yet. Propanol may be dehydrated to propylene. Propylene monomer is presently sold at 1200-1300USD/MT (*ICIS News, 2010*).

Higher alcohols synthesis concerns herein in particular the synthesis of higher alcohols from synthesis gas, synthesised in conjunction with methanol over a Cu based catalyst at high pressure in a synthesis loop at high pressure (around 100 bar) and about 300°C. The synthesis of higher alcohols may be described through the reaction types listed in below Scheme 7-2:

1. $CO + 2H_2 = CH_3OH$

2. $CH_3OH + 2n\ CO + H_2 = CH_3(CH_2)_nOH + n\ CO_2$

3. $CH_3(CH_2)_nOH + CH_3(CH_2)_mOH = CH_3(CH_2)_{m+n+1}OH + H_2O$

4. $CO + H_2O = CO_2 + H_2$

Scheme 7-2: 1. Methanol synthesis. 2. Propagation via CO insertion. 3. Condensation. 4. Water gas shift.

The overall higher alcohol synthesis is exothermic, and the reaction heat must be removed from the reaction zone in order to avoid catalyst overheating.

Typically the synthesis is conducted from synthesis gas with a CO/H_2 ratio of about 1, as this parameter has been found to be of great importance for the productivity of the higher alcohols over Cu/ZnO based catalysts (*Beretta et al., 1998, Mahdavi et al., 2005*). The function of CO is both to provide for carbon in the higher alcohol product and to remove reaction water through the water gas shift reaction.

Furthermore esters, aldehydes and ketones are observed as side-products as well. These may be hydrogenated to their corresponding alcohols.

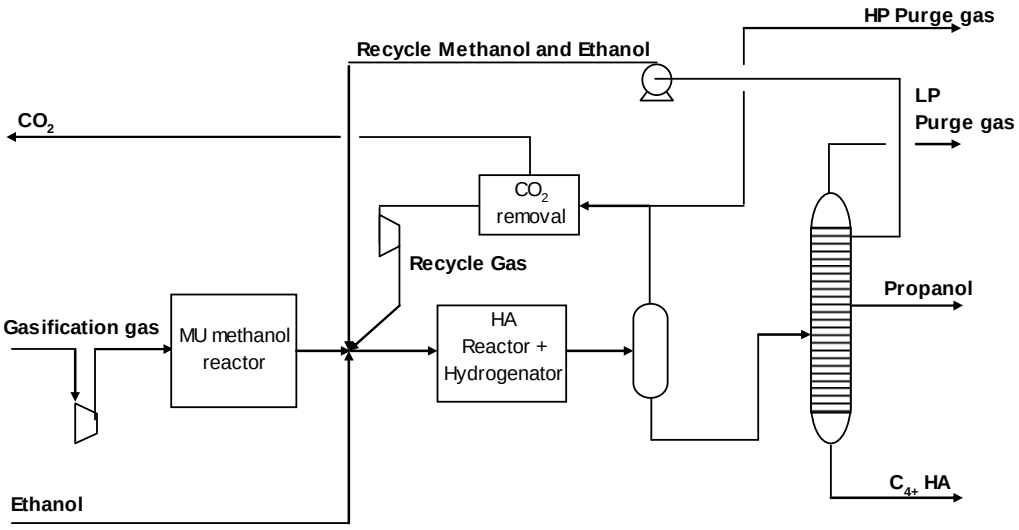

Figure 7-8: Schematic drawing of the higher alcohol synthesis.

Figure 7-8 shows a block diagram of a higher alcohol synthesis as described in literature (*Beretta et al., 1998*) with the modification that here all methanol and ethanol in the reactor effluent is recycled and ethanol is imported. Based on the increased selectivity to propanol the separation of this component in a side-draw is suggested. The co-feeding of ethanol has been shown here as an option.
The product distribution of the higher alcohols is indicative of chain propagation. In a literature study it appears that two major mechanisms for C-C coupling are suggested. There is a general agreement that the first C-C bonding from C1 species is the rate

limiting step. Two mechanisms are suggested in that respect. One is CO insertion and another is a condensation-like reaction where adsorbed intermediate precursors to methanol are the sources. In a study on Cu and ZnO surfaces it was found that the first C-C bound species was acetate, and it was formed on ZnO not on Cu. Common to the studies made on catalysts containing Cu and ZnO was that the mechanism for the first C-C suggested was condensation like. $Cu/ZnO/Al_2O_3$ catalysts studies for higher alcohols synthesis have been reviewed by *Slaa et al*. (1992). It is here reported that the activity of the catalyst with respect to methanol (and water gas shift) reaction was superior to the activity of higher alcohol formation, and the selectivity depends on the particular characteristics of the catalyst employed. It is well-known also that the methanol and water gas shift activity of a Cu catalyst correlates with the Cu surface area of the catalyst (*Ovesen et al., 1996,, Askgaard et al, 1995*).

The catalyst of the overall composition $Cu/ZnO/Al_2O_3$ may be perceived to possess a unification of more catalytic functions: hydrogenation, methanol formation, condensation and hydration in the higher alcohols synthesis. Therefore, an improved composition of the catalyst could be imagined to be found by changing for example the ratio of Cu to the other metals.

Further open questions are what effect the co-feeding of ethanol has on the product distribution, and to which extent the existence of ethanol at a higher concentration eases the conversion of C1 compounds, for example in the addition of C1 to ethanol resulting in propanol. Such dependences may be investigated in high pressure experiments and could constitute the alternative objectives of future experimental activities.

7.6.2 Alternative Bio-mass feedstock

Bio-ethanol is today produced by fermentation of sugar and starch primarily and not by fermentation of hydrolysate obtained from the 2nd generation lignocellulosic feedstock. In reality this means that presently the societal substantiation of converting bio-ethanol is questionable. The assumption that ethanol produced by fermentation is *de facto* a sound bio-mass based building block has only been discussed from the viewpoint that it possesses suitability, availability, economic potential for conversion to chemical and may be substantiated as environmentally friendly, having favourable C-factors close to 0 or below for a number of products. Furthermore, it represents a better choice than glycerol.

It has not been discussed herein until now that more than 1/3 of the carbon is lost at the outset in the fermentation process. Today, no other means of effectively converting monosaccharides or higher biomass based molecules to ethanol are known without going via synthesis gas, losing thereby the potential of retaining the chemical C-C bonds. An even better conservation of energy of naturally occurring sugars could be obtained if a heterogeneous catalyst could convert biomass sugars to a platform chemical, such as ethanol. Apart from the conservation of chemical C-C bond aspect, the energy requirement for the conversion of biomass feedstock may potentially also be reduced, if a higher concentration of the sugars is allowed here as compared to in the fermentation processes – a lot of energy is used for the heating and distilling off water from the fermentation broth. Recent research has for example provided for a process for making lactic acid from C_6 and C_3 sugars, taking an important scientific

short-cut if a high selectivity is attained (*Taarning et al., 2009*). Catalytic conversion of glucose and xylose, being the ethanol fermentation precursors, may be the better alternative to ethanol as a feedstock. It would be an interesting option to pursue. Therefore the selective conversion of sugars to value-added chemicals by heterogeneous catalysis could be regarded as an attractive route to pursue further along the strategy of this work.

7.7 Recapitulation and recommendations

The demand for energy and feedstock progressively grows unless political decisions force us to change the present projection (*International Energy Agency, 2009*). There will remain a need for oil, natural gas and coal based technologies for a long period still. The President of the United States, Barack Obama, has set an ambitious target of an 80% reduction of the CO_2 emission before 2050, which has been replicated in the EU (*European Commission, 2011*). Part of this may be reached through increased process efficiencies and CO_2 sequestration. The high level of efficiency already obtained in the fossil based technologies makes it difficult to gain a lot from increasing their efficiency further, and the CO_2 sequestration from off-gases is cumbersome and energy consuming. Therefore, the interest in CO_2 neutral sources will accelerate, if we maintain the CO_2 reduction targets and the growing need for energy and feedstock.

The green and sustainable technologies currently available for the production of chemicals are sparse. In order to meet the growing need for CO_2 reduction in chemical production this thesis pursues the quest for a process producing a value-added chemical from bio-mass by heterogeneous catalysis. The essence of the hypothesis pursued in this work is that, if it is possible to utilise the step-up of a more developed starting point, a biomass platform having conserved chemical C-C bonds, in the production of chemicals, a feasible process may be proposed.

Many factors influence the chance of success in process innovations, factors which all must be observed. I made use of the INSPIRE project management model in this explorative work, which progressed with constant iteration cycles over many interacting activities while being subjected to repeated change of the focus point. The use of experts in this respect secured a speed-up in the cycles of iteration, promoting the overview and the maturity of the project.

After down-selection of feedstock and product, a long study of the ethanol to acetic acid production route showed many promising aspects. Problem solution provided in association with the process development resulted in three patent applications as a first step to intellectual property right protection. The co-existence of ethanol and water indeed showed to be beneficial based on selectivity, activity and process considerations. Knowledge was built on one catalyst, Cu/Al_2O_3, which proved useful in the study of the next, a Cu/SiO_2 catalyst. A preliminary process evaluation based on this Cu/SiO_2 catalyst showed technical feasibility and initially competitiveness over the conventional carbonylation based process. However, market price developments off-set the margins for both technologies. In spite of the intense study, looking at the reaction system from many angles, some central investigations are still missing, some methods needs to be refined and the full potentials for the process have probably not yet been uncovered.

Therefore in conclusion the hypothesis proved true to a certain extent technically and investment wise. However, it failed marketwise. As the ethanol price seemingly has now linked up with the gasoline price and thereby the crude oil price a steadier delta P would have been warranted by choosing a chemical presently being based primarily on crude oil.

If the biomass based precursors to ethanol, C_6 and C_5 sugars, may be converted by heterogeneous catalysis to ethanol as a platform chemical or directly to value-added chemicals this would constitute a large step towards increased biomass conversion efficiency. As learned from the marketwise shortcomings an alternative product candidate may be related to the fuel production. Fuel additives are, obviously. By optimising a Cu based catalyst the selectivity in the conversion of bio-ethanol to a value-added chemical may be increased in a higher alcohols synthesis providing for a production competitive over the conventional. Such alternative investigations would also be sensible to make.

What happens, i.e. which biomass based productions become viable and how fast, depends on external factors such as market opportunities, CO_2 taxation and green subsidies or premiums.

References (alphabetic order)

Alapekkala, O., EurActiv, Unilever CEO: Sustainable sourcing 'doesn't have to cost more', 2010. Retrieved Feb. 10, 2011 from: http://www.euractiv.com/en/sustainability/unilever-ceo-sustainable-sourcing-doesnt-have-cost-more-interview-500644.

Alejandre, A., Medina, F., Sueiras, J.E., Preparation and study of Cu-Al mixed oxides via hydrotalcite-like precursors, Chem. Mater., 11 (1999) 939-948.

Amano, F., Suzuki, S., Yamamoto, T., Tanaka, T., One-electron reducibility of isolated copper oxide on alumina for selective NO–CO reaction, Appl. Catal., B, 64, 3-4 (2006) 282-289.

Askgaard, T.S., Nørskov, J.K., Ovesen, C.V., Stoltze, P., A Kinetic Model of Methanol Synthesis, J. Catal., 156 (1995) 229-242.

Azapagic, A., Carbon Footprint of Industrial Supply Chains, The University of Manchester, Manchester. Retrieved Dec. 21, 2010 from: http://www.sci.manchester.ac.uk/medialibrary/carbon_footprints_of_industrial_supply_chains-azapagic.pdf.

Banholzer, W.F., Watson, K.J., Jones, M.E., How Might Biofuels Impact the Chemical Industry, CEP, March (2008) 7-14.

Barrosso, M.N., Gomez, M.F., Arrúa, L.A., Abello, M.C., Reactivity of Aluminum Spinels in the Ethanol Steam Reforming Reaction, Catal. Lett., 109, 1-2 (2006) 13-19.

Beretta, A., Micheli, E., Tagliabue, L., Tronconi, E., Development of a Process for Higher Alcohol Production via Synthesis Gas, Ind. Eng. Chem. Res., 37 (1998) 3896-3908.

Bioenergy Feedstock Information Network (research organizations), Bioenergy and Biomass Frequently asked questions. Retrieved Jan. 18, 2011 from: http://bioenergy.ornl.gov/faqs/index.html.

Bohlmann, G.M., The Brazilian opportunity for biorefineries, Industrial Biotechnology, 2, 1 (2006) 127-132.

Burcham, M.M., Herman, R.G., Klier, K., Higher Alcohol Synthesis over Double Bed Cs-Cu/ZnO/Cr_2O_3 Catalysts: Optimizing the Yields of 2-Methyl-1-propanol (Isobutanol), Ind. Eng. Chem. Res., 37 (1998) 4657-4668.

Campbell, J.M., Nakamura, J., Campbell, C.T., Model studies of cesium promoters in water-gas shift catalysts: Cs/Cu(110), J. Catal., 136, 1 (1992) 24-42.

Cavallo, A., When the Oil Supply Runs Out, Science, 316 (2007) 980.

Chang, F.-W., Kuo, W.-Y., Lee, K.-C., Dehydrogenation of ethanol over copper catalysts on rice husk ash prepared by incipient wetness impregnation, Appl. Catal., A, 246 (2003) 253-264.

Chen, C.-S., Lai, T.-W., Chen, C.-C., Effect of active sites for a water-gas shift reaction on Cu nanoparticles, J. Catal., 273 (2010) 18-28.

Chen, L.-F., Guo, P.-J., Qiao, M.-H., Yan, S.-R., Li, H.-X., Shen, W., Xu, H.-L., Fan, K.-N., Cu/SiO_2 catalysts prepared by the ammonia-evaporation method: Texture,

structure, and catalytic performance in hydrogenation of dimethyl oxalate to ethylene glycol, J. Catal., 257 (2008) 172-180.

Choi, W.J., Glycerol-Based Biorefinery for Fuels and Chemicals, Recent Patents on Biotechnology, 2 (2008) 173-180.

Christensen, C.H., Rass-Hansen, J., Marsden, C.C., Taarning, E., Egeblad, K., The Renewable Chemical Industry, ChemSusChem, 1, 4 (2008) 283-289.

Chung, M.-J., Han, S.-H., Park, K.-Y., Ihm, S.-K., Differing characteristics of Cu an ZnO in dehydrogenation of ethanol: a deuterium exchange study, J. Mol. Catal., 79 (1993) 335-345.

Clark, J.H., Deswarte, F., Introduction to Chemicals from Biomass, Wiley, 2008, 24[a], 51[b].

Colley, S.W., Tabatabaei, J., Waugh, K.C., Wood, M.A., The detailed kinetics and mechanism of ethyl ethanoate synthesis over a Cu/Cr_2O_3 catalyst, J. Catal., 236 (2005) 21-33.

Corma, A., Iborra, S., Velty, A., Chemical Routes for the Transformation of Biomass into Chemicals , Chem. Rev., 107 (2007) 2411-2502.

Daniell, W., Schubert, U., Glöckler, R., Meyer, A., Noweck, K., Knözinger, H., Enhanced surface acidity in mixed alumina-silicas: a low temperature FTIR study, Appl. Catal., A, 196 (2000) 247-260.

Danish Energy Agency, Energy Statistics 2007, 2008.

Demirbas, A., Biofuels sources, biofuel policy, biofuel economy and global biofuel projections, Energy Convers. Manage., 49, 8 (2008) 2106-2116.

Dreyfus, H., Improvements in the manufacture of oxygenated organic compounds, GB 401269, 1933.

Ekvall, G. , Organizational Climate for Creativity and Innovation, Eur. J. Work Organ. Psy., 5, 1 (1996) 105-123.

European Commission, EU action against climate change, 2011. Retrieved Apr. 24, 2011 from: http://ec.europa.eu/climateaction/eu_action/index_en.htm.

European Environment Agency, How much bioenergy can Europe produce without harming the environment?, 2006.

Farm Energy Community, New Uses for Crude Glycerin from Biodiesel Production, 2010. Retrieved Feb. 25, 2011 from: http://www.extension.org/pages/New_Uses_for_Crude_Glycerin_from_Biodiesel_Production.

Faungnawakij, K., Shimoda, N., Fukunaga, T., Kikuchi, R., Eguchi, K., Cu-based spinel catalysts CuB_2O_4 (B = Fe, Mn, Cr, Ga, Al, $Fe_{0.75}Mn_{0.25}$) for steam reforming of dimethyl ether , Appl. Catal., A, 341, 1-2 (2008) 139-145.

Fernandez-Garcìa, M., Rodríguez-Ramos, I., Ferreira-Aparicio, P., Guerrero-Ruiz, A., Tracking down the reduction behavior of copper-on-alumina catalysts, J. Catal., 178 (1998) 253-263.

Fishhaut, E., Petrochemicals firms take a stand against oil price volatility, Market Focus, May 2003, EPRM (2003) 54-55.

Foerst, W., Ullmanns Encyklopädie, 6. Band, Urban & Schwarzenberg, München-Berlin, 1955, 783.

Froment, G.F., Bischoff, K.B., Chemical Reactor Analysis and Design, Wiley, New York, 1990.

Fu, Y., Hong, T., Chen, J., Auroux, A., Shen, J., Surface acidity and the dehydration of methanol to dimethyl ether, Thermochimica Acta, 434 (2005) 22-26.

Glazoff, M.V., Nanostructured Gamma Alumina from Amorphous Precursors, Port Allen, USA. Retrieved Dec. 27, 2010 from: http://www.nacatsoc.org/18nam/Posters/P054-Nanostructured%20Gamma%20Alumina%20from%20Amorphous.pdf.

Gold, T., The deep, hot biosphere, PNAS, 89, 13 (1992) 6045-6049.

Goldemberg, J., Coelho, S.T., Nastari, P.M., Lucon, O., Ethanol learning curve - the Brazilian experience, Biomass Bioenergy, 26, 3 (2004) 301-304.

Goodstein, D., The end of the age of oil, CaltechNews, 38, 7 (2005) .

Guan, Y., Hensen, E.J.M., Ethanol dehydrogenation by gold catalysts: The effect of the gold particle size and the presence of oxygen, Appl. Catal., A, 361 (2009) 49-56.

Guan, Y., Li, Y., van Santen, R., Hensen, E.J.M., Li, C., Controlling Reaction Pathways for Alcohol Dehydration and Dehydrogenation over FeSBA-15 Catalysts, Catal. Lett., 117, 1-2 (2007) 18-24.

Gubelmann-Bonneau, M., Process for the production of acetic acid by controlled oxidation of ethanol, US 5840971, 1998.

Gusi, S., Trifiró, F., Vaccari, A., Kinetic study of the reduction of copper-zinc-aluminum mixed oxide catalysts, React. Solid., 2 (1986) 59-71.

Hale, W.J., Haldeman, W.S., Method of producing organic acids, GB 287064, 1929.

Haner, C., Fenimore, E.P., Process for the manufacture of acetic acid, US 1911315, 1933.

Hansen, P.L., Wagner, J.B., Helveg, S., Rostrup-Nielsen, J.R., Clausen, B.S., Topsøe, H., Atom-Resolved Imaging of Dynamic Shape Changes in Supported Copper Nanocrystals, Science, 295 (2002) 2053-2055.

Happel, J., Chao, J.C., Mezaki, R., Thermodynamic equilibrium constant of ethyl alcohol-acetaldehyde-hydrogen system, J. Chem. Eng. Data, 19, 2 (1974) 110-112.

Hutchens, S.A., Benson, R.S., Evans, B.R., O'Neill, H.M., C.J. Rawn, Biomimetic synthesis of calcium-deficient hydroxyapatite in a natural hydrogel, Biomater., 27 (2006) 4661-4670.

ICIS News, J. Chang, Wacker ready with bioethanol route to acetic acid, 2008. Retrieved Dec. 28, 2010 from: http://www.icis.com/Articles/2008/03/19/9109481/Wacker-ready-with-bioethanol-route-to-acetic-acid.html.

ICIS News, Propylene Prices Continue to Rise, 2010. Retrieved Feb. 7, 2011 from: http://urethaneblog.typepad.com/my_weblog/2010/02/propylene-prices-continue-to-rise.html.

ICIS, ICIS Price Report: ACETIC ACID In Europe SPOT FD NEW, Copyright 2010, Reed Business Information Limited, 2010.

ICIS.com, Acetic Acid Production and Manufacturing Process. Retrieved Dec. 28, 2010 from: http://www.icis.com/v2/chemicals/9074780/acetic-acid/process.html.

Institute for Environment and Sustainability, Well-to-Wheels Analysis of Future Automotive Fuels and Powertrains in the European Context, WELL-to-WHEELS Report, Version 2c, 2007. Retrieved Jun. 16, 2009 from: http://ies.jrc.ec.europa.eu/WTW.

International Energy Agency, Key World Energy Statistics, International Energy Agency, Paris, 2009.

Inui, K., Han, S., Park, K., Ihm, S., Effective formation of ethyl acetate from ethanol over Cu-Zn-Zr-Al-O catalyst, J. Mol. Catal. A: Chem., 216 (2004) 147-156.

Iwasa, N., Takezawa, N., Reforming of Ethanol - Dehydrogenation to Ethyl Acetate and Steam Reforming to Acetic Acid over Copper-Based Catalysts, Bull. Chem. Soc. Jpn., 64 (1991) 2619-2623.

Janas, J., Gurgul, J., Socha, R.P., Dzwigaj, S., Effect of Cu content on the catalytic activity of CuSiBEA zeolite in the SCR of NO by ethanol: Nature of the copper species, Appl. Catal., B, 91, 1-2 (2009) 217-224.

Jenkins, B.M., Encyclopedia of Agricultural, Food and Biological Engineering, edited by D.R. Heldman, Taylor & Francis, 2003.

Joensen, F., Voss, B., Nerlov, J., Process for converting difficultly convertible oxygenates to gasoline, US 7820867, 2010.

Jørgensen, B., Christiansen, S.E., Thomsen, M.L.D., Christensen, C.H., Aerobic oxidation of aqueous ethanol using heterogeneous gold catalysts: Efficient routes to acetic acid and ethyl acetate, J. Catal., 251, 2 (2007) 332-337.

Kamble, V.S., Londhe, V.P., Gupta, N.M., Recent advances in basic and applied aspects of industrial catalysis, edited by T.S.R.P Rao, G.M. Dhar, Elsevier, Amsterdam, 1998, 815-828.

Kapteijn, F., Moulijn, J.A., Handbook of Heterogeneous Catalysis, Section 9.1, edited by G. Ertl, H. Knözinger, J. Weitkamp, 3, Wiley-VCH, Weinheim, 1997, 1359-1376.

Kauffman, G.B., Johann Wolfgang Döbereiner's Feuerzeug, Platinum Met. Rev., 43, 3 (1999) 122-128.

Kilos, B., Oxidative Dehydrogenation of Ethanol to Acetaldehyde on Supported Vanadium Oxide. Retrieved Dec. 28, 2010 from: www.nacatsoc.org/20nam/abstracts/O-S9-01.pdf.

Kim, T.-W., Song, M.-W., Koh, H.-L., Kim, K.-L., Surface properties and reactivity of Cu/γ-Al_2O_3 catalysts for NO reduction by C3H6: Influences of calcination temperatures and additives, Appl. Catal., A, 209, 1-2 (2001) 35-44.

Klier, K., Young, C.W., Nunan, J.G., Promotion of the water gas shift reaction by cesium surface doping of the model binary copper/zinc oxide catalyst, Ind. Eng. Chem. Fundamen., 25, 1 (1986) 36-42.

Knapsack-Griesheim Aktiengesellschaft, Process for the dehydrogenation of alcohols, GB 804132, **1958**.

Knapsack-Griesheim Aktiengesellschaft, Process for the dehydrogenation of alcohols, GB 825602, **1959**.

Kunkes, E., Methanol Synthesis from CO_2: Promoter and Presursor Phase Effects on the Performance of Cu/ZnO-based Catalysts, 2011. Retrieved from: www.7bgw.org/abstracts/79.pdf.

Kumar, P.A., Reddy, M.P., Ju, L.K., Hyun-Sook, B., Phil, H.H., Low temperature propylene SCR of NO by copper alumina catalyst, J. Mol. Catal. A: Chem., 291 (2008) 66-74.

Lachowska, M., Skrzypek, J., Ga, Mn and Mg promoted copper/zinc/zirconia - catalysts for hydrogenation of carbon dioxide to methanol, Stud. Surf. Sci. Catal., 153 (2004) 173-176.

Lee, H., ICIS pricing, Acetic Acid Prices and Pricing Information, 2010. Retrieved Feb. 7, 2011 from: http://www.icis.com/v2/chemicals/9074786/acetic-acid/pricing.html.

Legg, D.A., Adam, M.A., Improvements in and relating to copper catalysts, GB 166249, 1921.

Levenspiel, O., Chemical Reaction Engineering, 2nd Ed., John Wiley & Sons, New York, 1972.

Li, X., Iglesia, E., Selective Catalytic Oxidation of Ethanol to Acetic Acid on Dispersed Mo-V-Nb Oxides, Chem. Eur. J., 13 (2007) 9324-9330.

Liu, K., Tong, Z., Liu, L., Feng, X., Separation of organic compounds from water by pervaporation in the production of n-butyl acetate via esterification by reactive distillation, J. Membr. Sci., 256, 1-2 (2005) 193-201.

Liu, L., Ma, D., Chen, H., Zheng, H., Cheng, M., Xu, Y., Bao, X., Methane dehydroaromatization on Mo/HMCM-22 catalysts: effect of SiO_2/Al_2O_3 ratio of HMCM-22 zeolite supports, Catal. Lett., 108, 1-2 (2006) 25-30.

Luo, L., van der Voet, E., Huppes, G., An energy analysis of ethanol from cellulosic feedstock corn stover, Renewable Sustainable Energy Rev., 13 (2009) 2003-2011.

Ma, Y., Sun, Q., Wu, D., Fao, W.-H., Deng, J.-F., A gel-oxalate co-precipitation process for preparation of Cu/ZnO/Al2O3 ultrafine catalyst for methanol synthesis from CO_2+H_2: (II) effect of various calcination conditions, Appl. Catal., A, 177 (1999) 177-184.

Maciver, D.S., Tobin, H.H., Barth, R.T., Catalytic Aluminas I. Surface Chemistry of Eta and Gamma Alumina, J. Catal., (1963) 485-497.

MacLean, A.F., Process for catalytic dehydrogenation of alcohols to carbonyl compounds, US 2634295, 1953.

Mahdavi, V., Peyrovi, M.H., Islami, M., Mehr, J.Y., Synthesis of higher alcohols from syngas over Cu-Co_2O_3/ZnO, Al_2O_3 catalyst, Appl. Catal., A, 281 (2005) 259-265.

Mailhe, A., Procéde de préparation de l'acide acétique, FR 526567, 1921.

Marcinkowski, A.E., Henry, J.P., Catalytic dehydrogenation of ethanol for the production of acetaldehyde and acetic acid, US 4220803, 1980.

Meshbesher, T.M., Method for oxidizing lower alkanols to useful products, US 4457809, 1984.

Moroz, O.M., Gonchar, M.V., Sibirny, A.A., Efficient bioconversion of ethanol to acetaldehyde using a novel mutant strain of the methyltrophic yeast Hansenula polymorpha, Biotechnology and Bioengineering, John Wiley & Sons, 68, 1-2 (2000) 44-51.

Mousdale, D.M., Biofuels, CRC Press, Boca Raton, 2008, 6, 16, 20, 24, 37, 252.

Murray, R.F., Rhodes, D.W., Technical report: DOE Contract Number AT(10-1)-205, Phillips Petroleum Co., 1962, abstract.

Natural Resources Defense Council, Ethanol: Energy Well Spent, 2006. Retrieved Feb. 28, 2011 from: www.nrdc.org/air/transportation/ethanol/ethanol.pdf.

Ndou, A.S., Plint, N., Coville, N.J., Dimerisation of ethanol to butanol over solid-base catalysts, Appl. Catal., A, 251, 2 (2003) 337-345.

Obana, Y., Uchida, H., Sano, K., Catakyst for production of acetic acid or acetic acid and ethyl acetate, process for its production and proces for production of acetic acid or acetic acid and ethyl acetate, US 6867164, 2005.

Ostgard, D., Sauer, J., Freund, A., Berweiler, M., Hopp, M., van Heertum, R., Girke, W., Raney copper, US 6794331, 2003.

Ovesen, C.V., Clausen, B.S., Hammershøi, B.S., Steffensen, G., Askgaard, T., Chorkendorff, I., Nørskov, J.K., Rasmussen, P.B., Stoltze, P., Taylor, P., A Microkinetic Analysis of the Water-Gas Shift Reaction under Industrial Conditions, J. Catal., 158 (1996) 170-180.

Patrick, V., Gavalas, G., Structure and Reduction and Mixed Copper-Aluminum Oxide, J. Am. Ceram. Soc., 73, 2 (1990) 358-369.

Perego, C., Bortolo, R., Zennaro, R., Gas to liquids technologies for natural gas reserves valorization: The Eni Experience, Catal. Today, 142 (2009) 9-16.

Pfeffer, M., Wukovits, W., Beckmann, G., Friedl, A., Analysis and decrease of the energy demand of bioethanol-production by process integration, Appl. Therm. Eng., 27, 16 (2007) 2657-2664.

Phatak, A.A., Delgass, W.N., Ribeiro, F.H., Schneider, W.F., Density Functional Comparison of Water Dissociation Steps on Cu, Au, Ni, Pd, and Pt, J. Phys. Chem. C, 113 (2009) 7269-7276.

Plastemart.com, Feedstock Trends - Ethylene. Retrieved Dec. 28, 2010 from: http://www.plastemart.com/feedstock_graph.asp?cat=ETHYLENE.

Quincoces, C.E., Amadeo, N.E., González, M.G., Effects of Reduction and Regeneration Conditions on the Activity of CuO-ZnO Catalysts, Catalyst deactivation 1997: Proceedings of the international symposium, Cancun, Mexico, October 5-8, 1997, edited by C.H. Bartholomew, G.A. Fuentes, Elsevier, Amsterdam (1997) 535-541.

Ravinchandran, K., Outlook Challenging despite Modest Signs of Recovery, 2009. Retrieved Mar. 19, 2010 from: www.icra.in/Files/Pdf/Ticker/chemicals%20note-release.pdf.

RFA: Renewable Fuels Association, Statistics, Ethanol Industry Statistics, Annual World Ethanol Production by Country, 2010. Retrieved Feb. 28, 2011 from: http://www.ethanolrfa.org/pages/statistics.

Rüdinger, C., Eberle, H.J., Voit, H. , Wacker process on oxidative dehydrogenation, WO2008110468A1, 2008.

Sanchez-Sanchez, M.C., Yerga, R.M.N., Kondarides, D.I., Verykios, X.E., Fierro, J.L.G., Mechnistic Aspects of the Ethanol Steam Reforming Reaction for Hydrogen Production on Pt, Ni, and PtNi Catalysts Supported in g-Al_2O_3, J. Phys. chem. A, 114 (2010) 3873-3882.

Santacesaria, E., Gelosa, D., Carrà, S., Basic Behavior of Alumina in the Presence of Strong Acids, Ind. Eng. Chem., Prod. Re. Dev., 16, 1 (1977) 45-47.

Sato, T., The thermal transformation of Gelatinous Aluminium Hydroxide, ZAAC, 391, 2 (2004) 167-173.

Satterfield, C.N., Heterogeneous Catalysis in Industrial Practice (2nd ed.), Krieger Publishing, Melbourne, USA, 1996.

Scott, D.S., Lee, W., Papa, J., The measurement of transport coefficients in gas-solid heterogenenous reactions, Chemical Engineering Science, 29 (1974) 2155-2167.

Shapouri, H., Gallagher, P., USDA's 2002 Ethanol Cost-of-Production Survey, Agricultural Report Number 841, United States Department of Agriculture, 2005, 4.

Shimada, T., Sakata, K., Homma, T., Nakai, H., Osaka, T., Density functional theory study on the oxidation mechanisms of aldehydes as reductants for electroless Cu deposition process, Electrochim. Acta, 51 (2005) 906-915.

Shustorovich, E., Bell, A.T., An analysis of methanol synthesis from CO and CO_2 on Cu and Pd surfaces by the bond-order-conservation-Morse-potential approach, Surf. Sci., 253 (1991) 386-394.

Sieling, K., Christen, O., Effect of preceding crop combination and N fertilization on yield of six oil-seed rape cultivars (Brassica napus L.), Eur. J. Agron., 7, 4 (1997) 301-306.

Sklar, T., Ethanol from waste an opportunity for refiners, Oil & Gas Journal, June (2008) 54-59.

Slaa, J.C., van Ommen, J.G., Ross, J.R.H., The synthesis of higher alcohols using modified Cu/ZnO/Al2O3 catalysts, Catal. Today, 15 (1992) 129-148.

Sokolskii, D.V., Vozdvizhenskii, V.F., Kuanyshev, A.S., Kobets, A.V., Acetaldehyde adsorption in aluminium oxide, React. Kinet. Catal. Lett., 5, 2 (1976) 163-168.

Stull, D.R., Westrum, E.F., Sinke, G.C., The Chemical Thermodynamics of Organic Compounds, Wiley, New York, 1969, 439-440.

Stötzel, J., Lützenkirchen-Hecht, D., Frahm, R., Kimmerle, B., Baiker, A., Nachtegaal, M., Beier, M.J., Grunwaldt, J.-D., Reduction and re-oxidation of Cu/Al_2O_3 catalysts investigated with quick-scanning XANES and EXAFS, J. Phys. Conf. Ser., 190 (2009) 012153.

Sun, J.T., Metcalfe, I.S., Sahibzada, M., Deactivation of Cu/ZnO/Al_2O_3 Methanol Synthesis Catalyst by Sintering, Ind. Eng. Chem. Res., 38 (1999) 3868-3872.

Susnitzky, D.W., Carter, C.B., The formation of copper aluminate by solid-state reaction, J. Mater. Res., 6, 9 (1991) 1958-1963.

Svensmark, H., The Chilling Stars - A New Theory of Climate Change, Icon Books Ltd., 2007.

Taarning, E., Saravanamurugan, S., Holm, M.S., Xiong, J., West, R.M., Christensen, C.H., Zeolite-catalyzed Isomerisation of Triose Sugars, ChemSusChem, 7 (2009) 625-627.

Tanaka, Y., Utaka, T., Kikuchi, R., Sasaki, K., Eguchi, K., Water gas shift reaction over Cu-based mixed oxides for CO removal from the reformed fuels, Appl. Catal., A, 242, 2 (2003) 287-295.

Thomsen, A.B., Thomsen, M.H., van Maarschalkerweerd, C., Skytte, K., Olsen, H.S., Christensen, B.H., Zacchi, G., Risø Energy Report 6, Future options for energy technologies, edited by H. Larsen and L.S. Petersen, Ch. 7.5, Bioethanol for transport , Risø National Laboratory, Technical University of Denmark, 2007, 49-53.

Tomaki, Y., Masami, S., Preparation of acetic acid from ethanol or acetaldehyde, JP 57102835, 1982.

Tu, Y.J., Li, C., Chen, Y.-W., Effect of chromium promoter on copper catalysts in ethanol dehydrogenation, J. Chem. Technol. Biotechnol., 59, 2 (2004) 141-147.

Tu, Y.J., Chen, Y.-W., Effects of Alkali Metal Oxide Additives on Cu/SiO_2 Catalyst in the Dehydrogenation of Ethanol, Ind. Eng. Chem. Res., 40 (2001) 5889-5893.

U.S. Energy Administration Information, Weekly U.S. Retail Gasoline Prices, Regular Grade. Retrieved Feb. 7, 2011 from: http://www.eia.doe.gov/petroleum/data_publications/wrgp/mogas_home_page.html.

Ullmann, F., Enzyklopädie der technischen Chemie, Vierter Band (2nd ed.), Ann Arbor, Michigan, USA, 1943, 653.

Ullmann, F., Enzyklopädie der technischen Chemie, Vierter Band, Urban & Schwarzenberg, Berlin, 1917, 1-27.

United Nations, Brundtland report (Our Common Future) A/RES/42/187, Oxford University Press, 1987. Retrieved Dec. 27, 2010 from: http://www.un.org/documents/ga/res/42/ares42-187.htm.

United Nations, Kyoto Protocol, 1998. Retrieved Dec. 27, 2010 from: http://unfccc.int/kyoto_protocol/items/2830.php.

Venezia, A.M., La Parola, V., Pawelec, B., J.L.G. Fierro, Hydrogenation of aromatics over $Au-Pd/SiO_2-Al_2O_3$ catalysts; support acidity effect, Appl. Catal., A, 264 (2004) 43-51.

Viksø-Nielsen, A., Cellulose-to-Ethanol conversion technology, 2009. Retrieved Dec. 28, 2010 from: http://www.bioenergy.novozymes.com/learn-more-about-bioethanol/presentations/.

Wainwright, M.S., Proceedings on Alcohol Fuels, 8, (1978) 1-5.

Weissermel, K., Arpe, H., Industrial Organic Chemistry (4th ed.), Wiley-VCH GmbH & Co, 2003, 171-174, Ch. Alcohols.

Werpy, T., Petersen, G., Top Value Added Chemicals from Biomass Volume I - Results of Screening for Potential Candidates from Sugars and Synthesis Gas, U.S. Department of Energy, 2004.

World Coal Association, Where is coal found?. Retrieved Dec. 27, 2010 from: http://www.worldcoal.org/coal/where-is-coal-found/.

Wysocki, R.K., McGary, R., Effective Project Management (3rd ed.), Wiley, Indianapolis, 2003, Ch. 1, 2, 19.

Appendix A Ethanol conversion and sustainability

Contents

A.1 The 2nd generation bio-ethanol plant energy consumption estimate

Especially the production of ethanol from cellulosic/hemicellulosic feedstocks, the so-called 2nd generation production, is of interest as the production of ethanol from this resource does not compete with food production. However, when it comes to the limited availability of land field, a competition exists anyway, of whether energy crops or food should be produced. Only the biomass waste streams which are not suitable in food production may be counted as truly non-competing.
Typically the bio wastes such as corn stover and bark from trees also have alternative uses. Part of the corn stover generated must be ploughed into the ground in order to maintain arability of the land field. Bark from trees is for example presently being fed to bark boilers providing green energy for paper mills or being used for the production of wood pellets (*Siitonen et al.*).
Common to all these 2nd generation biomasses is that the composition of it makes it unattractive as a food source. The typical contents of lignin, cellulose and hemicellulose are high, whereas the content of sugar and starch is low.

The biomass feedstock must be pre-treated, under the concern of the formation of inhibitors, to open the biomass structure, making the fibres accessible for chemical or enzymatic hydrolysing agents. For example it may be advantageous to remove the lignin component of the biomass prior to the hydrolysis step by means of alkali and oxygen treatment (*Thomsen et al., 2007*). Other lignocellulosic material like wood has to be treated by means of steam explosion to open the lignocellulosic structure, due to its high content of lignin. Normally the lignin (solids) are removed after hydrolysis.

In the hydrolysis step the polysaccharides cellulose and hemicellulose are hydrolysed to obtain the C_6 and C_5 sugars, respectively, which may be fermented at a high yield into ethanol by means of Bakers yeast or other selective strains according to the reactions in Scheme A-1 :

$$C_6H_{12}O_6 \rightarrow 2\ C_2H_5OH + 2\ CO_2$$

$$3C_5H_{10}O_5 \rightarrow 5\ C_2H_5OH + 5\ CO_2$$

Scheme A-1: Fermentation of C_6 and C_5 sugars.

Thus ideally 2/3 of the carbon in the sugars is recovered in the ethanol.

Furthermore depending on the efficiency of the hydrolysis and the fermentation steps it may be desired to divide these into dedicated hemicellulose and cellulose hydrolysis, and C_5 and C_6 sugar fermentation. However, for economic reasons ideally as few process steps as possible is advantageous, if the sufficient yield of sugars is obtained from the biomass. In the aim for such economising it has also been suggested to combine the steps of enzymatic hydrolysis and fermentation in the so-called simultaneous saccharification and fermentation step, SSF. However, this requires a compromise of the optimal conditions for the enzymes and the fermentation strain (*Thomsen et al., 2007*).

Lately Novozymes has presented their version of a 2nd generation ethanol plant taking a starting point in corn stover (*Viksø-Nielsen, 2009*). They advocate

1) a pre-treatment with diluted acid and steam to open up the lignocellulosic structure, liberate the hemicellulose sugars and make the remaining cellulose accessible for the enzymes. Removal of toxic components is done by overliming. 2) The pre-treatment step is then followed by the dedicated enzymatic hydrolysis of the cellulose fraction to release glucose. 3) Solids (lignin) are then separated prior to the fast fermentation step where both the C_5 and C_6 sugars are converted to ethanol.

The main processes of the Novozymes 2nd generation bio-ethanol plant are shown in Figure A-1:

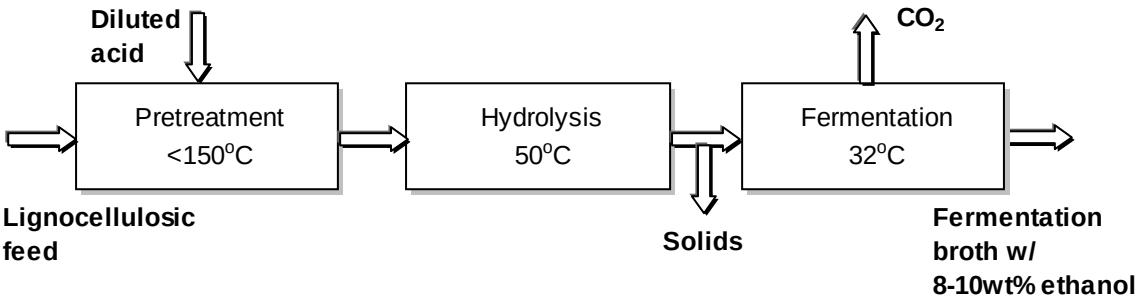

Figure A-1: The conversion of lignocellulosic material into ethanol rich broth may be divided into the primary steps of pre-treatment, hydrolysis and fermentation.

The raw ethanol obtained from the fermentation (fermentation broth, beer) containing 8-10wt% ethanol is distilled to produce 35wt% ethanol in a beer column and 94wt% ethanol in a rectifier. The ethanol rich product from the rectifier is then dried, typically by adsorption on molecular sieves, to 99.7wt% pure ethanol, as literally anhydrous ethanol is needed for the gasoline blending (*Pfeffer et al*., 2007).

Below Table A-1 shows the summary of a rough material and energy mass balance based on the principle by Novozymes as described above. It has been assumed that the lignocellulosic material is corn stover containing 15wt% water and that the dry biomass composition contains 25wt% hemicellulose and 37wt% cellulose (*National Renewable Laboratory*). 70% of the polysaccharides are converted to monosachharides by hydrolysis (*Viksø-Nielsen, 2009*), say 90% of the monosaccharides are fermented into ethanol and 1% of the ethanol is lost during distillation and drying to obtain anhydrous.

The supply of energy required for pre-treatment, hydrolysis and distillation has been assumed provided from an auxiliary boiler, producing steam with a thermal efficiency of 80%. Table A-1 shows the energy consumptions looked up or calculated for the individual conversion steps in the production of bio-ethanol.

Table A-1: Survey of energy uses in the production of 2nd generation bio-ethanol.

Unit operation	Relative Mass (T)	Wet mass (T)	Specific Energy Input (MJ/MT ethanol)	Energy Input (% of total)
Agriculture, transport and cutting	1 biomass	1.18	5769*	32
Pretreatment	0.25 hemicellulose 0.37cellulose	3.33	937**	5
Dedicated hydrolysis	0.12 C_5 sugar 0.35 C_6 sugar	3.33	4846***	27
Solids separation and wash	0.12 C_5 sugar 0.35 C_6 sugar	2.97	0	0
Fermentation	0.218 ethanol	2.87	0	0
Distillation	0.216 99.9wt% ethanol	0.216	5900****	34
Waste water			268	1
Total			17720	100

* An average value of energy use for agriculture of cellulosic biomass=1300 MJ/MT biomass from *Natural Resources Defense Councli (2006)*.
** Injection of 8 bar saturated steam at 170°C, credit of condensate calories
*** Indirect heating. 2 reheats of batch to 50°C.
**** Azeotropic distillation *(Madson and Monceaux)*

Comparing above primary energy input with the LHV energy of ethanol=26.8GJ/MT the NEB according to Eq. 1-2 may be calculated as = 26.8/18=1.5, if fossil fuels are used both for agriculture, transport and the unit operations in the 2nd generation bio-ethanol plant. If however it is foreseen that biomass, for example lignin may be used as the source of heating in the bio-ethanol plant the NEB value rises to 4.4, which was used in the C-factor paper, Appendix A.3.

Appendix A.1. References

Madson, P.W, Monceaux, D.A., Fuel Ethanol Production, http://www.bioethanol.ru/images/bioethanol/Fuel%20ethanol%20production%20-%20Katzen.pdf

National Renewable Energy Laboratory, Lignocellulosic Biomass to Ethanol Process Design and Economics Utilizing Co-current Dilute Acid Prehydrolysis and Enzymatic Hydrolysis for Corn Stover, 2002.

Natural Resources Defense Council, Ethanol: Energy Well Spent, 2006. Retrieved Feb. 28, 2011 from: www.nrdc.org/air/transportation/ethanol/ethanol.pdf.

Pfeffer, M., Wukovits, W., Beckmann, G., Friedl, A., Analysis and decrease of the energy demand of bioethanol-production by process integration, Appl. Therm. Eng., 27, 16 (2007) 2657-2664.

Siitonen, S., Possibilities of Reducing CO_2 Emissions in the Finnish Forest Industry, Finnish Forest Industries Federation, 2002. Retrieved Dec. 28, 2010 from: www.forestindustries.fi/Infokortit/reducingco2emissions/.../default.aspx.

Thomsen, A.B., Medina, C., Ahring, B., Risø Energy Report 2, New and emerging bioenergy technologies, edited by H. Larsen, J. Kossmann and L.S. Petersen, Ch. 6.4 Biotechnology in ethanol production, Risø National Laboratory, Technical University of Denmark, 40-44.

Viksø-Nielsen, A., Cellulose-to-Ethanol conversion technology, 2009. Retrieved Dec. 28, 2010 from: http://www.bioenergy.novozymes.com/learn-more-about-bioethanol/presentations/.

A.2 Personal contribution to paper and Paper: Zeolite-catalyzed biomass conversion to fuels and chemicals

Personal contribution to EES perspective paper (by Bodil Voss)

Ethanol

Ethanol may be produced biochemically (fermentation) from many carbohydrate sources such as sugar cane, corn, sugar beet, cereal grains and potatoes but also hydrolysates of lignocellulosic feedstocks (so-called 2nd generation) may be fermented to obtain ethanol. The production of bioethanol for fuel has increased dramatically in the US, Brazil, China and EU recently with a total annual global production of 52 million MT in 2008 [B1]. Vehicles can run unmodified on a blend of gasoline with up to 10% dry ethanol.

The raw ethanol obtained from the fermentation (fermentation broth) is distilled to produce 94wt% ethanol, which is then dried to >99.7wt% pure ethanol, as anhydrous ethanol is needed for the gasoline blending. Distillates of ethanol with concentrations of 10-94wt% primarily balanced by water may be withdrawn from the distillation based purification. The removal of water from the ethanol is a heat demanding process sparking an interest in the use of hydrous ethanol.

*Ethanol to a variety of product*s

The most widely used catalyst HZSM-5 catalyses the conversion of ethanol into a range of products the distribution of which varies with temperature and the addition of promoters.

Derouane et al [B13] proposed a simplified reaction scheme (see Scheme A-2) for the formation of diethyl ether, ethylene and C3+ hydrocarbons on zeolites.

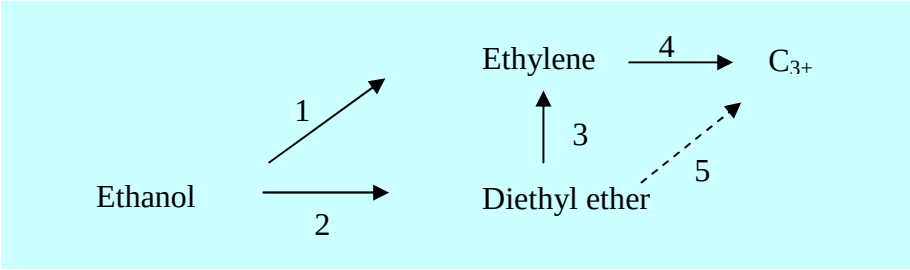

Scheme A-2: Reaction scheme for ethanol conversions on zeolites.

Barthos et al [B12] showed how the selectivity towards the different products of ethanol conversion on ZSM-5 varies with temperature from 100-700°C. Common to all zeolites the first product diethyl ether drops off from 200°C, while ethylene and propylene increase. Depending on the SiO_2/Al_2O_3 ratio the aromatics also start emerging above 200°C at low selectivities as compared to the olefins (>60%) but with the highest aromatics selectivity of xylenes and C9+ (2-4%). Benzene starts off at a higher temperature. The lower acidity of the zeolite with the highest SiO_2/Al_2O_3 ratio is reflected in a lower selectivity toward the formation of aromatics. The modification of HZSM-5 with Mo_2C increases the benzene selectivity amongst aromatics and makes

the ethylene selectivity diminish from about 65% above 400°C, in general increasing the aromatics selectivity. Addition of Re and Pt to ZSM-5 caused a dramatic decay of ethylene at 700°C leading to significant production of methane, hydrogen and CO according to:

$$C_2H_4 + H_2O = CO + CH_4 + H_2$$

Scheme A-3: Cracking of ethylene on zeolite ZSM-5 in the presence of water at 700°C.

In summary the preferred temperature regions for the conversion of ethanol into various products on HZSM-5 is depicted in Figure A-2 as:

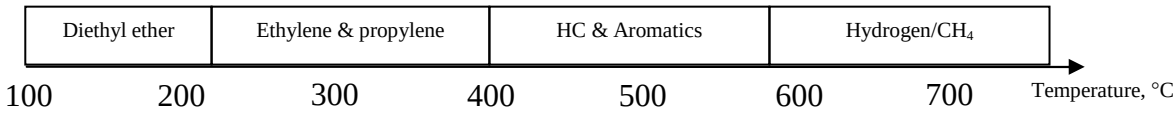

Figure A-2: The temperature regions for the maximum conversion of ethanol to products on HZSM-5

Modifications such as addition of promoters may shift the operating ranges.

Ethanol to Diethylether

As is well known diethyl ether may be used as a diesel fuel. Apart from excellent cold-start properties diethyl ether reduces the formation of NO in the exhaust gases from the diesel engines. In an experimental study on a single cylinder, four stroke, water-cooled DI diesel engine diethyl ether was co-fed with LPG as an ignition improver. Diethyl ether was found to lower the cylinder gas temperature reducing the NO in the exhaust gas by about 65% as compared to diesel at full load [B10].

IR spectra showed in a very early study [B11] how both Brønsted and Lewis acid sites catalyse the conversion of ethanol to diethyl ether. Low calcined zeolites having both types of sites show the highest activity and the lowest optimum temperature for diethyl ether. From TPD for diethyl ether adsorption over HZSM-5 (calcined at 540°C) it was found that diethyl ether was not desorbed at temperatures over 200°C in accordance with its low presence above that temperature under catalytic testing. The phosphoric acid treated ZSM-5 showed no coke formation. A reaction mechanism of the reaction between an adsorbed ethoxy species with a gas phase ethanol molecule was postulated. In the more recent study [B12] the coupling between two adsorbed ethanols yielding diethyl ether is suggested. Two zeolites with a SiO_2/Al_2O_3 of 80 and 280 respectively were compared. The lower number of Brønsted sites on the 280 version was reflected in a lower activity at low temperature, however in both cases the formation of diethyl ether diminished from 200°C and ceased at 300°C. Takahara et al [B14] showed that the formation of diethyl ether only requires weak acid sites.

Diethyl ether has recently been proposed as an ignition enhancer in internal combustion engines, where the diethyl ether is formed by dehydration of an ethanol containing fuel over a zeolite in a preconversion step before injection [B18].

Ethanol to Ethylene

Ethylene is a bulk chemical, for example being used for polyethylene. Ethylene may be obtained with a high selectivity over H-ZSM5 at lower temperature (250-300°C) than the hydrocarbons (350-400°C). The presence of water in the feed has been found [B6] to enhance the catalyst activity and selectivity for ethylene over diethyl ether. This is suggested to be due to a moderation of the Brønsted sites responsible for the dehydration activity.

Another catalyst active in the dehydration of ethanol is alumina. It was earlier established that TiO_2 modified alumina increased the ethylene activity over the unmodified alumina, and in a recent study the parallel phenomenon was observed for a zeolite 4A catalyst [B7]. Zeolites as compared to aluminas convert ethanol to ethylene at far lower temperatures, 250-300°C vs 350-400°C.

Nano-scale HZSM-5 zeolite [B8] has shown a better stability in converting bio-ethanol into ethylene. Over 300-400 h on stream (240°C) the activity and selectivity was observed to be constant for the nano-scale zeolite, vaguely dropping off from 500h, while microscale HZSM-5 within 60h suffered from a reduced activity and selectivity, dropping off more drastically at about 120h time on stream.

The dehydration route from ethanol to ethylene is insignificant for countries with a developed petrochemical industry. In developing countries however, where cheap ethanol is available it plays a rôle as a supplement to petroleum derived ethylene [B15].

Although the sales prices of ethanol and ethylene favour the sale of ethanol rather than polyethylene, self-sufficiency in the supply of ethylene for downstream polyethylene production may create overall viability.

Ethanol to hydrocarbons

The production of hydrocarbons from ethanol over ZSM-5 zeolite catalysts has been studied in continuation of the findings of methanol transformation into hydrocarbons (MTG) [B2]. The so-called ETG (Ethanol-To-Gasoline) yields same product distribution, whereas a higher deactivation rate is found. The faster deactivation is counteracted when hydrous ethanol is used. A hydrocarbon pool behaviour of the catalyst in the ETG process in parallel to the MTG process was observed with high yields of alkylated aromatics. According to the hydrocarbon pool theory the cavities of the zeolites host cyclic organic species from which the gasoline products originate through alkylation and cracking reactions. Both ethyl and methyl substituted benzenes were found in the dissolved zeolite catalysts after conversion of ethanol. The similarity to the MTG product distribution was ascribed to the lower reactivity of the ethyl substituted species in the hydrocarbon pool.

The shape selectivity of zeolite catalysts and the Fischer-Tropsch activity of iron have been sought combined through the incorporation of iron into the zeolite structure. In a recent work [B3] the optimum yield of C_{5+} products was obtained with samples of 0.3-0.5 wt% Fe over those with about 2wt% Fe. The substitution of part of the framework aluminium by iron was found to lower the deactivation rate.

Also the importance of the zeolite pore architecture has been investigated [B4]. Large pores (HFAU and HBEA) gave faster deactivation of the Brønsted sites resulting in very low C3+ activity. Medium pore HZSM-5 showed a maintained high activity in spite of a 55% loss of microporosity and 94% loss of Brønsted acidity, indicating that the pore mouth reactivity is dominant. The coke found are polyaromatics and is more condensed on large pore zeolites than for HZSM-5. Another structural parameter, namely the Si/Al ratio was found to influence. A higher selectivity for liquid hydrocarbons was obtained for Si/Al equal to 1 or 3 rather than 2 atoms in the elementary cell [B5].

Ethanol to Hydrogen

The possibility of utilising bio-ethanol for fuel cells on-board vehicles is also dealt with in the research on zeolites. Novel Rh and potassium-modified Rh catalyst supported on NaY zeolite showed hydrogen product yields of more than 60%. As opposed to oxide supported Rh catalysts able to run from 450-850°C the NaY supported Rh catalyst shows good conversion to hydrogen from about 300°C [B19].

A process for the reforming of ethanol to form hydrogen over a zeolite with Pt, Pd or Cu supported on a HZSM-5 zeolite has been proposed [B20]. A temperature of about 800°C is recommended in order to achieve a high CH_4 conversion.

Alkylation with Ethanol

The ability of zeolites to catalyse alkylation is recognised already in the hydrocarbon pool mechanism. Alkylation with ethanol has industrial interest for example the conversion of benzene into ethylbenzene. Applying zeolite ITQ-22 as described in [B9], formed by a structure of intersecting 8, 10 and 12 ring channels exhibits higher selectivity to diethyl benzene as does the industrially used catalyst based on ZSM-5. The higher selectivity is explained by a tailored pore structure of the multipore catalyst that allows primary products to escape before being further alkylated due to steric hindering and the specific siting of the Brønsted acid sites in the channel intersections.

Para-selectivity in the alkylation on benzene with ethanol into diethyl benzene has been studied for HZSM-5 by means of a nitridation pretreatment. The HZSM-5 samples investigated were flushed with NH_3 at 700°C. Pyridine-IR spectroscopy revealed that nitridation took place primarily in the Brønsted acid sites. The stability of the modified catalyst was found to be higher although with a lower initial activity. Remarkably higher selectivity towards para-diethyl benzene was found with increasing nitrogen incorporation [B24].

NO reduction

Zeolites have been found useful for the reduction of NO with ethanol in exhaust gases from lean-burn gasoline and diesel engines [B21].

Butanol

Analogously to ethanol butanol may be produced biochemically (fermentation) from the same feedstocks as ethanol. Furthermore, a niche lignocellulosic feedstock such as wheat straw, rice straw and switch grass may be applied for the co-fermentation to acetone-butanol and ethanol (3:6:1) (ABE), which is beneficial for keeping a low production cost. This is due to the ability of the ABE fermentation cultures to convert the hydrolysate sugars from lignocellulosic feedstock [B21]. Butanol has the advantage over ethanol as a gasoline supplement that it blends well with gasoline at higher concentration and it has higher energy content per volume.

Butanol to hydrocarbons

Recently it was found that the addition of butanol or other higher alcohols to a methanol (or dimethyl ether) feed increases the reactivities of the oxygenate feed. This may be due to light olefins, formed by dehydration of the higher alcohols, acting as precursors sustaining the hydrocarbo pool.[B25]

Alkylation with Butanol

The features of hierarchical zeolites with all pore size-regimes provide high catalytic activity and selectivity for alkylation of phenol with tert-butanol. A higher phenol conversion and a higher selectivity to 2,4 di (t-butyl) phenol was achieved as compared to the values obtained over conventional HZSM-5 and Al-MCM-41 with the phenol fed in a ratio 1:2.5 tert butanol at 145°C [B22]. The macro pores of hierarchical zeolites offer easier transport and access to active sites.

Esterification with butanol

Industrial esterification conversions typically involve using mineral liquid acids such as sulphuric acids. As an alternative, the use of a solid acid offers immobilisation and a non-corrosive medium. While ion-exchange resins are prone to degradation at higher temperatures and suffer from swelling zeolites like Y, X, BEA, ZSM-5 and MCM-41 constitute attractive alternatives. In a test reaction of esterification of acetic acid with butanol (at 75°C, liquid phase) zeolites in general show high reusability and activity [B23]. Amongs the zeolites tested, HUSY zeolite with a Si/Al ratio of 20 gave the highest activity.

Alcohol conversion perspectives

The main interest on alcohol conversion over zeolites is presumably going to be within olefins. Ethylene and propylene are continually being used as monomers or monomer precursors for the production of plastics. The energy intensity of the petroleum derived ethylene is likely to be penalised with heavy taxes in the future, increasing the feasibility of the alternative ethanol conversion route. Ethanol conversion over zeolites offers the benefits of water tolerance - in fact water co-fed serves as a coke suppressor.

In a period where the world converts to alternative fuels for cars, the high-energy-density gasoline/diesel may not be exchangeable for ethanol, electricity or hydrogen in for example aeroplanes until further technological development has taken place. Green gasoline may be produced from the gasification of biomass to obtain syngas and the subsequent conversion via methanol and the well-known MTG synthesis, or via the direct TIGAS route. But alternatively hydrous ethanol obtained from fermentation of lignocellulosic material may be converted via the ETG process as discussed above, the latter being the greener route.

With an alternative set of chemical building blocks as compared to Today's petroleum derived new chemical routes to obtain desired end-products chemicals may be called for. The prospects of incorporating active metals into the zeolite framework, the shape-selectivity of zeolites and their ability to be tailored for special features, for example in alkylation with alcohols, may help overcome the hurdles of converting from petroleum based to renewable based flowcharts [B26].

Appendix A.2 References

B1 - www.**ethanol**rfa.org/industry/statistics/
B2 – Roger Johansson et al, The Hydrocarbon Pool in Ethanol-to-Gasoline over HZSM-5 Catalysts, Catal Lett (2009) 127:1-6
B3 – Valmir Calsavara et al, Transformation of ethanol into hydrocarbons on ZSM-5 zeolites modified with iron in different ways, Fuel 87 (2008), 1628-1636
B4 – F. Ferreira Madeira et al, Ethanol transformation over HFAU, HBEA and HMFI zeolites presenting similar Brønsted acidity, Applied Catalysis A: General 367 (2009) 39-46.
B5 – Y.I Makarfi et al, Conversion of bioethanol over zeolites, Chem Eng. J. (2009), doi: 10.1016/j.cej.2009.06.001
B6 – Cory B. Phillips et al, Production of Ethylene from Hydrous Ethanol on H-ZSM-5 under Mild Conditions', Ind. Eng. Chem. Res. 1997, 36, 4466-4475
B7 – Liang-Peng Wu et al, The fabrication of TiO_2 supported zeolite with core/shell heterostructure for ethanol dehydration to ethylene, Catalysis Communications 11 (2009) 67-70
B8 – J. Bi et al, High effective dehydration of bio-ethanol into ethylene over nanoscale HZSM-5 zeolite catalysts, Catal. Today (2009), doi: 10.1016/j.cattod.2009.04.016
B9 – Avelino Corma et al, The benefit of multipore zeolites: Catalytic behaviour of zeolites with intersecting channels of different sizes for alkylation reactions, Journal of Catalysis 268 (2009) 9-17.
B10 – N.K. Miller Jothi et al, Experimental studies on homogenenous charge CI engine fuelled with LPG using DEE as an ignition enhancer, Renewable Energy 32 (2007), 1581-1593.
B11 – Deng Jingfa et al, Acidic Properties of ZSM-5 zeolite and Conversion of Ethanol to Diethyl ether, Applied Catalysis, 41 (1988) 13-22
B12 – R. Barthos et al, Decomposition and Aromatization of Ethanol on ZSM-Based Catalysts, J. Phys. Chem. B 2006, 110, 21816-21825
B13 – E.G. Derouane et al, Elucidation of the Mechanism of Conversion of Methanol and Ethanol to Hydrocarbons on a New Type of Synthetic Zeolite, J. Catal. 53 (1978) 40-55.

B14 – I. Takahara et al, Dehydration of ethanol into ethylene over solid acid catalysts, Catal Lett. 105 (2005) 249-252
B15 – K. Weissermel et al, Industrial Organic Chemistry, Wiley (2003), p 63.
B16 – http://www.farmfoundation.org/projects/documents/lau.ppt#256,1,SHORT-RUN DENSITY FORECAST FOR ETHANOL AND MTBE PRICES
B17 - Market focus, eprm, May 2003, p 54-55

Paper:
REVIEW www.rsc.org/ees | Energy & Environmental Science

Zeolite-catalyzed biomass conversion to fuels and chemicals

Esben Taarning,*[a] Christian M. Osmundsen,[ab] Xiaobo Yang,[a] Bodil Voss,[a] Simon I. Andersen[a] and Claus H. Christensen[a]

Received 22nd March 2010, Accepted 1st October 2010
DOI: 10.1039/c004518g

Heterogeneous catalysts have been a central element in the efficient conversion of fossil resources to fuels and chemicals, but their role in biomass utilization is more ambiguous. Zeolites constitute a promising class of heterogeneous catalysts and developments in recent years have demonstrated their potential to find broad use in the conversion of biomass. In this perspective we review and discuss the developments that have taken place in the field of biomass conversion using zeolites. Emphasis is put on the conversion of lignocellulosic material to fuels using conventional zeolites as well as conversion of sugars using Lewis acidic zeolites to produce useful chemicals.

Introduction

Zeolites are crystalline materials composed of SiO_4 and $[AlO_4]^-$ tetrahedra. The negative charge of $[AlO_4]^-$ tetrahedra is compensated by a cation, maintaining the overall electroneutrality of the zeolite. Charge compensation with H^+ renders the zeolite highly acidic, which is useful for many catalytic applications. An important feature of zeolites is their microporosity. Many zeolites contain a multidimensional microporous system which has similar dimensions as small molecules. This microporous system allows small reactant molecules to diffuse into the zeolite crystal, thereby allowing access to internal acid sites. The microporous system also adds another important feature to the zeolites, namely shape-selectivity. The size-restraints of the micropore channels can in some cases restrict the formation of large and often unwanted products. This is the case for the isomerisation of xylene mixtures, where *o*- and *p*-xylene are formed predominantly over the more bulky and unwanted *m*-xylene isomer.[1] Alkylation of benzene with ethylene is another important industrial example.[2] However, most importantly, zeolites are some of the most widely used heterogeneous catalysts for the valorization of hydrocarbon streams in refineries and petrochemical facilities.[3,4] The most important example is the use of zeolite catalysts in fluid catalytic cracking (FCC), which supplies about 45% of the global gasoline pool by the cracking of larger hydrocarbon into the gasoline range.[5] Zeolites also find use as catalysts for the conversion of oxygen containing compounds, and there are many examples of zeolite catalyzed acylations, esterifications and dehydrations.[5] Of particular importance is the zeolite catalyzed conversion of oxygenates to hydrocarbons. Most known is the conversion of methanol to gasoline (MTG) but many other oxygenates, including ethanol and pyrolysis oil, can also be converted into hydrocarbons that can be used as gasoline.

Biomass has in the past decade become an increasingly important resource for the production of transportation fuels and chemicals.[6] This utilization is primarily based on biochemical transformations, such as fermentation to produce ethanol from sugars. Biomass conversion based on zeolite catalysis is an alternative approach which could find broad application, especially for the conversion of lignocellulose to transportation fuels and sugars to chemicals. This perspective describes recent developments in this area.

Lignocellulose

Lignocellulosic biomass is the most abundant bio-resource available and consists of three major components: cellulose, hemicellulose and lignin (Table 1). Cellulose is a linear crystalline polymer composed of glucose units. Due to its high crystallinity, cellulose is very difficult to hydrolyse to glucose. Hemicellulose is different from cellulose since it is a branched amorphous polymer that is made of different pentose and hexose units. Due to the branching and its amorphous nature hemicellulose is easier to hydrolyse into monosaccharides than cellulose. Lignin is the largest

[a]*Haldor Topsøe A/S, Nymøllevej 55, 2800 Kgs, Lyngby, Denmark. E-mail: esta@topsoe.dk*
[b]*Department of Physics, Technical University of Denmark, Anker Engelundsvej 1, 2800 Kgs, Lyngby, Denmark*

Broader context

We review the use of zeolites for the conversion of biomass to fuels and chemicals. Zeolites are crystalline microporous aluminosilicate materials that are useful in many applications ranging from use as detergents, ion exchange applications, adsorbents and catalysis. Zeolite catalysis has in particular found use in the upgrade of petroleum to high-quality fuels. However, since biomass is a very different feedstock from petroleum, new approaches are needed if zeolites are to play the same role in the conversion of biomass. In recent years, biomass conversion has attracted tremendous focus and zeolites could play a role in a thermochemical biomass conversion scenario. Selective transformation of sugars to lactic acid derivatives is another area where zeolites can be envisioned to become important catalysts in a future bio-based society.

Table 1 Composition of different lignocellulosic feedstocks[7]

Lignocellulosic material	Cellulose (%)	Hemicellulose (%)	Lignin (%)
Corn cobs	45	35	15
Wheat straw	30	50	15
Rice straw	32	24	18
Fresh bagasse	33	30	19
Switchgrass	45	31	12

non-carbohydrate component of lignocellulosic biomass. It is an amorphous polymer of aromatic allylic alcohols that is very resilient towards hydrolysis and cannot be utilized by fermentation.

Many strategies exist for the conversion of lignocellulose to fuels. Second generation bioethanol can be produced by pretreating lignocellulose to open it up for a subsequent enzymatic hydrolysis. This facilitates the release of monosaccharides which can be fermented into ethanol. This process enables non-edible lignocellulose to be used as a source for ethanol, although lignin remains unutilized. Gasification of lignocellulose is a different strategy which enables all the carbon containing species present in the lignocellulose to be utilized, including lignin. The lignocellulose is heated to temperatures in the range of 800–1000 °C in the presence of a small amount of oxygen. This facilitates the complete break-down into CO/CO_2, H_2 and H_2O. The syngas thus produced can be converted into Fisher–Tropsch diesel or to

Esben Taarning

Esben Taarning is a research chemist at Haldor Topsøe A/S, working on the conversion of biomass to fuels and chemicals using heterogeneous catalysis. He received an MSc degree in chemistry from the University of Copenhagen in 2005 and in 2009 the PhD degree from the Technical University of Denmark after which he has worked for Haldor Topsøe A/S. The topic of his PhD thesis is the development of green and sustainable chemical reactions.

Xiaobo Yang

Dr Xiaobo Yang, holding BSc and MSc degrees of Fudan University, Shanghai, China, obtained his PhD in Chemical Technology in 1999 from University of Kaiserslautern, Germany, under the supervision of Prof. Stefan Ernst with a thesis on the host/guest chemistry of zeolites. Then he held a number of research positions at academic and industrial institutions, working on zeolite synthesis and characterization, among them at ENSCMu with Prof. Henri Kessler, and at University of Pennsylvania with Dr David Olson. Since 2008 Dr Yang has been working at Haldor Topsoe A/S as a Research Chemist on catalytic conversion of biomass to chemicals.

Christian M. Osmundsen

Christian Osmundsen received an MSc in chemical engineering from the Technical University of Denmark (DTU). He is currently a PhD student at the department of physics at DTU under the Catalysis for Sustainable Energy (CASE) Initiative. The focus of the project is the development of methods for converting biomass, in particular carbohydrates, into chemicals and fuels by catalytic means. The work is performed in collaboration with Haldor Topsøe A/S.

Bodil Voss

Bodil Voss (b. Feb. 14th 1967) is finishing an industrial PhD project in April 2011 on the conversion of biomass to chemicals by heterogeneous catalysis at Haldor Topsøe A/S (Denmark), a world leading supplier of catalysts and technological designs within the fields of bulk chemicals production and environmental processes and in collaboration with the Technical University of Denmark (DTU). Bodil Voss graduated as a Bachelor of Chemical Engineering from DTU in 1990 (Ingeniørakademiet). She was employed at Haldor Topsøe A/S immediately after obtaining her degree and has been working there for 20 years.

methanol which can be used to produce gasoline using the MTG process.[8]

Pyrolysis oil from lignocellulose

Pyrolysis of biomass is yet another strategy for the utilization of lignocellulose. By heating lignocellulose in the absence of oxygen, it can be converted into gaseous, liquid and solid materials. The relative distribution of each depends on process parameters such as residence time, temperature and heating rate. In general, long residence times of 15–30 minutes and low temperatures, around 400 °C, favor the formation of solid charcoal whereas flash pyrolysis with residence times shorter than 1 second and temperatures around 500 °C favor the formation of the liquid pyrolysis oil.[9,10] Pyrolysis facilitates the spontaneous occurrence of dehydration reactions, retro-aldol reactions and many radical reactions. In flash pyrolysis, high temperatures ensure efficient depolymerization while short residence time minimizes the effect of secondary reactions which otherwise would lead to further thermal decomposition of the pyrolysis oil, resulting in a reduced liquid yield. Yields of liquid pyrolysis oil in the range of 70–75% are obtainable using flash pyrolysis.

The most important reason to transform lignocelluloses into pyrolysis oil is that it becomes a liquid, which makes further processing less problematic. Pyrolysis achieves a partial breakdown of the macromolecular components of lignocellulose to smaller components such as sugar monomers and decomposition products of these. The lignin part is also depolymerized to some extent, and aromatics such as guaiacols and phenols are typical components found in pyrolysis oil. However, a large part of the lignin and some of the polysaccharides are converted into char, which is difficult to process further.

The elemental composition of pyrolysis oil generally resembles that of the parent lignocellulosic feedstock.[10] Pyrolysis oil is a viscous black liquid with a similar appearance as crude oil. However, it is fundamentally different in many regards (Table 2). Pyrolysis oil can be considered a micro-emulsion of various oxygenates such as carboxylic acids, ketones and aldehydes in water and it is immiscible with hydrocarbons. The presence of carboxylic acids renders the pyrolysis oil acidic, with typical pH values in the range of 2–2.5. Over time, the aldehydes and ketones undergo aldol condensation reactions under these acidic conditions. This causes the pyrolysis oil to change composition and viscosity over time and its acidic nature makes storage difficult due to corrosion issues. Pyrolysis oil has a slightly higher energy density than its parent lignocellulosic precursor but only an energy density of about 40% of that of diesel at 25% water content.

Zeolite upgrading of pyrolysis oil

Through proper separation techniques a number of useful chemicals can be retrieved from pyrolysis oil.[13] However, the sheer number of components present complicates this approach. Indeed, more than 400 different components have been identified in the oil, and the use of pyrolysis oil as a fuel substitute seems to be a more reasonable strategy.[14,15] So far, pyrolysis oil has only been used as fuel in a limited number of applications, such as stationary ones.[16,17] Pyrolysis oil is not useful as a liquid transportation fuel due to the many undesirable characteristics described unless it is upgraded to a more stable fuel product. One way to upgrade pyrolysis oil is by converting it to gasoline using a zeolite catalyst. This facilitates the conversion of pyrolysis oil to a hydrocarbon fraction which resembles gasoline.

When vapors of pyrolysis oil are passed through a bed of zeolite catalyst at 300–500 °C they are converted to hydrocarbons along with the formation of H_2O, CO_x and coke. This process thus resembles the MTG process to a great extent. In general, coke formation is much more pronounced when pyrolysis oil is used as feed compared to methanol, and in the order of 30% of the carbon in the feed ends up as coke on the zeolite. The primary reason for this is that pyrolysis oil contains less effective

Simon I. Andersen

Simon Ivar Andersen is the Reservoir fluid chemistry discipline manager at Schlumberger DBR Technology Center, Edmonton, Canada. Previously he has been principal research scientist and responsible for a program on renewable chemistry at Haldor Topsoe A/S, Denmark. Before joining Topsoe he was an associate professor in applied thermodynamics Dept. Chem. Eng. Technical University of Denmark. His research interests have been within phase behavior, colloidal chemistry and analysis of complex mixtures such as petroleum as well as catalysis.

Claus H. Christensen

Claus Hviid Christensen is Chief Executive Officer at LORC (Lindoe Offshore Renewables Center) that is leading the turnaround of the Danish shipyard Lindoe from ship construction to renewable energy technology. Before this, Claus Hviid Christensen was Vice President, R&D at Haldor Topsoe A/S with responsibility for emerging technology. He came to this position after founding the Danish Center of Excellence for Sustainable and Green Chemistry at the Technical University of Denmark, where he was Professor of Chemistry. Claus Hviid Christensen is also co-founder of Amminex A/S that develops ammonia and hydrogen storage technologies.

Table 2 Characteristics of pyrolysis oil and diesel fuel (40 °C and 25% water)[11,12]

Physical property	Pyrolysis oil	Diesel fuel
Moisture content	20–30 wt%	0.1 wt%
pH	2.0–2.5	—
Density	1.2 kg L^{-1}	0.94 kg L^{-1}
Elementary analysis (wt%)		
C	55–58	85
H	5–7	11
O	35–40	1
N	0–0.2	0.3
Ash	0–0.2	0.1
HHV as produced	16–19 MJ kg^{-1}	40 MJ kg^{-1}
Viscosity	40–100 cp	180 cp
Solids (char) (wt%)	0.1–0.5	1.0
Vacuum distillation residue	Up to 50 wt%	1 wt%

hydrogen than methanol or ethanol. It is simply a too highly oxidized feed to be converted solely into hydrocarbons, and excess carbon is therefore deposited as coke. The effective hydrogen of a feed can be assessed by the use of Chen's effective H/C ratio concept as defined by (H − 2O)/C.[18] Feeds having high H/C ratios in general lead to less coke formation than those having lower ratios. Thus, for methanol the effective H/C ratio is 2, while for pyrolysis oil it is below 0.5.

Oxygen is removed over the zeolites in the form of H_2O, CO or CO_2. The ideal situation for a highly oxidized feed such as pyrolysis oil is to remove most of oxygen in the form of CO_2, as this would effectively enhance the H/C ratio and thus lead to reduced coke deposition. However, different organic components tend to lose oxygen in different ways (Table 3). In general, alcohols and phenols lose oxygen in the form of H_2O, whereas aldehydes, formates and carbohydrates primarily lose oxygen as CO and H_2O. Carboxylic acids lose oxygen as CO_2 and H_2O. Acetic acid is therefore a useful component for the formation of hydrocarbons, even though its effective H/C ratio is 0.

Bakhshi and co-workers have tested different catalysts such as H-ZSM-5, H-Y, mordenite, silicalite-1, alumina–silica and various $AlPO_4$ molecular sieves, for pyrolysis oil upgrading in a fixed-bed reactor at temperatures in the range of 290–410 °C.[20,21] H-ZSM-5 was found to be superior to other catalysts, giving a 34 wt% organic fraction relative to the pyrolysis oil feed. This fraction was found to contain 87% hydrocarbons, with toluene and xylenes being the dominant species present. In contrast, when using a less acidic silica alumina catalyst, the organic fraction decreased to 25 wt% relative to the pyrolysis oil feed. In addition, the organic fraction contained fewer hydrocarbons (54%) with aromatics only constituting a minor fraction of these relative to aliphatics. This suggests that the less acidic silica alumina catalyst is not as effective a hydrogen transfer catalyst as the H-ZSM-5 and the aliphatics formed are not converted into the thermodynamically favored aromatics. Also, since aromatics have a lower H/C ratio than aliphatic hydrocarbons, more hydrogen has to be put into the aliphatics, which reduces the overall formation of hydrocarbons from pyrolysis oil due to its low hydrogen content. Another strategy that has been used is to co-feed pyrolysis oil with a hydrogen-rich compound in order to reduce the amount of coke formed and increase the amount of carbon that ends up as gasoline. In a study, Dao *et al.* co-fed methanol with furfural, a model compound representing pyrolysis-oil, at a mass ratio of 70/30.[22] Here the yield of deoxygenated hydrocarbons increased from below 10% to ~40 wt%, illustrating the beneficial role of increasing the hydrogen content of the feed.

Gayubo *et al.* have studied model compounds in order to investigate the molecular pathways taking place in the zeolites when processing pyrolysis oil.[23–25] Using an H-ZSM-5 zeolite as the catalyst, model compounds representing most of the species present in pyrolysis oil were examined. Here it was found that alcohols undergo dehydration at low temperatures (~250 °C) to form olefins which are converted into alkanes and aromatics at higher temperatures. Acetaldehyde forms large amounts of thermal coke prior to contact with the H-ZSM-5 catalyst, illustrating the unstable nature of many aldehyde components. Acetone initially transforms into isobutene and at higher temperatures this is further transformed into heavier olefins and aromatics and alkanes. Acetic acid was found to undergo ketonization to acetone and CO_2 and thus follows the reaction pathway of acetone. Phenol is much less reactive than the other substrates and is only partially converted to propene and butenes at temperatures of 400 °C; its conversion does not markedly change with temperature. 2-Methoxyphenol thermally decomposes in the heating zone, leading to the formation of coke, but it is not easily converted over the H-ZSM-5 even at 450 °C. From the insight gained when using these model compounds, it is speculated by Gayubo *et al.* that it could be worthwhile to remove aldehydes and phenolics from the pyrolysis oil prior to conversion over the zeolite in order to reduce the amount of coke formed.

Alternatively, from the view point of process design, FCC type riser reactors could be employed where on-site regeneration of coked catalysts is an option. This approach is widely used in the petroleum industry when processing heavy feedstocks and the coke is not completely lost since the heat released by coke-burning is used to supply heat for the process. The use of FCC catalysts, *e.g.* H-Y zeolite, has been studied by Vasalos *et al.*[26,27] In this study, the pyrolysis oil initially underwent a thermal

Table 3 Formation of H_2O, CO and CO_2 for various organic species over a H-ZSM-5 zeolite[19]

	Oxygen in gas phase (%)		
Feed compound	H_2O	CO	CO_2
Methanol	100	0	0
Dimethyl ether	100	0	0
Guaiacol	96	3	1
Glycerol	92	7.5	0.5
Xylenol	93	6	1
Eugenol	89	9	2
Anisole	88	12	Trace
2,4-Dimethyl phenol	87	12	1
o-Cresol	80	17	3
Starch	78	20	2
Isoeugenol	77	19	4
Glucose	75	20	5
Dimethoxymethane	73	6	21
Xylose	60	35	5
Sucrose	56	36	8
n-Butyl formate	54	46	0
Diphenyl ether	46	46	8
Furfural	14–22	75–84	2.5–3.0
Methyl acetate	54	10	36
Acetic acid	50	4	46

hydrotreament, resulting in a liquid yield of up to 42 wt%, with up to 85 wt% oxygen removed while 6.5 wt% oxygen remained in the hydrotreated product.[26] The hydrotreated pyrolysis oil can be separated by distillation, with the light distillate having properties compatible with petroleum gasoline or diesel and can be used directly as blend stocks to the corresponding petroleum fractions. The heavy fraction of the hydrotreated pyrolysis oil can be mixed into the petroleum FCC feeds, such as vacuum gas oils. Experimental results show that co-feeding of this hydrotreated pyrolysis oil with vacuum gas oil at 2.5 wt% can increase the yields of light cycle oil by 1 wt% with the concurrent formation of 0.5 wt% more coke.[27]

Catalytic fast pyrolysis

Pyrolysis processes can be carried out in the presence of a catalyst in order to obtain a more desirable hydrocarbon product in place of pyrolysis oil. An obvious benefit of using a catalyst such as a zeolite is that conversion of lignocellulose to gasoline takes place in a single step, thereby simplifying the process by avoiding condensation and re-evaporation of the pyrolysis oil. The principles in catalytic fast pyrolysis are the same as those for non-catalytic fast pyrolysis; lignocellulose is rapidly heated to a temperature between 300 and 700 °C using a short residence time and then rapidly cooled in order to achieve high liquid yields and prevent the formation of unwanted by-products. The catalyst ensures further cracking of the pyrolysis intermediates and oxygen removal in the form of H_2O, CO or CO_2 resulting in the formation of hydrocarbons.

Using a forestry residue biomass from beech wood, Lappas *et al.* carried out experiments to compare fast pyrolysis with catalytic fast pyrolysis using a FCC catalyst, *i.e.* Re-USY zeolite.[27] With the catalyst, pyrolysis oil yields decreased from *ca.* 75% to 45–50%, while yields of both gas and char almost doubled. However, the oil product obtained in the catalytic process was found to contain 50% more hydrocarbons and significantly less oxygenates than in the absence of catalyst, thus illustrating that upgrade of the pyrolysis oil occurs simultaneously as the pyrolysis reaction. The oxygen was removed primarily in the form of water in this study, resulting from the zeolites' ability to catalyze dehydration reactions due to its strong acidity. Samolada *et al.* have introduced a number of measurable factors which can be used as criteria to evaluate the effectiveness of the catalytic fast pyrolysis processes.[28] These are: loss of organics (LO), stability index (SI) and water generation (WG). The LO criteria relates to carbon efficiency and the other factors define the efficiency of oxygen removal. Different catalysts, such as H-ZSM-5 and Re-USY, mesoporous Al-MCM-41, alumina, and supported Fe/Cr catalysts, were tested for catalytic fast pyrolysis using a model biomass mixture. Here it was found that alumina hardly exhibits any catalytic role with respect to improving the fuel property of the liquid product. MCM-41 was found to be comparably inactive, probably due to the poor structural stability and its low acidity. Zeolites, especially H-ZSM-5, are effective oxygen removal catalysts, although at the expense of organics yield; in comparison with *e.g.* aluminium containing Al-MCM-41,[29,30] or Al-MCM-41 synthesized from zeolite seeds,[31] H-ZSM-5 produces more H_2O, indicating its stronger dehydration tendency due to its stronger acidity.

Catalytic fast pyrolysis of sugars is a topic that has been investigated by Huber and co-workers. Zeolites H-Y, β, and H-ZSM-5, silicalite-1 and a silica–alumina have been tested for the catalytic fast pyrolysis of glucose at 600 °C.[32,33] H-ZSM-5 gives the highest yields of aromatics and other (partially) de-oxygenated organics, along with by-products such as CO, CO_2, H_2O and coke. The primary product on silica–alumina is coke. The highest achievable aromatic yield over H-ZSM-5 is *ca.* 30% based on carbon, while approximately a similar amount of carbon ending up as coke.

Using the same H-ZSM-5 catalyst Huber and co-workers further studied the conversion of xylitol, cellulose and cellobiose. The more reduced xylitol was found to give higher yields of hydrocarbons (48%) compared to the glucose-based substrates. This is highly interesting, since glucose can be viewed as being xylitol + CO. Thus, if glucose is first decarbonylated to xylitol, higher gasoline yields should be obtainable. The aromatic product was analyzed and found to contain *ca.* 45% naphthalene, 20% toluene, others are benzene, alkylbenzene, and up to 5% indene.

Fast pyrolysis and catalytic fast pyrolysis are currently hot topics of research and development, but no commercial scale technology has been demonstrated yet. Current state of the art gasoline yields are in the order of 50% of what is theoretically possible. Challenges are two-fold. On the one hand, highly efficient methods have to be developed to deal with the large amounts of coke. An adaptation of the riser reactor technology applied in FCC processes should be a solution under consideration. On the other hand, to realize rapid heating and short residence time on a reasonably large throughput of feedstock requires sophisticated reactor design. Many different ideas are under investigation, such as fluidized beds, rotating cones, microwave heating, *etc.* Realistic leads will soon emerge.

Conversion of pyrolysis oil to a hydrocarbon fuel that can be used as a transportation fuel is an important field of research. An interesting strategy that has not been discussed here is hydrotreatment of the pyrolysis oil using HDO catalysts to form a more fuel-like product.[34,35] This is more desirable from a carbon-perspective, since more carbon ends up in the final hydrocarbon product rather than as coke on the catalyst. However, zeolite catalysis could take an important step forward by achieving a better control of how the oxygen is expelled from the pyrolysis oil. If a larger fraction of oxygen is expelled in the form of CO or CO_2, more hydrogen would be accessible for hydrocarbon formation and consequently less carbon would deposit on the zeolite.

Catalytic conversion of sugars to lactates

The isomerisation of C_3-sugars to lactic acid, which is thermodynamically more stable, is catalyzed by aqueous acids at temperatures of 250–300 °C. However, moderate yields are obtained at best.[36] Lewis acidic catalysts such as $SnCl_2$ have been demonstrated to be highly active and selective catalysts, achieving a methyl lactate yield of 89% for the conversion of glyceraldehyde in methanol at 90 °C.[37] Unfortunately, the use of a homogeneous catalyst is not practical with respect to catalyst recycling and product purification, and a heterogeneous catalyst would therefore be preferable. It has recently been demonstrated that Lewis acidic zeolites such as Sn-β have unique catalytic

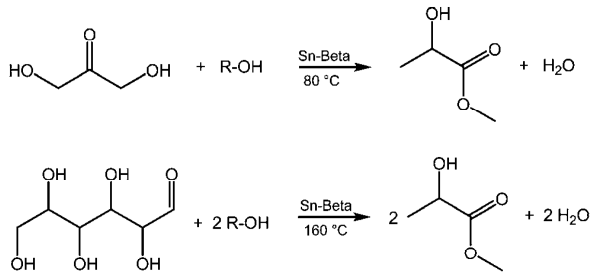

Scheme 1 The conversion of trioses and hexoses to methyl lactate is catalyzed by Lewis acidic zeolites such as Sn-Beta.

activity and are capable of converting C_3- and C_6-sugars directly into lactate esters (Scheme 1).[36,38] The solvent defines which lactate derivative is formed; water leads to the formation of lactic acid whereas methanol leads to methyl lactate.

For C_3-sugars, a quantitative yield of methyl lactate can be obtained in methanol at 80 °C,[36] while yields in the range of 40–65% are achieved when using glucose, fructose or sucrose as the substrate at somewhat higher temperatures (160 °C).[38] Lower yields are generally obtained when water is used as solvent, which could be resulting from autocatalytic decomposition reactions catalyzed by the formed lactic acid. The reaction pathway from C_3-sugars to lactate products is believed to proceed through a preliminary dehydration step, leading to the formation of pyruvaldehyde. Since pyruvaldehyde is highly reactive, it will be present as its hydrate in water and its hemiacetal in methanol. Isomerisation of these species *via* a 1,2-hydride shift leads to the formation of lactic acid and methyl lactate (Scheme 2, path A).

It has been confirmed that aqueous pyruvaldehyde is also converted into lactic acid using Sn-β as a catalyst, thus supporting the hypothesis that this is a preliminary intermediate.[39] In this context it was found that aqueous pyruvaldehyde is transformed at lower temperatures than the C_3-sugars, suggesting that the dehydration of C_3-sugars to pyruvaldehyde is the rate limiting step in the overall reaction. The 1,2-hydride shift resembles the MPVO-redox reaction to a great extent, and Sn-β has previously been demonstrated to be a highly active MPVO-catalyst.[40] Low levels of tin oxide can be incorporated into the β structure during zeolite synthesis, and Si–Sn ratio is typically in the order of 90 : 1 to 200 : 1. Since tin is tetravalent, charge compensation is not an issue and Sn-β is therefore not Brønsted acidic. Instead, the discrete tin atoms have Lewis acidic properties and can coordinate to carbonyl and alcohol groups. These functional groups are widely found in natural compounds, and in particular in carbohydrates. A tentative mechanism for 1,2-hydride transfer mediated by a hydrolysed Sn-site is shown in Scheme 3.

Although Lewis acidic zeolites such as Sn-β and Ti-β are superior catalysts for the conversion of C_3-sugars to lactate derivatives, conventional aluminium containing Y and β zeolites can also be used.[39,41] Higher reaction temperatures are generally required for conventional zeolites (110–120 °C) and the product selectivity depends greatly on the nature of the aluminium present in the zeolite. Strongly dealuminated zeolites containing a large degree of extra-framework aluminium have high selectivities towards lactate products. In contrast, zeolites which are Brønsted acidic in nature exhibit low selectivities towards lactates and increased selectivity for the formation of pyruvaldehyde dimethyl acetal. This effect has been illustrated for an Al-β zeolite (Si : Al 65 : 1) which yielded 74% pyruvaldehyde dimethyl acetal and 3% methyl lactate from dihydroxyacetone in methanol at 115 °C. The same zeolite was tested in a comparable experiment after steam treatment at 750 °C for 20 hours. Here, the pyruvaldehyde dimethyl acetal yield had dropped to 18% while 32% methyl lactate was formed.[36] This difference in product selectivity is caused by the inability of framework aluminium to catalyze the 1,2-hydride shift of pyruvaldehyde methyl hemiacetal leading to methyl lactate. Instead, further acetalization occurs, and pyruvaldehyde dimethyl acetal becomes the main product (Scheme 2, path B).

C_6-Sugars decompose when heated with an aluminium containing zeolite such as Al-β. However, Lewis acidic zeolites such as Sn-β, Ti-β and Zr-β are capable of converting C_6-sugars into lactic acid derivatives.[38] Since C_6-sugars such as glucose, fructose and sucrose are much more abundant than C_3-sugars, this increase in scope is highly important. The overall reaction pathway is believed to involve glucose–fructose isomerisation followed by a retro-aldol reaction of fructose forming the two C_3-sugars, glyceraldehyde and dihydroxyacetone (Scheme 4). The retro-aldol reaction is the rate determining step. These C_3-sugars are then converted into methyl lactate as described previously. This overall reaction pathway starting from glucose thus resembles the biological glycolysis pathway. Similar yields of methyl lactate are obtained when using either glucose (43%) or fructose (44%), suggesting that the two are in equilibrium under the reaction conditions. Surprisingly, higher yields of methyl lactate are achieved from sucrose (65%) compared to the monosaccharides. The ability of Sn-β to catalyze glucose–fructose isomerisation in water was recently reported by Moliner *et al.*[42] When comparing different Lewis acidic materials, Sn-β and Ti-β were found to be more active than other tin and

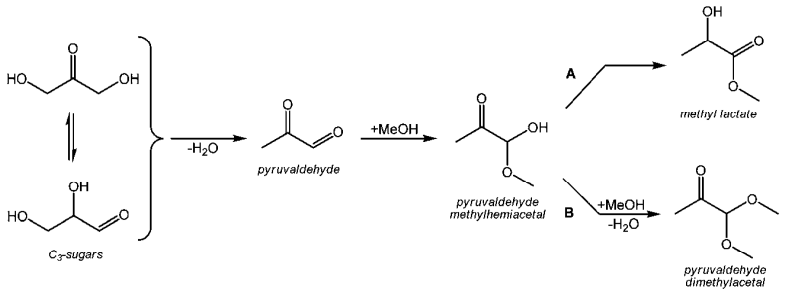

Scheme 2 Proposed reaction pathway for the conversion of trioses to methyl lactate and pyruvaldehyde dimethylacetal.

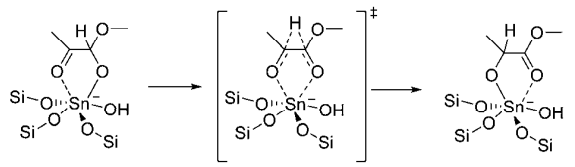

Scheme 3 Tentative transition state mechanism for the 1,2-hydride shift leading to isomerisation of pyruvaldehyde methyl hemiacetal to methyl lactate.

titanium containing materials. This further illustrates how Lewis acidic zeolites might find use as catalysts in carbohydrate conversion.

Currently, little is known about the carbohydrate chemistry catalyzed by Lewis acidic zeolites. However, the ability of the materials to catalyze MPVO-type hydride shifts, retro-aldol reactions and facile dehydration reactions while not having the strong and destructive Brønsted acidic properties of conventional zeolites makes them useful catalysts for converting carbohydrates to different compounds. The Lewis acidic zeolites further have the advantage that they are thermally very stable and can be calcined and reused many times.[38]

These promising characteristics make them real alternatives to fermentation based processes for the production of lactic acid. Currently, lactic acid is produced by fermentation of primarily glucose.[44] Since it is necessary to maintain a neutral pH in the fermentation broth, calcium hydroxide is added continuously to precipitate the formed lactic acid. After the fermentation has completed, sulfuric acid is added to reform the acid. The lactic acid is then converted to methyl lactate and purified by distillation.[44–46] The need for stoichiometric amounts of sulfuric acids and the large amounts of calcium sulfate produced as a by-product (approx. 1 ton per ton of lactic acid)[44] make this process less than ideal from an environmental standpoint. In comparison, catalytic production of methyl lactate does not result in the formation of stoichiometric amounts of salt waste and the fact that methyl lactate is formed directly could simplify the purification of it. However, a racemic lactate product is formed when using catalysts, where the fermentative approach yields a stereochemically pure product. This might limit the use of catalytically produced lactates to non-polymer applications.

Dehydration of sugars to furan compounds

Dehydration of pentoses to yield 2-furancarboxaldehyde, furfural, and hexoses to yield 5-hydroxymethylfurfural, HMF, has been studied for more than a hundred years. Furfural is produced on an industrial scale (approx. 200 000 t a^{-1}) from agricultural wastes, by hydrolysis followed by dehydration in aqueous acids at high temperatures.[43] HMF in contrast is not produced in large scale, although much research has gone into finding viable production methods. HMF can be produced analogously to furfural by dehydration of fructose or hydrolysis/dehydration of inulin, but the high costs of the substrate compared with comparable chemicals derived from petroleum make large scale production of HMF unattractive, thus HMF is primarily produced for use in the production of a few high value chemicals.[43] Both furfural and HMF, however, can be converted to a number of interesting chemicals by known processes, and thus have potential for use as platform chemicals.[44] Scheme 5 shows a number of industrially interesting chemicals that can be produced from HMF. HMF can be oxidized to furan-2,5-dicarboxylic acid, FDCA, which can be used as a replacement for terephthalic acid in the production of polymers,[45] making it interesting as a starting material for the production of biomass-derived polymers. Transportation fuels can be produced by hydrogenolysis of C–O bonds over a copper–ruthenium catalyst to produce 2,5-dimethylfuran (DMF). This compound is insoluble in water, and has a 40% higher energy density than ethanol,[46] making it an interesting alternative for gasoline blending. Alternately liquid alkanes can be produced by condensation reactions between acetone and either HMF or furfural, followed by hydrogenation, over a bi-functional catalyst, such as Pd/MgO–ZrO_2.[47,48]

The industrial production of HMF is typically performed in a homogeneous system using aqueous sulfuric acid as the catalyst. This approach leads to the formation of a number of by-products, formed by fragmentation and condensation reactions,[45] as well as polymeric by-products, known as humins.[44] The use of a homogeneous catalyst is not optimal, and much research has gone into finding alternative solid catalysts, such as zeolites or acidic resins. Rivalier *et al.* compared several different zeolites, such as zeolite β, ZSM5, Y, and mordenite, and found clear differences in conversion and selectivity, with mordenite

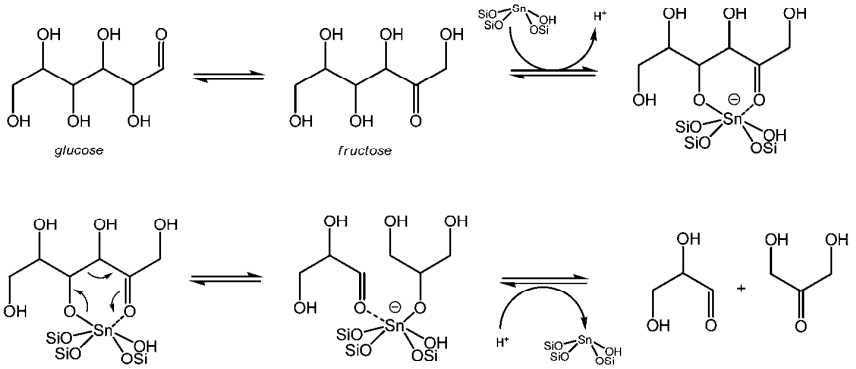

Scheme 4 Proposed reaction pathway for the conversion of glucose to trioses involving isomerisation to fructose, followed by a retro-aldol reaction of fructose leading to dihydroxyacetone and glyceraldehyde.

giving the best selectivities at more than 90%.[49] In a study by Moreau *et al.* the effect of the Si/Al ratio on the conversion and selectivity of the process was investigated;[50] a maximum yield of 70% was obtained, when using a zeolite with a Si/Al ratio of 11. In this process HMF was continuously extracted using methyl isobutylketone, MIBK. HMF can rehydrate to give levulinic acid,[51] and since this reaction is also acid-catalyzed removal of the formed HMF to a neutral phase can be used to avoid further reaction. The partition coefficient in the used system, however, necessitates the use of large volumes of the extraction phase (1 : 5 water to MIBK) making purification of the product costly. An alternative approach relies on the use of other solvents than water to perform the reaction, coupled with continuous removal of the formed water. In a work by Shimizu *et al.* water-free DMSO was used as solvent and the reaction was performed at reduced pressure to boil off any water formed during the reaction.[52] Using zeolite H-β, yields of up to 97% HMF were achieved, when the reaction was performed in an inert atmosphere, while at standard atmospheric pressure, the yield dropped to 51%. Both aldo- and ketohexoses can be utilized as substrate for HMF production. The reaction pathway from glucose and fructose is given in Scheme 6.

The dehydration can occur both through cyclic intermediates and through acyclic intermediates. Considering only the chemistry of the process, the use of ketohexoses, such as fructose, is generally preferred, as the reaction is both more efficient and selective.[51] In the dehydration of glucose, the enolization step is very slow, and thus becomes the rate determining step. The use of glucose further complicates the process, in that oligosaccharides with reducing groups can form, which react with intermediates or HMF itself, thereby reducing the overall yield.[51] However, glucose is much cheaper than fructose, and a change to a process based on glucose, or some polysaccharide of glucose, as substrate would go a long way in making the process more feasible from an industrial standpoint.

Glycerol

Glycerol is produced on large scale as a by-product in biodiesel production and its production is projected to grow even further as biodiesel production increases. Biodiesel production by transesterification is accompanied by the co-production of approximately 10% glycerol. This currently results in the co-production of more than 1 million tons of crude glycerol per year. There is a limited market for high-purity glycerol in the pharmaceutical sector, but this is not able to absorb the large quantities of glycerol produced. In recent years, though, glycerol has found new applications and the chemical companies Solvay and Dow have started using glycerol for the production of epichlorohydrin. Much research has been aimed at converting glycerol into different high-value chemicals. Glycerol transformation using dehydration, hydrogenation, oxidation and etherification as well as acetal and ketal formations have been reported in the literature. Of these, acetalisation and esterification lead to products that can be used as fuel additives, cosmetics, surfactants, plasticizers and pharmaceuticals while the other reactions aim at bulk-type chemical products such as acrolein, 1,3- and 1,2-propandiol. Also acetol, 3-hydroxypropanal, propylene oxide, glyceraldehyde and lactic acid are possible products from glycerol.[53–55]

Acid catalyzed dehydration of glycerol in liquid and gas phase has received much attention.[56] Acrolein has limited use but it can be transformed into acrylic acid, a very important commodity chemical, by oxidation. Typical catalysts used for the dehydration of glycerol are metal oxides and zeolite catalysts. The boiling point of glycerol is 290 °C and it is thermally unstable at this high temperature. Catalytic glycerol dehydration reactions, however, often require temperatures in the range of 250–350 °C, so catalyst deactivation due to glycerol by-product formation, coke deposition and acrolein polymerization are all complicating issues. These issues are taken into account by the use of a catalyst that can be regenerated by calcination. The catalyst life-time can be

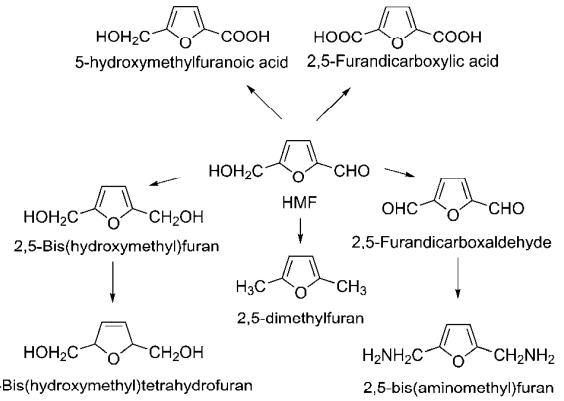

Scheme 5 Overview of industrially interesting chemicals that can be produced from HMF.[43,44,46]

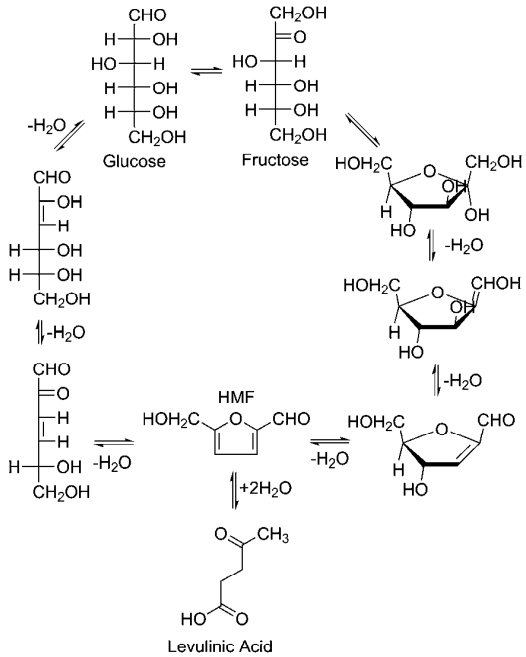

Scheme 6 Pathways for the dehydration of glucose and fructose to HMF.[44]

improved by using diluted glycerol rather than pure glycerol. This is particularly true in liquid phase dehydration of glycerol, but dilution with water can often also be used to minimize coke-formation in vapour phase dehydrations. Kartryniok *et al.* recently gave an excellent review on glycerol dehydration in gas phase showing that zeolites (H-ZSM-5, H-ZSM-11 and H-β) all give 100% glycerol conversion and acrolein selectivities in the range of 70–83% at temperatures of 330–360 °C.[56] Corma *et al.* have used a FCC type reactor for glycerol conversion and showed that low temperatures (350 °C) give higher acrolein yields over H-ZSM-5 than using higher temperatures (500 °C).[57] However, even at 350 °C there is a significant build-up of coke. Yoda and Ootawa showed by FT-IR analysis that on H-ZSM-5 the secondary hydroxy group in glycerol interacts preferentially with the OH of the zeolite, leading to acrolein being formed selectively.[58] Liquid phase glycerol dehydration is somewhat slower and polymerization of acrolein may hamper the industrial application. The acrolein selectivity found for zeolite catalyzed dehydrations are generally slightly lower than those obtained when using many metal oxides. The lower selectivity is likely caused by the higher acidity of the zeolites compared to metal oxides. When operating in a temperature regime where zeolites are known to form hydrocarbons, coke and hydrocarbon formation is likely to occur simultaneously with the dehydration, thus lowering the acrolein selectivity.

Terpenes

Terpenes are hydrocarbon compounds found in many places in nature. The basic building block of terpenes is the isoprene unit; terpenes consisting of between 1 and 8 isoprene units are found in the resins secreted from a wide variety of plants, in essential oils, and in pigments, while higher terpenes, polyterpenes, are found in latexes.[59] Derivates of terpenes are known as terpenoids. Compared to other biomass resources, the available amount of terpenes is relatively low, and the price relatively high, thus most terpenes are used directly, *e.g.* as fragrances or flavors. Some terpenes, and terpenoids, are, however, produced on a large scale and find use as solvents and as starting materials for the production of fine chemicals.[44]

The isomerisation of citronellal to isopulegol (Scheme 7), an intermediate step in the industrial production of menthol, can be performed using Sn-β with almost quantitative yields of pulegols.[60] Industrially, the production of isopulegol is much more interesting than the other pulegols, thus a high diastereoselectivity is important; using Sn-β it is possible to obtain approximately 85% isopulegol. The current industrial yield is 92%, however, this is achieved using a homogeneous, water-sensitive catalyst.

Another example is the isomerisation of α-pinene to camphene (Scheme 8); camphene has a large number of uses, *e.g.* as an intermediate for the production of fragrance materials, acrylates, terpene–phenol resins, as well as a solvent for varnishes. The industrial production is performed using a TiO_2 catalyst, yielding a complex reaction mixture of camphene, limonene, tricyclene, flenchenes and bornylene.[44] Due to the low reaction rate, a number of other catalysts have been investigated for the reaction, such as zeolites β, ZSM-5, mordenite, and Y. For zeolite Y, yields of over 40% camphene, along with 23% limonene, have been reported, at 85% conversion.[61]

Dehydration of alcohols

Ethanol is the largest biochemical produced today and its growth is estimated to continue for many years. Due to the large scale of ethanol production, ethanol can be viewed as a potential feedstock for the production of other compounds, in the same way as naphtha is today. In general, dehydration of ethanol using zeolites leads to the formation of diethyl ether, ethylene or gasoline, depending on the reaction conditions (Fig. 1).

Derouane *et al.* and others have studied the conversion of methanol and ethanol over H-ZSM-5 zeolite at different temperatures.[62–65] At low temperatures (150–200 °C), diethyl ether is the dominant species formed, whereas higher temperatures (200–300 °C) lead to the formation of ethylene instead. At temperatures above 250 °C, higher hydrocarbons form and at temperatures above 300 °C the higher hydrocarbons constitute the majority of the product composition (Fig. 1). At temperatures above 350 °C, the product composition resembles that seen for methanol, where a large fraction of the hydrocarbons is aromatic species. The most notable difference is that ethylated aromatics are formed, rather than the methylated aromatics seen in the MTG reaction.

Diethyl ether is a diesel fuel with excellent cold-start properties and the ability to reduce NO_x emissions in the exhaust gas from diesel engines and has the potential to be an important bio-fuel in the future.[66] Diethyl ether formation is catalyzed by both Brønsted and Lewis acidic sites and even weakly acidic sites have been demonstrated to be effective catalysts for the formation of diethyl ether.[62,65]

Ethylene is the most important chemical produced, with an annual production exceeding 100 million tons. Currently, ethylene is produced from petroleum and natural gas, either by steam cracking of naphtha or from ethane dehydrogenation. Ethylene can also be obtained from ethanol by dehydration, and commercial scale production of bio-ethylene began in 2009 in

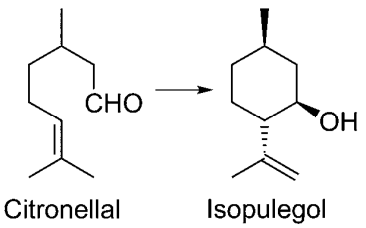

Scheme 7

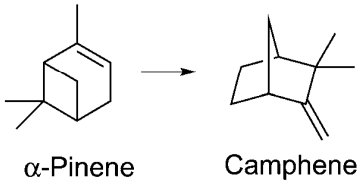

Scheme 8

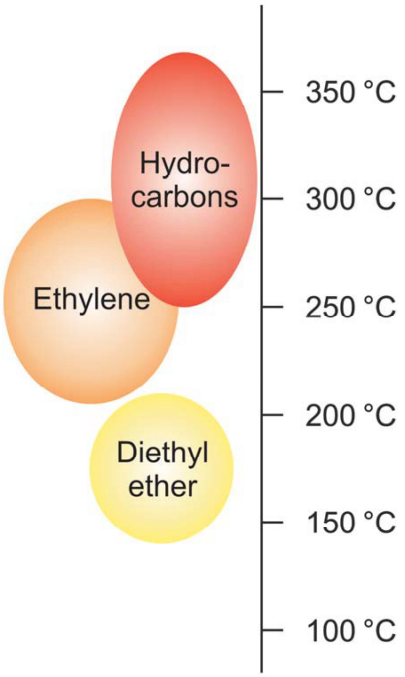

Fig. 1 Product selectivity at various temperatures for the conversion of ethanol over H-ZSM-5.

Brazil.[67] Ethylene can be obtained in high selectivity over H-ZSM5 zeolite catalysts at temperatures in the range of 250–300 °C. As is the case for many zeolite catalyzed processes, catalyst deactivation due to coke formation eventually occurs and the catalyst has to be calcined in order to regenerate its activity. Hierarchical zeolites, such as nanocrystalline H-ZSM-5, exhibit significantly improved lifetimes compared to conventional H-ZSM-5 for ethylene production at 240 °C. Thus, a lifetime in the order of 500 hours has been reported for nanocrystalline H-ZSM-5, compared to a lifetime of 120 hours for conventional microcrystalline H-ZSM-5.[68] The presence of water in the feed has been found to moderate the strongly acidic sites and enhance the catalyst activity and selectivity towards ethylene.[69] Furthermore, water often has a diminishing effect on the rate of coke formation and can thus be an instrument to improve the catalyst lifetime. The use of aqueous rather than anhydrous ethanol will reduce the feed cost. However, ethylene production will likely only be viable in countries such as Brazil, where a large source of cheap ethanol is available.[70]

Conversion of ethanol to gasoline has been studied in continuation of the findings of the MTG process.[71] The ETG process leads to a hydrocarbon product similar to that obtained in the MTG reaction, consisting primarily of monocyclic aromatics in the C_7–C_{10} range together with C_{5+} alkanes, which can be used directly as gasoline. According to the hydrocarbon pool theory the cavities of the zeolites host cyclic organic species from which the gasoline products originate through alkylation and cracking reactions.[71] Analysis of the organic species present in spent H-ZSM-5 zeolites has been carried out by dissolution of the zeolite crystal in hydrofluoric acid followed by extraction and GC analysis. This analysis shows that they consist of both ethylated and methylated aromatics. This is slightly different from the MTG reaction, in which only methylated aromatics, such as hexamethylbenzene, are present in the micropores.[71–73] The importance of the zeolite pore architecture has been investigated.[69] Zeolites having large pores (FAU and BEA) undergo a rapid deactivation of the Brønsted acidic sites, resulting in very low C_{3+} activity. In comparison, H-ZSM-5 with its smaller pores exhibits a comparable slow deactivation, analogous with what is observed in the MTG process. However, deactivation on H-ZSM-5 is more pronounced for ETG relative to MTG.[71] The deposited coke consists of polyaromatics and is more condensed on large pore zeolites than on H-ZSM-5.[74] Using ion exchanged zeolites can also change the lifetime and product selectivity. In a recent study the yield of C_{5+} products was found to increase when 0.3–0.5 wt% Fe was exchanged into the H-ZSM-5 zeolite.[75]

Conversion of higher alcohols such as butanol or propanol to gasoline can be achieved using a H-ZSM-5 zeolite. The production of gasoline from these higher alcohols is easier than from methanol or ethanol, since only mildly acidic sites are needed. Even after the strongly acidic sites have deactivated, production of highly branched C_6–C_9 olefins from 1-propanol takes place without the formation of aromatics.[76] These olefins can be hydrogenated into high-octane gasoline. Co-feeding methanol with butanol has also been shown to have a beneficial effect on the production of gasoline from methanol, allowing lower reaction temperatures to be used.[77] This increased activity for methanol conversion in the presence of butanol could be an effect of butanol being able to maintain the carbon-pool more effectively at lower temperatures than methanol.

Outlook

The discovery of zeolites has improved the global energy supply tremendously, allowing a higher gasoline production from oil than what was previously possible. Zeolites are today an integral part of any oil refinery and although zeolites initially emerged as catalysts for the conversion of petroleum, they are likely to play an important role in future bio-refineries as well. No matter how bio-refineries will be based, zeolites will have a role to play. Zeolites can be used for the production of gasoline from methanol (gasification), ethanol (fermentation) and oxygenates (pyrolysis), thereby covering the most likely bio-refineries. Zeolites can also be used for the production of olefins, either from methanol, in the MTO process, or by dehydration of ethanol, propanol and butanol. Finally, zeolites could replace, or supplement, biochemical processes in some cases, *e.g.* for the production of lactates from carbohydrates.

Gasoline production from pyrolysis oil is cost-attractive since this does not require a gasifier or a fermentation and distillation facility, which is the case for the gasification and fermentation based scenarios. However, the serious coking issues described illustrate that this is very difficult to realize. The fundamental problem is that too little hydrogen is available in pyrolysis oil, which results in the deposition of coke on the catalyst, rather than the formation of hydrocarbons. It would be a major breakthrough within zeolite catalysis if the fate of oxygen in the pyrolysis oil could be controlled to a greater extent. If oxygen was expelled primarily as CO_2 rather than water, this would result in a higher hydrogen content of the feed and reduce the

coking significantly. This could improve the productivity of gasoline from pyrolysis oil and improve the catalyst life-time.

Other advances within zeolite catalysis are likely to emerge from new zeotype materials such as stannosilicates (Sn-β) and titanosilicates (TS-1, Ti-β) which have already been demonstrated to be highly active and selective catalysts for the conversion of carbohydrates. These materials have very different catalytic capabilities than conventional aluminosilicate zeolites and seem more compatible with the fragile nature of carbohydrates. These materials have the potential to be broadly applied within biomass conversion in the future.

Acknowledgements

The Catalysis for Sustainable Energy initiative is funded by the Danish Ministry of Science, Technology and Innovation.

References

1 A. A. Kaeding, C. Chu, L. B. Young, B. Weinstein and S. A. Butter, *J. Catal.*, 1981, **67**, 159–174.
2 G. Bellussi, G. Pazzuconi, C. Perego, G. Girotti and G. Terzoni, *J. Catal.*, 1995, **157**, 227–234.
3 A. Corma, *Chem. Rev.*, 1997, **97**, 2373–2419.
4 A. Corma, *Chem. Rev.*, 1995, **95**, 559–614.
5 *Handbook of Heterogeneous Catalysis*, ed. G. Ertl, H. Knözinger, F. Schüth and J. Weitkamp, Wiley-VCH, 2nd edn, 2008.
6 C. H. Christensen, J. Rass-Hansen, C. C. Marsden, E. Taarning and K. Egeblad, *ChemSusChem*, 2008, **1**(4), 283–289.
7 R. L. Howard, E. Abotsi, E. L. Jansen van Rensburg and S. Howard, *Afr. J. Biotechnol.*, 2003, **2**(12), 602–619.
8 M. Stöcker, *Microporous Mesoporous Mater.*, 1999, **29**(1–2), 3–48.
9 A. V. Bridgwater, *Appl. Catal., A*, 1994, **116**, 5–47.
10 A. V. Bridgwater and G. V. C. Peacocke, *Renewable Sustainable Energy Rev.*, 2000, **4**, 1–73.
11 A. V. Bridgwater, *Chem. Eng. J.*, 2003, **91**, 87–102.
12 D. C. Elliott and G. F. Schiefelbein, *Prepr. Pap. - Am. Chem. Soc., Div. Fuel Chem.*, 1989, **34**, 1160.
13 H. Chum, J. Diebold, J. Scahill, D. Johnson, S. Black, H. Schroeder and R. E. Kriebich, *ACS Symp. Ser.*, 1989, **385**, 135–151.
14 S. Czernik and A. V. Bridgwater, *Energy Fuels*, 2004, **18**, 590–598.
15 C. Branka, P. Giudicanni and C. D. Blasi, *Ind. Eng. Chem. Res.*, 2009, **42**, 3190–3202.
16 M. E. Boucher, A. Chaala and C. Roy, *Biomass Bioenergy*, 2000, **19**, 337–350.
17 M. E. Boucher, A. Chaala, H. Pakdel and C. Roy, *Biomass Bioenergy*, 2000, **19**, 351–361.
18 N. Y. Chen, T. F. Degnan, Jr and L. R. Koenig, *CHEMTECH*, 1986, **16**, 506–511.
19 J. Diebold and J. Scahill, *ACS Symp. Ser.*, 1988, **376**, 297–307.
20 R. K. Sharma and N. N. Bakhshi, *Energy Fuels*, 1993, **7**, 306–314.
21 J. D. Adjaye, S. P. R. Katikaneni and N. N. Bakhshi, *Fuel Process. Technol.*, 1996, **48**, 115–143.
22 L. H. Dao, M. Haniff, A. Houle and D. Lamothe, *ACS Symp. Ser.*, 1988, **376**, 308–316.
23 A. G. Gayubo, A. T. Aguayo, A. Atutxa, R. Prieto and J. Bilbao, *Energy Fuels*, 2004, **18**, 1640–1647.
24 A. G. Gayubo, A. T. Aguayo, A. Atutxa, R. Prieto and J. Bilbao, *Ind. Eng. Chem. Res.*, 2004, **43**, 2610–2618.
25 A. G. Gayubo, A. T. Aguayo, A. Atutxa, R. Prieto and J. Bilbao, *Ind. Eng. Chem. Res.*, 2004, **43**, 2619–2626.
26 M. C. Samolada, W. Baldauf and I. A. Vasalos, *Fuel*, 1998, **77**, 1667–1675.
27 A. A. Lappas, S. Bezergianni and I. A. Vasalos, *Catal. Today*, 2009, **145**, 55–62.
28 M. C. Samolada, A. Papafotica and I. A. Vasalos, *Energy Fuels*, 2000, **14**, 1161–1167.
29 E. F. Iliopolou, E. V. Antonakou, S. A. Karakoulia, I. A. Vasalos, A. A. Lappas and K. S. Trian, *Chem. Eng. J.*, 2007, **134**, 51–57.
30 E. Antonakou, A. Lappas, M. H. Nielsen, A. Bouzga and M. Stöcker, *Fuel*, 2006, **85**, 2202–2212.
31 K. S. Triantafyllidis, E. F. Iliopoulou, E. V. Antonakou, A. A. Lappas, H. Wang and T. J. Pinnavaia, *Microporous Mesoporous Mater.*, 2007, **99**, 132–139.
32 T. R. Carson, T. P. Vispute and G. W. Huber, *ChemSusChem*, 2008, **1**, 397–400.
33 T. R. Carlson, G. A. Tompsett, W. C. Conner and G. W. Huber, *Top. Catal.*, 2009, **52**, 241–252.
34 D. C. Elliot, E. G. Baker, J. Piskorz, D. S. Scott and Y. Solantausta, *Energy Fuels*, 1988, **2**, 234–235.
35 D. C. Elliot and A. Oasmaa, *Energy Fuels*, 1991, **5**, 102–109.
36 E. Taarning, S. Shunmugavel, M. S. Holm, J. Xiong, R. M. West and C. H. Christensen, *ChemSusChem*, 2009, **7**, 625–627.
37 Y. Hayashi and Y. Sasaki, *Chem. Commun.*, 2005, 2716–2718.
38 M. S. Holm, S. Saravanamurugan and E. Taarning, *Science*, 2010, **328**, 602–605.
39 R. M. West, M. S. Holm, S. Shunmugavel, J. Xiong, Z. Beversdorf, E. Taarning and C. H. Christensen, *J. Catal.*, 2010, **269**, 122–130.
40 A. Corma, M. E. Domine, L. Nemeth and S. Valencia, *J. Am. Chem. Soc.*, 2002, **124**, 3194–3195.
41 K. P. F. Jannsen, J. S. Paul, B. F. Sels and P. A. Jacobs, *Stud. Surf. Sci. Catal.*, 2007, **170**(B), 1222–1227.
42 M. Moliner, Y. Román-Leshkov and M. E. Davis, *Proc. Natl. Acad. Sci. U. S. A.*, 2010, **107**, 6164–6168.
43 F. W. Lichtenthaler, Carbohydrates, in *Ullmann's Encyclopedia of Industrial Chemistry*, John Wiley & Sons, Inc., 2003.
44 A. Corma, S. Iborra and A. Velty, *Chem. Rev.*, 2007, **107**, 2411–2502.
45 B. Kamm, *Angew. Chem., Int. Ed.*, 2007, **46**, 5056–5058.
46 Y. Román-Leshkov, C. J. Barret, Z. Y. Liu and J. A. Dumesic, *Nature*, 2007, **447**, 982–986.
47 C. J. Barret, J. N. Chheda, G. W. Huber and J. A. Dumesic, *Appl. Catal., B*, 2006, **66**, 111–118.
48 G. W. Huber, J. N. Chheda, C. J. Barret and J. A. Dumesic, *Science*, 2005, **308**, 1446–1450.
49 P. Rivalier, J. Duhamet, C. Moreau and R. Durand, *Catal. Today*, 1995, **24**, 165 171.
50 C. Moreau, R. Durand, S. Razigade, J. Duhamet, P. Faugeras, P. Rivalier, P. Ros and G. Avignon, *Appl. Catal., A*, 1996, **145**(14), 211–224.
51 J. Lewkowski, *ARKIVOC*, 2001, 17–54.
52 K. Shimizu, R. Uozumi and A. Satsuma, *Catal. Commun.*, 2009, **10**, 1849–1853.
53 C.-H. Zhou, J. N. Beltrami, Y.-X. Fan and G. Q. Lu, *Chem. Soc. Rev.*, 2008, **37**(3), 527–549.
54 A. Behr, J. Eitling, K. Irawadi, J. Leschinski and F. Lindner, *Green Chem.*, 2008, **10**, 13–30.
55 F. Jerôme, Y. Pouilloux and J. Barrault, *ChemSusChem*, 2008, **1**, 586–613.
56 B. Kartryniok, S. Paul, M. Capron and F. Dumeignil, *ChemSusChem*, 2009, **2**, 719–730.
57 A. Corma, G. W. Huber, L. Sauvanaud and P. O'Conner, *J. Catal.*, 2008, **257**, 163–171.
58 E. Yoda and A. Ootawa, *Appl. Catal., A*, 2009, **360**, 66–70.
59 M. Eggersdorfer, Terpenes, in*Ullmann's Encyclopedia of Industrial Chemistry*, John Wiley & Sons, Inc., 2000.
60 A. Corma and M. Renz, *Chem. Commun.*, 2004, 550–551.
61 C. M. López, et al., *Catal. Lett.*, 1999, **62**, 221–226.
62 J. Deng, G. Zhang, S. Dong, H. Pan and H. Wang, *Appl. Catal.*, 1988, **41**, 13–22.
63 R. Barthos, A. Széchenyi and F. Solymosi, *J. Phys. Chem. B*, 2006, **110**, 21816–21825.
64 E. G. Derouane, J. B. Nagy, P. Dejaifve, J. H. C. van Hoof, B. P. Spekman, J. C. Védrine and C. Naccache, *J. Catal.*, 1978, **53**, 40–55.
65 I. Takahara, M. Saito, M. Inaba and K. Murata, *Catal. Lett.*, 2005, **105**, 249–252.
66 K. Kuzuoka and K. Junichi, *US Pat.*, 20080282998, 2008.
67 http://www.rsc.org/chemistryworld/News/2008/March/31030801.asp.
68 J. Bi, X. Guo, M. Liu and X. Wang, *Catal. Today*, 2010, **149**, 143–147.
69 C. B. Phillips and R. Datta, *Ind. Eng. Chem. Res.*, 1997, **36**, 4466–4475.
70 K. Weissermel and H. J. Arpe, *Industrial Organic Chemistry*, Wiley, 2003, p. 63.
71 R. Johansson, S. L. Hruby, J. Rass-Hansen and C. H. Christensen, *Catal. Lett.*, 2009, **127**, 1–6.

72 M. Bjørgen, S. Svelle, F. Joensen, J. Nerlov, S. Kolboe, F. Bonino, L. Palumbo, S. Bordiga and U. Olsbye, *J. Catal.*, 2007, **249**, 195–207.
73 M. Bjørgen, F. Joensen, K.-P. Lillerud, U. Olsbye and S. Svelle, *Catal. Today*, 2009, **142**, 90–97.
74 F. F. Madeira, N. S. Gnep, P. Magnoux, S. Maury and N. Cadran, *Appl. Catal., A*, 2009, **367**, 39–46.
75 V. Calsavara, M. L. Baesso and N. R. C. Fernandes-Machado, *Fuel*, 2008, **87**, 1628–1636.
76 U. V. Mentzel, S. Shunmugavel, S. L. Hruby, C. H. Christensen and M. S. Holm, *J. Am. Chem. Soc.*, 2009, **131**(46), 17009–17013.
77 F. Joensen, P. E. H. Nielsen, N. C. Schiødt, T. V. W. Janssens and B. Voss, WO 2008071291, 2008.

CHEMSUSCHEM

DOI: 10.1002/cssc.200900215

C Factors Pinpoint Resource Utilization in Chemical Industrial Processes

Bodil Voss, Simon Ivar Andersen, Esben Taarning,* and Claus Hviid Christensen[a]

This Full Paper illustrates the use of the C factor (CO_2/product mass ratio) as a parameter to evaluate the CO_2-burden of a product. The C factor contains information of the total amount of CO_2 emitted in order to produce a product, and thus enables a direct comparison of different processes from a CO_2 aspect. We illustrate how this simple concept can be used to evaluate different resource types and processes. The C factors for different chemicals such as methanol, synfuels, and acetic acid are calculated for oil, coal, natural gas, and biomass. Based on these calculations, the combination of biomass and natural gas is an attractive alternative to coal, leading to products that have significantly lower C factors.

Introduction

Biomass is becoming an increasingly significant resource for the production of transportation fuels and is projected to compose more than 5% of the global fuel supply within a decade.[1] The interest in utilizing biomass comes primarily from the desire to minimize CO_2 emissions associated with the combustion of fossil fuels as well as the wish to diminish a national dependence on foreign oil. Currently, ethanol produced by fermentation of glucose and sucrose accounts for the majority of the fuel made from biomass. Processes for making synfuels, that is, fuels made from other feedstocks than oil but with the main characteristics of conventional gasoline and diesel fuels, have been known for many decades. However, lately new processes for making synfuels from biomass have emerged.[2] In order to compare the different fuel types, the "well-to-wheel" concept (WtW) has been introduced.[3] The mileage versus the CO_2 emissions for various alternative fuels is compared in order to benchmark these against oil-based fuel types. The more holistic life cycle assessment (LCA) concept has been applied to many products, including chemicals, and is used for the evaluation of a particular product on a "cradle-to-grave" basis.[4] Thus, a full LCA of a product will contain information of the environmental impact that is caused by the production, distribution, existence, and decomposition of a product. LCA methodologies have in some cases been adapted to analyze only a shorter timespan of a product, for example the "gate-to-gate" timespan.[5]

Today, we utilize about 5% of our oil recovery for the production of chemicals. The utilization of biomass as an alternative resource for the production of chemicals offers new options, because the biomass feedstock features well-defined chemical functionalities, warranting a shorter process route to some end-products as compared to conventional fossil feedstocks. Many new chemicals and processes for the production of chemicals originating from biomass have been developed in recent years.[6] Meanwhile, biomass is also being utilized for the production of biofuels on a vast scale and the most optimal use of biomass, and resources in general, from a CO_2 perspective is easily obscured by the many options available. To gain insight into the optimal resource use a less detailed and faster evaluation method than the LCA concept is needed.

We have recently introduced the "C factor" (CO_2/product mass ratio) as a measure for the CO_2 burden associated with a particular product.[7] The C factor is simply the overall mass-specific CO_2 emission associated with the manufacture of a particular product, and any product can in principle be labeled with a C factor. The C factor is less holistic than the full LCA, taking into account only the CO_2-emissions involved in the "cradle-to-gate" life of a product. The further "gate-to-grave" contributions of a product will of course be equal for similar chemical compounds and independent of how the compound was obtained. Thus, the C factor can be used as a direct indicator to assess the climate impact of the production of a chemical compound. In an evaluation of different reactions and, hence, process routes as well as layouts to a given chemical compound with a relatively large CO_2 impact in the fate after the "gate," the application of a more elaborate "cradle-to-cradle"-type LCA may result in a somewhat obscured result. In the case of a small process C factor this will be completely overshadowed by the large downstream impact of the chemical plant. Global bulk chemicals produced in large quantities may have small C factors (e.g., acetic acid production) but even the selection amongst different routes may have a large impact on the total CO_2 burden on the atmosphere. Unlike the monetary price, the C factor is not affected by fluctuations in resource prices and it can, in view of the future strategies for reducing our global CO_2 emissions, be a useful gauge for the overall viability of a particular process and product. As future production costs will most likely include high CO_2 taxes, a

[a] B. Voss, Dr. S. I. Andersen, Dr. E. Taarning, Prof. C. H. Christensen
Haldor Topsøe A/S
Nymøllevej 55, 2800 Kgs. Lyngby (Denmark)
Fax: (+45) 4527 2999
E-mail: esta@topsoe.dk

direct measure for the CO_2 emissions associated with a product or a process will be a useful assessment tool.

We exemplify the use of the C factor for the production of different bulk scale chemicals. By using this tool we show that comparison between various resources becomes simple. We also illustrate that biomass in some cases is the best resource to use for the production of chemicals in C factor terms. Figure 1 depicts the combination of various resource feedstocks to platform chemicals/compositions, and the further conversion to the four products we have examined.

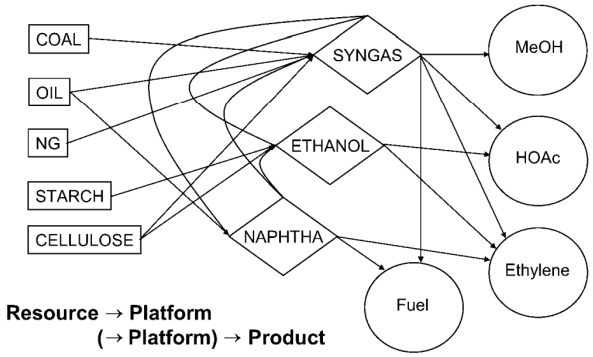

Figure 1. Overview of combinations of resources, platforms, and products investigated in this work. The conversion of source into products may go via one or more platforms.

The Climate Factor

C factor

The C factor provides information on the total mass of CO_2 emitted to the atmosphere to produce one kilogram of a particular end product using a well-defined process. The C factor depends on the emission contributions of all the individual steps involved in producing a product, such as resource extraction, transportation, and pretreatment as well as the contribution from converting the resource to the product using a specific process. It is not our aim to make a full description, that is, specify every single emission of CO_2 that may occur from the various utilities, for example small consumers of electricity, and/or the outside battery limit expenditures of energy, but rather to account for the main sources of CO_2 emissions.

As illustrated above, the conversion of a resource into a chemical may go via one or more platform chemicals or compositions, common for more end-products. For reasons of clarity, it may be useful to keep a distinction between the resource-related C factor (C_{res} factor), and the overall C factor. Furthermore, where a platform chemical/composition is involved, this may favorably be extracted for the convenience of producing C factors for other end products. Note that the unit of the C factor is per mass of the resource, platform, or end product in question.

Where useful, a process-related C factor, C_{proc} factor, reflecting the CO_2 emissions for heating, product loss, and other aspects of the conversion steps to the end product may also be extracted, as a mere balance between the overall C factor and the C_{res} factor, recalculated to the end product basis. The C factor obviously depends on the efficiency of the process, because a product loss will necessitate the use of a larger amount of resources to start with and thereby increase the C factor. Furthermore, both the flue gas content of CO_2 coming from the required energy input to the process and the CO_2 removed through the adjustment of the conversion media are also sources of CO_2 emission. The CO_2 emitted during the transport of a product from the production site to the end user is not considered in this paper, as we will focus on resource conversion. Moreover, this number may not differ significantly between products produced from fossil resources and products produced from biorenewables.

The resource-related C factor value is calculated as the CO_2/resource mass ratio for the resource at the site of the plant when it is ready to be converted. In effect the C_{res} factor may be regarded as a zeroth-platform C factor. This figure thus provides information on the CO_2 emissions required to extract, transport, and pretreat the resource prior to any processing. Naturally it will vary from region to region and will be very different for different resource types. For coal, the C_{res} factor primarily reflects the emissions for mining, transportation, and crushing, whereas for biomass it depends on agricultural emissions, transportation, and pretreatment. This figure also includes the CO_2 uptake of the biomass, which acts as a "CO_2 subsidy" for this resource type. The C_{res} factor value chosen may have a big effect on the resulting overall C factor, depending on the process in which the resource is converted.

In the following, an overview is given of the three major resources: biomass, petroleum and natural gas, and coal.

Biomass

Biomass in general comprises all biorelated material, whereas the utilization requires that we divide it into different classes. Gasification is very versatile and can be based on all types of carbon-containing materials including wood, municipal waste, and manure. For the generation of platform chemicals, for example ethanol, by fermentation the presence of carbohydrate structures, in particular sugars, as a source of nutrition is required. This highly limits the present species of crops available for efficient ethanol production by fermentation. However, with improvements of the biocatalytic processes for breaking down cellulose and hemicellulose, the availability of resources may expand significantly. We have designated the sugar/starch biomass as first-generation biomass, and have termed the latter, primarily containing cellulose and hemicellulose, second-generation biomass.

The exploitation of biomass resources involves numerous production steps, and the efficiency is highly dependent on the source material as well as geographic conditions and regional logistics. The processes involve farming, harvesting, transport to centralized process units, processing, and transport to consumers. In case chemicals are made from an intermediate platform chemical, for example ethanol, it may further be transported to an even more centralized processing plant if

CHEMSUSCHEM

economy of scale is of importance. In terms of the CO_2 impact, the cultivation of forest and grasslands may, as pointed out in various reports, have a direct negative impact on the environment owing to the liberation of vast amounts of CO_2 during such farming processes. Economy of scale may also be affected as, for example, the gathering of biomass for fermentation or gasification is limited by distance. Most reports mention a radius of 50 km as the average zone of potential gathering material. At higher distances, the cost of transportation may become a significant burden to the viability of the resources because of the crops' high water contents. The processing of different crops in the most efficient manner will become an issue in a future biobased scenario. In a EU report,[3] it was concluded that the large variations in energy consumption in the production of ethanol from various crops (wheat, wheat straw, sugar beets, sugar cane, and others) results in situations where the use of biomass especially for fuel purposes is more justified by the savings on fossil fuels than on an actually more efficient process, even in terms of CO_2 impact. The actual ratio of energy contained in the product lower heating value (LHV) to energy expended, the so-called net energy balance (NEB; MJ_{out}/MJ_{in}), may reach about 0.6 for the conversion of sugar beet into ethanol.[8] In comparison, for the conversion of conventional fossil feedstocks into fuel, this ratio is approximately 6. Cellulosic (and lignocellulosic) biomass comprises straws, stem fibres, stover, saw dust, and other materials that may be considered waste material from a primary production, as well as willow which is produced for the dedicated supply as a cellulosic feedstock. In this study we have not put a farming and transport CO_2 burden on the waste biomass category. The resource factor for the cellulosic biomass is accordingly calculated as the original amount of CO_2 sequestered from the atmosphere per kilogram of cellulosic raw material.

In spite of a lower NEB foreseen for biomass-based ethanol compared to crude oil distillates, the application of biomass for the production of chemicals may have certain advantages. As the biomass-based feed into the sequence of conversion processes to product is often at a higher level of chemical functionality relative to fossil feeds, the production route to a chemical may be much shorter.

Petroleum and natural gas

The energy consumption and the CO_2 burden related to recovering, treating, and transporting petroleum and natural gas are dependent on a number of factors, such as reservoir geology, applications of secondary production methods (e.g., water flooding, gas injection, and others), oil viscosity and density, treatment of gas before transportation, and of course the transportation distance. When gas injection involves CO_2, this sequestration should be taken into account in the resource C factor, but as the use of this production technology is currently applied only in very few places, we may overall consider this a special case that has little impact on the overall CO_2 emissions from the petroleum industry. The CO_2 emissions from oil and gas production are related to surplus gas flaring, compressor/pump workings, and other factors. On off-shore production platforms most of the energy required is generated from natural gas turbines and, hence, on the basis of regional production numbers, one may estimate the CO_2 release related to this gas consumption. However, as gas and oil are often co-produced, one should not discern between CO_2 related to gas and to oil as such. In such cases, we will apply a number based on the total mass of hydrocarbon products. The numbers reported by the Danish Energy Authorities indicate a CO_2 resource C factor of 0.09 kg(CO_2) kg(oil or gas)$^{-1}$ for the Danish North Sea production region.[9] This estimate of the C resource for oil and gas may seem conservative taking into account the more complex nature of an off-shore operation as those performed in Denmark, Norway, the Gulf of Mexico, and other regions. However, on-shore wells also apply energy-demanding water flooding methods (injection of water to recover oil). A recent report on water consumption in oil production cites that 74.7% of on-shore operations in the USA are currently under secondary recovery schemes (water flooding).[10] In other words, these operations require a large energy input as the volume basis of injection water to oil is often as high as 5. The C factor of 0.09 kg(CO_2) kg(oil or gas)$^{-1}$ is thus justified as a figure that is not only conservative but also indicates the direction that the petroleum recovery industry is taking in terms of energy spent/mass of oil recovered.

On the other hand, this is highly dependent on the nature of the reservoir, for example, the energy and CO_2 burden of producing syncrude in Canada from oil sands is much higher. Our estimation does not include the heteroatom content (NSO) which, especially for heavy oil, may be as much as 15% wt.[11]

The production of natural gas fields is assumed to have an energy consumption of about 2% of the total gas, and the consumption due to the common transport over very long distances may be in the range 6–10% (Well-to-Wheel analysis, EU report[12]).

When not converted locally as a feedstock for chemicals, natural gas production alone will have a similar C_{res} factor as oil and gas production. In our case it was estimated to be 0.08 kg(CO_2) kg(natural gas (NG))$^{-1}$.

Coal

The C_{res} factor for coal primarily depends on the energy required for coal extraction, transportation, and crushing. The extraction energy for coal has been reported in terms of energy return-on-investment (EROI) as being between 1:30 and 1:75.[13,14] Thus, in order to extract 1 tonne of coal, an energy equivalent to 13–33 kg of coal is required. For the calculations in this paper, it is assumed that an energy equivalent of 20 kg of coal (281 MJ) is required to mine 1 tonne of coal. The contribution from transportation depends on the distance from the mining site to the plant and the mode of transportation. In this paper the coal is assumed to be transported 500 km by train from the mouth of the mine to the plant. The energy intensity for coal transportation by train has been taken as 0.23 MJ t^{-1} km^{-1} to give a total energy contribution of 115 MJ t^{-1}.[14] Finally, the energy intensity for coal crushing is esti-

mated to be 10 MJ t^{-1}.[15] The total energy contributions add up to 406 MJ t^{-1} of coal. This energy is assumed to be supplied in the form of natural gas. Based on these assumptions the C_{res} factor for coal is 0.02 kg(CO_2) kg(coal)$^{-1}$.

In Table 1 we have compiled the magnitudes of C_{res} factors for the different resources considered here, based on literature surveys.

Table 1. C_{res} factors for various resources.

Resource type	kg(CO_2) kg(resource)$^{-1}$	Refs.
Crude oil[a]	0.09	[9]
Natural gas	0.08	[9]
Coal	0.02	[13–15]
Biomass	−1.89	[16]

[a] Recovered offshore using water injection.

C Factor Calculation

To provide fast but reliable C factor numbers for the platform chemicals and the overall C factors of end products for various process routes, a starting point has been taken in with the relevant C_{res} factor (as described above). This is combined with the relevant process steps with their respective process yields and energy uses to achieve a platform or end-product chemical. Where the end-product is achieved via a platform chemical/composition the end-product C factor has been calculated by chaining the platform calculations to describe overall processes, that is, the C factor of a platform chemical may be regarded as the C_{res} factor for the subsequent conversion step. Figure 2 shows this principle and examples of the emission of CO_2 from different generic steps.

Some of the process steps are well-described by full mass balances, whereas others are described by yield and energy inputs at best. When the full mass balance is known, the C factor may be easily obtained by reading the mass rate numbers of the CO_2 emitted from the combined process and dividing these by the production rate. In most cases full mass balances are not easily available. CO_2 is generally emitted from fuel, which can be unconverted feed (yield issues). From the process step CO_2 is emitted either through conversion or, in the case of gasification, the adjustment of the so-called module by removal of CO_2 (adjustment issues). In the following this is covered in more detail, combining it into equations readily applicable for other cases. Examples are given on different approaches and effects of the degree of detailed knowledge of a process.

In case several desirable products are formed in a single process, a shared C factor for the desirable products can be calculated by treating the products as one type. The fraction of carbon not converted into a desirable product is considered as a fuel or a waste stream that will contribute to the CO_2 emissions. If the fuel requirement for the process is equal or less than the required energy, the net energy input is zero. Energy required for the process step is calculated based on LHVs of the fuel applied. In case a process step uses oxygen, the consumption of power in the plant is added as well, using a conversion factor of 11.3 MJ kWh^{-1}. In most cases, the energy input has been converted to the amount of CO_2 emitted from the combustion of 100% methane as fuel with a carbon content of 1 kmol kmol^{-1} natural gas, except when the energy input obviously comes from another fuel source.

Accordingly, the most basic C factor (kg(CO_2) kg(product)$^{-1}$) for a product produced through a single conversion step is calculated according to Equation (1):

$$\text{C factor} = \frac{C_{res}}{\text{yield} \cdot F} + \frac{1 - \text{yield}}{\text{yield} \cdot F} \cdot CO_2(\text{equiv. feed}) + CO_2(\text{adj}) + \frac{E - E_{credit}}{LHV} \cdot CO_2(\text{equiv. fuel}) \quad (1)$$

where "yield" is the fraction, on a C basis, that is converted into the desired product; F is the theoretical amount of product produced per amount of feed (kg product/kg feed); CO_2(adj) is the CO_2 adjusted in the special case of a CO_2 removal step in, for example, a gasification process unit (kg(CO_2) kg(product)$^{-1}$; see below); E is the external energy input necessary per kilogram product (MJ/kg product); E_{credit} is the export of energy per kilogram of product (MJ kg(product)$^{-1}$); LHV is the lower heating value of the fuel (typically natural gas; MJ kg(fuel)$^{-1}$); and CO_2(equiv) is the amount of CO_2 emitted through the combustion of the feed or fuel, respectively, per its amount (kg(CO_2) kg(fuel)$^{-1}$).

E_{credit} expresses the credited energy rate of the fuel which would be required for producing the actual export energy form, for example, steam, electricity, or power. Therefore a corresponding efficiency correction must be made. The description of two steps rather than one is obtained by specifying the C factor calculated in the first step as the new C_{res} and applying the equation again for the second step. By means of the above principle, a number of routes to chemicals via various platforms have been investigated. Table 2 summarizes the conversion factor values applied in the present study.

In order to make the C factors from each conversion step comparable, that is, to compare their relative contribution to a final, overall C factor, the indi-

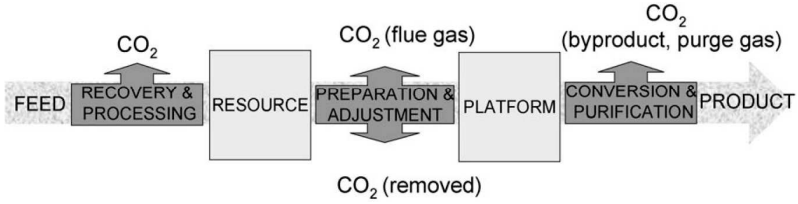

Figure 2. CO_2 is emitted in numerous steps from feed to product. In addition to the C factor describing the overall CO_2 emission, a C factor for each of the resources and platforms provides a detailed picture.

CHEMSUSCHEM

Table 2. Conversion factors used for calculating C factors.

Description	Conversion factor	Unit
Additional fuel source, NG LHV	35.8	$MJ\,Nm^{-3}$
Normal gas volume	22.414	$Nm^3\,kmol^{-1}$
NG C content	1	$kmol(C)\,kmol(NG)^{-1}$
Thermal efficiency@120 bar steam[a]	60	%
ASU energy consumption[b]	372	$kWh\,tonne(O_2)^{-1}$
Shaft power energy	11.3	$MJ\,kWh^{-1}$

[a] 1 bar = 10^5 Pa. [b] ASU: air separation unit.

vidual C factors of the resources or platforms must be compensated by the theoretical conversion factor *F* of the particular step:

$$C_{platform}\ \text{factor}(\text{endproduct}, \text{basis}) = \frac{C_{platform}\ \text{factor}(\text{platform}, \text{basis})}{F}\quad (\text{kg}(\text{product})\,\text{kg}(\text{resource})^{-1}) \tag{2}$$

In this way the loss of feed in a process step through a yield lower than 100% is attributed to the process step where the carbon is lost.

The process-related C factor, C_{proc} factor, may then be calculated as the balance between the overall C factor and the resource-related C factor recalculated as indicated above:

$$C_{proc}\ \text{factor} = \frac{\text{C factor} - C_{res}\ \text{factor}}{F}\quad (\text{kg}(\text{product})\,\text{kg}(\text{resource})^{-1}) \tag{3}$$

The pitfalls are that process steps that in reality are completely integrated are treated independently by the C factor method. For example, in the production of methanol from natural gas, the synthesis gas step, which provides the synthesis gas feed for the methanol synthesis, also provides heat and power to the methanol synthesis and purification unit by steam generation. At the same time the unconverted synthesis gas and byproduct streams from the methanol synthesis and purification units provide energy for the heat-consuming reforming process. Therefore, in cases where this is not accounted for in the C factor, this will come out less attractive (more CO_2 emitted per mass of product) compared to cases where the process integration and energy exports are included. It remains a challenge to keep things simple and still provide good C factors, and the inclusion of purge gas (fuel) and steam credits in the C factor method will require access to detailed information. Yet, the product yield of a process in combination with knowledge of the fuel abilities of the waste stream indicate whether extra external energy input is needed for the process step and this may, as shown in the example below, compensate for the lack of detailed knowledge.

How to calculate the C factor for a product

Example 1: Methanol synthesis from natural gas.

This example covers the calculation of the C factor using various degrees of detailed knowledge of the process. In the case of methanol production from natural gas, synthesis gas (syngas) is a platform chemical/composition. In large-scale methanol production, syngas is typically prepared by autothermal reforming (ATR). To make an efficient synthesis the so-called module, namely the molar ratio $M = (H_2 - CO_2)/(CO + CO_2)$ of the syngas is adjusted to a value just above 2, whilst at the same time the CO_2 level of the make-up gas to the methanol synthesis has to be low. A CO_2 removal process is typically placed in the synthesis gas preparation section for the proper adjustment of the syngas to obtain the desired module value. Figure 3 is a simplified process scheme for the production of methanol from natural gas.

As previously established, the C_{res} for pretreated natural gas equals 0.08 kg kg(NG)$^{-1}$, assuming 100% CH_4. From the mass balance on a process flow diagram of an ATR-based synthesis gas preparation, it is found that 1.9 kg syngas (syngas calculated as $H_2 + CO$ with an average mole mass of 32.04/3 = 10.68 kg kmol^{-1}) is produced per kilogram natural gas. Further the CO_2 emitted through the flue gas from a fired heater providing preheating and the CO_2 emitted from the CO_2 removal corresponds to 0.21 kg kg(syngas)$^{-1}$. The air separation unit supplying oxygen for the autothermal reformer provides 0.65 kg(O_2) kg(syngas)$^{-1}$. This oxygen demand needs to be converted into energy and therefore an additional CO_2 term. Accordingly the C factor for the preparation of synthesis gas (module = 2) from natural gas is outlined in Table 3.

If a full process flow diagram is available for the conversion of natural gas into methanol a C factor of 0.34 kg(CO_2) kg(methanol)$^{-1}$ can be obtained in the same manner. Apparently, there is a conflict here: Why is the C factor for methanol production lower than the C factor of its platform feed? The explanation to this is that in reality the methanol synthesis sec-

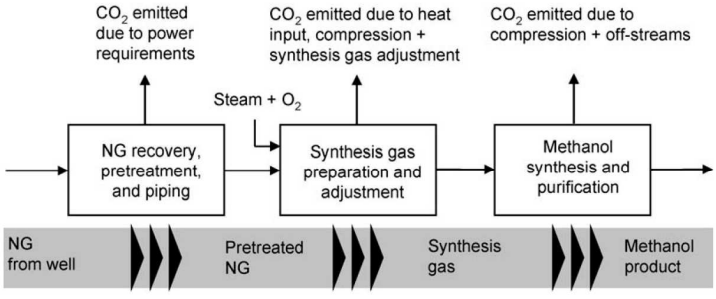

Figure 3. The conversion of natural gas (NG) to the product methanol goes via the resource platform 'pretreated natural gas' and the chemical composition platform 'synthesis gas'.

Table 3. C factor calculation for conversion of natural gas into syngas.

C factor	Contribution
C_{res}/F	0.08 [kg(CO_2) kg(NG)$^{-1}$]/1.9 [kg(syngas) kg(NG)$^{-1}$]
Fuel and adjustment	+0.21 [kg(CO_2) kg(syngas)$^{-1}$]
Energy oxygen plant	+0.65 [kg(O_2) kg(syngas)$^{-1}$]/1000 [kg t^{-1}] ·372 [kWh t(O_2)$^{-1}$] ·11.3 [MJ kWh^{-1}]/35.8 [MJ Nm^{-3}]/22.414 [Nm^3(NG) kmol(NG)$^{-1}$] ·1 [kmol(C) kmol(NG)$^{-1}$] ·44 [kg(CO_2) kmol(C)$^{-1}$]
Total	0.40 kg(CO_2) kg(syngas)$^{-1}$

tion generates carbon-poor fuel gas (which saves some of the natural gas fed to the synthesis gas preparation), and the synthesis gas preparation unit has an export of steam which could ideally be credited to its C factor with a more detailed C factor scope.

Another approach is taken when a process flow diagram for the methanol synthesis is not available. Then one will have to rely on yield and energy input only. It is well known that the carbon-efficiency of syngas conversion in a methanol synthesis is typically in the order 90–95% and a purification loss of 1% is foreseen. Overall, then the methanol yield is about 94% or 0.94. The unconverted feed (syngas) is easily combustible and the waste stream may to a large extent replace natural gas for fuel. It is also known that the methanol synthesis is generating heat, approximately balancing the heat input needed for product purification, and that the upstream conversion step generates steam for the power for compression. Therefore the estimated external heat input is set equal to zero (Figure 4). An estimate of a C factor will then be made according to the following calculation:

$$\text{Cfactor} = \frac{0.40(\text{kg}(CO_2)\,\text{kg}(\text{syngas})^{-1})}{0.94 \cdot 1(\text{kg}(\text{methanol})\,\text{kg}(\text{syngas})^{-1})} = 0.43\ \text{kg}(CO_2)\,\text{kg}(\text{methanol})^{-1} \quad (4)$$

The numbers 0.34 and 0.43 kg(CO_2) kg(methanol)$^{-1}$ result from a relatively detailed estimate and a less-detailed estimate of the C factor, respectively. Therefore a certain margin should be allowed for when comparing C factors.

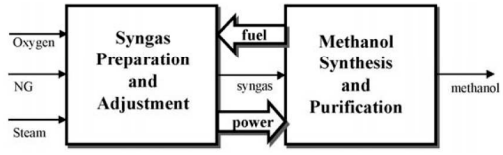

Figure 4. In integrated processes such as methanol production from natural gas there is an exchange of utilities across the process steps, influencing the C factor estimate.

Example 2: Ethanol from carbohydrate and cellulosic biomass by fermentation

This example uses the net energy balance (NEB) value often reported in, for example well-to-wheel reports, to generate the energy demand and, hence, the CO_2 emission from a process.

As a special case, the production of ethanol by fermentation takes numerous steps which have been studied in detail already. We start by assuming that roughly two-thirds of the carbon extracted from the atmosphere ends up as a useful product, for example as ethanol, and that one-third of the carbon is reemitted as CO_2 during the fermentation process. Then, by converting the NEB value from the literature into an external energy input required, a platform or end-product C factor for ethanol may be calculated.

As discussed earlier the NEB for ethanol production varies to a large extent. In many processes, the main energy source available may currently be the use of natural gas, exempting ethanol production from sugar cane where a small energy surplus production is observed. In the latter case the bagasse is used as an energy source for fermentation and distillation, and the production considered self-sustained in terms of energy, not including farming and harvesting. When the latter two are included in the NEB calculation this may increase to between 1.8 and 2.4 (MJ MJ^{-1}) dependent on the source. Dias de Oliveira et al.[17] suggested a value of 3.7 for sugar-cane-derived ethanol and 1.1 for corn-derived ethanol. Mousdale has given an excellent overview of the pros and cons in these calculations,[8] which in turn affect estimates of C_{res} considerably.

In the calculations presented herein, first-generation glucose-containing biomass processed by fermentation to ethanol was given a NEB of 1.2, whereas a value of 4.4 was used for the conversion of second-generation, cellulose-based material. Both values have been reported by Mousdale, with substantial deviations that highly affect the economy on all levels of biomass processing. The C factor for the first-generation ethanol with NEB = 1.2 may as an example be calculated as shown in Table 4. In comparison, the C factor for the ideal reaction ($CO_2 + 3\,H_2O \rightarrow EtOH + 3\,O_2$) is −1.91 kg($CO_2$) kg(ethanol)$^{-1}$.

In summary, the use of C factors as a tool takes some experience and a sound judgment. The level of detailed information does affect the accuracy and therefore, also in the comparison of different routes to the same product, caution should be ex-

Table 4. First-generation ethanol production from carbohydrates by fermentation.

C factor	Contribution
Fermentation carbon in ethanol	−1 [kg(CO_2) kg(CO_2)$^{-1}$]/{2/3·(46 [kg-(ethanol)]/(2·44) [kg(CO_2)])}
Fermentation emission	1 [kg(CO_2) kg(CO_2)$^{-1}$]·{1−(2/3))/(2/3)·(46 [kg-(ethanol)]/(2·44 [kg(CO_2)])}
CO_2 from energy demand based on NEB	1/1.2 [MJ(ethanol) MJ(LHV)$^{-1}$]·26.8 [MJ-(ethanol) kg(ethanol)$^{-1}$]/35.8 [MJ-(LHV) Nm(NG)$^{-3}$]/22.414 [Nm^3 kmol^{-1}]·44 [kg-(CO_2) kmol^{-1}]
Total	−0.68 kg(CO_2) kg(ethanol)$^{-1}$

ercised. As previously mentioned, steam credits are not subtracted. This will of course, in a larger petrochemical or biorefinery scenario, be a benefit to the calculated C factor. Neither electricity consumers nor all CO_2 evolved in terms of plant or machinery manufacture are accounted for and therefore C factors are not as accurate as LCA numbers. On the other hand, C factors can be used as simple indicators when LCA information is either not required or detailed information not accessible.

Table 5. C factors to alternative routes to preferred end-products.

End product	Resource	Platform	$C_{platform}$ factor	C factor	Refs.
Ethylene	Oil	Naphta	0.4	1.9	[9, 18–22]
	NG	Syngas	0.4	1.1	[9, 18, 23]
	Biomass (1st gen.)	Ethanol	−0.7	−0.7	[8]
	Biomass (2nd gen.)	Ethanol	−1.6	−2.2	[8]
Gasoline/synfuel	Oil	Naphtha	0.4	0.4[a]	[9, 18]
	NG	Syngas	0.4	1.9	[9, 18]
	Coal	Syngas	2.0	6.5	[13–16, 18, 24]
	Coal + NG	Syngas	0.6	2.4	[9, 13–15, 25]
	Biomass (2nd gen.)	Syngas	0.1	1.0	[8, 26, 28]
	Biomass (2nd gen.) + NG	Syngas	0.0	0.3	[8, 26, 28]
Acetic acid	NG	Syngas	0.4	0.3	[9]
	Coal	Syngas	1.4	0.9	[13–16]
	Biomass (1st gen.)	Ethanol	−0.7	0.1	[8]
	Biomass (2nd gen.)	Ethanol	−1.6	−0.6	[8]
Methanol	NG	Syngas	0.4	0.3	[9, 29]
	Coal	Syngas	0.9	2.2	[13–16]
	Coal + NG	Syngas	0.6	0.6	[9, 13–16, 24]
	Biomass (2nd gen.)	Syngas	0.1	0.0	[8, 27]
	Biomass (2nd gen.) + NG	Syngas	0.0	−0.1	[8, 9, 28]
Ethanol	Oil	Naphtha	0.4	1.6	[9, 18, 30]
	Biomass (1st gen.)	Ethanol	−0.7	−0.7	[8]
	Biomass (2nd gen.)	Ethanol	−1.6	−1.6	[8]

[a] The C factor for gasoline from oil is based on a conventional refining pathway.

Results and Discussion

Table 5 lists the resulting C factor values for a number of end products and their respective platforms for a selection of feedstocks. In most cases a high level of process insight has been used to calculate the information given.

Eventually the CO_2 conserved in the product is released again and returns to the CO_2 cycle. The accumulation time or the temporary storage time of CO_2 through solidification in materials depends highly on the product. It is clear that practically biofuels do not store the CO_2 temporarily bound. On the other hand, as a replacement all together it saves the emission otherwise resulting from the burning of petroleum derived fuels in engines. Whether or not there is a net premium to gain depends on a more thorough calculation. Some chemicals end up in products that do not degrade over 100 years, principally sequestering CO_2. On the other hand, should we welcome an ever-increasing amount of waste?

The situation may be that an end product may be obtained primarily from a certain platform material. In such a case it should be evaluated which resource may ideally be used for the provision of the platform material. In a CO_2-taxation-dominated economy, the C factor will make an indication of the proper choice.

Synfuel

As an example the CO_2 emissions in the production of gasoline from the straight-forward refining of crude oil have been analyzed. Furthermore they have been established in the alternative routes of reforming natural gas or gasifying coal or biomass to synthesis gas proper for synfuel production, followed by the conversion of such synthesis gas to synthetic gasoline, namely via either of the synfuel routes: Fischer–Tropsch (FT) or the TIGAS (Topsøe Integrated Gasoline Synthesis) processes, uniformly taken as processes with a yield of 80% with no extra heat input needed. Figure 5 shows the synthesis gas platform C factor details recalculated to the end product basis of the production of the alternative naphtha/synfuel from oil, natural gas, coal, biomass, and combinations.

Utilization of coal as a resource for the production of synfuels results in the highest C factor value by far. For the idealized reaction $3C + 2H_2O = 2\text{“}CH_2\text{”} + CO_2$ the C factor is 1.57 kg-(CO_2) kg(synfuel)$^{-1}$. A break-down of the obtained C factor for the production of module 2 syngas reveals that the major CO_2 burden lies in the adjustment of the coal gas, that is, the CO_2

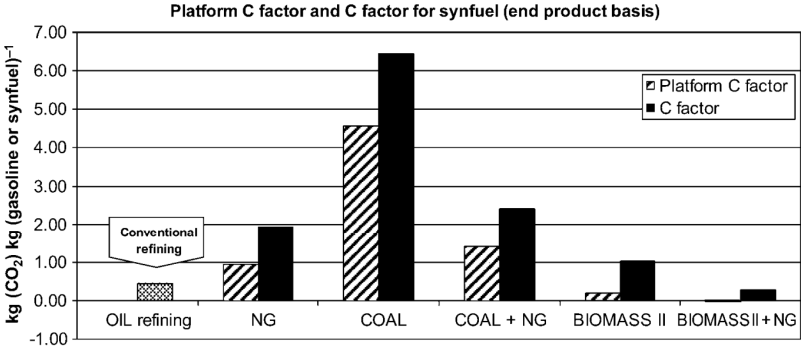

Figure 5. The CO_2 burden on the production of syngas as a synfuel platform in the coal to synfuel route heavily influences the resulting total C factor.

removal, resulting from the coal gasification (Figure 6). Figure 7 shows the corresponding process break-down.

In other words, the potential of reducing CO_2 emission in the process steps from the coal resource to synthesis gas lies

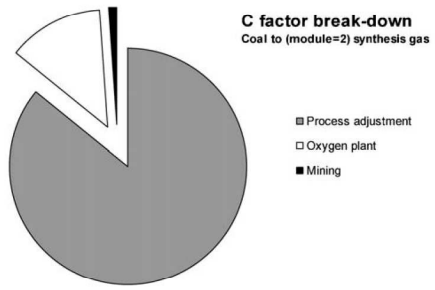

Figure 6. The CO_2 emission contribution from the platform C factor comes from the process adjustment, that is, the direct CO_2 removal in order to obtain module 2 synthesis gas as platform composition.

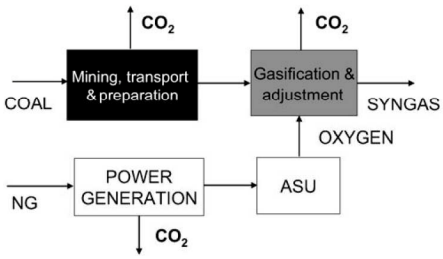

Figure 7. Detailing of process steps. The C factor for the conversion from coal to the syngas platform can be broken down into CO_2 emitted due to mining, transport, and crushing of coal, gasification and composition adjustment of the syngas, and the CO_2 emitted in generating the power needed for the air separation unit (ASU) to provide oxidant to the gasification process.

in the disintegration step of coal; the gasification step. Today the gasification takes place at high temperatures, resulting in a synthesis gas relatively rich in CO_2 because of a high CO/H_2 ratio in the original unadjusted raw synthesis gas. One way of reducing CO_2 would be to lower the disintegration temperature, reducing both the CO_2 level of the synthesis gas and reducing the oxygen consumption for the process, in turn reducing the power consumption for the air separation unit. Such lowering of the gasification temperature through the use of a catalyst has been looked into for the evident reason that it saves energy.[26]

WtW studies of the EU report a greenhouse gas (GHG) emission of 0.18 g and 0.36 kg CO_2 per kilometer driven in a passenger diesel car for a gas-to-liquid (GTL) and a coal-to-liquid (CTL) synfuel, respectively.[3] Anticipating a diesel density of 0.82 kg L^{-1} and a fuel consumption of 5 L per 100 km, the resulting emissions are 4.4 and 8.8 kg(CO_2) kg(synthetic diesel), respectively, using the two different fuels. These numbers compares reasonably with the numbers calculated by means of the C factor method, namely 5.0 and 9.6 kg(CO_2) kg^{-1}, if the emission during combustion is 3.1 kg(CO_2) kg(diesel)$^{-1}$.

Natural gas may also provide synthesis gas through one of the reforming technologies available: steam reforming. However, compared to the ideal synthesis gas composition for methanol or synfuel production it is too rich in hydrogen. Thus, by combining the coal gasification and natural gas steam reforming technologies in parallel in the right proportions, one ends up with a close-to-ideal synthesis gas composition. Hereby, the drawback of both processes becomes a common advantage, rendering coal as a reasonably good resource. In a specific example aiming at synthesis gas adjusted for synfuel or methanol production, 30% of the synthesis gas is supplied from the gasification of coal and 70% from the steam reforming of natural gas, or expressed through a mass-based feed ratio (natural gas/coal) = 1.1 kg kg^{-1}. In this case, the platform (syngas) C factor is reduced by a factor of 4 as compared to coal, to the level of the platform C factor for natural conversion.

This principle has been utilized in the Hynol process (Figure 8),[25,28] where the product stream of coal being gasified at high pressure and yielding synthesis gas with a high level of

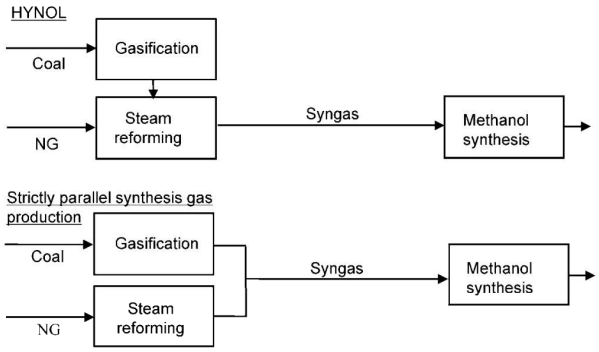

Figure 8. The Hynol process utilizes the benefits of combining feedstocks for methanol production. For gasification processes with a low methane slip the strictly parallel layout is preferable.

methane is in a second step processed together with a natural gas feed in order to eventually achieve a synthesis gas composition well-suited for the synthesis of methanol. The fact that the methanol synthesis is enhanced at higher pressures makes it beneficial also to provide for the synthesis gas at high pressure. Coal gasification at high pressure induces a high methane leakage. In the Hynol process the methane leakage from the gasifier is reduced in the downstream reformer. In cases where the gasification provides for a synthesis gas low in methane a more beneficial layout is obtained by operating the preparation of synthesis gas strictly in parallel.

An alternative feedstock to coal in a combined gasification process co-fed with natural gas is biomass. Indeed, our results show that this layout provides for a C factor of 0.3 kg(CO_2) kg(synfuel)$^{-1}$, competing with gasoline obtained through the refining of oil. In other instances, the routes available may not only go from different resources but also via different plat-

CHEMSUSCHEM

forms. With the future perspectives of the CO_2-taxation-dominant economy, we must observe the possibilities emerging through the re-introduction of biomass as a resource.

Acetic acid

Acetic acid is another product that over time has been produced by numerous routes. Acetic acid is a commodity chemical which is produced in excess of 8×10^6 MTa^{-}. About 65% is produced through carbonylation of methanol obtained from natural gas conversion. The suggested route for renewables using ethanol as a platform can be either direct oxidation via acetaldehyde or by using the dehydrogenation route. Of the two, the dehydrogenation is known not to generate CO_2, while the oxidation route leads to a certain degree of full combustion of the ethanol feedstock to CO_2. Therefore, the dehydrogenation route could become a preferred route, if the energy consumption is sufficiently competitive with the oxidation route. The carbonylation route such as the Monsanto process or Cativa process involves complex production plants.

We have compared the production of acetic acid from the overall conversion via methanol or ethanol. Methanol is obtained from natural gas or from coal gasification. In the two cases, the C factor for the MeOH becomes 0.3 and 2.0 kg(CO_2) kg(methanol)$^{-1}$, respectively. The resulting C factor for acetic acid production from natural gas is 0.3, taking into account a fully integrated plant design. Acetic acid may be obtained from synthesis gas produced from coal gasification by adjusting the hydrogen-to-CO ratio to a value just above 1 (removal of CO_2 is necessary). The 1:1 synthesis gas is then split approx. 50:50, where one split fraction is used for the production of CO while the remainder constitutes part of the make-up for the methanol synthesis. Pure CO may for example be obtained from the split stream in a cold box, where the balance hydrogen-rich stream may be combined with the partial make up stream for the methanol synthesis enriching it to an appropriate composition (module 2 as described above). A C factor of 0.9 kg(CO_2) kg(acetic acid)$^{-1}$ is obtained anticipating such a route. In comparison the C factor for the ideal reaction $C+H_2O\rightarrow H_2+CO\rightarrow{}^1/_2\,AcOH$ is 0. However in reality the gasification of coal takes place through an oxidation process involving oxygen, which produces CO_2. Alternatively, looking at renewable resources and starting from ethanol it seems that anticipating an acetic acid yield of 95% and an external energy input of 2.5 Gca Mt(acetic acid)$^{-1}$ (LHV basis), the CO_2 emission is competitive already with a narrow net energy balance of first-generation ethanol (NEB = 1.2) produced from sugar or starch; a C factor of 0.1 kg(CO_2) kg(acetic acid)$^{-1}$ is calculated for the dehydrogenation route versus the C factor for the conventional natural-gas-based process involving methanol carbonylation of 0.3 kg(CO_2) kg(acetic acid)$^{-1}$. Maturing the biomass conversion of cellulose into an ethanol technology allows in all instances for a much greener process with an overall negative CO_2 impact. Anticipating a net energy balance of 4.4, an abatement of 0.6 kg(CO_2) kg(acetic acid)$^{-1}$ is obtained. In comparison, the C factor for the ideal reaction $CO_2+H_2O\rightarrow{}^1/_2\,AcOH+O_2$ is -1.47 kg(CO_2) kg(acetic acid)$^{-1}$.

Ethanol versus gasoline as transportation fuel

An issue which is hard to get around is the question of ethanol as a gasoline substitute. Apart from the debate on whether ethics allow us to fuel cars with a chemical that originates from food resources, we may ask if it is feasible from a CO_2 emission point of view?

As to mileage, anticipating that only 0.70 kg of gasoline must be fed in order to equal one kilogram of ethanol combusted in a gasoline engine, the CO_2 emission of a first generation ethanol is 1.8 kg(CO_2) kg(gasoline equivalent)$^{-1}$, or approximately half the amount of CO_2 emitted by combusting one kilogram of gasoline produced from crude oil. Meanwhile, the net energy balances of first-generation ethanol productions are subject of much debate. If the energy output is anticipated as only 60% of the energy input, the CO_2 emissions are equal in the two cases, gasoline and first-generation ethanol, per kilometer driven. On these grounds, especially the production of first-generation biomass for fuel may take fierce competition from exploiting the arable land against the alternative essential crops such as grain or other biomass productions of higher priority. Furthermore, the fuelling of vehicles with 100% ethanol requires motor retrofits.

As mentioned before synfuel produced through the combined gasification of natural gas and second-generation biomass has a C factor comparable with gasoline or diesel produced from crude oil. This may be a good alternative route to synfuel not requiring any modification of the engines. Waste gasification may also further be considered. A second-generation ethanol is superior to any of the above-mentioned scenarios.

Ethylene

The C factor for ethylene heavily varies, remarkably, depending on the resource chosen for its manufacture. Ethylene can be made from dehydration of first- and second-generation bioethanol. As discussed in Example 2, the energy consumption for these are represented by the net energy balance numbers 1.2 and 4.4, respectively, meaning that the route from second-generation biomass has a lower (more negative) platform C factor for ethanol. Taking a starting point in these platform values, -0.7 kg(CO_2) kg^{-1} for first-generation and -1.6 kg(CO_2) kg^{-1} for second-generation biomass, and assuming a yield of 95% and including corrections for mass change through conversion of ethanol to ethylene the numbers for the feed and loss sum to -1.2 kg(CO_2) kg^{-1} and -2.6 kg(CO_2) kg^{-1}, respectively. Then, with the inclusion of the energy consumption the C factors for the ethylene end product are -0.7 kg(CO_2) kg^{-1} and -2.2 kg(CO_2) kg^{-1} for first- and second-generation biomass, respectively. The CO_2 credit obtained by the usage of the biomass source (via the extraction of CO_2 from the atmosphere) is amplified due to relatively high carbon content (weight fraction) as compared to an alternative product, for example, acetic acid. At the same time, the production of ethylene from crude oil is heavily energy-consuming. This leads to a high disparity of the ethylene C factor by comparing a second-generation biomass

to the conventional production route, −2.2 vs. 1.9 kg(CO_2) kg-(ethylene)$^{-1}$.

The so-called carbon footprint of ethylene is reported to be about 1.8–1.9 kg(CO_2) kg(ethylene)$^{-1}$, consistent with a C factor of 1.9 kg(CO_2) kg(ethylene)$^{-1}$ from naphtha cracking. Recently Johnson et al. pointed out that for the polyethylene industry carbon footprint analysis gives highly diverse results due to different approaches in the analysis of steam cracker contributions.[31] However, although the two results for ethylene compared herein appear to be similar, it was not reported if any gate-to-grave or polyethylene conversion was included in the calculations.

Figure 9 compares the C factors for production of ethylene, gasoline, acetic acid, methanol, and ethanol from various sources, compiling the above discussion into one single comparison. The size of the circles used reflects to some degree the uncertainty involved in the calculations, without being specific for each case. Seven different resources or combinations of resources have been analyzed, showing that second-generation (cellulosic) biomass, because of the high NEB and low C_{res} in all cases, results in very favorable C factors for most processes, except for gasoline production.

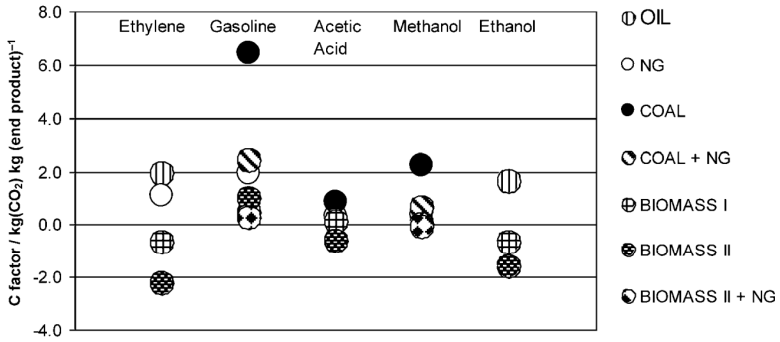

Figure 9. Survey of the overall C factors for several end products produced from various resources.

As indicated in the above examples, the C factor is given with a rather large uncertainty depending on the knowledge of the process and in terms of the resource as well. As such, caution should be exercised in the comparison of two alternative process routes if the degree of detailed knowledge is not the same and if the magnitudes are close.

Conclusions

Different processes or routes to similar products can be evaluated and compared regarding the CO_2 impact through the C factor, which gives the produced mass of CO_2 per mass of product. To be able to compare different resources in the analysis (i.e., fossil and biomass-related), we have introduced a resource-related C factor, C_{res} factor (including recovery, mining, processing, and transport of the resource) which links to a C_{proc} factor, the latter accounting for fuel uses and feed losses through the conversion of the resource in the chemical process scheme.

LCA methodologies have been applied in the literature to several of the products or processes analyzed in the present paper.[32] However, many of these studies apply different LCA methodologies and the direct comparison of results from different sources may be affected significantly by this. A study by the "Hysociety" reports these differences for the LCA of hydrogen vehicles. Based on this we have refrained from evaluating the proposed C factor against complete LCAs. Other simple measures of sustainability such as the *E* factor[33] evaluating waste generation or the mass efficiency approach are to some extent integrated in our calculations as we consider all carbon containing byproducts and unconverted feed as sources of energy which, hence, becomes converted into a CO_2 contribution.

The C factor can be used for the assessment of the climate impact of a particular process as well as in the comparison of different processes. The C factor is particularly useful in cases where the more extensive LCA is not needed.[34] The C factor of the end product can only be calculated with an uncertainty, which increases as the level of detailed knowledge of a process decreases. Hence, caution should be exercised when processes of comparable C factors are examined. In the case of acetic acid and gasoline production from a variety of sources, it is indeed possible to see substantial differences in the C factors related to both resource and the conversion route selected. A bulk chemical, such as acetic acid, can according to our calculations be produced at a much lower C factor based on renewable resources compared to the current predominant use of methanol carbonylation.

In general, C factors are not that difficult to calculate from basic knowledge of process parameters, such as energy requirement and yields of intermediates and product. We therefore suggest this parameter as a means of measuring and comparing processes where the use of full life cycle analysis is not required or meaningful.

Acknowledgements

Financial support from the Danish Agency for Science Technology and Innovation is gratefully acknowledged.

Keywords: biomass · carbon dioxide · renewable resources · sustainable chemistry · synfuels

[1] A. Demirbas, *Energy Convers. Manage.* **2008**, *49*, 2106–2116.
[2] Y. Román-Leshkov, C. J. Barrett, Z. Y. Liu, J. A. Dumesic, *Nature* **2007**, *447*, 982–985.

[3] *Well-to-Wheel and Well-to-Tank Report, Version 2c*, Institute for Environment and Sustainability, **2007**. Available from http://ies.jrc.ec.europa.eu/WTW (accessed November 2009).
[4] T. Geerken, S. Lassaux, R. Renzoni, V. Timmermans, *Review of Hydrogen LCAs for the Hysociety Project* **2004**, http://www.vito.be/VITO/OpenWoDocument.aspx?wovitoguid=53F587DD-9100-4E5A-983C-5DCC2B9F8F62 (accessed November 2009).
[5] C. Jimínez-Gonzaílez, S. Kim, M. R. Overcash, *Int. J. Life Cycle Assessment* **2000**, *5*, 153–159.
[6] E. Taarning, I. S. Nielsen, K. Egeblad, R. Madsen, C. H. Christensen, *ChemSusChem* **2008**, *1*, 75–78.
[7] C. H. Christensen, *ChemSusChem* **2008**, *1*, 283.
[8] D. M. Mousdale, *Biofuels—Biotechnology, Chemistry, and Sustainable Development*, CRC **2008**.
[9] http://www.ens.dk/da-DK/UndergrundOgForsyning/Olie_og_gas/Data/Produktionsoversigter/Sider/Forside.aspx (accessed November 2009).
[10] M. Wy, M. Mintz, M. Wang, S. Arora, *Argonne National Laboratory Report ANL/ESD/09–1*, **2009**.
[11] J. G. Speight, *The Chemistry and Technology of Petroleum, 4th Ed.*, CRC, Boca Raton, **2007**.
[12] W.Kleinitz, personal communication, **2009**.
[13] C. J. Cleveland, R. Costanza, C. A. S. Hall, R. Kaufmann, *Science* **1984**, *225*, 890–897.
[14] P. Purohit, A. K. Tripathi, T. C. Kandpal, *Energy* **2006**, *31*, 1321–1331.
[15] The energy intensity for coal crushing is based on figures from the Pennsylvania Crusher Corporation: http://www.penncrusher.com/Size_Reduction/power_requirements.cfm (accessed November 2009).
[16] C. Higman, M. van der Burgt, *Gasification*, Elsevier, Amsterdam **2003**.
[17] M. E. Dias de Oliveira, B. E. Vaughan, E. J. Rykiel, Jr., *BioScience* **2005**, *55*, 593–602.
[18] T. Ren, *Energy* **2006**, *31*, 817–833.
[19] S. J. Stanley, *Petrotech* **2009**, 416.
[20] *Energy Use and Energy Intensity of the US Chemical Industry*, **2000**. Available from http://www.osti.gov/bridge/servlets/purl/773773-UFjL87/webviewable/773773.pdf (accessed November 2009).
[21] J. P. Wauquier, *Crude Oil Petroleum Products Process Flowsheets*, Gulf, Houston, **1995**.
[22] W. F. Banholzer, *CEP*, March **2008**, S7–S14.
[23] J. Q. Chen, *Catal. Today* **2005**, *106*, 103–107.
[24] V. Ramanathan, *AP-2488 Research Project 239, Final Report*, July **1982**.
[25] Meyer Steinberg, *BNL-65453 (DOE)*, **1997**.
[26] M. A. Caballero, *Ind. Eng. Chem. Res.* **1997**, *36*, 5227–5239.
[27] S. P. Babu, *Biomass Gasification for Hydrogen Production–Process Description and Research Needs*. Available from http://www.ieahia.org (accessed November 2009).
[28] Y. Dong, *Int. J. Hydrogen Energy* **1997**, *22*, 971–977.
[29] Foster Wheeler & Methanol Casale, *Methanol Solutions*, **2005**. Availabe from www.fwc.com/industries/pdf/Methanol_flyer_A4_final.pdf (accessed November 2009).
[30] K. Weissermel, *Industrial Organic Chemistry, 4th. Ed.*, Wiley-VCH, Weinheim **2003**.
[31] A. Azapagic, *Life Cycle Assessment: A Tool for Assessing and Improving Environmental Sustainability.* Available from http://www.york.ac.uk/org/gcn/pages/pdf/AdisaAzapagicManchester.pdf (accessed November 2009).
[32] M. Neelis, M. Patel, P. Bach, K. Blok, *Appl. Energy* **2007**, *84*, 853–862.
[33] R. A. Sheldon, *Green Chem.* **2007**, *9*, 1273–1283.
[34] M. A. Curran, *Life Cycle Assessment: Principle and Practice*, **2006**. Available from http://www.epa.gov/nrmrl/lcaccess/pdfs/600r06060.pdf (accessed November 2009).

Received: September 13, 2009
Revised: November 9, 2009

A.4 Survey over others and own contribution to present work

Table A-2: Survey of activities and contributions to the project.

Activity	Own work	Others work[f]
2nd gen. Bio-ethanol NEB, Appendix A.1	X	SIA, ESTA
Ethanol conversion over zeolites, Appendix A.2	X	
Article, EES, Appendix A.2	X	ESTA et al.
Resource discussion	X	
Article, ChemSusChem, Appendix A.3	X[a]	(SIA, ESTA)
Ethanol production price	X	
Gross margin analysis	X	
Acetic acid, history, use, state of the art	X	
Economics, Appendix B.1	X	
Ethanol to Acetic acid routes and technology	X	
Process assessment		
Flow diagram, Appendix D.2, specifications	X[e]	SIA
Cost estimate	X	SGK
Production price, Appendix D.6	X	
Screening set-up		
Glass set-up, run, Appendix D.1	X	
Basic catalyst preparations (precipitations)		ANSJ
Impregnations, special cat. Hardware	X	
Non quantitative analysis, GC-MS	X	
Other experimental set-ups		
Stability set-up, design, PFD, Appendix C.1	(X)[c]	NN
Other set-ups, design, PFD, safety, op. manual	X	
Catalyst preparations		ANSJ
Planning and method	X	
Run		XIYA, MBM, PJM, ANKA
Analysis methods and calibration		SIA, MBM, PJM, ANKA
Troubleshooting	X	Team
Principle, mass balance and equilibrium program	X	
Patent applications		
Water in recycle control, Appendix D.3	X[b]	(NCS)
Thermoneutral process, Appendix D.4	X[b]	(CHC, NCS)
Integration with VAM, Appendix D.5	X[b]	(RAMA)
Characterisation		
EXAFS, Appendix E.1	(X)[d]	JDG, APM, FMCA
All other		Analysis lab.
Article, Photon Science 2009, Appendix E.2	X[a]	APM, PABB, FMCA, JDG
Experimental and characterisation data analysis	X	
Modelling and kinetics	X	
DFT calculations		BUTE
Article, Applied Catalysis A, Appendix F.1	X	
Higher alcohols		
PFD, process considerations	X	
Experimental set-up, method, analysis		PL, BUTE, Analysis lab.
Catalyst preparation		SLJ
Planning	X	
Data analysis tool	X	

a) the article was written mainly by me, but supplemented and reviewed by others.

b) the applications were drafted by me solely, even if co-inventors were specified.

c) the stability set-up was made by rebuilding of an old unit.

d) I prepared the samples for EXAFS and provided the feeding system to the reduction experiment with ethanol.

e) I prepared the process flow diagram and made the majority of the equipment specifications, but SIA made the design calculation of the Distillation column F-1001.

f) The names according to the initials listed are: (ANKA) Anders Kallesøe, (ANSJ) Annika Schnack-Jensen, (APM) Anna Puig Molina, (BUTE) Burcin Temel, (CHC) Claus Hviid Christensen, (ESTA) Esben Taarning, (FMCA) Fernando Morales Cano, (JDG) Jan-Dierk Grunwaldt*, (NCS) Niels Christian Schjødt*, (PABB) Pablo Beato, (PL) Peter Lehrmann, (SGK) Søren Guldbæk Karlsen, (SIA) Simon Ivar Andersen*, (SLJ) Susanne Lægsgaard Jørgensen, (XIYA) Xiaobo Yang. * are my PhD project supervisors. All other are employees at Haldor Topsøe A/S.

Appendix B Conventional acetic acid route

Contents

B.1 The production price of acetic acid via carbonylation

B.1 The production price of acetic acid via carbonylation

The main sections of a conventional acetic acid plant comprise: reforming, CO_2 removal, CO separation (cold box or membrane), oxygenate synthesis and distillation or product recovery, acetic acid reactor/flash separator/OH MeI recovery, and distillation (light end, drying and heavies columns), as shown in Figure B-1.

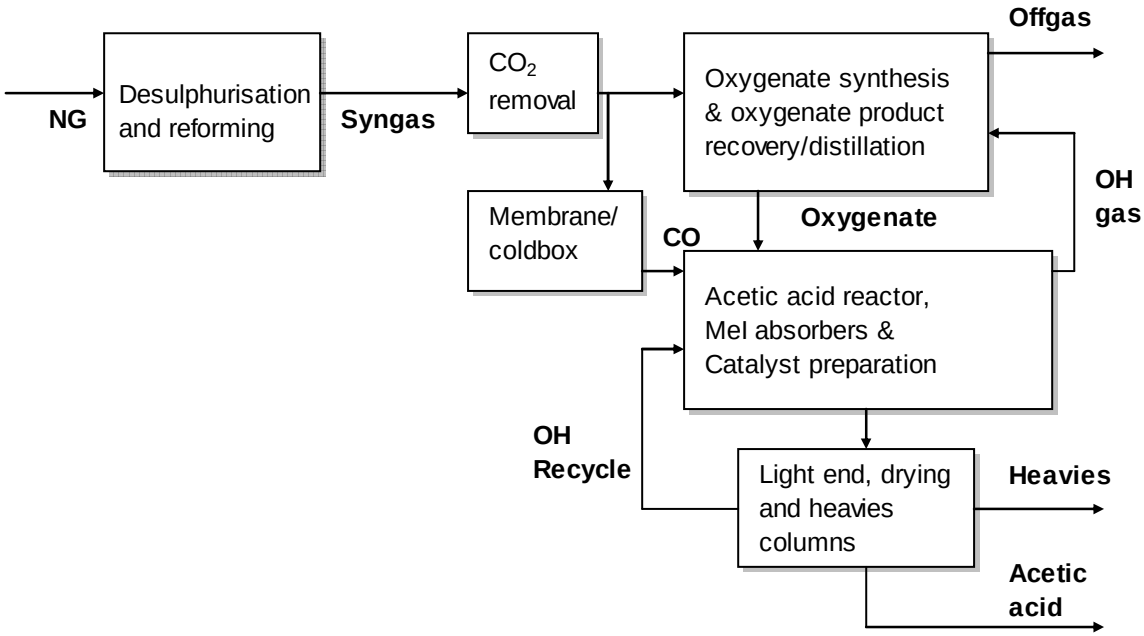

Figure B-1: The carbonylation route. Natural gas is fed and being prepared to syngas which is converted to oxygenate and CO respectively. The carbonylation takes place at about 35 bar and involves an expensive Rh catalyst and a carcinogenic co-catalyst methyl iodide which must be prepared batchwise on site and made up. HI which is in equilibrium with methyl iodide, methanol and water must be removed to less than 40 ppb in the final product to comply with typical acetic acid product specifications.

The primary make-up streams to the carbonylation section with the acetic acid reactor etc. are methanol and CO. The purity of the carbon monoxide supplied to the back-mixed reactor i.e. is important, though not crucial, for keeping a moderate synthesis pressure – a low purity can be paid off with a low utilisation of the carbon monoxide or an operating pressure increase. The requirements to the methanol feed purity are rather high, in order to avoid the formation of side-products which are difficult to separate.

The stabilisation of the Rh catalyst requires a certain water concentration of the reaction medium, which in turn complicates the separation and purification of the acetic acid in the complex downstream distillation section. A modernisation by Celanese of the above described rhodium catalytic system was made in the late 1970'es involving the catalyst stabilization by means of LiI, the improved catalyst being able to operate at a much lower water concentration. As an answer to this BP introduced a low water process too (Cativa) based on Ir replacing Rh and modified by the addition of ruthenium enhancing the reaction rate tremendously at low water conditions.

But in spite of the different developments the principle of the carbonylation based processes is the same and involves similar sections.

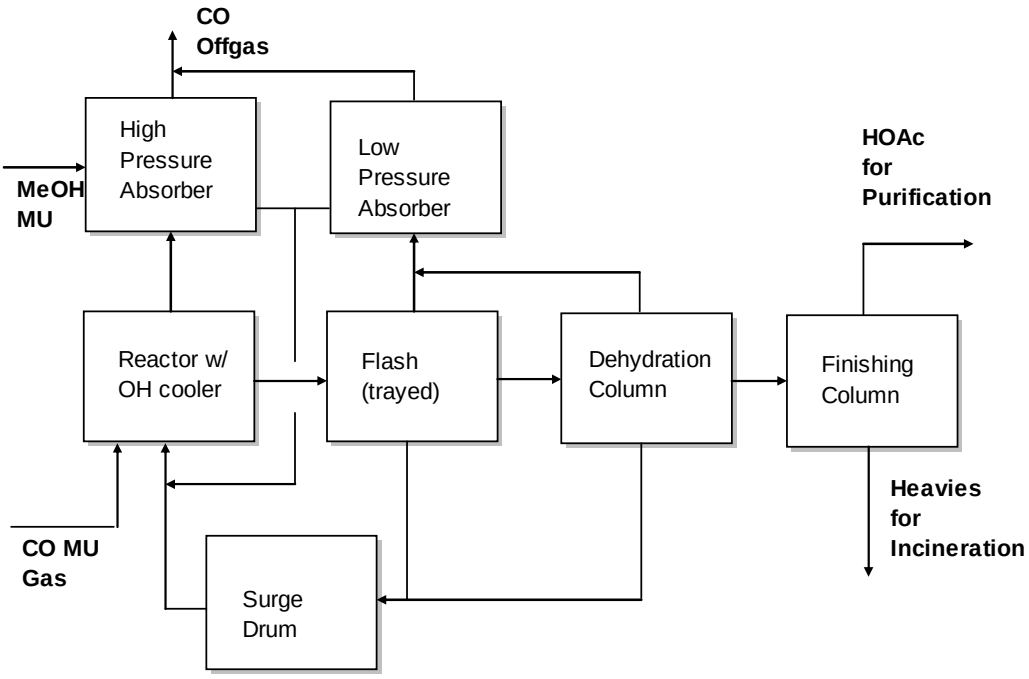

Figure B-2: Process scheme of the Acetica carbonylation process route. The low water carbonylation processes are similar to the original Monsanto process sections. The process development of the carbonylation process leading to an immobilisation of the Rh catalyst and the lower water content of the process has diminished the operating cost and investment.

Taking one of the highly mature low water processes, the Acetica process from Chiyoda, as an example (see Figure B-2) it has the advantage over the other low water carbonylation processes that the Rh catalyst is immobilised (*Chiyoda Corporation*). The Rh is supported on beads loaded into a bubble column which represents a simplification of the original Monsanto stirred tank reactor.
The OH gas is cooled and the gas phase is passed to a high pressure methyl iodide absorber, using make-up methanol as a solvent.
Apart from the reactor with OH reflux cooler operating at 60 bar, it comprises a flash distillation wherefrom a large fraction of the HI in the reactor effluent may be recovered together with the minute amounts of the Rh which may have been lost from the heterogeneous catalyst. Dissolved gases containing methyl iodide from the flash is sent to a low pressure absorber, while the methyl iodide top draw is recycled to the reactor through the recycle surge drum. The flash distillation corresponds to the original light ends column in the Monsanto process. The side draw rich in acetic acid is dewatered in a dehydration column, and heavies and traces of HI are removed in their finishing column.
Although the process developments have greatly improved on the original Monsanto process the reaction system still involves highly corrosive elements such as methyl iodide and HI.

We have at Haldor Topsøe A/S in-house information on the carbonylation route due to our acetic acid process development activities during the 90s. In a last version of our acetic acid process schemes with a production capacity of 300,000 MTPY based on

the carbonylation route, the carbonylation reactor runs under low water conditions (representing also today's state-of-the-art), relieving the requirements to downstream purification section in terms of equipment size. The corresponding investment figures from the 90s were updated with respect to the construction material prices today and the inflation rate. The fixed capital investment, the grand total capital requirement and the utility consumption figures in this work originates from this in-house study. The investment and utility consumptions figures used are estimated to be conservative, as the Topsøe integrated acetic acid process avoids the distillation of methanol prior to the carbonylation (*Joensen, 1998*).
Battery limits are at the supply of natural gas and at the export of acetic acid from day tanks.

In below Table B-1 the specific cost of feedstock and utility consumption is specified for each of the three carbonylation layouts. NGP designates the natural gas price in USD/GJ.

Table B-1: The key figures on investment and consumptions for a 300,000 MTPY acetic acid plant based on carbonylation. The identification by number of the plant types listed is corresponding to the plant layouts shown in Figure 2-1.

	1. Integrated	**2. With MeOH import**	**3. With MeOH and CO imports**
Grand total Investment (MM USD)	671	517	286
Simple Payback time (y)	10	10	10
SpecificConsumptionCost[a] (USD/MT)	34.1·NGP+25.5	22.5·NGP+132.	22.5·NGP+205.3

a) MeOH imported at a cost of 200USD/MT, incl. all utilities, incl. catalyst consumptions.

The utility prices used as basis is listed below in Table B-2.
Based on a few specifications of the individual process equipment items and selecting their material of construction the individual equipment costs were estimated by Questimate®. Such simple methods for estimating capital costs are discussed by *Turton et al.* The installed cost of the equipment items was calculated as the equipment cost times an individual installation factor reflecting the complexity of the installation. The accuracy of this method is estimated by our cost estimator to be ±30%, but the accuracy of the delta is higher when comparing examples, prepared by the same method.

The ISBL investment is the sum of the installed cost inside battery limits. OSBL investment comprises the cost of equipment outside battery limits, i.e. not directly process related, but related to the supply the utilities and to the plant area.
The total fixed investment, being the sum of ISBL and OSBL investments is calculated according to Eq. **B-1** by setting the ISBL investment to a certain fraction of the total fixed investment, TotalFixedInvestment, here 0.65:

$$TotalFixedInvestment = ISBL + OSBL = \frac{ISBLInvestment}{0.65} \quad \textbf{Eq. B-1}$$

The grand total investment is obtained according to Eq. B-2 by a 25% addition to the total fixed investment including thereby professional services and contingencies:

$$GrandTotalInvestment = 1.25 \cdot TotalFixedInvestment \quad \textbf{Eq. B-2}$$

The gate price of the product is then calculated according to Eq. B-3:

$$GatePrice = \frac{GrandTotalInvestment}{SimplePayBackTime \cdot AnnualCapacity} + SpecificConsumptionCost + FixedCost \quad \textbf{Eq. B-3}$$

where the AnnualCapacity is the annual acetic acid capacity in MTPY.

According to rules of thumb the FixedCost in Eq. B-3 is calculated according to Eq. B-4:

$$FixedCost = \frac{1.4 \cdot salaries + 0.04 \cdot ISBL + 0.03 \cdot OSBL + 0.02 \cdot FixedInvestment}{AnnualCapacity} \quad \textbf{Eq. B-4}$$

where the salaries= 3 shifts@200,000 USD/y=600,000USD/y.

Table B-2: Utility prices used for the calculation of the specific consumption cost, reflecting the actual energy price.

Unit price	Low	Medium	High
NG price (USD/GJ)	1	6	12
Desalinated water unit price (USD/m^3)	1.2	1.2	1.2
Sea cooling water unit price (USD/m^3)	0.01	0.01	0.02
Electric power unit price (USD/kWh)	0.02	0.14	0.28
Steam unit price (USD/MT)	4.5	7	10
Nitrogen unit price (USD/Nm^3)	0.02	0.02	0.02

Appendix B.1. References

Chiyoda Corporation, Acetic Acid Production Process (ACETICA). Retrieved Dec. 28, 2010 from: http://www.chiyoda-corp.com/technology/en/gtl/acetica.html.

Joensen, F., Process for the preparation of acetic acid from a synthesis gas of hydrogen and carbon monoxide, US 5840969, 1998.

Turton, R., Bailie, R.C., Whiting, W.B., Shaewitz, J.A., Analysis, Synthesis, and Design of Chemical Processes, 2nd ed., Prentice Hall PTR, New Jersey, 2003, 141-186.

Appendix C Experimental

Contents

C.1 Sketch of stability test set-up

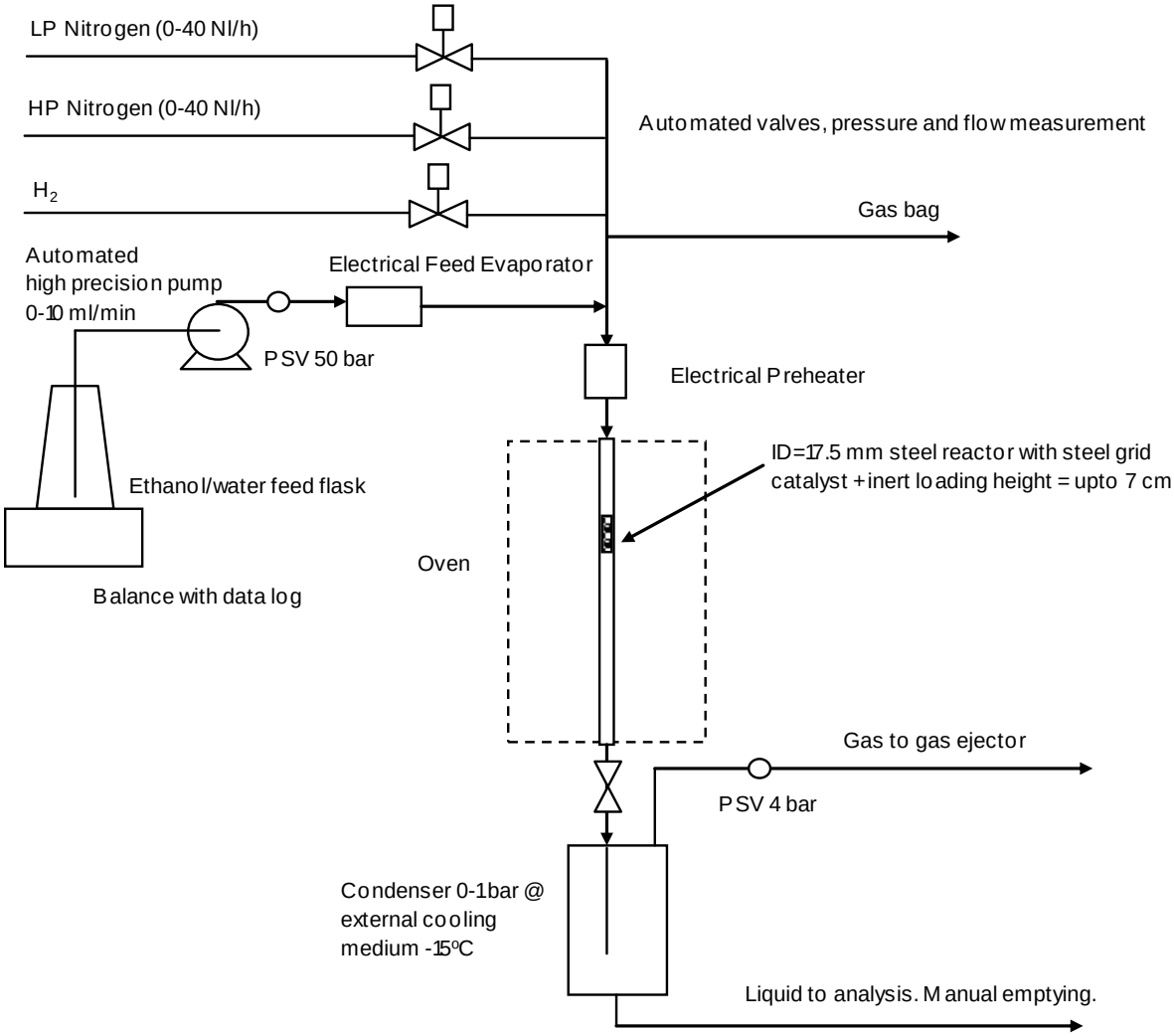

Appendix D Alternative Ethanol-to-acetic acid route and catalysts

Contents

D.1 Catalyst screening survey

Table D-1: A survey of the catalysts tested during catalyst screening, test conditions and results.

Catalyst ID Size (mm)	Set-up	Temperature (°C) **Time (h)**	Feed (molar) ($EtOH:H_2O:O_2$) **LWHSV (g/(g·h))**	Products	Comments
$Cu/ZnO/Al_2O_3$ 4.5 x 3.5	Screening 1.2 cm Glass	270, 320 **2**	50/50/0 **2.4**	Oxidation products (Condensation products)	Low mechanical stability
$Cu/ZnO/Al_2O_3$, 1% Ag 4.5 x 3.5	Screening 1.2 cm Glass	260, 320 300, 320 **2**	100/0/0 50/50 **2.4**	Oxidation products (Condensation products)	Low mechanical stability
20mol%$Cu/ZnO/Al_2O_3$ 4.5 x 4.5	Screening 1.2 cm Glass	200,230,270,280 290 320,360 290,300,330 **2**	100/0/0 75/25/0 50/50/0 25/75/0 **2.4**	Oxidation products Condensation products	Good mechanical stability
$MgAl_2O_4$ 4.5 x 3.5	Screening 1.2 cm Glass	300, 380 **2**	100/0/0 **2.4**	Condensation products	
Ag (1%) on TiO_2 8 mm Daisy	Screening 1.2 cm Glass	250, 350 **2**	100/0/0 **2.4**	Condensation products	Good mechanical stability Low conversion
Pd (1%) on silica 1/8” extrudates	Screening 1.2 cm Glass	270 – 320 **2**	100/0/0 **2.4**	Diethyl ether	Good mechanical stability High conversion
Cu/Al_2O_3- calc.550 6 x 6 mm	Screening 1.2 cm Glass	270 – 320 **2**	50/50/0, 100/0/0 **2.4**	Oxidation products (Condensation products)	Good mechanical stability High conversion
Cu/Al_2O_3- calc.850 5 x 5 mm	Screening 1.2 cm Glass	320 320 **2**	50/50/0, 100/0/0 50/45/5 **2.4**	Oxidation products (Condensation products)	Good mechanical stability High conversion
Cu/Al_2O_3- calc.1100 4 x 4 mm	Screening 1.2 cm Glass	270 – 320 **2**	50/50/0 **2.4**	Oxidation products (Condensation products)	Good mechanical stability Low conversion
$Cu/ZnO/Al_2O_3$, 2% K	Screening	270	50/50/0, 100/0/0	More condensation products	Low mechanical stability

4.5 x 3.5 mm	1.2 cm Glass	**2**	**2.4**		Low conversion
Cu/Al_2O_3- calc.850, 2% K 5 x 5 mm	Screening 1.2 cm Glass	320 **2**	100/0/0, 50/50/0 **2.4**	More condensation products	Good mechanical stability Low conversion
Cu/Al_2O_3- calc.850 5 x 5 mm	New set-up 8 mm glass	300 3 x 7	60/40/0 **3**	Escalating condensation products	Good mechanical stability. Deactivation.
Cu/Al_2O_3- calc.550 5 x 5 mm	New set-up 8 mm glass	300 2 @ 4 x 7	60/40/0 **3**	Escalating condensation products	Good mechanical stability. Deactivation.
Cu/Al_2O_3- calc.550 steamed @ 500°C for 5 h. 5 x 5 mm	New set-up 8 mm glass	300 3 x 7	60/40/0 **3**	Escalating condensation products. Dies suddenly.	Good mechanical stability
V_2O_5 on TiO_2	New set-up 2.7 cm Glass	200, 300 **5**	60/40/0 **0.7**	Huge amount of condensation products	Initial Acetic acid formation. Huge number/amount of side-products. Croton aldehyde.
Pt (1%), CeZr oxide, 3 x 3 mm	Screening 1.2 cm Glass	200, 320 **2**	50/45/5 **2.4**	Oxidation products (acetaldehyde)	Low mechanical stability Low conversion
Cu/CeO_2 4 x 4 mm	Screening 1.2 cm glass	320 2	50/50 **2.4**	Oxidation products And condensation products	Very low conversion
$Cu/ZnO/Cr_2O_3$ 4.5 x 4.5 mm	Screening 1.2 cm Glass	320 **2**	50/50 **2.4**	Oxidation products	High conversion Contains Cr
Cu/Al_2O_3- calc.850 1.4 x 1.4 mm	New set-up 8 mm glass	320 5 x 7	60/40 **3.4**	Oxidation products (butanol, butanoic acid)	High conversion Good stability (so far)
Pd (1%) WO_3/ZrO_2	Screening 1.2 cm Glass	320 **2**	50/50 **2.4**	Diethylether	Low conversion
ZrO_2 2 mm extrudates	Screening	320 **2**	50 HAc/50 H_2O **4.8**	Condensation products (oxidation products)	High conversion 2 phases
HSA alumina 1/16” trilobe extr.	Screening	320 **2**	50 HAc/50 H_2O **4.8**	HUGE amount of condensation product	2 phases, top phase dark brown
Cu/Al_2O_3- calc.850 5 x 5 mm	Screening 1.2 cm Glass	320 **2**	50 HAc/50 H_2O **2.4**	Oxidation products (Condensation products)	Good mechanical stability

					High conversion No ethyl acetate formed
Model catalyst 2.5wt% Cu on alumina 1/16” trilobe extr.	Screening	320 **2**	50/50 **2.4**	Condensation products	High conversion Dark brown droplets 2 phases
Raney Cu on Pyrex	Screening 1.2 cm glass	300 **2**	50/50 **9.6**	Oxidation products (very selective)	5.4 wt% acetic acid!!
Cu flakes/chips	Screening 1.2 cm glass	300-600 **4**	50/50 **2.4**	Acetaldehyde at very high temperature	Hopeless!!
Cu on HSA silica 4 x 6 mm cylinders	Screening 1.2 cm glass	320 **2**	50/50 **2.4**	Oxidation products (Condensation products)	Lower activity as compared to Cu/Al_2O_3-850 but sound product distribution.
Cu on Colloid Silica 4 x 6 mm cylinders	Screening 1.2 cm glass	320 **2**	50/50 **2.4**	Oxidation products (Condensation products)	Half the activity as compared to above HAS silica, but sound product distribution. Mechanically weak.
2500 wtppm Pt on TiO2 8 mm offwhite Daisies	Screening 1.2 cm glass	320 **2**	50/50, 50/45/5, $50HAc/45H_2O/5O_2$ **2.4**	DEE, acetaldehyde, butadiene Cyclopentanes Methanol, methyl Acetate, C_3-C_5 acids, aromatics	Very low activity. Yellow condensate. Small droplets of oily phase. Quite high activity on $HAc/H_2O/O_2$ feed and a lot of HOAc + side-products. Lower end of bed black at unload.
Pt (1%) on Cu/MnO_2 dark grey rings	Screening 1.2 cm glass	320 **2**	50/50, 50/45/5, $50HAc/45H_2O/5O_2$ **2.4**	Oxidation products. Diethoxy ethane. Very selective with ethanol/H_2O and opt. O_2. Activity increase with O_2 addition.	Low/medium activity. Still selective with ethanol/H_2O/O_2 3 times activity

				Selectivity lower with HAc	with O_2
Pt on alumina 3 mm balls, grey	Screening 1.2 cm glass	320 **2**	50/50, 50/45/5, 50HAc/45H_2O/5O_2 **2.4**	DEE, acetaldehyde, butadiene Cyclopentanes C_3-C_5 acids, aromatics	Very low activity. Modest activity on HAc/H_2O/O_2 feed to HOAc + side-products. Yellow products on glass equipment.
Pd on alumina balls 3mm, bright orange	Screening 1.2 cm glass	320 **2**	50/50, 50/45/5, 50HAc/45H_2O/5O_2 **2.4**	Low conversion (HAc+acetone+butanol) With acetaldehyde a huge amount of condensation products in top phase, oxidation products and side-products in bottom phase	Brown top phase Brown stuff on reactor inner wall
$CuMnO_2$	Screening 1.2 cm glass	320*2/280 **2**	50/50, 50/45/5, 50HAc/45H_2O/5O_2 **2.4**	Medium conversion, oxidation products + ketones, butanoic acid. Substantial activity increase on oxygen addition. With acetaldehyde feed a HIGH conversion of acetaldehyde to paraldehyde is obtained.	

D.2 Process flow diagram for the non-oxidative dehydrogenation of ethanol to acetic acid

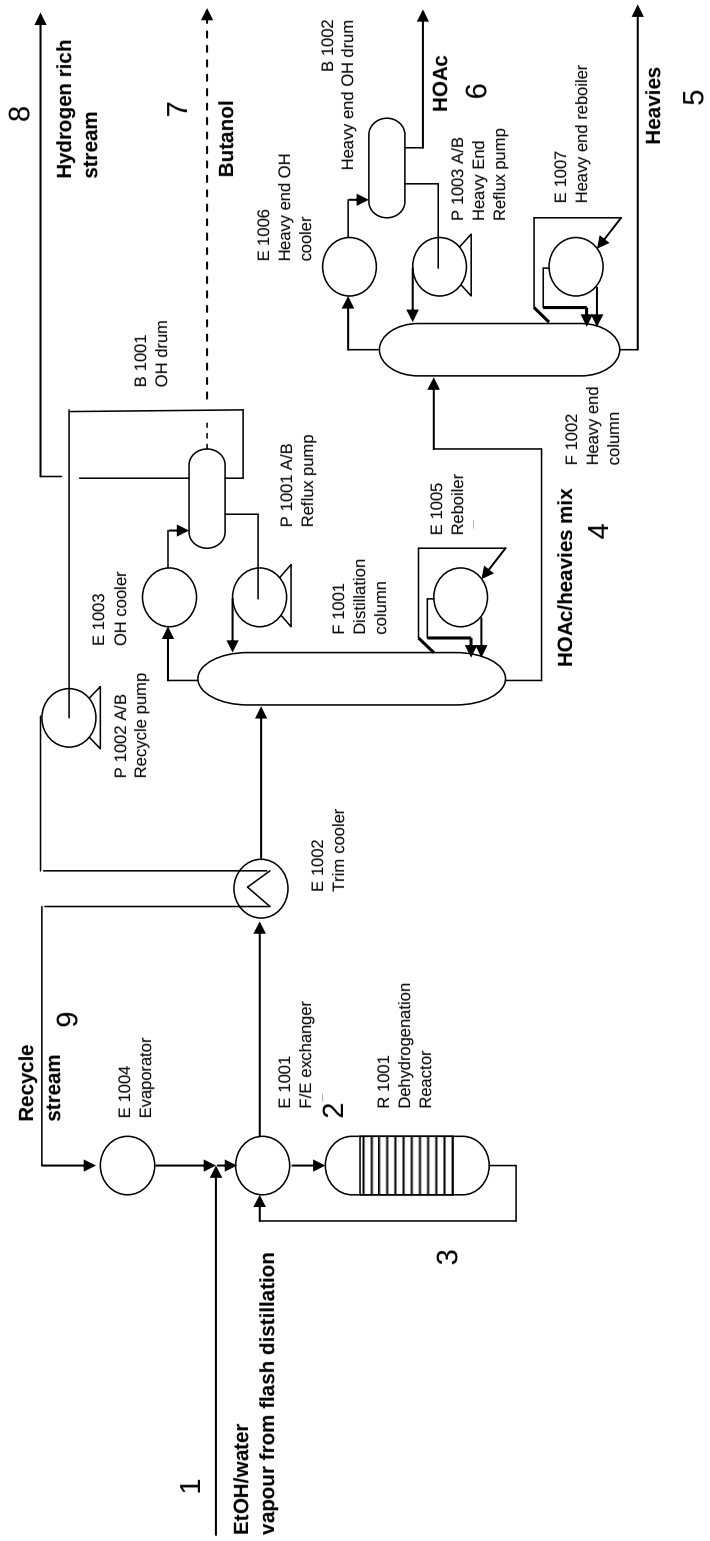

HEX	Duty (GJ/h)
E 1001	55.7
E 1002	41.8
E 1003	-147.6
E 1004	77.4
E 1005	100.2
E 1006	-21.4
E 1007	22.0
R 1001	36.1

Position	1	2	3	4	5	6	7	8	9
Pressure, bar g	2	1	1	0	0	0	0	0	2
Temperature, °C	125	305	320	118	161	118	20	20	65
Flow rate, kmol/h	1308	4832	5464	654	28	626	0	1308	3524
Composition (mol%):									
Ethanol	51.7	24.9	9.6	0	0	0	0	0	15.0
Water	48.3	50.2	33.3	0	0	0	0	0	51.0
Acetaldehyde	0	23.7	21.0	0	0	0	0	0	32.6
Ethyl acetate	0	1.1	1.0	0	0	0	0	0	1.5
Acetic acid	0	0	11.6	96.6	22.3	100.0	0	0	0
Hydrogen	0	0	23.2	0	0	0	0	100.0	0
1-Butanol	0	0	0.4	0	0	0	100.0	0	0
Heavies	0	0	0	3.4	77.7	0	0	0	0
MW, kg/kmol	32.52	31.94	28.25	61	81.88	60.05	74.12	2.02	31.73

D.3 Patent Application for the Water Balanced Non-oxidative Dehydrogenation of Ethanol to Acetic Acid

(19) Europäisches Patentamt
European Patent Office
Office européen des brevets

(11) **EP 2 192 103 A1**

(12) **EUROPEAN PATENT APPLICATION**

(43) Date of publication:
02.06.2010 Bulletin 2010/22

(51) Int Cl.:
C07C 51/00 *(2006.01)* ***C07C 51/44*** *(2006.01)*
C07C 53/08 *(2006.01)*

(21) Application number: **09013880.1**

(22) Date of filing: **05.11.2009**

(84) Designated Contracting States:
AT BE BG CH CY CZ DE DK EE ES FI FR GB GR HR HU IE IS IT LI LT LU LV MC MK MT NL NO PL PT RO SE SI SK SM TR
Designated Extension States:
AL BA RS

(30) Priority: **27.11.2008 DK 200801673**

(71) Applicant: **Haldor Topsoe A/S**
2800 Kgs. Lyngby (DK)

(72) Inventors:
- **Voss, Bodil**
  2830 Virum (DK)
- **Schiødt, Niels, Christian**
  2700 Brønshøj (DK)

(54) **Process for the conversion of ethanol to acetic acid**

(57) Process for the preparation of acetic acid comprising the steps of:
(h) providing a feed stream of water and ethanol;
(i) adding the feed stream to a recycle stream comprising unconverted ethanol and water;
(j) heating the admixture to a predetermined reaction temperature and passing the thus heated admixture over a catalyst being active in non-oxidative conversion of ethanol to acetic acid to obtain an effluent being rich in acetic acid;
(k) optionally cooling the effluent;
(1) separating the effluent into a stream rich in acetic acid being essentially free of water, a hydrogen containing stream, and a stream with unconverted amounts of ethanol, water and reactive derivates of acetic acid and optionally ethyl acetate;
(m) recycling the stream with unconverted amounts of ethanol and water to step (a);
(n) determining the amount of water in the recycle stream and adjusting the composition of the ethanol and water feed stream in step (a) to a water/ethanol mole ratio of between 0.3/0.7 to 0.6/0.4.

EP 2 192 103 A1

Printed by Jouve, 75001 PARIS (FR)

Description

[0001] The present invention relates to an improved process of converting a stream comprising ethanol and water to obtain a product rich in acetic acid. More particularly, the invention concerns the non-oxidative dehydrogenation of ethanol and water to obtain a product stream of acetic acid essentially free of water.

[0002] It has been known for several decades how to produce acetic acid from ethanol.

[0003] Ethanol can be produced from ethylene by hydrolysis and it may be produced by fermentation of sugars. Traditionally, hydrolysis of ethylene to produce ethanol has been performed to meet the technical use of ethanol, while fermentation of sugar containing matter is an ancient process the product of which is primarily used for household purposes. In the latter process, the ethanol produced is obtained in an aqueous solution in a concentration of 5-15% by weight along with fermentation by products and solids, the so-called broth.

[0004] Typically the ethanol is then distilled in two columns to obtain 96% ethanol and may finally be dried in a bed of zeolites to obtain anhydrous ethanol useful as an additive to gasoline.

[0005] As part of a new fuel supply development the capacity of bio-ethanol production for the use as gasoline additive has increased tremendously over the past 10 years, especially in Brazil and the US.

[0006] Ethanol can be converted by dehydrogenation to acetic acid via the oxidative and the non-oxidative route, viz.:

$$EtOH + O_2 = HOAc + H_2O \text{ (oxidative route)} \quad (1)$$

$$EtOH + H_2O = HOAc + 2\ H_2 \text{ (non-oxidative route)} \quad (2)$$

[0007] While the oxidative route is exothermic and not limited by equilibrium, the non-oxidative route is endothermic and equilibrium limited and proceeds via the intermediate acetaldehyde (HAc).

$$EtOH = HAc + H_2 \text{ (non-oxidative)} \quad (3)$$

[0008] It is known that e.g. copper is an active catalyst for the non-oxidative dehydrogenation of ethanol to acetic acid. Other catalysts like coal are capable to convert ethanol in the non-oxidative route to acetic acid.

[0009] Some of the catalysts being active in the non-oxidative route are active also in the esterification of ethanol and acetic acid, whereby ethyl acetate constitutes part of the product composition by the following reaction:

$$EtOH + HOAc = EtOAc + H_2O \text{ (non-oxidative)} \quad (4)$$

[0010] Examples of catalysts active in the oxidative conversion of ethanol to acetic acid are vanadium oxide, gold nanoparticles and supported palladium.

[0011] Suggestions of processes for the preparation of acetic acid from ethanol are sparse.

[0012] GB 287064 discloses an acetic acid process, where an alcohol such as ethyl alcohol is passed upward in a reactor column containing in a first bed with Ag doped Cu catalyst in its reduced state and in its oxidised state at the top of the reactor. The reduced catalyst is active in dehydrogenation of ethanol to acetaldehyde, which is oxidized by contact with the Cu oxide via acetaldehyde to acetic acid being withdrawn from the top of the reactor. Cu oxide is thereby reduced to copper. The Cu catalyst recovered from the bottom of the reactor may be reoxidized and recycled to the top of the reactor. This process employs a moving bed with Cu/CuO as catalyst and an oxygen carrier for the oxidation of ethanol to acetic acid via acetaldehyde.

[0013] Kanichiro Inui et al (Effective formation of ethyl acetate from ethanol over Cu-Zn-Zr-Al-O catalyst', Journal of Molecular Catalysis A: Chemical 216 (2004), page 147-156) describes Cu-Zn-Zr-Al-O as catalysts being active in the conversion of ethanol to ethyl acetate and to acetic acid in presence of water by non-oxidative route. It is mentioned that the selectivity to propanone decreases with increasing selectivity to acetic acid. Up to 15 wt% water in the feed is described, which corresponds to 31% on a mole basis. It is proposed that the reaction proceeds via acetaldehyde, hemiacetal and ethyl acetate to acetic acid through a final hydration.

[0014] JP 57102835 discloses a non-oxidative process for the production of acetic acid from ethanol in a first ethanol dehydrogenation reaction over a CuO and other oxidic catalysts and a hydrogen separation step. In a subsequent step acetic acid together with water is separated and acetaldehyde is separated from unconverted ethanol. This process may further comprise a second acetaldehyde dehydrogenation step to acetic acid with addition of additional water, wherein the product of this step is recycled to the hydrogen separation step and unconverted ethanol is recycled to the first ethanol dehydrogenation step.

[0015] Separation of acetic acid from water is an expensive process step which must be conducted in equipment being constructed of highly corrosion resistant material. A further disadvantage of the above process is addition of water in a second step in order to provide an oxidant for the conversion of acetaldehyde to acetic acid. The combined extraction

and addition of water in such a process scheme imposes a severe economic penalty.

[0016] The oxidative route does not offer the possibility of recovering essentially water-free acetic acid without the removal of water by-product.

[0017] It has now been found that acetic acid being essentially free of water can be produced by the non-oxidative route from an ethanol/water feed by adjusting the water content in the ethanol feed and adding water to the acetic acid preparation process exclusively together with the ethanol feed.

[0018] Pursuant to the above finding this invention provides a Process for the preparation of acetic acid comprising the steps of:

(a) providing a feed stream of water and ethanol;
(b) adding the feed stream to a recycle stream comprising unconverted ethanol and water;
(c) heating the admixture to a predetermined reaction temperature and passing the thus heated admixture over a catalyst being active in non-oxidative conversion of ethanol to acetic acid to obtain an effluent being rich in acetic acid;
(d) optionally cooling the effluent;
(e) separating the effluent into a stream rich in acetic acid being essentially free of water, a hydrogen containing stream, and a stream with unconverted amounts of ethanol, water and reactive derivates of acetic acid and optionally ethyl acetate;
(f) recycling the stream with unconverted amounts of ethanol and water to step (a);
(g) determining the amount of water in the recycle stream and adjusting the composition of the ethanol and water feed stream in step (a) to a water/ethanol mole ratio of between 0.3/0.7 to 0.6/0.4

[0019] The production of acetic acid from ethanol may involve production of by-products. In case these by-products or derivatives form azeotropes with the product mixture during the separation process, it may be beneficial to remove water along with the by-product. This is not considered extraction of water but parasitic loss of water.

[0020] The separation unit may be a conventional distillation column, where the hydrogen rich stream is retrieved from the gas phase in the reflux drum, the optional acetaldehyde containing stream is withdrawn from the top section of the distillation column and the stream containing the unconverted ethanol is withdrawn from an intermediate section of the column. The acetic acid rich stream is collected from the bottom of the distillation column.

[0021] In the process, n-butanol may be formed as a by-product. N-butanol is difficult to separate from acetic acid. By arranging a catalyst being active in the reaction of butanol with acetic acid to butyl acetate in the separation step, it is possible to convert n-butanol to n-butyl acetate and at the same time removing product water generated by the esterification of these.

[0022] Zeolites are active in the conversion of n-butanol and acetic acid to n-butyl acetate, thus a bed of zeolite catalyst may advantageously be installed in the distillation column. N-butyl acetate may in turn be removed from the acetic acid product by other means if desired.

[0023] If the separation step is performed in the distillation column at a pressure slightly below the pressure prevailing in the reaction step, temperatures from 118 up to about 150°C will be found in the bottom part of the distillation column corresponding to a temperature close to the boiling point of pure acetic acid.

[0024] The content of water in the recycle stream of the inventive process depends on the degree of conversion of the intermediate acetaldehyde (reaction 3) to acetic acid, the potential further conversion of the acetic acid with unconverted ethanol to ethyl acetate (reaction 4), the parasitic loss of water in a by-product removal and generated water from by-product or derivatives reactions.

[0025] In order to obtain a stable process producing acetic acid essentially free of water from an ethanol and water feed stream, water should only be fed in amounts that secures its complete consumption by the process.

[0026] An advantage of the present process is that the separation step results in an acetic acid product being essentially free of water during periods, where in principle the water content of the ethanol/water feed is too high as compared to above criterion. If the separation takes place in a distillation column an increase of the water content in the system may be counteracted by increasing e.g. the distillation column reflux ratio.

[0027] Further typical operation conditions comprise temperatures for the catalytic conversion of ethanol to acetic acid of 250-450°C, preferably about 250-350°C and an operation pressure of 0-10 bar, preferably 0-3 bar.

[0028] The adjustment of the amount of water in the ethanol feed stream may be managed by establishing a mass balance of the process giving a start target value of water content in the recycle stream, while increasing the water content in the feed after measuring the decrease of water content in the recycle stream and vice versa.

[0029] The water content in the recycle stream may be determined by e.g. an online dew point transmitter. Other principles of control may be applied as well.

[0030] According to the non-oxidative dehydrogenation reaction 2), equimolar amounts of ethanol and water are required at start conditions of the process.

[0031] An equimolar feed of ethanol and water corresponds to a 71.9 wt% ethanol and 28.1 wt% water mixture.

[0032] The equimolar feed may be obtained in a side stream from an ethanol plant producing bio-ethanol or fuel-ethanol, de-bottlenecking the process. As an example, such a side stream may be obtained as a vapour stream from a distillation section of an ethanol plant, whereby evaporation of the ethanol/water feed is avoided. It may be advantageous therefore to integrate the inventive process into an ethanol plant, where ethanol and water are present in suitable amounts and especially where the feed is vaporised.

[0033] The amount of water in the feed can be adjusted by adding small amounts of steam/water to an un-adjusted feed of ethanol being lean in water.

[0034] Suitable ethanol conversion catalysts are any catalyst being active in the conversion of ethanol to acetic acid via acetaldehyde dehydrogenation at the above conditions. Preferred catalysts include those which further catalyse the reaction of ethanol with acetic acid to obtain ethyl acetate. Examples of catalysts active in the dehydrogenation of ethanol to acetic acid are copper based, optionally in combination with zinc oxide, chromium oxide, manganese oxide, zirconium oxide and/or aluminium oxide or a catalyst comprising the above oxides supported on an inert carrier.

[0035] Figure 1 is a simplified flow sheet of an embodiment of the invention, where a stream of evaporated ethanol and water is used as fed to the process. The feed stream is mixed with an evaporated recycle stream primarily comprising unconverted ethanol, acetaldehyde, water and ethyl acetate.

[0036] In the following Example condensation products are higher boiling alcohols, subject to esterification in the distillation column provided by the active catalyst bed (e.g. HZSM-5) arranged within a distillation column.

[0037] Example 1, below, demonstrates that an adjusted feed stream of ethanol and water results in no extra additions or extractions of water for the production of acetic acid essentially free of water.

Example 1

[0038] Reference is made to Figure 1. A feed 10(1 kmol/h as per example) consisting of adjusted amounts of ethanol and water is added to an evaporated recycle stream 100. The admixture is preheated in feed-effluent heat exchanger 20 and further in preheater 30 in order to reach a proper reaction temperature of the reactor feed 40. The conversion of reactor feed 40 is carried out in acetic acid reactor 50 in presence of a copper aluminate catalyst. The reactor effluent 60 leaving at 320°C is cooled in the F/E exchanger 20 before being passed to distillation column 70. In the distillation column acetic acid product and higher alcohols (heavies) are withdrawn from the bottom of the column in line 80 while hydrogen rich co-product 90 is withdrawn from the overhead of the column. An intermediate boiling fraction comprising acetaldehyde, ethyl acetate, ethanol, water which forms recycle stream 100 is withdrawn as a liquid either from the column overhead together with hydrogen and separated from hydrogen in separator 85. Recycle stream 100 may preferable be withdrawn from column 70 at a lower tray, as shown by the dotted line.

[0039] Table 1 summarizes the numbers of a mass balance in the above process being operated with an adjusted ethanol/water feed.

Table 1

Stream no.	10	40	60	80	90	100
Weight %						
Water	26.0	28.0	20.4			28.8
Ethanol	74.0	30.3	9.1			12.7
Acetaldehyde		38.4	38.8		18.0	53.9
Ethyl acetate		3.2	3.2			4.5
Acetic acid			26.1	95.9		
Hydrogen			1.8		82.0	
Condensation products			0.7	4.1		
Flow rate Kg/h	32.8	119.0	114.0	30.6	2.5	81.2

Claims

1. Process for the preparation of acetic acid comprising the steps of:

(a) providing a feed stream of water and ethanol;

(b) adding the feed stream to a recycle stream comprising unconverted ethanol and water;
(c) heating the admixture to a predetermined reaction temperature and passing the thus heated admixture over a catalyst being active in non-oxidative conversion of ethanol to acetic acid to obtain an effluent being rich in acetic acid;
(d) optionally cooling the effluent;
(e) separating the effluent into a stream rich in acetic acid being essentially free of water, a hydrogen containing stream, and a stream with unconverted amounts of ethanol, water and reactive derivates of acetic acid and optionally ethyl acetate;
(f) recycling the stream with unconverted amounts of ethanol and water to step (a);
(g) determining the amount of water in the recycle stream and adjusting the composition of the ethanol and water feed stream in step (a) to a water/ethanol mole ratio of between 0.3/0.7 to 0.6/0.4

2. Process of claim 1, wherein the effluent of step (c) further contains acetaldehyde.

3. Process of claim 1, wherein the predetermined reaction conditions in step (c) comprise an operation temperatures for the catalytic conversion of ethanol to ace tic acid of 250-450°C, preferably about 250-350°C and an operation pressure of 0-10 bar, preferably 0-3 bar.

4. Process of claim 1, wherein the acetic acid rich stream is separated from the effluent in step (e) by means of distillation in a distillation column being provided with a bed of a zeolitic catalyst.

5. Process in accordance with anyone of the preceding claims, wherein the feed stream of water and ethanol is a side-stream from an ethanol-plant.

6. Process of claim 5, wherein the side-stream is with drawn from a distillation section of the ethanol-plant.

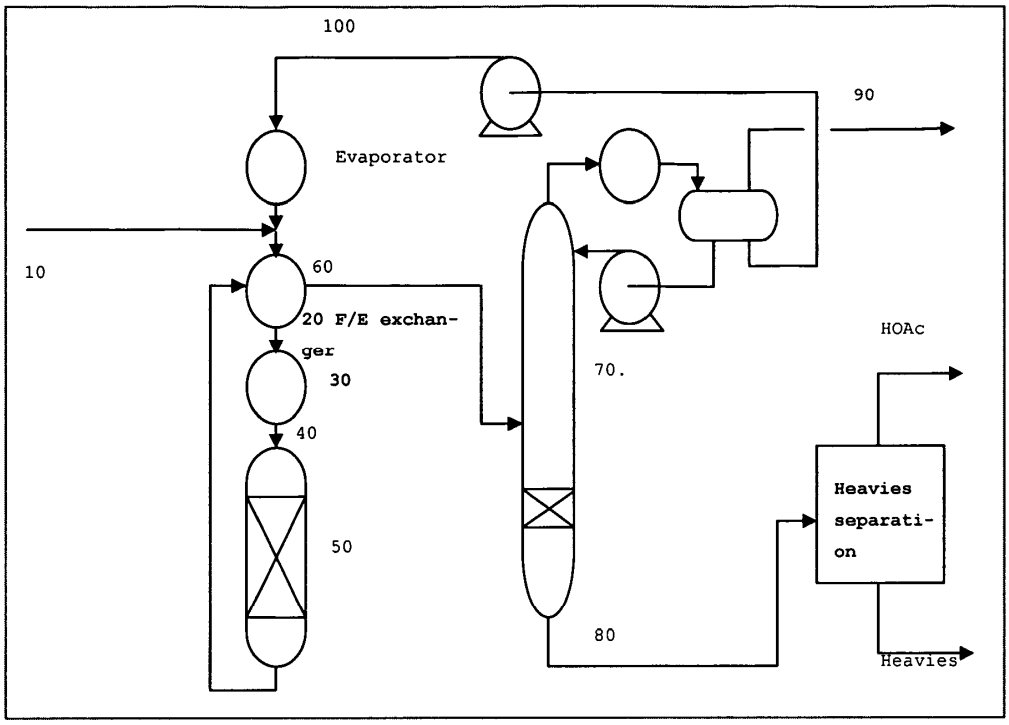
100
90
Evaporator
10
60
20 F/E exchan-
ger
30
40
50
70.
HOAc
Heavies
separati-
on
80
Heavies

Figure 1

EP 2 192 103 A1

Europäisches Patentamt
European Patent Office
Office européen des brevets

EUROPEAN SEARCH REPORT

Application Number
EP 09 01 3880

DOCUMENTS CONSIDERED TO BE RELEVANT

Category	Citation of document with indication, where appropriate, of relevant passages	Relevant to claim	CLASSIFICATION OF THE APPLICATION (IPC)
X Y	US 2 184 555 A (KENYON WILLIAM O) 26 December 1939 (1939-12-26) * the whole document *	1-3,5-6 4	INV. C07C51/00 C07C51/44 C07C53/08
Y	US 6 730 806 B2 (WU KUO-CHING [TW] ET AL) 4 May 2004 (2004-05-04) * claims 6,8,10,11; examples 1,3 *	4	
A	US 1 951 280 A (HALE WILLIAM J ET AL) 13 March 1934 (1934-03-13) * the whole document *	1-6	
A	US 2 690 993 A (MCGRATH HENRY G) 5 October 1954 (1954-10-05) * the whole document *	4	

TECHNICAL FIELDS SEARCHED (IPC)
C07C

The present search report has been drawn up for all claims

Place of search	Date of completion of the search	Examiner
Munich	18 March 2010	Bedel, Christian

CATEGORY OF CITED DOCUMENTS

X : particularly relevant if taken alone
Y : particularly relevant if combined with another document of the same category
A : technological background
O : non-written disclosure
P : intermediate document

T : theory or principle underlying the invention
E : earlier patent document, but published on, or after the filing date
D : document cited in the application
L : document cited for other reasons

& : member of the same patent family, corresponding document

1

EPO FORM 1503 03.82 (P04C01)

ANNEX TO THE EUROPEAN SEARCH REPORT ON EUROPEAN PATENT APPLICATION NO. EP 09 01 3880

This annex lists the patent family members relating to the patent documents cited in the above-mentioned European search report. The members are as contained in the European Patent Office EDP file on
The European Patent Office is in no way liable for these particulars which are merely given for the purpose of information.

18-03-2010

Patent document cited in search report	Publication date	Patent family member(s)	Publication date
US 2184555 A	26-12-1939	NONE	
US 6730806 B2	04-05-2004	TW 575557 B	11-02-2004
		US 2003109742 A1	12-06-2003
US 1951280 A	13-03-1934	NONE	
US 2690993 A	05-10-1954	NONE	

EPO FORM P0459

For more details about this annex : see Official Journal of the European Patent Office, No. 12/82

REFERENCES CITED IN THE DESCRIPTION

This list of references cited by the applicant is for the reader's convenience only. It does not form part of the European patent document. Even though great care has been taken in compiling the references, errors or omissions cannot be excluded and the EPO disclaims all liability in this regard.

Patent documents cited in the description

- GB 287064 A **[0012]**
- JP 57102835 B **[0014]**

Non-patent literature cited in the description

- **Kanichiro Inui et al.** Effective formation of ethyl acetate from ethanol over Cu-Zn-Zr-Al-O catalyst. *Journal of Molecular Catalysis A: Chemical,* 2004, vol. 216, 147-156 **[0013]**

D.4 Priority Patent Application for the partly oxidative dehydrogenation of ethanol to acetic acid

(19) Europäisches Patentamt
European Patent Office
Office européen des brevets

(11) EP 2 194 036 A1

(12) EUROPEAN PATENT APPLICATION

(43) Date of publication:
09.06.2010 Bulletin 2010/23

(51) Int Cl.:
C07C 45/38 *(2006.01)* ***B01J 8/04*** *(2006.01)*

(21) Application number: **09013879.3**

(22) Date of filing: **05.11.2009**

(84) Designated Contracting States:
AT BE BG CH CY CZ DE DK EE ES FI FR GB GR HR HU IE IS IT LI LT LU LV MC MK MT NL NO PL PT RO SE SI SK SM TR
Designated Extension States:
AL BA RS

(30) Priority: **27.11.2008 DK 200801672**

(71) Applicant: **Haldor Topsoe A/S**
2800 Kgs. Lyngby (DK)

(72) Inventors:
- **Christensen, Claud, Hviid**
  3540 Lynge (DK)
- **Schiødt, Niels, Christian**
  2700 Brønshøj (DK)
- **Voss, Bodil**
  2830 Virum (DK)

(54) **Process and reactor for the thermoneutral conversion of ethanol to acetic acid**

(57) Process for the production of acetic acid comprising the steps of:
(a) passing a feed stream containing ethanol and water together with a predetermined feed rate of an oxygen containing atmosphere in presence of one or more catalysts being active in simultaneous non-oxidative and oxidative conversion of ethanol to a product stream with acetic acid;
(b) recovering from the product stream a stream of acetic acid;
(c) optionally recovering reactive derivatives of acetic acid and recycling these to step (a).

A reactor for use in the process comprises a first and at least a second fixed catalyst bed with a catalyst being active in simultaneous non-oxidative and oxidative conversion of ethanol to acetic acid;
inlet means for a fed stream comprising ethanol, water and a first portion of an oxygen containing atmosphere to the first catalyst bed;
between the first and at least second catalyst bed inlet means for a second portion of the oxygen containing atmosphere and means for distributing and mixing the second portion of the oxygen containing atmosphere into an effluent of partly converted feed stream from the first catalyst bed; and
means for passing the partly converted feed stream and admixed with the oxygen containing atmosphere into the at least second catalyst bed.

EP 2 194 036 A1

Printed by Jouve, 75001 PARIS (FR)

Description

[0001] The present invention relates to a process for the conversion of ethanol and water to a product rich in acetic acid. More particularly, the invention is a process for combined oxidative and non-oxidative dehydrogenation of ethanol to acetic acid.

[0002] Different methods for the preparation of acetic acid from ethanol have been known for many years.

[0003] Ethanol can be produced from ethylene by hydrolysis, and it may be produced by fermentation of sugars. Typically, hydrolysis of ethylene to ethanol has been preferred primarily to meet the technical use of ethanol, while fermentation of sugar containing matter is an ancient process the product of which is primarily used for household purposes. In the latter process the ethanol produced is obtained in an aqueous solution in a concentration of 5-15% by weight along with fermentation by products and solids, the so-called broth.

[0004] Typically, the ethanol is then distilled in two columns to obtain 96% ethanol and may finally be dried in a bed of zeolites to obtain anhydrous ethanol useful as an additive to gasoline.

[0005] As part of a new fuel supply development the capacity of bio-ethanol production for the use as gasoline additive has increased tremendously over the past 10 years, especially in Brazil and the US.

[0006] Ethanol can be converted by dehydrogenation to acetic acid via the oxidative and the non-oxidative route, viz.:

$$(1)\ EtOH + O_2 = HOAc + H_2O \quad \text{(oxidative route)}$$
$$(2)\ EtOH + H_2O = HOAc + 2\,H_2 \quad \text{(non-oxidative route)}$$

[0007] The oxidative route is exothermic ($-\Delta H^{l}$ = 439 kJ/mol) and not limited by equilibrium and the non-oxidative route is endothermic ($-\Delta H^{l}$ = -44 kJ/mol) and equilibrium limited producing acetaldehyde as an intermediate.

[0008] It is known that e.g. copper is an active catalyst for the non-oxidative dehydrogenation of ethanol to acetic acid. Other catalysts like coal are capable to convert ethanol in the non-oxidative route to acetic acid.

[0009] Some of the catalysts active in the non-oxidative route are active also in the esterification of ethanol and acetic acid, whereby ethyl acetate constitutes part of the product composition. Typical by-products in the non-oxidative route are coupling reaction products ketone, aldehyde and alcohol products, e.g. propanon, butanal and butanol.

[0010] Examples of catalysts active in the oxidative conversion of ethanol to acetic acid are vanadium oxide, gold nanoparticles and supported palladium.

[0011] Suggestions of processes to make acetic acid from ethanol are sparse.

[0012] GB 287064 discloses an acetic acid process, where an alcohol such as ethyl alcohol is passed upward in a reactor column containing in a first bed an Ag doped Cu catalyst in its reduced state and in its oxidised state at the top of the reactor. The reduced catalyst provides for dehydrogenation of ethanol to acetaldehyde, which is oxidized by contact with Cu oxide to acetic acid being withdrawn from the top of the reactor. Cu oxide is thereby reduced to copper. The Cu catalyst recovered from the bottom of the reactor may be reoxidized and recycled to the top of the reactor. This process employs a moving bed with Cu/CuO as catalyst and an oxygen carrier for the oxidation of ethanol to acetic acid via acetaldehyde.

[0013] Kanichiro Inui et al (Effective formation of ethyl acetate from ethanol over Cu-Zn-Zr-Al-O catalyst', Journal of Molecular Catalysis A: Chemical 216 (2004), page 147-156) describes Cu-Zn-Zr-Al-O as catalysts being active in the conversion of ethanol to ethyl acetate and to acetic acid in presence of water by non-oxidative route. It is mentioned that the selectivity to propanone decreases with increasing selectivity to acetic acid. Up to 15 wt% water in the feed is described, which corresponds to 31% on a mole basis. It is proposed that the reaction proceeds via acetaldehyde, hemiacetal and ethyl acetate to acetic acid through a final hydration.

[0014] JP 57102835 discloses a non-oxidative process for the production of acetic acid from ethanol in a first ethanol dehydrogenation reaction over a CuO and other oxidic catalysts and a hydrogen separation step. In a subsequent step acetic acid together with water is separated and acetaldehyde is separated from unconverted ethanol. This process may further comprise a second acetaldehyde dehydrogenation step to acetic acid with addition of additional water, wherein the product of this step is recycled to the hydrogen separation step and unconverted ethanol is recycled to the first ethanol dehydrogenation step.

[0015] When carrying out a non-oxidative synthesis of acetic acid from ethanol, the catalyst may be arranged in an adiabatic reactor or in a heated reactor. The adiabatic reactor type is cheap to operate, however, a large temperature decrease over the reactor results in a lower product yield or requires high internal cooling rate or recycle rate in order to limit the temperature decrease over the reactor.

[0016] The heated reactor is an expensive alternative due to its more complicated construction. Furthermore, a heat source is required to supply the heat for the reaction.

[0017] The conversion of ethanol to acetic acid via the oxidative route is strongly exothermic. Due to the strong exothermic nature the reaction must be performed in a reactor type provided with efficient heat removal means, i.e. high

areas of heat transfer are mandatory, which results in an expensive design. Furthermore, risks of temperature run-away and general selectivity problems are negative results of strong exothermic reactions.

[0018] In contrast to the above discussed reaction types, a process without a heat requirement, a so called thermoneutral process, does not require special means of heat supply or heat removal in the reactor. Ideally, if a chemical process takes place at a temperature higher than ambient, a slightly exothermic process supplies heat for the preheating of the feed by heat exchange with the hot reactor effluent having a temperature higher than the feed.

[0019] Processes where the adiabatic temperature increase is moderate or low are considered to be thermoneutral. In context with the invention, reactions having a ΔH^{l} and specific heat capacity of the reactants resulting in an adiabatic change of the temperature between about -25 to 25°C are considered thermoneutral.

[0020] The general object of this invention is to provide a process for the production of acetic acid, wherein a feed stream of ethanol and water is converted to acetic acid in a thermoneutral manner.

[0021] It has been found that a feed stream comprising ethanol, water and oxygen can be converted over a bed of reduced copper based catalyst at thermoneutral conditions with a high yield of acetic acid and considerably reduced formation of carbon dioxide compared to the oxidative acetic acid reaction. The condition of such a process require adjustment of the oxygen content in the feed in such manner as to allow for a thermoneutral process without suffering a severe loss of selectivity.

[0022] Pursuant to the above findings, the present invention is a process for the production of acetic acid comprising the steps of:

(a) passing a feed stream containing ethanol and water together with a predetermined feed rate of an oxygen containing atmosphere in presence of one or more catalysts being active in simultaneous non-oxidative and oxidative conversion of ethanol to a product stream with acetic acid according to the following reaction:

$$CH_3CH_2OH + yH_20 + xO_2 = CH_3COOH + 2(1\text{-}x)H_2 + y\text{-}(1\text{-}2x)H_20\ ,$$

wherein
x is the molar ratio of oxygen to ethanol,
y is the molar ratio of water to ethanol, and
wherein
y is at least (1-2x);
(b) recovering from the product stream a stream of acetic acid;
(c) optionally recovering reactive derivatives of acetic acid and recycling these to step (a).

[0023] Typical operation temperatures for the catalytic conversion of ethanol to acetic acid are 250-450°C, preferably about 250-350°C. The operation pressure is between 0 and 10 bar, preferably 0-3 bar.

[0024] A thermoneutral process in accordance with the previous definition is controlled by the molar ratio of oxygen to ethanol.

[0025] The amount of the oxygen containing atmosphere is preferably adjusted so that the exit temperature from the reaction is higher than the inlet temperature in order to supply heat for preheating of the feed stream with the hot product stream.

[0026] The dehydrogenation reactions of ethanol to acetic acid proceed by the following reaction schemes:

$$CH_3CH_2OH + H_2O = CH_3COOH + 2H_2 \text{ (endothermic, non-oxidative)}$$

$$2xH_2 + x\ O_2 = 2x\ H_2O \text{ (exothermic oxidation of hydrogen)}$$

where x is the fraction of ethanol converted by the oxidative reaction (1)

[0027] A balance of the standard heats of reaction requires a stoichiometry representing 91% non-oxidative and 9% oxidative, i.e. x=0.09, or $CH_3CH_2OH + 0.82H_2O + 0.09\ O_2 = CH_3COOH + 1.82H_2$.

[0028] In a thermoneutral process being within the scope of the invention, x may deviate from 0.09 and still provide for a temperature increase/decrease of less than 25°C. Preferably, the molar ratio of oxygen to ethanol is between 0.0045 and 0.25.

[0029] The by-product formation of CO_2 proceeds according to the reaction scheme:

$$CH_3CH_2OH + 3\ O_2 = 2\ CO_2 + 3\ H_2O$$

[0030] The utility of the process depends on the selectivity towards acetic acid instead of carbon dioxide in the oxidative conversion part of ethanol to acetic acid.

[0031] A stoichiometric ratio of ethanol to water in a thermoneutral process for the conversion of ethanol and water to acetic acid can be adjusted in e.g. a side stream from an ethanol plant producing bio-ethanol or fuel-ethanol, thereby de-bottlenecking the ethanol production. Such a side-stream may advantageously be obtained as a vapour stream withdrawn from the distillation section of the ethanol plant, whereby a need for evaporation of the ethanol/water feed is avoided. The amount of oxygen to be added for obtaining a thermoneutral process is moderate and appropriate ratios may be obtained by adding compressed atmospheric air to the process.

[0032] It may therefore be advantageous to integrate the process according to the invention into an ethanol plant, where ethanol and water are present in suitable concentrations and especially where the feed is vaporised.

[0033] The hydrogen co-product generated during the process may be recovered from the product mixture in a hydrogen rich stream by conventional methods such as phase separation, distillation, membrane etc.

[0034] The recovered hydrogen rich stream can be passed to a fuel cell in order to convert chemical energy to electrical power and heat. Advantageously, the fuel cell is of a type where the heat generated is removed at a temperature which can supply the heat needed in the ethanol plant or the acetic acid plant, e.g. for distillation reboiler or preheating. Another advantage of combining the acetic acid plant with a fuel cell is that the air supply is common to the dehydrogenation process as well as to the fuel cell. In both processes the air is preferably supplied at a pressure slightly above atmospheric pressure, e.g. 1-5 bar. By employing the air blower for the supply of air to both units, a reduction of the inventory is achieved. Thus, in a preferred embodiment of the invention the hydrogen rich product from the dehydrogenation process is passed to a fuel cell for the generation of electricity and heat, the fuel cell being supplied with air for the oxidation of the fuel from an air blower supplies additionally air to the acetic acid process.

[0035] Catalyst/s being useful in the process according to the invention are any being active in the conversion of ethanol to acetic acid via the oxidative and non-oxidative route. The group of useful catalysts include those which further catalyse the conversion of ethanol with acetic acid to obtain ethyl acetate. Examples of catalysts active in the dehydrogenation of ethanol with water to acetic acid are Cu based, optionally in combination with zinc oxide, chromium oxide, manganese oxide, zirconium oxide and/or aluminium oxide, or a catalyst comprising the above supported on an inert carrier.

[0036] The invention provides furthermore a reactor for the thermoneutral production of acetic acid as described hereinbefore.

[0037] The reactor according to invention comprises a first and at least a second fixed catalyst bed with one or more catalysts being active in simultaneous non-oxidative and oxidative conversion of ethanol to acetic acid; inlet means for a feed stream comprising ethanol, water and a first portion of an oxygen containing atmosphere to the first catalyst bed; between the first and at least second catalyst bed inlet means for a second portion of the oxygen containing atmosphere and means for distributing and mixing the second portion of the oxygen containing atmosphere into an effluent of partly converted feed stream from the first catalyst bed; and
means for passing the partly converted feed stream and admixed with the oxygen containing atmosphere into the at least second catalyst bed.

[0038] The above invention will be described in more detail in the below Examples 1 and 2.

[0039] In Example 1, a product stream rich in acetic acid is prepared by passage of a feed composition having a stoichiometry corresponding to a thermoneutral dehydrogenation of ethanol to acetic acid over a bed of catalyst being active both in the oxidative and the non-oxidative dehydrogenation of ethanol and water for the preparation of the acetic acid product.

Example 1

[0040] In an experimental setup a feed stream of 52.7% ethanol, 47.3% water was fed at a rate of 21.4 g/h by a HPLC pump. The feed stream was evaporated, mixed with O_2 at a rate of 0.77 Nl/h and passed over a $CuAl_2O_4$catalyst at 320°C and atmospheric pressure in gas phase together with a nitrogen carrier gas stream at a feed rate of 11.5 Nl/h. The product obtained from the conversion was fractioned into a condensate and a gas fraction. The produced condensate was formed at rate of 16.9 g/h and had a composition of 55.95% H_2O, 14.66% acetic acid, 20.12% acetaldehyde, 8.39% ethanol, 0.62% ethyl acetate and less than 0.3% coupling by-products. The gas fraction was formed at a rate of 21.2 Nl/h having a composition of 54.19% N_2, 0.73% CO_2, 11.11% acetaldehyde and 33.96% hydrogen.

[0041] As can be calculated from above figures the selectivity of ethanol to acetic acid or reactive derivatives is 98.8%.

Example 2

[0042] The experiment in Example 1 was repeated; however, oxygen was added in two portions. In an experimental setup a feed stream of 52.7% ethanol, 47.3% water was fed at a rate of 21.4 g/h by a HPLC pump, mixed with O_2 at a rate of 0.385 Nl/h and passed over 5 g of the catalyst at 320°C and atmospheric pressure in the gas phase together with a nitrogen carrier gas stream at a feed rate of 11.4 Nl/h. The product obtained from the first conversion was mixed

with further a second portion of O_2 at a rate of 0.385 Nl/h and passed over second bed of the catalyst maintained at 320°C. The product obtained from the second conversion was cooled and fractioned into a condensate and a gas fraction. A condensate rate of 17.1 g/h with a composition of 56.33% H_2O, 14.55% acetic acid, 19.98% acetaldehyde, 8.27% ethanol 0.61% ethyl acetate and less than 0.3% coupling by-products was obtained. A product gas rate of 20.9 Nl/h was measured with a composition of 55.1% N2, 0.25% CO_2, 11.4% acetaldehyde and 33.3% hydrogen.

[0043] As can be calculated from above figures the selectivity of ethanol to carbon dioxide of 0.4% is found, which is only one third of the selectivity found with one addition of oxygen.

Claims

1. Process for the production of acetic acid comprising the steps of:

   (a) passing a feed stream containing ethanol and water together with a predetermined feed rate of an oxygen containing atmosphere in presence of one or more catalysts being active in simultaneous non-oxidative and oxidative conversion of ethanol to a product stream with acetic acid according to the following reaction:

   $$CH_3CH_2OH + yH_20 + xO_2 = CH_3COOH + 2(1\text{-}x)H_2 + y\text{-}(1\text{-}2x)H_20\ ,$$

   wherein
   x is the molar ratio of oxygen to ethanol,
   y is the molar ratio of water to ethanol and wherein
   y is at least (1-2x);
   (b) recovering from the product stream a stream of acetic acid;
   (c) optionally recovering reactive derivatives of acetic acid and recycling these to step (a).

2. Process of claim 1, wherein the feed rate of the oxy gen containing atmosphere corresponds to a molar ratio of oxygen to ethanol is between 0.0045 and 0.25.

3. Process of claims 1 and 2, wherein the oxygen containing atmosphere is air.

4. Process in accordance with anyone of the preceding claims, wherein the feed stream of water and ethanol is a side-stream from an ethanol-plant.

5. Process of claim 4, wherein the side-stream is withdrawn from a distillation section of the ethanol plant.

6. Reactor for the thermoneutral conversion of ethanol to acetic acid comprising a first and at least a second fixed catalyst bed with a catalyst being active in simultaneous non-oxidative and oxidative conversion of ethanol to acetic acid;
   inlet means for a fed stream comprising ethanol, water and a first portion of an oxygen containing atmosphere to the first catalyst bed;
   between the first and at least second catalyst bed inlet means for a second portion of the oxygen containing atmosphere and means for distributing and mixing the second portion of the oxygen containing atmosphere into an effluent of partly converted feed stream from the first catalyst bed; and
   means for passing the partly converted feed stream and admixed with the oxygen containing atmosphere into the at least second catalyst bed.

EP 2 194 036 A1

Europäisches Patentamt
European Patent Office
Office européen des brevets

EUROPEAN SEARCH REPORT

Application Number
EP 09 01 3879

DOCUMENTS CONSIDERED TO BE RELEVANT

Category	Citation of document with indication, where appropriate, of relevant passages	Relevant to claim	CLASSIFICATION OF THE APPLICATION (IPC)
X	US 4 220 803 A (HENRY JOSEPH P [US] ET AL) 2 September 1980 (1980-09-02) * column 2, line 1 - line 28; claims; examples *	1-5	INV. C07C45/38 B01J8/04
X	US 3 248 453 A (BEYRARD NORBERT R) 26 April 1966 (1966-04-26) * figures *	6	
A	US 5 840 971 A (GUBELMANN-BONNEAU MICHEL [FR]) 24 November 1998 (1998-11-24) * claims; examples *	1-5	
A	US 1 911 315 A (CARL HANER ET AL) 30 May 1933 (1933-05-30) * page 2, line 92 - page 3, line 20 *	1-6	

TECHNICAL FIELDS SEARCHED (IPC)
C07C
B01J

The present search report has been drawn up for all claims

Place of search	Date of completion of the search	Examiner
Munich	30 March 2010	Bedel, Christian

CATEGORY OF CITED DOCUMENTS
X : particularly relevant if taken alone
Y : particularly relevant if combined with another document of the same category
A : technological background
O : non-written disclosure
P : intermediate document

T : theory or principle underlying the invention
E : earlier patent document, but published on, or after the filing date
D : document cited in the application
L : document cited for other reasons

& : member of the same patent family, corresponding document

EPO FORM 1503 03.82 (P04C01)

3

ANNEX TO THE EUROPEAN SEARCH REPORT ON EUROPEAN PATENT APPLICATION NO. EP 09 01 3879

This annex lists the patent family members relating to the patent documents cited in the above-mentioned European search report. The members are as contained in the European Patent Office EDP file on
The European Patent Office is in no way liable for these particulars which are merely given for the purpose of information.

30-03-2010

Patent document cited in search report	Publication date	Patent family member(s)	Publication date
US 4220803 A	02-09-1980	NONE	
US 3248453 A	26-04-1966	CH 409917 A	31-03-1966
		DE 1193493 B	26-05-1965
		ES 267230 A1	01-11-1961
		FR 1271069 A	08-09-1961
		GB 923041 A	10-04-1963
		LU 40131 A	15-11-1961
		NL 264761 A	
US 5840971 A	24-11-1998	CO 4410241 A1	09-01-1997
		FR 2716450 A1	25-08-1995
		ZA 9501331 A	23-10-1995
US 1911315 A	30-05-1933	NONE	

EPO FORM P0459

For more details about this annex : see Official Journal of the European Patent Office, No. 12/82

REFERENCES CITED IN THE DESCRIPTION

This list of references cited by the applicant is for the reader's convenience only. It does not form part of the European patent document. Even though great care has been taken in compiling the references, errors or omissions cannot be excluded and the EPO disclaims all liability in this regard.

Patent documents cited in the description

- GB 287064 A **[0012]**
- JP 57102835 B **[0014]**

Non-patent literature cited in the description

- **Kanichiro Inui et al.** Effective formation of ethyl acetate from ethanol over Cu-Zn-Zr-Al-O catalyst. *Journal of Molecular Catalysis A: Chemical,* 2004, vol. 216, 147-156 **[0013]**

D.5 Patent Application for the Integrated VAM process

US 20110137074A1

(19) **United States**

(12) **Patent Application Publication** (10) **Pub. No.: US 2011/0137074 A1**

Voss et al. (43) **Pub. Date: Jun. 9, 2011**

(54) **PROCESS FOR THE PRODUCTION OF ACETIC ACID ETHYLENE AND VINYL ACETATE MONOMER**

(76) Inventors: **Bodil Voss**, Virum (DK); **Rachid Mabrouk**, Malmo (SE); **Claus Hviid Christensen**, Lynge (DK)

(21) Appl. No.: **12/963,402**

(22) Filed: **Dec. 8, 2010**

(30) **Foreign Application Priority Data**

Dec. 8, 2009 (DK) PA2009 01291

Publication Classification

(51) **Int. Cl.**
C07C 67/54 (2006.01)

(52) **U.S. Cl.** **560/248**

(57) **ABSTRACT**

An integrated process for the production of acetic acid, ethylene and vinyl acetate monomer comprising the steps of:

(a) evaporating at least part of an ethanol feed stock

(b) producing in a first reaction zone a first product stream comprising acetic acid by oxidative or partly oxidative dehydrogenation of ethanol feed stock;

(c) producing in a second reaction zone a second product stream comprising ethylene from an ethanol feed stock;

(d) reacting in a third reaction zone an acetic acid reaction stream containing at least a portion of the acetic acid from the first reaction zone with an ethylene reaction stream containing at least a portion of the ethylene product from the second reaction zone and with oxygen to a third product stream comprising vinyl acetate monomer;

(e) passing at least a portion of the third product stream to a distillation section and isolating at least a portion of the vinyl acetate monomer;

(f) supplying at least part of reaction heat from the third reaction zone to provide heat for evaporating at least part of the ethanol feed stock in step (a);

(g) supplying at least part of reaction heat from the first reaction zone to provide heat for producing the second product stream in the second reaction zone in step (c) and for distilling of the third product stream in the distillation section in step (e).

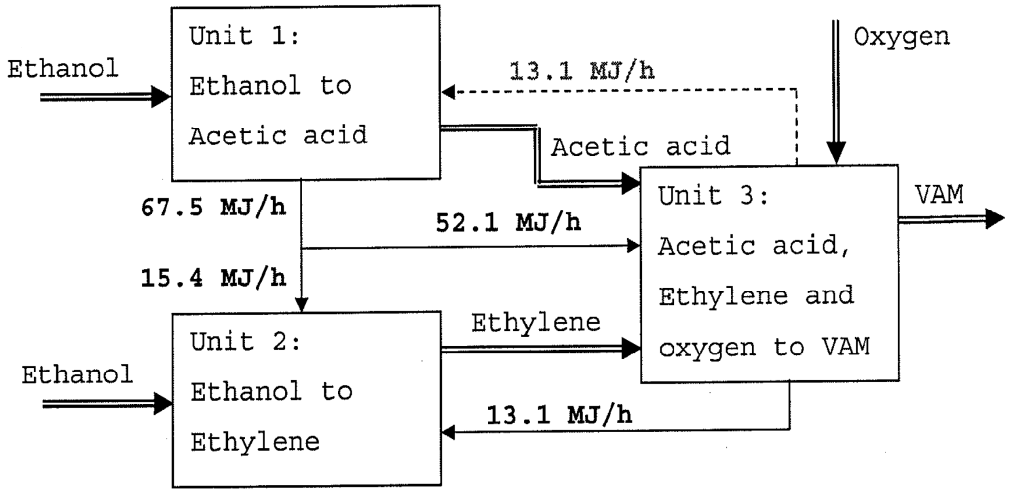

Patent Application Publication Jun. 9, 2011 US 2011/0137074 A1

Figure 1

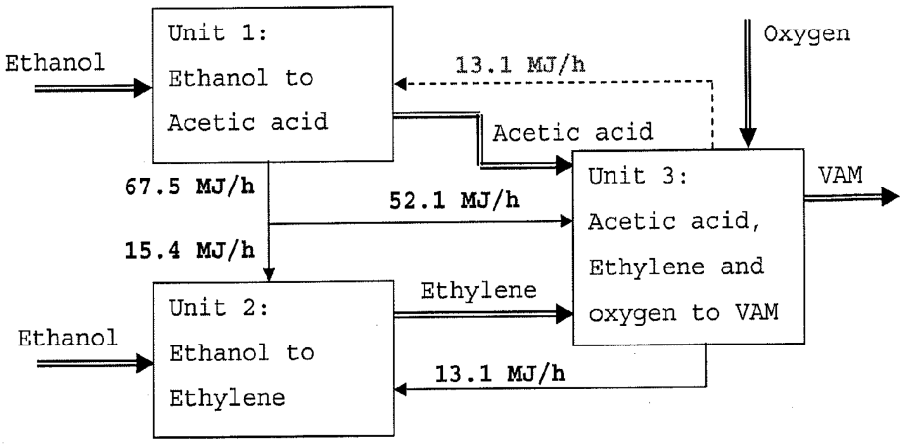

US 2011/0137074 A1 Jun. 9, 2011

PROCESS FOR THE PRODUCTION OF ACETIC ACID ETHYLENE AND VINYL ACETATE MONOMER

[0001] This invention relates to an improved process for the preparation of ethylene and acetic acid being and use of these compounds as feed stock in the production of vinyl acetate monomer (VAM). In particular, the invention is directed to internal supply of heat to the VAM process by an integrated process comprising heat transfer between all steps of the process.

[0002] Since the 1960's processes were developed for the production of VAM from ethylene, oxygen and acetic acid in presence of catalysts comprising Pd optionally doped with Au, Rh or Cd and promoted with alkali acetate by the following reaction:

$$C_2H_4+CH_3COOH+½O_2=VAM+H_2O$$

[0003] This reaction is accompanied by the detrimental side reaction of complete ethylene oxidation:

$$C_2H_4+3O_2=2CO_2+2H_2O$$

[0004] Due to the sensitivity of the catalyst, the temperature must be kept below a certain temperature depending on the actual catalyst.

[0005] In addition to the above catalysts, other catalysts being useful in the production of VAM are known in the art. Examples of such catalysts are mentioned in U.S. Pat. No. 6,022,823, U.S. Pat. No. 6,057,260 and U.S. Pat. No. 6,472,556. The catalysts may be supported on carriers including silica, silica-alumina or other metal oxides.

[0006] Typically, the upper temperature limit in the VAM synthesis is 200° C. and the lower temperature limit is 130° C. Below 130° C. the activity of the catalyst is insufficient and there exists a risk of condensation of acetic acid. This leaves a relatively small range of feasible operating temperatures for the VAM synthesis.

[0007] In addition to concerns about catalyst stability and activity, the selectivity for formation of the desired VAM product decreases with increasing temperature.

[0008] The VAM reaction proceeds exothermically with production of heat. Thus, in order to maintain a proper temperature profile in the reaction zone within the allowed temperature range, means for the management of the reaction heat must be provided through external or internal removal of heat. Different means for heat management are being applied in the industry or mentioned in connection with the production of VAM.

[0009] Conventionally, a tube and shell reactor with the catalyst contained inside the tubes and with boiling water on the outer shell side is applied. In such a reactor the heat of reaction is removed by generation of low pressure steam with a temperature being equal to the tube wall temperature. In order to prevent the temperature to rise above 200° C. inside the catalyst bed, the boiling water temperature is typically not higher than about 180-185° C., sometimes less than 160° C.

[0010] A drawback of the boiling water cooled reactor is that the temperature of the process generated steam varies over time. The deactivation of the VAM catalyst over time is compensated by increase of the operating temperature, which requires an increased boiling water temperature.

[0011] Alternatively, the catalytic conversion according to the above reaction may take place in a fluidised bed reactor based process, where a substantially constant temperature is obtained in the catalyst bed due to back-mixing of catalyst particles and reaction medium. The fluidised bed operation is a rather expensive process with high requirements to mechanical stability of the catalyst particles.

[0012] Another method of maintaining the operating temperature below 200° C. is staged addition of cooler oxygen or other reactants to the process, as mentioned in US 2006/0116528 A1.

[0013] The quench arrangement provides several advantages. By the staged oxygen addition, a higher conversion of ethylene per pass is possible, because more oxygen can be added observing the limitations on oxygen concentration (set to avoid the risk of explosion), the reduction of selectivity and thereby potential temperature run-away. Additionally, an improved temperature control is obtained by the direct cooling through addition of cool oxygen feed. Furthermore an improved activity may be obtained when keeping the average ethylene partial pressure higher. Cooling channels may be arranged adjacent to the channels containing the catalyst particles, further improving the temperature control and minimising the need for internal cooling through inert recycling.

[0014] As a main disadvantage, the quench reactor produces less steam than a boiling water reactor and it is a complex equipment.

[0015] Common to the known methods for the removal of reaction heat by steam generation in the VAM process is that the process-generated steam temperature is too low for the steam can used in the distillation section of the VAM unit downstream of the VAM reactor. The VAM distillation section needs a heating medium such as low/medium pressure steam at 160 to 250° C. in order to be operable. Typically steam is imported to the VAM facility in order to cover the VAM plant steam deficit. The steam condensate is returned/exported from the VAM distillation section.

[0016] An improved process-generated steam quality is obtained by compressing the process-generated steam as disclosed in US 2008/0234511 A1. Thereby the quality of the process generated steam and its pressure level is changed to provide saturated steam qualities at 160-200° C., often superheated up to 250° C. Steam compression is, however, an expensive method and the steam deficit for the distillation section is only halved.

[0017] Another method of heat supply to a VAM plant is to transfer heat required from a neighbouring acetic acid plant, either through heat exchange or via generated steam as heat transferring medium. WO 2005/092829 suggests transferring a portion of heat produced during the production of acetic acid to a VAM feed stream and/or to the VAM distillation section.

[0018] Despite of the above discussed efforts, a need remains to design a process for the preparation of VAM with a sufficient heat supply to the distillation section.

[0019] As mentioned above, the feed stock in the VAM process is acetic acid, ethylene and oxygen.

[0020] Oxygen is conventionally produced in oxygen plants involving low temperature distillation.

[0021] Ethylene may be produced by different methods. As an example, ethylene may be obtained through steam cracking of naphtha, through the conversion of methanol in the so-called MTO process with a mixture of ethylene and propylene as products, or it may be produced with high selectivity and yield in the ethanol dehydration reaction:

$$CH_3CH_2OH=CH_2CH_2+H_2O$$

[0022] The dehydration of ethanol to ethylene proceeds endothermic and is industrially carried out in a heated fixed bed catalytic reactor typically at a temperature in the range of 300-450° C.

[0023] Examples of catalysts being active in dehydrating of ethanol to ethylene include zeolites and supported or unsupported metal oxides such as ZnO/Al_2O_3, FeO/Al_2O_3, Mn_2O_3/Al_2O_3.

[0024] Water containing ethanol may be used as a feed stock for the dehydration of ethanol to ethylene.

[0025] Ethanol feed stock can be produced by fermentation of carbohydrate containing materials. In this process the ethanol product is obtained in an aqueous solution with an ethanol concentration of 5-15% by weight together with fermentation by-products and solids, the so-called broth.

[0026] Ethanol can be converted by dehydrogenation to acetic acid via the oxidative and/or the non-oxidative route, according to the following reaction schemes:

$EtOH+O_2 \Rightarrow HOAc+H_2O$ (oxidative route, 180-320° C.) (1)

$\Delta H^{\circ} = -439$ kJ/mole

$EtOH+H_2O \rightleftharpoons HOAc+2H_2$ (non-oxidative route, 250-350° C.) (2)

$\Delta H^{\circ} = +44$ kJ/mole

[0027] Whereas the oxidative route is exothermic and not limited by equilibrium, the non-oxidative route is endothermic and equilibrium limited and proceeds via intermediate acetaldehyde formation.

[0028] Copper or copper based materials are suitable catalysts for the non-oxidative dehydrogenation of ethanol to acetic acid. Other catalysts e.g. coal capable of converting ethanol at non-oxidative conditions to acetic acid, are mentioned as well in the literature.

[0029] Examples of catalysts active in the oxidative conversion of ethanol to acetic acid are vanadium oxide, nano-gold particles and supported palladium.

[0030] The conversion of ethanol to acetic acid may be carried out by a combination of the oxidative and the non-oxidative reaction.

[0031] It has now been found that the processes for the preparation of acetic acid, ethylene and the VAM process can advantageously be integrated or combined, so that the heat requirements of the VAM distillation section are met, while at the same time excess heat from the VAM process is used in the acetic acid and/or the ethylene processes.

[0032] Pursuant to this finding, this invention provides an integrated process for the production of acetic acid, ethylene and vinyl acetate monomer comprising the steps of:

[0033] (a) evaporating at least part of an ethanol feed stock

[0034] (b) producing in a first reaction zone a first product stream comprising acetic acid by oxidative or partly oxidative dehydrogenation of ethanol feed stock;

[0035] (c) producing in a second reaction zone a second product stream comprising ethylene from an ethanol feed stock;

[0036] (d) reacting in a third reaction zone an acetic acid reaction stream containing at least a portion of the acetic acid from the first reaction zone with an ethylene reaction stream containing at least a portion of the ethylene product from the second reaction zone and with oxygen to a third product stream comprising vinyl acetate monomer;

[0037] (e) passing at least a portion of the third product stream to a distillation section and isolating at least a portion of the vinyl acetate monomer;

[0038] (f) supplying at least part of reaction heat from the third reaction zone to provide heat for evaporating at least part of the ethanol feed stock in step (a);

[0039] (g) supplying at least part of reaction heat from the first reaction zone to provide heat for producing the second product stream in the second reaction zone in step (c) and for distilling of the third product stream in the distillation section in step (e).

[0040] By the term "partly oxidative dehydrogenation" as used hereinbefore and in the following is meant a combination of the above described oxidative and the non-oxidative route as shown by reaction (1) and (2)

[0041] An advantage of the invention is that the heat of reaction being formed during the VAM producing reaction is used in the evaporation of ethanol feed stock for the formation of ethylene and acetic acid and the heat of reaction from the ethylene and acetic acid reactions is at the same time used in the distillation of the VAM raw product, so that there will be no heat export to an external process unit.

[0042] A further advantage of the invention is that the ethanol feed stock in the step (a) and (b) may contain water.

[0043] The reaction heat being formed in the first reaction zone during the oxidative or partly oxidative dehydrogenation of ethanol is preferably transferred to the second reaction zone to supply heat for the endothermic dehydration of ethanol to ethylene and to the VAM distillation section. Simultaneously, the reaction heat being formed in the third reaction zone is preferably transferred to the first and/or the second reaction zone.

[0044] The supply of heat to the various reaction zones may proceed according to any known means of heat transfer. A preferred method in the inventive process is an indirect heat exchange between the media to supply/absorb heat or via a heating agent carrier. Typically the heating agent is steam, but other agents like thermo-stabile oils, like Dowtherm® may also be used.

[0045] In an embodiment of the invention, reaction heat from the VAM synthesis section is used to generate steam from boiler feed water in a boiling water cooled reactor and/or a boiler. The steam, a 160° C. saturated steam, may be flashed to a stream of superheated steam better suited as heating agent for the evaporation of ethanol in a heat exchanger (evaporator). The steam is transferred to the ethanol evaporator/s in the acetic acid and/or ethylene processes. The reaction heat from the acetic acid process is used to generate steam in a boiler and/or a boiling water cooled reactor at a higher temperature level, e.g. 320° C., a part of which is transferred to a steam heated ethylene reactor and the remainder is flashed to the appropriate temperature levels of the VAM distillation section, about 250° C. and 200° C., respectively.

[0046] Suitable catalysts for the various reactions in the process according to the invention are well known in the art as discussed hereinbefore.

[0047] In further an embodiment, the two ethanol feed stock streams may contain water, and optionally at different concentrations between 0-90 wt %, primarily balanced by ethanol. Minute amounts of by-products in the ethanol feed streams being tolerable under the concern of the synthesis in question and the VAM synthesis may be present as well.

[0048] In still an embodiment, only part of the acetic acid and ethylene production is used as feed streams for the VAM synthesis.

[0049] Further aspects and features of the invention will be illustrated in more detail in the following Examples

EXAMPLE

[0050] This is an example of the present invention which demonstrates the heat integration is made possible through the process integration of three process units with reference to FIG. **1** in the drawings.

[0051] Process stream lines are indicated by double lined arrows and heat transfer lines are indicated by single line arrows.

[0052] Two feed stream lines of pure ethanol are provided from an external ethanol source (not shown).

[0053] In unit 1 acetic acid is prepared by conversion of a first ethanol feed stream via the oxidative or at least partly oxidative reaction, resulting in at least 217 kJ/mole reaction heat or 67.5 MJ/h at a temperature of 320° C.

[0054] In unit 2 a second ethanol feed stream is dehydrated to ethylene at 300° C., wherein the reaction heat produced in unit 1 is transferred to unit 2. In unit 2 the heat provided from unit 1 serves both to the isothermal dehydration of ethanol (14.7 MJ/h) and to the feed preheating from e.g. 280° C. (0.6 MJ/h) to the reaction temperature, and losses (0.1 MJ/h).

[0055] In unit 3 vinyl acetate monomer (VAM) is produced by conversion of acetic acid, ethylene and oxygen with a selectivity to VAM of 99% from acetic acid and 94% from ethylene.

[0056] The heat exported from the VAM unit 3 is used as heat of evaporation of the ethanol feed stock (13.1 MJ/h) in unit 2. The amount of steam for heating the VAM distillation corresponds to an energy flow of 52.1 MJ/h transferred from the first unit as 320° C. hot saturated steam, being flashed to the preferred operating temperatures 200 and 250° C., respectively.

[0057] The example represents one embodiment of the invention. In another embodiment the heat exported from the VAM unit may be used as heat of evaporation in unit 1. This alternative is indicated with dotted lines in FIG. **1**.

1. An integrated process for the production of acetic acid, ethylene and vinyl acetate monomer comprising the steps of:

(a) evaporating at least part of an ethanol feed stock

(b) producing in a first reaction zone a first product stream comprising acetic acid by oxidative or partly oxidative dehydrogenation of ethanol feed stock;

(c) producing in a second reaction zone a second product stream comprising ethylene from an ethanol feed stock;

(d) reacting in a third reaction zone an acetic acid reaction stream containing at least a portion of the acetic acid from the first reaction zone with an ethylene reaction stream containing at least a portion of the ethylene product from the second reaction zone and with oxygen to a third product stream comprising vinyl acetate monomer;

(e) passing at least a portion of the third product stream to a distillation section and isolating at least a portion of the vinyl acetate monomer;

(f) supplying at least part of reaction heat from the third reaction zone to provide heat for evaporating at least part of the ethanol feed stock in step (a);

(g) supplying at least part of reaction heat from the first reaction zone to provide heat for producing the second product stream in the second reaction zone in step (c) and for distilling of the third product stream in the distillation section in step (e).

2. The process of claim **1**, wherein the ethanol feed stock being evaporated in step (a) is fed to the first reaction zone.

3. The process of claim **1**, wherein the ethanol feed stock being evaporated in step (a) is fed to the second reaction zone.

4. The process of claim **1**, wherein the at least part of the reaction heat being removed from the first reaction zone is supplied to the second reaction zone by means of steam via a steam system.

5. The process of claim **1**, wherein the at least part of the reaction heat from the third reaction zone is supplied by means of steam via a steam system.

6. The process of claim **4**, wherein high pressure steam condensate being formed by transferring heat in the steam system to the second reaction zone is flashed to create steam at a lower pressure, which is passed to the distillation section in step (e) for the supply of heat.

7. The process of claim **4**, wherein high pressure steam condensate formed by the steam transferring heat to the second reaction zone is recycled to the first reaction zone to absorbing heat by forming high pressure steam.

8. The process of claim **1**, wherein the ethanol feed stock contains water.

9. The process of claim **1**, wherein the ethanol feed stock being used in steps (c) and (d) originates from a single ethanol source.

10. The process of claim **1**, wherein the ethanol feed stock being used in steps (a) and (b) originates from one or more distillates of ethanol produced through the fermentation of carbohydrates.

* * * * *

D.6 The production price of acetic acid via non-oxidative dehydrogenation of ethanol

A rough representation of a generic 300,000 MTPY ethanol non-oxidative dehydrogenation acetic acid plant is shown in Appendix D. 3. Reference is made to this in the below process description. The mass balance of the utility side has not been calculated in the flow diagram, but the individual utility consumptions have been included in the estimation of the production price. The degrees of conversion and the amount of catalyst needed in the dehydrogenation reactor is based on the screening experiment on the Cu spinel catalyst fed with a space velocity of 3g/(g·h) at 320°C.
Battery limits are at the supply of a flash distilled 60/40 ethanol water feed and at the export of acetic acid from day tanks (as in the carbonylation process).

Process description.
The ethanol to acetic acid plant is imagined to lie next to a 2nd generation ethanol plant (see Appendix A.1). Below is described the unit operations between the import of ethanol and the export of acetic acid to day tanks.
Ethanol/water vapour is imported as a side draw from the distillation column of the 2nd generation bio-ethanol plant and mixed with a recycle stream of unconverted ethanol, intermediate acetaldehyde, ethyl acetate and water. The admixture is heated in the F/E Exchanger E-1001, to 305°C and feed to the inlet of the tubular Dehydrogenation Heated Reactor, R-1001, loaded with catalyst pellets active in the dehydrogenation of ethanol to acetic acid. The reactions taking place in the reactor are shown in Scheme 3-1. Due to the overall endothermic reaction conducted heat must be supplied to the reactor. The catalyst pellets are placed in a bed penetrated by tubes fed with high pressure steam condensing at 330°C. The effluent enriched in acetic acid exits R-1001 at 320°C and is cooled by the reactor feed in F/E exchanger E-1001 to 141°C and further to 67°C in Trim cooler E-1002 before being sent to the separation section. In the separation section the reactor effluent is distilled in Distillation Column F-1001. The highest boiling compounds, product acetic acid and heavy compounds represented by butanoic acid, are withdrawn from the bottom of the column and sent to the second distillation column Heavy End Column F-1002. Butanol is removed by a butanol removal means. In the OH drum B-1001 of F-1001 co-product hydrogen is separated from the remainder stream of unconverted ethanol, acetaldehyde, ethyl acetate and water, and exported. The remainder stream mentioned above is pressurised in Recycle Pump P-1002 A/S, heated in E-1002 by the hot distillation feed and finally evaporated in Evaporator E-1004 by means of condensing low pressure steam, before being recycled and mixed with the ethanol/water import.
In the Heavy End Column F-1002 the product acetic acid is recovered in the top of the column, while the heavy compounds are withdrawn in the bottom of F-1002 and sent to an incinerator.

Production price.
The ISBL equipment items have been specified by means of so-called one-line specs. Based on these a cost estimate with accuracy ±30% has been prepared. The reactor has been designed on the basis that a STY of 0.5 kg/(kg·h) at EOR conditions may be obtained for the catalyst. SS 317 has been anticipated to withstand the corrosive environment in the plant, apart from the heavy end column where Hastelloy has been specified.

The result from the cost estimation of ISBL is enclosed in below Table D-2 which also gives the utility consumptions calculated for the above described 300,000 MTPY ethanol to acetic acid plant. Reference is made to Eq. **B-1**, Eq. B-2, Eq. B-3, Eq. B-4 and Table B-2 shown in Appendix B.1. EtOHP designates the ethanol feedstock price in USD/MT.

Table D-2: Survey of key numbers for the calculation of the acetic acid gate production price by the non-oxidative dehydrogenation of ethanol. 95% selectivity to ethanol is assumed.

	Non-oxidative dehydrogenation of Ethanol
Grand total Investment (MM USD)	97
Simple Payback time (y)	10
Specific consumption cost[a] (USD/MT)	0.844·EtOHP+5.45

a) Incl. catalyst and utilities.

Appendix E Cu spinel catalyst characterisation

Contents

E.1 Extra scans from the Lund XAFS in situ reduction of Cu spinel catalyst and 2.5 wt% Cu/Al_2O_3 model catalyst.

a) XAFS scans recorded at 24-37°C

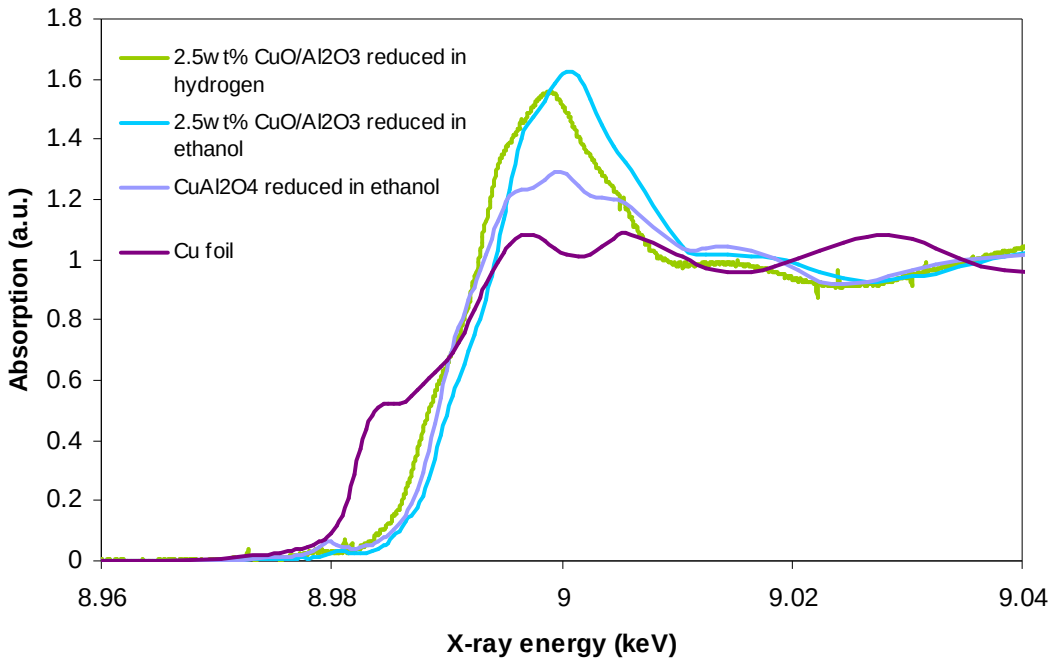

b) XAFS scans recorded at 286-316°C

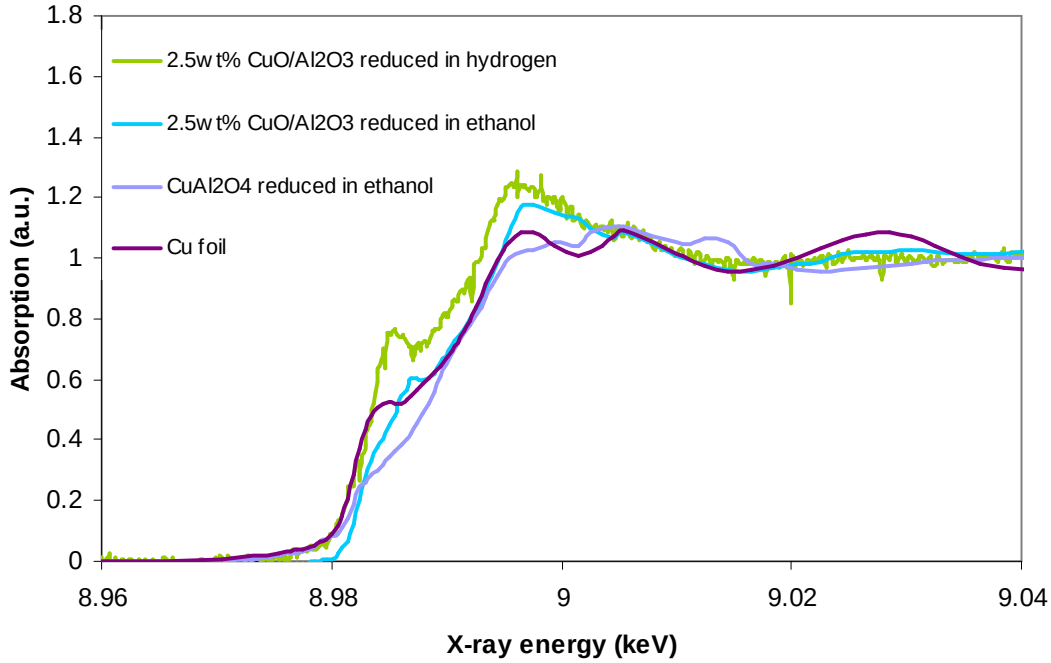

E.2 Report, HASYLAB Annual Report 2009 (online):

CuO/Al_2O_3 catalyst investigated by EXAFS

B. Voss, A. Puig-Molina, P. Beato, F. Morales-Cano, J.-D. Grunwaldt[1]

Haldor Topsøe A/S, Nymøllevej 55, DK-2800 Kgs. Lyngby, Denmark

[1]Department of Chemical and Biochemical Engineering, Technical University of Denmark, Søltofts Plads, Bygning 229, 2800 Kgs. Lyngby, Denmark

This report illustrates the behaviour of Cu during the stages of reduction with ethanol on a CuO/Al_2O_3 catalyst with a low Cu loading (2.5wt%). Through in situ experiments carried out at beamline X1 at HASYLAB it was found that the Cu reduces via its oxidation state (I) in ethanol similarly to reduction in hydrogen (3% H_2/N_2), and that very small Cu particles were obtained on the alumina surface.

Introduction

The objective of this study is to investigate the reduction of CuO/Al_2O_3 catalysts with the reducing agents ethanol and hydrogen. The CuO/Al_2O_3 catalyst system has found a wide use. For example, low loaded CuO/Al_2O_3 catalysts have been found useful in automotives for the reduction of NO to N_2 in the presence of oxygen [1], due to its preferential Cu(I) state when exposed to reducing conditions. However the complete reduction of Cu to its metallic state deactivates the NO decomposition over the Cu catalyst. Furthermore, the selective catalytic reduction of NO with a reducing agent already present in the exhaust appears advantageous. Considering the potential use of ethanol as an environmentally benign fuel for lean-burn gasoline engines, this makes ethanol an attractive reducing agent candidate for the reduction of NO. In addition, CuO/Al_2O_3 has been investigated for its use as an ethanol reforming catalyst for the production of hydrogen [2].

Therefore it is important to investigate whether the oxidation state, the structure of the reduced Cu species, and the degree of dispersion of the metallic Cu particles are affected by the reaction medium chosen, e.g. hydrogen or ethanol. It is also known that converting CuO/Al_2O_3 to Cu(II) spinel $CuAl_2O_4$ before reduction may enhance the dispersion of Cu on the alumina surface.

Experimental

The reduction experiments were conducted in situ at the X1 station at HASYLAB in a tailor-made reactor set-up with a gas feeding system providing nitrogen or $3\%H_2/N_2$ gas. Ethanol was introduced via a high precision Isco syringe pump, evaporated and mixed with nitrogen carrier gas. 50 mg of crushed 2.5wt% Cu/alumina sample in the 100-150 micron sieved fraction was used in the experiments. The catalyst was reduced in ethanol and in $3\%H_2/N_2$, respectively. EXAFS and QEXAFS around the Cu K-edge were recorded at RT before and after reaction and during heating to 380°C (ramp rate: 5°C/min). EXAFS spectra were also acquired after exposure to ethanol/water at 300°C.

Results and Discussion

The XANES spectra of the fresh sample shows the presence of Cu as Cu(II). The lack of a shoulder on the rising absorption edge points to a spinel structure (see figure 1). The detailed EXAFS analysis confirmed the formation of a $CuAl_2O_4$ spinel.

The XANES spectra (see figure 2) show that Cu(II) reduces to Cu(0) via Cu(I) when reduced in either hydrogen or ethanol as shown by the typical Cu(I) feature in the rising edge of the XANES spectra collected at 220°C.

By means of the Cu-Cu coordination number (6.9-8.2) it can be estimated that the average size of the Cu particles in the samples after operating conditions is about 10-16Å, with a tendency of larger Cu particles in the sample reduced with ethanol. Note however that a small contribution of a Cu-O shell is also observed in the Fourier transformed EXAFS spectra with a Cu-O bond distance of 1.96-1.98Å. This could be due to the presence of unreduced Cu (I), a Cu support interaction or a thin oxygen layer covering the Cu particles.

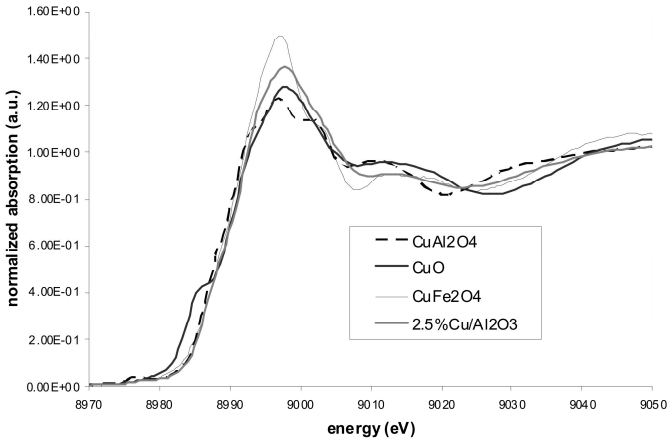

Figure 1.The XANES spectra indicate that the Cu in the 2.5% Cu/Al_2O_3 is most likely in a spinel structure.

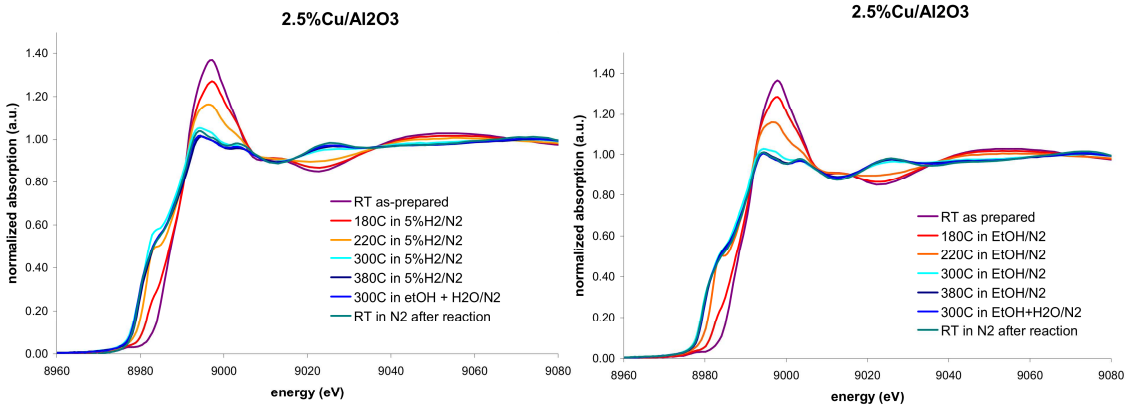

Figure 2. Left: reduction in hydrogen. Right: Reduction in ethanol. The Cu(II) reduces to Cu(0) via Cu(I) indicated by the spectra recorded at 220°C.

It seems that the CuO/Al_2O_3 catalyst may be reduced as gently in ethanol as it is reduced in hydrogen. It is therefore also assumed that ethanol may be used as a reducing agent over a low loaded CuO/Al_2O_3 catalyst in the reduction of NO. Similarly it is found that ethanol may be applied as reducing agent as an alternative to hydrogen for CuO/Al_2O_3 catalysts used for steam reforming of ethanol.

References

[1] Tae-Won Kim et al, Applied Catalysis A: General **210** 35-44 (2001).
[2] M. Noelia Barroso et al, Catalysis Letters **109** 13-19A (2006).

Appendix F Cu/SiO_2 catalyst kinetics

Contents

F.1 Paper:

Applied Catalysis A: General 402 (2011) 69–79

Contents lists available at ScienceDirect

Applied Catalysis A: General

journal homepage: www.elsevier.com/locate/apcata

Kinetics of acetic acid synthesis from ethanol over a Cu/SiO_2 catalyst

Bodil Voss[a,*], Niels Christian Schjødt[a], Jan-Dierk Grunwaldt[b], Simon Ivar Andersen[a], John M. Woodley[c]

[a] Haldor Topsøe A/S, Nymøllevej 55, DK-2800 Kgs. Lyngby, Denmark
[b] Institute for Chemical Technology and Polymer Chemistry, Karlsruhe Institute of Technology (KIT), Kaiserstr. 12, 76128 Karlsruhe, Germany
[c] Department of Chemical and Biochemical Engineering, Technical University of Denmark (DTU), DK-2800 Kgs. Lyngby, Denmark

ARTICLE INFO

Article history:
Received 1 February 2011
Received in revised form 18 May 2011
Accepted 19 May 2011
Available online 2 June 2011

Keywords:
Ethanol dehydrogenation
Acetic acid
Cu crystal
Kinetics
Step sites

ABSTRACT

The dehydrogenation of ethanol via acetaldehyde for the synthesis of acetic acid over a Cu based catalyst in a new process is reported. Specifically, we have studied a Cu on SiO_2 catalyst which has shown very high selectivity to acetic acid via acetaldehyde compared to competing condensation routes. The dehydrogenation experiments were carried out in a flow through lab scale tubular reactor. Based on 71 data sets a power law kinetic expression has been derived for the description of the dehydrogenation of acetaldehyde to acetic acid. The apparent reaction order was 0.89 with respect to water and 0.45 with respect to acetaldehyde, and the apparent activation energy was 33.8 kJ/mol. The proposed oxidation of acetaldehyde with hydroxyl in the elementary rate determining step is consistent with these both. Density Functional Theory (DFT) calculations show the preference of water cleavage at the Cu step sites. In light of this, an observed intrinsic activity difference between whole catalyst pellets and crushed pellets may be explained by the Cu crystal size and growth rate being functions of the catalyst particle size and time.

1. Introduction

Acetic acid is a bulk chemical which today is produced in amounts exceeding 10 million tons per year worldwide. The established production route has been dominated by the carbonylation of methanol which only relies on fossil sources [1]. In recent years, under the consideration of CO_2 neutrality and independence of fossil sources, the utilisation of biomass for chemical production has regained significant interest. The dehydrogenation of ethanol to acetic acid over Cu catalysts has been known for about a century [2], but ever since the highly selective carbonylation process was discovered the carbonylation route has attracted far the most interest due to its comparably cheap feedstock. Industrially the utilisation of ethanol as a feedstock for acetic acid production has survived the competition from the fossil feedstock based carbonylation process where cheap ethanol is available in large amounts. Less than 10% of the world's capacity of acetic acid is produced according to the route: dehydrogenation of ethanol to acetaldehyde followed by partial oxidation of acetaldehyde to acetic acid [2]. If not carefully operated, however, the two step ethanol route is hampered by a high loss of feedstock to the parasitic CO_2 production in the oxidation step.

As is well-known, but not industrialised, acetic acid may also be produced from ethanol in a single non-oxidative reaction step [3]. The non-oxidative dehydrogenation of ethanol to acetic acid may be described through the following reactions according to Eqs. (1) and (2).

$$CH_3CH_2OH \rightleftarrows CH_3CHO + H_2 \qquad \Delta H^\circ = 68.7\,\text{kJ/mol} \qquad (1)$$

$$CH_3CHO + H_2O \rightleftarrows CH_3COOH + H_2 \qquad \Delta H^\circ = -24.8\,\text{kJ/mol} \qquad (2)$$

Both reactions are equilibrium limited, implying that unconverted ethanol and acetaldehyde should be separated from the acetic acid product and recycled in an industrial process.

Depending on the catalyst activity the further esterification of ethanol with acetic acid may take place:

$$CH_3CH_2OH + CH_3COOH \rightleftarrows CH_3COOCH_2CH_3 + H_2O \qquad (3)$$

and butanol or other condensation side-products may be produced:

$$2CH_3CH_2OH \rightarrow C_4H_9OH + H_2O \qquad (4)$$

Many Cu catalysts, supported or non-supported, are able to convert ethanol to acetic acid. Especially Cr promoted Cu catalysts have been studied due to their regeneration and stabilising abilities, but the carcinogenic effects of Cr in its hexavalent form makes this promoter less desirable. The kinetics of the first conversion (Eq. (1)) has been investigated on unsupported Cu as well as Cr promoted Cu by Tu et al. [4], where it was found that the dehydrogenation of ethanol to acetaldehyde is a first order reaction in ethanol. An apparent activation energy of the non-promoted unsupported Cu

* Corresponding author. Tel.: +45 45272000; fax: +45 45272999.
E-mail address: bov@topsoe.dk (B. Voss).

0926-860X/$ – see front matter © 2011 Elsevier B.V. All rights reserved.
doi:10.1016/j.apcata.2011.05.030

catalyst of 51 kJ/mol was found. However, the data analysis by Tu et al. [4] appears to have been conducted without allow for the fact that the dehydrogenation reaction is equilibrium limited. Herein, it was assumed that the fraction of converted ethanol should be read as the fraction of ethanol converted divided by equilibrium ethanol conversion fraction, which would be the normal parameter subject to graphical analysis with equilibrium reactions. This would explain the high degree of conversion reported for ethanol. The chemical equilibrium for this reaction has been discussed [5,6].

However, in an overall ethanol to acetic acid process high catalyst selectivity to the desired product may be of even greater importance than a high activity, due to simpler product recovery section. We have found that Cu on SiO_2 is a highly selective dehydrogenation catalyst presumably due to its support neutrality, thereby inhibiting e.g. acid or base catalysed dehydration and condensation reactions.

The kinetics for the second conversion (Eq. (2)) on Cu has not been reported to our knowledge. Parts of the pathway and mechanism have been elucidated through conversion of intermediates, surface studies and isotopic labelling [7–11]. Furthermore, support for the mechanisms may be found in similar chemical conversions, where the difference between the reactions is merely the nature of the radical attached to the functional group. Cu catalysts are known to catalyse the dehydrogenation of methanol as well [12–14]; herein C1 is designated as the set of elementary reactions occurring on a Cu surface active in methanol reforming, while C2 has been designated as the set of elementary reactions involved in Cu surface catalysed ethanol reforming. Comparison between part of the C1 and C2 mechanisms on Cu has been suggested [7,8,10]. The C1 mechanisms are interconnecting methanol, water and formic acid in parallel while the C2 mechanisms are interconnecting ethanol, water and acetic acid. The common elementary surface reactions involved in water dissociation on Cu sites have furthermore been discussed [15–17].

In order to support the process development of the new acetic acid process, for example to properly design the synthesis reactors and establish the optimal reaction conditions, a kinetic model is needed. In this paper we have focused on the kinetic order of water and acetaldehyde in the conversion of acetaldehyde with water to acetic acid and hydrogen (Eq. (2)) and the correlations between the Cu crystal size and activity. DFT calculations have been made on the dissociation of water on Cu slabs. A kinetic discussion is made on the basis of mechanistic considerations. A power law expression is used to model the experimental data.

2. Experimental

2.1. Catalyst preparation

The Cu/SiO_2 catalyst used for this kinetic study was prepared by precipitation of $Cu(NO_3)_2$ with K_2CO_3 in a suspension of HSA-silica (specific surface area = 348 m^2/g) at pH 6.0. The precipitate was ripened at 333 K for 1 h, then filtered and washed with hot water until the filtrate had a conductivity of less than 0.1 mS/cm, and finally it was dried at 353 K. The powder (45.7 wt% Cu loading, 0.24 wt% K) was mixed with 3.3 wt% graphite as a lubricant and 5 mm × 6 mm ($h \times d$, height × diameter) cylindrical pellets were made from the catalyst powder, which were then calcined at 623 K for 2 h before use. In part of the experiment a sample of crushed catalyst pellets from a 1–3 mm sieve fraction was used in place of whole pellets.

Different batches of Cu/SiO_2 were made on the same recipe. One sample was used for equilibrium data, one for the prediction of reaction order. The whole pellets all originated from the same batch.

2.2. Catalyst characterisation

Theoretical DFT calculations were made in-house by using a Dacapo calculator on the simulation of a three-layer thick copper slab. The water binding energy was calculated by subtracting the energy of the relaxed copper slab and the water in the gas phase from the total energy of the water adsorbed on the copper slab.

X ray diffraction (XRD) was conducted in an X ray diffractometer with Cu Kα1 radiation of a wave length of 1.54 Å.

In situ reduction was conducted in Transmission Electron Microscope (TEM) on crushed catalyst powder in a Titan ETEM apparatus. The microscope was operated at 300 kV and tuned to a flat information transfer out to 20 mrad using the supporting SiN membrane window before conducting the experiment. The hydrogen source was Alphagas H_2. Imaging took place before and during exposure to app. 10 mbar H_2 at 608 K.

An EXAFS study on *in situ* reduction of a 100–150 micron sieve fraction of the crushed catalyst was conducted at the beamline X1 at HASYLAB. QEXAFS scans were recorded using a Si(1 1 1) double-crystal monochromator in continuous screening mode between 8500 and 9700 eV. The energy was calibrated using a Cu foil. The data were reported on an *in situ* cell as described in reference [18] and background removal and data fitting were conducted with the Win XAS software [19].

2.3. Catalyst testing

Dehydrogenation of ethanol mixtures was conducted in an 8 mm reactor tube installed in a ventilated temperature controlled oven. The catalyst was loaded either as (a) whole pellets (12 g cylindrical $h \times d$: 5 mm × 6 mm) in a single-pellet-string configuration with 3 mm glass balls as separators or (b) as crushed pellets (4 g, 1–3 mm sieve fraction) diluted with SiC in a 1:1 ratio on volume basis. The catalyst was activated in each case prior to the experiment with 5% H_2 in N_2 at 523 K and a flow rate of 900 Nml/min for 7 h. The liquid reactant was fed by means of a high precision pump (HPLC pump, LDC Analytical, ConstaMetric 3200) to an evaporator installed inside the ventilated oven. Preheated N_2 carrier gas was added from a mass flow controller at a ratio of either 333 or 666 Nml per ml of liquid feed to the evaporated feed before being introduced to the reactor. The inlet temperature and the reactor wall temperature were the same. The molar feed ratios of ethanol to water in the liquid feed were 60:40, 50:50, 40:60 and 20:80. In addition, 10% of an acetaldehyde and water mixture in a 50:50 molar ratio was co-fed in some experiments. The temperatures ranged from 553 to 613 K and the operating pressure was slightly above atmospheric.

The liquid products were sampled in a condenser cooled to 258 K by a cooling circuit. The gas flow rate at the exit of the condenser was measured by means of a flow meter and the condensate flow rate was calculated. Online GC was not obtainable due to the corrosivity of the product, potentially damaging the sample port (previous experience). The composition of the condensate was determined by means of a gas chromatograph (GC) with a flame ionisation detector (FID). Based on the measured composition and the assumption that acetaldehyde would be the only condensable escaping the condenser in significant amounts (established by analysis), a complete calculated mass balance could be established. The water and the acetic acid concentration in the condensate were double checked by titration.

Due to the hard to handle acetaldehyde the variation of acetaldehyde vs. water in the feed was in most cases obtained indirectly by feeding ethanol and water in different ratios, having observed that the dehydrogenation reaction of ethanol to acetaldehyde (Eq. (1)) is much faster than the dehydrogenation of acetaldehyde (Eq. (2)).

Minute side products (<0.2 mol%) count ethyl acetate, diethoxy ethane and ppm concentrations of n-butanol. All the unloaded cat-

alyst samples were analysed by means of XRD. The samples were passivated in 1% O_2/99% N_2 at room temperature before unloading.

For each series of kinetic experiments carried out on whole pellets for a given feed composition the temperature and flow rates were varied to provide kinetic data at varying contact times, and at each temperature the first flow rate was repeated in the end before changing the temperature in order to follow the deactivation of the catalyst. Each data point was compensated for deactivation assuming that the rate equations of both Eqs. (1) and (2) were influenced to the same degree, based on the Eq. (2) activity. The degree of deactivation was 0–50% dependent on temperature.

The resulting kinetic data sets comprise numbers for feed and effluent compositions, catalyst mass, inert mass, reactor length, temperature, pressure and flow rate. To include thermal transport effects and efficiently combine the analysis of the two consecutive conversions according to Eqs. (1) and (2) the kinetic data obtained were evaluated based on the data sets by contemporary integration in a one-dimensional wall cooled plug flow reactor model on the suggested power-law kinetics. The one-dimensional reactor software is developed in-house but in principle any one-dimensional reactor modelling software with appropriate integration accuracy may be used for this purpose. With the above mentioned one-dimensional reactor model it was possible to perform integration over the catalyst mass for each of the experiments, $n = 1, 2, 3, \ldots, N_{exp}$, where N_{exp} is the total amount of proper experiments, thereby calculating the product outlet concentrations.

An error function was defined with respect to all the data sets evaluated and to both the acetaldehyde and the acetic acid outlet concentrations in the individual data sets. The error function (Eq. (5)) expresses the sum of the squared sum of the relative deviation between the calculated outlet concentrations, y_{calc}, of acetaldehyde and acetic acid according to Eqs. (1) and (2) and the corresponding measured concentrations, y_{exp}, at the outlet of the reactor.

$$SSQ = \sum_{n=1}^{N_{exp}} \left(\sum_{i=HAc,\,HOAc} \frac{y_{calc,i} - y_{exp,i}}{y_{exp,i}} \right)^2 \quad (5)$$

By means of the Complex Box method and by varying the kinetic coefficients and activation energies in the suggested kinetic expressions used for calculating the outlet concentrations, a minimisation of the error object function value and a set of the correspondingly optimised variables were obtained.

3. Results

3.1. Catalyst characterisation results

XANES and EXAFS showed that the reduction of the CuO in the fresh catalyst sample the Cu/SiO_2 catalyst started at 488 K and was finalised at 510 K. Fig. 1 shows a selection of the EXAFS spectra recorded during the *in situ* reduction of the test sample.

Obviously complete reduction of Cu(II) to Cu (0) is obtained within a narrow temperature window leaving copper in its metallic state.

The formation of Cu particles on the surface of the SiO_2 support upon activation is supported by the analysis of the TEM images. Fig. 2 shows the Cu crystals formed on the SiO_2 surface when subjected to 11 mbar H_2 at 608 K.

Further investigation of the Cu crystal size by XRD (Scherrer equation) showed that substantially larger Cu crystals were formed on the whole pellets during reduction (160 Å compared to 110 Å on crushed pellets). Likewise the growth rate of the Cu crystals seems to be influenced by the size of the catalyst particle. Sintering due to water formed during reduction may be the explanation for the larger Cu crystals found on the whole pellets. Fig. 3a shows the size

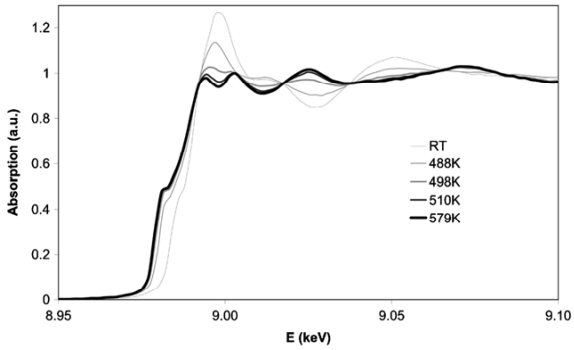

Fig. 1. EXAFS spectra obtained during *in situ* reduction of 50 mg 100–150 micron sieve fraction Cu/SiO_2 catalyst in 5% H_2 (flowing at a rate of 10 Nl/(min g)) at room temperature (298 K, RT), 488, 498 and 579 K. The spectrum at 579 K corresponds to Cu(0).

of the Cu crystals along the [2 0 0] direction (Cu D[2 0 0]) just after reduction, Fig. 3b shows an XRPD spectrum for a specific catalyst sample, and Fig. 3c shows the initial acetic acid formation rate of whole catalyst pellets compared with crushed catalyst pellets. Further sintering was observed after a number of hours on stream for whole pellets and crushed catalyst pellets.

In-house DFT calculations show that water preferably dissociates on Cu(2 1 1) surfaces, or step sites, the density of which decreases with the Cu particle size. The Cu(2 1 1) surface calculations give an energy barrier of 1.3 eV (125 kJ/mol) for the water dissociation reaction.

3.2. Pathway and equilibriums

In order to establish the pathways and equilibriums of the reaction system of Eqs. (1) and (2) a reaction profile experiment was initially made at high to very low liquid weight hourly space velocities, LWHSV (g/(g h)), expressing the load of liquid feed per time unit on the catalyst mass.

Fig. 4 shows the reaction profile found for the conversion of a feed mixture with the molar ratio of ethanol to water of 40:60.

The concentration profile in Fig. 4 (ethanol = EtOH, water = H_2O, hydrogen = H_2, acetaldehyde = HAc, acetic acid = HOAc) with acetaldehyde going through a maximum confirms acetaldehyde as a typical intermediate. As may be gathered, the reaction rate of the

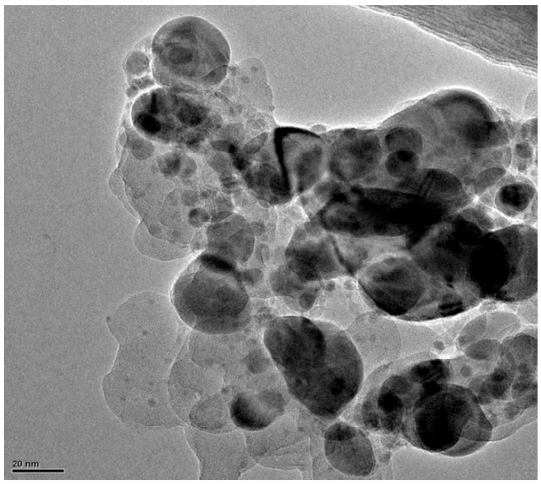

Fig. 2. TEM image showing Cu crystals of average size>100 Å (dark circular) on SiO_2 support (brighter shades) after *in situ* reduction at 335 °C in 10.5 mbar H_2.

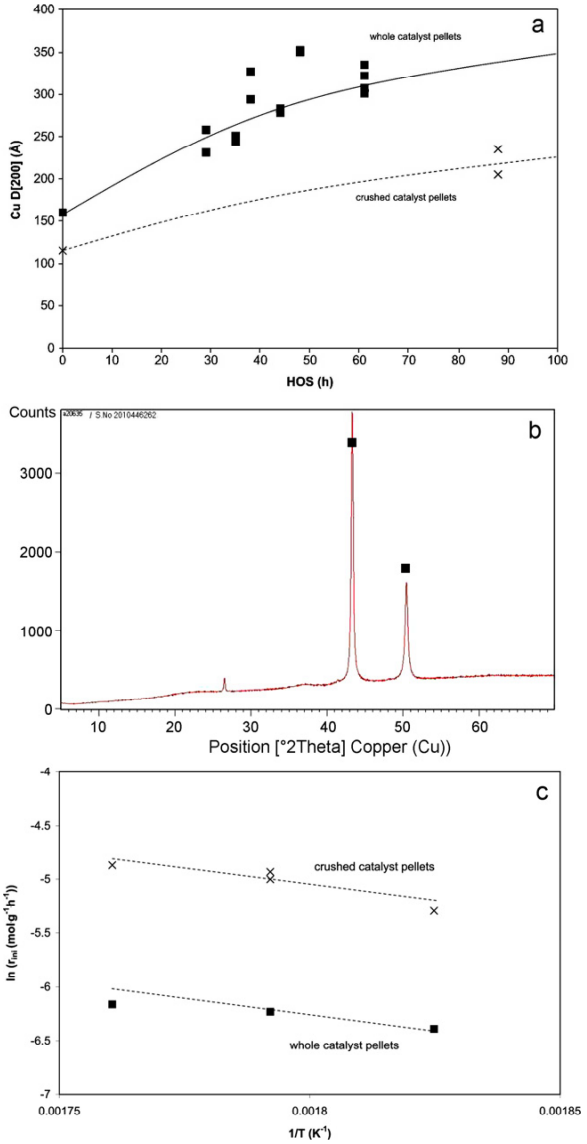

Fig. 3. (a) The Cu crystal size D[2 0 0] analysed by *ex situ* XRPD after reduction and operation. The resulting Cu crystal size depends on the catalyst particle size and time on stream. HOS is hours on stream. (b) An *ex situ* XRPD for a 1.4 mm Cu/SiO_2 catalyst particle reduced in 5% H_2 and operated for 61 h on a 40:60 ethanol/water molar feed diluted to 50% by nitrogen. (c) Arrhenius plot of the initial rates of acetic acid formation vs. inverse absolute temperature for a 40:60 ethanol/water feed.

dehydrogenation reaction of ethanol (Eq. (1)) is much faster than the dehydrogenation of acetaldehyde with water to acetic acid and hydrogen (Eq. (2)). Furthermore, the profile seems to level out at low LWHSV, indicating that the equilibrium is approached. In a kinetic evaluation the reaction rate is typically corrected with $(1-\beta)$ for considering a reaction approaching equilibrium, if it describes a first order conversion, where β is the reaction quotient divided by the corresponding equilibrium constant. Therefore, the equilibrium temperature function had to be estimated for this purpose.

The approximate reaction quotient, Q_{appr}, may be expressed as:

$$Q_{appr} = \frac{p_{H_2} \cdot p_{CH_3CHO}}{p_{CH_3CH_2OH} \cdot p^{\theta}} \quad (6)$$

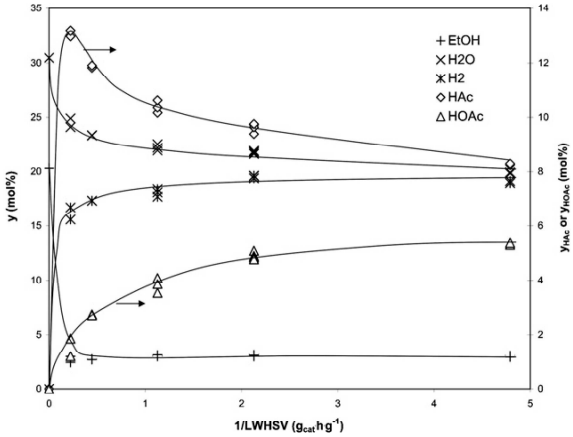

Fig. 4. The reaction profile of a 40:60 ethanol/water mixture diluted with N_2 to 50 mol% fed into a bed of crushed Cu/SiO_2 catalyst at an outlet temperature of 588 K at close to atmospheric pressure. Minor side-products e.g. ethyl acetate and n-butanol have been neglected in the figure. The concentrations (mol%), of the acetaldehyde (HAc) and acetic acid (HOAc) products may be found on the right abscissa.

where p_{H_2}, p_{CH_3CHO} and $p_{CH_3CH_2OH}$ are the partial pressures of hydrogen, acetaldehyde and ethanol, respectively, and p^{θ} is the gas standard state pressure (1.013 bar = 1 atm). At low LWHSV the approximate reaction quotient as calculated by Eq. (6) for the smoothed data at 588 K is about 0.7, at a total operating pressure of 1.05 bar.

The degree of conversion of acetaldehyde with water to acetic acid and hydrogen according to Eq. (2) was in all kinetic experiments so low that the reaction was far from equilibrium.

Feeding a mixture of acetaldehyde, being an intermediate, and water to the catalyst gave no ethyl acetate side-product, while acetic acid was produced, and the production rate of acetic acid was higher than if a mixture of ethanol and water was used as a feed. The result indicates that acetic acid may be produced directly from acetaldehyde and water, and that this is the primary route to acetic acid from ethanol and water.

3.3. Kinetic modelling

While the differential reactor type is the most preferred for kinetic investigations, sound approaches may be obtained also through integral reactors as long as a broad range of low to high degrees of conversions are obtained for a variation of feeds at different temperatures. With two consecutive reactions and minor side-reactions taking place, the smoothest analysis is obtained by using computer modelling. The reaction rate according to the reaction in Eq. (2) is so low that diffusion limitation is not controlling the observed rates even on whole catalyst pellets of the size used in our experiments. In such case, the application of a single-pellet string reactor type is favourable in that the reactor may be modelled more easily [20]. With a limited reactor volume and a slow reaction in question the degree of conversion would be too low for modelling of crushed catalyst at realistic ethanol partial pressures.

By applying a data fitting program using a non-linear optimisation method on the sum of squared relative errors between the observed and modelled product concentrations the kinetic parameters may be fitted.

Present experiments were conducted at initial ethanol partial pressures 0.11–0.26 bar and water partial pressures 0.18–0.45 bar. Acetaldehyde was in some cases co-fed at an initial partial pressure of 0.05 bar. In order to investigate its influence on the acetic acid formation rate the acetaldehyde partial pressure at low contact time

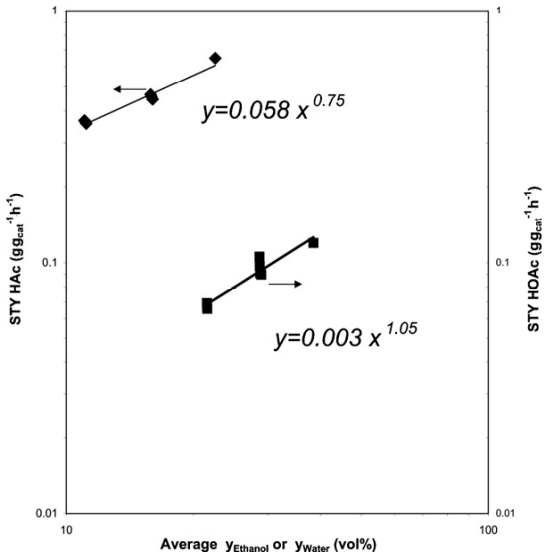

Fig. 5. Log–log plots of the acetaldehyde space-time yield (STY) vs. the average ethanol concentration and the acetic acid STY vs. the average water concentration, respectively, at 563 K and atmospheric pressure as a simple approach for determining the reaction orders in the kinetic expressions for Eqs. (1) and (2) for crushed pellets. Averages are arithmetic inlet to outlet.

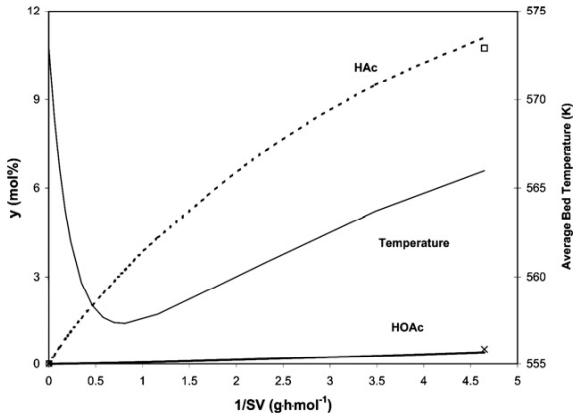

Fig. 6. The modelled conversions and the radial averaged temperature (lines) and the experimental values for acetaldehyde (square) and acetic acid (cross); y is indicated in mol%. The partial pressure of ethanol = 0.26 bar and the partial pressure of water = 0.39 bar in the feed. The feed/wall temperature = 573 K.

was further varied indirectly by varying the initial ethanol partial pressure. The temperature was varied between 553 and 613 K.

3.3.1. Crushed catalyst pellets

As mentioned above, the operation of the experimental reactor at close to isothermal conditions may be obtained with a bed of crushed catalyst pellets diluted with SiC, which has high thermal conductivity, 360 W/mK. Such experiments were conducted in order to observe the reaction order effects while minimising the effect of non-isothermal behaviour.

In one part of the experiment – on crushed catalyst – the ethanol/water ratio was fixed while its feed rate was changed keeping the nitrogen carrier gas flow rate and the temperature constant. Hereby, the partial pressures of the water and ethanol feed were changed, while the exit acetaldehyde concentration was almost constant.

The influence of the two varied reactants was investigated by plotting the space-time yields (STYs) of the products vs. the average of the reactants concentration log–log in a series of experiments conducted at 563 K, where the degree of conversion is rather low, hereby approaching differential analysis. Fig. 5 shows the plots to determine the reaction order of Eq. (1) with respect to ethanol and the reaction order of Eq. (2) with respect to water.

An approximation of the reaction order of the first rate equation (Eq. (1)) with respect to ethanol was obtained as the slope of the log–log depiction of the acetaldehyde STY, STY HAc, vs. the average ethanol concentration (arithmetic inlet to outlet) in vol%. The STY HAc value includes the amount of acetaldehyde which had further been converted to acetic acid. The reaction order with respect to ethanol is found to be 0.8 by this analysis. Apart from not being an actual but rather an average reaction rate, the STY does not compensate for the approach to equilibrium. β for Eq. (1) ranged from 0.05 to 0.15.

In the study by Tu et al. [4] conducted at 523–583 K the conversion of ethanol to acetaldehyde was found to take place according to a first order reaction in ethanol. Based on this literature evidence and the above finding, the rate equation for the dehydrogenation of ethanol to acetaldehyde (Eq. (1)) was assumed to be of first order in ethanol in the further data analysis.

According to the same method and based on the same data the log–log plotting of the STY of acetic acid, STY HOAc, vs. the average water vol% was made (Fig. 5) in order to indicate the reaction order with respect to water in Eq. (2). As mentioned above, during these experiments the acetaldehyde concentration in the effluent was almost constant. If as an approximation the acetaldehyde concentration profile is assumed constant in this series of experiments, we find a reaction order of water of 1.05, i.e. a close to first order dependence.

3.3.2. Whole pellets

Modelling an example of a conversion profile based on a first order reaction rate for Eq. (1) confirms that isothermal operation is not achieved. Fig. 6 shows the modelled conversion and temperature profiles for an example, where y is the concentration of acetaldehyde and acetic acid in mol%, respectively.

However, by means of the fact that Δt approaches 0 at low contact times the initial rates, r_{ini}, defined as the reaction rate of the feed composition of acetic acid formation for an infinitely low concentration of acetaldehyde may approximately be established from the depiction of y_{HOAc} vs. 1/SV irrespective of the non-isothermal behaviour. The r_{ini} values are found as the tangent slopes in 1/SV = 0.

Fig. 7 shows the log–log plot of experimental results of a series of feeds on whole pellets where the ethanol partial pressure was kept constant while the water partial pressure was varied. In effect, this variation of water partial pressure at constant ethanol implies a constant acetaldehyde concentration at a given, low contact time, as the Eq. (1) reaction rate is very high and is assumed being dependent on ethanol alone.

Note that both on crushed and sieved catalyst and whole catalyst pellets the reaction order of water is close to 1.

In a further series of experiments acetaldehyde was co-fed leading to a remarkable increase of the initial reaction rate to acetic acid. Therefore, overall a rate expression for Eq. (2) is suggested depending on both water, with a close to first order dependence, and acetaldehyde partial pressures.

3.4. Parameter fitting

As mentioned, the conversion of ethanol to acetaldehyde was assumed to be a first order reaction with respect to ethanol. The

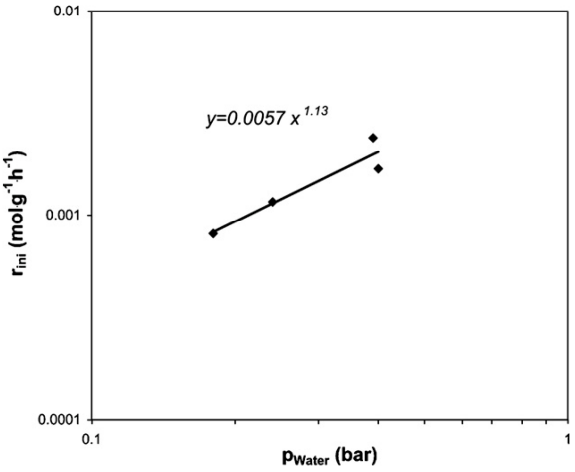

Fig. 7. The initial acetic acid formation rate vs. the partial pressure of water at toven = 573 K and constant ethanol pressure (0.26–0.265 bar) in the feed on whole catalyst pellets.

power law expression in accordance herewith may be expressed as follows:

$$-r_{CH_3CH_2OH,1} = A_1 \cdot \exp\left(\frac{-E_1}{RT}\right) \cdot p_{CH_3CH_2OH} \cdot (1-\beta_1) \quad (7)$$

where A_1 is the pre-exponential factor in mol/(g h bar), E_1 is the apparent activation energy in kJ/mol, $p_{CH_3CH_2OH}$ is the partial pressure of ethanol in bar, and β_1 is the observed reaction quotient divided by the equilibrium constant for Eq. (1).

Even with a certain reduction of the reaction rate due to diffusion limitation, the order of the reaction remains 1.

The reaction according to Eq. (2) was given a power law rate equation, with a dependence of acetaldehyde and water:

$$-r_{CH_3CHO,2} = A_2 \cdot \exp\left(\frac{-E_2}{RT}\right) \cdot p_{CH_3CHO}{}^{\gamma_{CH_3CHO}} \cdot p_{H_2O}{}^{\gamma_{H_2O}} \cdot (1-\beta_2) \quad (8)$$

where A_2 is the pre-exponential factor in mol/(g h bar$^{\Sigma\gamma}$), E_2 is the apparent activation energy in kJ/mol, p_{CH_3CHO} is the partial pressure of acetaldehyde in bar, p_{H_2O} is the partial pressure of water in bar, γ_{CH_3CHO} and γ_{H_2O} are the reaction orders with respect to acetaldehyde and water, and β_2 is the observed reaction quotient divided by the equilibrium constant for Eq. (2). The approach to equilibrium expressed by β_2 was in all cases almost negligible.

Using a one-dimensional reactor modelling program the above power law expressions were evaluated.

In the rate expression, Eq. (7), the pre-exponential factor, A_1, and the apparent activation energy, E_1, were allowed to vary, while in the rate expression, Eq. (8), both the pre-exponential factor, A_2, the apparent activation energy E_2 and the exponents, γ_{CH_3CHO} and γ_{H_2O}, were defined as variables.

The optimised parameters found for the 71 data sets with ethanol partial pressures 0.11–0.26 bar, water partial pressures 0.18–0.45 bar and acetaldehyde co-fed at up to 0.05 bar, diluted with N_2 carrier gas, and the temperatures ranging from 553 to 613 K, were as follows:

$A_1 = 3.53E_3$ mol/(g h bar) $E_1 = 43.7$ kJ/mol

$A_2 = 20.4$ mol/(g h bar$^{1.34}$)

$\gamma_{CH_3CHO} = 0.45$ $\gamma_{H_2O} = 0.89$ $E_2 = 33.8$ kJ/mol

Fig. 8 shows the parity plots for acetaldehyde and acetic acid respectively sorted in 3 selected reactor wall/inlet temperatures.

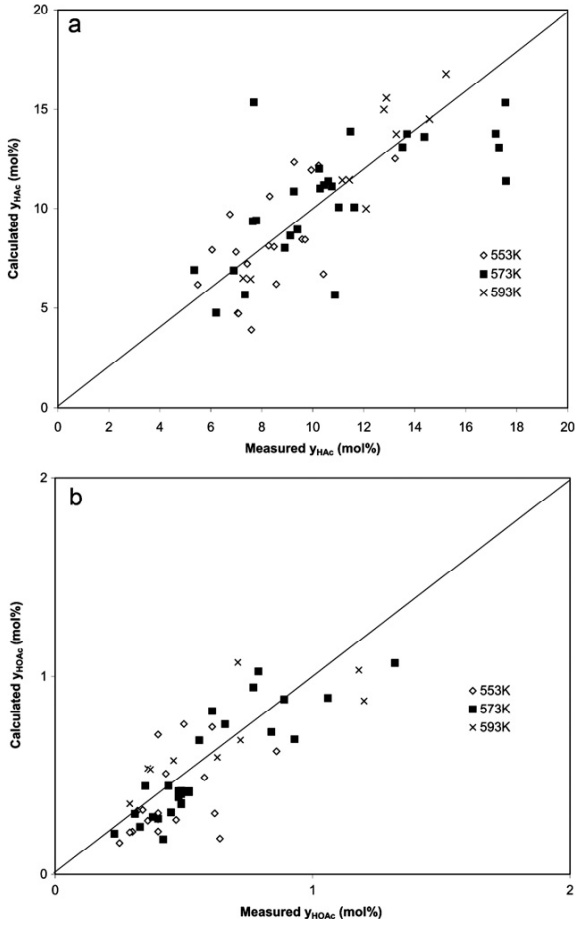

Fig. 8. Parity plots of calculated vs. measured concentration of the products acetaldehyde and acetic acid based on whole catalyst pellets. Upper: acetaldehyde. Lower: acetic acid. The plot points are sorted in three series corresponding to the reactor wall/feed temperature: diamonds 553 K, filled squares 573 and crosses 593 K.

The objective here was to study the kinetics for the conversion of acetaldehyde with water to acetic acid and hydrogen. As shown above in Fig. 6, the reactor was not operated completely isothermally. The integral analysis of the two rate expressions, Eqs. (7) and (8), was however accounting also for the actual temperature profile in the test reactor. From above parity plots Fig. 8 it is seen that no systematic deviation occurs with reactor wall/feed temperature variation. This indicates a good validity of the apparent activation energy found for the studied conversion kinetics.

For comparison, further kinetic data as to conversion, selectivity and stability of the Cu/SiO_2 catalyst are enclosed in Appendix A.

4. Discussion

4.1. Side-reactions and equilibrium

Using the present Cu/SiO_2 catalyst, only very limited side-reaction conversion to ethyl acetate and butanol via Eqs. (3) and (4) have been observed for the catalyst tested. In literature such side-products are typically reported [7,9].

At higher temperatures the ethanol may dehydrate to ethylene [21]. However, no such side-production of ethylene was observed in the temperature range 553–613 K.

Regarding the ethanol dehydrogenation (Eq. (1)), the approximate reaction quotient value of about 0.7 was found in present investigation at 588 K for low LWHSV, approaching equilibrium. This value corresponds closely to the equilibrium constant of 0.8 at 588 K obtained theoretically from the Stull et al. [5] thermochemical values as calculated by Happel et al. [6]. Happel argues that the departure from ideal behaviour is insignificant for Eq. (1) at the conditions given allowing the direct comparison of the approximate reaction quotient (Eq. (6)) at low LWHSV with the equilibrium constant value. The corresponding standard entropy and enthalpy of formation of acetaldehyde proposed by Stull et al. [5] are 264.2 J/(mol K) and −166.4 kJ/mol. Happel et al. [6] made a series of experiments based on the approaching of the Eq. (1) equilibrium from both sides at temperatures 456–533 K. They compared their own experimental values against various literature thermochemical and experimental data for this reaction. Happel et al. [6] also found that their equilibrium data agreed best with the thermodynamic values reported by Stull et al. [5]. These standard entropy and enthalpy values for acetaldehyde were therefore used in our data evaluation.

4.2. Mechanism

Up to now no kinetic model, empirical or microkinetic, for the conversion of acetaldehyde to acetic acid has been suggested in the literature. But some of the elementary steps have been reported. From one side it is difficult to determine a mechanism from an empirical kinetic expression. The other way round with some mechanistic information it gets easier to propose an empirical expression with greater validity. Reference is made to the Appendix B where mechanistic considerations are made based on the literature [7–13], comprising the corresponding C1 mechanisms. Appendix B also contains Table 1 showing the considered elementary reaction steps I–XVII on the Cu surface. Reference to these steps I–XVII in Table 1 are hereinafter made directly.

As learned in Appendix B, the formation of CH_3CHOO^* may, with a basis in the C1 elementary steps, be explained through the oxidation of an adsorbed acetaldehyde with adsorbed O^*, step VIII or adsorbed OH^* to H^* and CH_3CHOO^*, step IX, or it may be explained through a direct ethoxy route: ethanol dissociation into adsorbed ethoxy and H^*, the ethoxy being oxidised with adsorbed O^* to CH_3CHOO^* and adsorbed H^*, see steps I, II + VII. The CH_3CHOO^* then abstracts α-hydrogen, step X, and the acetate formed reacts with adsorbed hydrogen to acetic acid which desorbs, steps XI–XII.

Adsorbed oxygen or hydroxyl needed for these oxidations may be obtained by the dissociation of adsorbed water to OH^* and H^* on the Cu surface, followed by 2 adsorbed hydroxyls forming adsorbed water and atomic oxygen, steps XIII–XVI. Dihydrogen gas is formed by desorption of two adsorbed hydrogen, step XVII. The dissociation of water, step XIV, is known to be slow [13] and rate determining under typical water-gas shift conditions.

Accordingly, the reaction mechanism of ethanol dehydrogenation with water to acetic acid and hydrogen via acetaldehyde (Eqs. (1) and (2)) may be described through the discussed elementary steps of steps I–XVII.

4.3. Rate determining step

The dissociation of water on Cu surfaces (step XIV) is known [13] to be rate determining under typical water gas shift conditions in conjunction with the methanol reforming, C1 system.

We may note, however, that whereas a high activation barrier (84 kJ/mol) for the dehydrogenation of formaldehyde into formyl is predicted by Shustorovich [14] for the C1 system, the ready formation of adsorbed acetyl CH_3CO^* from acetaldehyde was observed in the C2 system on a Cu surface [11].

Furthermore, it is reported by Iwasa and Takezawa [7] that in the C1 system the dehydrogenation step of methanol to formaldehyde is rate determining over its further conversion to methyl formate or carbon dioxide, via formate. For the C2 system the dehydrogenation step to acetaldehyde is much faster than its further steps to acetic acid.

As the formation rate of acetic acid is higher from acetaldehyde than from ethanol, the alternative overall ethoxy route via step VII seems to not be the dominant. It is likely that the rate determining step is either of the oxidations in step VI, step VIII or step IX, or the dissociation of water, step XIV. Either which oxidant, O^* or OH^*, reacts with adsorbed acetaldehyde or acetyl, water must dissociate via elementary step XIV on the Cu surface to provide for these.

4.4. Reaction order

In analysing the Langmuir–Hinshelwood type reaction rate expressions for a proposed rate determining step, the denominator term ($1 + \sum$ adsorption terms) expresses the reduction of activity due to occupation of free sites by adsorbed species. Askgaard et al. [12] report that the coverage of the free Cu sites in the C1 system highly depends on the pressure of the active components. At 2 bar and 500 K the relative abundance of free sites is 0.88,

Table 1
Elementary reaction steps suggested for the dehydrogenation of ethanol via acetaldehyde to acetic acid on Cu, steps VII–XI based on C1 elementary reactions on Cu. * signifies a free Cu site.

	Elementary surface reaction	Type	Reference
I	$CH_3CH_2OH(g) + * = CH_3CH_2OH^*$	Ethanol adsorption	[8,11]
II	$CH_3CH_2OH^* + * = CH_3CH_2O^* + H^*$	Hydroxyl hydrogen abstraction	[8,11]
III	$CH_3CH_2O^* + * = CH_3CHO^* + H^*$	Ethoxy α-hydrogen abstraction	[8,11]
IV	$CH_3CHO^* = CH_3CHO(g) + *$	Acetaldehyde desorption	[7,8,11], this work
V	$CH_3CHO^* + * = CH_3CO^* + H^*$	Acetaldehyde α-hydrogen abstraction	[11]
VI	$CH_3CO^* + OH^* = CH_3COOH^* + *$	Acetyl hydroxyl oxidation	[11]
VII	$CH_3CH_2O^* + O^* = CH_3CHOO^* + H^*$	Ethoxy oxidation	[12]
VIII	$CH_3CHO^* + O^* = CH_3CHOO^* + *$	Acetaldehyde oxidation	[12]
IX	$CH_3CHO^* + OH^* = CH_3CHOO^* + H^*$	Acetaldehyde hydroxyl oxidation	[12]
X	$CH_3CHOO^* + * = CH_3COO^* + H^*$	Acetate formation	[12]
XI	$CH_3COO^* + H^* = CH_3COOH^* + *$	Acetic acid formation	[12]
XII	$CH_3COOH^* = CH_3COOH(g) + *$	Acetic acid desorption	[7,12], this work
XIII	$H_2O(g) + * = H_2O^*$	Water adsorption	[7,12,16,17]
XIV	$H_2O^* + * = OH^* + H^*$	Water dissociation	[7,12,16,17]
XV	$2OH^* = H_2O^* + O^*$	Hydroxyl disproportionation	[7,12,16,17]
XVI	$OH^* + * = O^* + H^*$	Hydroxyl dissociation	[7,12,16,17]
XVII	$2H^* = H_2(g) + 2*$	Dihydrogen formation	[7,12,16,17], this work

balanced primarily by coverage of adsorbed hydrogen. It may be argued then that at 0.5 bar of reactants and products and 553 K, i.e. four times lower pressure and a higher temperature, the free sites are by far the most abundant species. Assuming that the free sites are dominant, the adsorption terms become negligible, leaving basically a rate equation equal to the numerator term of the full Langmuir–Hinshelwood expression.

Whereas the conversion of acetaldehyde to acetic acid is rather slow the dehydrogenation of ethanol to acetaldehyde is so fast that pore diffusion limitation could influence the observed rate. Being a first order reaction intrinsically one would, however, still expect a first order behaviour in ethanol for the ethanol dehydrogenation under the influence of pore diffusion limitation, the observed activation energy being somewhat lower, depending on the pore branching.

We find an observed activation energy of 44 kJ/mol for the ethanol dehydrogenation, Eq. (1). Tu et al. finds an intrinsic activation energy for ethanol dehydrogenation to acetaldehyde on pure Cu of 51 kJ/mol. The two values are basically consistent keeping in mind that our value is slightly lowered due to the diffusion limitation in our whole pellet experiments. Shustorovich and Bell [14] calculates the activation energy barrier of the formation of methoxy from adsorbed methanol to be around 38 kJ/mol. The energy of hydrogen abstraction from ethanol should be similar; thus the calculated value by Shustorovich and Bell is consistent with the activation energies for Eq. (1) found experimentally.

The approximate determination of the apparent reaction order of 0.8 (see Fig. 5) in ethanol is consistent with the finding by Tu et al. [4] who report the reaction order with respect to ethanol to be 1.

Guan and Hensen [15] investigated the ethanol dehydrogenation on a silica supported gold catalyst. The reaction rate was found to be solely first order with respect to ethanol. The first order ethanol dependence without the dependence of hydrogen is consistent with a Langmuir–Hinshelwood expression with negligible adsorption terms assuming that the first hydrogen abstraction is the rate determining step [22].

For the acetaldehyde conversion, Eq. (2), we find an apparent reaction order of water close to unity. However, a dependence of acetaldehyde was found as well. A reaction order for the reaction in Eq. (2) close to unity for water (see Fig. 5) may reflect that the elementary step XIV is rate limiting. Under this assumption, a reaction order higher than 0 with respect to acetaldehyde reflects that the dissociation of water in step XIV is not much slower than is the oxidation of acetaldehyde or acetyl. However, the dissociation energy of adsorbed water on step sites was found to be 125 kJ/mol by means of DFT calculations, which is far from the apparent activation energy 34 kJ/mol as found experimentally for Eq. (2). Wang et al. have reported water dissociation energies of 100–123 kJ/mol for the Cu(1 1 0), Cu(1 0 0) and Cu(1 1 1) surfaces [23]. Due to this discrepancy, we do not believe that water dissociation is the rate limiting step in Eq. (2).

Colley et al. found that the activation energy for the dehydrogenation of adsorbed acetaldehyde to acetyl is much smaller than the desorption of acetaldehyde leading to low concentrations of acetaldehyde in the gas phase. We do, however, see very high concentrations of acetaldehyde in our reaction system where adsorbed acetaldehyde or acetyl possibly reacts with dissociated water, O* or OH*. This indicates that the acetaldehyde or acetyl oxidations (Table 1, steps VI, VIII or IX) have considerable activation barriers. Therefore, it is most likely that either the oxidation with O* or OH* of adsorbed acetaldehyde or hydroxyl oxidation of acetyl is rate determining.

The assumption of acetaldehyde or acetyl oxidation being the rate determining step does indeed result in a Langmuir–Hinshelwood expression, based on one site type, where the observed numerator has a reaction order of 1 both with respect to water and acetaldehyde. Furthermore a reaction order with respect to hydrogen of −½ is found assuming acetaldehyde oxidation with adsorbed hydroxyl, OH*, to be rate determining, while the hydrogen reaction order was found to be −1 for acetaldehyde oxidation with atomic oxygen, O*, or acetyl oxidation with adsorbed hydroxyl as the rate determining step, respectively.

Elementary steps XIII–XVII were studied on a Cu[1 1 1] surface by Phatak et al. [16] and it was found that the coverage of OH* is a factor of 10^6 as high as the O* coverage. In a more recent study by Chen et al. [17] it was found that hydroxyl even binds stronger on Cu[3 2 1] step sites. Therefore, most likely the oxidation takes place by means of adsorbed hydroxyl, OH*.

As mentioned, the intrinsic reaction rate model has hydrogen dependence as well. Hydrogen was varied as a process parameter however being proportional to the acetaldehyde partial pressure in most cases. Assuming that the rate determining step is the oxidation of adsorbed acetaldehyde with hydroxyl, the corresponding Langmuir–Hinshelwood expression may explain the observed near 0.5 dependence of acetaldehyde if the apparent reaction order reflects in reality an overall acetaldehyde and hydrogen dependence and if the adsorption terms are truly negligible. Eq. (9) expresses the forward Langmuir–Hinshelwood reaction rate for Eq. (2) being far from equilibrium, based on the above assumption.

$$-r_{CH_3CHO,L-H,forward} = \frac{k \cdot (p_{H_2O} \cdot p_{CH_3CHO})/p_{H_2}^{1/2}}{(1 + \sum \text{adsorption\_terms})^2} \quad (9)$$

where k is the resulting apparent rate constant and p_{CH_3CHO}, p_{H_2O}, p_{H_2} are the partial pressures of acetaldehyde, water and hydrogen.

Assuming the pathway would go through acetyl oxidation with hydroxyl, the overall acetaldehyde and hydrogen reaction order of the numerator alone is 0, which does not correspond well with the overall dependence of acetaldehyde and hydrogen found by optimisation.

Furthermore, a positive dependence of the total pressure would be expected from any of these terms. However, increasing the operating pressure by a factor of 10 caused serious deactivation of the catalyst, presumably due to sintering, so this information was veiled by an overlaying deactivation phenomenon.

The dependence in acetaldehyde (and hydrogen) could thus be explained by the oxidation of adsorbed acetaldehyde with hydroxyl as the primary pathway and the rate determining step, in agreement with the suggestion by Iwasa and Takezawa [7]. Citing Ovesen et al. [13] different mechanisms can lead to the same overall kinetic expression. But based on more indications, the two most likely pathway candidates finally down-selected actually have different reaction order sets, of which one set has a superior fit with the power-law expression found. Best consistence is therefore found for acetaldehyde oxidation with hydroxyl.

The validity of the derived power-law rate equation for the conversion of acetaldehyde (Eq. (8)) may be limited to feeds with approximately equimolar amounts of acetaldehyde and hydrogen.

4.5. Reduction influence

As mentioned, in aiming for more isothermal operation some experiments were conducted on crushed catalyst under which conditions the catalyst seemed to have a 3 times higher intrinsic activity for the conversion of acetaldehyde to acetic acid. The discrepancy cannot be explained by diffusion limitation, as judged from the observed reaction rate, reaction order and the apparent activation energy for the two catalyst sizes tested.

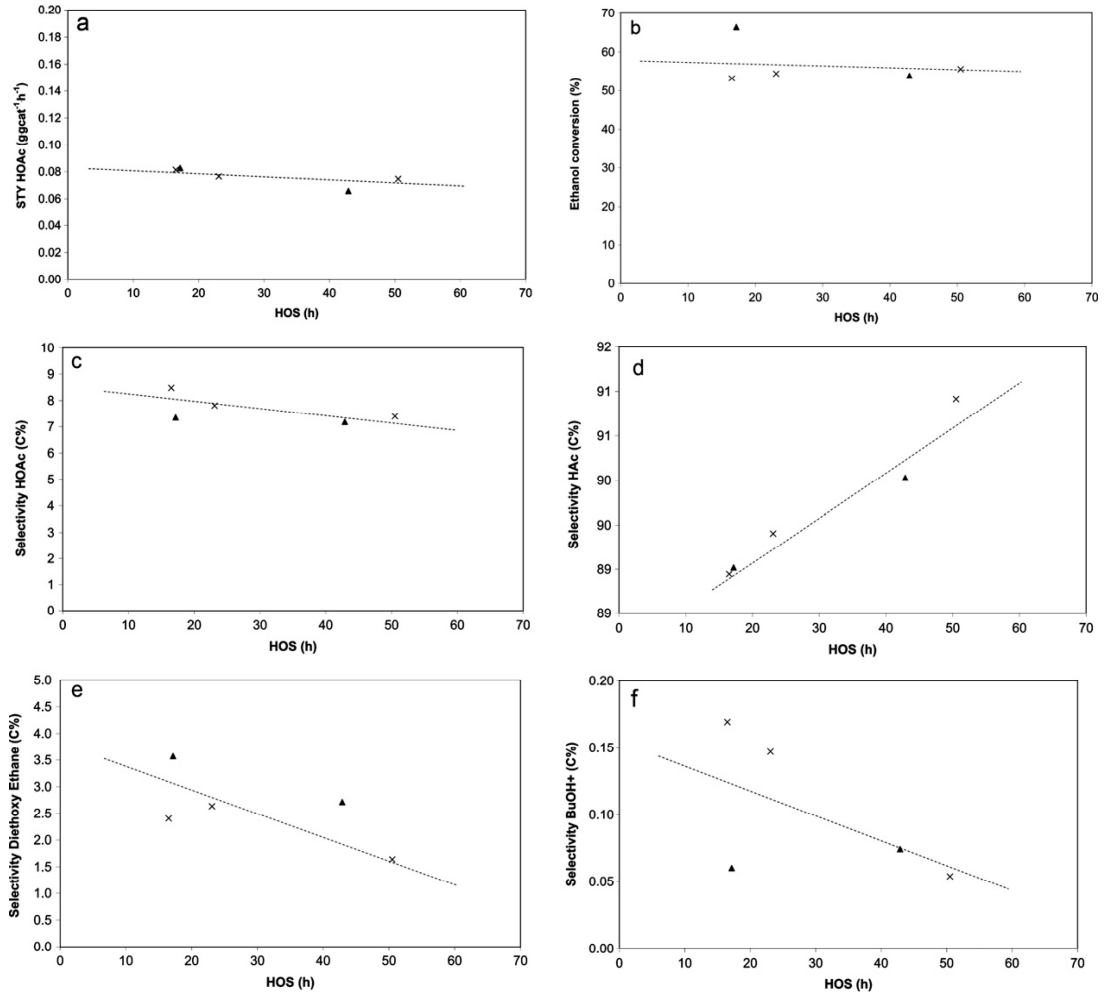

Fig. 9. (a) STY_{HOAC}, (b) ethanol conversion and (c–f) product selectivities vs. time on stream for reaction conditions LWHSV = 0.4–0.5 g/(g h) for a 40:60 ethanol:water feed at t_{bed} = 290–300 °C.

Using the information from the DFT calculations on Cu surfaces the cleavage of water primarily takes place on step sites. According to Guan and Hensen [15], studying dehydrogenation of ethanol on gold surfaces, the density of step sites is expected to depend inversely on the particle size above a certain optimum nanoparticle size; and for constant Cu amount the Cu surface area also depends inversely on Cu crystal size.

Above best consistence with experiments was found for acetaldehyde oxidation with hydroxyl as the rate determining step, having a high dependence of water in the corresponding rate equation. If Cu step sites are the predominant active sites for the cleaving of water the primary coverage of hydroxyl species used in the oxidation of acetaldehyde is also on the step sites. The almost doubling of the Cu crystal size may then, together with the inverse dependence of the density of Cu step sites, account for the reduction of the reaction rate with a factor of 3.

The XRD on the catalyst reveal that the catalyst is influenced by a sintering phenomenon during reduction such that Cu crystals of almost double size are obtained for whole pellets as compared to crushed pellets (1–3 mm sieve fraction). Similarly, the growth rate during operation is affected but the most predominant effect is induced under reduction. It may be argued that reduction water plays a role.

5. Conclusion

Cu/SiO_2 is a selective and well-suited catalyst for acetic acid synthesis from ethanol, the Cu being present as metallic copper particles on the silica support as confirmed by TEM, EXAFS and XRD. DFT calculations show the preferential cleavage of water at Cu step sites.

The reaction quotient of 0.7, approximating the equilibrium constant, at 588 K for ethanol dehydrogenation to acetaldehyde and hydrogen was found to agree well with the equilibrium constant value estimated from the thermochemical data reported by Stull et al. [5].

The suggested reaction order of 1 with respect to ethanol for the dehydrogenation of ethanol to acetaldehyde was supported by the experiments in present study. The apparent activation energy of the non-intrinsic kinetic expression for dehydrogenation of ethanol to acetaldehyde is as expected slightly lower than the intrinsic value reported in literature for pure Cu.

An intrinsic empirical kinetic power law expression for the dehydrogenation of acetaldehyde to acetic acid was derived. The apparent reaction order of water close to unity and the apparent reaction order of acetaldehyde and hydrogen overall of 0.45 tentatively suggest that hydroxyl based oxidation of acetaldehyde can be the rate determining step.

The relationship between the Cu crystal size and the intrinsic activity found is consistent with the suggestion of the hydroxyl oxidation as the rate determining step, and the preferential cleaving of water on step sites as found by DFT.

Acknowledgments

We thank Berit Hinnemann and Burcin Temel, Haldor Topsøe A/S, for their efforts on DFT calculations as well as Charlotte Ovesen, Haldor Topsøe A/S, for mechanistic discussions, Robin Christensen and Xenia Faber for XRPD analysis and Stig Helveg, Haldor Topsøe A/S, for *in situ* TEM analysis of the Cu/SiO_2 catalyst.

This work is part of an industrial PhD study under the CHEC and PROCESS Research Centers at the Department of Chemical and Biochemical Engineering at the Technical University of Denmark in collaboration with Haldor Topsøe A/S, financed by Haldor Topsøe A/S and the Danish Council for Technology and Innovation.

Finally we acknowledge HASYLAB at DESY, Hamburg, for beamtime and DANSCAT and the EU for financial support of the beamtime (Contract AII3-CT-2004-506008).

Appendix A.

In this appendix we provide further considerations on the experimental basis and some additional catalytic data.

In a first round, the Cu/SiO_2 catalyst was tested as crushed pellets sieve fraction diluted with SiC in order to establish as close to isothermal as possible conditions for equilibrium experiments. However, running on crushed catalyst results in low particle Reynolds Number (Re_p) down to 10 ($Re_p = d_h G/\mu$, where d_h is the hydraulic diameter, G is the gas mass velocity per cross section of empty tube and μ is the fluid viscosity) in the 8 mm reactor with the catalyst mass and flow rate limitations given. Therefore, due to the dependence on proper modelling most of the kinetic experiments were conducted with whole pellets in a single-pellet string configuration at $Re_p \approx 60–250$, making a modelling of the conversion reasonably trustworthy. Furthermore, from the observed reaction rate of acetaldehyde conversion to acetic acid (based on the Weisz–Prater Modulus) no significant internal diffusion limitations are expected.

Fig. 9a–f shows the activity (STY), conversion and product selectivity vs. hours on stream for whole pellets.

Appendix B.

In this appendix we have a discussion on the suggested reaction mechanisms based on literature findings.

As to the reaction pathway Inui et al. [9] suggest that over a Cu–Zn–Zr–Al–O catalyst acetic acid is produced from ethanol through acetaldehyde in agreement with Eq. (1) but that acetaldehyde reacts to hemiacetal and further to ethyl acetate, which then hydrolyses to acetic acid in disagreement with Eq. (2). Based on our work it is assumed that acetic acid is produced primarily through the reaction of acetaldehyde with water over a Cu catalyst, which was also supported by Iwasa and Takezawa [7].

Breaking the conversions into elementary steps the likelihood of the suggested reaction pathway may be elucidated.

Table 1 shows a survey of elementary reactions established or proposed as parallels to elementary reactions for C1 conversions. Herein * signifies a free Cu surface site.

The initial mechanism for the abstraction of hydrogen from ethanol to obtain acetaldehyde has been studied in the literature [8,11].

The initial conversion of ethanol to acetaldehyde is suggested to take place via steps I and II followed by another hydrogen abstraction step, see step III. Steps I and II in combination and step III were shown in temperature dependent ethanol adsorption studies (TDSS) on Cu/Cr_2O_3 by Colley et al. [11]. The dominant abstraction of α-hydrogen from adsorbed ethoxy on Cu in step III was confirmed by Chung et al. [8] by isotopic labelling.

As observed in our experiment acetaldehyde desorbes as an intermediate, step IV.

Furthermore, Colley et al. found that acetaldehyde easily dehydrogenates into acetyl, step V, and that acetyl reacts with ethoxy to ethyl acetate. Very small amounts of ethyl acetate were found in our work in the conversion of ethanol over Cu/SiO_2 indicating a low coverage of either ethoxy or acetyl. Assuming a considerable coverage of acetyl the reaction of an adsorbed acetyl with hydroxyl to CH_3COOH^* may be suggested, step VI.

Iwasa and Takezawa [7] suggest the nucleophilic addition of water (OH) to adsorbed acetaldehyde as the pathway for acetic acid formation. They further made comparisons to the methanol system studied over Cu based catalysts and found several similarities. Therefore, in screening for more possible pathways inspiration has been found in the corresponding C1 system conversions, i.e. methanol (MeOH) reforming ($MeOH + H_2O = 3H_2 + CO_2$) or synthesis being catalysed on Cu surfaces in conjunction with the water gas shift reaction ($CO + H_2O = H_2 + CO_2$). Support to the valid comparison of the methanol and ethanol systems of reaction pathways over Cu catalyst may be found in a work by Shimada et al. [10] where the oxidation of formaldehyde and acetaldehyde, were studied. Chung et al. [8] expects analogies between ethanol and methanol dehydrogenation mechanisms due to their identical distance between the α-hydrogen and the oxygen under the consideration of configurational constraints.

The elementary reaction pathways for methanol and shift active Cu catalysts have been studied by Ovesen et al. [13] and Askgaard et al. [12]. In the C1 system, the elementary steps underlying the synthesis of methanol over Cu catalyst, where the side-product formaldehyde is found, is explained by the dissociation of adsorbed oxidised formaldehyde hydrate, H_2COO^*, on a free site to form $HCHO^*$ and O^* by Askgaard et al. [12], the methanol synthesis taking place in a C1 system, while ethanol is a C2 compound. Thus, in the reverse direction, the oxidation of the adsorbed formaldehyde to the oxidised formaldehyde hydrate is implicitly suggested in the C1 system, and the further steps of its decomposition to H^* and adsorbed formate, and the final decomposition of formate to CO_2 and H_2 were verified at 470 K. As opposed to formate as a product in the C1 system acetate in the C2 system is a very stable compound which may easily be hydrogenated to acetic acid.

Following the suggested pathways for formaldehyde to formate by Askgaard et al. the formation of oxidised acetaldehyde hydrate CH_3CHOO^* is assumed possible, being the precursor to acetate and acetic acid.

References

[1] K. Weissermel, H.-J. Arpe (Eds.), Industrial Organic Chemistry, fourth ed., Wiley, Weinheim, 2003, pp. 171–174.
[2] W. Foerst, Ullmanns Encyklopädie, 6. Band, Urban & Scharzenberg, München-Berlin, 1955, p. 783.
[3] Y. Tomiaki, S. Masami, JP57102835.
[4] Y.-J. Tu, C. Li, Y.-W. Chen, J. Chem. Technol. Biotechnol. 59 (1994) 141–147.
[5] D.R. Stull, E.F. Westrum, G.C. Sinke, The Chemical Thermodynamics of Organic Compounds, Wiley, New York, 1969, pp. 439–440.
[6] J. Happel, J.C. Chao, R. Mezaki, J. Chem. Eng. Data 19 (2) (1974) 110–112.
[7] N. Iwasa, N. Takezawa, Bull. Chem. Soc. Jpn. 64 (1991) 2619–2623.
[8] M.-J. Chung, S.-W. Han, K.-Y. Park, S.-K. Ihm, J. Mol. Catal. 79 (1993) 335–345.

[9] K. Inui, T. Kurabayashi, S. Sato, N. Ichikawa, J. Mol. Catal. A 216 (2004) 147–156.
[10] T. Shimada, K. Sakata, T. Homma, H. Nakai, T. Osaka, Electrochim. Acta 51 (2005) 906–915.
[11] S.W. Colley, J. Tabatabaei, K.C. Waugh, M.A. Wood, J. Catal. 236 (2005) 21–33.
[12] T.S. Askgaard, J.K. Nørskov, C.V. Ovesen, P. Stoltze, J. Catal. 156 (1995) 229–242.
[13] C.V. Ovesen, B.S. Clausen, B.S. Hammershøi, G. Steffensen, T. Askgaard, I. Chorkendorff, J.K. Nørskov, P.B. Rasmussen, P. Stoltze, P. Taylor, J. Catal. 158 (1996) 170–180.
[14] E. Shustorovich, A.T. Bell, Surf. Sci. 253 (1991) 386–394.
[15] Y. Guan, E.J.M. Hensen, Appl. Catal., A 361 (2009) 49–56.
[16] A.A. Phatak, W.N. Delgass, F.H. Ribeiro, W.F. Schneider, J. Phys. Chem. C 113 (2009) 7269–7276.
[17] C.-S. Chen, T.-W. Lai, C.-C. Chen, J. Catal. 273 (2010) 18–28.
[18] J.-D. Grunwaldt, M. Caravati, S. Hanneman, A. Baiker, Phys. Chem. Chem. Phys. 6 (2004) 3037–3047.
[19] T. Ressler, J. Synchrotron Radiat. 5 (1998) 118–122.
[20] D.S. Scott, W. Lee, J. Papa, Chem. Eng. Sci. 29 (1974) 2155–2167.
[21] S. Freni, N. Mondello, S. Cavallaro, G. Cacciola, V.N. Parmon, V.A. Sobyanin, React. Kinet. Catal. Lett. 71 (2000) 143–152.
[22] R.M. Rioux, M.A. Vannice, J. Catal. 216 (2003) 362–376.
[23] G.-C. Wang, J. Nakamura, J. Phys. Chem. Lett. 1 (2010) 3053–3057.